

AD-A161 539

NPS -67-85-008

NAVAL POSTGRADUATE SCHOOL

Monterey, California



PROCEEDINGS OF THE 1985 ONR/NAVAIR

WAVE ROTOR RESEARCH AND

TECHNOLOGY WORKSHOP

MAY 1985

DTIC FILE COPY

Approved for public release; distribution unlimited

Prepared for: OFFICE OF NAVAL RESEARCH
ARLINGTON, VA 22217
NAVAL AIR SYSTEMS COMMAND
WASHINGTON, DC 20361

DTIC
ELECTE
OCT 22 1985

85 10 21 105

A

NAVAL POSTGRADUATE SCHOOL

Monterey, California

Rear Admiral R. H. Shumaker
Superintendent

D. A. Schrady
Provost

The workshop which is reported herein was held at the Naval Postgraduate School on 26 & 27 March 1985 and was supported by the Office of Naval Research (Mechanics Division), under the cognizance of K. Ellingsworth and by Naval Air Systems Command (Code 310E) under the cognizance of G. Derderian. The program and sessions were chaired by R. Shreeve. Coordination of all arrangements before and during the workshop, transcription of the discussion and compilation of these proceedings was provided by A. Mathur with the assistance of M. Rigterink. The projectionist was J. King and R. Phillips provided video recording.

The proceedings were compiled and edited under Navy Contract Number N62271-85-M-0423. Publication of the Proceedings does not constitute endorsement of the opinions individually expressed by the participants.

Reproduction of all or part of this report is authorized.

This report was prepared by:

Ramond P. Shreeve
R. P. SHREEVE
Director, Turbopropulsion
Laboratory

Atul Mathur
A. MATHUR
Project Engineer
EXOTECH Inc.

Reviewed by:

H. F. Platzer
H. F. PLATZER
Chairman,
Department of Aeronautics

Released by:

J. Dyer
J. DYER
Dean of Science and Engineering

DISCLAIMER NOTICE

THIS DOCUMENT IS BEST QUALITY PRACTICABLE. THE COPY FURNISHED TO DTIC CONTAINED A SIGNIFICANT NUMBER OF PAGES WHICH DO NOT REPRODUCE LEGIBLY.

UNCLASSIFIED

SECURITY CLASSIFICATION OF THIS PAGE (When Data Entered)

REPORT DOCUMENTATION PAGE		READ INSTRUCTIONS BEFORE COMPLETING FORM
1. REPORT NUMBER NPS-67-85-008	2. GOVT ACCESSION NO. AD-A161539	3. RECIPIENT'S CATALOG NUMBER
4. TITLE (and Subtitle) PROCEEDINGS OF THE 1985 ONR/NAVAIR WAVE ROTOR RESEARCH AND TECHNOLOGY WORKSHOP		5. TYPE OF REPORT & PERIOD COVERED 1st Jan - 31st March 85 FINAL REPORT
		6. PERFORMING ORG. REPORT NUMBER
7. AUTHOR(s) R. P. SHREEVE & A. MATHUR (EDITORS)		8. CONTRACT OR GRANT NUMBER(s) N0001485WR24208 N0001985WR51147
9. PERFORMING ORGANIZATION NAME AND ADDRESS NAVAL POSTGRADUATE SCHOOL MONTEREY, CALIFORNIA 93943		10. PROGRAM ELEMENT, PROJECT, TASK AREA & WORK UNIT NUMBERS 61153N; RR024-03-02
11. CONTROLLING OFFICE NAME AND ADDRESS OFFICE OF NAVAL RESEARCH 800 N. QUINCY STREET ARLINGTON, VIRGINIA 22217		12. REPORT DATE MAY 1985
		13. NUMBER OF PAGES
14. MONITORING AGENCY NAME & ADDRESS (if different from Controlling Office)		15. SECURITY CLASS. (of this report) UNCLASSIFIED
		15a. DECLASSIFICATION/DOWNGRADING SCHEDULE
16. DISTRIBUTION STATEMENT (of this Report) Approved for public release; distribution unlimited.		
17. DISTRIBUTION STATEMENT (of the abstract entered in Block 20, if different from Report)		
18. SUPPLEMENTARY NOTES		
19. KEY WORDS (Continue on reverse side if necessary and identify by block number) WAVE ENGINES WAVE ROTOR TECHNOLOGY GAS WAVE TURBINE ENGINES PRESSURE EXCHANGERS		
20. ABSTRACT (Continue on reverse side if necessary and identify by block number) An overview, presentations and discussion in a 26/27th March 1985 workshop held at the Naval Postgraduate School, "to provide the input necessary for an assessment of the prospects for the useful exploitation of wave rotors in gas turbine engines", are documented.		

DD FORM 1473

1 JAN 73

EDITION OF 1 NOV 65 IS OBSOLETE
S/N 0102-014-6601

UNCLASSIFIED

SECURITY CLASSIFICATION OF THIS PAGE (When Data Entered)

TABLE OF CONTENTS

	page
I. INTRODUCTION AND SUMMARY	1
II. AUTHOR PRESENTATIONS	5
(In order presented)	
i. Kantrowitz, A., 'Wave Engines' (Opening Address)	5
 <u>SESSION 1 - PRESSURE EXCHANGERS</u>	
ii. Kentfield, J. A. C., 'The Pressure Exchanger; An Intro- duction, Including a Review of the Work of Power Jets (R & D) Ltd'.	9
iii. Berchtold, M., 'The Comprex®'	50
iv. Matthews, L., 'The Gas Dynamics of Pressure Wave Super- chargers' (transcription of presentation)	75
v. Thayer, W., 'The MSNW Energy Exchanger Research Program'.	85
 <u>SESSION 2 - WAVE ENGINES</u>	
vi. Moritz, R., 'Rolls-Royce Studies of Wave Rotors (1965- 1970)'	116
vii. Pearson, R., 'A Gas Wave-Turbine Engine Which Developed 35 HP and Performed over a 6:1 Speed Range'	125
viii. Mathur, A., 'A Brief Review of the G. E. Wave Engine Program of 1958 - 1963)'	171
ix. Weber, H. E., 'Shock-Expansion Wave Engines - New Directions for Power Production'	194
 <u>SESSION 3 - RESEARCH AND APPLICATIONS STUDIES</u>	
x. Mathur, A., 'Design and Experimental Verification of Wave Rotor Cycles'	215
xi. Eidelman, S., 'Gradual Opening of Axial and Skewed Passages in Wave Rotors'	229
xii. Wilson, D. G., 'Wave Rotors as Substitutes for Gas-Turbine Diffuser-Combustor Systems'	250
xiii. Zubatov, N., 'Application of Wave Energy Exchanger to Industrial and Energy Systems'	261

xiv.	Rostafinski, W., 'Comparison of the Wave-Rotor-Augmented to the Detonation-Wave-Augmented Gas Turbine'	271
------	------------------------------------------------------------------------------------------------------------------	-----

SESSION 4 - ENGINE PERFORMANCE CALCULATIONS

xv.	Berchtold, M., 'The Compres [®] as a Topping Spool in a Gas Turbine Engine for Cruise Missile Propulsion'	284
xvi.	Taussig, R., 'Wave Rotor Turbofan Engines for Aircraft'	291
xvii.	Pearson, R., 'Performance Predictions for Gas Turbine-Wave Engines Including Practical Cycles with Wide Speed Range'	329
III.	DISCUSSION SESSION	379
i.	Discussion Following Prof. Pearson's Talk	379
ii.	General Discussion	386
Appendix A	Spalding, D. B., 'Remarks on the Applicability of Computational Fluid Dynamics to Wave-Rotor Technology' . .	403
Appendix B	Workshop Program	407
Appendix C	List of Attendees	410
	Distribution List	415

DATE	<input checked="" type="checkbox"/>
TIME	<input type="checkbox"/>
LOCATION	<input type="checkbox"/>
J. J. J. J.	
By	
Distribution	
Availability Codes	
Dist	Avail d/or Special
A-1	23



INTRODUCTION AND SUMMARY
R. P. Shreeve (Chairman)

The concept of a "wave engine", or of the use of a "wave rotor" component in an engine, is often unknown even to engineers who are both active and expert in the technology of conventional engines. The first reaction of a gas turbine engineer is probably that the wave rotor is a "partial admission" device. This is true. However, more importantly, it is also a self-cooling device. The rotor has simple, straight passages in which one gas compresses another by wave propagation and the gas flow both into and out of the stationary ports is, in principle, steady.

The earliest mention of such concepts was in the first decade of this century. Before the conventional gas turbine became successful, wave engines were examined with comparable expectations. They are reexamined now for two compelling reasons. First, the performance of conventional gas turbine engines is inherently constrained to the maximum cycle temperature which steady state operation of the turbine will allow. This constraint especially depresses the performance of small and medium-sized engines wherein it becomes difficult to design efficient and effectively-cooled turbomachinery. Second, in contrast to what was available when the gas turbine engine was first developed, computer-numerical methods for the construction of wave processes and analysis of unsteady flow processes can now be developed in a useful way.

Certain individuals have enthusiastically advocated the development of wave engines for many years. Others have 'found' wave engines only recently. Since 1969, the General Power Corporation in the U.S. has attempted the development of a prototype engine. Also, a research and exploratory experimental program was carried out by Mathematical Sciences Northwest (now Spectra Technology Inc.).

At intervals, different agencies of the U. S. Government have been approached for support for wave engine development programs. The interest of DARPA (Defense Advanced Research Projects Agency) was first expressed in 1981. A Navy-sponsored program to develop an understanding of wave-rotor science and technology was initiated at the Naval Postgraduate School in 1982, and the present workshop is an outgrowth of the latter program.

The announced purpose of the workshop was to bring together an international group who are, or who have been, involved in research studies or applications of gas-gas, or gas-shaft, energy exchange through wave propagation in rotor passages. It is intended that the workshop serve to define the current levels of understanding, capability and interest in the field, and to provide the input necessary for an assessment of the prospects for the useful exploitation of wave rotors in gas turbine engines.

The 2-day meeting had a total of 53 participants with representation from industry, universities and government agencies. Participation from abroad included Brown-Boveri (BBC) Ltd., Rolls-Royce Ltd., Cambridge University and University of Calgary. The program was organized into sessions dealing with pressure exchangers, wave engines and research and applications studies. The total volume of information transmitted was surprisingly large. A comprehensive review has not yet been possible. The following paragraphs give only a general outline of the proceedings and some of the highlights.

The keynote speaker, Professor Arthur Kantrowitz emphasized two main points; first, that travelling waves are inherently more effective in increasing gas pressure at a given Mach number than are steady state processes; second, that the key problem of leakage between stator and rotor can be readily overcome by using active clearance control.

In the first session Professor John Kentfield gave an introduction to the wave-rotor concept and to various types of wave energy exchangers, and reviewed the early work done in England at Power Jets (R&D) Ltd. (Additional comments on the Power Jets work were contributed by Professor D. B. Spalding of Imperial College and are given in Appendix A). A thorough presentation of the Brown-Boveri (BBC) Complex as an engine supercharger, its origins and present commercial success, was made by Professor Max Berchtold. Dr. L. Matthews then described the current BBC research and development program. Specifically, an experimental rig has been built and is operating in which laser anemometry is used to investigate the accuracy of computational descriptions of the unsteady flows. Finally, the analytical and experimental work to demonstrate an efficient gas pressure exchanger was described by Dr. W. J. Thayer. A direct energy transfer efficiency of 80-85% is projected to be possible based on this experience.

Four wave-engine development programs were presented in the second session. First, Professor Ron Pearson of the University of Bath described what was probably the first successful wave engine. After first building a very small engine (which was exhibited and which resembled a small sewing machine in size and shape), he designed and built for Ruston-Hornsby a machine which operated successfully prior to 1960 when first switched on. The engine produced 35 Horsepower and operated over a 6:1 speed range. This pioneering effort was not published at the time but was in fact a clear demonstration of the feasibility and potential of wave engines. Feasibility is not an issue; how best to exploit the concept in an engine and what levels of performance are attainable, are the questions that must be addressed. Dr. Atul Mathur followed Prof. Pearson with an account of a five year wave engine development program carried out by the General Electric Company. This very thorough program was terminated in 1963 at the point of success when the company decided, as a policy, to terminate all work on small engines. Work at Rolls-Royce in Gt. Britain in the mid 60's, to adapt the Complex design to a helicopter engine was described by Mr. R. R. Moritz and illustrated by a movie. Finally, the design and development status of the General Power Corporation engine was presented by Prof. H. E. Weber with comments by Prof. Max Berchtold. (Mr. Richard R. Coleman was unable to attend)

In "Research and Applications Studies", the work at the Naval Postgraduate School was presented in two talks. Dr. Atul Mathur described a Random Choice Method (RCM) code for preliminary design of wave rotor cycles and a wave turbine experiment now in progress. Dr. Shmuel Eidelman showed results obtained with a Godunov-Euler (EGE) code for the 2D unsteady port opening process. The latter work clearly demonstrated the necessity for either modeling or computing the transient effects of port opening and suggested that the effects might be minimized by selecting the passage skewing angle in correct relation to the design wheel speed. Results of potential applications studies were contributed by Prof. D. G. Wilson and Prof. N. Zubatov. The latter described industrial applications studied in the U.S.S.R. A comparison of the performance of a wave-turbofan engine (derived from a

study reported by R. Taussig) with that of an as-yet-unproven concept involving detonative combustion, for a 1000lb thrust engine operating at $M=.75$ was presented by Dr. W. Rostafinski of NASA Lewis Research Center. SFC's below .65 were projected for both engines.

The final three presentations dealt explicitly with the projected benefits of incorporating pressure exchangers, or shaft-work-producing wave-energy exchangers, in gas turbine engines. Prof. Berchtold first presented the results of studies based on the incorporation of a Comprex as a topping spool in both a helicopter and a cruise missile engine. An improvement in thermal efficiency from 21 to 26% with power output increasing from 420 to 550 horsepower was projected in the first case, and an SFC of .95 lb/hr.lb at 300lb. thrust in the second. Potential improvements can be expected to the above figures as ceramic rotors are perfected.

Dr. Robert Taussig, from recently published work, gave results of studies of small gas turbine-wave engines which projected TSFC in the range 0.68 to 0.75 lb/hr.lb. for engines in the 600-1000 lb thrust category.

Finally, Prof. Pearson, after describing the methods which he uses to calculate performance and to design for speed range ("half wave plateau" method), gave projections for the performance of what he terms a combined "GAS WAVE TURBINE-GAS TURBINE"(GWT-GT) engine in which the GWT (with shaft work output), rather than the pure pressure exchanger considered in the two previous talks, is incorporated as a topping unit in the gas turbine cycle. Prof. Pearson's calculations showed that a 10cm. diameter rotor, operating as a naturally-aspirated unit could output 17KW of shaft power with a thermal efficiency of 40%. In a small by-pass jet engine application (600lb. thrust at $M=.65$), an SFC of .71 to .73 lb/hr.lb was predicted to be achievable.

While the stimulus for holding the workshop had been to define the potential for flight applications of wave rotors, Prof. Pearson concluded his presentation by showing potentially important applications of the GWT-GT to coal gasification and to combined cycle electrical power generation. In each case, the GWT, in principle, overcame a limitation in present schemes.

The discussion following the sessions provided opportunity for comment, statements of opinion and recommendations. It is noted that the discussion took place based on what had been heard and retained, and without access to the written material contained in the present volume. Speakers generally conceded that a proven potential exists, and comments dealt with what needed to be done now. The recommendation was made to pursue first only applications in which the wave rotor offered distinct benefits over existing technology. Engine company representatives were clearly interested in the predictions of improved SFC's, but wanted data from tests in order to perform their own assessment of what they could do with current technology. One problem was that companies do not have engineers available at the moment to assign to the development of higher-risk technology. A very convincing case would have to be made.

Comments were made concerning the success of Prof. Pearson's engine in comparison with that of the GPC. Professor Pearson's own explanation was that he had taken a more conservative approach, making his mistakes and learning on the first, very small scale machine, and then designing the second one for speeds at which stresses would not be constraining. In comparison, the GPC

approach involved much higher engineering risks.

Professor Pearson commented that, given the opportunity, he could build a wave engine that would be better than the last one, and that it would work first time as predicted. He also added that he had learned never to persist with a poor design, but always to start again. This could have been a reason for the lack of success in the Rolls-Royce program, which sought to adapt an existing unit to a quite different task.

A full transcription of the discussion is given in Section IV*. In closing the opinion was expressed that an engine re-demonstration was required in order that the development of the technology could receive the attention and support that appear to be warranted.

Dr. Kantrowitz proposed that a committee be formed to ensure that the momentum of interest generated by the workshop be conserved, and that the government have access to a panel to which it can turn for guidance. The Chairman undertook to act on this proposal and the Workshop was adjourned.

*Note: As was announced in advance to the participants, the discussion was recorded on video tape and voice recorder for transcription into the proceedings. In transcribing the recording, minor changes have been made only in grammar, in order to improve readability. The editors hope that this meets with the approval of the participants.

WAVE ENGINES

Arthur Kantrowitz, Thayer School, Dartmouth College

It has long been suspected that compressions and expansions based on wave processes can be made MORE efficient than the corresponding steady flow processes. One basis for this hope can be seen from the first slide (see Fig. C,4b), which compares the pressure ratio necessary to stop a moving gas in a steady process e.g. a perfect diffuser with that necessary to stop a gas, moving at the same speed, with a compression wave or a shock wave. Pressure ratios up to about 10 can be obtained with smaller gas velocities and thus hopefully with smaller friction losses, in unsteady processes. Learning to use waves to make more efficient heat engines is therefore an important opportunity. It is my opinion that central to the achievement of useful wave engines is the invention of effective components which would allow the designer more latitude.

Two classes of wave engines have recieved significant attention. The first is the Schmidt tube which propelled the WWII Buzz bomb. This engine was cheap to make but it has never, as far as I know, achieved high efficiency or long life. In an effort to address the second difficulty it would be useful to design an efficient aerodynamic valve i.e. a check valve without moving parts. To deal with this problem, I will describe the Cascade Diode (U. S. Patent #2,925,830: issued 1960).

The second class of wave engines is the wave rotor which is the primary subject of this workshop. One of the important problems with this device has been the leakage losses produced by clearance between rotor and stator. To control this clearance in the presence of high temperatures and thermal expansions I will describe a thermally actuated clearance control (U. S. Patent #2,665,058: issued 1954).

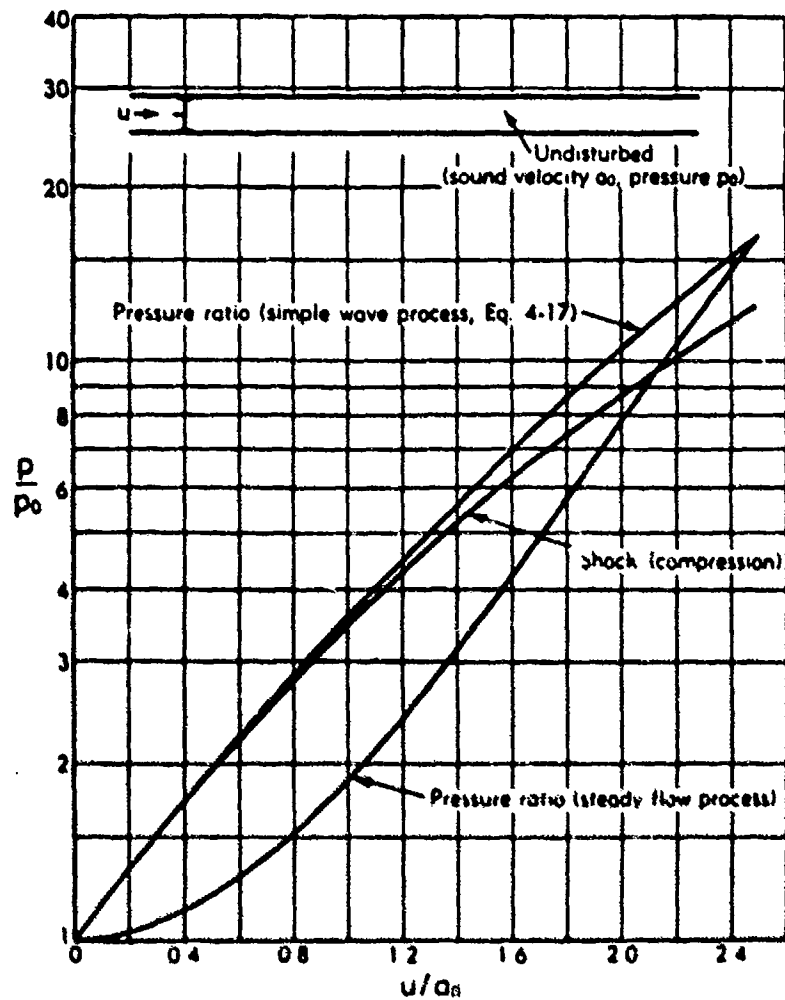
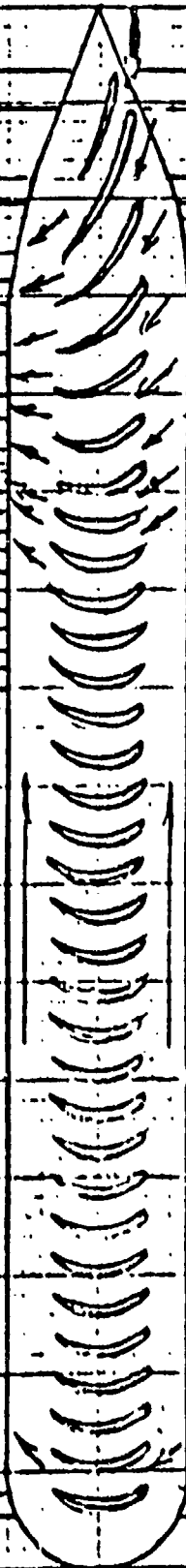


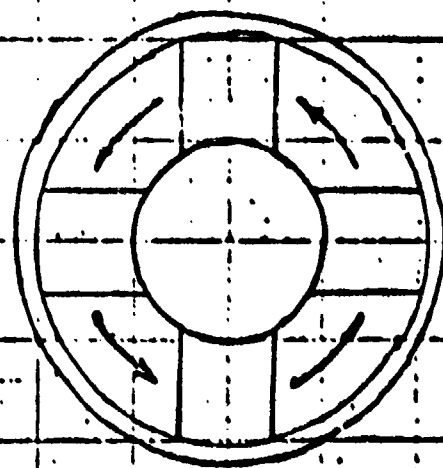
Fig. C.16. Pressure ratio obtained when a gas is accelerated to a velocity u by a compressive simple wave. This is compared with the ratio of stagnation to static pressures for a steady flow process in which the transition is accomplished using both P and Q waves. For comparison the pressure ratio produced by a sudden acceleration to a velocity u , which produces a shock, is also plotted. $\gamma = 1.4$

REVERSED FLOW

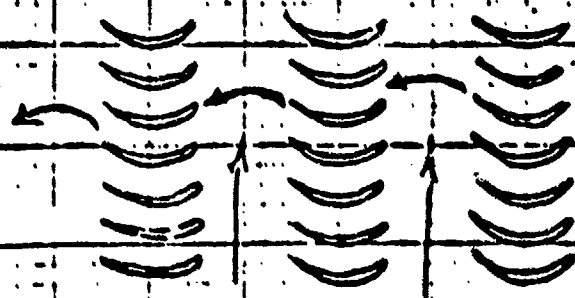


LONGITUDINAL SECTION

CASCADE DIODE



AXIAL CROSS SECTION



DEVELOPED VIEW

FORWARD FLOW

Kantrowitz 8v78

Jan. 5, 1954

A. KANTROWITZ
CONSTRUCTION FOR CONTROLLING CLEARANCE AND
POSITIONS OF PARTS BY THERMAL ACTUATORS

2,665,058

Filed June 1, 1950

2 Sheets-Sheet 1

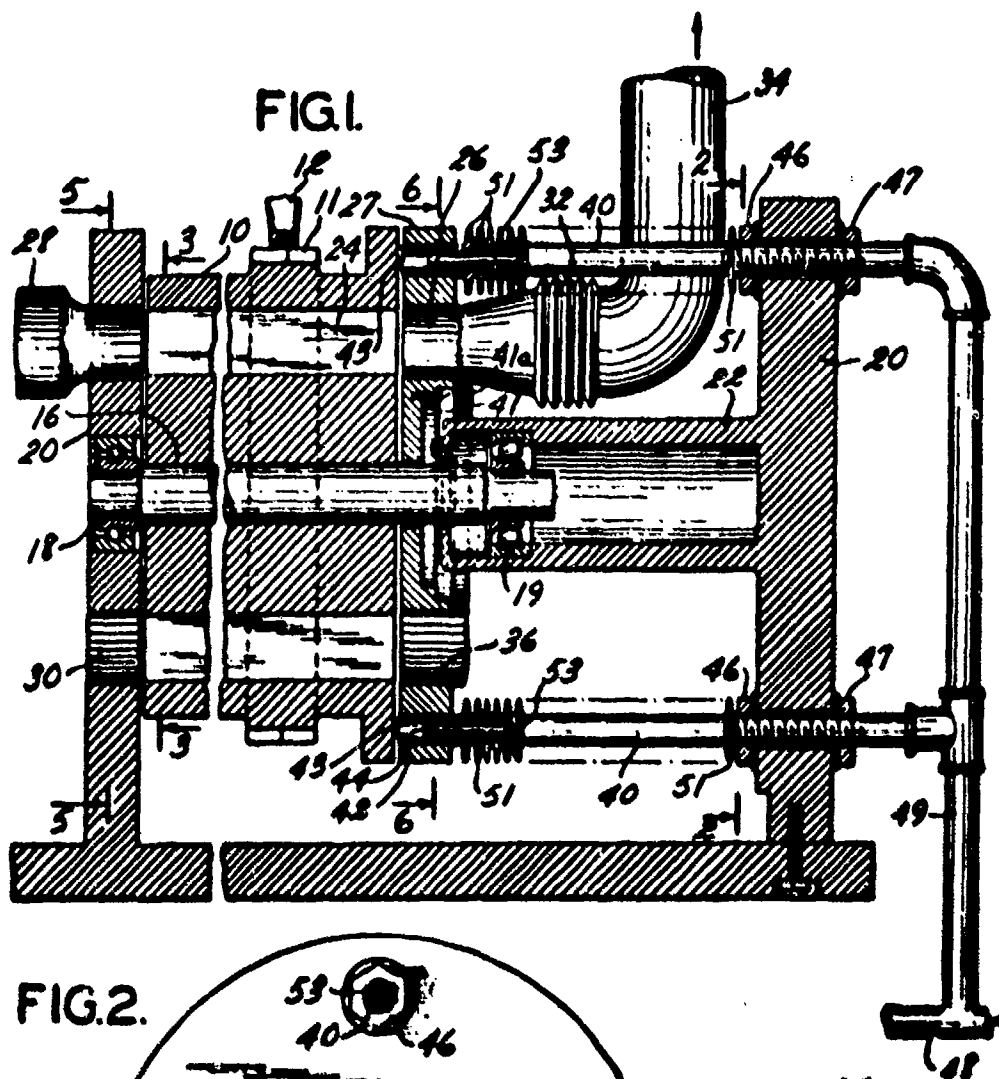


FIG. 2.

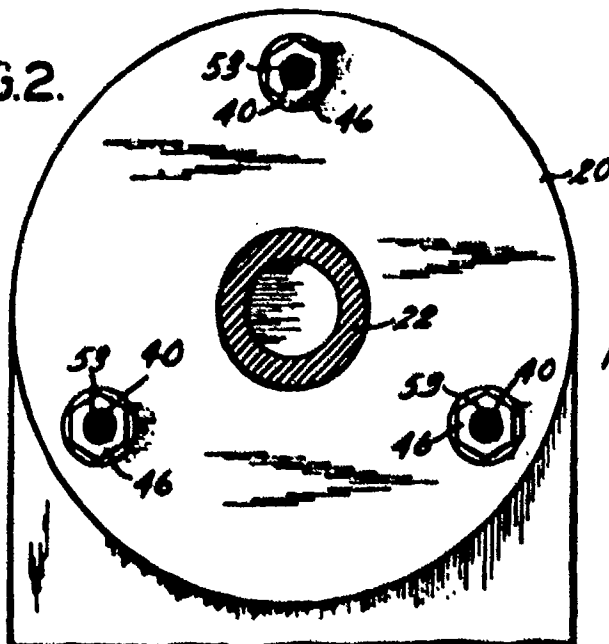


FIG. 3.

INVENTOR
Allen Kantrowitz
BY *Henry Young*
ATTORNEY

THE PRESSURE EXCHANGER: AN INTRODUCTION
INCLUDING A REVIEW OF THE WORK OF
POWER JETS (R & D) LTD.

J.A.C. Kentfield
Department of Mechanical Engineering
University of Calgary
Calgary, Alberta, Canada

ABSTRACT

The potential of pressure-exchangers to perform useful cycles involving the compression and expansion of gaseous flows is discussed briefly and an outline is given of the activities of Power Jets (R & D) Ltd. in the pressure-exchanger field. The bare bones of the dynamic pressure-exchanger concept are introduced in a simplified manner designed to focus attention on the most basic wave processes such as cell filling and cell emptying. Results are presented of cell filling and emptying tests carried out by Power Jets (R & D) Ltd. Various pressure-exchanger cycles, many of which were subsequently tested experimentally, are described in a basic manner prior to presenting data obtained from tests sponsored by Power Jets (R & D) Ltd. Finally, the results of some detailed, comprehensive, cycle analyses are presented for comparison with the results of experiments. It was concluded that, in the most general sense, the results of the Power Jets tests agreed fairly closely with advanced theoretical analysis and that dynamic pressure exchangers perform well. The outstanding need is to identify practical applications where the special properties of pressure exchangers are used to best advantage.

THE PRESSURE EXCHANGER: AN INTRODUCTION
INCLUDING A REVIEW OF THE WORK OF
POWER JETS (R & D) LTD.

J.A.C. Kentfield
Department of Mechanical Engineering
University of Calgary
Calgary, Alberta, Canada

ABSTRACT

The potential of pressure-exchangers to perform useful cycles involving the compression and expansion of gaseous flows is discussed briefly and an outline is given of the activities of Power Jets (R & D) Ltd. in the pressure-exchanger field. The bare bones of the dynamic pressure-exchanger concept are introduced in a simplified manner designed to focus attention on the most basic wave processes such as cell filling and cell emptying. Results are presented of cell filling and emptying tests carried out by Power Jets (R & D) Ltd. Various pressure-exchanger cycles, many of which were subsequently tested experimentally, are described in a basic manner prior to presenting data obtained from tests sponsored by Power Jets (R & D) Ltd. Finally, the results of some detailed, comprehensive, cycle analyses are presented for comparison with the results of experiments. It was concluded that, in the most general sense, the results of the Power Jets tests agreed fairly closely with advanced theoretical analysis and that dynamic pressure exchangers perform well. The outstanding need is to identify practical applications where the special properties of pressure exchangers are used to best advantage.

NOMENCLATURE

a	Local acoustic velocity
l	Length of a pressure-exchanger cell
\dot{m}	Mass flow rate
\dot{m}_s	Mass flow rate required to fill cells at inlet port stagnation conditions
M^*	Axial component of Mach number ($\equiv \frac{u}{a}$)
p	Static pressure
P	Stagnation pressure

P_R	Static pressure ratio (Fig. 11)
q	Heat flow rate
t	Time
t_{CELL}	Time required to expose, or cover, a cell end
T	Stagnation temperature
T_R	Static temperature ratio (Fig. 11)
u	Local gas velocity
x	Coordinate directed along a pressure-exchanger cell
γ	Ratio of specific heats
$\Delta t'_{CELL}$	Dimensionless cell width $\{\equiv \frac{t_{CELL} a_{PORT}}{l}\}$
η	Product of the isentropic efficiencies of compression and expansion (equalizer and divider cycles)
η_{COMP}	Isentropic efficiency of compression
μ	Non-dimensional bulk input $\{\equiv [(\dot{m}T)_{HIN} - (\dot{m}T)_{HOUT}] / (\dot{m}_s T_{LIN})\}$
ρ	Fluid density

Subscripts

a, b etc.	State point locations
IN, OUT	Inflow, outflow
PORT	Port condition
ref	Reference condition

Components Identified in Figures

C	Compressor
H	High pressure port
L	Low pressure port
M	Medium pressure port
T	Turbine

INTRODUCTION

The former British company Power Jets (Research and Development) Ltd., with Prof. D.B. Spalding of Imperial College as consultant, performed, and sponsored, research and development work in the pressure exchanger field between approximately 1952 and 1965. Power Jets inter-

est in pressure exchangers appears to have been sparked by the pioneering work of G. Jendrassik, former chief engineer of the Gantz diesel engine company of Budapest, Hungary. Jendrassik, in parallel with but independently of, Seippel in Switzerland was an originator of pressure-exchanger systems or more correctly dynamic pressure-exchanger systems since pressure waves were utilized.

Some earlier pressure-exchanger concepts pre-dating the work of Seippel and Jendrassik did not make use of pressure wave effects [1,2]. Pressure exchangers which do not utilise pressure waves are sometimes termed static, or semi-static, pressure exchangers. A broader and more general overview of the history of pressure exchangers than can be given here is due to Azoury who covers the subject up to 1965 [3].

A REPRESENTATIVE PRESSURE EXCHANGER

Pressure-exchanger is the generic name given to a class of machine which utilizes non-steady compressible flow phenomena to perform a variety of useful, cyclic, processes. An essential feature of pressure-exchangers is a cellular component usually constituting the rotor of the machine. It is, perhaps, most convenient to describe the essential structure of a typical pressure-exchanger and, subsequently, to investigate the principles of the device. Equipped with this knowledge it is then possible to consider the potential advantages and disadvantages of pressure-exchangers and hence show why there is currently an increasing interest in machines of this type.

A pressure-exchanger, in its most common form, comprises two basic components:

- a) a rotor of cellular construction, as mentioned previously,
- b) a stator containing gas ports in the end faces. The end plates of the stator are mounted as closely as possible to the rotor consistent with the avoidance of rubbing.

Figure 1 is a diagram of the basis of most pressure exchangers. Only one port is shown in each end plate merely to illustrate the essential features of the device. Figure 2 is a schematic cross-section of a simple pressure exchanger: only a single port-and-duct is shown.

In practice the outer sleeve, apparent in Fig. 1 and 2, is sometimes arranged to be telescopic, as was the case with the Power Jets

machines. This allows the clearances between the rotor and the end plates to be maintained at constant, or very nearly so, pre-determined values despite changes in rotor temperature. The end plates move closer together, or further apart, as the rotor cools or heats up respectively. A simpler alternative technique, less suited to transient situations, is to control the temperature of a non-telescopic sleeve such that correct clearances are maintained.

A means is provided to rotate the rotor; this may consist of an electric motor coupled to the rotor by, say, a belt transmission. Alternatively rotors can be made self driving as will be explained later. In either case the power required to maintain rotor rotation in a correctly designed pressure-exchanger is very small; it is nearly zero. The function of the driving means is merely to overcome bearing friction and rotor windage. There is always the inherent possibility in pressure-exchangers of rotating the "stator" and fixing the "rotor". this arrangement rarely seems to be convenient but it should, at least, be kept in mind.

So far only the hardware has been considered. Imagine, for example, that the rotor is spinning and that the cells contain gas at rest relative to the rotor.

If a port, for example the one on the left in Fig. 1 is supplied with fluid (gas) at a pressure higher than that in the cells then gas will enter each cell as it passes the port. The inflow will compress the contents of each cell in turn and will set it in motion to the right. The rotor can be made self driving by arranging an inlet port at a sufficient incidence to the rotor such that the inflow impinges on the cell walls.

Consider, as the alternative to cell filling, what happens when a pressure lower than that prevailing in the cells exists in a port. The port may be regarded as connected to a sink or low pressure reservoir, by the duct coupled to it. Fluid leaves the cells via the port and passes to the reservoir. If, for example, the right hand port of the basic pressure-exchanger of Fig. 1 is connected, via the duct, to a sink then outflow will occur from each cell as it passes the port. The outflow sets the contents of the cells in motion such that fluid flows out to the right, the consequent expansion lowering the pressure

of the cell contents remaining.

It can be seen, in this way, that by cutting ports in the end plates and connecting these to appropriate high or low pressure reservoirs fluid will enter, or leave, the rotor in a pre-arranged sequence. In most pressure-exchangers the frequency with which cells pass the ports is such that flow in the ports is (substantially) steady, the non-steady flow being confined to the cells.

It remains to be shown that such an arrangement can be made to perform useful functions of practical interest. However before proceeding further to consider the potential advantages and disadvantages of pressure exchangers a more detailed study of the basic cell filling and emptying wave processes is required.

BASIC WAVE EVENTS

Wave processes in dynamic pressure exchangers are normally analysed, as was the case for the Power Jets units, by the method-of-characteristics as applied to one-space-dimensional, time dependent, flow [4]. This procedure, which is extremely powerful, can be arranged to take into account variation of entropy, wall frictional effects, heat transfer, the finite time taken to uncover, or cover, a cell end, cell partition thickness, and finally leakage between the cell end faces and the stator end plates. It is also possible to accommodate the possibility of employing tapered cells of non-uniform cross-sectional area [3,5,6,7]. These procedures have also been adapted for digital computation [8,9,10]. The method-of-characteristics is too long and complex to be considered further here. However, a very simple theoretical treatment of idealised, one-dimensional nonsteady compressible flow is possible which gives at least an indication of the dominant physical and quantitative flow features.

Consider, for example, the filling of a single cell of the rotor shown in Fig. 1 and 2 as comparable to the transient filling of a tube of uniform cross-sectional area with a valve at the end capable of opening, or closing, instantaneously and having an unobstructed flow area equal to the cross-sectional area of the container. A cell modelled in this way, which is assumed to have adiabatic walls, is shown in Fig. 3(a). When the pressure of the fluid at rest in the cell is

less than that of the surroundings sudden opening of valve X (Fig. 3(a)) at the left hand end of the cell results in fluid rushing into the cell and initiating a rightward moving discontinuity or compressive wave. In front (i.e. to the right) of the wave the fluid is that which was in the cell originally and it is at rest relative to the pressure-exchanger rotor. Behind (i.e. to the left) of the wave the fluid has been compressed, and set in uniform motion to the right, whilst fluid from the duct flows into the cell through the fully open valve X. The compressive wave propagates rightwards faster than the rightwards flow velocity prevailing behind the wave. In the limit, for infinitesimally weak waves, the wave propagation velocity will be the acoustic velocity in the undisturbed flow. When the rightward moving wave reaches the closed end of the tube all the fluid in the tube, that is the original contents of the tube plus the fluid that flows in through valve X, is travelling to the right at the inflow velocity through valve X.

Since the rightward flow obviously cannot continue through the closed right hand end of the cell, a reflected compression wave is generated at the right hand end wall. This serves to compress, further, the contents of the cell and to bring the flow to rest. The reflected wave propagates leftwards against the direction of inflow. Provided there is no entropy discontinuity between the fluid added to the tube and the original contents of the fluid interface is transparent to the reflected leftward moving wave which continues to propagate until it reaches valve X. If at this moment valve X is closed instantaneously the fluid trapped within the cell will all be at rest and at a higher pressure than that of the surroundings. Such a phenomenon can be shown to be consistent with the requirements of the First Law of Thermodynamics.

The sequence of the events during the filling process can be plotted on a distance (x), time (t) basis, otherwise known as a wave diagram, and this has been done in Fig. 3(b). In Fig. 3(b) a closed end is represented by shading and an open end by the absence of shading. Hence the period during which valve X should be open or a cell communicates with the port, can be deduced immediately from the $x \sim t$ diagram provided the wave propagation velocities are known.

The reverse process to filling, that is cell emptying where the initial pressure in the cell exceeds that of the surroundings, is depicted on the $x \sim t$ plane in Fig. 4. Here the illustration of the model cell, shown in Fig. 3(a), has been omitted since it contributes nothing to the $x \sim t$ diagram showing the physical events. Essential differences between the filling and emptying processes are that the pressure waves occurring during emptying are both of the expansion type and, with valve X located at the left, outflow occurs to the left.

It can be seen that had the cell of Fig. 3(a) been drawn with the valve at the right hand end, and the closed end at the left, the flow and wave propagation directions would be the reverse of those shown in Fig. 3(b) and 4. The nature of the wave events occurring would otherwise be the same.

In a real device valve X cannot be expected to open or close instantaneously nor can friction between the moving fluid and the internal surfaces of the tube be eliminated. However apart from these differences the situations depicted in Fig. 3 and 4 can be shown to approximate reality for relatively weak pressure waves.

Having obtained an impression of the physical nature of the flow for the particular cases of filling and emptying it is now possible to analyze, quantitatively, a more general situation where a single, weak, isentropic, pressure wave propagates through a fluid in a region where the flow velocity in the x direction is u in front of the wave.

Derivation

Applying the conservation of mass principle between fixed stations A and B of the duct shown in Fig. 5 during a time interval δt in which a weak pressure wave travels an elemental distance δx ;

Net mass inflow during δt = mass accumulation during δt , i.e.

$$(u + \delta u)(\rho + \delta \rho) A \delta t - \rho u A \delta t = \delta \rho A \delta x \quad (1)$$

but:

$$\delta x = (a + u) \delta t \quad (2)$$

thus from (1) and (2)

$$(u + \delta u)(\rho + \delta \rho) - u\rho = \delta \rho (a + u)$$

or after expansion:

$$u\rho + \rho\delta u + u\delta\rho + o(\delta^2) - u\rho = a\delta\rho + u\delta\rho$$

Thus after simplification and ignoring terms of order δ^2

$$\rho\delta u = a\delta\rho$$

or

$$\delta u = a \frac{\delta\rho}{\rho} \quad (3)$$

Assuming that the wave is isentropic:

$$\left(\frac{a}{a_{\text{ref}}}\right)^{\frac{2}{\gamma-1}} = \frac{\rho}{\rho_{\text{ref}}} \quad (4)$$

and from logarithmic differentiation of equation (4):

$$\left(\frac{2}{\gamma-1}\right) \frac{\delta a}{a} = \frac{\delta\rho}{\rho} \quad (5)$$

substituting for $\delta\rho/\rho$ in equation (3) from (5):

$$\delta u = \left(\frac{2}{\gamma-1}\right) \delta a \quad (6)$$

Integrating equation (6) without limits, when δ is vanishingly small, and subsequently rearranging:

$$a - \left(\frac{\gamma-1}{2}\right) u = \text{CONSTANT} \quad (7)$$

For a compression wave propagating against the flow, as depicted in Fig. 6, it can be shown by a similar analysis that:

$$a + \left(\frac{\gamma-1}{2}\right) u = \text{CONSTANT} \quad (8)$$

The results given by equations (7) and (8) can be shown to cover all individual, or simple, isentropic waves including expansion wave cases not represented in either Fig. 5 or 6. Thus combining equations (7) and (8):

$$a \pm \left(\frac{\gamma-1}{2}\right) u = \text{CONSTANT} \quad (9)$$

Equation (9) is the required result; the positive or negative signs arise, for positive u , as indicated in Fig. 7.

Construction of $u \sim a$ Diagrams

Equation (9) shows that, on a $u \sim a$, or state, plane, all possible combinations of a and u for a particular value of the CONSTANT can be represented by two inclined straight lines, one with a positive

slope, the other with a negative slope. If the a (ordinate) scale is made $2/(\gamma-1)$ times that used for the u (abscissa) scale, then one line has a slope of $+45^\circ$, the other a slope of -45° . Plotting similar pairs of lines for other discrete values of the CONSTANT on the R.H.S. of equation (9) results in a mesh of lines having slopes of $\pm 45^\circ$ as shown in Fig. 8.

The $u \sim a$ (state) and accompanying $x \sim t$ (wave) diagrams for a typical filling process, such as that illustrated in Fig. 3(b), are presented in Fig. 9. Figure 10 shows the corresponding $u \sim a$ and $x \sim t$ diagrams for an emptying process such as that depicted in Fig. 4. It can be seen from both Fig. 9 and 10 that the labelling identifying the corners of the $u \sim a$ diagrams also represents the corresponding flow regimes between the waves on the $x \sim t$ plane. To improve clarity, compression waves are represented on the $x \sim t$ plane as solid lines and expansion waves by chain-dotted lines.

Mach numbers and pressure ratios can be deduced easily from the $u \sim a$ plane. For example with reference to Fig. 9 or 10:

$$M_b^* = \frac{u_b}{a_b} \quad \text{and} \quad \frac{p_b}{p_a} = \left(\frac{a_b}{a_a} \right)^{\frac{2\gamma}{\gamma-1}}$$

The latter expression is justified because the flow is assumed to be isentropic. It is generally desirable, for most real pressure exchanger situations, not to exceed a pressure ratio of about 2:1 for an individual wave, and hence a port Mach number of about 0.5, in order to minimise the adverse effects of irreversibilities. In the most general sense, this conclusion is confirmed from the results of comprehensive basic cell filling and emptying tests conducted by Power Jets using air as the working fluid. These results are presented, in terms of static temperature versus static pressure ratio, in Fig. 11. The "first part of filling" refers to the first compression wave of a filling process, the "second part of filling" refers to the reflected wave: likewise for emptying. It can be seen, from Fig. 11, that the magnitude of departures from the isentropic increases as the static pressure ratio increases.

ADVANTAGES AND DISADVANTAGES OF PRESSURE EXCHANGERS

It is now possible to make a qualitative assessment, at least tentatively, of the potential advantages and disadvantages of pressure exchangers compared with turbo-machines based on the structural and performance characteristics of pressure-exchangers outlined so far.

Advantages:

- i) Robust construction.
- ii) Generally low rotational speed compared with turbo-machines; too high a rotational speed will obviously not permit the occurrence of adequate cell filling or cell emptying.
- iii) Isentropic efficiencies of compression and expansion comparable with those of turbo-machines: this follows if efficient cell filling and emptying processes are encouraged.
- iv) less prone to erosion damage, due to solid particles or liquid droplet ingestion, than turbomachinery. The velocity of the working fluid in a pressure exchanger relative to the hardware is typically about 1/3 of values commonly met with in turbo-machines; this implies that the kinetic energy of a particle of prescribed mass is only about 10%, in a pressure exchanger, of values attainable in typical turbo-machines.
- v) Ability to withstand higher temperature than say, gas turbines without recourse to structural cooling. The hottest parts of the rotor of a pressure-exchanger are usually only exposed to the maximum working temperature for a portion of the running time; in some cases these regions are also in contact with cool working fluid such as, for example, scavenge air.
- vi) Non-surfing performance characteristics of pressure-exchangers; pressure-exchangers do not surge in the manner customarily associated with axial or centrifugal turbo-compressors.
- vii) A rapid response to operational transients.
- viii) Possibly a lower first cost than some competitive equipment.

Disadvantages:

- i) Low mass flow rate per unit of frontal area compared with turbo-machinery, particularly in relation to axial flow turbo-machines.
- ii) Not primarily suitable for the direct production of shaft power output without the use of a power turbine. In some cases a power turbine can be combined with the pressure-exchanger cellular rotor.
- iii) Noise generation; due to the non-steady flows occurring within them, pressure-exchangers are inherently noisy and therefore require careful muffling or silencing. The noise produced is predominantly of high frequency, usually say 1 to 5 k hertz, and can, therefore, be dealt with fairly easily by absorption devices.
- iv) Significant cyclic fatigue loading conditions often prevail particularly within the cellular rotor.

PRESSURE-EXCHANGER CONFIGURATIONS

Dynamic pressure-exchangers can be configured to perform a wide variety of useful tasks. Seven particular configurations studied to a greater or lesser extent by, or for, Power Jets, are shown in an idealised form in Fig. 12 to Fig. 18 inclusive. In each case the ports of the pressure exchanger are identified by labelling them with reference to the function of each port in accordance with the following code:

L ≡ low pressure	} subscripts "IN" or "OUT" are employed to identify inlet or outlets respectively.
M ≡ medium pressure	
H ≡ high pressure	

In order to simplify the diagrams each wave, compression or expansion, is identified as a single line. As before solid lines are used for compression waves and chain-dotted lines for expansion waves. Particle paths are represented as dotted lines. Wave interactions at interfaces are ignored. For each cycle illustrated a turbo-machine capable of performing the same task is shown, diagrammatically, alongside the dynamic pressure-exchanger which is drawn on the distance \sim time plane. It should be borne in mind that, because the wave processes are cyclic, the top of each distance-time, or wave diagram can be considered to be

looped around and joined to the bottom or, alternatively, each wave cycle is repetitive.

Figure 12 shows the basic configuration of a machine which can serve as a low pressure-ratio gas generator or air compressor or internal-combustion-engine supercharger. The cycle involves two scavenging processes, one at the low pressure of the cycle, the other at the high pressure condition. The low pressure scavenge process serves to replace products of combustion exhausting from the machine with an induced air flow from the surroundings. The high pressure scavenge process results in discharging air, which has been compressed, into the high pressure circuit whilst receiving products of combustion from the same circuit. The cycle involves, in essence, two compression and two expansion waves. A scavenge process can be thought of, in terms of pressure waves, as a two-wave process. Sometimes the low pressure scavenge outlet port is made much wider than the inlet as shown in the inset.

A similar cycle, but with a heat rejection and mass injection replacing the heat addition process, is shown in Fig. 13. This machine can serve as an air-cycle refrigerator. The "output" flow is the cooled low pressure stream leaving the unit.

Figure 14 is another configuration suitable for use as a gas generator, air compressor or supercharger. The arrangement differs from that of Fig. 12 by virtue of the addition of transfer passages each connecting an emptying process to a filling process. The purpose of transfer passages is to increase the overall pressure ratio of the machine without recourse to high gas Mach numbers in the ports of the system. Two transfer passages are shown in Fig. 14: at least in principle there is no restriction on the number of transfer passages that can be used.

A pressure-exchanger equalizer is depicted in Fig. 15. This machine serves a similar function to an ejector or to the turbo-compressor unit shown in the diagram. This cycle is interesting in that it is one which is wholly dependent on wave dynamics: there is no comparable cycle for a non-dynamic, or static pressure-exchanger. A similar remark can be made in relation to the pressure-exchanger divider cycle shown in Fig. 16. This cycle takes as an input a medium pressure stream and

divides it into two outflowing streams one at a higher and the other at a lower stagnation pressure than the input flow. There are potential uses for such devices in pressure-boosting applications and in natural-gas distribution grids.

Figure 17 illustrates a simple pressure-gain combustor concept. Here combustion of a fuel/air mixtures takes place, at constant volume, within the cells of the pressure-exchanger. The resultant pressure rise results in the discharge or products of combustion at a higher stagnation pressure than the stagnation pressure of the entering air flow. The fuel flow can be added to the entering air stream in a number of ways. There are obvious potential problems relating to developing a satisfactory combustion system within the confines of a pressure-exchanger cell. Figure 18 depicts an alternative form of pressure-gain combustor, also equivalent to a constant-volume combustor, employing a conventional, steady flow, combustor in the high pressure circuit of the machine. Potential applications for the systems shown in Fig. 17 and 18 relate, for example, to gas turbine usage to replace conventional steady flow combustors with units capable of generating a stagnation pressure increase. The foregoing examples do not represent an exhaustive inventory of possible pressure-exchanger configurations; the applications are, however, sufficiently varied to give some idea of the wide range of uses to which pressure-exchangers can be put.

PRESSURE-EXCHANGER CONFIGURATIONS TESTED EXPERIMENTALLY

Power Jets sponsored single-cell tests to obtain fundamental cell filling and emptying data [11] and subsequent filling and emptying tests using a cellular rotor; the collapsed results of many of these latter tests are shown in Fig. 11. Tests, with supporting analyses, were also carried out to establish the overall characteristics of low and high pressure scavenging processes [7].

In addition to fundamental tests of individual wave processes Power Jets sponsored, or carried out, tests of a number of functional, complete, pressure exchangers. These efforts were directed primarily at four systems:

- 1) gas generator configurations along the lines of that illustrated diagrammatically in Fig. 12; machines of this kind

were tested, at various stages of the program, as gas generators, diesel engine superchargers and as a pressure-firing system for a steam boiler,

- ii) air cycle refrigerators of the type shown in Fig. 13. Apart from test-bed trials prototype units of this kind were used for mine cooling in South African and India,
- iii) equalizers (Fig. 15); extensive test-bed running was undertaken to establish the overall characteristics of such cycles.
- iv) dividers (Fig. 16); again extensive test-bed running was carried out to establish cycle characteristics experimentally.

Proceeding to look, in turn, at each of the four previous examples in more detail.

Gas generators

Typical representative results obtained with a Power Jets gas generator are shown in Fig. 19. The unit was of the most simple type and did not, for example, feature transfer ports (Fig. 14).

Control was by varying the fuel flow quantity; there was no bleed-off of hot gas or compressed air from the H.P. circuit. The fall-off of the isentropic compression efficiency, η_{COMP} , (upper curve family) was due to hot gas mixing with the compressed air delivered into the H.P. loop this effect becoming ever more significant as the H.P. scavenge ratio (centre diagram) increased towards, or exceeded, unity. The estimate of η_{COMP} was based on the temperature rise of the air (due to compression in the pressure-exchanger) by measuring stagnation temperature at the L.P. inlet and H.P. outlet ports.

The lower curve family shows the non-dimensional bulk input u versus pressure ratio. The straight dotted line is the theoretical, non-dimensional, bulk input for a waveless (static) pressure-exchanger. Better results than those shown in Fig. 19 have been reported by Power Jets [12]. A fairly close correlation between theory and practice is also on record [13].

Coolers

At least two dynamic pressure-exchanger coolers were built by Power Jets (R and D) Ltd. These units were later operated as deep-mine environmental air-cooling devices. Figure 20 is an illustration of the first prototype unit. The pressure-exchanger and water-cooled heat-exchanger are in the foreground. The portion of the mine ventilating duct in which the unit was located is shown in the upper part of the photograph. The make-up air flow to the high pressure circuit was tapped from the mine compressed air supply.

In each of the two prototype units the rotor was made self-driving by angling the high-pressure inlet to give the entering flow an incidence angle of approximately 10° to the cell walls at the operating speed. The coefficient of performance (cooling duty divided by the isentropic work of compression of the make-up air) was 1.2 for the second prototype unit. Noise levels were controlled by use of acoustic splitters which proved adequate to make the noise of the installed units insignificant compared with typical mine noise levels. See the contribution by Barnes to the written discussion of reference [3] for further details of the mine cooler system.

Equalizers

Figure 21 shows an experimentally obtained performance map for an equalizer, using air as the working fluid, in which the dimensionless cell width $\Delta t'_{\text{CELL}} \approx 0.36$ [14]. Figure 22 is a comparative performance map obtained by analytical means not based on the method-of-characteristics [15]. The discrepancy between Fig. 21 and 22 was thought to be due to the wider cell width, $\Delta t'_{\text{CELL}} \approx 0.54$, employed to obtain the analytically derived curves.

Amongst the applications considered for equalizers one was to use the device as a thrust augmentator for either a turbo-jet or low bypass ratio turbo fan. For an application of this nature the high-pressure inlet flow to the equalizer would be the engine efflux. The low pressure flow would be drawn from the surroundings. The results of an approximate analysis based on equalizer experimental performance, of the expected thrust augmentation versus overall pressure ratio is presented in Fig. 23. It can be seen that the characteristics of the

device indicate that a good performance is only possible for fairly low values of P_H/P_L .

Dividers

The experimentally obtained performance map of a divider is presented in Fig. 24 for a machine having a dimensionless cell width of: $\Delta t'_{\text{CELL}} \approx 0.36$ [14]. A corresponding theoretically obtained performance map, for $\Delta t'_{\text{CELL}} = 0.54$, is presented in Fig. 25. The method used for establishing this theoretical map was the same as that used for the analytically derived equalizer map of Fig. 22 [15].

Figure 26 shows the test rig from which both the equalizer and divider experimental performance characteristics were obtained. Detailed method-of-characteristics analyses were also performed for both the equalizer and the divider cycles in which account was taken of friction, finite cell wall thickness, finite cell width and leakage. The result of this work, which is available elsewhere [16], are not reproduced here.

POTENTIAL APPLICATIONS

It seems essential, if pressure exchangers are to be commercially successful, to find applications where these devices can excel uniquely. It does not seem, to the writer, to be worth developing a pressure-exchanger based solution to a problem which can be solved equally well, or indeed nearly as well, by an existing, developed, machine or system. It would appear, for example, that the success being achieved by the Comprex unit of Brown Boveri in the vehicle supercharging field is due largely to the very rapid, almost instantaneous, response of the Comprex to changes in engine operating conditions, an area where the turbo-charger is less responsive, and the work carried out by Brown Boveri to reduce the sensitivity of the Comprex to changes of engine speed. Installationally, the Comprex is slightly less easy to accommodate than a turbo-charger due to the need to arrange a drive for the rotor; clearly in those cases where it is employed it is felt that the slight installational inconvenience is outweighed by the performance advantages.

It appears to the writer that pressure exchangers may have considerable advantages, due to a perception that they have a high erosion resistance and possibly a low first cost, in simple, moderate thermal efficiency, power plants employing fuels, such as pulverised coal or residual oil, less well suited to gas turbines or reciprocating engines. A plant of the proposed type would probably employ a gas generator with perhaps two transfer passages, similar to that of Fig. 14, with a simple, fairly low maximum temperature power turbine. A possible arrangement is shown schematically in Fig. 27. A power plant of this type may find application in locomotives or ships. It is known, for example, that the People's Republic of China is currently using a large number of coal-fired steam locomotives. The desire has been expressed to replace these with other types of coal burning machines of about twice the thermal efficiency. This implies that an overall thermal efficiency of about 16 to 20% is required. Currently coal-fired Stirling engines are being studied as possible alternative prime movers [17]. Possibly a pressure exchanger based power plant would be suitable and may require less development than a relatively "high tech" Stirling engine.

Another field where pressure exchangers may have a unique role to play is as pressurised combustors for coal, or residual-oil, fired steam boilers. Again the special features commending pressure exchangers for such applications are a high erosion resistance and, possibly, a lower first cost than otherwise comparable turbo-machinery. The pressure exchanger required is a gas generator type unit, possibly without transfer ports, along the lines of that shown in Fig. 12.

Pressure exchangers may have a part to play in the development of pressure-gain combustors, or so called topping spools, for gas turbines: in many such systems the blading of a turbo-machine counterpart is too small for satisfactory operation thereby giving an advantage to the pressure exchanger. Two such pressure exchanger systems are shown in Fig. 17 and 18. Whilst the system of Fig. 18 is closer to currently available technology it is apparently less compact than that of Fig. 17. The challenge in developing the system of Fig. 17 is clearly that of establishing good combustion conditions in a device which will also function as a pressure exchanger. The combustion-in-

cell concept does not rely constantly on the igniter. Spalding has suggested, if this system were ever to be developed, the use of a pocket in the stator, possibly in the vicinity of the igniter, to transport products of combustion upstream to cells approaching the combustion zone. In this way the igniter is only required for start-up [18].

What appears to be a good practical application of the pressure exchanger divider has been proposed by Barnes [19]. This application relates to pumping-energy recovery in natural-gas distribution networks. Since the system has already been subjected to analysis and the results of this work are available [19] it will not be described here. The special pressure exchanger properties commending this application are the absence of surge problems, rapid response to transients and equipment robustness.

CONCLUSIONS

An overview has been presented, very briefly and with many omissions, of the work on pressure exchanger development sponsored, and carried out by Power Jets (R & D) Ltd., assisted by Prof. D.B. Spalding and others, over a period of approximately thirteen years. An attempt was also made to introduce the concept of the dynamic pressure exchanger in as simple a manner as possible.

A survey of some of the experimental results available from the Power Jets work, and comparison with relevant theoretical analyses, indicates that, in the most general sense, pressure exchangers work satisfactorily in practice. It appears to be of paramount importance, when attempting to identify potential applications for pressure exchangers, to take into account the special properties, and performance characteristics, of these machines which fit them uniquely for the proposed tasks. In this way competition with existing, fully developed, equipment is avoided.

REFERENCES

1. KNAUFF, R. British Patent No. 2818, 1906.
2. LEBRE, A.F. British Patent No. 290 669, 1928.

3. AZOURY, P.H. An Introduction to the Dynamic Pressure Exchanger. Proceedings, Volume 180, Part 1, No. 18. Institution of Mechanical Engineers 1965.
4. RUDINGER, G. Nonsteady Duct Flow: Wave Diagram Analysis. Dover Publications, New York, 1969.
5. JENNY, E. Unidimensional Transient Flow with Consideration of Friction, Heat Transfer and Change of Section. Brown Boveri Review, 57, No. 11, p. 447, 1950.
6. SPALDING, D.B. Wave Effects in Pressure Exchangers, Part II, Power Jets (Research and Development) Ltd., Rept. No. 2202/x 41, 1955.
7. SPALDING, D.B. Filling, Emptying, and Transfer Processes in a Pressure Exchanger of Finite Cell Width, Power Jets (Research and Development) Ltd., Rept. No. 2222/x 46, 1956.
8. JONSSON, V.K., MATTHEWS, L. and SPALDING, D.B. Numerical Solution Procedure for Calculating the Unsteady, One-Dimensional Flow of Compressible Fluid. ASME paper 73-FE-30, 1973.
9. MATTHEWS, L. An Algorithm for Unsteady Compressible One-Dimensional Fluid Flow. M.Sc. dissertation, Imperial College of Science and Technology, University of London, October 1969.
10. CRONJE, J.S. and KENTFIELD, J.A.C. A Numerical Procedure for the Analysis of One-Space-Dimensional Non-Steady Compressible Flow. Proceedings, 7th Australian Hydraulics and Fluid Mechanics Conference, Brisbane, pp. 346-439, August 1980.
11. AZOURY, P.H. The Dynamic Pressure Exchanger-Gas Flow in a Model Cell, University of London, Ph.D. Thesis, 1960.
12. 'Pressure exchanger progress', The Oil Engine and Gas Turbine, 32 (No. 371), 35, 1964.
13. AZOURY, P.H. High-pressure and Low-pressure Scavenge in a Pressure Exchanger of Finite Cell Width, Power Jets (Research and Development) Ltd., Rept. No. 2263/Px 10, 1961.
14. KENTFIELD, J.A.C. The Performance of Pressure-Exchanger Dividers and Equalizers. ASME Journal of Basic Engineering, Series D, Vol. 91, No. 3, pp. 361-368, 1969.
15. KENTFIELD, J.A.C. An Approximate Method for Predicting the Performance of Pressure Exchangers. ASME paper 68-WA/FE-37, 1968.

16. KENTFIELD, J.A.C. An Examination of the Performance of Pressure Equalizers and Dividers, University of London, Ph.D. Thesis, 1963.
17. WALKER, G. KENTFIELD, J.A.C., JOHNSON, E., FAUVEL, R. and SRINIVASAN, V. Coal-Fired Stirling Engines for Railway Locomotive and Stationary Power Applications. Institution of Mechanical Engineers Proceedings, Vol. 197, No. 46, 1983.
18. SPALDING, D.B. Private communication, 1968.
19. KENTFIELD, J.A.C. and BARNES, J.A. The Pressure Divider: A Device for Reducing Gas-Pipe-Line Pumping-Energy Requirements. Proceedings, 11th IECEC, pp. 636-643, AIChE., 1976.

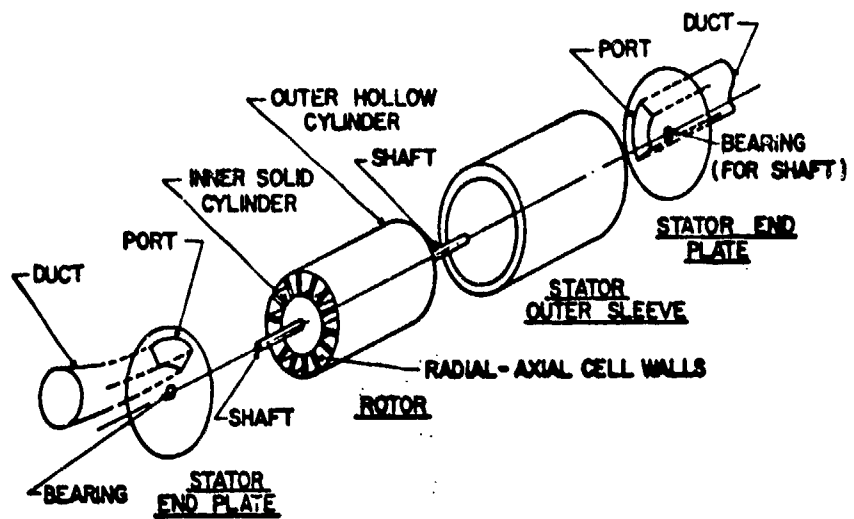


Fig. 1 Basic arrangement of a simple pressure exchanger

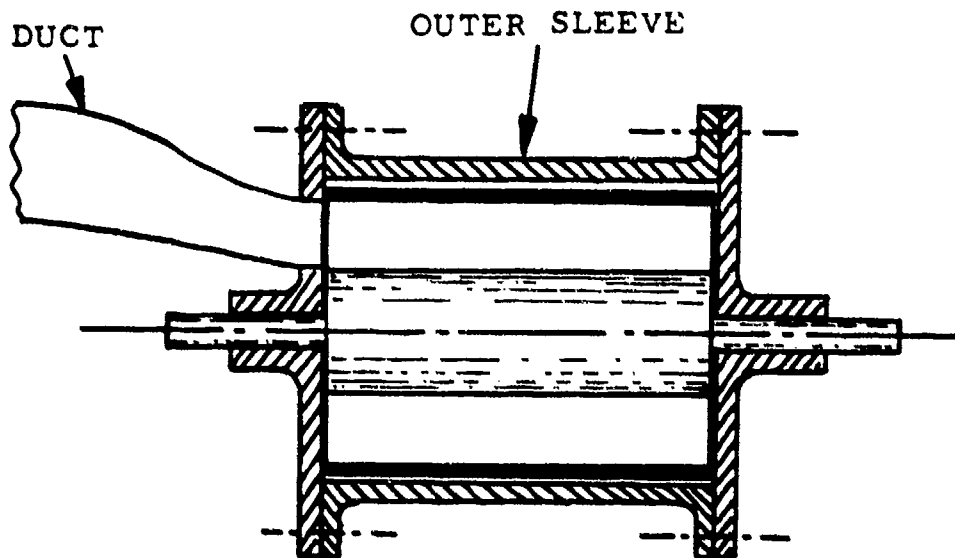


Fig. 2 Cross-section of a simple pressure exchanger

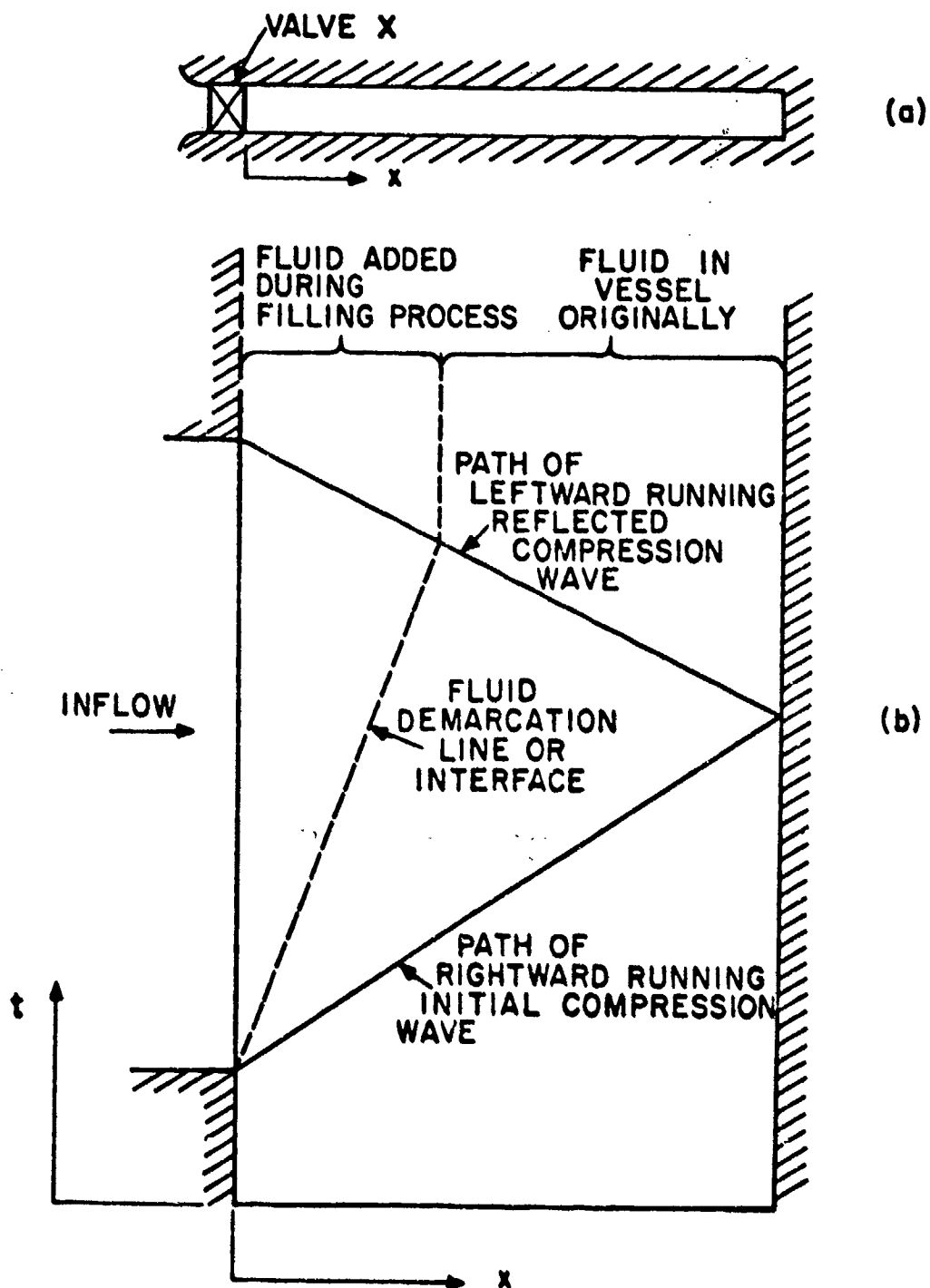


Fig. 3 A typical gas dynamic filling process,
 (a) tubular container with valve at left hand end,
 (b) wave ($x \sim t$) diagram for filling process.

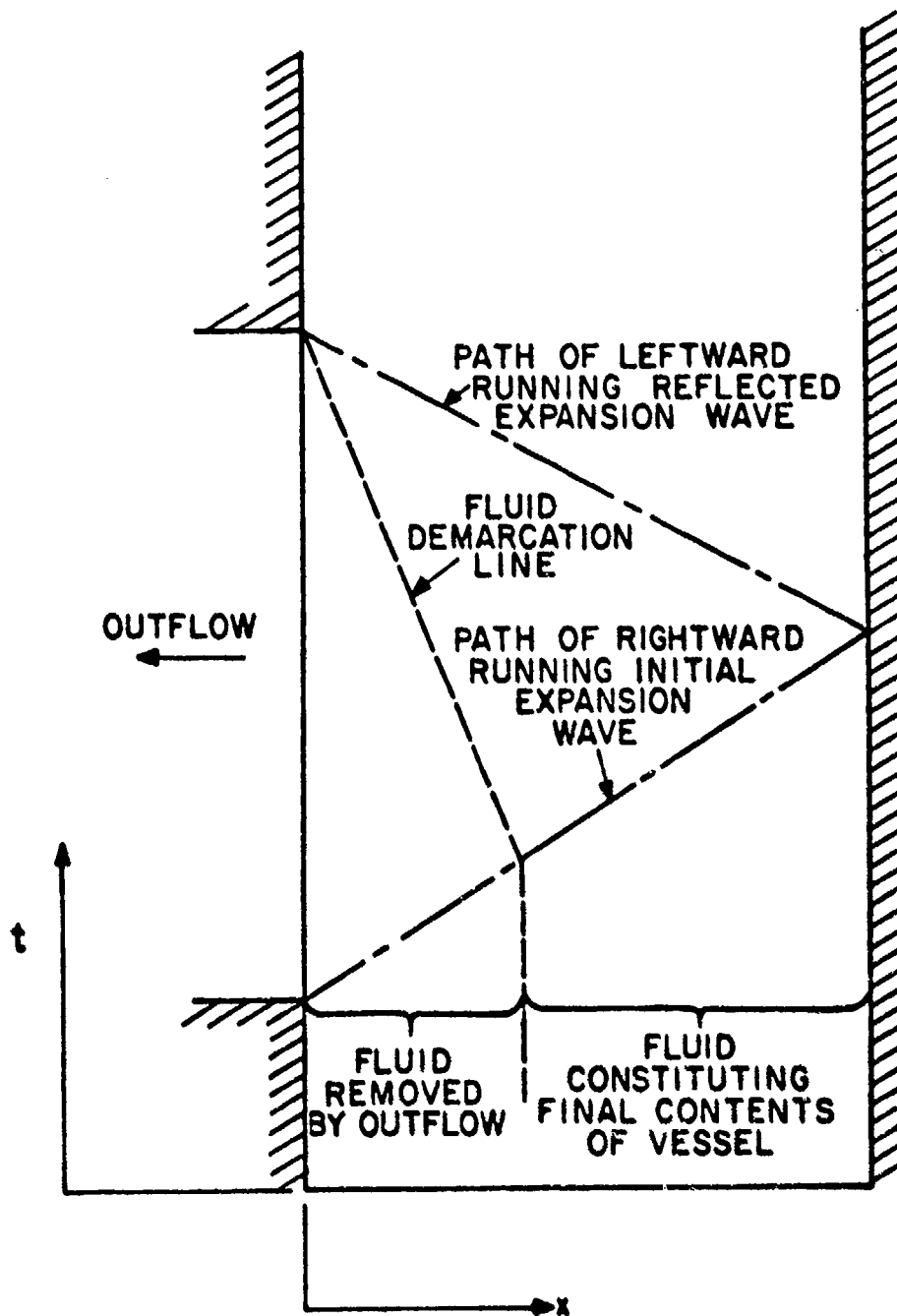


Fig. 4 Wave diagram for a typical emptying process.

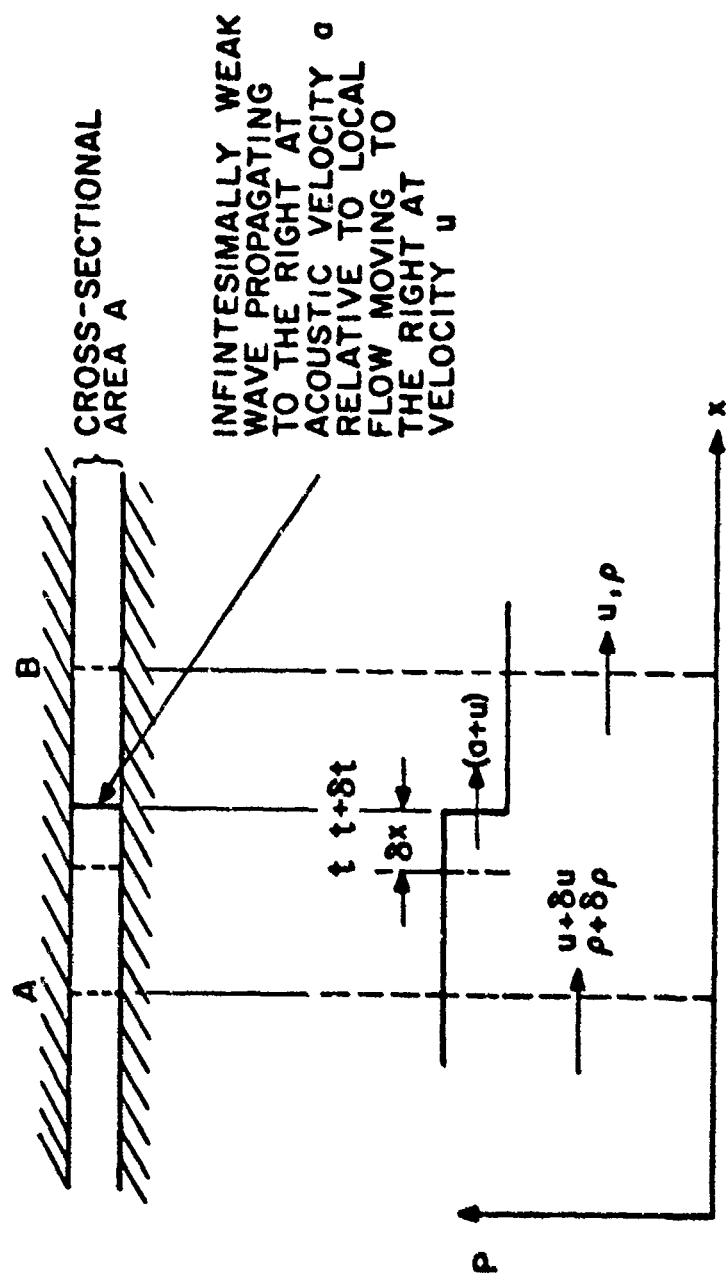


Fig. 5 Elemental isentropic wave propagating to the right in gas flowing in the same direction.

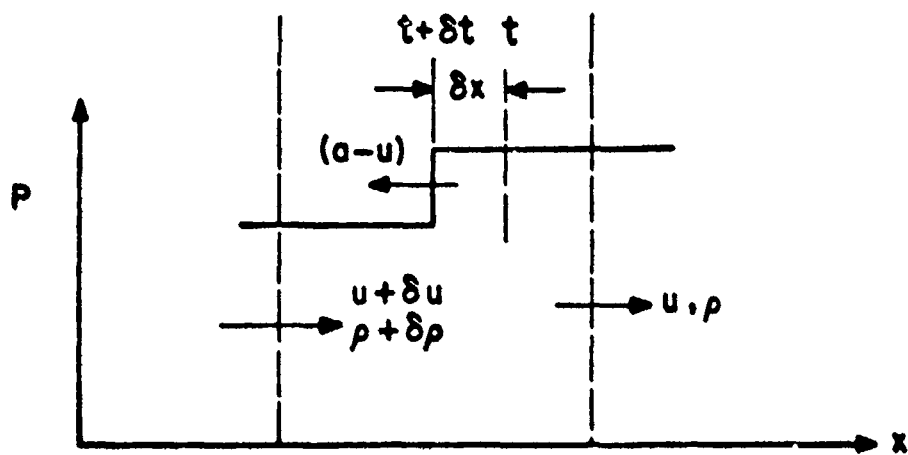


Fig. 6 Elemental isentropic wave propagating to the left in gas flowing in the opposite direction.





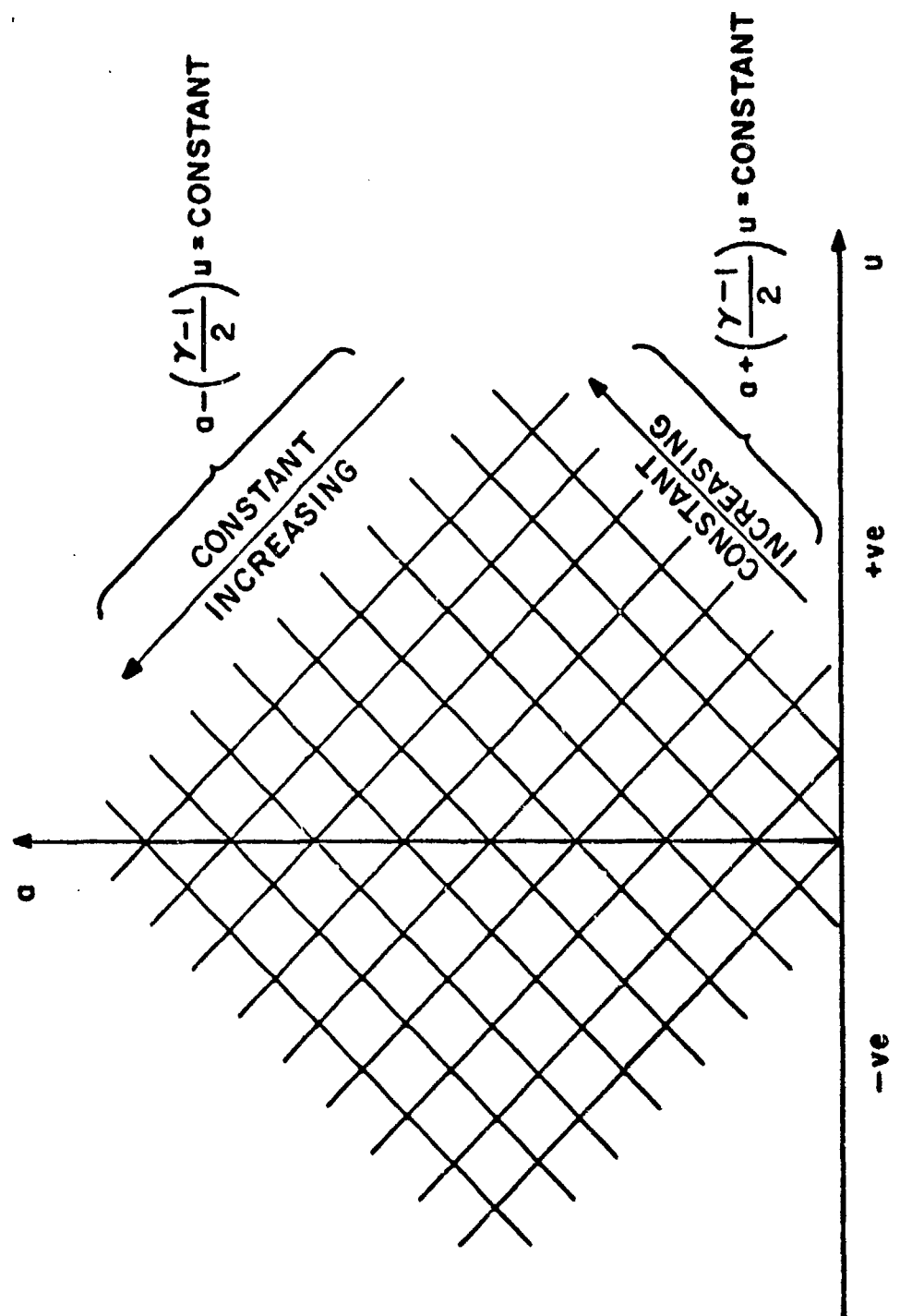
COMPRESSION WAVES	EXPANSION WAVES
  $a - \left(\frac{\gamma-1}{2}\right)u = c$ $a + \left(\frac{\gamma-1}{2}\right)u = c$	  $a + \left(\frac{\gamma-1}{2}\right)u = c$ $a - \left(\frac{\gamma-1}{2}\right)u = c$
<p style="text-align: center;">$c \approx \text{CONSTANT}$ u IS POSITIVE FOR FLOW TO THE RIGHT</p>	

Fig. 7 Isentropic pressure waves and corresponding equations.



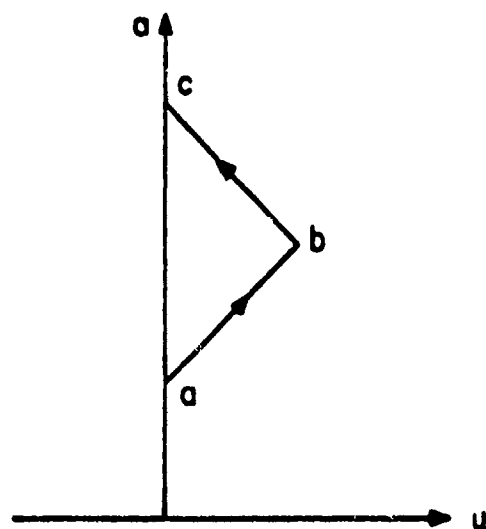
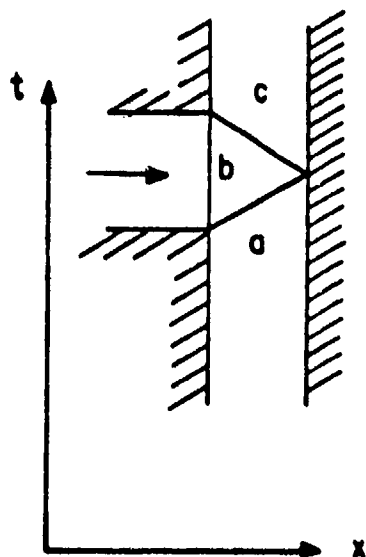


Fig. 9 Filling process on $x \sim t$ and $a \sim u$ diagrams.

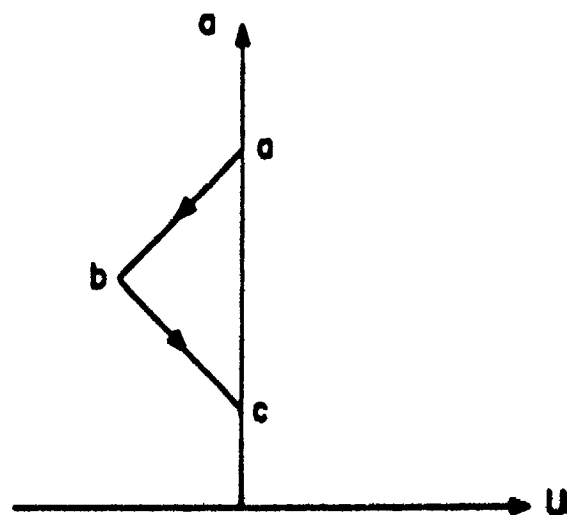
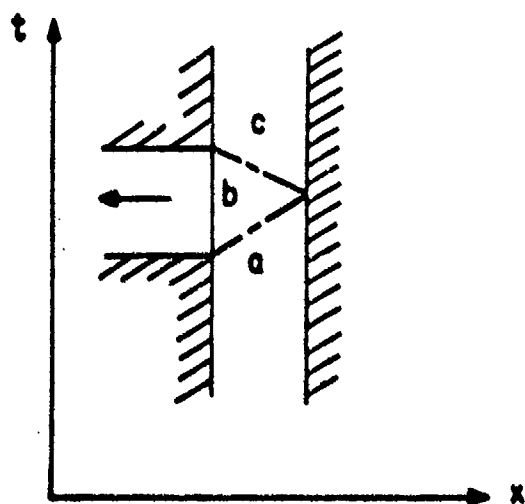


Fig. 10 Emptying process on $x \sim t$ and $a \sim u$ diagrams.

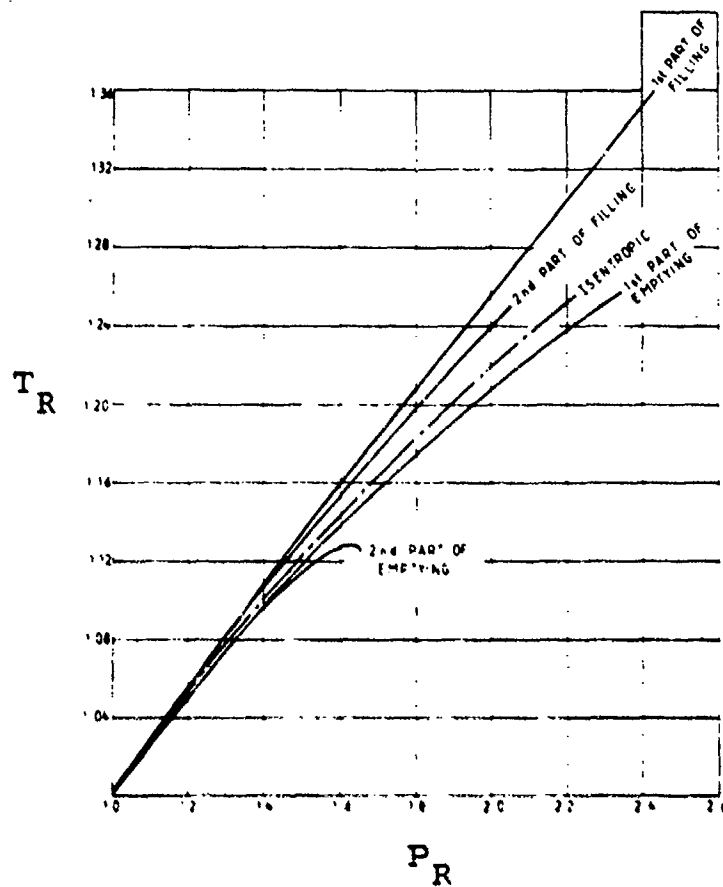


Fig. 11 Experimentally obtained static temperature ratio (T_R) versus static pressure ratio (P_R) relationships
 $(\Delta t'_{\text{CELL}} \approx 0.54, \quad \gamma = 1.4)$

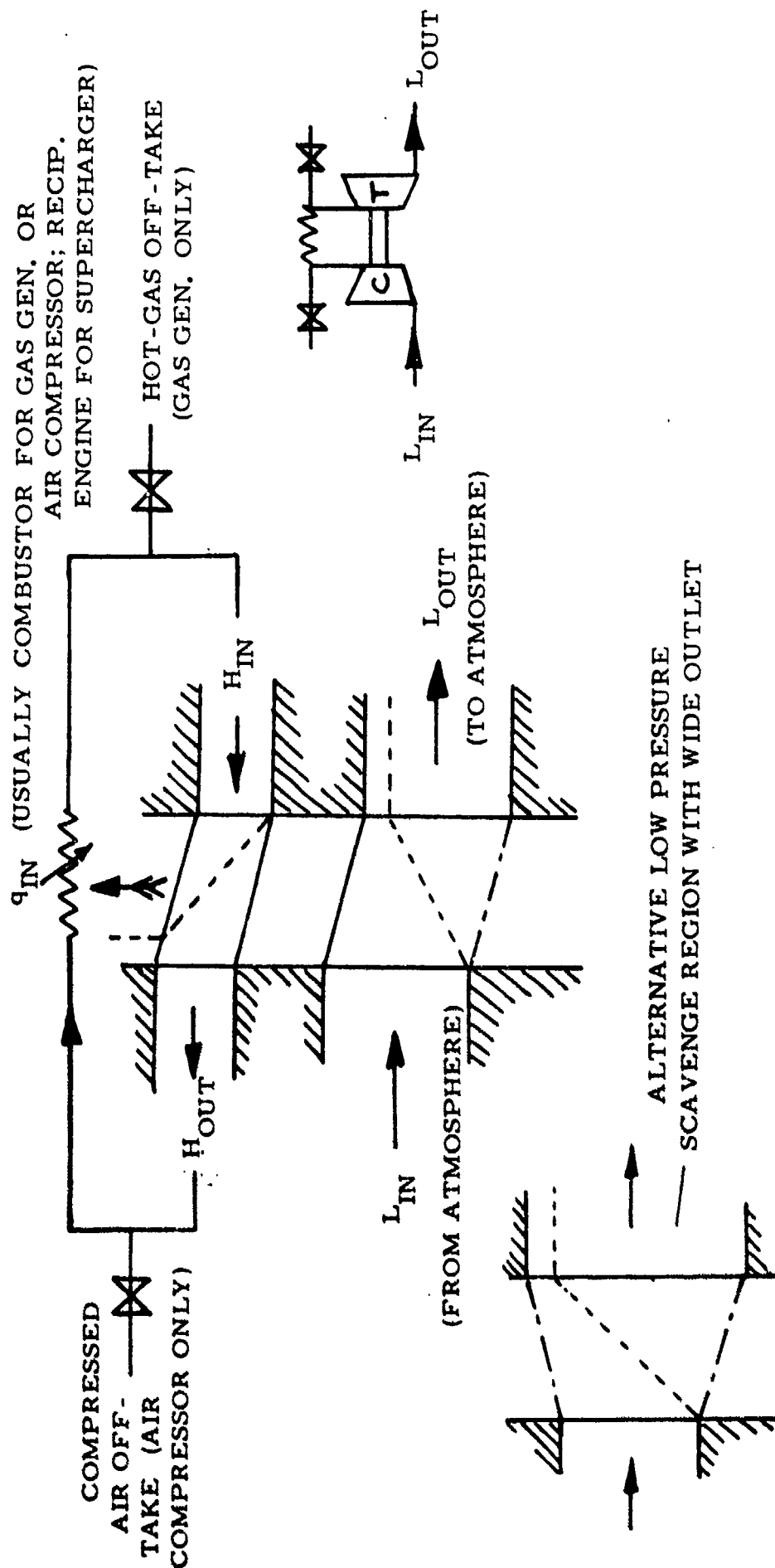


Fig. 12 A gas generator, air compressor or supercharger configuration utilizing dynamic pressure exchange.

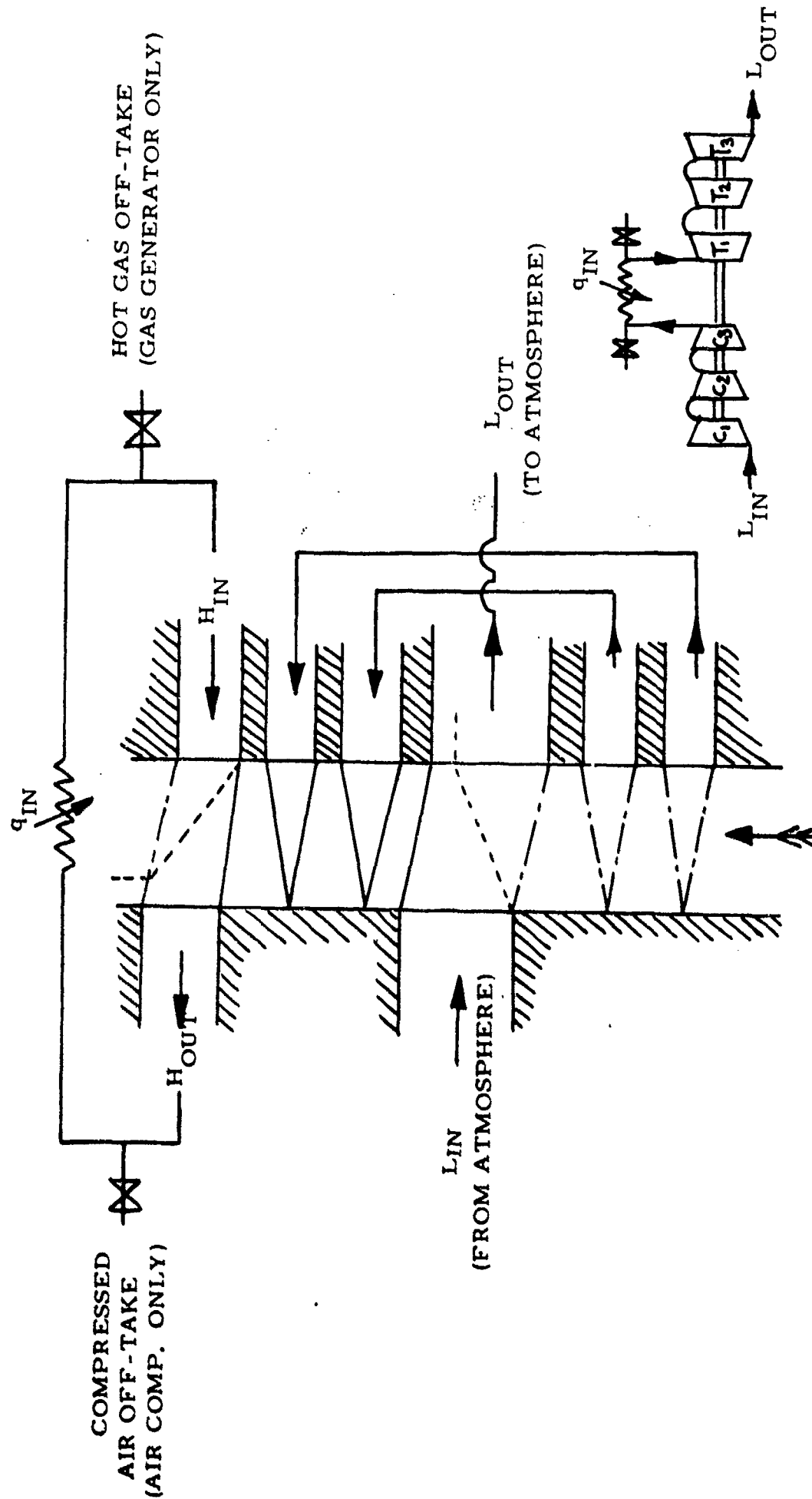


Fig. 14 A gas generator, air compressor or supercharger configuration incorporating two transfer passages.

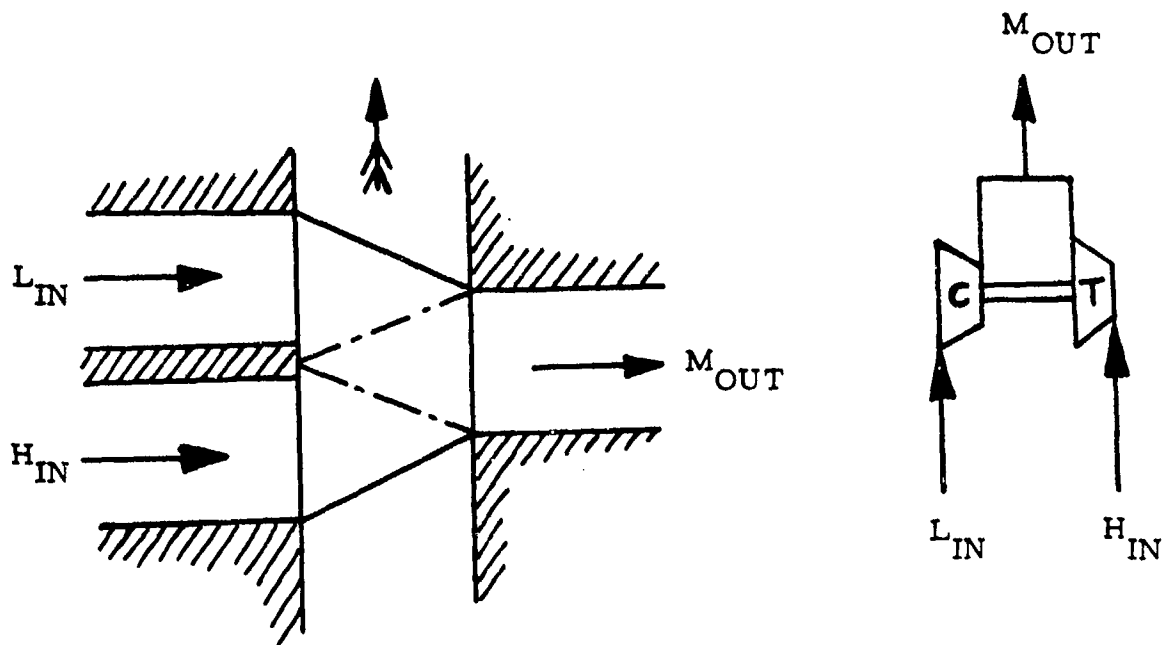


Fig. 15 Pressure-exchanger equalizer configuration.

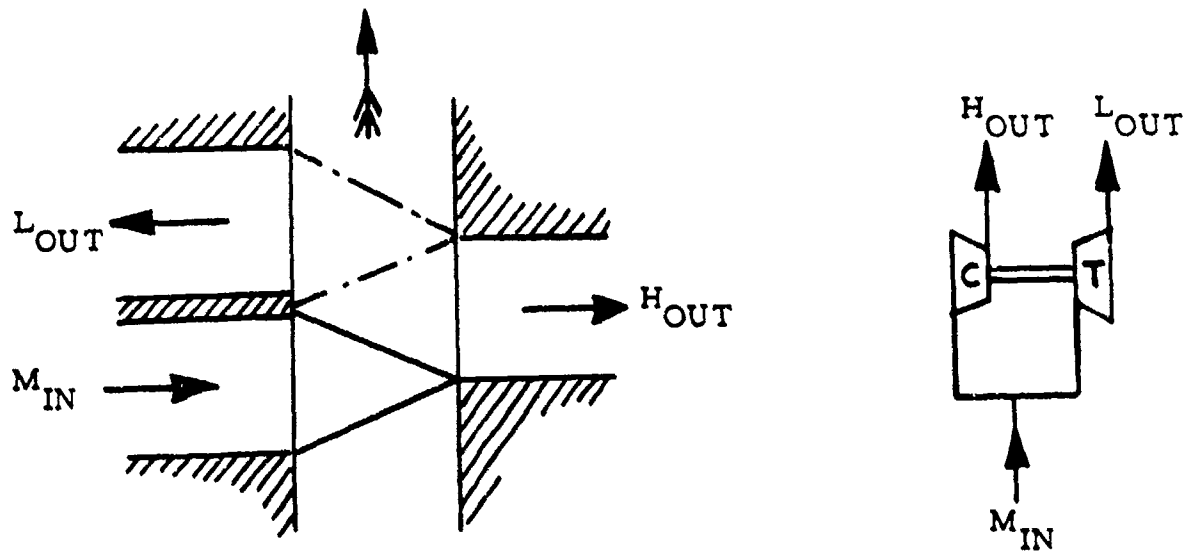


Fig. 16 A pressure-exchanger divider configuration.

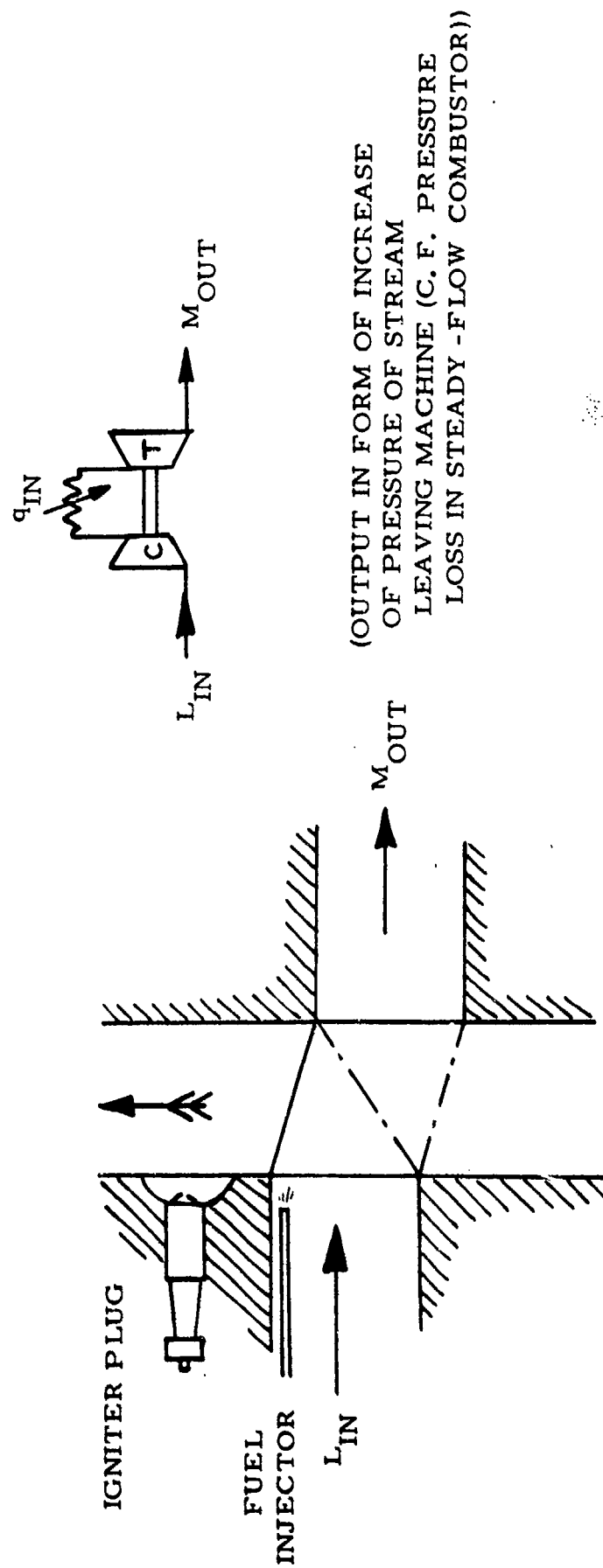
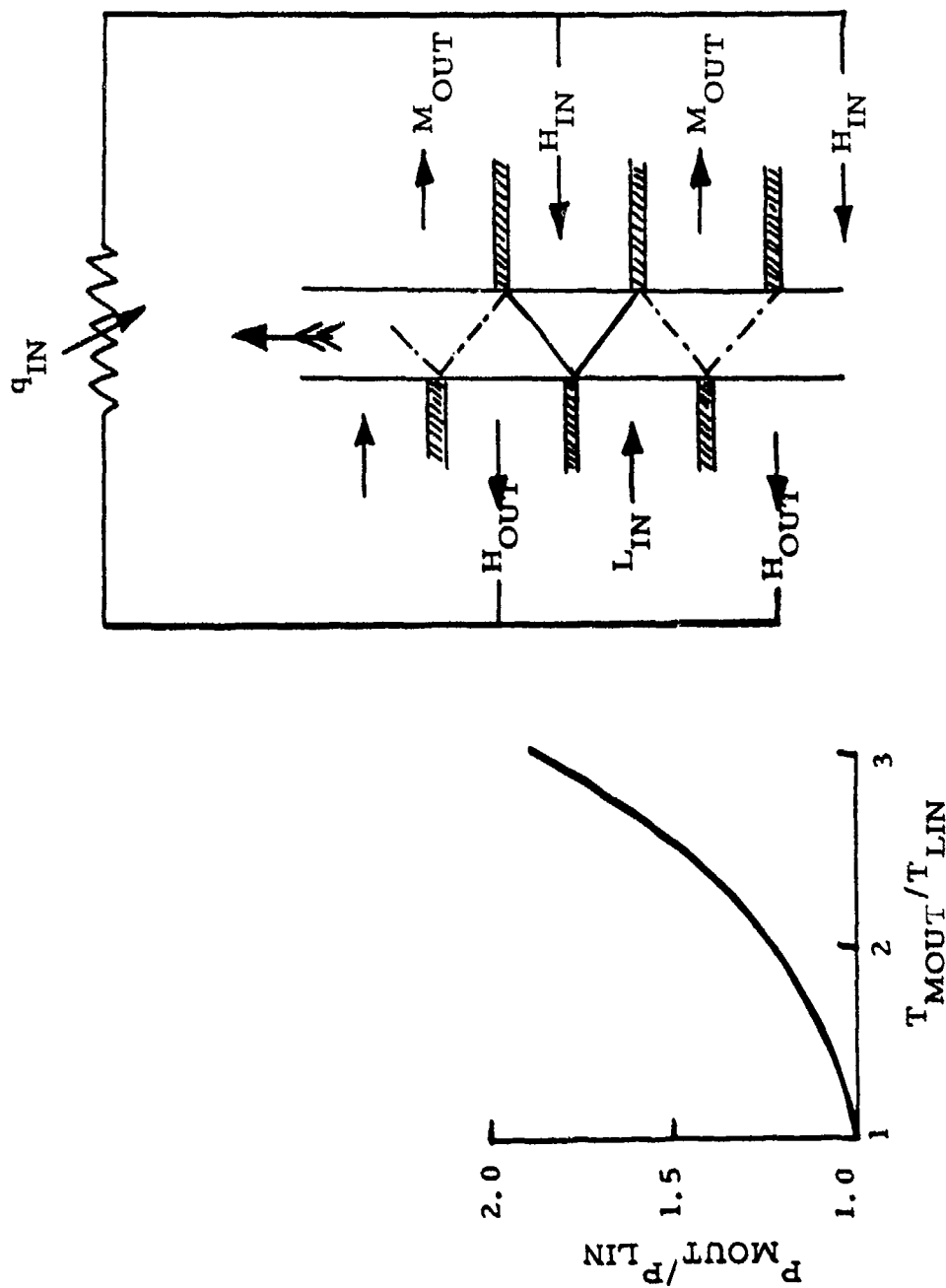


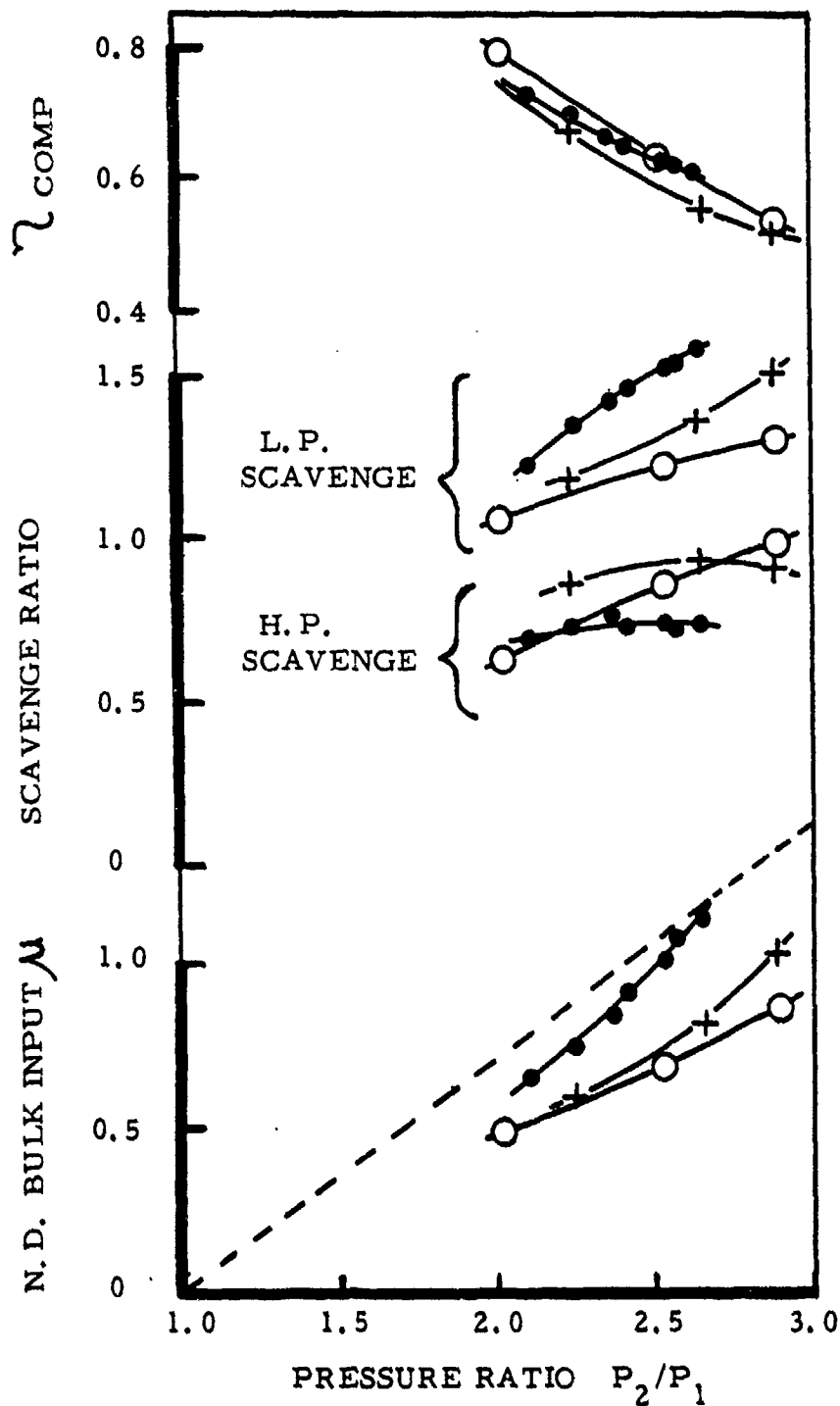
Fig. 17 A pressure-gain combustor using pressure exchange.



IDEAL, AIR-CYCLE PERFORMANCE
OF SYSTEMS OF FIG. 17 & 18.

Fig. 18 An alternative pressure-gain combustor of the pressure exchanger type.

Note the provision of multiple sets of ports - this can be done for most pressure exchangers.



CODE	SPEED REV/MIN
—●—	4500
—+—	5000
—○—	6000

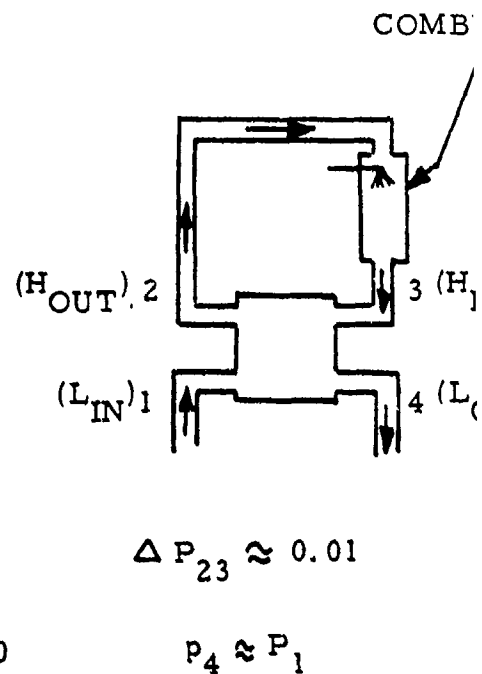


Fig. 19 Performance of a simple dynamic pressure exchanger operating as a gas generator (early Power Jets test). Rotor diameter approximately 8" (203mm), length 11" (279mm).

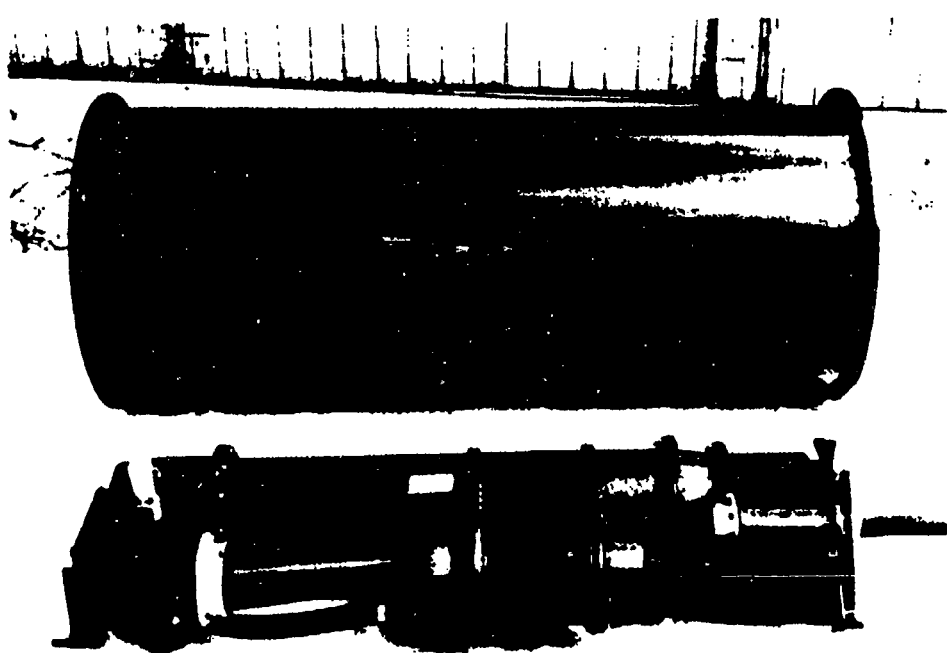
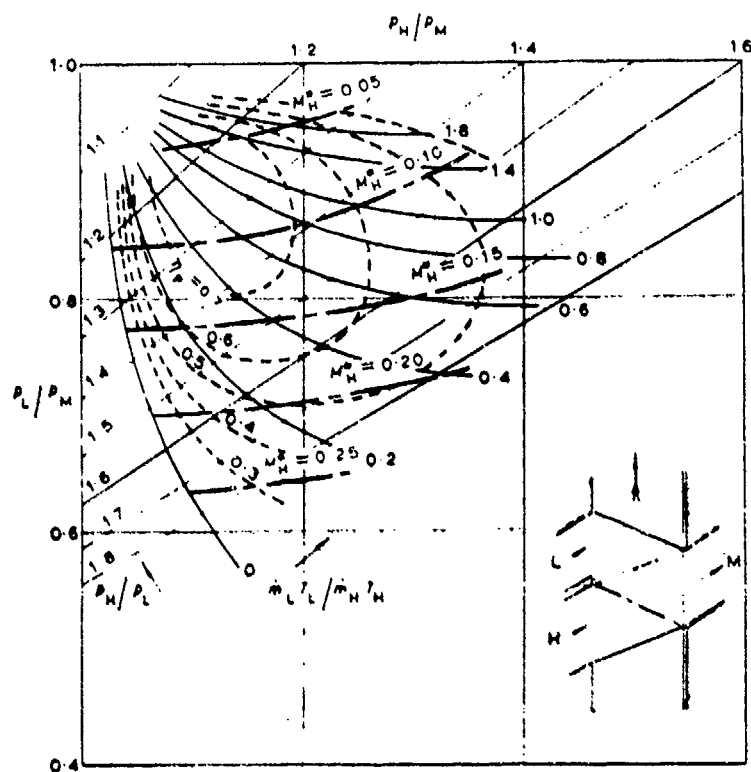


Fig. 20 Power Jets prototype pressure-exchanger mine cooler air-cycle refrigerator.



Experimental conditions:

$T_H = 308 \text{ K}$, $p_L \approx 1 \text{ atm}$, $T_L/T_H \approx 0.95$
 Rotor speed = 5500 rev/min
 H port width = 47
 M port width = 48
 L port width = 43
 phasing = 24

Fig. 21 Experimentally obtained equalizer performance map
 $\Delta t'_{\text{CELL}} \approx 0.36$, using air as the working fluid ($\gamma = 1.4$)

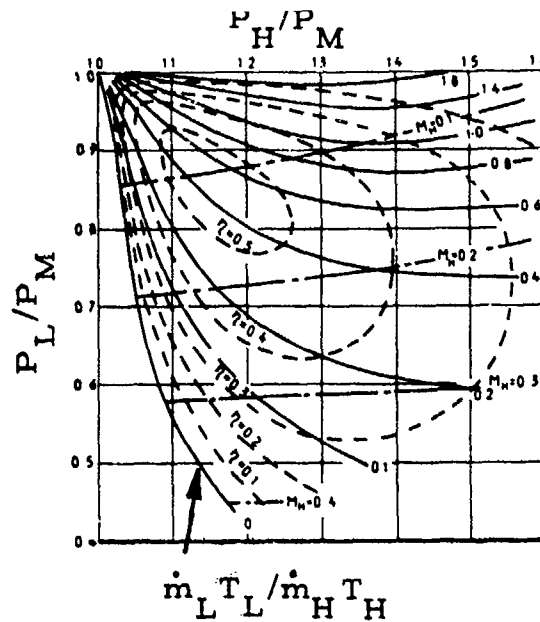


Fig. 22 Predicted performance of an equalizer ($\Delta t_{\text{CELL}} \approx 0.54$).

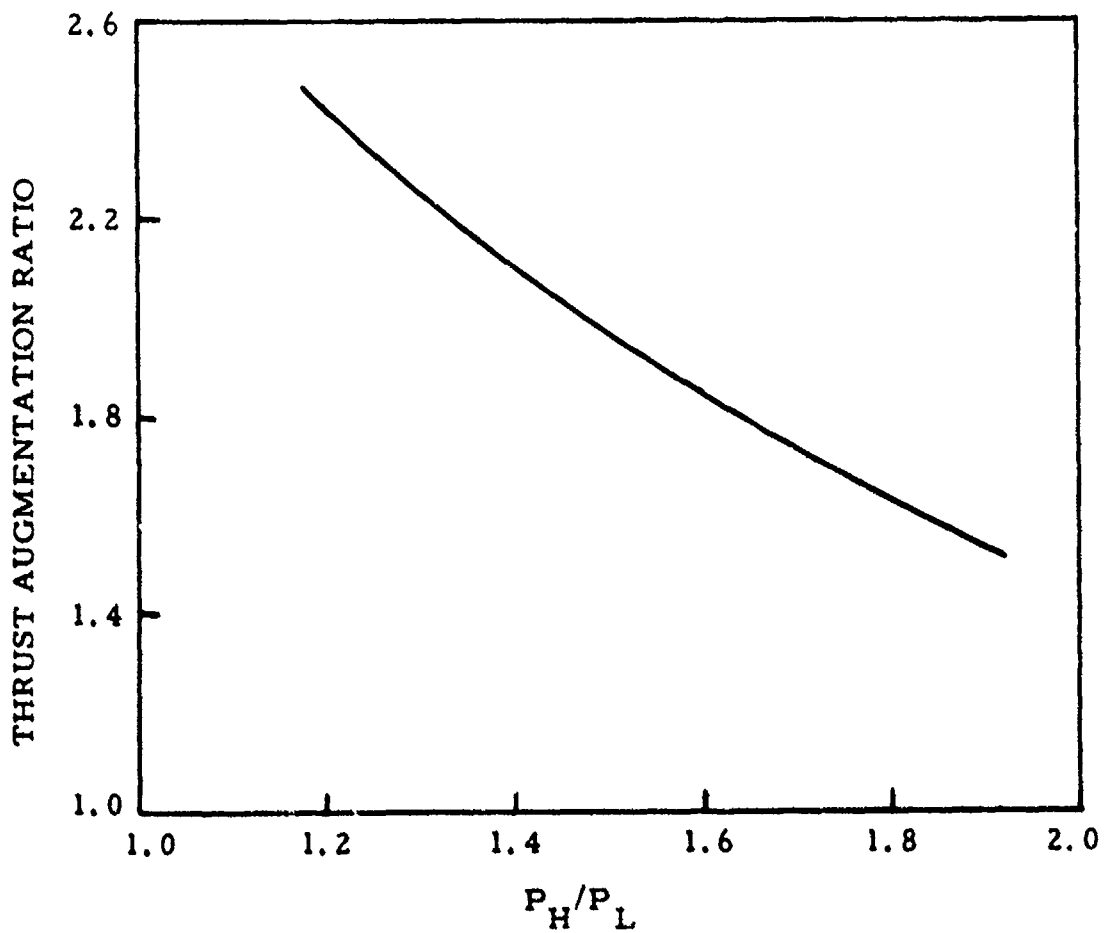


Fig. 23 Thrust augmentation performance of an equalizer based on experimentally measured characteristics.

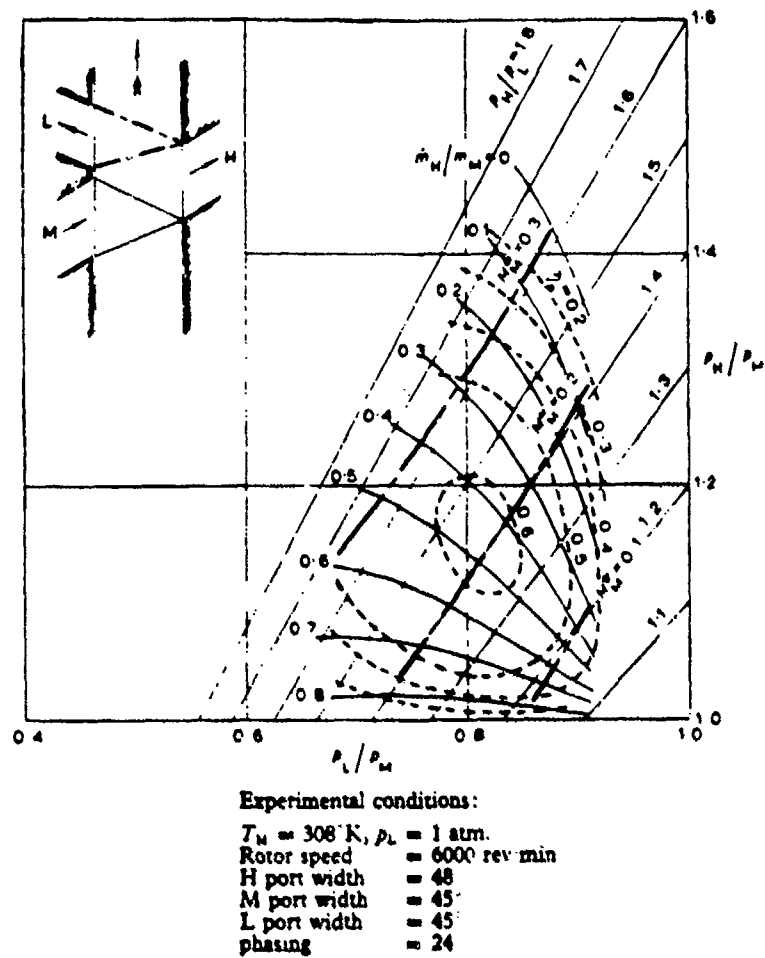


Fig. 24 Experimentally obtained performance of a pressure-exchanger divider, with $\Delta t_{\text{CELL}} \approx 0.36$, using air as the working fluid ($\gamma = 1.4$).

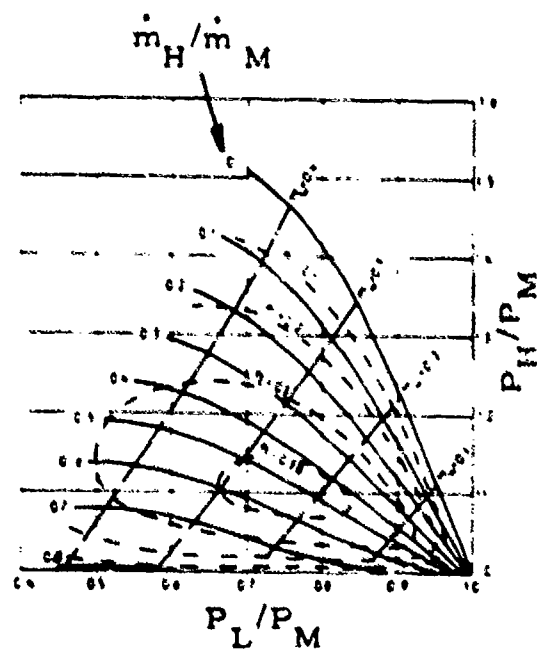


Fig. 25 Predicted performance of a divider ($\Delta t_{\text{CELL}} \approx 0.54$)

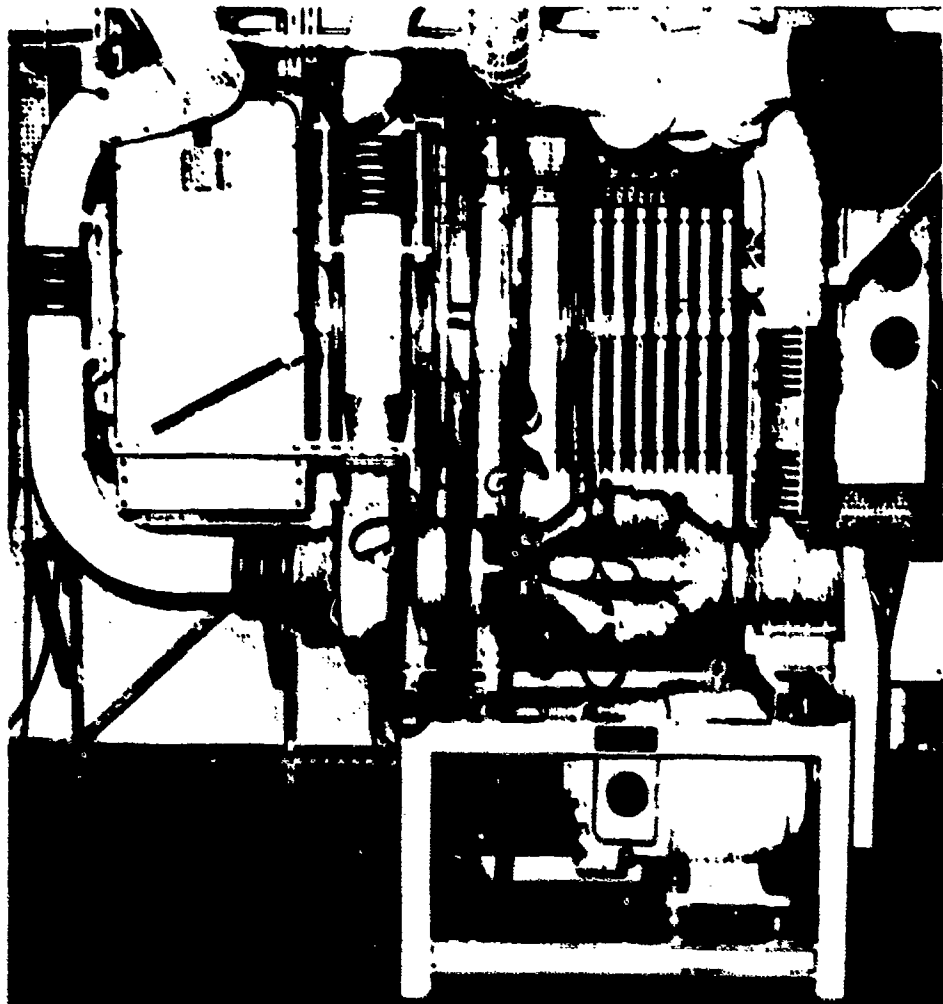


Fig. 26 The Power Jets pressure-exchanger divider/equalizer test rig as installed at Imperial College, University of London.

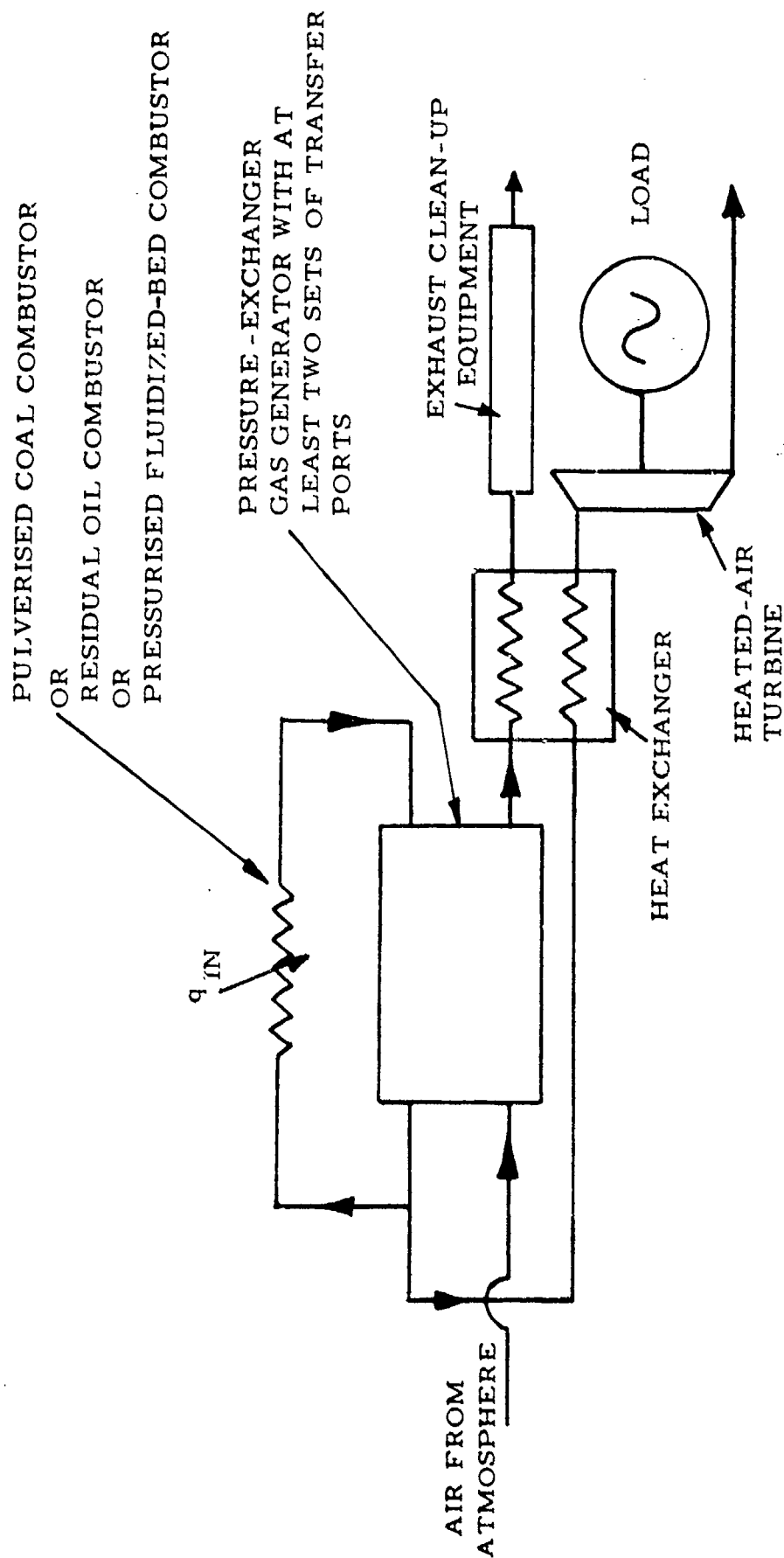


Fig. 27 Proposed moderate thermal efficiency, poor-fuel, power plant for locomotive or marine propulsion.

T H E C O M P R E X

Summary

The Comprex for supercharging Diesel engines in passenger cars represents a practical utilization of the wave rotor concept. Turbocharging has long been introduced in locomotive and ship-Diesel engines for increasing the power output. Today turbosupercharger have also become standard equipment on trucks and tractors. The matching of the pistonengine- and the turbomachine characteristic does not cause particular problems, as multispeed transmissions allow engine operation in a narrow speed range. The high vehicle masses do not seem to demand rapid load response. In passenger Diesel cars the engine has to work in a wider speed range and rapid response to load change is mandatory. This feature can be felt most distinctly when comparing two diesel cars, one Comprex- and the other turbo-charged.

The characteristic of the Comprex can be adapted to the particular requirement of a high torque in the normal engine operating speed range of a naturally aspirated engine. This can be realized with a particular stator porting design. In addition to the intake- and exhaust ports there are stator pockets with immediate mass reinjection into the rotor. This allows the Comprex to match the engine mass-flow demand, when it is driven over a belt. At constant air-fuel ratio the engine intake manifold pressure and thus the torque stay about constant over a wide engine speed range. The manifold pressure raises as fast as the exhaust temperature increases. As the air pressure is generated by the compression wave the rotor speed does not first have to change.

As the Comprex supercharged car can be driven at lower engine speed the will be an advantage in fuel consumption and noise. The Comprex can be built with low flow capacity without a loss in performance due to detrimental Reynolds number effects.

The wave rotor is produced by casting with uneven partition spacing for lowering the single frequency noise energy. With simple acoustic means in the intake- and exhaust ducts the vehicle noise can be held down to acceptable levels. The low rotor tip speeds will eventually permit the use of ceramic, which offers the advantage of low weight, low cost and almost no thermal expansion. Clearances between rotor and stators, which affect losses, can be held smaller.

Brown Boveri is selling units to go into the Opel Diesel car, the first to benefit from wave rotor technology.

SUPERCHARGING WITH COMPREX

Prof. M. Berchtold, Swiss Federal Institute of Technology,
Zürich / Switzerland

History

The idea of interchange of energy by direct impingement of gases dates back to the time at the beginning of this century when Büchi proposed exhaust gas driven turbosupercharging of Diesel engines. A patent of Burghard describes the cell rotor admitting gases through segmented stator ports. The idea forgotten came up again in the late thirties when the principle was used as a heat pump with air as the working fluid. Brown Boveri who was building the device for a customer realized that design modifications were needed to account for nonsteady flow phenomena. The patent by C. Seippel describes the operation and the timing requirements. Later, the pressure wave energy exchanger named Comprex to indicate its capability of compressor-expander was used as the upper stage of a gasturbine engine. Whereas good efficiencies were obtained, rotors could not be built to stay together. In the early fifties, the potential of the Comprex as a Diesel engine supercharger was recognized. After the first units were constructed and tested on vehicular Diesel engines in the USA, Brown Boveri in Switzerland initiated a concentrated effort to develop the Comprex to meet the requirements of its practical realization.

The Principle of Operation

The schematic arrangement of the Comprex as exhaust gas driven Diesel engine supercharger is shown in Fig. 1. The rotor B has straight axial channels of constant cross section, also called cells. The stators on both sides of the rotor have segmented openings registering with the rotor passages. The ducting F for air entering the rotor and for the discharge of compressed air E are connected to the cold stator. The duct for compressed hot gas D and the duct for hot gas discharge G are connected to the hot stator. The rotor assumes essentially a valving function. The belt drive C is needed to overcome bearing-, windage- and friction-losses. The energy exchange comes from direct interaction of the gas to be expanded, passed on to the air to be compressed.

The mode of operation can best be explained considering the axial rotor channels to be unwrapped into the projection plane Fig. 2. The ports in the cold stator on the left side and the ports in the hot stator on the right side are stationary. The duct E for the compressed air connects to the engine intake manifold E. The duct D for the exhaust gas collected in the exhaust manifold A leads into the rotor. The turning of the rotor is represented by the rotor cells moving from the top on down. The ports thus open and close according to the schedule determined by the geometrical location of the ports and the downward speed of the rotor. The requirements for the timing of the compression- and expansion-waves are best understood by the description of the cycle.

The explanation begins on top of Fig. 2 where the rotor is filled with air at rest below ambient pressure. The cell opening to the exhaust gas port

allows the gas to enter the rotor due to the large pressure difference. The air at rest has to be pushed forward producing a compression wave. The wave front progressing faster than the speed of sound simultaneously compresses and accelerates the air. As the wave reaches the cold stator, the discharge port is opened and allows the compressed air to enter the stationary duct E leading to the engine intake manifold E. The kinetic energy is partly converted into pressure. The speed of the gas and the speed of the compressed air are about equal. This also is the speed of the interface. As Fig. 2 indicates, this speed is far below the speed of the compression wave. It is this physical phenomenon which makes the efficient transfer of energy by direct interaction possible.

The compressed air discharge port closes prior to the arrival of the interface preventing exhaust gas to be recirculated into the engine. Some of the air which has been contaminated due to mixing at the interface remains in the rotor cell. As the exhaust gas intake port is closed a rarefaction or expansion wave is generated. The deceleration of the gas to standstill at the wave front occurs with the simultaneous expansion. Now the rotor is filled with exhaust gas and some air, both at rest. The pressure is still considerably above ambient. This remaining pressure furnishes the energy to scavenge the cell, namely to replace the exhaust gas by air. The opening of the exhaust gas discharge port induces the second rarefaction or expansion wave, thus generating the outflow into the exhaust duct G. First the gas and then the air in contact is being traversed by the expansion wave. The full content of the rotor cell is set in motion. At this time the air intake opens and the inertia of the gas column draws in the air. As the cell has been scavenged the exhaust discharge port is being closed. Prior to this time the air intake has also been closed, thus producing another, however rather weak expansion wave decelerating the air to standstill. The pressure of the air at rest is subambient. The cell is now ready for the next cycle.

The pressure of the air obtained in the intake manifold E is determined by the strength of the compression wave which again is a function of the engine exhaust discharge pressure. This again depends on the exhaust gas temperature leaving the engine. As the mass-flows to and from the engine are essentially equal, the power to be gained by the expansion of the hot exhaust gas is sufficient to obtain a somewhat higher pressure of the cold air to be compressed. Part of the surplus power covers the inefficiencies. There are losses due to the finite clearance between rotor and stators. Furthermore, there are losses due to incomplete recovery of kinetic energy of the compressed air in the duct E and of the exhaust gases leaving the rotor through duct G. Losses are caused also during opening and closing of the cells passing the radial edges of the stator ports. The effect of heat exchange superimposed to the compression and expansion energy exchange makes the processes non-adiabatic. This is a distinct difference from the adiabatic compression and expansion in turbomachines. Work dissipation due to flow friction on the cell walls brings a further deviation from the isentropic changes of state. The losses due to irreversibilities in the compression wave are insignificant. The design point including

the total of all losses reveals overall combined energy efficiencies of 74 %. This makes the Comprex competitive with turbosuperchargers.

Matching the Comprex to Engine Demands

A practical supercharger has to function over a wide operating range. Vehicular engines in particular are rather challenging in this respect.

The rotor as shown above has to be driven by the engine. V belts are well accepted on vehicular engines for generator-and-fan drives. This, however, makes the Comprex speed range as wide as the engine speed range, namely up to 1:4. At low Comprex speed, the main compression wave arrives far too early at the cold stator with the result that the compression wave is being reflected at the closed end of the rotor cell creating a high pressure of no use. This wave returning to the exhaust gas intake disrupts the timing with the effect of flow reversal and with a complete breakdown of performance. A number of simple means have been found which help to overcome the disadvantage of wave mistiming. The wide speed operation has been realized by the use of additional stator ports which, however, are not connected to any duct. The ports allow the air in the rotor to flow out and to enter the rotor into the adjacent cell. In the case of the early arrival of the compression wave, only partial reflexion occurs. The reflected wave arrives at the hot stator at the time the inflow of exhaust gas into the rotor has started. The wave prevents the inflow over a segment of the port. The flow of exhaust gas is reduced which matches the lower flow at reduced engine speed. This appears to the engine to have the same effect as variable geometry of a turbocharger. A similar pocket is supplied with exhaust gas. The secondary wave generated by this pocket enters into a corresponding pocket in the cold stator. The effect of these pockets sustains scavenging of the rotor cells at low rotor speeds. In Fig. 3 the essential components of a Comprex unit are shown. The main ports and the axiliary ports (as pockets) are visible. The letters indicating the ports agree with the duct designation of Fig. 1. The letters HIK refer to the pockets. The stators, contrary to Fig. 1 and 2, are built to produce two complete cycles per revolution of the rotor. This has the advantage of symmetry in the stator design. At equal rotor speed the rotor length is half which makes the unit lighter and more compact.

The Comprex having a porting configuration to give a wide speed range fortunately meets the massflow demand of the engine. This results in a nearly constant engine intake manifold pressure for constant exhaust gas temperature in a reasonably wide speed range of the engine.

The requirements for passenger car- and truck-engines as well as the capability of rapid load changes are being discussed in the second part of the paper.

In the supercharger version the peak efficiency has to be sacrificed in favour of the wide speed range capacity. Yet the efficiencies are competitive with turbosuperchargers which need bypass blowoff valves causing a considerable loss in efficiency at high engine speed.

The Comprex can be analysed theoretically using the method of characteristics. The assumption of onedimensional flow can be refined to take care of partial opening losses, leakage losses, as well as heattransfer- and friction-losses. Integration of the theoretical intake- and exhaust velocity profiles gives remarkably precise duplication of measured performance. The cycle calculation using the graphical method of characteristics is rather a demanding and time consuming process. Whereas it is possible to computerize the calculations, it is still difficult to introduce complicated boundary conditions such as pockets since massbalances will have to be fulfilled for the main ports as well as for the pockets. The graphical method of analysis can be made with grossly simplified assumptions. It is most instructive since it allows to understand the phenomena which determine basically the functioning of the Comprex.

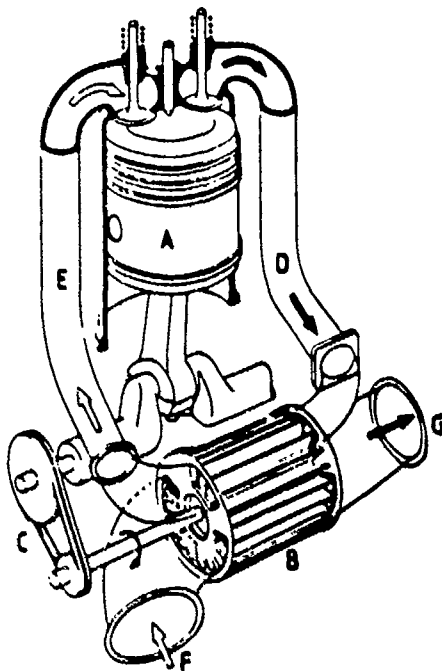
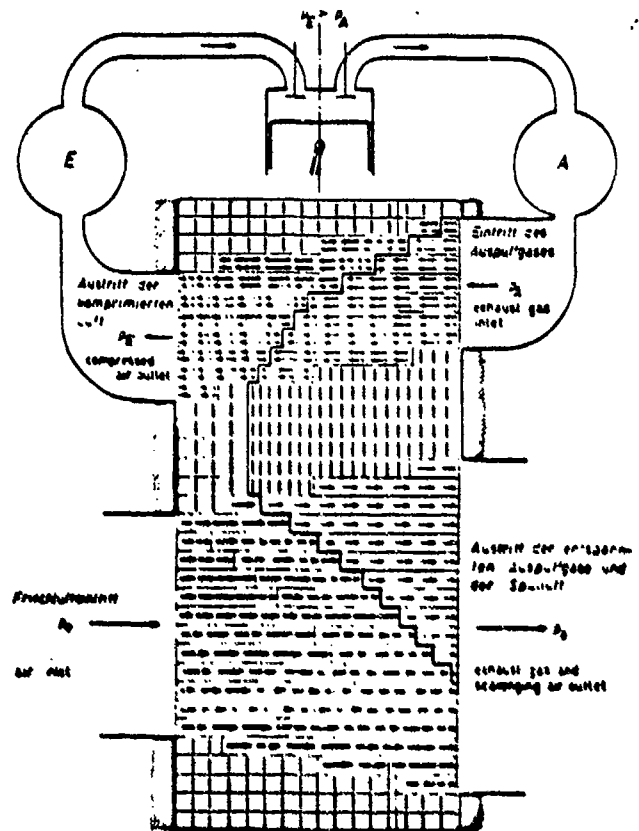


Fig. 1. COMPREX Pressure-wave Machine as a supercharger

- A Engine
- B Cell-wheel
- C Belt drive
- D High-pressure gas
- E High-pressure air
- F Low-pressure air
- G Low-pressure gas



- 1 Luft in Ruhe Druck p_0 at rest pressure
- 2 Spül- und Komprimierung in Ruhe (recirculation and compression at rest)
- 3 Luft in Bewegung (low pressure air in motion)
- 4 Komprimierung (compression)
- 5 Spül- und Komprimierung (recirculation and compression)
- 6 Teilweise komprimierte Auspuffgas in Ruhe (partially compressed exhaust gas at rest)
- 7 Komprimierung (compression)
- 8 Komprimierung (compression)
- 9 Komprimierung (compression)
- 10 Komprimierung (compression)
- 11 Komprimierung (compression)
- 12 Komprimierung (compression)
- 13 Komprimierung (compression)
- 14 Komprimierung (compression)
- 15 Komprimierung (compression)
- 16 Komprimierung (compression)
- 17 Komprimierung (compression)
- 18 Komprimierung (compression)
- 19 Komprimierung (compression)
- 20 Komprimierung (compression)
- 21 Komprimierung (compression)
- 22 Komprimierung (compression)
- 23 Komprimierung (compression)
- 24 Komprimierung (compression)
- 25 Komprimierung (compression)
- 26 Komprimierung (compression)
- 27 Komprimierung (compression)
- 28 Komprimierung (compression)
- 29 Komprimierung (compression)
- 30 Komprimierung (compression)
- 31 Komprimierung (compression)
- 32 Komprimierung (compression)
- 33 Komprimierung (compression)
- 34 Komprimierung (compression)
- 35 Komprimierung (compression)
- 36 Komprimierung (compression)
- 37 Komprimierung (compression)
- 38 Komprimierung (compression)
- 39 Komprimierung (compression)
- 40 Komprimierung (compression)
- 41 Komprimierung (compression)
- 42 Komprimierung (compression)
- 43 Komprimierung (compression)
- 44 Komprimierung (compression)
- 45 Komprimierung (compression)
- 46 Komprimierung (compression)
- 47 Komprimierung (compression)
- 48 Komprimierung (compression)
- 49 Komprimierung (compression)
- 50 Komprimierung (compression)
- 51 Komprimierung (compression)
- 52 Komprimierung (compression)
- 53 Komprimierung (compression)
- 54 Komprimierung (compression)
- 55 Komprimierung (compression)
- 56 Komprimierung (compression)
- 57 Komprimierung (compression)
- 58 Komprimierung (compression)
- 59 Komprimierung (compression)
- 60 Komprimierung (compression)
- 61 Komprimierung (compression)
- 62 Komprimierung (compression)
- 63 Komprimierung (compression)
- 64 Komprimierung (compression)
- 65 Komprimierung (compression)
- 66 Komprimierung (compression)
- 67 Komprimierung (compression)
- 68 Komprimierung (compression)
- 69 Komprimierung (compression)
- 70 Komprimierung (compression)
- 71 Komprimierung (compression)
- 72 Komprimierung (compression)
- 73 Komprimierung (compression)
- 74 Komprimierung (compression)
- 75 Komprimierung (compression)
- 76 Komprimierung (compression)
- 77 Komprimierung (compression)
- 78 Komprimierung (compression)
- 79 Komprimierung (compression)
- 80 Komprimierung (compression)
- 81 Komprimierung (compression)
- 82 Komprimierung (compression)
- 83 Komprimierung (compression)
- 84 Komprimierung (compression)
- 85 Komprimierung (compression)
- 86 Komprimierung (compression)
- 87 Komprimierung (compression)
- 88 Komprimierung (compression)
- 89 Komprimierung (compression)
- 90 Komprimierung (compression)
- 91 Komprimierung (compression)
- 92 Komprimierung (compression)
- 93 Komprimierung (compression)
- 94 Komprimierung (compression)
- 95 Komprimierung (compression)
- 96 Komprimierung (compression)
- 97 Komprimierung (compression)
- 98 Komprimierung (compression)
- 99 Komprimierung (compression)
- 100 Komprimierung (compression)

Fig. 2. Unwrapped Rotor Cells Wave Propagation and Air-resp. Gas-flow schedule.

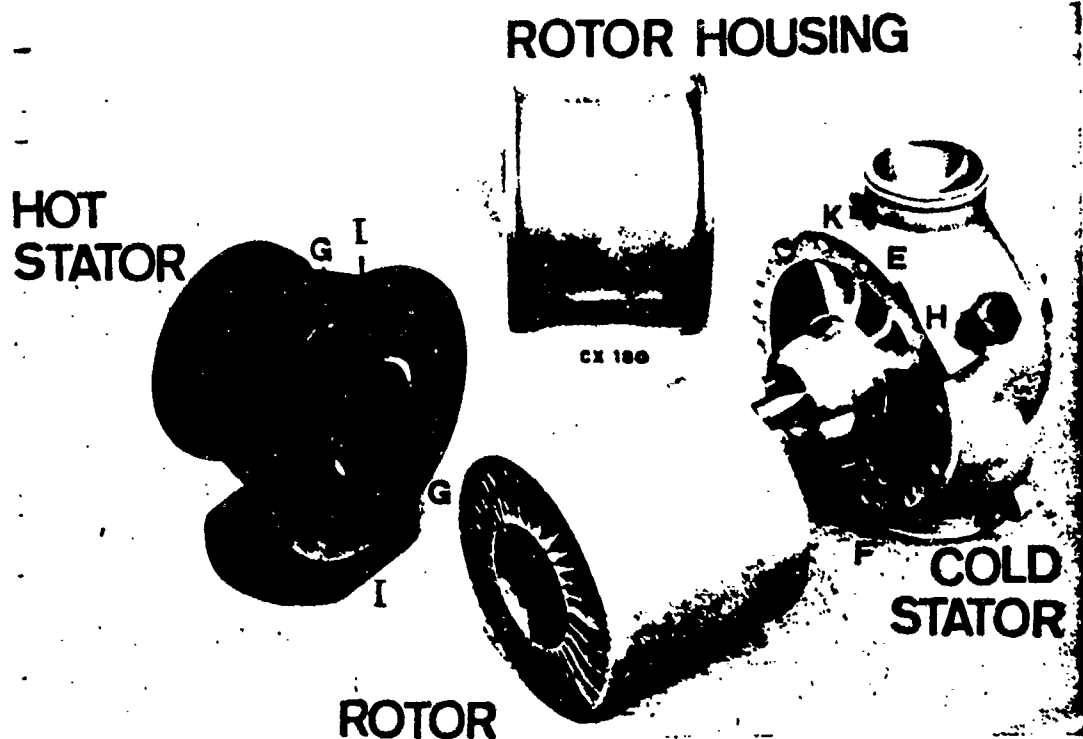


Fig.3. Components of the Comrex.

Ports D,G,E,F are connected to Ducts D,G,E,F Fig.1.

D Exhaust gas from engine

G Exhaust gas discharge

F Air inflow from ambient

E Compressed air flow to engine

Pockets H,I,K are energized at low rotor speed
and provide energy for scavenging the cells.

Bibliography

1. E. Jenny: Berechnung und Modellversuche über Druckwellen grosser Amplituden in Auspuffleitungen, Dissertation ETH 1949, Zürich
2. G. Rudinger: Wave Diagrams for Nonsteady Flow in Ducts, G. van Nostrand Co, Inc. 1955, New York
3. H.V. Hoerler: Abschätzung der Verluste in instationär gasdynamischen Kanaltrommel-Drucktauschern, Dissertation ETH, 1969, Zürich
4. G. Zehnder: Calculating Flow in Pressure Wave Machines, Brown Boveri Review No. 4/5, 1971.

SUPERCHARGING WITH COMPREX. APPLICATION AND EXPERIENCE

Prof. Max Berchtold, ETH, Zürich; Andreas Mayer, Brown Boveri, Baden

Introduction

Today almost all Diesel engines of power output higher than 400 kW are turbosupercharged. Brown Boveri has contributed significantly in raising the level of supercharging technology. A triplication of the power output compared to the naturally aspirated engine of equal displacement has become an accepted standard.

Supercharging is broadly applied to Diesel engines for trucks, buses, farm machinery and earth moving equipment. Here the operational requirements are more demanding due to the frequent load changes and the wide engine speed range. The reason for the wide use of the Diesel engine is the high fuel economy and the long durability. The passenger car Diesel which has become more widely considered has to meet the challenge of high fuel economy. The requirements for the wider engine speed range and the instantaneous load response are well recognized. Noise levels, acceptable for trucks, have to be reduced substantially. The emission levels reached in spark ignited engines only with sophisticated exhaust gas after treatment, are met by the Diesel engine with respect to carbon dioxide and hydrocarbons. Nitric oxide and particulates, however, as well as the unpleasant odour are of primary concern.

The low Diesel engine power output compared to gasoline engines of equal weight makes supercharging mandatory. The Compres pressure-wave supercharger has proven its capability to meet these requirements of the passenger car Diesel engine.

Tests of supercharging Diesel engines with the Compres go back over 20 years. The first prototype units have been tested and evaluated in a vehicular application in 1969 on a heavy duty truck, built by the Saurer Company in Switzerland. The performance expectations have been met. A number of problems, however, had to be solved to make this new device suitable for practical use and to become competitive in price with the conventional exhaust gas driven turbocompressor.

Manufacturing Technology

In order to meet durability at low cost, a rotor casting process had to be developed. A tremendous effort led to a sophisticated technique, capable of producing rotors which have numerous advantages over the older rotor construction, using sheet metal blades brazed into slots in the hub and the shroud. The casting technique allows to form the blade joints at the hub and the tip without local stress concentration. The intermediate shroud permits the stresses due to different temperatures between the hub and the shroud to be relieved. Previously this has been obtained by curved blades in radial direction. The alloy for the rotors is of a low coefficient of thermal expansion. Furthermore, it has a high oxidation resistance. Operating gas temperatures up to 850° C can readily be handled. The casting facility is shown in Fig. 1.

Precision casting techniques also are being applied to the stator castings. The porting geometry meets the tolerance requirements without expensive machining operations.

The Comprex rpm being between 8000 and 25000 depending on the airflow capacity, presents no problem to bearing design. The bearings are supplied by the engine oil pump. Rubbing seals are used to prevent oil from entering the air passages or dirt to get into the oil return line. The partially segmented Comprex, Fig. 2, shows the shaft and bearing arrangement.

Refinements in the stator design have resulted in a substantial weight reduction. The unit is supported by the exhaust gas collector, an arrangement well proven by the mounting of turbo superchargers.

Noise emission

The previous sheet metal rotor produced a narrow frequencyband noise of a rather penetrating character. The effective dampening to a permissible level turned out to be difficult. Cells of uneven width in random pattern gave a significant reduction in noise. The cast rotor with the intermediate shroud in variable cell width and shifted cell partitions also for reasons of stress relief gave an even greater noise reduction of 10 db. The additional means for treatment of the remaining noise can thus be less effective. The noise emission spectra for the two different rotors is shown in Fig. 3.

Exhaust Gas Recirculation

Diesel engines operating at low bmep produce NO_x even though the mean temperature is far below the stoichiometric combustion end temperature. The burning, however, always takes place at the zone of stoichiometric mixture. The local burning temperature therefore is as high as at full load. A reduction of the reaction heat thus calls for a reduction of oxygen concentration. This is obtained by exhaust gas recirculation, reducing the stoichiometric peak cycle temperature determining the NO_x equilibrium. A simple valving- and control system is used to have some exhaust gas bypassed into the engine at part load. At full load, the recirculation which causes a reduction of power output is undesired. Fortunately, the Comprex by its principle of operation has a sufficient amount of internal exhaust gas recirculation in the particular desired engine operating regime. Fig. 4 indicates the amounts of recirculation for different operating conditions. The NO_x reduction comes to 20 % at low load.

Potential Power Output Gain by Supercharging

The requirements for the supercharging of Diesel engines depend on the application. Passenger car engines are the most demanding. The high torque at low engine speed, combined with the request of rapid load response is typical. Whereas the turbosupercharger, combined with a turbine bypass valve,

is capable of building up a sufficient manifold pressure at low speed, it is not giving the response. At high engine speed, the limited turbine flow capacity calls for opening the bypass in order to prevent the manifold pressure from exceeding permissible limits. The compressor stability, however, remains to be a problem.

In the case of a more narrow speed range, such as in traction engines with multiple speed gearboxes, the waste gate hookup can be used to a pressure ratio level of 3. About the same limitations exist for the Comprex as far as speed range and pressure ratio. Fig. 5 shows the ranges for passenger car and truck engines.

As special engine applications call for higher levels of supercharging, two stage supercharging appears to be the best solution to meet the vehicular requirements. It has been found that the combination of the Comprex as the low pressure stage and a turbocharger as the high stage offers significant advantages both with respect to high speed range and high response. A peak bmep level of 27 bar ata at a manifold pressure ratio up to 6 has been demonstrated. The tests have confirmed the performance expectations. A six cylinder Caterpillar engine has been used which has been equipped with a fuel pump of higher capacity and with shorter pistons reducing the compression ratio to 12. Furthermore, it became necessary to install a device for adjustment of the injection timing.

Cooling of the charge air lowers the peak cycle pressure in all cases and thus the thermal loading of the critical engine components.

Comprex Superchargers for Wide Range of Engine Capacity

At the first stage of development, a series of Comprex units has been designed to meet the range of power output from 80 to 450 kW (Fig. 6 and 7). The units are of geometrical similar design. They have been extensively tested for endurance both in teststand- as well as in vehicular use. Life expectancy of 8 to 10000 hours is well within reach. The only wear has been found in the shaft rubbing seals. During engine overhaul, these parts can easily be replaced. The V belt for the rotor drive matches the belt life of the generator- and fan belt drives. Trucks have been operated over two million kilometers at satisfactory reliability (Fig. 8).

Comprex supercharging of passenger car engines has been started relatively recent. 1978, an Opel 2,1 liter Diesel engine has first been tested with the Comprex. Excellent response at low speed engine up to a high torque were the convincing features of this first test. In the further development, the Comprex was adapted to meet the higher engine speed range. The somewhat lower supercharging levels, sufficient for passenger car engines, allowed to increase the flow capacity for a given rotor size. Thus, a smaller Comprex matches the demands of the same engine.

As light weight passenger cars need less power (engines of the 1 liter class), smaller units have been added to the existing series. The power

range has thus been extended down to 30 kW. This Comprex is equivalent in weight to the turbochargers of equal capacity (Fig. 9 and 10).

A comparison of efficiencies can be seen at Fig. 11. It should be pointed out that there is no efficiency deterioration with down-sizing. The efficiencies given refer to a representative average engine operating point. The compression efficiency based on an isentropic temperature rises as high as 90 %. The combined efficiency reaches 56 % at the best point. One should realize that the wide speed range calls for a sacrifice in peak performance. In the case of optimized performance for narrow range or single point operation, the combined efficiency reaches 74 % which amounts to component efficiencies in the middle eighties.

The Comprex for Vehicular Diesel Engines

Present capabilities of the Comprex:

- Engine RPM range for full torque 1: 5
- Engine RPM range between idling 1:10
 and max. power
- Exhaust temperatures up to 850° C
- No low volume limitation (no Surge)
- Automatic altitude correction
- Instantaneous response under all operating conditions

The Comprex can meet the requirements of the passenger car Diesel engine.

The Comprex offers the greatest advantage in cases where frequent and instant load changes are of significance, combined with a wide engine speed range operation.

Fig. 12 shows the torque curves for different levels of supercharging. In single stage supercharging peak mean, effective pressures up to 20 bars are possible, whereas two stage (combined Comprex turbosupercharger) supercharging yields up to 28 bars.

The largest Comprex units are designed to be used in earth moving equipment. In this application, the capability of producing a high torque, a low engine speed without delay in torque rise is of primary concern. The frontend loader is shown in Fig. 13. Fig. 14 refers to a typical work cycle of loading, transporting and unloading. The best judgment can be made by comparing the performance of the same piece of equipment using the same Diesel engine, the same power shift transmission in one case with the Comprex and in the other with a turbosupercharger. The maximal fuel input for both injection pump is the same. The performance advantage of the Comprex over the turbocharger becomes apparent. The gain in transportation volume was established to be between 9 and 16 %. The difference was due to the ability of the driver. In cases of a more demanding mission, the advantage of the Comprex was even more pronounced. If one considers the cost (equipment amortisation, wages and fuel), the cost difference of the Comprex vs the turbocharger is totally insignificant. The drivers expressed their favorable opinion regarding the advantages due to the higher load capability.

Ploughing Tractor

Again the specific power requirement of this type of equipment is well suited for a Comprex supercharged Diesel engine. The Finish Company Valmet has been the first engine and tractor builder to install the Comprex as standard equipment. The production advantage is particularly significant since the thrust force to push the plough varies as much as 50 %, depending on the compactness of the earth. The ability to continue the operation through a segment of increased resistance is of primary importance. The capability of a substantial torque rise with decreasing engine speed represents the essential feature. In case of a stall with turbocharged engines, the tractor has to start up again loosing time and thus production. As fluctuations occur at short intervalls, stalls can become very frequent. Operating at part load at a lower gear ensures the availability of extra thrust to pull through a higher drag section. This means lower utilization of the equipment. More time is needed for ploughing the same area. A power shift gear can overcome some of the disadvantages. However, the added Comprex cost offsets the price of the power shift gear. The Valmet tractor is shown in Fig. 15.

A Steyr Daimler Puch Tractor has been tested with a Comprex utilizing compressed air intercooling. In this case, the torque rise was as much as 38 %. This allowed the tractor to operate at lower engine speed at the normal ploughing speed with a considerable fuel saving. The high torque at low speed engine proved to start up the tractor without excessive clutch abuse.

The Comprex in the Truck Engine

Modern direct injection engines are known for their high efficiency. A further improvement, thus, can only be realized by lowering the engine speed at equal power which means a torque increase by rising the manifold pressure. This again is the domain of the Comprex, capable to lower fuel consumption without additional control means such as a waste gate. Lowering the speed also lowers noise emission. The advantage of fewer gear shiftings and the use of a gear box with fewer stages should be considered in evaluating the economy of the Comprex supercharger.

The Comprex in the Passenger Car

The introduction of Diesel engines in passenger cars has primarily been initiated by the attractive fuel economy. The fact that this engine realizes a stratified charge concept makes it also more favorable with respect to emissions without the need for expensive devices for exhaust gas after treatment. The lower power output at equal displacement and equal weight calls for supercharging. The torque shape and response should be as good as with the standard gasoline engine. The Comprex meets this requirement. The passenger car engine has its most frequent use in the middle range of rpm at about one third of its peak torque. At this regime, the thermal efficiency of the gasoline engine is about two thirds of the peak efficiency. The Comprex supercharged Diesel engine, both with indirect and direct injection at equivalent part load, has a thermal efficiency equal or better than the gasoline engine at peak torque.

The fuel savings with Diesel powered passenger cars are therefore substantial. The mixture enrichment in the gasoline engine warmup period makes up for a 20 % fuel consumption increase in the first 5 km. The Diesel engine does not need such modifications.

In 1978, the first Comprex supercharger fitted to a passenger car engine had the Comet combustion chamber. The torque curve 1, Fig. 16 shows the moderate gain reached at that time which agreed with the torque curve of the turbocharged engine. In driving the car, the response made the car seem considerably more powerful.

Based on the experience with Comprex supercharged truck engines, the bmep compared to naturally aspirated engines was still quite moderate. Due to the larger engine speed range of passenger cars, compared to the relatively narrow speed range of truck engines, made the torque at low engine speed fall off below acceptable levels. High torques at one quarter of the max. engine speed are taken for granted in gasoline engines. In this range additional development efforts were concentrated. It was found that strong pressure pulsations occurred in the engine exhaust gas collector which disturbed the Comprex performance. A modification of the stator geometry has been established to correct this disadvantage. Curve 2 in Fig. 16 indicates the substantial gain. At the same time, the flow capacity has been increased thus allowing to reduce the rotor diameter from a diameter of 112 mm to 93 mm. A Comprex weight reduction to about 60 % of the previous weight, needless to say, brings several advantages.

The intake manifold pressure ratio in the low speed range is now between 1.4 and 1.5. If a charge air cooler is incorporated, a density ratio of about 1.4 means a bmep of 10 bar at .25 of peak engine speed. In the mean engine speed range a bmep of nearly the double of its naturally aspired counterpart was obtained. At max. engine speed, the bmep gain is falling to about 30 to 40 %. Here the cycle peak pressure represents the limiting factor. One should be aware that engine size and gear box ratios should be selected carefully. In doing this, the criterion of available excess power at a car speed of 40 km/h to produce an acceleration of $0,7 \text{ m/sec}^2$ should be considered. This would permit a reduction of the engine displacement in the Opel engine to 1,64 liter or to increase the vehicle mass proportionally. The fuel consumption has been measured on the vehicle dynamometer with a 2 liter engine assuming the heavy vehicle. The expected fuel consumption for the Opel with the 1,64 displacement engine has then been established by calculation. The results are presented in Fig. 17 as a comparison.

In order to fully benefit from the potential fuel saving with no sacrifice in car performance, the following requirements will have to be met:

- A high degree of supercharging in the entire engine operating speed range.
- Availability of full torque within 0.5 sec.
- High thermal efficiency in the medium engine speed range at a bmep level of 4 bar to be within 10 % to the peak efficiency of 32.6 % (equal to 260 gr/kWh). Future direct engines will be 15 % better.

High torque at low engine speed allows engine utilization with very much lower noise emissions.

The Comprex has received much attention lately for its potential use in passenger car Diesel engines. The 3 liter 6 cylinder engine in the Daimler-Benz as well as the 1.2 liter 3 cylinder engine in the VW represents the extremes of the wide range of application evaluation. Both engines with indirect and direct injection, with and without charge air cooling are being tested. There are cars with manual gear shift and with automatic transmission. Engines have to be designed sufficiently rugged to be supercharged to a manifold pressure ratio of 2. Air cleaner and exhaust mufflers have to be laid out for low pressure drop at the larger air and exhaust gas flows.

An application of a small Diesel engine supercharged by the Comprex is being tested in the Steyr-Daimler-Puch jeep. This vehicle, shown in Fig. 18, demonstrates the specific advantages of the new system having a high torque in the full range of engine speed.

Fig. 19 represents a typical Comprex installation on a vehicular Diesel engine. In order to simplify the beltdrive, the Comprex is placed in such a way that the belt pulley is in the plane of the V beltdrive for the electric generator. The Comprex is bolted to the exhaust gas collector. This eliminates the need for flexible expansion joints. As the drive power is quite small, the belt force driving the Comprex rotor is insignificant. An idler pulley is used to adjust the belt tension. The piping of the compressed air is flexibly mounted with rubber sleeves. For starting the engine, a simple small alternate air intake valve is provided in the compressed air duct. The spring loaded valve opens automatically by the vacuum when the engine is turned over by the electric starter. The over all installation is simple since there is no need for a hot bypass valve with controls. Also no control means are necessary to limit the fuel input during transients.

Summary

The Comprex represents a new principle suitable to supercharge vehicular Diesel engines with requirements for a wide speed range operation and for rapid response to load changes. The device operating at low speed is simple in its design. Emission- and the noise standards can be met.



Fig.1 Complex Rotor Casting Facility

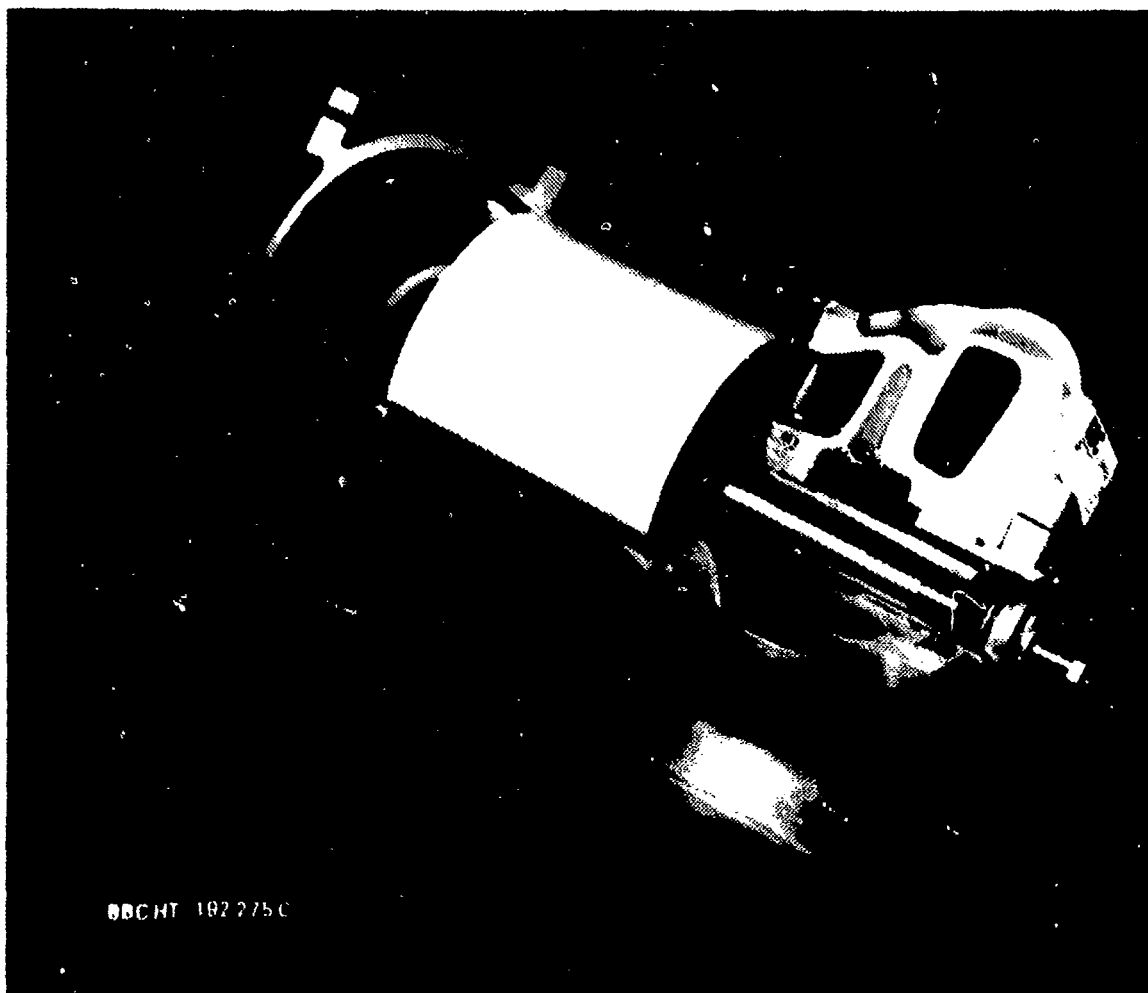


Fig. 2 Compro Supercharger

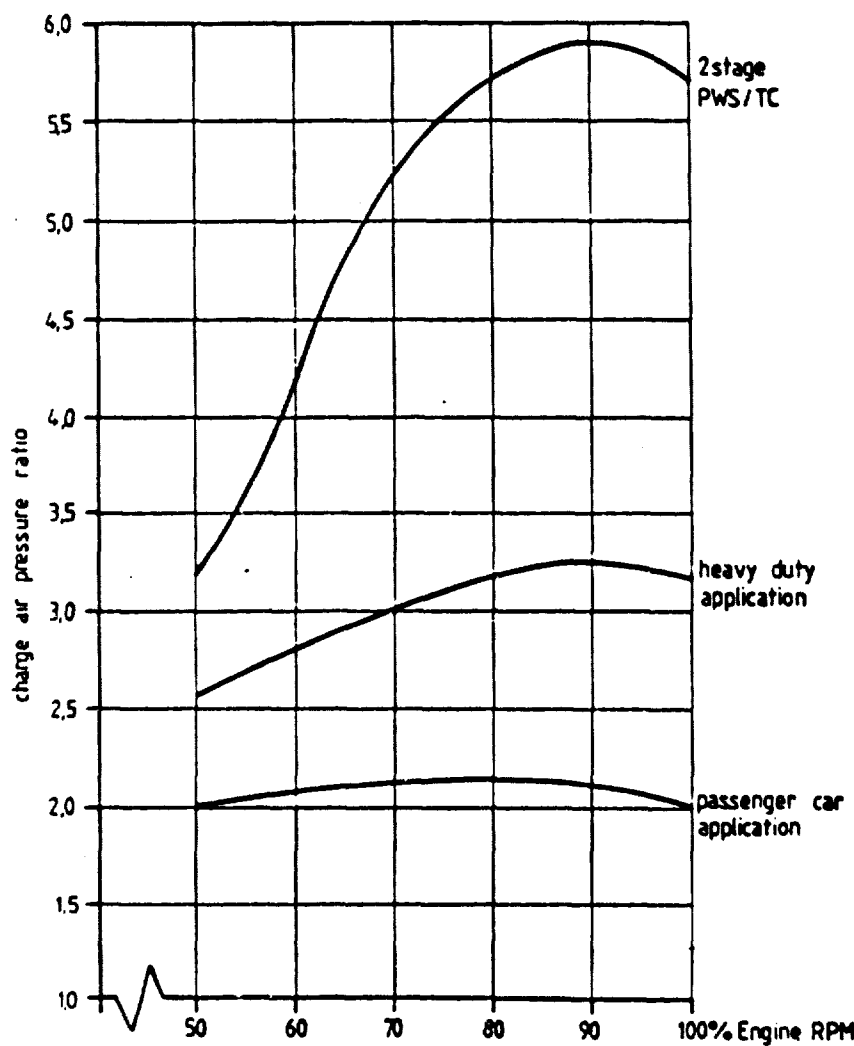
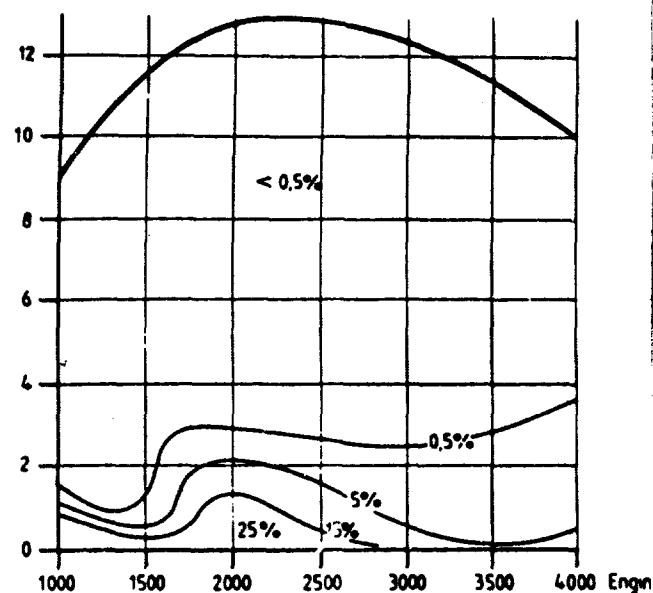
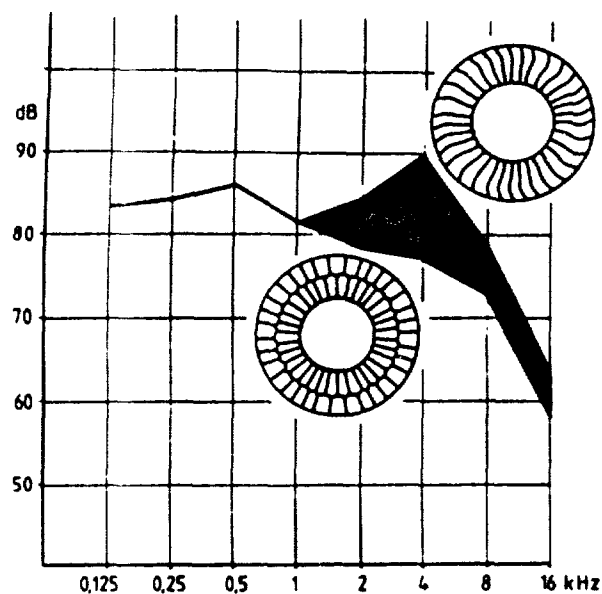


Fig. 5. Supercharging Pressure Ratio vs Engine Speed with Comrex Supercharging.

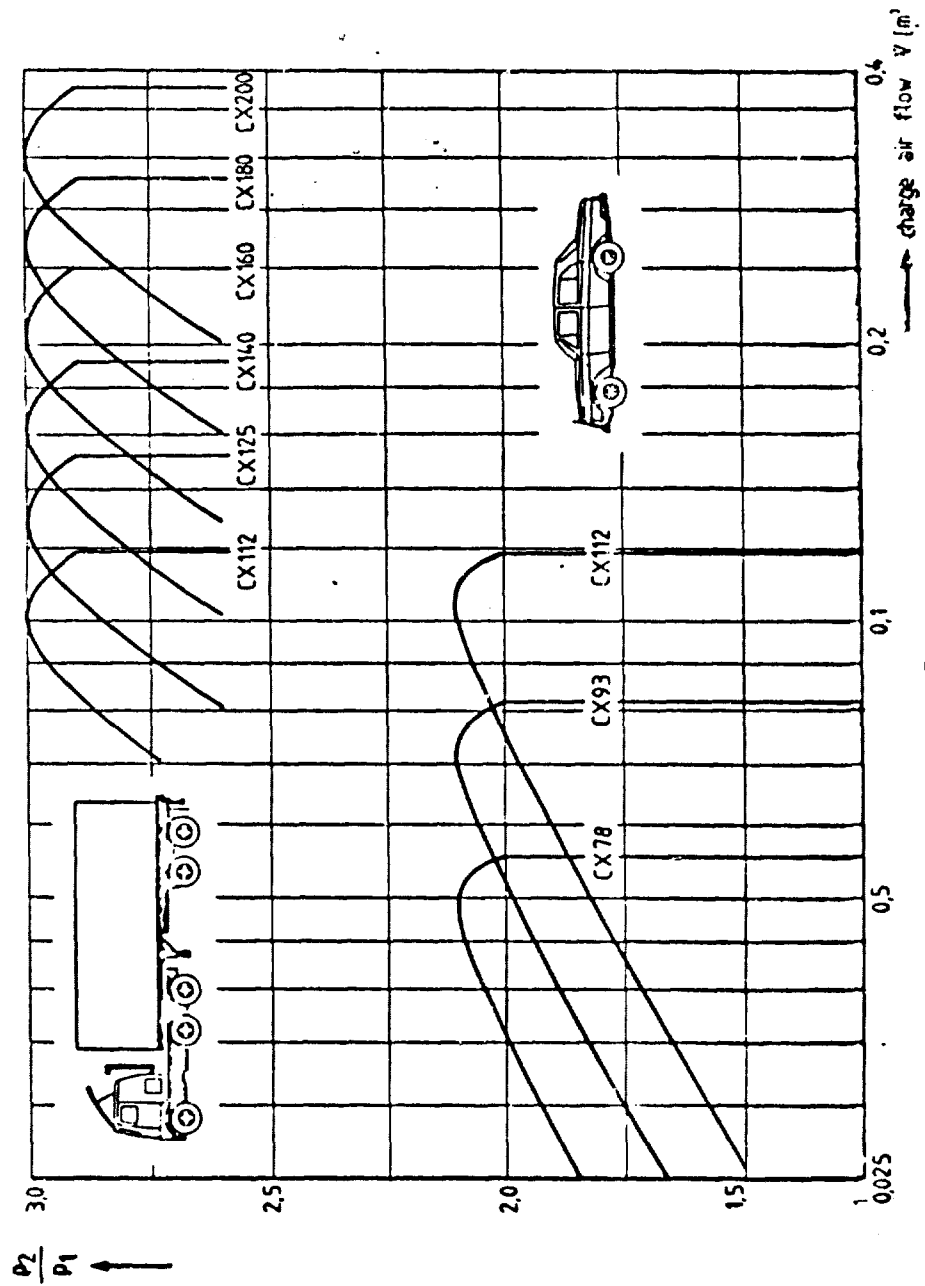


Fig. 6

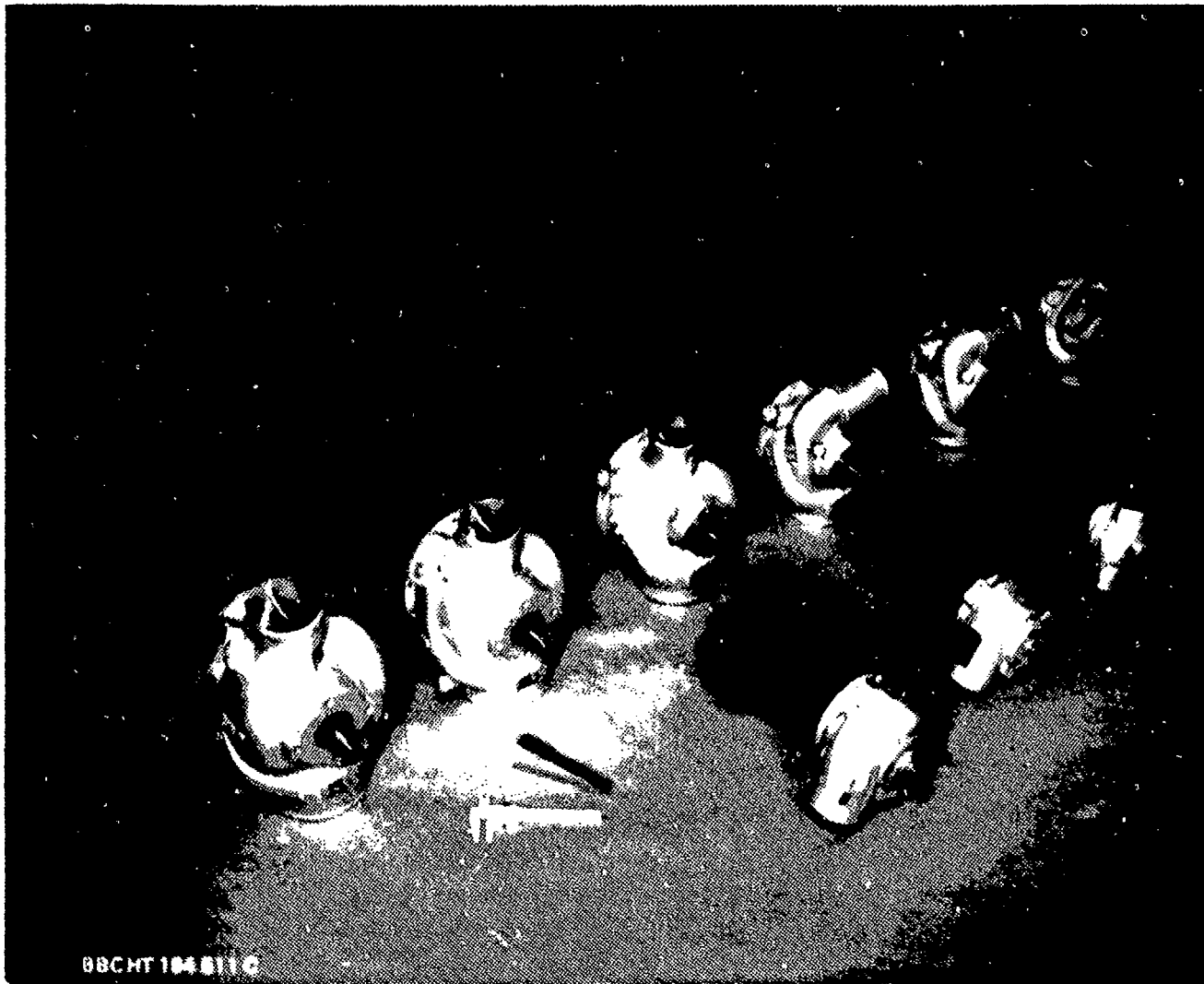


Fig. 7 Comprex Supercharger Models



Fig.8. Saurer Truck with Complex Supercharger.

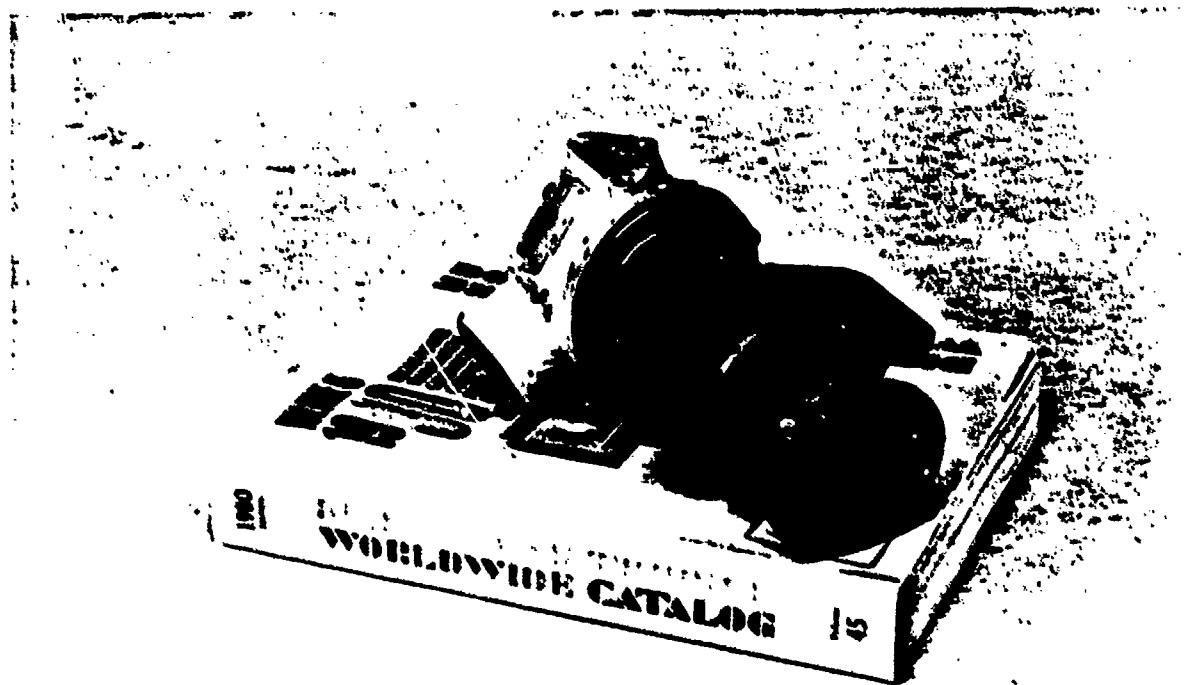


Fig.9. Small capacity Complex for Passenger Cars Diesel Engine.

Commercial vehicle range

	Nominal engine output [kW]	Weight [kg]
CX 200	250 - 450	40
CX 180	200 - 350	32
CX 160	160 - 280	24
CX 140	125 - 225	18
CX 125	100 - 180	14
CX 112	80 - 140	12

Car range

CX 112	60 - 90	10,5
CX 93	42 - 62	7,0
CX 78	30 - 45	5,7

Fig.10. List of Compres Model Sizes with Engine Power Rating.

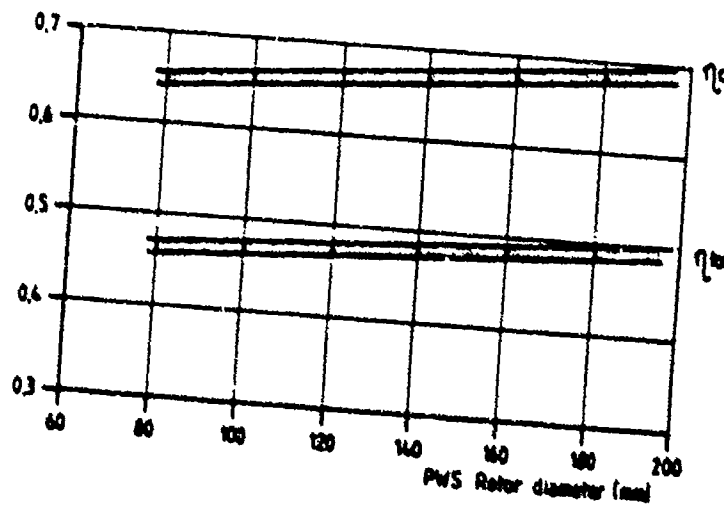


Fig.11. Equivalent Compres Efficiency vs. Compres Size
Compression Efficiency
Overall Efficiency.

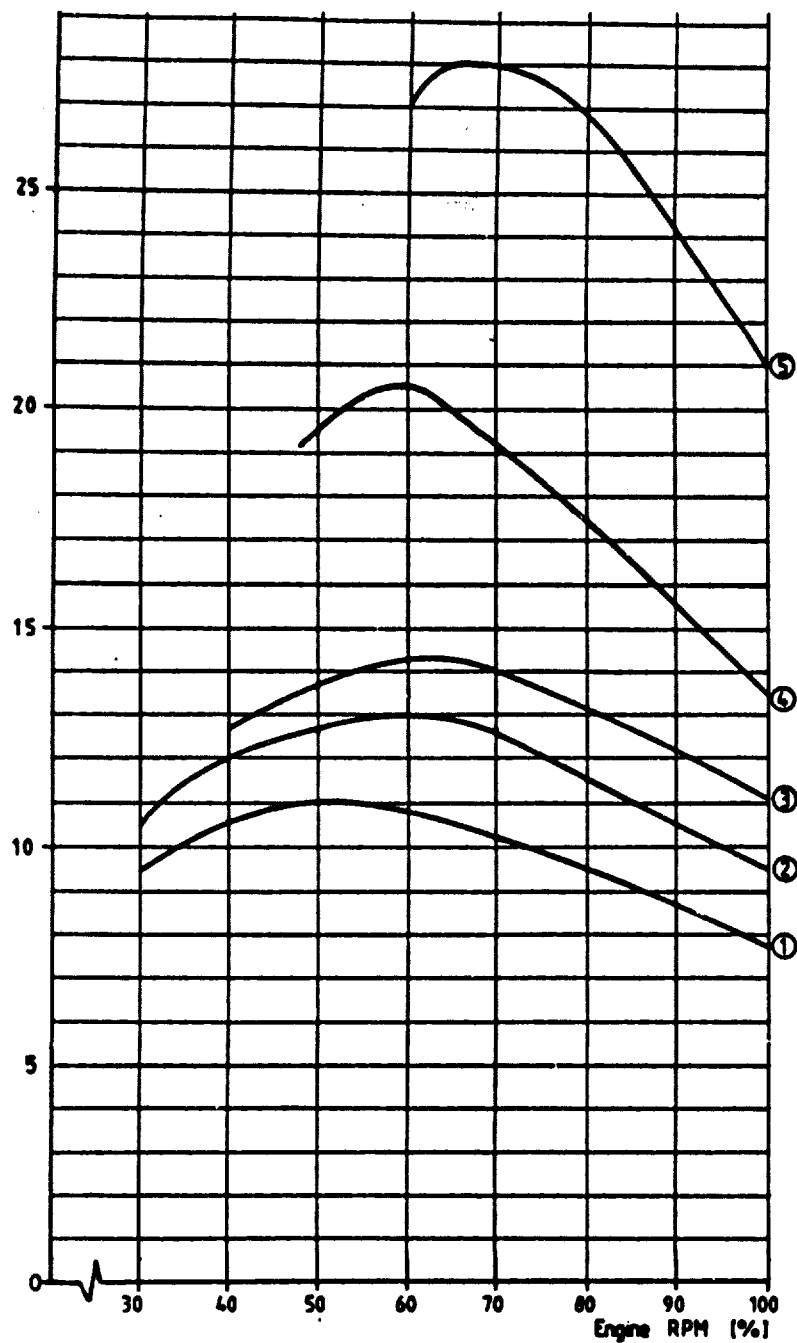


Fig.12. Mean effective Pressures vs. Engine speed for different levels of Compres Supercharging.

Identification of curves:

Intercooling is applied in all cases except Curve 1.

- 1) Passenger Car
- 2) Passenger Car
- 3) Truck Engine
- 4) Heavy Duty Truck Engine
- 5) Heavy Duty Truck Engine with Compres and Turbocharger.

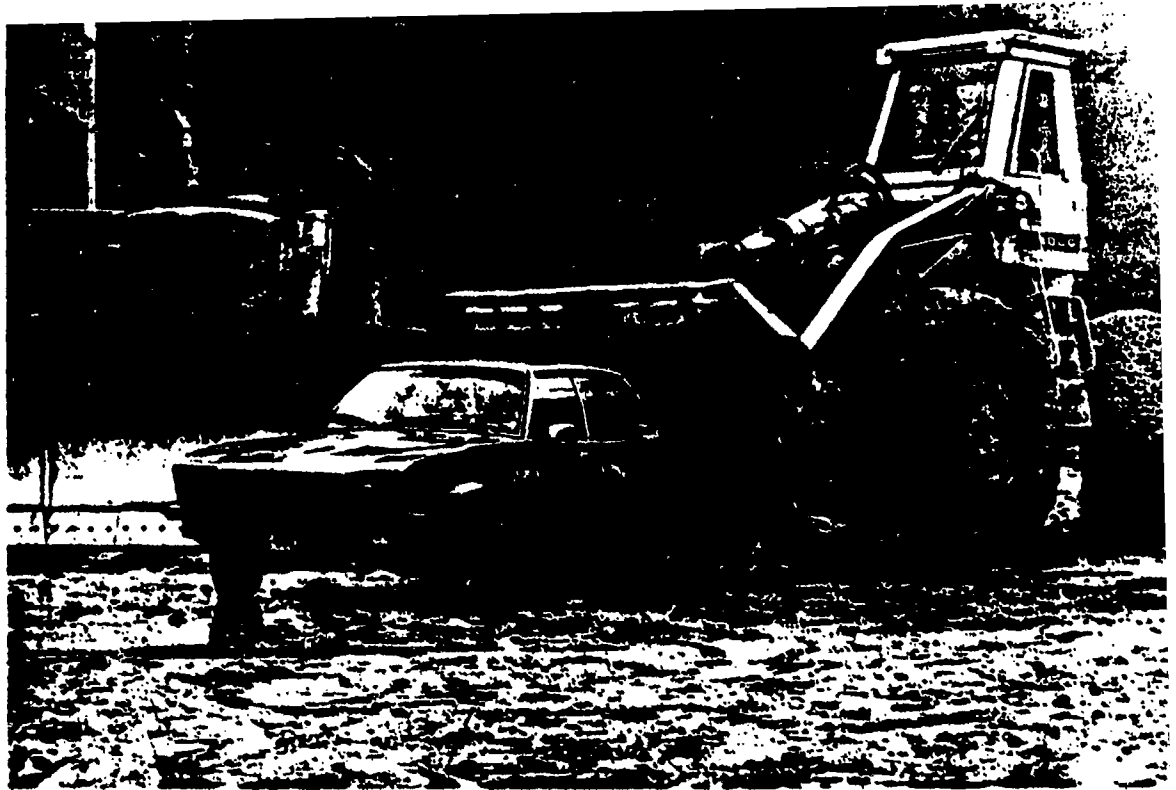


Fig.13. Frontend Loader.

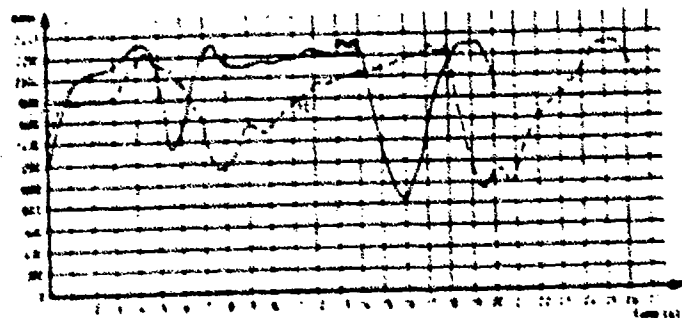
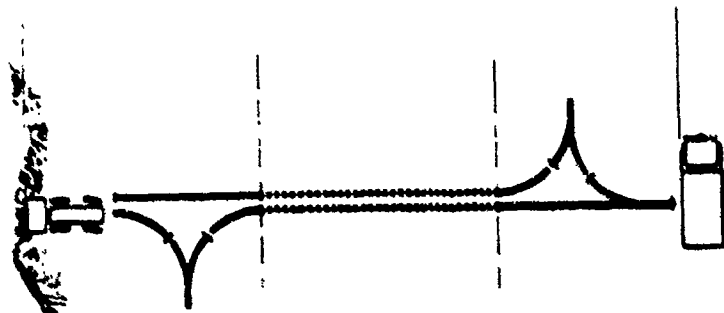


Fig.14. Frontend Loader Mission.



Fig.15. Valmet Tractor.

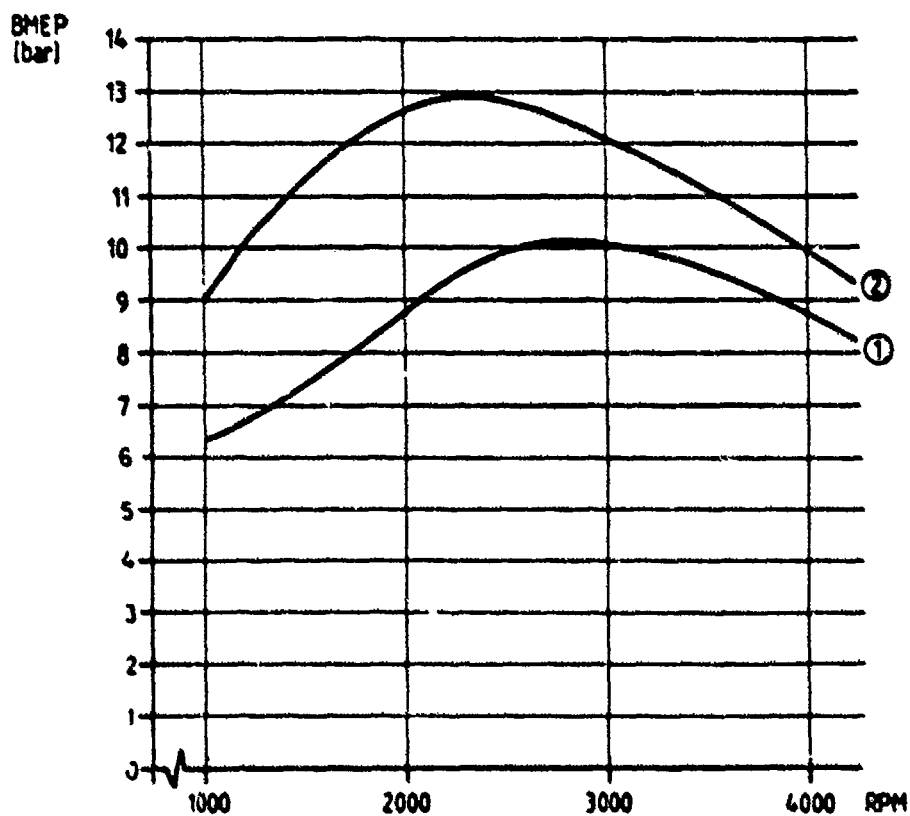


Fig.16. Comparison of BMEP Curves vs. Engine speed
 1) First Test of Comprex on Opel IDI Engine
 2) Improved Matching of Comprex on Opel IDI Engine.

Inertia weight : 3000 lb

<u>Fuel economy</u>	<u>2,3 l</u>	<u>1,64 l</u>
Urban Test	30,0	36,8 mpg
Highway Test	38,8	44 mpg
CFE	33,4	39,7 mpg

<u>Emissions</u>		
HC	0,26	0,31 gpm
NO _x	0,64	0,79 gpm
CO	1,5	1,01 gpm
Particulates	0,32	0,48 gpm

<u>Drive-by Noise</u>	
(ISO 362)	74 dBA

Fig.17. Opel Record Passenger Car Performance and US Emission Test Comparison for equal Car weight and different engine sizes.



Fig.18. Steyr - Daimler - Puch
4-wheel - Drive Experimental Car.

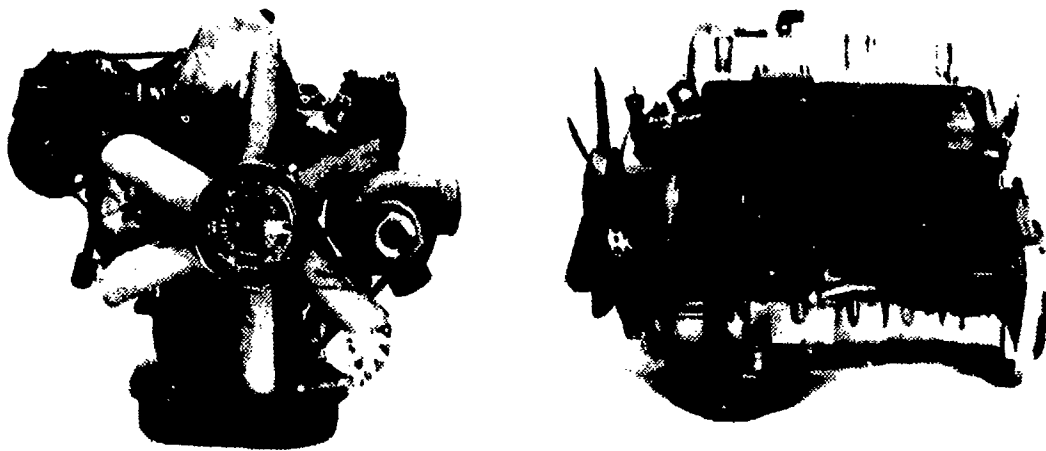


Fig. 19 Complex Installation on Vehicular Diesel Engine

Gas Dynamics of Pressure-Wave Supercharging

Dr.L.Matthews, BBC Brown Boveri, Baden,Switzerland

The aim of this project is to achieve a further improvement in the design of pressure-wave (PW) machines through a detailed investigation of the aerodynamics. Such an optimisation is only possible by applying sophisticated measurement techniques and advanced computational methods.

PW machines can be utilised wherever an exchange of energy is necessary, possibly accompanied by heat transfer and/or mass transfer. The supercharging of automobile engines is an application where considerable energy economy can be realised by direct transfer of energy from the exhaust gases to the inlet air. The BBC Brown Boveri COMPREX[®] supercharger is such a PW machine and the theme of this study.

The intensive Comprex development activity ranges from testing road vehicles, experiments in engine test cells and combustion rigs to basic research of the PW process in the "MessComprex" test rig. The MessComprex is an idealized PW machine which permits an individual investigation of the gas dynamics phenomena. In a first step the study is confined to the driver-gas and the driven-gas end is sealed off.

The experimental research of the PW process is split into three activities based on the measurement technique employed:

- Global measurements and measurements of the boundary conditions in the inlet and outlet ports. The flow parameters were obtained by traversing a 3-hole probe with integral thermo-element.
- Laser-velocimetry: non-intrusive investigation of the unsteady flow in the rotating cell passages. The velocity and turbulence vectors at several axial, circumferential and radial positions were measured at different rotational speeds and pressure ratios inside a specially constructed glass rotor.
- Transient pressure measurements in the rotor cell passages using miniature piezo-resistive transducers. The periodic pressures at 5 axial positions revealed the intricacy of the PW process.

The above measurements provide empirical inputs to the computational model and serve the calibration of the computer program. The program calculates the one-dimensional, unsteady, laminar, compressible flow using the Lax-Wendroff scheme with flux correction of the PW fronts. The basic PW process is well simulated by such a computational procedure. The details of the superimposed disturbances originating from the cell-filling process, flow recirculations, boundary layers, secondary flow and high turbulence levels cannot however be fully simulated. It is proposed to study these with a two-dimensional finite-volume algorithm such as suggested by McCormack.

The detailed experimental investigation of the idealized PW process yielded an unique and valuable pool of data. The newly gained insight should help the imminent commercial break through of the COMPREX[®] pressure-wave supercharger. This research was funded by NEFF (Swiss National Energy Research Fund) and BBC Brown Boveri.

The following is a transcription from tape of Dr. Lebius Matthews' talk.

The figures could not be included.

Well gentlemen, I come from Switzerland and one of the first things I did in this country was to sit down in front of the television set to look at the academy award presentations; I thought I could take some tips from the way the stars went about it. What I noticed is that they always thank everybody and say that everything has only been possible because of the work of others and this is very true in my case. I am here as the representative of a company, and the work I will be showing has been done in large part by my colleagues. I also want to say that it constitutes a great honor to be here in this illustrious company and to be put in the same session with Professors Kentfield, and Berchtold. That gives me a clue to tell you something about my background. I have a doctorate from Imperial College, and during that period I had the chance to work with Professor Kentfield and also Professor Spalding. Later I worked in the research laboratories of General Electric Company, and now for the past decade I have been with BBC Brown-Boveri in their research laboratories in Baden, Switzerland. Because I have not had the chance to coordinate my presentation with some of the things you have already heard, there could be a certain amount of overlap, and I was distressed to find that I even have some of the same pictures which Professor Berchtold showed, but that means we may get to lunch a bit quicker, because I can just flash those. I will be showing some slides to begin with, and this part represents the work that we as a company, as a whole have done. Then later on, I have a few transparencies which are a sneak preview of the work which I have been doing in the very recent past. May I have the first slide please? (A view of the Comprex Rotor) This picture is already very familiar to you and Professor Berchtold has already pointed out to you the reasons why this particular construction has been adopted, he has also told you how this variable pitching helps to spread the noise over several frequencies. This kind of construction is mechanically advantageous, and yet another reason for having this inbetween shroud, as it has been called today, is that we are now aware that there are radial fluctuations of pressure. By splitting up the radial height, you are effectively cutting the amplitude of the sound. And so this is how a rotor now looks. To give you an idea of size, the diameter of this can be less than 4 inches (98mm), to be precise, and the length is roughly the same as the diameter. A very wide spectrum of work is being done at BBC. There is the work which we are doing with vehicles on the road, and this picture shows it. Here is the truck driving along and there are two of my colleagues making noise measurements. Now, Professor Kentfield had said that noise was a possible disadvantage of this machine, and I can proudly claim that we as a company, have licked this problem and in fact we are able to meet the most stringent road regulations. By chance, they happen to be most stringent in Switzerland. We are meeting the noise regulations everywhere. There is no unpleasantness at all in the sound these machines make. It certainly has a distinctive note, but I think that gives it a touch of class, because anyone driving such a vehicle can now be proud that he has this special tone. This is the Earth moving machine, or one like the one which Professor Berchtold showed. And here you can see the engine side by side with the vehicle itself. The Comprex itself is here and is belt driven.

This is a vehicle engine, I believe it is one from Chrysler, but I am not sure, I think it is about a 3 liter engine and the Comprex itself is installed up there.

This is a slide of an engine test bed where the Comprex is being tested, with the engineer sitting in the control room; the engine is behind the glass walls, and is connected to a water brake, and with that I want to come down to the next lower level of our testing. The first level is on the road, vehicles which are actually running and being driven thousand miles a day, in fact we have cars that are on the road, 24 hours of the day, driven in three shifts. This is the second level where we have the Comprex running in engine test cells.

This is a closer view of the engine which you saw on the previous slide with the comprex mounted on it. Because it is instrumented for testing, there are a lot of cables and pipes and signal carrying transmitters all over the place. (A machine inside an actual car would not be so cumbersome).

We have got a little bit closer to it and you can see the ducting carrying the gasses to and from the Comprex.

With this I would like to come to the third level of our research and development activity, and that is that we not only test the Comprex on road vehicles, and in engine test cells, but also machines which are fitted to combustion rigs. There is no engine there, but we burn fuel and push it through the comprex and make very detailed tests, varying all the geometry and parameters. This here is the comprex itself. This is one of the stators, this is the other stator, this is the shiny casing around the shroud, and you can see the pipes which are bringing the gases to, and carrying them away from the Comprex.

This is a picture which you have seen in another form from both the two previous speakers, and they have done me a service by introducing you to some of the conventions which we use. Namely that we present the diagram in the form of the open duct rotor, a developed view. And this slide helps you to see the process as it goes along. The convention that is used here is that the red represents the hot gases, and the blue the fresh air, and if you look at the intensity of the color, you can guess the intensity of the pressure of this gas. Those are the exhaust gases coming from the engine, marked here as gas high pressure. This is the inlet port on the gas side, and then the high pressure which is about 2 bars begins to enter the cell. This line which you see here is the compression wave which originates from this edge, and when it is correctly laid out at the point at which this compression reaches the air side, the fresh air side, that should be the point at which the air, which is on this side and has been compressed by the compression wave, can now be pushed out into the port carrying the charge back to the engine. The compression wave reflects from this edge as a secondary wave, causing a further rise in pressure. It comes here to the gas side and is now reflected as an expansion wave, the point where this expansion wave reaches this end, is the point when this port should be closed. You see that when it is correctly laid out the interface doesn't quite reach the air end before this end is closed off. Now one goes into this phase and here there are expansion waves. At this point, the opening of the exhaust discharge occurs which sets off another expansion wave. The gas which is inside the cell is now pushed out,

and fresh air is now induced through this port. This exhaust port is made sufficiently wide so that a fair amount of scavenging air is drawn through which helps to completely refresh the contents of the cell. So at this point the cell is full of clean fresh air, and the whole process starts again from the top. Now, one of the subtle features of our machine are these pockets, that is the compression pocket here, an expansion pocket, and the gas pocket, and these geometrical construction features are what helps our machines to maintain performance at off design speeds.

Here we are zooming in on the high pressure process as we call it, that is the top part of the previous picture. These machines run at about 15,000 R.P.M at design speed, which means that the rotor completes one revolution in four milli-seconds. We have shown the cells drawn at different positions and these positions are 15 microseconds apart. The time if you like, is running downwards. This is a cell which is full of quiescent fresh air at a pressure slightly below atmospheric. This cell is exposed to the gas inlet. The compression wave races into this cell at about sonic speed, and behind the compression wave the pressure rises. Naturally the compression wave runs at speeds considerably higher than the speed at which the gas itself is flowing. This means that pressure is transferred much faster than the mass. This is good for us because that means we have a very rapid and sudden increase in pressure. Here we can see in some detail the compression wave being reflected, and at this point you see the stop signal which is released, and we have actually drawn some fans here to show the expansion waves. This expansion wave is the signal for the closing of the cell, so when the cell has reached this point, and before the interface has reached the air end, it is closed off and we are left with this air cushion. This air cushion has the function of insulating the air side casing from the hot gases, which are kept on this side. Here we want to draw attention to another feature. The cell walls are heated by the exhaust gases which have been allowed to flow in there. Later on the same cells are filled with cold air, which means the cells are being warmed and cooled alternately, and very rapidly, and therefore they assume a mean temperature, and therefore all the material problems are much simpler than they are for example, in the turbines.

This is a zoom view of the low pressure side (it continues from where we left off before). Reading from top to bottom, there is the air cushion, and the quiescent decompressed gas, which has been decompressed by the expansion waves running in it. At this point this edge sets off an expansion fan. What we have not shown are the further reflections of this fan, they go on very weakly and are still present. What is important for us, is that fresh air is sucked in, and the exhaust gases are allowed to flow out, after having been expanded. Here you see the scavenging process taking place. The expansion fan is being set off from this inlet edge, which gives the signal here for the gas outlet port to be closed.

With that I want to come to the fourth and most basic level of our research and development activity; a laboratory piece of equipment which is a model machine, referred to internally as the MeJcomprex. 'MeJ' comes from the German word to measure, and not from the english word messy. In fact, it is a very clean and idealized machine and you can already notice some of the idealizations which we have. We have only a single deck of cells. The cells are equally spaced, and you see the aspect ratio is nearly one to one. These are the various geometric idealizations which we have made. Another

idealization is that we work only with air and not with hot gases. In the first phase we have shut off one end of this so that we only look at part of the process. Now the question is, what do we hope to achieve by this? And the answer is, we want to look at the most idealized process because only if you have understood this, and only if you are able to compute this idealized gas dynamic process, do you have any hope of understanding the more complex processes which take place in the real machine. We find it convenient to work with air because we know the thermodynamic properties of air perfectly. What advantages do we have in such a machine? We can instrument it and it is a very highly instrumented machine. For example we have rotating pressure transducers fitted into it, and we get signals out so we know what the transient pressures are inside of the rotor. Another feature is, this particular one has a glass shroud. It is not our intention to sell any machine with a glass shroud, it's only to help us look into it literally to find out what is going on. We use laser anemometry to measure the instantaneous velocities inside the cells.

This is the Meßcomprex (Meß being German for 'to measure') or the model complex test rig, and as I said it is a laboratory piece of equipment, and far removed from the road machines. The rotor itself is here, we have shrouded it up quite carefully because we once had a nasty experience of the glass shroud bursting. We have an electric motor to drive it, on which we have a speed control. One side of it is temporarily blocked off. On this table here, we place our laser (I will show some slides on that), and we bring air in and take it away through flexible pipes. Here we have manometer columns, and a compressor there to provide high pressure air, which is the simulation of the exhaust gases; we have coolers, bypasses, mufflers, and a whole bank of thermal elements which are being fed into the thermal register block.

Here we see the machine in more detail. The actual rotor is inside there. And this shows how the gases, or the air, in our case, is fed into it. One of the features we have in our laboratory machine is that the complete stator can be rotated. The reason we need to rotate the stator (the stator is not rotating but can be rotated during an experiment), is so you do not have to move around it with a laser in order to look at the velocities at different positions. To avoid doing that, we just swivel the entire machine, stator and all, while the rotor is rotating, and that is why we have a fairly complex arrangement here.

Here are some of the instruments that we are using. The scale here is in centimeters, from there to there it is one inch or 2.5cm. These are miniature instruments which we have here, this is the pressure transducer, it's a piezo-resistive transducer with built in temperature compensation, and we have 5 of these which are fitted into the rotor, and the signals are taken out using mercury slip rings. This one is a very small 3 hole pitot tube that has 3 holes in there, they are all made with half a millimeter diameter hypodermic tubing and there is also a minute thermoelement in it. We use this to traverse the stator ports to measure the air velocities in the ports.

This is the rotor laid bare. Here is the laser beam pointed into the cells into the rotor. After our previous unfortunate experiences, we bandaged up the glass rotor and let just that bit open there where we wanted to look into it, we used to take this bandaging apart and move it to different places. Now we have it all padded up with foam and so on, so it can get the bits of glass if it breaks.

A slightly closer view shows the laser beam, and if you look very carefully you will see that there are two spots, and that is significant because, what we are using is the so called laser 2 focus technique. The principle is very simple, one has two spots of light, very close together actually, and what one is measuring is the time of light. The air is seeded with particles as I told you, and one starts a clock when a particle moves through a start beam, and then one stops a clock when one has moved through the stop beam. You can imagine that this is no simple process, this timing is done in the nanosecond range.

This shows the laser gun with this lens, and here we have an arrangement with which we generate the tracer particles. These have to have a controlled diameter smaller than $1/2$ a micrometer, in order that they are small enough to reasonably follow the flow which they are representing.

These are the electronics which we need in order to make these kind of instantaneous velocity measurements. I think I told you that the entire rotor turns around in six milliseconds and the cell passing frequency is about 20 microseconds. In that short period of time, we have further broken down each cell into about ten different windows into which we look to obtain the velocities. We are investigating an event which is in the microsecond range, we are making time of light measurements in the nanosecond range, and in order to obtain any kind of meaningful measurements, we have to do it statistically because there is the chance that the stop beams could be activated by a particle which had not previously passed through the start beam, or that the particle that does pass through the start beam does not pass through the stop beam, so in order to cope with all of these eventualities, we had to do 2 things. One is to rotate the stop beam around the start beam, so that we can, in an initial pass determine the most likely direction of the flow. The second thing is we have to go about it statistically, in that we wait for 2,000 events and we represent these 2,000 events on a histogram which you can see faintly on this video screen here, and have a histogram like this, we can read off the most probable velocity at that point. So in here we have all the timing, electronics, processing, and the digital PDP-11 computer which we then use later on to store and process the data which we previously had collected.

This shows the histograms in more detail each one was collected for a different flow direction. The only purpose for showing it is to show that it is sufficiently peaky that we believe our velocity readings with it with a great amount of confidence.

I also told you that we were making measurements of the transient pressures inside the rotor. While the rotor is turning we are able to tell what the pressures are instantaneously inside that rotor. And this is the transient data logger that we are using for this purpose. This is a broad overview of some aspects of the development activity which we are carrying on, with some particular emphasis on the model complex, because that is the model I am most closely associated. Now if I have whetted your appetite sufficiently I could show you some of the results that we have collected, or a small sample of them. This shows dramatically the kind of measurements that we are making. This is our rotor, and in the first phase of our study we have closed off one end of the rotor, studying only the process by which high pressure gas enters the rotor cells, expands and leaves. We use a laser to measure the velocities inside the rotating cell. We use these transducers that are built into the

wall to measure the pressures inside this rotating cell. We also use a three hole pitot probe to find out what the velocities are inside the ports leading to and from the rotor. These are the measurements we have made in the stator, this is the stator outlet port where the expanded gases leave for one particular combination of pressure and speed. We have drawn the vectors and to give you an idea, that much is 100m/s, so the air which is leaving the rotor, creates a region of separated flow in the stator. Perhaps we haven't designed the stator perfectly. The vectors show that there is not only an axial component in the velocity, but also a tangential component in the velocity. We found that because we are only studying a part of the process, there were regions in the stator where reversed flow was taking place. This was where the expansion waves had reflected, and come back, and were creating a reverse flow into the rotor, and then again going out into the stator. Here we have plotted the axial velocities, that is the dependent variable, and this is the independent variable which is the position of the probe inside the stator, and this is the region where we found that under certain circumstances back flow into the rotor was taking place. This of course will not take place in the real machine because in the lab machine one side is closed off.

We also measured the temperatures. The temperature profile in the stator is shown here. And once again, the vertical axis is the independent variable, that is the probe position, and this horizontal axis is the temperature, and due to the expansion shortly after the air rushes out into the stator in our cold machine, we have temperatures which have fallen to about -20° , and I think Professor Kentfield has touched on this; among all the other applications, one could use the comprex as a refrigerator, as well, by simply splitting the cold and the hot streams. This is the density profile which we have calculated from the temperature and pressure measurements.

We have also measured the tangential velocities in the stator. There are some unfortunate negative tangential velocities under certain conditions. This is being caused by a separation bubble which we found present in our stator. This is the pressure profile and it looks quite constant and very neat. That is the static pressure after it has been expanded, just slightly below atmospheric due to the back pressures.

Here we have plotted the static enthalpy, and here the entropy, and this I find very interesting. In spite of all the temperature and velocity profiles, it has a very constant entropy profile, which means that we are simply switching energy between temperature and pressure.

This is the situation when we have a higher inlet pressure than in the frames I showed previously, which were for 1.5 bar; this one is for 1.9 bar, and here we come up with a small surprise, which once we think about it, is not so strange, and that is that we have supersonic flow in the stators. This is caused by the fact that the cells are not opened up instantaneously, opened or closed, even though it is all occurring at high speed; nevertheless the cell is open gradually and due to this gradual opening there is a burst of supersonic flow which comes shooting out into the stator until the cell is fully open and then it goes back to subsonic flow. Here I am talking about the actual velocities and not the pressure waves. It is obvious that the pressure waves move at more than sonic speeds, but we also found that under certain conditions we could have localized patches of supersonic flow in the stators. One can see here that the velocities are on the order of about 400m/s, that is

about Mach 1.2 or Mach 1.3.

This is the schematic of our basic two focus technique. We start with two laser beams which have first been split, then reflected twice, and then focused in this measurement plane to 2 focal points. Behind the plane where the measurement is taking place, there are reflections coming off the rotor wall; we have had problems with those but have also discovered how to electronically sort them out. A particle passing through here triggers a signal when it passes through this beam, and when it passes through the next focal point, it sends off another signal. The signals collected go through a screen here which cuts off everything except the signals coming from the two focal points, then enter a photo detector and into the rest of the electronics.

These are the kinds of measurements we have been making. Once again, the vertical axis is the independent variable, and if you like, you can think of this as a cell, these are the cell walls, this broken line shows the edge of the cell wall, that is from here to here is the pitch of the cell and we plot here, on this frame, the axial velocities, and then on this frame the relative tangential velocities. What I mean by the relative tangential velocities is that from the measured absolute tangential velocity, we subtract the tangential velocity at which the rotor itself is running, so that we know the relative tangential velocity inside one particular cell.

Mr. Y

How close to the cell wall are you measuring?

The cell width is about 10mm. So here, about 2mm from the cell wall. It is difficult to get very close to the cell wall because of the reflections which start coming off the cell wall. By the way the electronics is sophisticated enough to chop the measurement, so what we do is, as the cell wall comes by we shut off the laser, and turn it on again as soon as we are into the cell wall. This is done with a Bragg cell, and needless to say it takes place at extremely high speed, but anyway we are continuously chopping it and opening it, and with this kind of technique we have been able to measure a velocity profile. Mind you this is an instantaneous velocity profile. Inside a cell, that picture shows an axial velocity profile, and the bottom picture shows a tangential velocity profile. Now in order for the one-dimensional calculations to be any good, this tangential velocity profile should be 0 and constant, and in this situation it is just at the point where the air is beginning to flow into the cells, and this is the proof.

We are not only in a position to measure the axial and tangential velocities in the cell, but we are also in a position to measure the turbulence level inside the cells. In this particular measurement they are acceptably small, 4% for the stream wise turbulence and 5% for the cross-wise turbulence. Those arrows are the statistical measure of the uncertainty with which we are making these measurements. One of the beauties of this statistical two focus technique is that we know how good our measurements are. We know within what band and with what confidence we have our values. The value which is written down is the value which prevails at the middle of the cell.

This is the situation which prevails when the cell has rotated through 5° , or

the cell is half open now. These measurements have been made at an axial position about one inch downstream of the stator, and here the axial velocity profile looks like this, it's considerably higher than before; previously it was 35m/s, now it is 56m/s, because the flow is picking up speed there. We no longer have 0 tangential velocity. It is true that in the center of the cell it is only 5m/s but at certain points it is only about 20m/s. This shows us that the assumptions about one-dimensional flow do have their limitations.

This is the situation after the rotor has turned 10° from the first position, which means the cell is completely exposed to the flow. We now see fairly significant relative tangential velocities, and the axial velocity has picked up further.

And this is a composite of some of the measurements we have made. You can almost see, if you imagine, the wave has run from here to here, this is our closed end, then it has reflected back here, so the velocities pick up and then the reflecting wave comes back and now they are pointing the other way. And you will observe that there are significant tangential components.

Here we have plotted just the axial velocities, once again this is the inlet which now faces 34° , and that is the outlet. Until now we have not made a lot of measurements because we have spent a lot of time developing the experimental techniques which we have applied and which we believe are unique. Here is a comparison which has been made between the axial velocities which we have measured, and those which our computer programs tell us, and it looks very good, much to my surprise.

And now going on to our transient pressure measurements. We have an instrumented rotor, with five pressure transducers spread along the axial length; this shows the position of 0° on the rotor and is where the flow enters the cells; at 34° it is closed off, at 140° it is opened and at 250° it is closed again. As I said, from here, to here it is 6 milliseconds, so we have transducers with a useable frequency of 100KHz. In order not to confuse the picture too much, I have only plotted 3 of these. The green one is nearest to the stator, about one inch away from the stator. This one which is not colored at all is about 3 inches from the stator, and the orange one is about 5 inches from the stator. Here we can see what happens to the pressure waves, the cells are exposed to the inlet and the pressure shoots up at once, almost as good as those drawings Prof. Kentfield showed you, where one saw a step rise in the pressure. They actually do have a terrific step rise in pressure, and then there is a period where the first transducer just maintains the pressure, because the pressure wave is now traveling from left to right towards the closed end. But then the reflected compression wave comes back, and then we get the next boost in pressure; so in the first stage we boost from 1 to 2 bars and then in the next stage we boost from 2 to 3 bars. Now if you look at the orange line, and that is the transducer that is furthest away from the inlet, it has taken a while for the pressure wave to move from this position to this position. That is why this rise occurs much later. But, here you don't see that step anymore because being closer to the closed end, the reflected wave slams it almost immediately after the primary wave has hit it, and so we see this enormous and continuous increase in pressure. Between here and here, both ends are closed, and the pressure waves are running back and forth inside the cell. You see a general fall off in the pressure level; this is caused by the unfortunate leakage which we try our best to keep as small as

possible, but it is nevertheless there. At this point the cell is open, and the green transducer which is in the position nearest the port, indicates a pressure drop straight away. It is very interesting how steeply and quickly it can fall, and after a suitable interval the pressure of the transducer at the mid position falls off, and lastly the pressure falls off at the position furthest away from the inlet. Then here you can see a flow region where the pressure has fallen considerably below atmospheric, if these measurements are to be believed, to a pressure of $1/2$ a bar; this is the region for which this idealized machine caused the reverse flow in the stators. And then there are all of these further wiggles and the cycle starts again.

Now here I have sketched a situation which could occur when the rotor is running at less than design speed. When the rotor is running at 60% of design speed, then the reflected wave comes back relatively quicker, and this is because the waves are running back and forth at the same speed. No matter what speed the rotor is turning, but because the rotor is turning that much more slowly, the reflected wave has prematurely come back to the inlet end and this could then of course cause loss of pressure and reverse flow into the inlet.

These are the transient signals which we have measured under such a situation at 60% of rated speed. Here one sees the same phenomenon as before, if you just look at the green line here you start at one bar, the primary compression wave boosts the pressure to 2 bars, the reflected pressure wave boosts to 3 bar (tape ends).

Here are some comparisons between the experiment and the computation, and these show where we stand at the moment. Naturally with all the computations, with all the numerical smearing which takes place, we can't hope to catch all the expansion fans, and the secondary features of the flow, so we lose all of this detail, which actually exists in the experiment. But we are very pleased that we got this step and this level in general right.

This one is for another operating condition with slightly lower pressures. Again we are able to compute the broad features of the flow extremely well; we haven't got our leakage model absolutely right yet, at least not up to this point. Meanwhile we have used the empirical information we have collected, in order to improve our leakage model and to make sure we can match it.

This is for another operating condition, and the remarks I made before hold true for this one also; however we are also working on more advanced techniques in computation. We are in the process of programming a full method of characteristics code, which we hope will give us many more details than we would otherwise have. We are also programming a 2-D McCormack type code to give us the details of the flow which occurs through cells which are only partly opened or partly closed. That was just a broad overview of some of the things we do, and a detailed view of some of the things I have done, and to go back to what I said earlier, I have to thank all my colleagues who made it possible.

THE MSNW ENERGY EXCHANGER RESEARCH PROGRAM

William J. Thayer
Spectra Technology, Inc.
Bellevue, Washington 98004

Measurements and numerical modeling of energy, or pressure, exchanger flow and performance were carried out to characterize controlling processes and to maximize the efficiency of a small test device. The laboratory energy exchanger was developed and tested under steady external flow conditions to study sensitivity to a number of flow and configuration parameters. This machine operated at a pressure ratio of approximately 2.5 and transferred approximately 100 kW of power between two impedance-matched streams. Measurements were made of both overall flow and performance parameters and of flow details. These measurements included dynamic measurements of pressure within the rotor throughout numerous rotation cycles, end wall pressure measurements, temperature distributions in the inlet and outlet ports, gas sampling in the exit ports where contact surfaces left the rotor, and overall average mass flow, temperature, and recovery pressures in all inlet and outlet ports. These data were used to evaluate the work transfer efficiency, η , which is related to a compressor and turbine efficiency product, and equivalent turbine and compressor efficiencies. Tests demonstrated a maximum work transfer efficiency of 74 percent, equivalent to compressor and turbine efficiencies of 75 and 97 percent, respectively. These tests also showed the sensitivity of these efficiencies to the controlled parameters.

A one-dimensional, unsteady flow model was developed for the energy exchanger. Equations for mass, momentum, and energy conservation in both the unsteady internal flow region and steady external ports were solved using numerical techniques. Appropriate boundary conditions were applied at the blank end walls and the rotor/port boundaries. Losses due to inflow and outflow effects, leakage, friction, and heat transfer were included in this model. The SHASTA algorithm was used in this numerical analysis. Comparisons of computed parameters with detailed pressure measurements and overall performance have largely verified this model of energy exchanger flow. Together, the computer projections and test data provide a clear understanding of the dominant flow processes and controlling parameters. Projections using the unsteady flow code indicate that transfer efficiencies of 80 to 85 percent can be expected from future energy exchangers.

ENERGY EXCHANGER PERFORMANCE MEASUREMENTS AND PROJECTIONS

William J. Thayer III
Spectra Technology, Inc.
Bellevue, Washington 98004

ABSTRACT

An experimental and analytical investigation of energy, or pressure, exchanger flow processes was conducted to quantify controlling mechanisms and to maximize the efficiency of these devices. Energy exchangers are rotating, axial flow machines that utilize unsteady gasdynamic processes to directly transfer work between two gas streams. These machines simultaneously perform functions analogous to a gas turbine and a compressor. A single-stage test device was developed and used to conduct steady flow tests at compression and expansion pressure ratios of approximately 2.5. The test energy exchanger transferred approximately 100 kW of power and demonstrated overall transfer efficiencies as high as 74 percent. An unsteady one-dimensional flow code was developed and used to calculate test device performance and to project large-scale energy exchanger operating characteristics. The computer model agreed well with measured overall performance and detailed flow data. Projections using this code indicate that efficiencies to 80 percent are feasible for the test energy exchanger and to 85 percent for large-scale devices.

I. INTRODUCTION

The term "energy exchanger" originated with Hertzberg⁽¹⁾ in his early work to apply unsteady, gasdynamic processes to power generation. The energy exchanger is a gasdynamic wave machine similar to the Comprex, invented and patented by Seippel in 1946. The energy exchanger performs the function of a mechanically coupled gas compressor and turbine, transferring work to compress one gas stream while extracting work from another expanding gas stream. However, the transfer of work between these streams is fluid-dynamic, and shaft work is not a required transfer mechanism between the streams. Since

this device transfers the potential for doing work from one gas stream to another, it could equally well be called a "work exchanger" or "pressure exchanger."

Many applications of wave machines have been proposed since their inception. These have included applications to internal combustion engine supercharging, wind tunnel test facilities, chemical processing, high temperature compression, and other transfer processes between gas streams. The development and application of wave machines has been extensively reviewed by Rose.⁽²⁾ Several new applications of the energy exchanger to power generation cycles have been studied by Spectra Technology, Inc. (STI), formerly Mathematical Sciences Northwest, Inc.⁽³⁾ These applications included its use as a high pressure, high temperature top stage for a gas turbine topping-steam bottoming cycle using coal-derived fuels; use as a high temperature air compressor for a coal-burning MHD power plant; and use as a "dirty" gas expander/air compressor for pressurized, fluidized bed (PPB) fired coal-burning power plants. The applications in MHD and combined cycle plants appear to be quite competitive with other advanced approaches to these power generation cycles. The energy exchanger offers distinct advantages in terms of overall plant efficiency, simplicity, and durability relative to gas turbines in PPB cycles using conventional compressors, turbines, and gas clean-up techniques.⁽³⁾ These studies show that operation of the energy exchanger at work transfer efficiencies (related to the product of compressor and turbine adiabatic efficiencies) of 75 percent or higher is required for effective application of this technology in power generation applications.⁽³⁾ As discussed below, results of testing and computer projections indicate that the energy exchanger will operate at efficiencies of 75 to 85 percent when this technology is further developed and implemented in large-scale devices.

The energy exchanger employs unsteady flow processes to transfer power from one gas stream to another. Energy exchangers can be configured with one expansion/compression cycle per revolution on the rotor, as was the test machine described in Section III, or with two or more cycles, as depicted in Figure 1. A number of long narrow gas passages, which behave very much like shock tubes, are mounted on the periphery of a rotating drum. Two gas streams

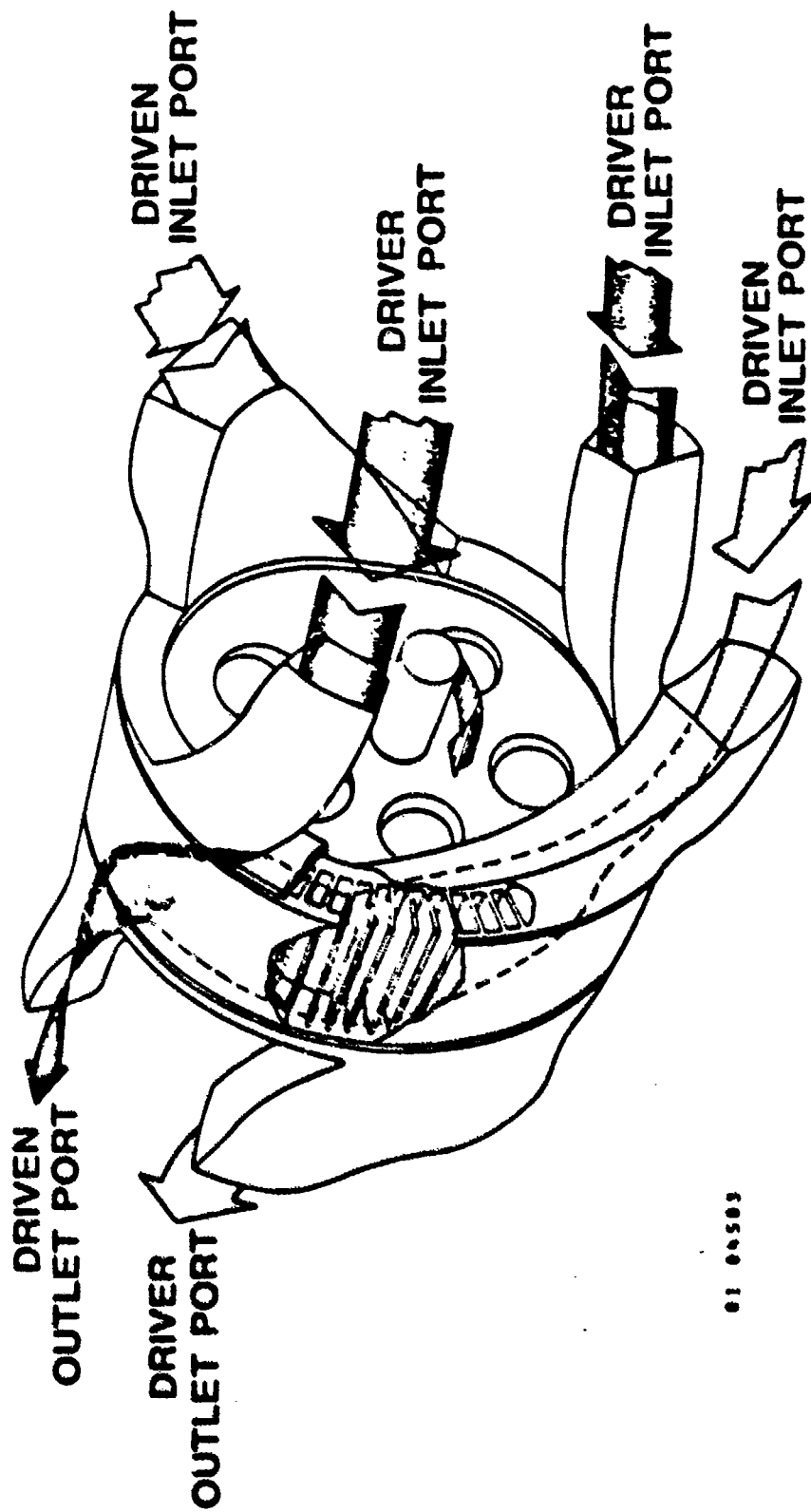


Figure 1. Energy Exchanger Configuration with Two Expansion and Compression Cycles on One Rotor.

flow steadily into the rotor through ports in the stationary endwalls, transfer power by means of the steady port flows and a pressure wave system that is repetitively established in each tube, and then flow steadily into the outlet ports. Motion of the tubes past the stationary inlet and outlet ports and regions of closed endwall is used to establish the unsteady flow processes within the rotating tubes of wave machines. The initially low pressure gas, called the "driven" stream after shock tube nomenclature, enters the rotor through a large port, is compressed by pressure waves within the rotor tubes, and leaves the rotor at high pressure through the smaller driven stream outlet port in Figure 1. A continuous stream of high pressure gas, called the "driver" stream, enters the rotor through a small inlet port, transfers its power to the driven stream through unsteady flow processes on the rotor, and exhausts from the rotor through a low pressure port. In most applications, the high pressure driven gas stream will pass through a combustor, heat exchanger, or other heat source and return to the energy exchanger as the driver stream. The operation of the energy exchanger and other wave machines is discussed in considerable detail in References 3 and 4. Through the use of proper rotor, port, and endwall configurations and operating conditions, work transfer between the driver and driven streams can be made very efficient. Both the experiments and code projections discussed below indicate that energy exchangers can have high efficiencies and other favorable operating characteristics that will make these machines very useful in power generation and propulsion applications.

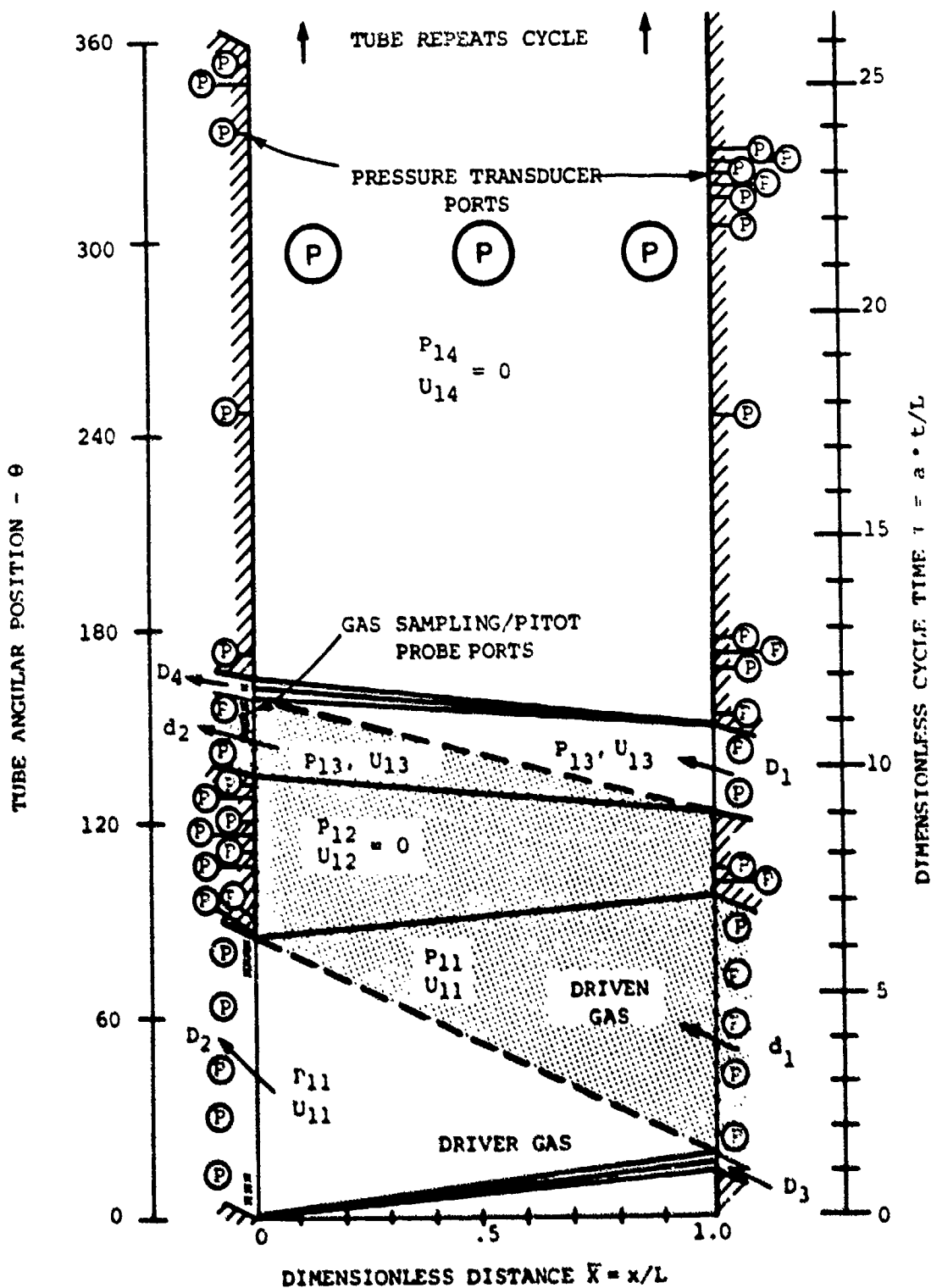
This paper summarizes the test and computational results of the earlier program.⁽³⁾ The test energy exchanger was configured as described in Section III, and tests were conducted for a wide range of conditions. The clearances between the rotor and stationary inlet and outlet ports were minimized to limit leakage. Wave management ports were used to cancel undesired reflections of compression and expansion waves, improve inlet and outlet flow uniformity, and reduce associated losses. In addition, effects of port widths, rotor speed, and flow conditions have been studied to identify configurations and conditions of highest efficiency and to determine sensitivities to flow parameter variations. Instrumentation, including pressure transducers mounted on the rotor, was used to identify flow problems and mechanisms which govern the energy exchanger work transfer efficiency.

The best configuration and operating parameters tested produced a transfer efficiency of 74 percent.

The energy exchanger unsteady flow code, which was described in an earlier paper⁽⁴⁾ and in Reference 3, has been used to calculate internal flow conditions and overall performance for a range of configurations and operating conditions of the test energy exchanger. As discussed in Section IV, computed energy exchanger flows agree very well with overall performance measurements and with detailed measurements of flow property variations during each tube rotation. This agreement has verified that the dominant mechanisms have been adequately modeled and has provided confidence in the accuracy of the code for projecting energy exchanger performance in other operating and machine-size regimes. Computations indicate that energy exchangers with throughput and operating conditions comparable to the test device could operate at transfer efficiencies of 80 percent if relatively minor changes were made in the basic wave system and configuration. As discussed in Section V, additional calculations indicate that large-scale energy exchangers could operate with efficiencies to approximately 65 percent at conditions similar to those tested.

II. ENERGY EXCHANGER UNSTEADY FLOW CODE

The projections of energy exchanger performance discussed below were made using a computer program that was developed to model energy exchanger flows. The overall wave system represented the six-port energy exchanger configuration shown in Figure 2. Note that this figure also contains instrument locations, which will be described in Section III. Energy exchanger performance and flow details could be computed with only the primary flow ports operating, i.e., the high pressure driver gas inlet D_1 , the low pressure driver outlet D_2 , the low pressure driven gas inlet d_1 , and the high pressure driven gas outlet port d_2 . Either of the wave management, or tuning, ports D_3 and D_4 could be operated at prescribed conditions or eliminated from the computation, as desired. The amount of "dead space", i.e., the blank stator walls that were not needed for wave formation and control, could be arbitrarily set. The large dead regions shown in Figure 2 for the test apparatus wave diagram were the largest actually used in computing energy



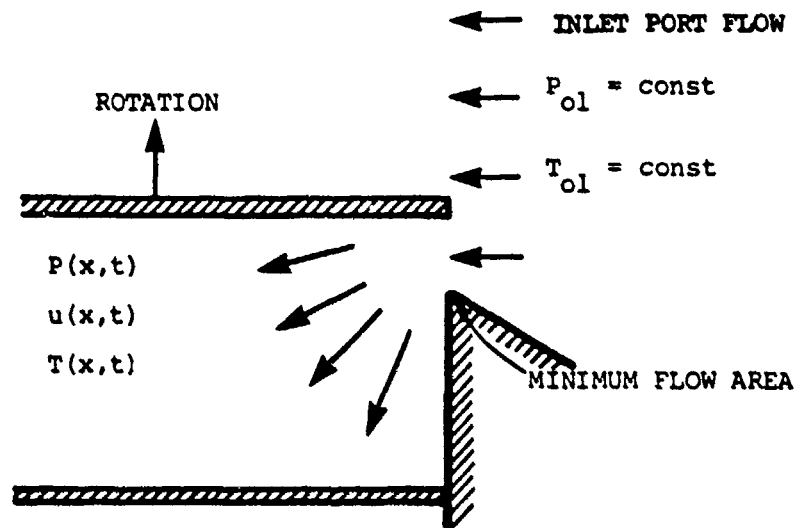
81 04678

Figure 2. Ideal Wave Diagram for Test Energy Exchanger With Instrument Locations.

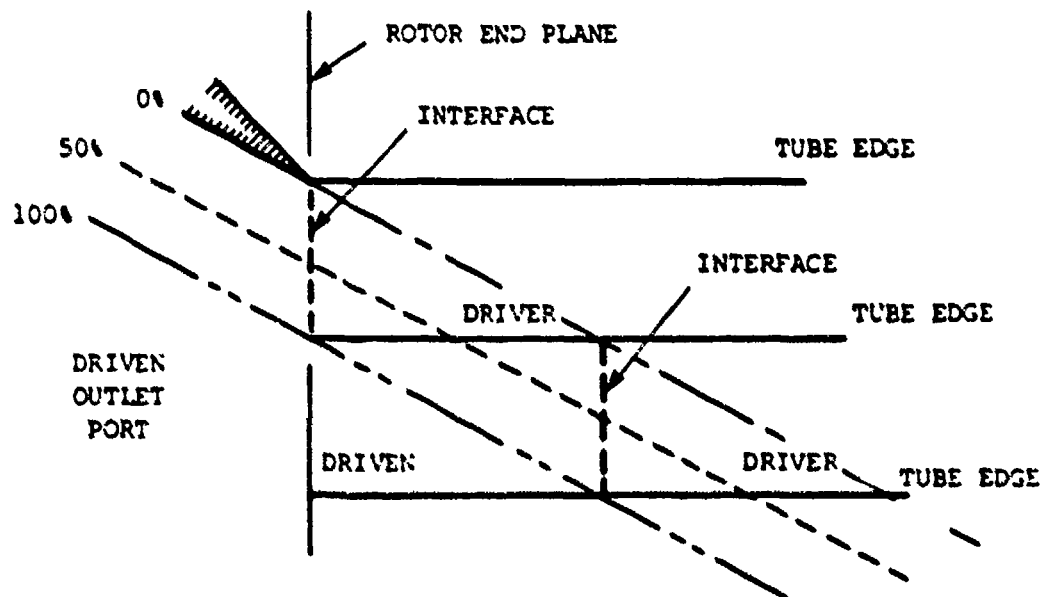
exchanger performance. This large dead region was incorporated into the test apparatus to allow for an additional set of inlet and outlet ports, which were never installed. The dead regions were generally reduced to that actually required for a closed wave system during computations of maximum energy exchanger performance. The energy exchanger flow code is described in detail in References 3 and 4. Its major features are summarized in this section.

The flow within tubes on the energy exchanger rotor was modeled using the standard, one-dimensional unsteady flow equations. Terms were included to calculate wall friction and heat transfer processes using correlations for steady, turbulent pipe flows. The one-dimensional unsteady tube flow equations were solved numerically using the flux correlated transport technique.⁽⁵⁾ This technique is accurate and stable in regions of high property gradients, such as shock waves and interfaces between different gases, and allows calculations to be carried out over many cycles. Thus, operational transients and approach to steady-state operation of the energy exchanger can be accurately calculated. The accuracy of the unsteady flow algorithm was verified by comparisons of code calculations with analytical solutions of the shock tube problem and wave reflections from blank walls and open ended tubes, as discussed on Reference 3.

The internal, unsteady tube flow equations were coupled at the rotor boundaries to steady flow equations governing the external manifolds. The effects of the finite rate of tube opening to the ports, inflow and outflow loss mechanisms, and endwall leakage flows, as indicated in Figure 3(a), were included at the rotor boundaries. This aspect of the flow modeling was probably the most critical in developing an accurate fluid dynamic representation of the dominant unsteady flow processes and the principal losses, many of which are two- or three-dimensional in nature. The finite rate of tube opening and closing generally spread compression and expansion waves over an axial distance of several tube widths, instead of the infinitesimal thickness shown in Figure 2. This also delayed wave arrival at the opposite rotor endplane significantly relative to early method of characteristics calculations based on the start of tube opening. Losses which occurred during tube opening and closing, such as throttling due to pressure



(a) Inlet Tube End During Tube Opening



(b) Ideal Driver/Driven Gas Interfaces Leaving Rotor

Figure 3. Tube and Port Configuration During Tube Opening and Closing Events

imbalances, significantly reduced efficiencies at high pressure ratio operation.

The models which incorporated the boundary conditions for both endplanes were "quasi-steady" in nature in that the steady flow equations were used at each time step to relate some of the flow properties at the boundary point just inside the rotor to specified external flow parameters. The time dependent equations were simultaneously used to relate the remaining unknown flow properties at these boundary points to those in the "region of influence" of the previous time step and the adjacent grid points at the current time step. Separate sets of simultaneous equations were derived for the inlet and for the outlet ends of the rotor for normal flow conditions, i.e., inflow in an inlet port and outflow in an outlet port. Additional equations, corresponding subroutines, and logic for distinguishing types of flow conditions were developed to compute rotor boundary conditions for nonstandard conditions, such as reversed flow from the rotor back into an inlet port and from an outlet port back onto the rotor. These conditions occurred when pressure waves impinged on the ports during off-design operation and when undesired waves were present due to improper port locations, when wave management ports were not used, and when port flow conditions produced excessively strong or weak waves which were not cancelled as planned.

All of the inlet port flows external to the rotor were treated as nonuniform, steady flow regions which originated at a uniform stagnation condition, P_0 and T_0 , an unspecified distance from the rotor. The velocity, static temperature, and static pressure at the rotor boundary were computed at each time step by using, in part, the steady, compressible flow equations for a streamtube originating at the specified uniform, external, total pressure and temperature. Losses due to leakage through the rotor-stator clearance gap, incorrect matching of gas and rotor tangential velocity, and throttling associated with the pressure imbalance across the reduced inflow area during tube opening and closing were incorporated into the steady flow equations at the rotor boundary. Losses due to transient pressure imbalances between adjacent external and internal regions were evaluated using this quasi-steady flow formulation and the assumption of no recovery of excess dynamic head. Only losses due to leakage and excessive tangential gas velocity were applied

when the tubes were fully open to the inlet ports and reversed flow was absent. Stagnation pressure losses in the inlet ports due to velocity differences between adjacent streamtubes were assumed negligible in this initial formulation, although computed results for off-design conditions showed that this was probably not a reasonable assumption at times.

The boundary condition at the rotor exit plane differed considerably from that at the inlet end, but the loss mechanisms were identical. The outlet ports were treated as regions of uniform, specified static pressure, with the other flow variables computed via the unsteady flow internal to the rotor. It was assumed that there was no recovery of velocity head in the outlet diffusers and ducts due to the generally nonuniform flow at the rotor exit plane. Sets of simultaneous equations were solved, at each time step, to match the internal unsteady flow to the quasi-steady external port flow, as at the rotor inlet plane. The boundary condition equations were treated independently as required in each port and blank endwall region and in transition regions between ports and between ports and endwall regions.

Energy exchanger performance computations were carried out by following a single rotor tube through several revolutions of the rotor. Steady state operation, i.e., port inflow and outflow rates and wave strengths repeatable from cycle to cycle, was approached after approximately three revolutions. The total mass and enthalpy flow into and out of each port was determined by integrating the appropriate velocity, density, specific enthalpy product over the port area. The efficiency with which the energy exchanger extracts work from the driver stream and transfers it to the driven stream is represented by the work transfer efficiency η_{EE} . This efficiency was defined as the ratio of the increase in expansion work ideally extractable from the driven stream as it is processed by the energy exchanger to the expansion work ideally extractable from the incoming driver stream. For the test energy exchanger, this can be expressed as

$$\eta_{EE} = \frac{\dot{W}_{id2} - \dot{W}_{id1}}{\dot{W}_{id1} + \dot{W}_{id3}} \quad (1)$$

where $\dot{W}_{i(n)}$ is the work rate that could be generated by expansion through an

ideal turbine from the state of interest to a reference pressure (ambient pressure for all tests and computations). The subscripts d1, d2, D1, and D2 refer to the driven inlet and outlet streams and the driver inlet and outlet streams, respectively. The subscripts D3 and D4 refer to the inlet and outlet streams for the wave management ports, respectively. For ideal gases with constant specific heats, the ideal expansion work terms can be written as

$$\dot{W}_{in} = \dot{m}_n c_{pn} T_n \left[1 - \left[\frac{P_a}{P_{on}} \right]^{\gamma_n - 1/\gamma_n} \right] \quad [2]$$

where \dot{m}_n , c_{pn} , T_n , γ_n , and P_{on} are, respectively, the mass flow rate, specific heat, temperature, specific heat ratio, and stagnation pressure of the stream of interest, and P_a is the reference pressure. The work and efficiency terms were evaluated in the code by suitably integrating computed flow properties across the inlet and outlet ports. Leakage to atmosphere through the clearance regions between the rotor and endwalls was treated using the steady flow equations governing compressible gas flow with friction at each time step. Total leakage was determined by integrating the leakage throughout a complete revolution. The complete unsteady flow code was verified to the extent possible by comparisons with measurements made during the test program described below. This energy exchanger flow code is believed to model the dominant flow processes with sufficient accuracy that projections of performance and evaluations of configuration and operating parameter dependence can be dependably made. This will be apparent in comparisons with test results, as discussed in Section IV.

III. ENERGY EXCHANGER TEST APPARATUS

Tests were conducted using an energy exchanger and test facility which were developed to demonstrate high efficiency, to provide data for code verification, and to provide a better understanding of energy exchanger flow. The test energy exchanger, flow facility, and measurement techniques are shown schematically in Figure 4 and described briefly below. More detailed descriptions are available in References 3 and 4.

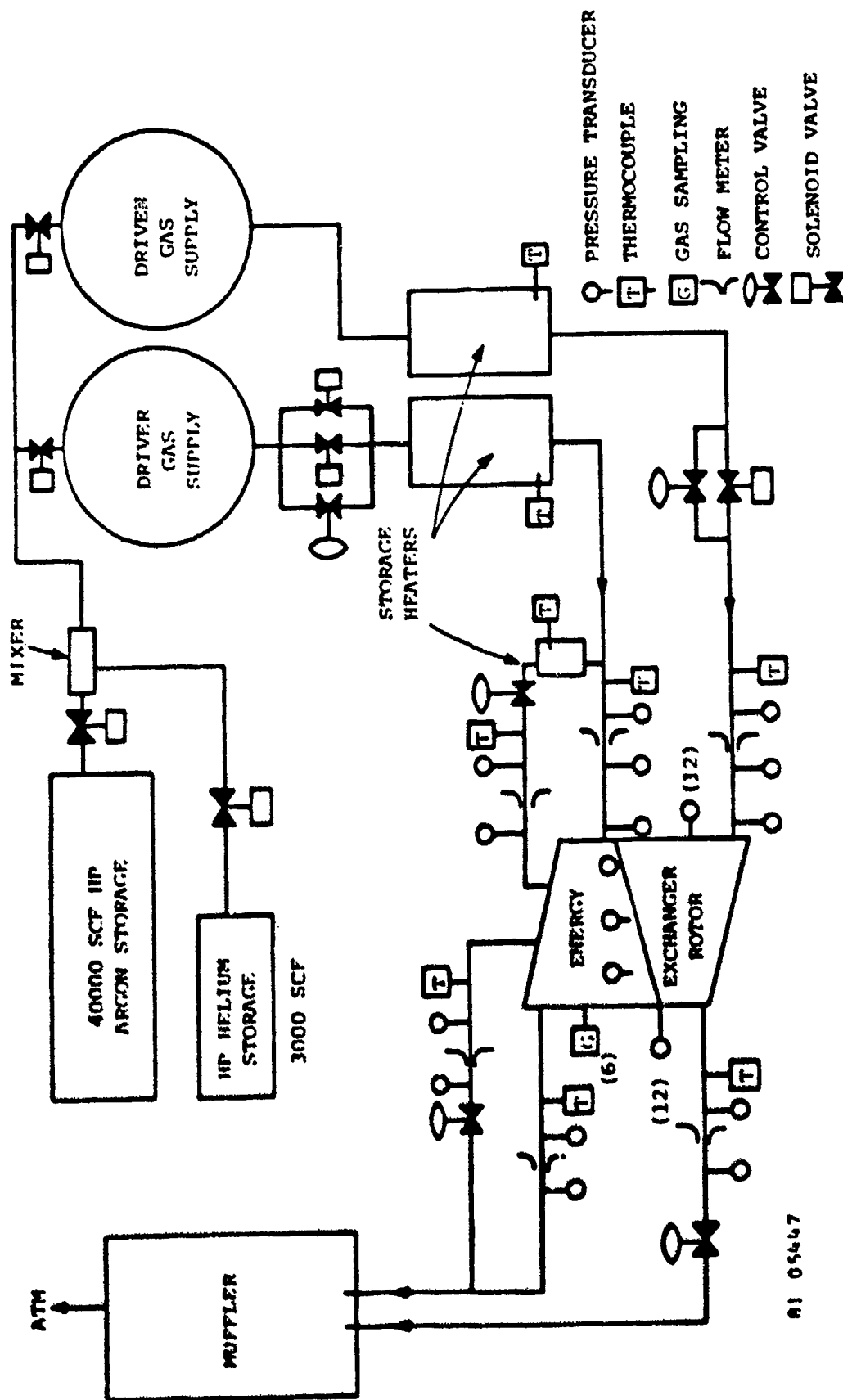


Figure 4. Energy Exchanger Blowdown Test Facility

The test energy exchanger shown in Figure 5 transferred approximately 100 kW between the driver stream and the driven stream. These two streams had matched acoustic impedances, analogous to contact surface tailoring in shock tubes, to simplify the wave system by which power was transferred. The expanding driver stream entered the rotor at a pressure of 25.3 kPa (36.9 psia) and temperature of 525 K and left the rotor at approximately ambient pressure. The work done by this stream was largely used to compress the driven stream from approximately ambient conditions through a pressure ratio of approximately 2.5. Mass flow rates of the driver and driven streams were in the range of 0.8-1.1 kg/sec. In addition, two small port flows were used during some tests to cancel pressure waves at critical rotor locations and, thus, to provide more uniform port flows and higher transfer efficiency. These wave management, or tuning, ports were located near the driven gas inlet and outlet ports, as shown in Figure 2, and required approximately 25 and 80 gm/sec of flow, respectively, to cancel the principal expansion waves. It should be noted that the port widths and locations were designed on the basis of an ideal method-of-characteristics analysis that was done before the unsteady flow code described in Section II was operational. The locations of the inflow and outflow ports, rotor size, tube size, and other configuration parameters are given in Table 1. The clearance between the rotor and the stationary flow ports was initially 0.033 cm (0.013 inch) but was reduced to 0.010-0.013 cm (0.004-0.005 inch) for most of the tests reported here. The design rotor speed was 1960 rpm, and tests were conducted for a speed range to 10 percent above and below this value.

All tests were carried out at steady-state operating conditions. The test facility that was developed for this program operated for six seconds during each test. Gases and thermal energy for each test were stored in pressure vessels and storage heaters, respectively. Steady flow conditions were established during the first second of each test by using an appropriately designed valving and flow system. These conditions were maintained during the remainder of each test by the programmed opening of control valves. Prior to each test, the rotor and all inlet and outlet ports and piping were heated to constant temperatures corresponding to steady-state conditions. This eliminated the thermal starting transient and ensured that test conditions did not change during each test. This facility made possible

Table 1

PRIMARY TEST DEVICE DIMENSIONS

Rotor length	40 cm
Rotor diameter	45 cm
Gas passage outer diameter	40.75 cm
Gas passage inner diameter	32.75 cm
Number of tubes	100
Blade width	0.15 cm
Rotor/endwall clearance	0.033 cm, 0.012 cm
Driver outlet port location	0°-83°
Driven inlet port location	17°-97°
Driver inlet port location	121.9°-148°
Driven outlet port location	134°-157.2°
Inlet wave management port location	12.3°-17.0°
Outlet wave management port location	157.2°-163°

HIGH PRESSURE
INLET MANIFOLD
(DRIVER IN)

LOW PRESSURE
INLET MANIFOLD
(DRIVEN IN)

INLET
TUNING
PORT

PRESSURE
TRANSDUCER
PORTS

ROTOR

HIGH PRESSURE
OUTLET MANIFOLD
(DRIVEN OUT)

OUTLET
TUNING
PORT

ROTOR GAS
PASSAGES

END WALL
DEAD SPACE

relatively low cost, repeatable testing of the energy exchanger at steady-state conditions.

Flow meters, thermocouple probes, and pressure transducers were used to monitor inlet and outlet mass flow rates, pressures, and temperatures at low velocity regions upstream of the inlet manifolds and downstream of the outlet diffusers, as shown in Figure 4. The energy exchanger work transfer efficiency η_{EE} , equivalent compressor efficiency η_{CE} , and turbine efficiency η_{TE} were evaluated from these data using equations given in References 3 and 4. The work transfer efficiency was defined as the increase in ideal expansion work of the driven stream divided by the total ideal expansion work of the driver stream and other input streams used to accomplish the work transfer. Leakage was calculated as the difference between the measured total inlet and outlet mass flow rates. Twenty-four pressure transducers, indicated by P in Figure 2, located on the inlet and outlet endwalls were used to measure steady pressures at various fixed angular locations of the tube rotation. In addition, three pressure transducers were installed in one rotor tube at locations near the inlet, at the centerplane, and near the outlet. They were used to measure the time varying pressure throughout the tube rotation. Signals from these high frequency response Kulite transducers were transferred from the rotor to stationary external amplifiers and data recording equipment through a low-noise slip ring assembly. Gas samples were taken at locations marked by X in Figure 2 from the outlet port regions where the interfaces between driver and driven gases left the rotor and were analyzed using a gas chromatograph. These data were used to monitor interface locations and to determine the degree of mixing between streams.

The entire test control, data acquisition, and data reduction sequence was carried out using a PDP-11 minicomputer system. The steady-state flow data were measured, digitized, and stored in computer memory every 1/30 second throughout each test. The high frequency data from the pressure transducers mounted on the rotor and a timing/position signal were measured, digitized, and stored at 25 μ sec intervals for 0.2 second periods during each test. Four channels of a transient digitizer were used to acquire and store this data for transfer to and reduction by the minicomputer after each test. All data from each test were permanently stored on floppy disks after each test.

Computations to determine efficiency, mass flow rates and leakage, pressure distributions, and histories were carried out shortly after each test.

IV. TEST RESULTS AND COMPARISONS WITH CODE CALCULATIONS

Testing of the energy exchanger was conducted for several configurations and over a range of operating conditions. Configuration changes included variation of the clearance between rotor and endwalls, incorporation of wave management ports near the driven gas inlet and outlet ports, and increasing the area of the main driven stream outlet port. Operating parameters that were varied during the test program included driver and driven gas inlet pressures, driven gas outlet pressure, rotor speed, and flow rates through the wave management ports. The energy exchanger flow code was used to compute detailed flow parameters and the overall performance of a number of test conditions. The data are discussed and compared with computations in this section.

Overall Performance Data and Computations

The major configuration changes had significant effects on the work transfer efficiency and flow through the energy exchanger. Decreasing the clearance between the rotor and stationary port faces reduced the leakage from approximately 12 percent of the total input flow rate to 3-4 percent as predicted by the leakage model, and provided a substantial efficiency improvement. This may be seen by comparing the lower two curves of Figure 6, where the dependence of the energy exchanger work transfer efficiency η_{EE} on the driven stream outlet pressure P_{D2} is shown. The low leakage tests, for which data is shown in Figure 6, were conducted at a driver inlet total pressure of 2.71 atm, a driven stream inlet stagnation pressure of 1.08 atm, and a driver outlet pressure of 1.00 atm. The rotor speed of 1790 rpm gave a higher efficiency than the design speed of 1960 rpm. Both inlet and outlet wave management ports were closed for these tests. The maximum efficiency was approximately 70 percent for driven outlet pressures in the range of 2.2 to 2.4 atm for the low clearance configuration, approximately 11 efficiency points higher than the high leakage case. The mass flow rate into the driven outlet manifold decreased continuously as its back pressure was raised for

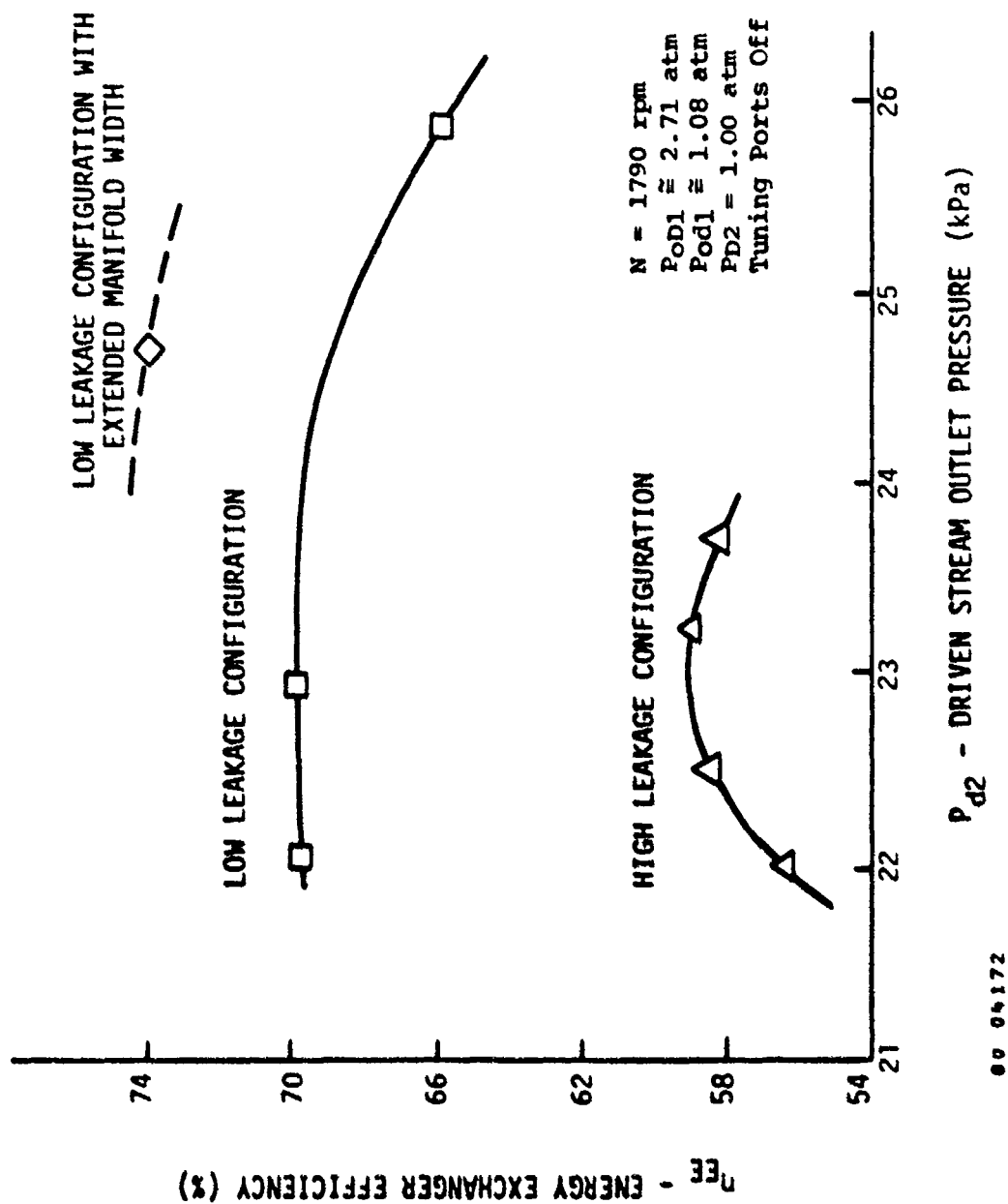


Figure 6. Comparison of Energy Exchanger Efficiency Variation with Backpressure for Low and High Leakage Configurations

both configurations, and caused a decrease in efficiency as the pressure ratio was increased. It should be pointed out that the test energy exchanger had no mechanical or thermal problems operating at the low rotor-manifold clearance, once the device had been properly aligned. No contact occurred during the rapid pressurization and flow transients of the tests, although some motion of the manifolds could be detected.

A port configuration change was suggested by exercising the unsteady flow code on the test energy exchanger and closely related geometries. Since decreased driven stream outflow rates were observed experimentally at high back pressures (see Figure 6), the possibility of increasing this flow rate by extending the high pressure outflow port was evaluated. An 11 percent increase in mass flow rate and efficiency was predicted to result from a 15 percent increase in this manifold width. Unfortunately, resources were not available to disassemble the test device, to fabricate a new high pressure outflow manifold, diffuser, and ducting, and to reassemble and realign the test device. To examine the effectiveness of increased manifold width, the outlet wave management port, D_4 in Figure 2, ducted into the main high pressure port, D_2 , to provide matched recovery flow conditions in the low velocity duct downstream of the device. This increased the outflow area by approximately 22 percent, substantially more than that predicted as optimal by the code. For this condition, an 8 percent improvement in efficiency was predicted. The measured high pressure outflow rate increased by approximately 10 percent and provided an efficiency rise to $\eta_{EE} = 74$ percent, as shown in the uppermost curve in Figure 6. Tests were conducted at only one condition for this configuration due to the difficulty in matching flows and to the lateness in the test program of this test series. However, higher efficiencies could be expected if tests were conducted to optimize performance with respect to back pressure and speed.

A comparison of measured and computed energy exchanger efficiency is made in Figure 7 for the range of pressure ratios of the driven and driver streams used in the low leakage tests of Figure 6. Here PR_C is the compression pressure ratio, i.e., the ratio of the driven outlet stagnation pressure P_{od2} to the driven inlet stagnation pressure P_{od1} . PR_T is the expansion pressure ratio, i.e., the ratio of the driver inlet stagnation

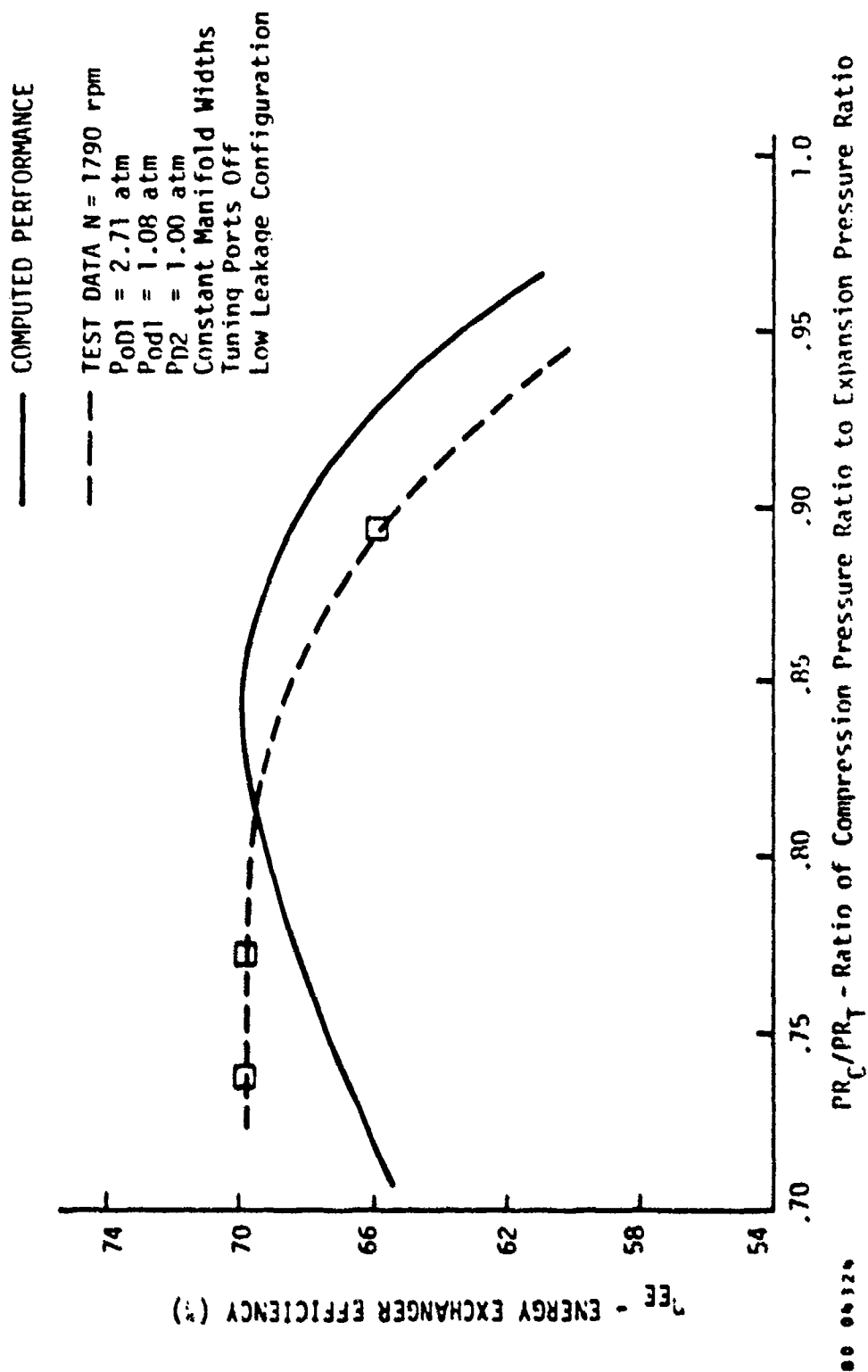


Figure 7. Comparison of Computed and Measured Energy Exchanger Efficiency

pressure P_{OD1} to the driver outlet static pressure P_{D2} , which was nearly ambient. Variation in this ratio of compression-to-expansion pressure ratios was accomplished experimentally by varying the back pressure of the driven outlet stream, P_{OD2} , while maintaining all other parameters at approximately constant conditions. The experiments showed that efficiency was relatively constant at pressure ratios less than approximately 0.8. At higher pressure ratios, the efficiency dropped quite rapidly due to a decrease in mass flow rate into the constant width, high pressure outlet manifold. The relative magnitude of the computed work transfer efficiency is in quite good agreement with the experimental data, although the code predicted a drop in efficiency at lower pressure ratios that was not observed in experiments. The difference between predicted and measured efficiencies is believed to be due to variable pressure and reversed flow conditions that occurred in portions of the ports under certain operating conditions. These nonuniform flow conditions became greater at the lower pressure ratios. Fortunately, the actual device performance seemed to be less sensitive to these nonuniformities than was predicted. Since constant stagnation or static pressures were assumed to exist across the inlet and outlet ports, respectively, in the computer model, discrepancies between experiments and the code are not surprising at conditions which produced nonuniform external flows and pressure distributions. Upgrading of the code to include a two-dimensional manifold/port flow model would be very desirable to better model actual flow conditions. However, the general agreement between the predicted and measured efficiencies gives enough credibility to the code that predictions can reasonably be made to determine the effects of device configuration and operating parameter changes.

Detailed Flow Measurements and Computations

Very good agreement also was seen between measured and computed pressures within the rotor tubes as they rotated through repetitive cycles. These comparisons are made for tests at conditions both without (Figure 8) and with (Figure 9) flow through the wave management ports. Pressures were measured on the rotor using high frequency response pressure transducers located in one tube at positions 3 cm from the inlet manifolds, at the rotor center plane, and 3.5 cm from the outlet endplane of the rotor. Pressures on

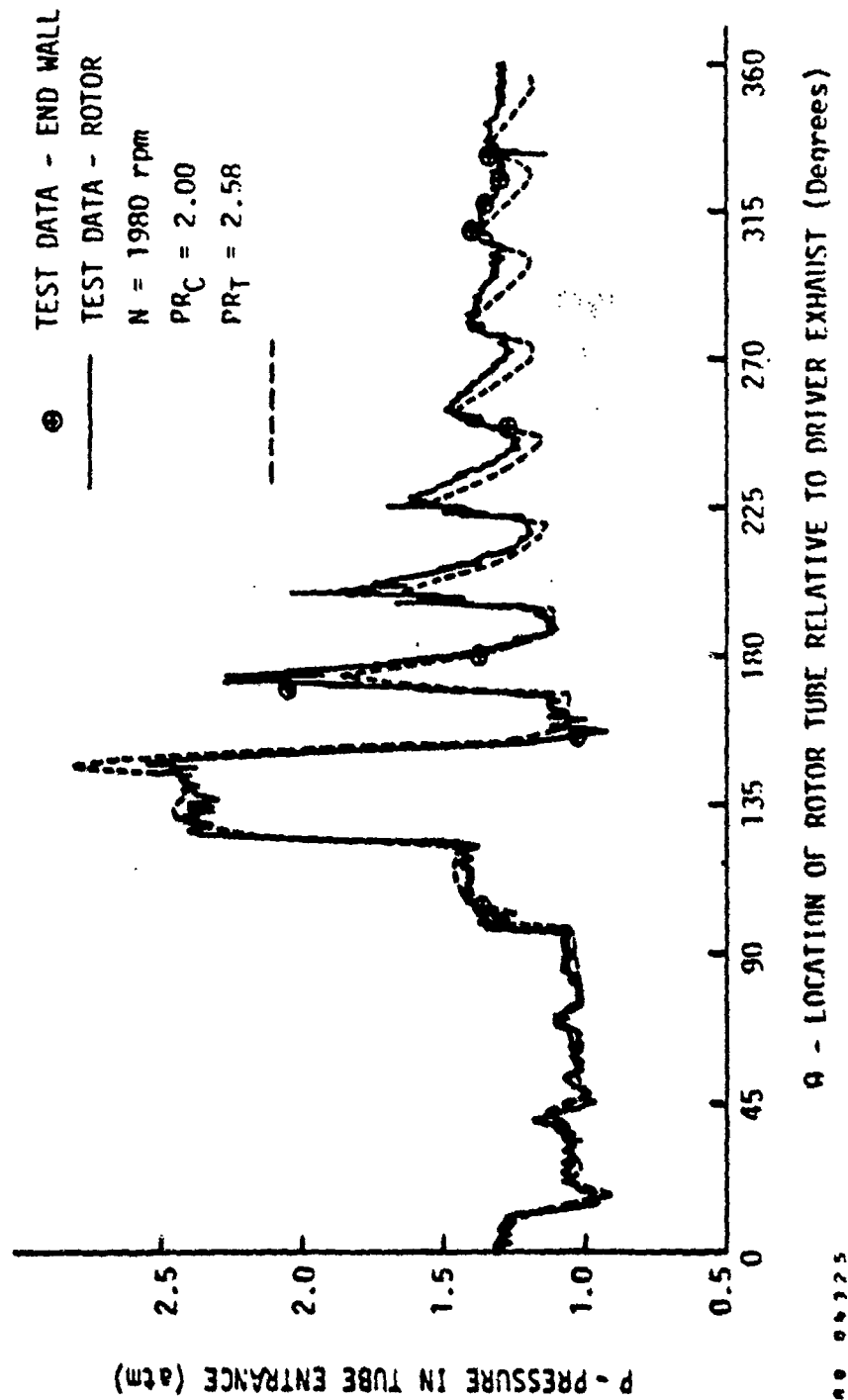
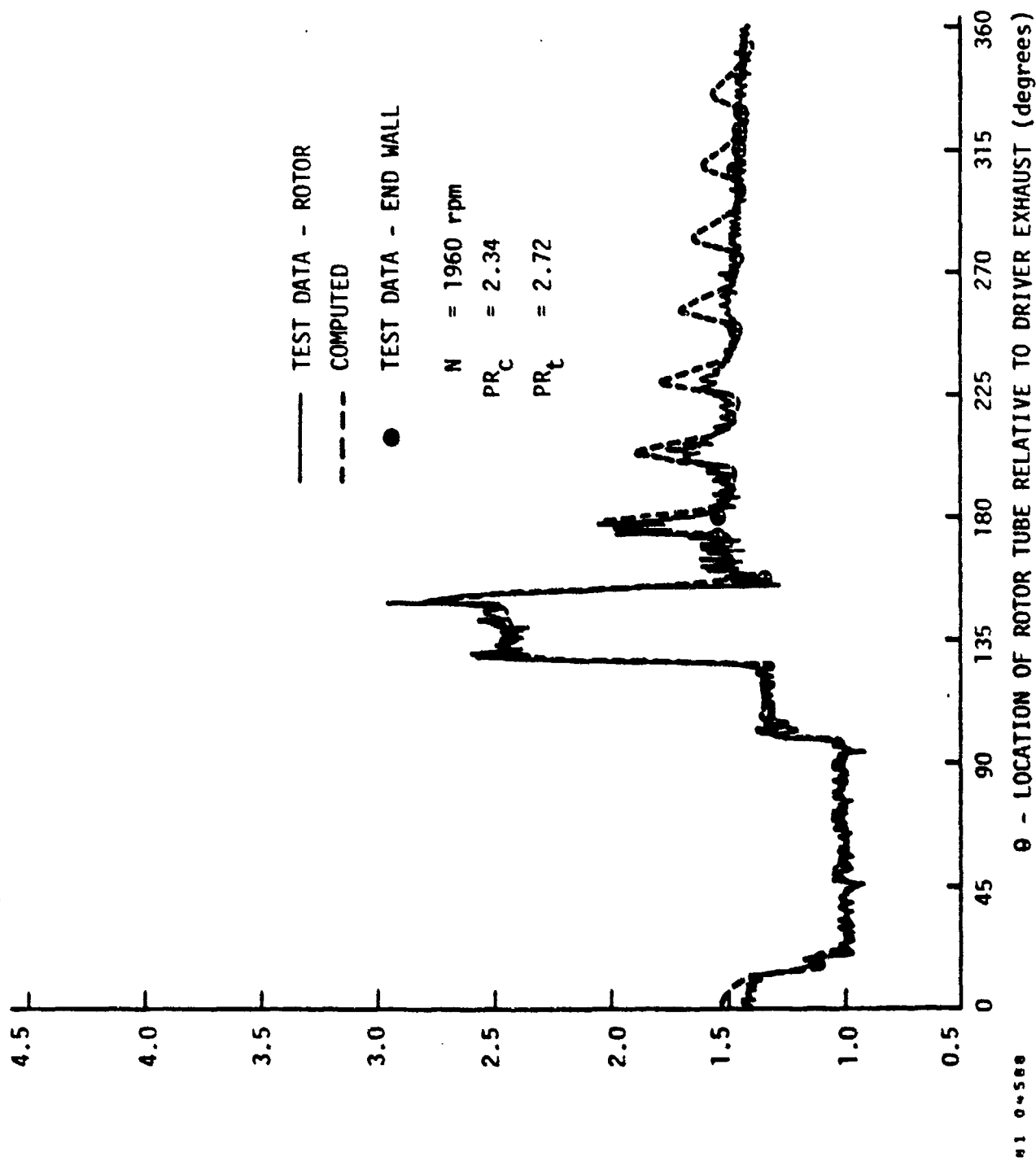


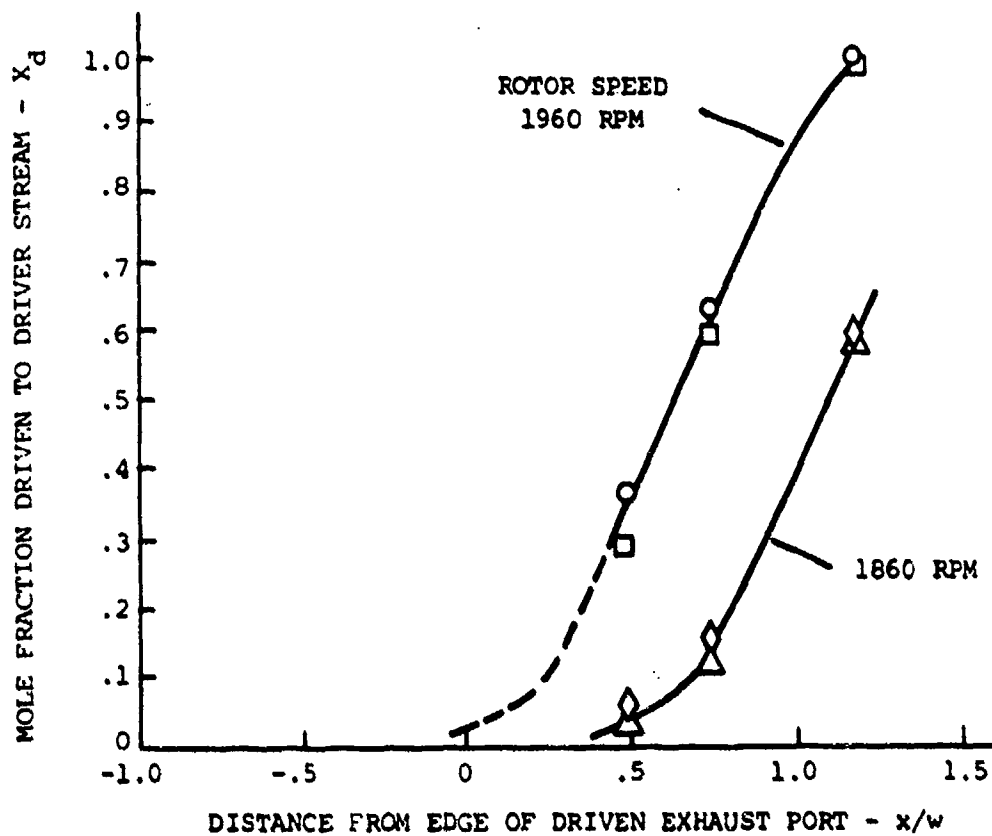
Figure 8. Comparison of Measured and Computed Pressure History Without Wave Management



the rotor at the inlet end of the rotor are shown as a function of tube angular position, θ , through one rotation (solid curve). The zero angle location was designated to be at the start of the low pressure, driver gas exhaust port. Pressures measured at fixed locations on the inlet manifold plane also are shown as discrete data points on these figures. Pressures measured continuously on the rotor and at the adjacent endplane are in very good agreement, although some high frequency noise is evident for the on-rotor data. The computed pressures at the pressure transducer location are shown as dashed curves in these figures. Agreement between computed and measured pressure histories is quite good in the active portion of the cycle (i.e., $\theta < 160^\circ$). Comparison of Figures 8 and 9 demonstrates the effectiveness of the wave management ports in canceling pressure disturbances.

The pressure data from endwall and on-rotor transducers and the computed flow properties led to a greatly increased understanding of the operation of real energy exchangers and the dominant wave mechanisms. Principal waves and loss mechanisms have been identified and are discussed in detail in Reference 3. Computed pressure, velocity, and overall performance characteristics of the test energy exchanger, such as those cases described above, agreed well with test data and led to a detailed understanding of energy exchanger operation and sensitivity to many operating parameters. In the later portion of the test program when the code was operational and its accuracy established, similar predictions guided changes in device operation to optimize performance. Additional calculations were used to predict performance improvements that would be expected to derive from changes in the test device configuration and scale, as discussed in the following section.

Gas samples taken from probes located in the outlet ports immediately adjacent to the downstream face of the rotor, as shown in Figure 2, provided a description of the location and thickness of the contact surfaces between the driver and driven gases. Typical data are shown in Figure 10, where the mole fraction of driven gas in driver gas has been plotted as a function of location in the outlet port. The location has been nondimensionalized by dividing by a rotor tube width, w . These data indicate that the mixing layer between gases was approximately one tube width, as indicated in Figure 3(b).



81 04633

Figure 10. Composition of Gas Stream Near Location Where Interface Leaves Rotor.

Test conditions were usually specified so that the high pressure contact surface did not leave the rotor at locations within the driven gas outlet port, d_2 . This procedure was followed to eliminate the erroneously high transfer efficiencies that would result from injecting significant quantities of hot driver gas into the driven gas stream. The locations of the contact surface in the high pressure outlet region varied as the inlet and outlet pressures and the rotor speed varied. In general, their locations were reasonably predicted by the unsteady flow code, as verified by gas sampling measurements. All performance test data reported above (Figures 6-9) came from tests in which the high pressure contact surface was not located in the high pressure outlet port, d_2 .

V. PERFORMANCE PROJECTIONS

The energy exchanger flow code was used to predict performance changes which would be associated with configuration changes to the test device and for scale changes to potential power system components. Projections indicate that a 100 kW energy exchanger of the scale of the test device could operate with a work transfer efficiency of greater than 80 percent. Large-scale devices operating at similar flow conditions could transfer power between gas streams with an efficiency approaching 85 percent.

A major improvement in efficiency of the test energy exchanger was projected if the driven gas outlet manifold were increased somewhat in width. This can be seen in Figure 11. Here the projected efficiency is plotted as a function of the area ratio, A_{d2}/A_{D1} , where A_{d2} is the driven gas outlet area and A_{D1} is the driver gas inlet area. Since the rotor tubes, inlet, and outlet ports have constant and equal height, this area ratio is identical to the angular width ratio of the ports. In these computations, the variation in outlet port area was accomplished by extending or contracting the angular extent of the port symmetrically about the port centerline. These calculations were done for a driven-to-driver pressure ratio, PR_C/PR_T , of 0.95 and a rotor speed identical to that of Figure 7. Note that at this pressure ratio, the projected and measured efficiencies were substantially below the maximum seen in Figure 7 for the test device area ratio of 0.89 and a pressure ratio of 0.84. The inlet wave management port was used in the calculations of

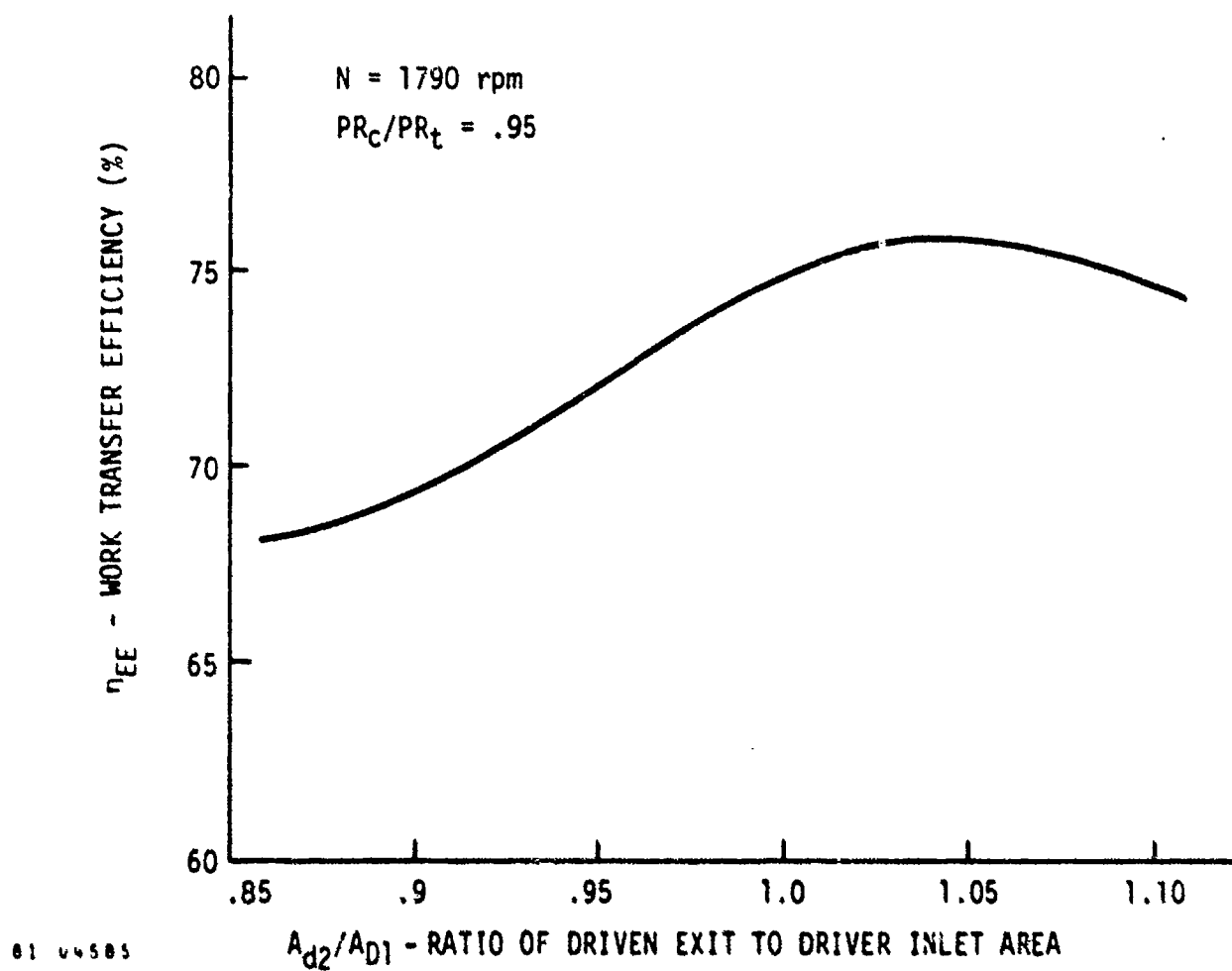


Figure 11. Predicted Variation of Transfer Efficiency With Driven Stream Port Width.

Figure 11, resulting in an improvement in efficiency of 4 percentage points with respect to the equivalent pressure ratio and test device area ratio in Figure 7. For reference, an area ratio of 0.935 would be specified for an ideal wave system. The transfer efficiency was projected to increase by approximately 6 percentage points to 76 percent if the high pressure outlet port area were increased from the test ratio of 0.99 to approximately 1.05, where performance is projected to optimize at this operating condition.

Several other configuration changes were projected to further increase the efficiency. Reducing the regions of blank endwall from that used in the test device to the minimum required for operation would reduce leakage to less than 1 percent of the total flow and improve the efficiency by 3 to 4 efficiency points. Changing the low pressure port widths and locations slightly to optimize real energy exchanger operation would improve efficiency by almost one efficiency point. Moving the high pressure ports relative to one another is projected to have a similar effect. The energy exchanger code indicates that the combined effect of all of these changes would provide a transfer efficiency of 80 percent for an optimized, 100 kW size energy exchanger.

Additional calculations have been made to evaluate the potential efficiency of large energy exchangers. The devices considered were similar to the optimized small energy exchanger and operated at similar conditions, but were scaled up to handle 100 to 1000 times more flow. Projections indicate that work transfer efficiencies as high as 85 percent may be feasible for such large-scale devices.

ACKNOWLEDGMENTS

The work described in this paper was sponsored by the U.S. Department of Energy Basic Energy Sciences Division under Contract DE-AC06-78-ER01084.

REFERENCES

1. R.C. Weatherston and A. Hertzberg, "The Energy Exchanger: A New Concept for High Efficiency Gas Turbine Cycles," ASME Journal of Engineering for Power, 1966.
2. P.H. Rose, "Potential Applications of Wave Machinery to Energy and Chemical Processes," Shock Tubes and Shock Waves, Proceedings of the 12th International Symposium on Shock Tubes and Waves, A. Lifshitz and J. Rom, Editors (Magnes Press, 1980).
3. W.J. Thayer et al., Energy Exchanger Performance and Power Cycle Evaluation: Experiments and Analysis, Final Report DOE/ER/01084-1, April 1981.
4. W.J. Thayer et al., "Measurements and Modeling of Energy Exchanger Flow," Energy To The 21st Century, Proceedings of the 15th Intersociety Energy Conversion Engineering Conference, Seattle, Washington, August 1980, p. 2368.
5. J.P. Boris and D.L. Book, "Solution of Continuity Equations by the Method of Flux Corrected Transport," Chapter 11, Volume 16, Methods of Computational Physics (Academic Press, New York, 1976).

ROLLS-ROYCE STUDY OF WAVE ROTORS,

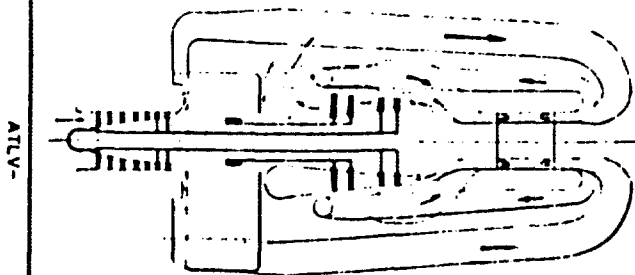
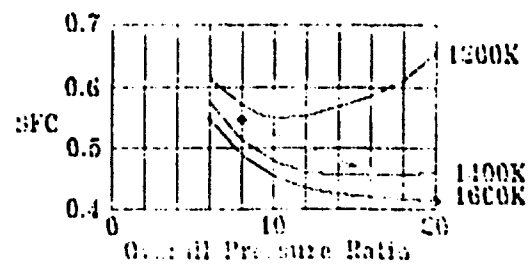
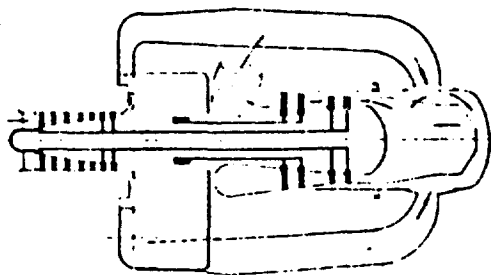
1965 - 1970

Robert Moritz

- Helicopter engine chosen for first demonstrations :
 - Low R -> large SFC gain
 - Existing blading efficiency low
 - Wave rotor durability gain
 - Relatively easy engine changes
- Preliminary rig testing at lower temperature and pressure.
- Design carried out in consultation with Prof. Berchtold.

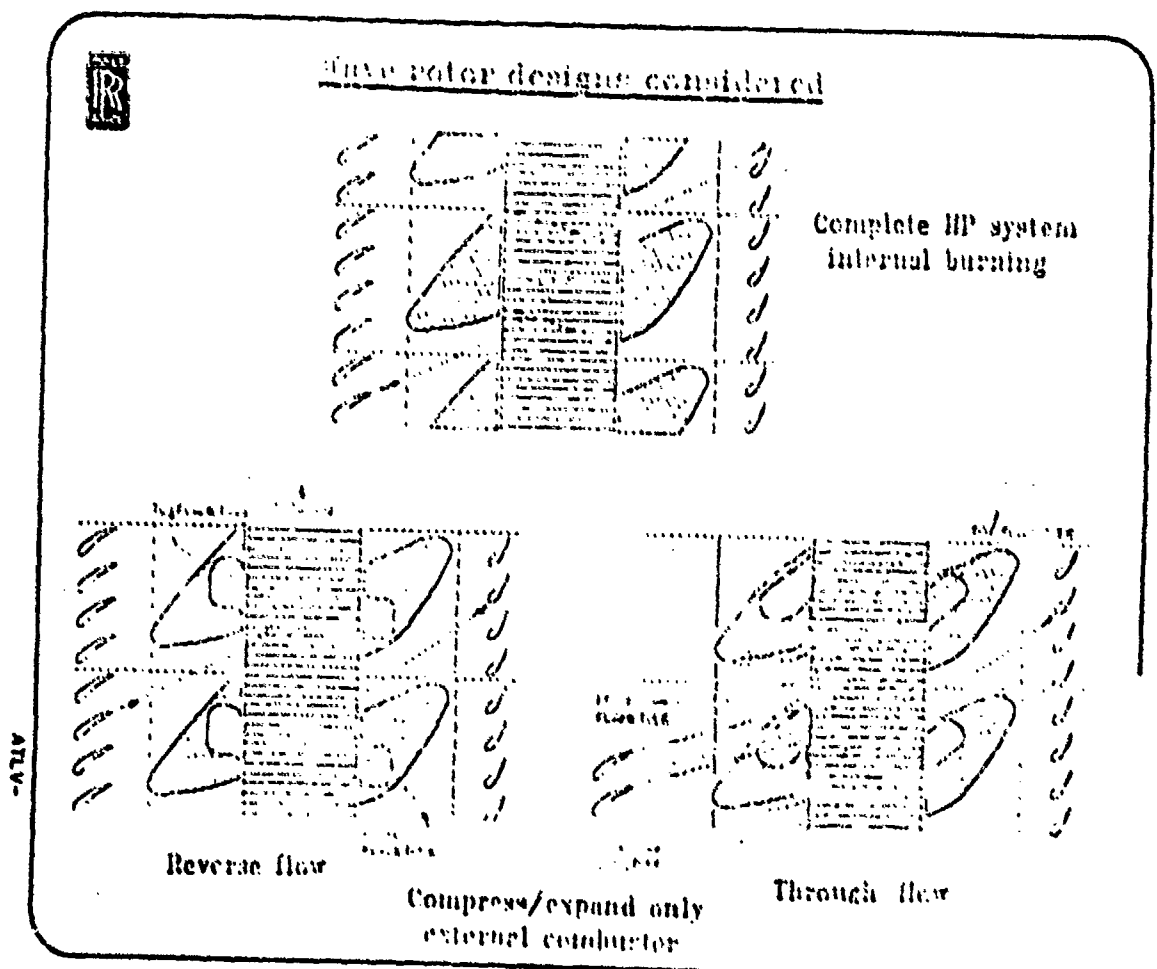


Addition of wave rotor to a helicopter engine.



Reproduction
best available copy.

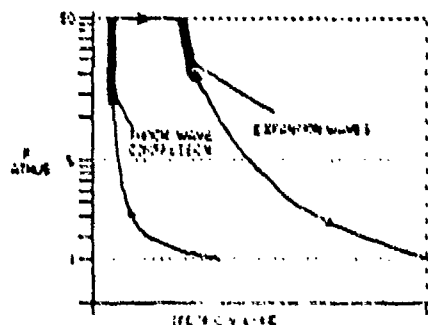
- In-rotor burning not pursued as low efficiency and instability are likely.
- Thru-flow keeps rotor and port temps low but associated heat transfer spoils compression effy.
- Reverse flow chosen for efficiency with accepted mechanical burden.



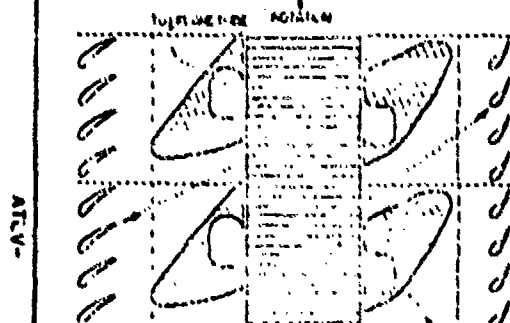
- Function is to replace compressor and turbine of HP spool.
- Successful design must therefore have a winning combination of simplicity and efficiency relative to existing 'steady' flow machines.



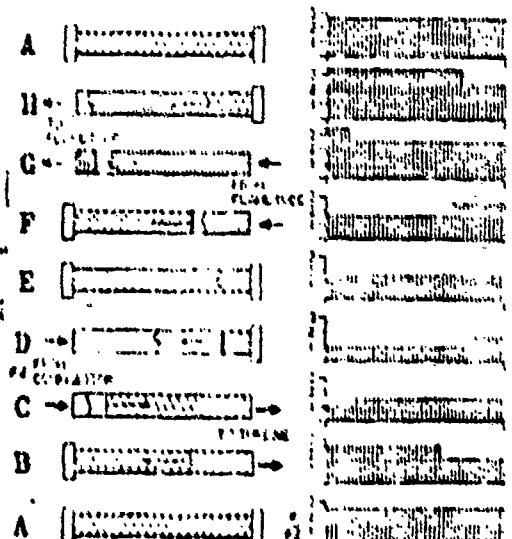
Wave rotor plus separate combustor replacing conventional HP system.



Role of wave rotor in engine cycle



Wave rotor layout



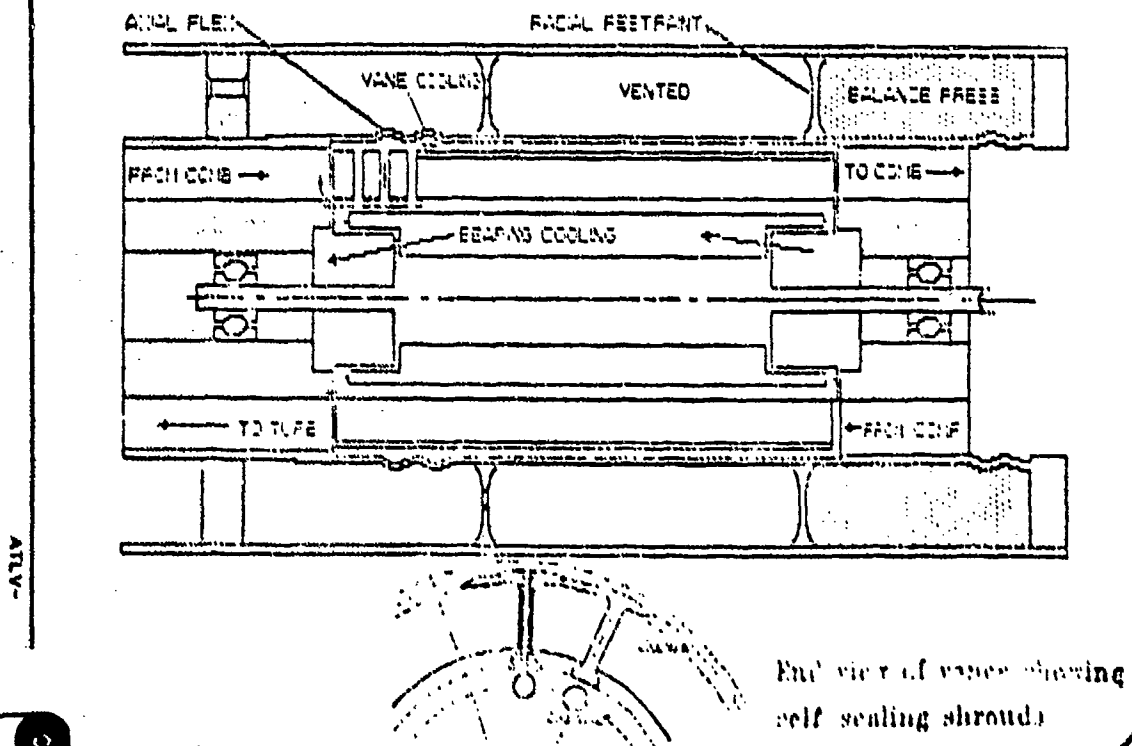
Sequence of events in wave rotor

best available copy.

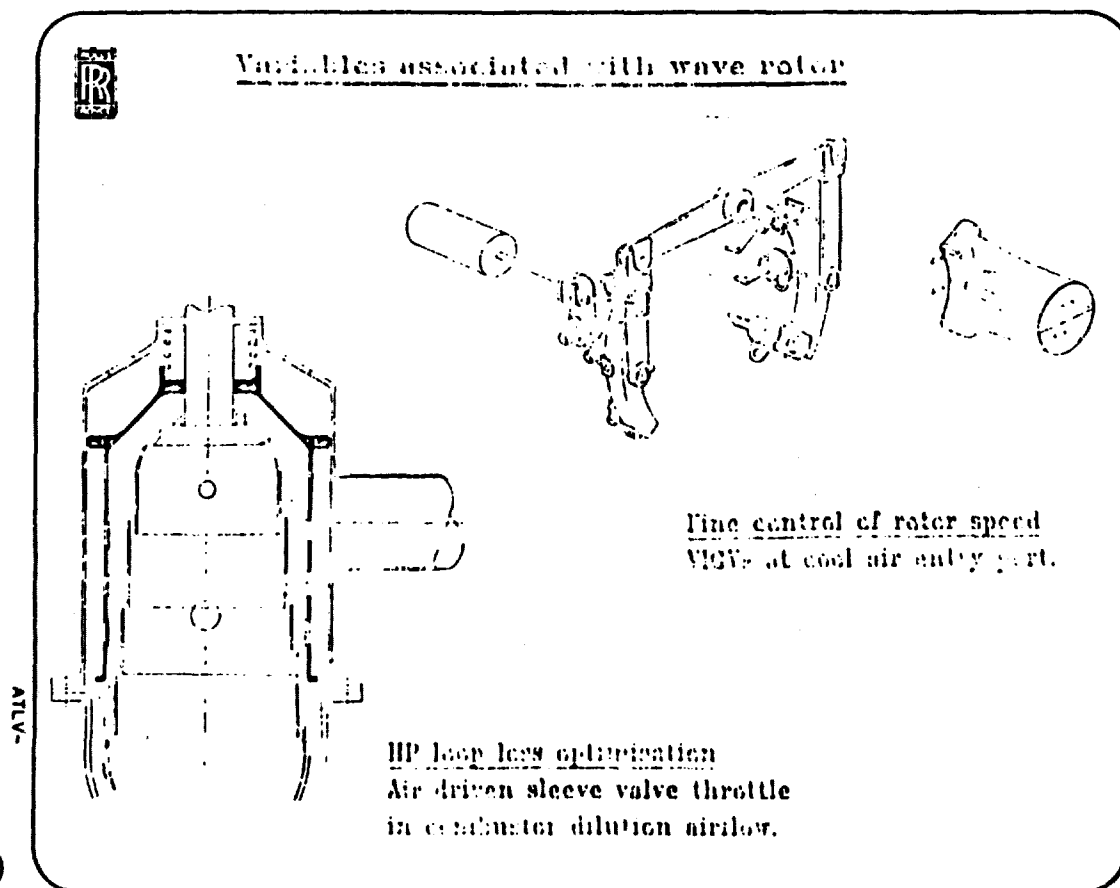
- 6 inch length rotor expands 0.079
.001 clearance both ends costs 17 P
- Each end tied to its ports by a
thrust bearing. Casing flexibility
stops fight, radial diaphragms
restore stiffness.
- Vanes require wall cooling
- Seal and service air details are as
complex as a regular gas turbine.



Wave rotor mechanical features



- Wave velocity (fixed by temperature) and rotor speed must be matched to about $\pm 5\%$.
- Rotor speed is fixed by gas work input, which is changed as VICV angle is adjusted
- For adequate low speed work, and optimum performance, HP loop loss must be adjusted ... max at min T
- Sleeve valve in combustor gives this adjustability.

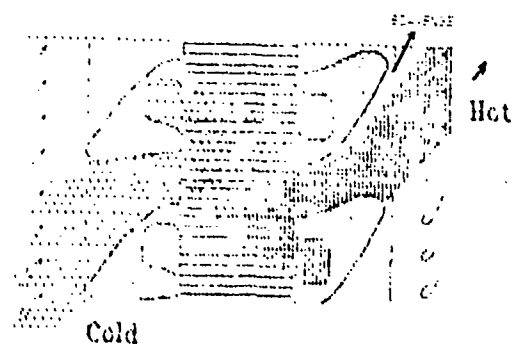


Wg design

- Preliminary 3-cycle rotor
- Simplified wave design (design program developed later)
- Simplified mechanics ... did not have proposed floating scheme.

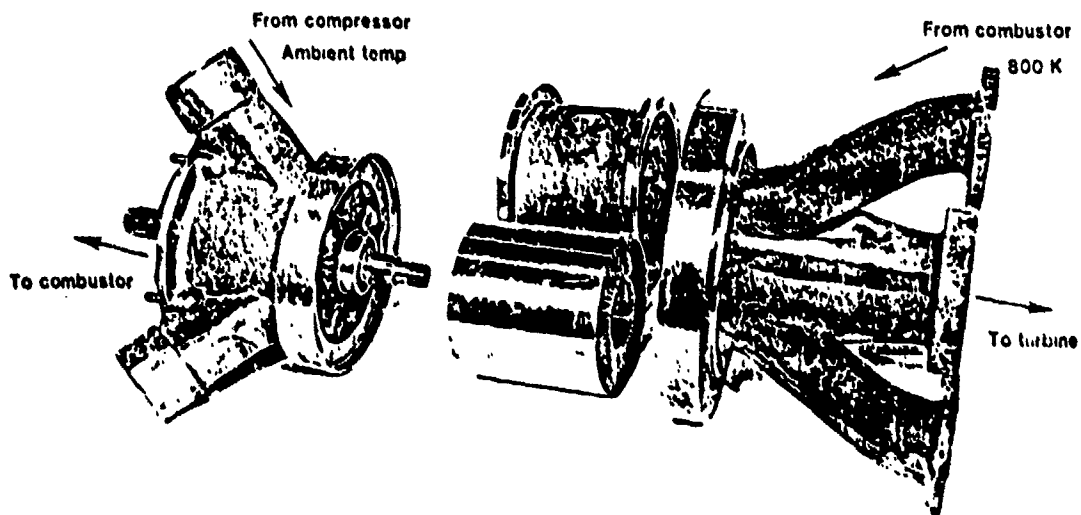
In testing

- Variety of port timings and end to end rotations tested (125 builds)
- 23, 34 & 46 cell rotors. Thick & thin vane tested
- Variable IGVs and HP loop loss investigated
- Speed, P.T and scavenge varied



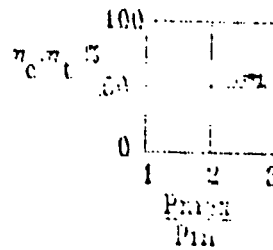
12

WAVE ROTOR TESTED BY ROLLS-ROYCE CIRCA 1967

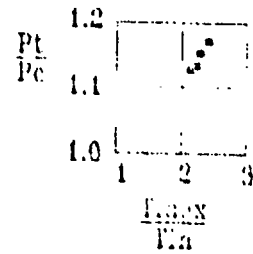


Key results

- Optimum performance poor
- VIGVs caused severe loss
(R dropped from 1.16 to 1.10)
- Prone to mechanical failure of
vanes ... max 40hr endurance
- Better quality design not tested



Conventional: $\eta_c, \eta_t = .77$



$P_t/P_c=1.5$

$T_{02}/T_{01}=2.2$

14

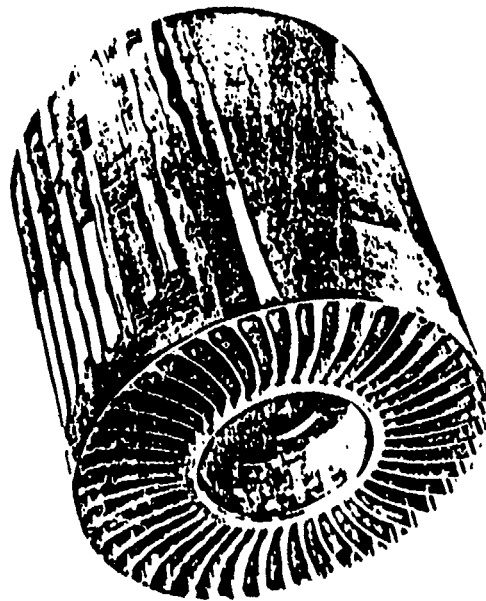
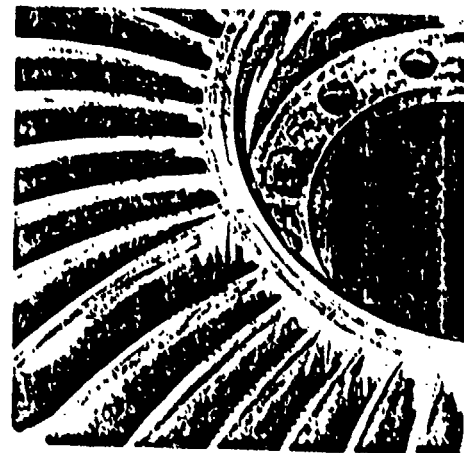


FIG. 1
General view of rotor



Conclusions. 1970

- * Advances in 'steady' flow component design lessen appeal of wave rotor
- * Rig results show both aerodynamic and mechanical shortcomings.
- * Major effort would be needed to make the concept servicable.
Design complications include :

- * May not start conveniently.
(eg starter motors could be required for HP & LP spools)
- * Rotating component durability
- * Fuel system more complex
- * Variables need careful control

A GAS WAVE-TURBINE ENGINE WHICH DEVELOPED 35 H.P.
AND PERFORMED OVER A 6:1 SPEED RANGE.

R.D. Pearson, University of Bath, U.K.

March 1985.

Summary

An engine of 9 inch rotor diameter and 3 inch length was operated for about 300 hours developing a gas energy output of 24 horse power when used in the mode of pure pressure exchange and 35 horse power in its design mode as a shaft power machine.

The engine used pressure wave processes for compression and expansion during its single cycle per revolution in the known manner of pressure exchange but power was developed from the difference in whirl momentum of gases entering and leaving the rotor in the manner of a turbine.

Special design features were incorporated which enabled a wide operating speed range to be accommodated without recourse to adjustable stator porting. Prior to this development such machines were considered operable only over very narrow ranges of speed or needed slideable stator ports and these would have involved excessive cost and mechanical complication together with increased maintenance and reduction in reliability.

The engine started at the first attempt accelerating unassisted from 3,000 RPM to its maximum safe speed of 18,000 RPM. It ran with extremely stable speed and was very controllable. A thermal efficiency of only ten percent was recorded but the engine was naturally aspirated and had no assistance from scavenge fans. Low pressure scavenge fell short of requirements and provides a main explanation for failure to achieve design power. Also the machine contained no heat resisting metals except for the combustor liner. Even so, pressure ratios of up to 4.5:1 were attained.

In view of the limitations considerable potential for development could be inferred and it is tragic that the source of funding was severed just when success seemed so close.

LIST OF FIGURES

1. Explosion Turbine
2. Cell ring rotating explosion turbine
3. Vortex valve and test
4. Explosion turbine with receiver
5. Single cell pressure exchanger cycle.
6. "COMPREX" as High Pressure stage of a Gas Turbine
7. Measurements of deflection at partial cell opening
using a water analogue channel.
8. Chart for estimating rarefaction generation in cells
at partial opening.
9. Position Diagram for Pressure Exchange Engine (GWT)
10. High Pressure Scavenging Effectiveness.
11. Low Pressure Scavenging Effectiveness.
12. Power-Speed Characteristic.
13. Thermal Efficiency - Power Characteristic.

LIST OF PLATES

1. Assembled view of Home Made Pressure Exchange Engine
of $2\frac{1}{2}$ inch Rotor Diameter.
2. Exploded view of the same $2\frac{1}{2}$ inch Rotor Machine.
3. Exploded view of Factory built 9 inch Rotor size machine.
4. Assembled view of Factory built Pressure Exchange Engine
of 9 inch Rotor Diameter.
5. The 9 inch Rotor size Engine fitted with Hydraulic
Dynamometer.
6. 9 inch diameter Pressure Exchange Rotor viewed from the
inlet end and showing the Gear Tooth Coupling.
7. 9 inch Diameter Rotor viewed from the rear.
8. Rear view of the 9 inch Rotor after suffering an
accidental overspeed and showing damage.
9. Developed Porting Diagram with Design Data.
10. Details of rear and front Stator Plates.

INTRODUCTION

A Personal History of Pressure Exchange.

The first person will be used for this section since it is the most appropriate. This historical record has not been given before but it seems the best way of answering many questions which my readers are likely to be asking such as "Why was this programme not pursued following early successful demonstration?" or "Why did no publication of the work appear at the time?" Also there are many lessons to be drawn from the errors made. I have decided to start right at the beginning and then I was 13 years old!

Early Experiments

My father was a science schoolteacher with a very strong engineering bent. He had a fully equipped modelling workshop and spent his spare time making model petrol engines complete with magnetos or coils. So I had an early advantage. He showed me how to make small steam turbines from tin cans. They had thin flexible shafts and shook violently as they passed through their critical speeds. Later, much to his subsequent dismay, he demonstrated how a can could be exploded by using a gas/air mixture.

My response was to try driving a turbine by successive explosions using a fan to scavenge the combustion space. The arrangement is shown in Fig.1. The explosions were too weak and it proved far more difficult to achieve an adequate repetition rate than I ever imagined. I thought it a good idea to try first to improve explosive power. Perhaps if one tin can exploded into a second, thereby compressing a combustible mixture, the desired improvement would arise. The result exceeded my wildest expectations. The stillness of the summer evening was shattered by the report and the primary stage - a two pound treacle tin - vanished. It was then observed apparently motionless but tumbling at a high altitude - probably two to three hundred feet in the air. Explosion of a single can will only lift the lid about four feet. All excited I gave dad a demonstration and felt squashed to see the enthusiasm not shared. Indeed he went grey and stern and forbade any further combustion trials with the available town's gas. So from that time on all work had to be carried out in secret whilst dad was out flying his model aeroplanes.

Ideas for double chamber exploders for driving turbines were followed by

strings and then the ends were joined to form a circle. The idea was for each chamber or "cell" to explode into the next and there were to be about twenty cells in the hope that by the time the explosion had travelled round the circle a gas air mixture would have refilled them so the explosion would become continuous. After that the ring would be mounted on a shaft so that with a tangential outlet from each cell the whole device would spin like a Catharine wheel (Fig. 2).

I thought non-return valves would be needed to prevent the explosion going backwards. Others would prevent discharge to the inlet. But these requirements would involve an excessive number of moving parts. Perhaps "centrifugal force" could be utilised - we had just learned about it at school. A thing I called a "vortex valve" was made in tinplate and tested by hanging plates on cotton threads from a high shelf. One plate was close to the inlet, the other opposite the outlet of a combustion cell. This is shown in Fig. 3. It proved very effective, the "inlet" plate hardly moving whilst the outlet plate hit the shelf. I never finished the ring cell model, losing confidence that it would work because I had no idea how fast air or the explosion would travel. I know now that the vortex valves would not be needed and still think the general idea feasible, but have never tried it out.

Indeed problems of mixture strength control could be easier since flow would be steady at the centre where air and fuel would be admitted. The device could be easily mass produced needing no fine clearances or accurate manufacture. It might one day find application in gas turbines as toppers or in combined steam cycle plant using gasified coal, since no dilution air would be required. It is the need for dilution which prevents combined gas - steam cycles achieving more than about 3 percentage points improvement in thermal efficiency despite considerable extra complication. I went back to single chambers.

I knew turbines worked best with steady flow so the next step involved a receiver fitted with non-return valve. Explosions pumped gas into the receiver (Fig. 4).

My First Pressure Exchanger.

Then I had an inspiration. I could solve the difficulty of intermittent combustion by using the receiver as a steady flow combustor

if I used a rotary valve to dump spent gas from the explosion chamber, now converted to a compression cell, and carried out compression by opening this to the receiver.

Two scavenging stages were now needed. One at atmospheric pressure to purge the cell of combustion products and replace these with a fresh air charge, the other at maximum cycle pressure to transfer the compressed air to the combustor and replace it with high pressure hot combustion products. Fans were to be used for each to effect transfer but the cells were to be made long and narrow so that gas inertia could assist. I did not trust this to be effective on its own as I had no knowledge for estimating its magnitude.

The cycle is illustrated schematically in Fig. 5 and pressure-volume diagrams are included to illustrate the processes of compression by pressure equalisation and expansion by cell isolation followed by the opening of one end.

Energy was clearly released by each of these processes and if turbines were incorporated power could be extracted. Two important facts however were evident. First even if all this power were wasted the device could still provide a positive output by bleeding air from the combustor. Second, if this power was tapped it provided nearly twice the output of a purely constant volume explosion device working between the same pressure limits.

The perfect gas law could be applied to the cell states at the points of completion of low and high pressure scavenge in order to estimate the combustion pressure which ought to be attained :

$P_1 V_1 = m_1 R T_1$ refers to end of LP scavenge, and

$P_2 V_2 = m_2 R T_2$ refers to end of HP scavenge, but

R is the gas constant so by division :-

$$\frac{P_2}{P_1} = \frac{m_2}{m_1} \cdot \frac{T_2}{T_1}$$

The cycle pressure ratio was therefore independent of the cycle repetition rate. It would increase with combustion temperature and reduce as m_2 reduced by bleeding air from the combustor.

This was my first pressure exchanger and had only one stationary cell. I never finished making it because a multiple cell version evolved. Then I turned it inside out. The stationary ring of cells became a rotor, the rotary valve the stator. And then I added transfer passages connecting expansion to compression processes to improve compression efficiency. A shrouded rotor was used and with slots in the shroud for interaction with these transfer passages. The latter were tuned to the same frequency to further improve efficiency so I called it a "resonic cascade compressor".

All this was made very difficult by the attitude of my father whom I greatly respected. But he was totally opposed to my experimentation since it was "cranky and ridiculous and could never work because if any of these ideas were any good they would have been worked on already".

How right he was. By the time the model was finished and ready for test I was an undergraduate about to take a London External degree by study in evening school at the local Chesterfield Technical College. I had by this time some six years workshop experience as a works apprentice at a colliery engineering factory. I felt a sudden urge to visit the local reference library, something I had not done for over a year. The first book I noticed was a new periodical "The Oil Engine and Gas Turbine". It fell open at a page entitled "Pressure Exchanger" and I remember thinking what a good name this would have been for my machine. I was crestfallen after reading the article as I recognised it as a greatly advanced version of my own scheme. It was my first introduction to the idea of utilising wave processes in the rotor cells. I had ignored wave action in the these yet had carefully designed waves into the stator transfer passages! The article described a Brown Boverie machine for fitting to a gas turbine railway engine. The concept is illustrated in Fig. 6. The upper figure is a rotor development showing cells moving from left to right. Owing to this motion waves in the cells have an inclined absolute direction, the inclination increasing with rotor speed. Since port edges are timed to match waves as shown, the speed is fixed for a given design of porting. Cells containing combustion products above air inlet pressure arrive at port 3 opening one end to exhaust k and creating a rarefaction wave from 3 to 4 where the air inlet is timed to open.

Since gas velocities are much lower than those of wave fronts a so called "contact surface" between incoming air and exhaust gas I_4 projects into the cells to form low pressure scavenging, whereby they are refilled. The gas velocity is generated by decompression as the wave passes.

Similarly high pressure scavenging is initiated by opening to the outlet from the combustor, port G, compression wave 1 to 2 is generated by opening cells to edge 1 and contact surface I_1 is formed between incoming high pressure hot gas and outgoing compressed air. Other waves 7 to 8 and 5 to 6 arise as port edges close and stop the flow. Such rotor developments are now known as "Wave Position Diagrams".

I managed to obtain about five pounds per square inch pressure and at least the flame was supported in the combustor but I had lost interest, knowing my design to be obsolete.

After graduation I joined NGTE to learn about real gas turbine engines but not much interest could be raised there regarding pressure exchange. I rented a workshop in Leicester and used the old $2\frac{1}{2}$ inch rotor for some experiments, using it to try and obtain power by explosive combustion in the rotor cells. These had their outlets swept back at 45 degrees so could act as reaction blading for explosively induced pressure rise. A stator pocket was provided to induce compression and ignition. Gas/air mixture was introduced at the intake. No power was generated though spectacular displays of flame emerged from the exhaust.

My First "Gas Wave Turbine" or "Pressure Exchange Engine".

But by this time I had developed a method of wave plotting after reading an IMechE paper by Bannister and Mucklow. This led me to realise the Brown Boveri machine had limitations which could be bettered. In particular, transients caused by the interaction of finite cell width and port edges needed careful analysis. I also evolved a wave plan which would permit operation over a wide speed range without adjustable porting. Energy would be wasted unless the rotor ran at high speed as then unavoidable high speed transient jets could be converted to rotor work. Hence what I now call a "Gas Wave Turbine" or G.W.T. was born. Also for a given number of cells per cycle, friction of gases flowing

through the rotor would reduce as design speed increased. This was because rotor length must vary inversely with RPM. Hence rotors ought to run as fast as possible. Analysis then showed it difficult to obtain pressure exchange without shaft work when designed for wide speed range. An optimum arrangement had no gas bleed from the combustor.

Then a most useful paper by A. Kantrowitz (2) appeared. It compared a theoretical graphical method somewhat similar to my own with experimental data obtained from a cell rotor operated with compressed air. Only half the rotor cycle was utilised to allow die-away of residual waves before the next cycle started. This answered my main question in the affirmative. I now knew I could make a running engine because the theoretical method would adequately predict real working.

I left to go it alone. My father had now changed his attitude and encouraged this. I would devote six months to making a small running demonstration engine and with this would have little trouble attracting the funding needed for a full scale commercial venture.

Or so I thought! In the event it took 9 months just to develop the combustor to achieve satisfactory performance. It was three years before even short demonstration runs were achieved. I had decided the application to choose was an alternative propulsion unit for small pleasure boats. Here novelty would be important and existing single cylinder outboard motors were often hard to start and caused unpleasant vibration. Starting of my turbines would be no trouble and they would be vibrationless. Poor fuel consumption expected in the early stages would be a minor consideration.

But now for the major error of judgement! To cut corners and save time I decided to build the new engine around the old 2 1/2 inch pressure exchanger rotor. This had taken much time to construct, it needed only a new running shroud, and I wished to avoid the expenditure of as much time as possible. Had I not compromised thus I think I would have achieved success in about a year with a much better engine to show at the end.

Never compromise by trying to make do with old rotors! Start again from scratch.

This rotor had only 16 cells which was far too few a number as I knew perfectly well. Cell opening and closing losses would be excessive so I decided to start by investigating these. I constructed a wooden cell model for use in a water channel. This was conveniently provided by damming up the stream at the bottom of my parents' garden. The model is illustrated in Fig. 7 together with the test results. A sliding wedge represented a stator port and deflection of the fluid leaving the cell outlet was measured for two cases, one representing a high angle nozzle of 70° , the other representing a cell having an outlet angle of 42° .

Deflection is caused by partial opening and causes severe loss of power. The results were used also for determining boundary conditions at partial port opening for predicting pressure wave development in the cells. For this purpose the results are transformed to the chart shown in Fig. 8.

Subsequent wave plotting appeared to indicate that a workable design could be achieved. The engine was built, the rotor being dynamically balanced on a crudely constructed purpose made machine. It took a long time and many modifications before self sustained accelerations were achieved.

A photograph of the finished engine is shown in Plate 1 and Plate 2 shows it dismantled.

Low pressure scavenge was totally inadequate and had to be boosted by four injectors bleeding compressed air from the combustor. Also some variable geometry had to be fitted. These were two position vanes to provide a low and a high speed range. In the end acceleration could be achieved unassisted from 5000 RPM to 24,000 RPM but this was the low speed range. Design speed was 45,000 RPM but this was never reached owing to poor features of mechanical design which resulted in seizures and bearing failures caused by heat soak on shutdown.

High pressure scavenging appeared to be adequate once the low pressure scavenge was assisted by the injectors. Combustion was intermittent and erratic until this was done. Also a low pressure pre-scavenge duct had been added and also made considerable improvement. This can be

seen in Plate 1 near the bottom. The combustor is at the top. The engine had a transfer duct between HP scavenge and LP pre-scavenge which effected partial expansion by abstracting residual air for re-introduction at cell outlets via high angle nozzles. These provided a drive by making use of most of the energy available from the pressure equalisation process prior to high pressure scavenge. Simultaneously this air fed in with opposite cell ends closed, generated most of the required pressure rise.

No fan assistance was ever given to either of the scavenging stages despite the 'S' shaped cells. These were angled forward at inlet to give minimum incidence during scavenge, were axial for the most part and bent back at 42° at the rear, so providing substantial reaction with consequent impedance to scavenging flow. It is not surprising that difficulties of development were experienced.

PRIOR ART

A businessman and owner of several companies, Mr.G.E. Hooton, was interested in promoting the project. He organised the formation of a development company in conjunction with Ruston and Hornsby Ltd. of Lincoln and Dr. G.B.R. Fielden, FRS, then their technical director, gave this his enthusiastic support. The new company was called "Rotary Power Ltd." and I was Technical Director. All funding was provided by Ruston's. They first made a very thorough patents search and provided a stack of documents more than three inches thick. It made very depressing reading. About 80% of all the ideas I had worked on were described. It was like reading a history of my own thinking. The story began in 1906 with two patents by Knauff (3)(4) which anticipated first a shaft power machine and second a so called Lebre type static pressure exchanger (very similar to my "resonic cascade compressor"). It was, however, not until 1929 that the essential wave nature of the unsteady processes were designed in by Hans Burghard (5) and this anticipated the work of Seippel (6) whose "comprex" patent of 1941 is well known and was part of the Brown Boverie attempt to develop the railway loco engine mentioned earlier.

It is usual in research to first review all existing literature relating to the field to avoid duplication of effort. My experience leads me to think that this should be delayed several months at least so that the

newcomer can start with a completely open mind. He may find an important alternative approach to which his mind could be blocked if exposed too soon to prior art.

A 9 inch Rotor Size Experimental Gas Wave Turbine

The design principles used in the 2 $\frac{1}{2}$ inch model were refined and a new engine designed with careful attention to detail. This would have to work straight away without the mechanical limitations experienced earlier. A kinetic design was decided upon so that the bearings would be supported on a cool frame and this would also carry the hot stators. It was hoped that thermal distortions could be controlled this way and make it unnecessary to have more than one thermodynamic cycle per revolution - another way of balancing thermal effects. The latter is undesirable because it doubles the number of cells needed and so halves the cell wall thickness. Since pressure exchange involves cyclic pressure variation the cell walls are subjected to alternating stresses making a perfect fatigue machine. Fatigue stresses increase with the square of the number of thermodynamic cycles per revolution, if wall thickness/pitch ratio is fixed, and so a single cycle is safest. The mechanical design is illustrated in Plate 3 giving an exploded view whilst the assembled version is given in Plate 4. The 4 inch bore metering nozzle shown in the foreground enabled the airflow induced during low pressure scavenge to be measured. The smaller downward facing inlet provided cooling air to the rotor shaft in order to limit thermal expansion. The rotor, shown in Plates 6 and 7 had thin walled obtuse cones connecting with the shaft for limiting heat soak and this also minimised axial expansion. The entire rotor was made from "Fortiweld", a material only slightly more heat resistant than mild steel. Jessops H46, a ferritic turbine disc material, had been selected but could not be obtained in reasonable time. The more exotic nimonics or other turbine blade metals were avoided because one aim was to demonstrate that cheaper non strategic materials were acceptable.

A stator ring (third item from left Plate 3) connected stators with the cool frame and was cast in light alloy, but apart from the combustor liner and bronze bearings all other parts were made in mild steel.

The combustor was a scaled down Ruston TA design and was developed separately by a Ruston team. It is interesting that this "elbow

chamber" evolved an antichamber at the rear just as the one I developed for the smaller model. It was found essential for operation over a wide fuel/air ratio range.

The stators were complex as shown in detail in Plates 9 and 10. Ports were subdivided more than would have been the case for a prototype, the idea being to assess flow details by separate measurement in each sub-duct. This turned out to be a mistake because it made the engine look very ugly. Later this appeared to be a primary reason for rejection by Rolls Royce. Some of their top men witnessed what I considered to be a convincing demonstration run, but they were clearly unimpressed and it was obvious that they considered the machine bizarre. It would have been better to have designed a cheaper, simpler and more elegant machine for demonstration without bothering too much about data acquisition. This should have been allocated to the next machine built.

The ports shown in Plate 10 can be identified from the development shown in Plate 9 since the cc inlet 12 (to combustor) is at 3 o'clock for the rear stator (Left Plate 10) and the c.c. outlet 12A at 9 o'clock (right). Rotor movement is clockwise referred to the rear stator. The high angle driving nozzles are at 12 o'clock and these are followed by a high pressure prescavenge outlet arranged to give good high pressure scavenge over a wide speed range. For the same reason a low pressure prescavenge duct at 4 o'clock on the front stator (LPPS) is fitted. The very small holes are static tapplings for pressure measurement.

As in the $2\frac{1}{2}$ inch machine no scavenge fans were used. In consequence a rapid slowing of cell gas occurs during low pressure scavenge resulting in high speed discharge to the first ports 5 and 6 followed by lower speed flow to 8 and 9. This is why the exhaust ducts are split and have different angles as measured from the axial direction. High pressure scavenge is not affected in this way due to the density of air discharged being greater than that of hot gas admitted.

In Fig.9 a wave position diagram shows the port development more clearly. Most waves have been omitted for clarity but the main wave fronts are shown with F marking the foot and H the head so F marks the start and H the end of pressure and gas speed change over a wave front. M marks the "half wave" point and two M lines have a plateau of constant

state linking them showing that a wave has been deliberately arranged to develop in two stages with tolerance to speed variation in mind.

Solid lines indicate compression waves, when two merge a shock S such as at 4 is generated, dashed lines are rarefactions and chain dashed are contact surfaces between air and hot combustion products. It used to require eight to twelve weeks at 6 days/week 10 hours/day to plot a single design diagram in the detail required. All waves refer to the leading cell wall as datum and it needs to be borne in mind that the same state exists over one pitch of the cell as it carries through the cycle. The wave foot F arises as soon as a cell leading wall opens past a port edge, e.g. wave (22) caused by opening to first exhaust L_{01} , but wave head H arises one pitch later at the point of full opening. The position of initiation of intermediate points is found using Fig. 8B.

The full pressure amplitude ($\pi_F - \pi_H$) is first determined and $(\pi_F - \pi)/\pi_H$ found. This might be .09 for example. Then the wave starting points for the $1/4$, $1/2$, $3/4$ and $7/8$ fractions of full wave amplitude can be read off. In this case the $y/8$ values would be .15, .33, .56 and .82 respectively and so tend to crowd toward the opening point giving a concave shape to a π -time pressure profile. A similar chart for compression wave generation can be plotted and yields the opposite - a convex π -time profile.

Identification of Ports and Stages (Fig. 9)

Suffix 1 is the inlet stator or the outlet.

L_{11} to L_{01} is high speed low pressure scavenge

L_{12} to L_{02} is low speed low pressure scavenge

N_R produces a transient depression to reflect as F(6)M for providing insensitivity to rotor speed.

R_i - compression pocket with driving nozzles.

P_{11} - high pressure prescavenge inlet

R_0 " " " outlet.

This combination gives insensitivity to rotor speed variation for high pressure scavenge.

The compression pocket R_i is fed from both R_0 and from R. The latter collects remaining air mixed with some hot products from cells

undergoing expansion after leaving the high pressure scavenging stage. H_0 is the compressed air outlet connecting with the steady flow gas turbine type combustor.

P_{H1} is a high angle nozzle fed with air drawn from outside the combustor liner.

H_1 is the main hot gas outlet from the combustor providing high pressure relatively free from unwanted carry over waves. This also occurs over a wide range of rotor speed.

Power Measurement

I had intended constructing a matching dynamometer for power measurement but was strongly advised by the board of directors to purchase a proprietary machine which would be fully developed. I should not waste my time developing ancillary equipment. Although I could not fault this logic I had a very strong feeling of apprehension regarding this policy. As will be described this "hunch" should have been heeded and from other similar experiences it is my strong recommendation that such strong hunches should not be dismissed lightly.

In the event a Heenan and Froude DPX 190 hydraulic dynamometer was sold to us rated for use up to 20,000 RPM.

First Trials

Plate 4 shows the engine alone ready for the first trial. A small compressed air pipe can be seen far right. This ended in a small starting air jet which impinged on the rotor blades and was sufficient to spin it to 3,000 RPM. The combustor was ignited by opening a valve on the calor gas cylinder and firing a spark plug. Gas oil was then admitted and the calor gas shut off.

The engine immediately responded accelerating to full design speed of 16,100 RPM at the very first attempt. Everyone was very excited at such a promising beginning and the dynamometer was hurriedly fitted.

Next day the first power measurements were made and Dr. Fielden brought in Sir Frank Whittle, inventor of the first British jet engine, to witness this. And the following day saw a demonstration to the entire Ruston Board some twenty strong.

Then disaster struck! After some few minutes the machine screeched to a sudden stop from 18,000 RPM giving off a red shower of sparks.

But it was not the engine, this remained intact and undamaged. It was Heenan and Froude's "fully developed" proprietary dynamometer which had seized! It turned out to have a bearing life of three to five hours. We had been sold a low speed machine and all the firm had done was fit high speed bearings. They had no knowledge or experience of high speeds nor had they any high speed test facility. They had simply relied on us to find out how well it worked. So much for a fully developed article. This was instrumental in the ultimate winding up of the project.

ENDURANCE TESTING IN PRESSURE EXCHANGE MODE

The board, alarmed at evidence of unreliability, required the engine to be put on endurance tests. To satisfy this as well as I was able the sight glass of the combustor was replaced with a $\frac{3}{4}$ inch orifice and the engine run as a pure pressure exchanger with gas bleed. This was equivalent to 24 horse power at a pressure ratio of 2.4. Any further increase would have caused overspeed since this condition provided the maximum of 18,000 RPM. However this subjected the rotor to adequate thermal transient stresses with the inlet temperature exceeding 1000°C. Some 300 hours of running with frequent starts and stops were achieved without sign of distress.

FINAL TESTS

During this time an air brake was designed and constructed as a crash programme working overtime and through the night. Eventually brake load could be re-applied and research continued. This new brake performed well and needed no development. It was direct coupled and used a spare supercharger impeller of $10\frac{1}{2}$ inch tip diameter. A swung casing enabled accurate measurements to be made by torque reaction.

Unfortunately the technician in charge of endurance testing had become tired of the frequent starts and stops needed for refuelling. He fitted a bypass system to enable change to a second fuel tank to be made without stopping. As soon as he tried it a design fault caused full fuel flow to be suddenly injected to the combustor, causing a violent overspeed which wrecked the rotor. The damage is shown in Plate 8 and

the failure mode is of interest.

The shroud ring had been steel brazed with SPM2 alloy powder to the rotor tips. These were made with $1/4$ " wide platforms for increase of brazed joint area. Only one joint failed as seen at 8 o'clock. Remaining failures were through solid blade material with tears starting at the roots. Clearly a safe failure mode was achieved as compared to the catastrophic kind which would have resulted from drum failure.

TEST RESULTS

As a consequence only preliminary performance results were obtained but analysis of these was informative and encouraging.

Scavenging effectiveness is shown in Figs.10 and 11 plotted against speed of rotation. In both cases effectiveness is defined as the actual flow volume achieved divided by the flow which would just admit or remove an air mass given by the product of ambient air density and cell volume passing rate. The high pressure scavenge effectiveness shown in Fig.10 had to be inferred from measurements of fuel flow and combustion temperature rise but the low pressure scavenge effectiveness was metered with no allowance for mixing effects which caused some air to be lost in the exhaust. The results show that the design aim was almost achieved and that very satisfactory operation over a wide speed range of 6:1 obtained. The design point marked + is shown corresponding with a pressure ratio of 5.43 but the maximum achieved was limited to 4.2 owing to excessive leakage and poor low pressure scavenge. This would reduce high pressure scavenging effectiveness as a secondary effect. It will be observed that these parameters both increase as pressure ratio increases so that it can be inferred by extrapolation that the values would be close to design aims if the two defects could have been remedied.

The excessive leakage resulted from unexpectedly large axial rotor displacements during thermal transients which forced increased axial clearances to be allowed. Some 7 to 15% of total flow is estimated to have been lost as leakage. The mass loss and incomplete scavenge then combined together to cause the gas inlet temperature to increase prematurely to a limiting value of 1050°C at a pressure ratio of 4.2. The maximum rotor temperature was then 450°C as measured by "thermindex

paints" and was the limit for the "fortiweld" rotor material. These values can be compared with design figures of gas inlet temperature 747°C and pressure ratio 5.43 with rotor temperature 380°C.

OVERALL PERFORMANCE

The combined effect of excessive leakage and consequential underscavenge resulted in failure to reach design performance and thermal efficiency. In Fig. 12 shaft horsepower is plotted against speed of rotation from the experimental results. A maximum output of 35 HP was achieved at 16,100 RPM as compared with the 55 HP expected and is sufficiently close to be regarded as encouraging in view of the mismatching caused by the excessive gas temperatures resulting from underscavenging and leakage. The wide speed range is again evident and it must be stressed that this was achieved using no variable porting of any kind. The rising torque characteristic would only be suitable for alternator, propeller, fan or compressor drives but wave machines have the advantage over gas turbines of not being limited to slow accelerations by surge.

Fig. 13 shows a thermal efficiency of nearly 10% (on GCV) which is low but could be improved by development. Part load values show much lower fall off than for an equivalent gas turbine. Thermal efficiency is plotted against power output for one gas inlet temperature and speed varied to give best results. A curve taken at a constant speed of 17,000 RPM is also given showing a steeper fall off at part load. It should be noted that the efficiency curves relate to a maximum temperature of only 1070°K (800°C, or 1470°F). The results were taken a long time ago and some appear to not have been retained. Values at the highest temperature of 1250°K must have given higher efficiencies. I am sure slightly over 40 HP was achieved and extrapolation of the power curve of Fig. 12 to 18,000 RPM shows this ought to have been possible. Also from memory I recall a maximum pressure ratio of 4.5 being recorded.

Some exhaust traversing was carried out to determine the temperature profile at various radii. This indicated much greater mixing of air and exhaust gas during scavenge than had been expected, since although measurements were indicating failure of the theoretical "contact surface" between air and exhaust gas to reach cell ends, a rapid fall in temperature started to occur at about 60% exhaust port opening. This indicates the need for increasing design overscavenge.

Average exhaust temperatures were, however, consistently about 50°C above maximum rotor values. This is an important advantage since this type of engine will be used in practice as a high pressure high temperature stage and the exhaust needs to be as hot as possible. For uncooled gas turbines, of course, the exhaust temperature is necessarily much less than the maximum rotor value and so the wave machine has been demonstrated to possess an important advantage.

Winding Up of the Project

It is most unfortunate that Rustons ran into financial difficulties just as demonstration of feasibility was achieved. They had to cut back and long term research and development is always the first to be shed. I was no longer permitted access to their premises and the equipment was crated and despatched to me at Chesterfield. I found it quite impossible to attract further funding since nobody was even remotely interested. I had the entire crate scrapped without even looking inside, which was a terrible waste.

I wrote a paper "An Experimental Pressure Exchange Engine and its Future Possibilities" for the I.Mech.E. This was delivered at the Rolls Royce Welfare Hall, Derby and won the graduate's prize for that year. However, it was never published being rejected ultimately by the assessors on grounds of "inadequate experimental results".

I spent a year trying to restart the project also partly constructing a very small machine intended as a model jet propulsion engine of 12 oz. design thrust and building a valveless pulse combustor of 1 1/4 pound thrust running at 330 Hz. The pulse combustor was intended to ultimately provide a pressure gain to replace steady flow chambers. This would permit greater deflection in the cells and so improve GWT performance. But these efforts were useless for furthering my career prospects. I decided to abandon pressure exchange.

The traumatic effect of failure caused a depression lasting many years. Later I carried out more work on valveless pulse combustors with some success. A postgraduate, Ross Harley, carried out a computer study under my direction to apply the method of characteristics to this field. Useful wave maps could be computer drafted and this was published in 1971 at "The First International Symposium on Pulsing Combustion" at

Sheffield. Later a single orifice pulse combustion burner was also simulated. On test this was developed to high performance. It regularly achieved a twelve percentage pressure gain measured as steady flow after its smoothing system and in one test seventeen percent was recorded. Peak pressures were 3 atmospheres absolute at 12% pressure gain. Frequency was 200 Hz which proved too high for easy starting.

It had always been intended to build up to a test of a rotary multiple cell ring or "Rotary mode pulse combustor" but to date this has never been attempted.

FUTURE APPLICATIONS

Gas Wave Turbines could ultimately find application as toppers for both gas and steam turbines. Combined cycle proposals to date involve conventional gas turbines which have limited exhaust temperatures. In consequence they are applied with most of the energy path in parallel with the steam cycle making it impossible to achieve much improvement in fuel economy. It is only expected for example that the current 38% efficiency of an all steam station such as Drax B would be raised to 41% for combined cycles. With a gas wave topper true series operation of energy path would arise and is potentially capable of raising thermal efficiency therefore to 55% according to recent evaluations.

Similarly as toppers for gas turbines efficiencies could be raised to an estimated 45%.

An advanced GWT should in future achieve a pressure ratio of 12 so that boosted to 4 atmospheres by turbocharging, combustion pressures of 48 ATM or even above should be possible. Such easily attainable high pressures make application to coal gasification attractive. Other applications such as military and jet propulsion units for aircraft and missiles also seem attractive. Details of such evaluation are to be presented in a separate document.

CONCLUSION

Although design targets for an experimental Gas Wave Turbine were not reached, results obtained were on the whole most encouraging. It was conclusively proved that wave machines could operate over a wide speed range and deliver useful power without assistance and without any form

of variable porting whatever. This was achieved also without any fan boosting of either of the two scavenging stages. Failure to achieve design point appears to be partly due to inadequate control of clearances and to poor low pressure scavenging. It is confidently believed that these problems could be adequately solved by development.

The project showed also that the method of characteristics used with care and taking proper account of the effects of cell width results in an accurate matching of exit duct angles to gas velocities. Diffuser recovery efficiencies of 60% had been assumed for design and results show that these are approximately correct.

Further development is justified but the next engine should have assistance in the low pressure scavenging stage.

A personal history of development of the project has been presented by which it is hoped to usefully transmit some of the experience gained.

R.D. Pearson

March 1985

- (1) BANNISTER, F.K. (University of Nottingham).
"Pressure Waves in Gases". Akroyd Stuart Memorial Lectures, 1958.
(Note. This is not the I.Mech.E. paper which did not include characteristics).
- (2) KANTROWITZ, A., HERTZBERG, A., McDONALD, E.E. and RESLER, E. Jr.
"Heat Engines based on Wave Processes". Graduate School of
Aeronautical Engineering, Cornell University, Ithaca, N.Y.
Mar.21, 1949.
- (3) KNAUFF, L. British Patent No. 2819 (1906)
(Shaft Power Machine).
- (4) KNAUFF, L. British Patent No. 8273 (1906)
(Lebre Type Pure Pressure Exchanger).
- (5) BURHARD HANS. British Spec. No. 485,386 1929.
- (6) SEIPPEL CLAUDE. British Spec. No. 553,808 1941.
- (7) PEARSON, R.D. and HOOTON.
"Improvements in Pressure Exchangers".
British Patent No. 843,911 June 30th 1955.

Also under the same names the following list of other
Specifications :-

British Patent No. 803,659 Jan 13 1954
803,660 Oct 29 1958
843,912 June 30 1955
843,913 " " "
843,914 " " "

of variable porting whatever. This was achieved also without any fan boosting of either of the two scavenging stages. Failure to achieve design point appears to be partly due to inadequate control of clearances and to poor low pressure scavenging. It is confidently believed that these problems could be adequately solved by development.

The project showed also that the method of characteristics used with care and taking proper account of the effects of cell width results in an accurate matching of exit duct angles to gas velocities. Diffuser recovery efficiencies of 60% had been assumed for design and results show that these are approximately correct.

Further development is justified but the next engine should have assistance in the low pressure scavenging stage.

A personal history of development of the project has been presented by which it is hoped to usefully transmit some of the experience gained.

R.D. Pearson

March 1985

Acknowledgements

The author was indebted to Dr. G.B.R. Feildon CBE, FRS for his support. He was then Technical Director at Ruston and Hornsby Ltd. The assistance of others on the staff at that company is also appreciated. The financial support of Mr. G.E. Hooton was an important factor which enabled the project to begin.

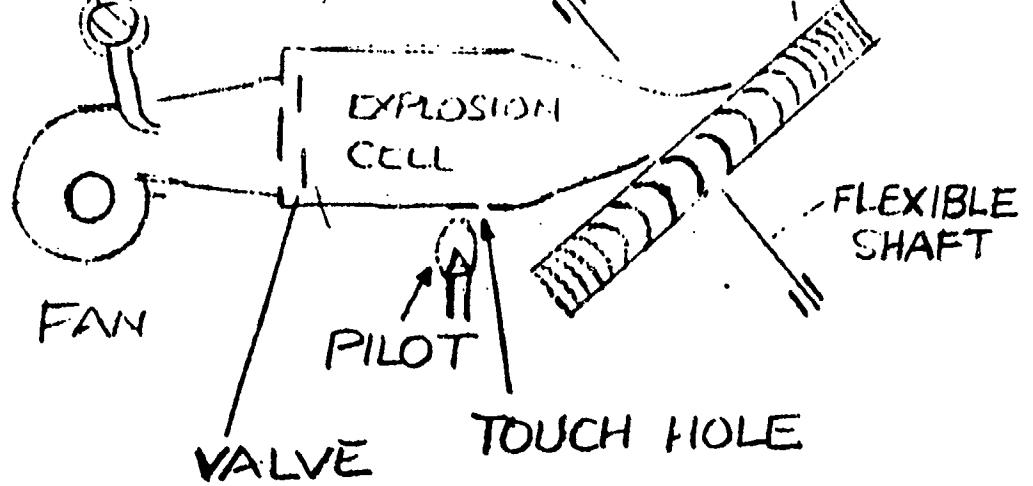


FIG 1 EXPLOSION TURBINE

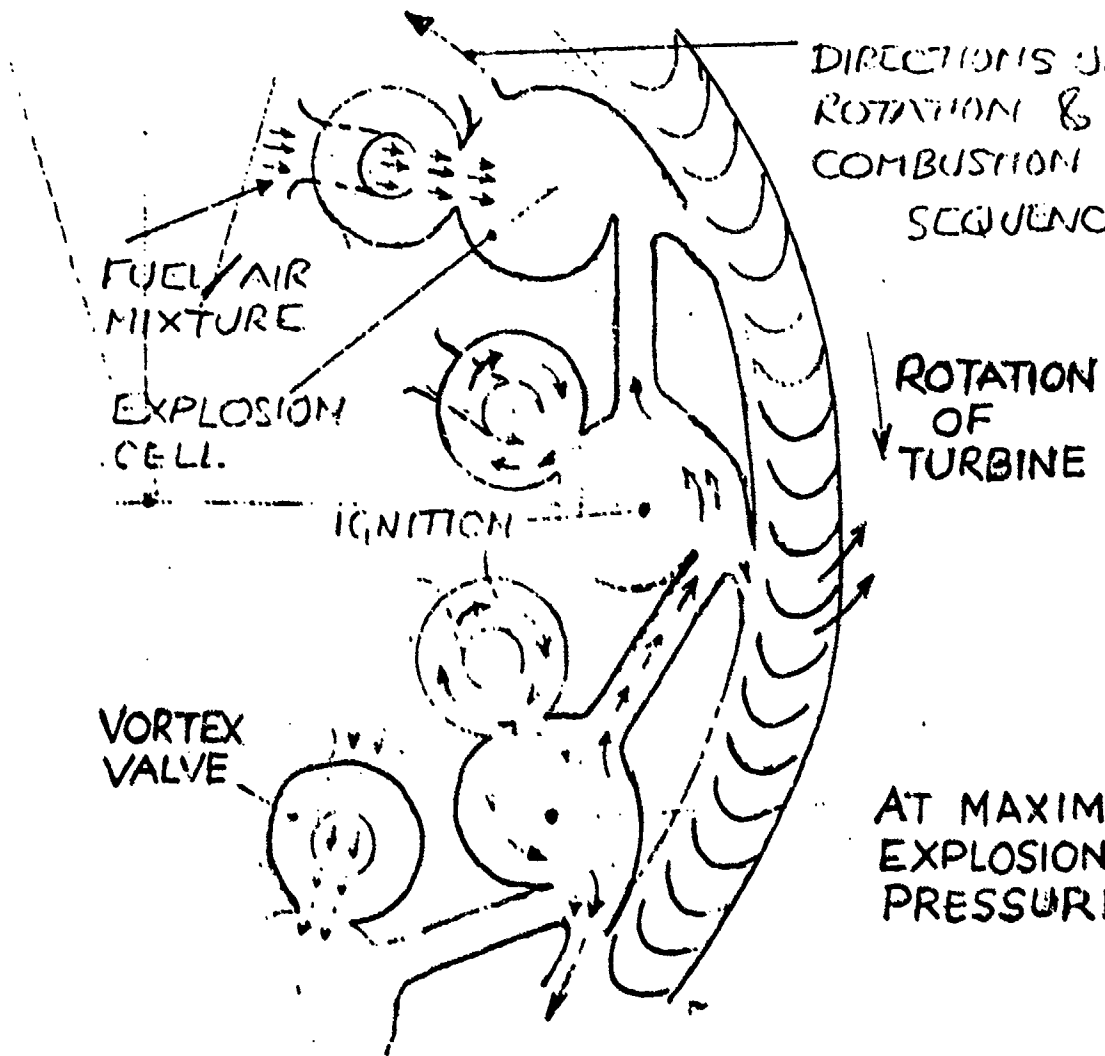


FIG. 2 CELL RING ROTATING EXPLOSION TURBINE

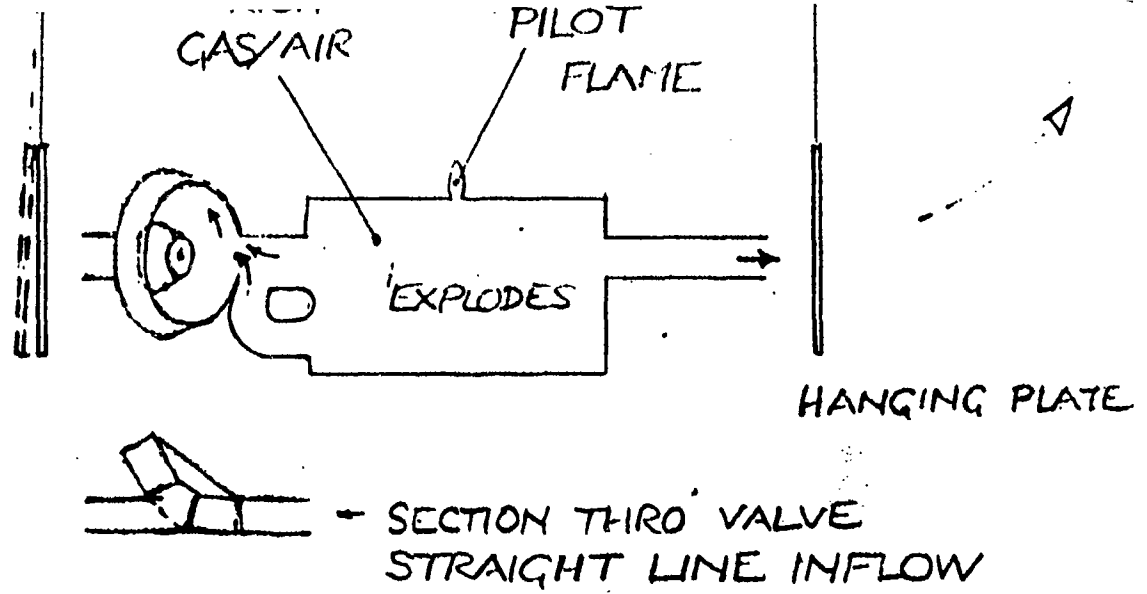


FIG. 3 VORTEX VALVE & TEST

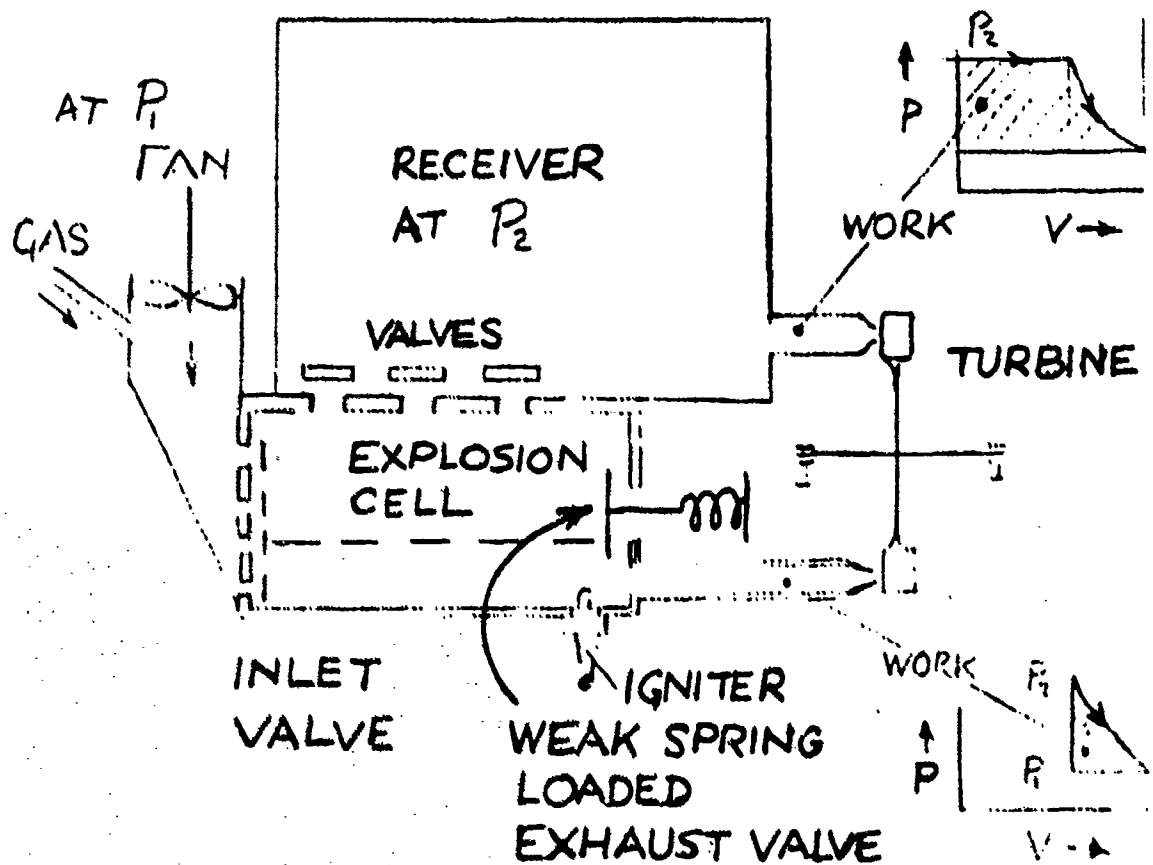


FIG. 4 EXPLOSION TURBINE
WITH RECEIVER

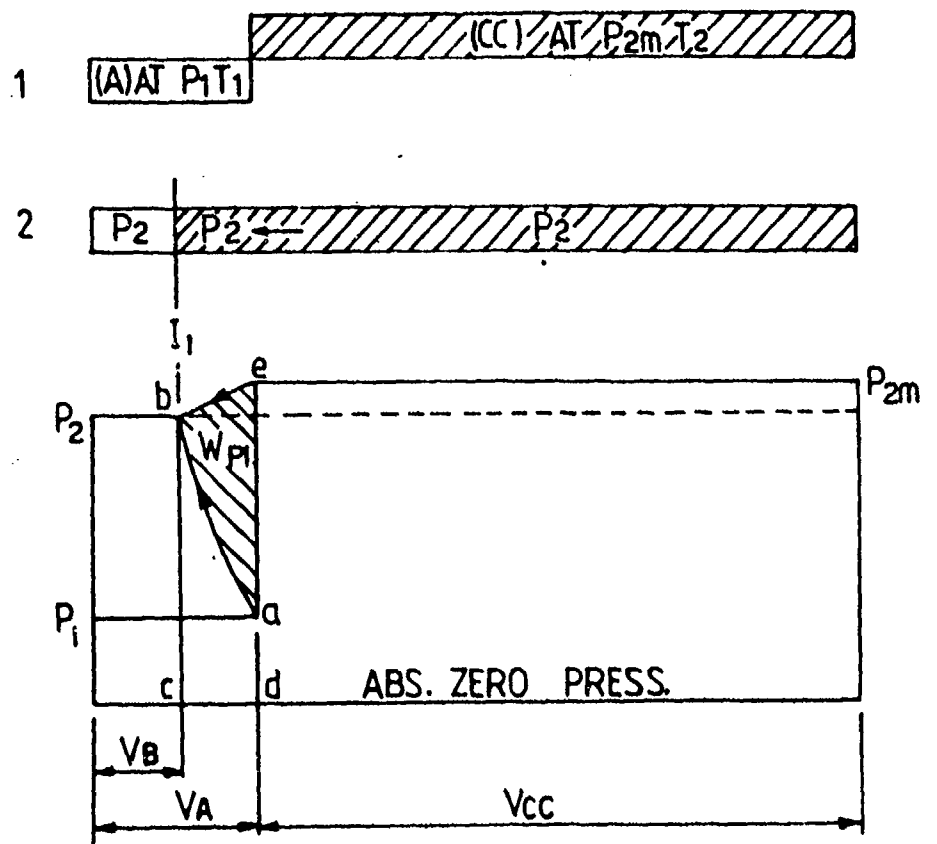


FIG.5(a) COMPRESSION BY PRESSURE EQUALISATION

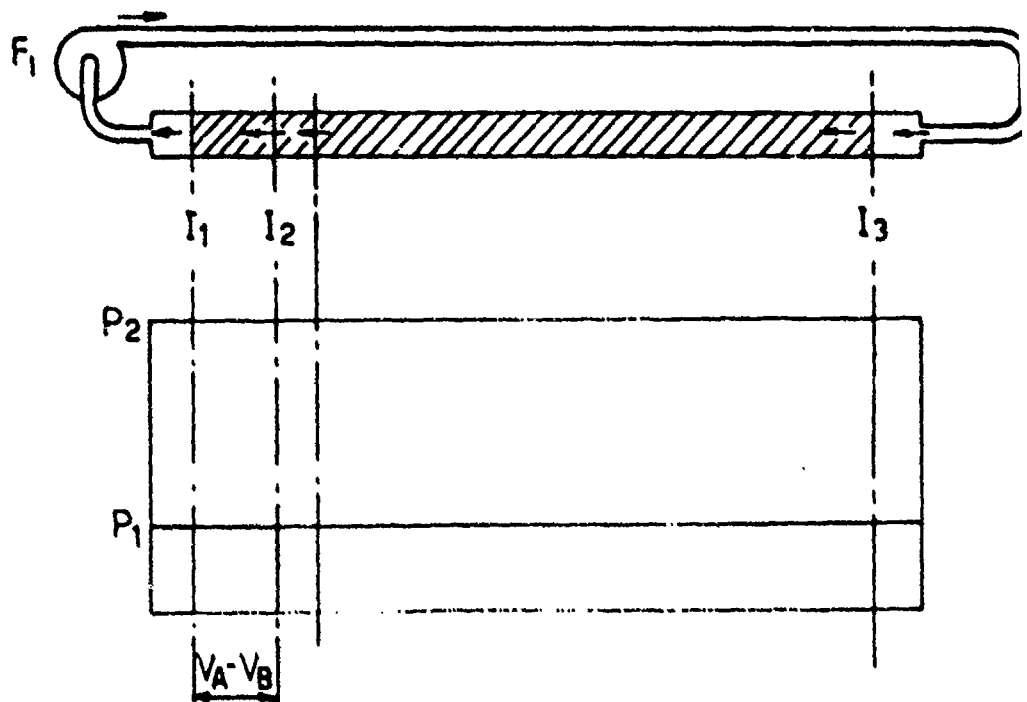


FIG.5 (b) HIGH PRESSURE SCAVENGE

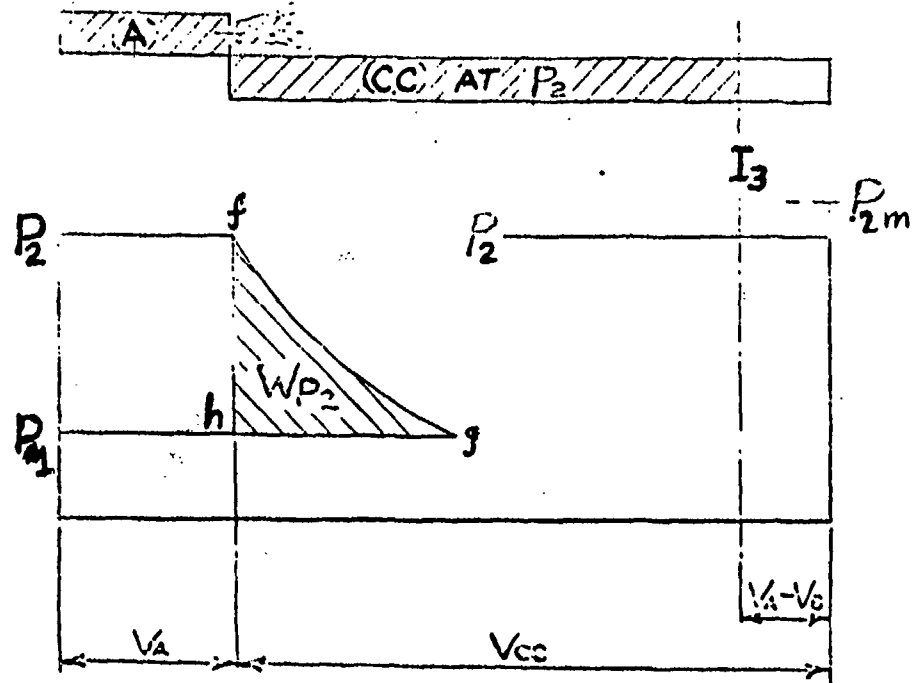


FIG.5.C EXPANSION

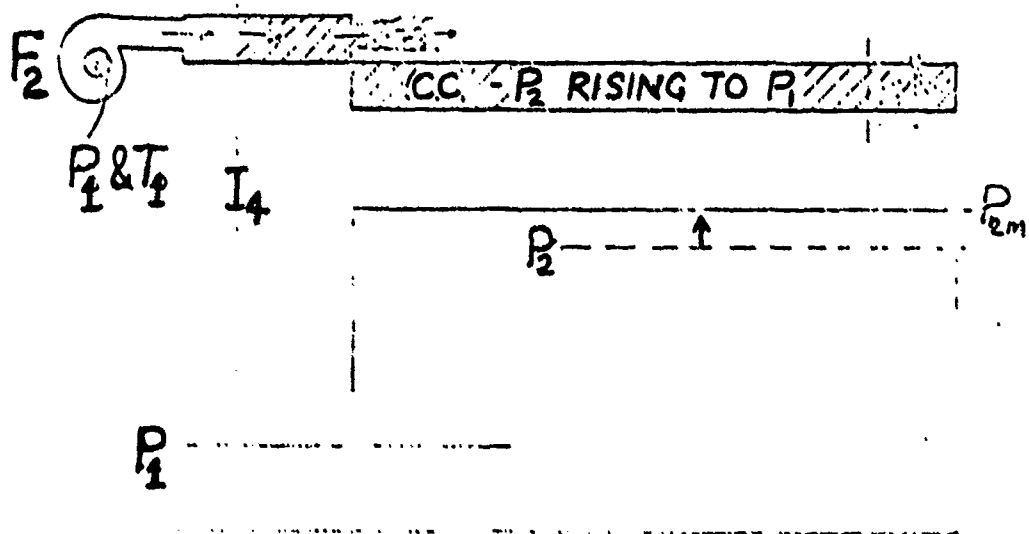
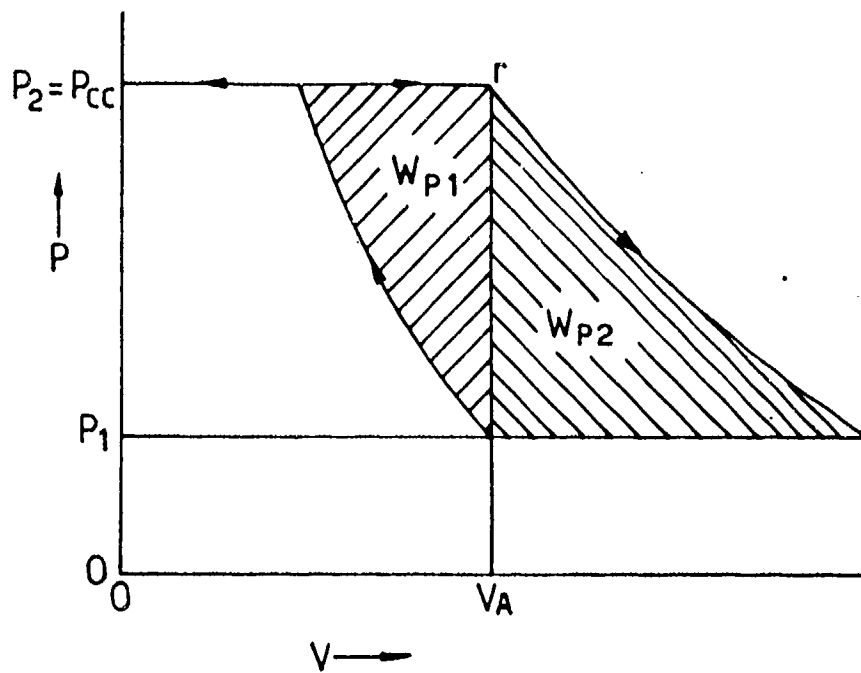


FIG.5d LOW PRESSURE SCAVENGE



CONDITIONS FOR
EQUILIBRIUM

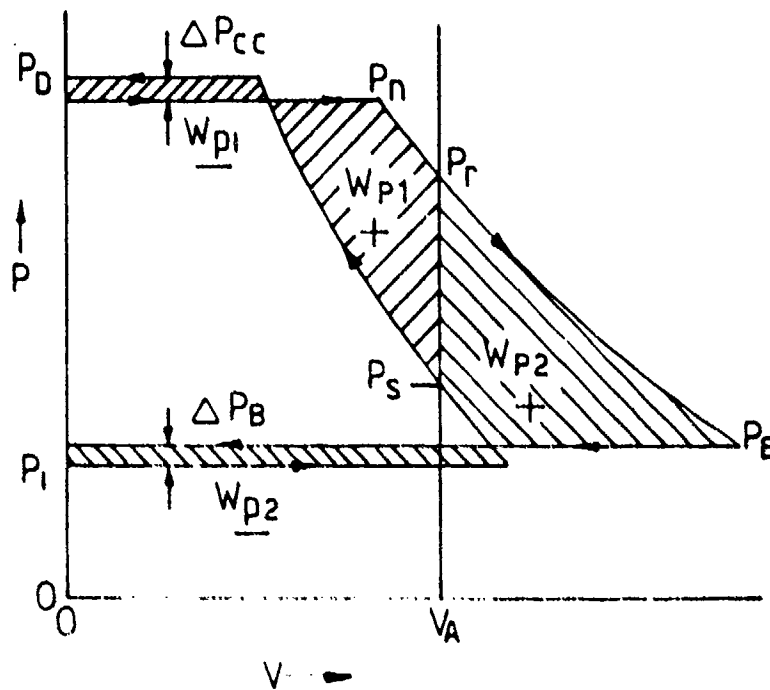
$$P_1 V_A = M_1 R T_1$$

&

$$P_2 V_A = M_2 R T_2$$

$$\therefore \frac{P_2}{P_1} = \frac{M_2 T_2}{M_1 T_1}$$

FIG 5(e) BASIC SIMPLE CYCLE



$$P_s V_A = M_s R T_s$$

&

$$P_r V_A = M_r R T_r$$

$$\therefore \frac{P_r}{P_s} = \frac{M_r T_r}{M_s T_s}$$

FIG 5 (f) GENERAL CYCLE

SEIPPEL'S COMPREX

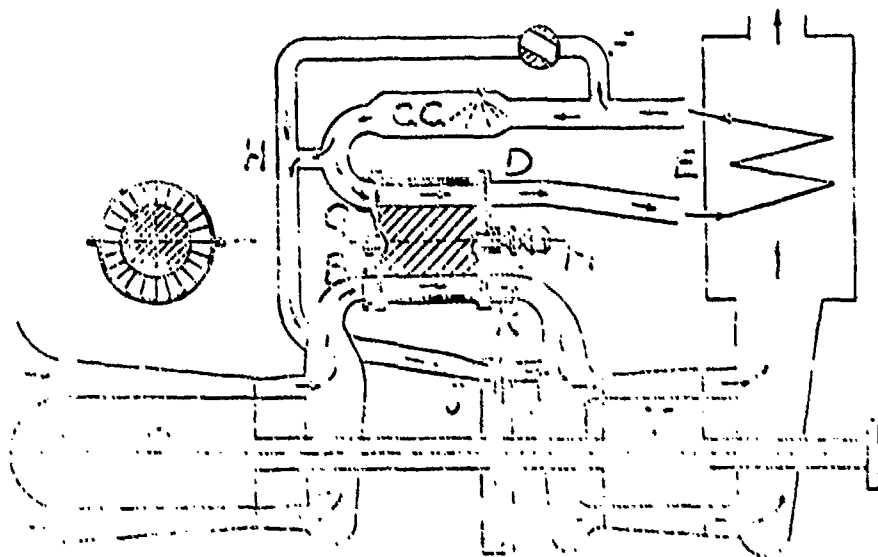
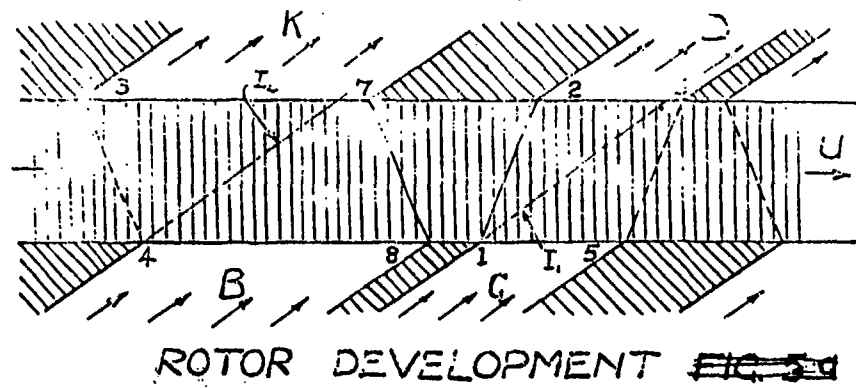
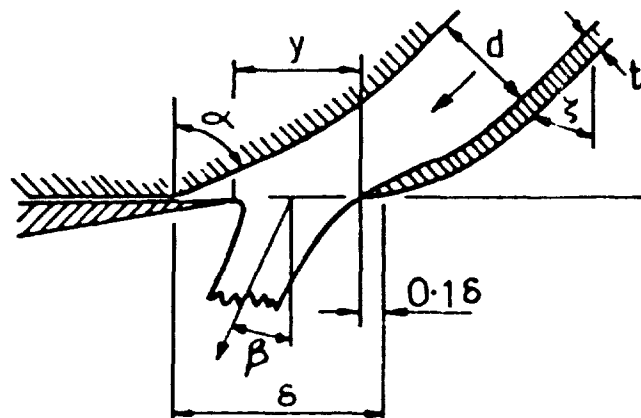
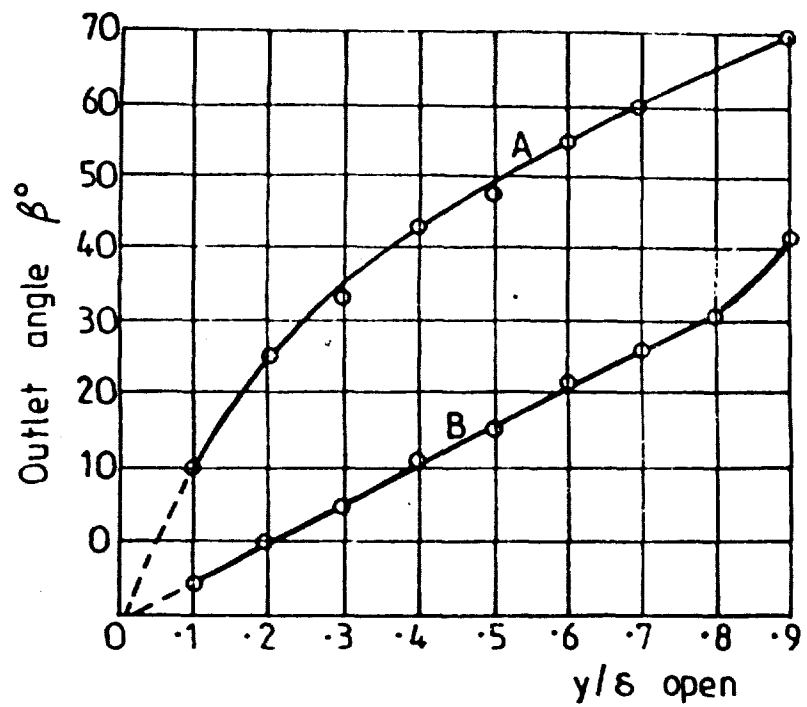


FIG. 6 COMPREX AS HIGH PRESSURE STAGE OF A GAS TURBINE



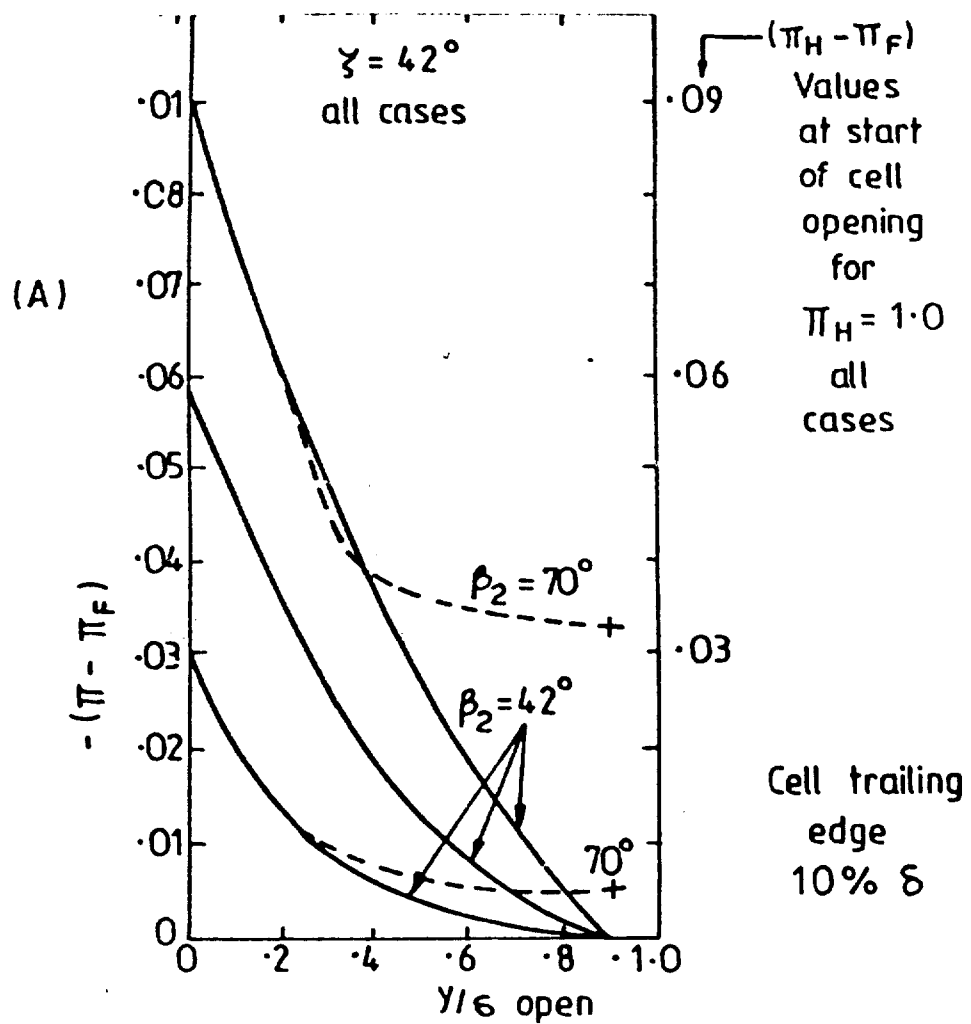
A - $\zeta = 42^\circ$ $\alpha = 70^\circ$

B - $\zeta = 42^\circ$ $\alpha = 43^\circ$

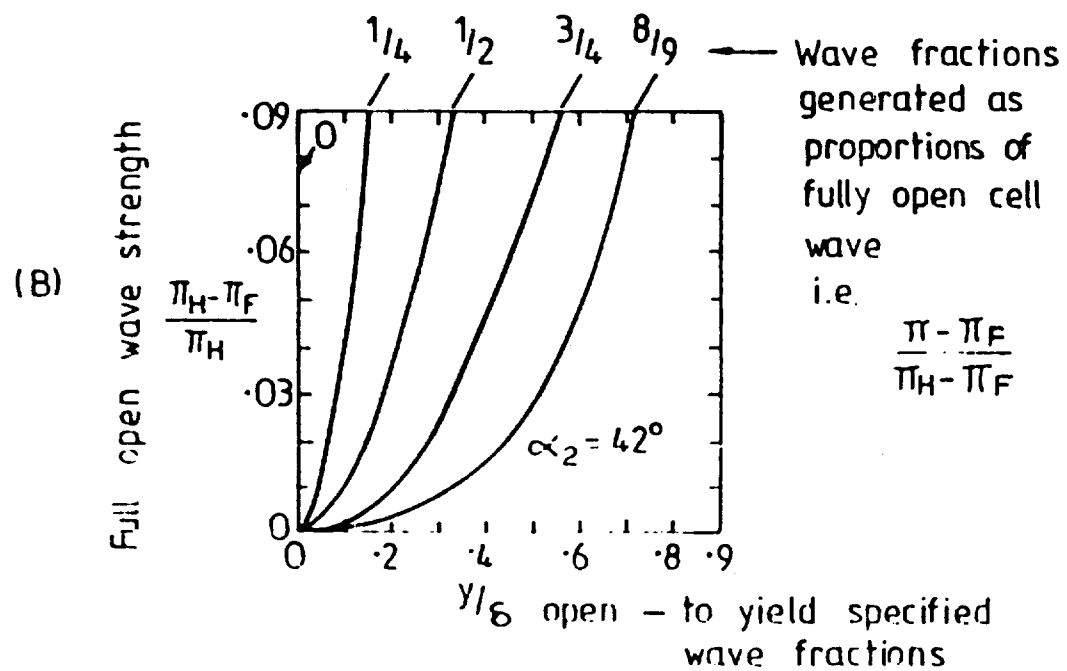
$$\frac{a}{a+t} = 0.75$$

$\delta = 1.0''$, $H = 1.65''$ (Water approach depth)

FIGURE 7. CELL OUTLET DEFLECTIONS AT PART OPENINGS
DETERMINED FROM WATER CHANNEL TESTS



(B) is derived from (A)



Use generalised Chart (B)

FIGURE 8. CHARTS FOR ESTIMATING THE DEGREE OF CELL OPENING NEEDED TO GENERATE SPECIFIED RADEFACTION WAVES.

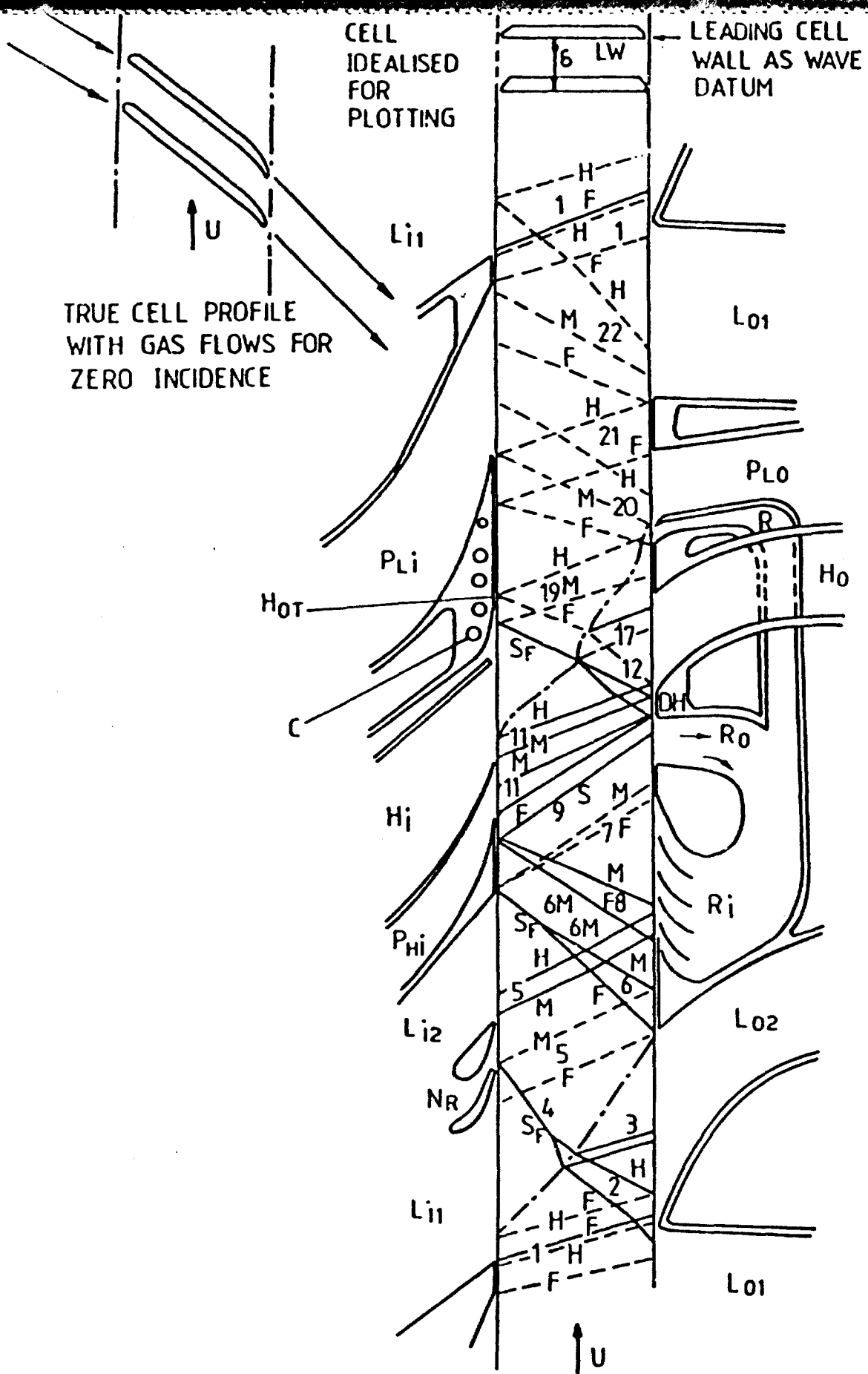


FIG.9 POSITION DIAGRAM FOR PRESSURE EXCHANGE ENGINE

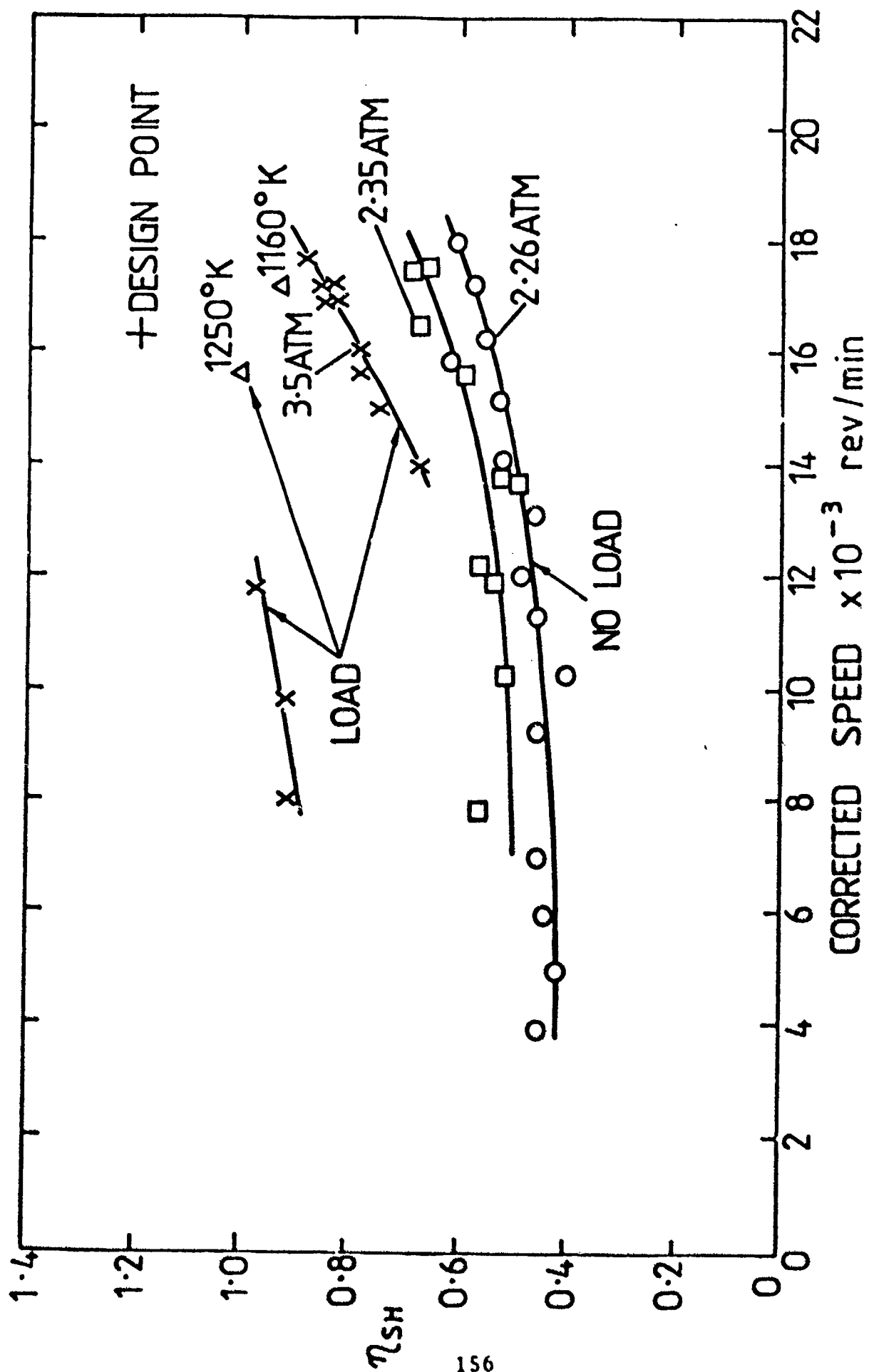


FIG.10 HIGH PRESSURE SCAVENGE EFFECTIVENESS η_{sh}

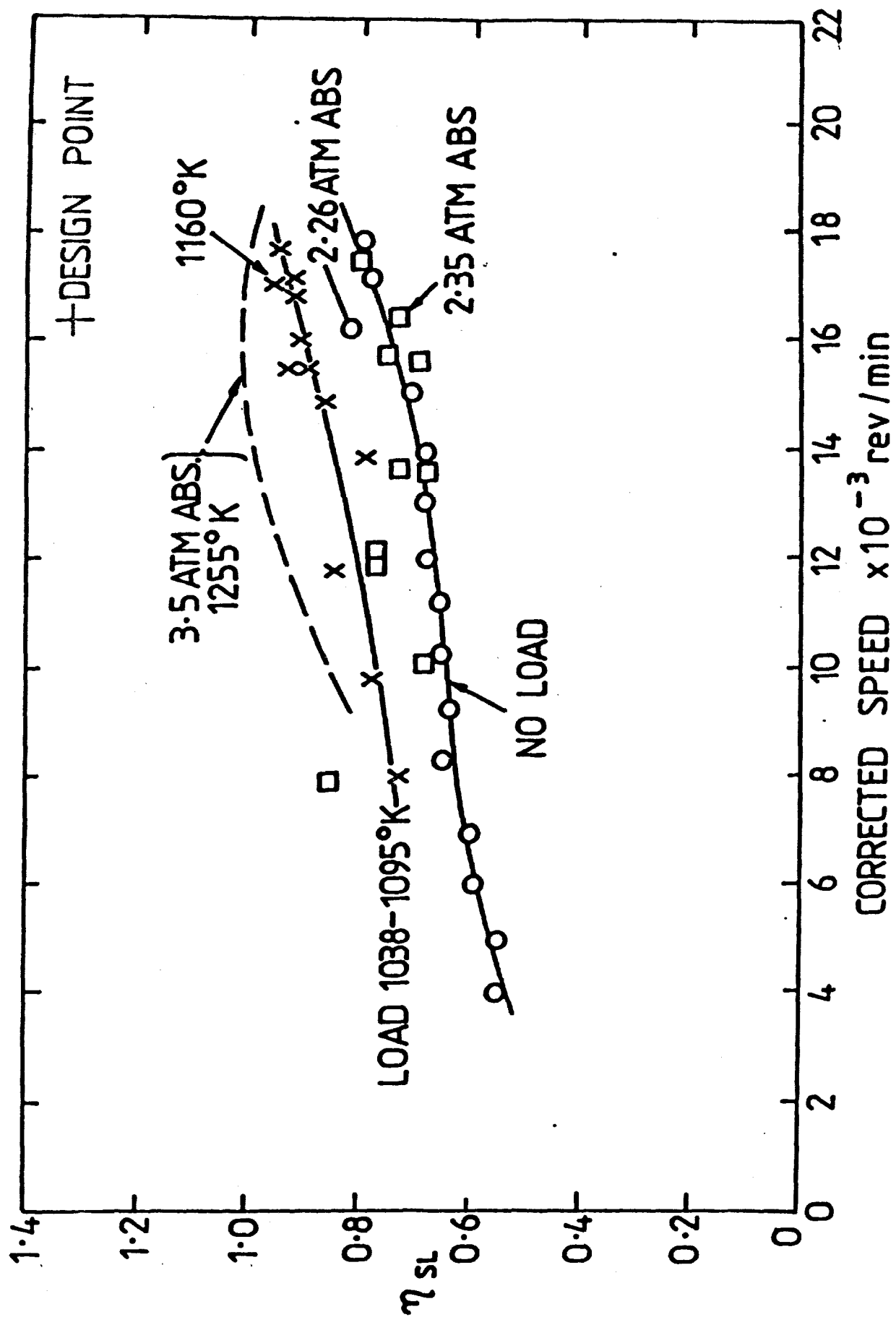


FIG.11 LOW PRESSURE SCAVENGE EFFECTIVENESS η_{sl}

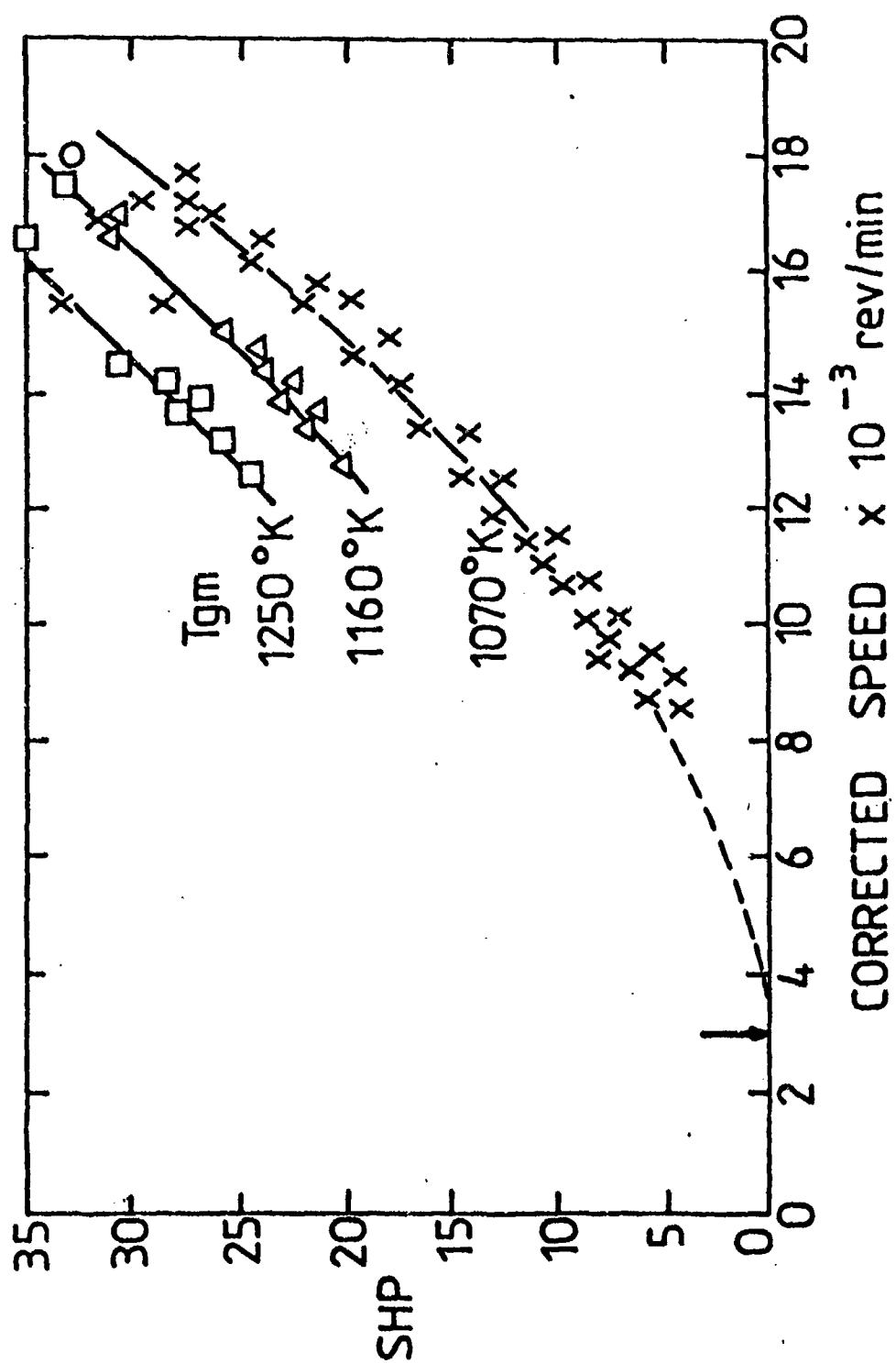


FIG.12 POWER - SPEED CHARACTERISTIC

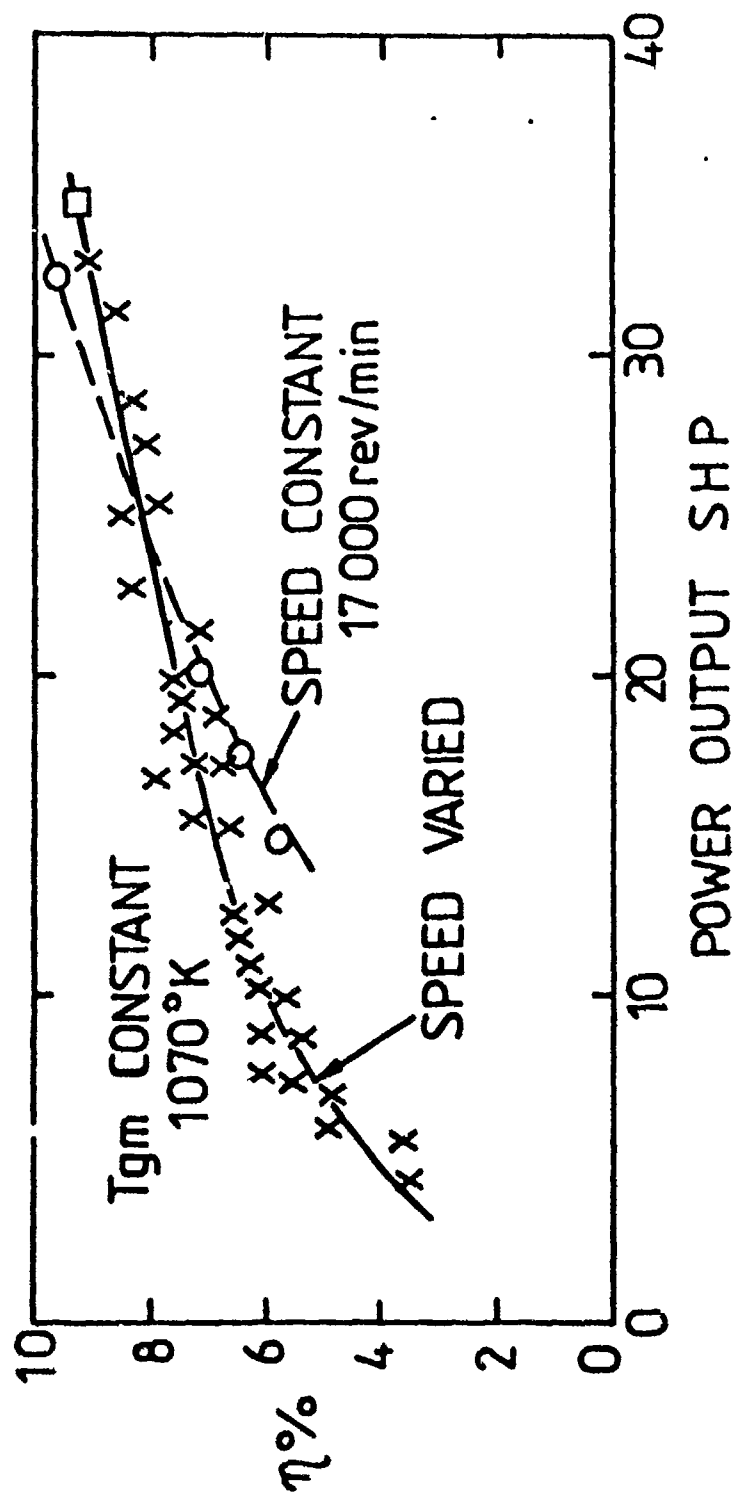


FIG. 13 THERMAL EFFICIENCY (η) - POWER CHARACTERISTIC

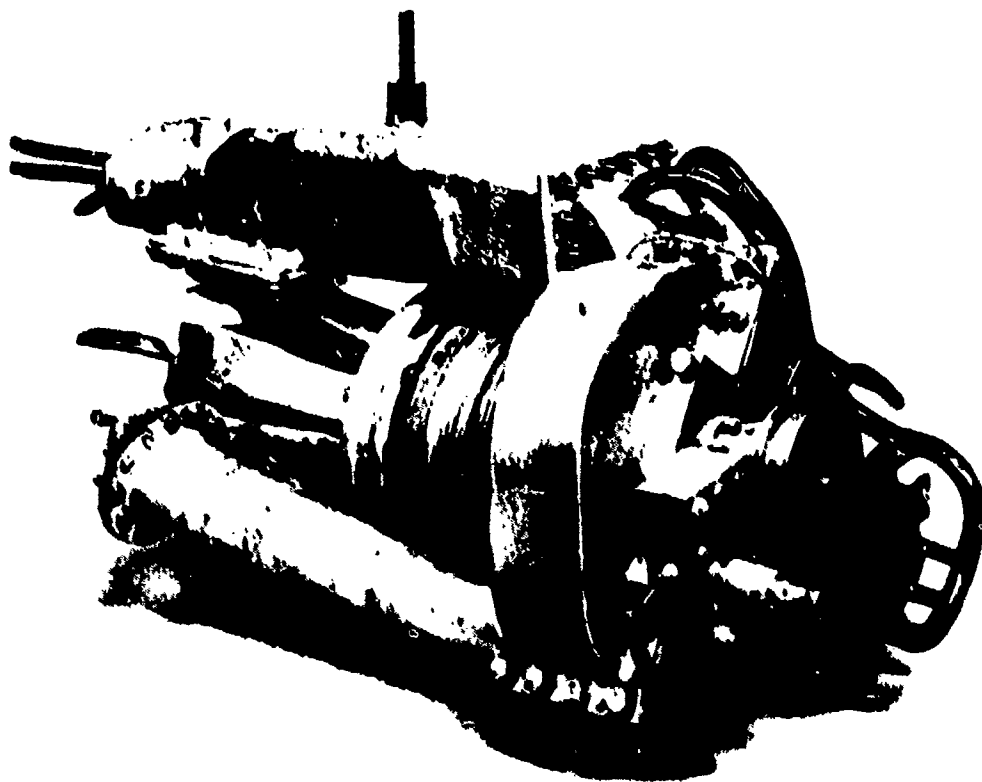


PLATE 1 ASSEMBLED VIEW OF HOME MADE PRESSURE EXCHANGE ENGINE OF
2 $\frac{1}{2}$ INCH ROTOR DIAMETER.

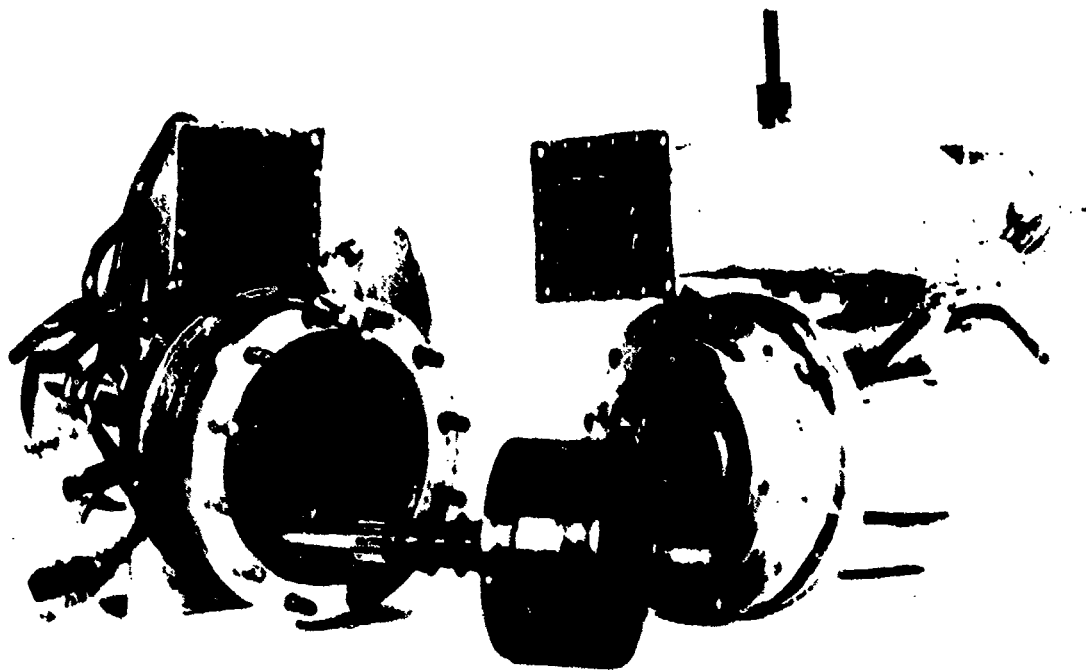


FIGURE 2 EXPLODED VIEW OF THE 1/2 INCH DIO MACHINE.

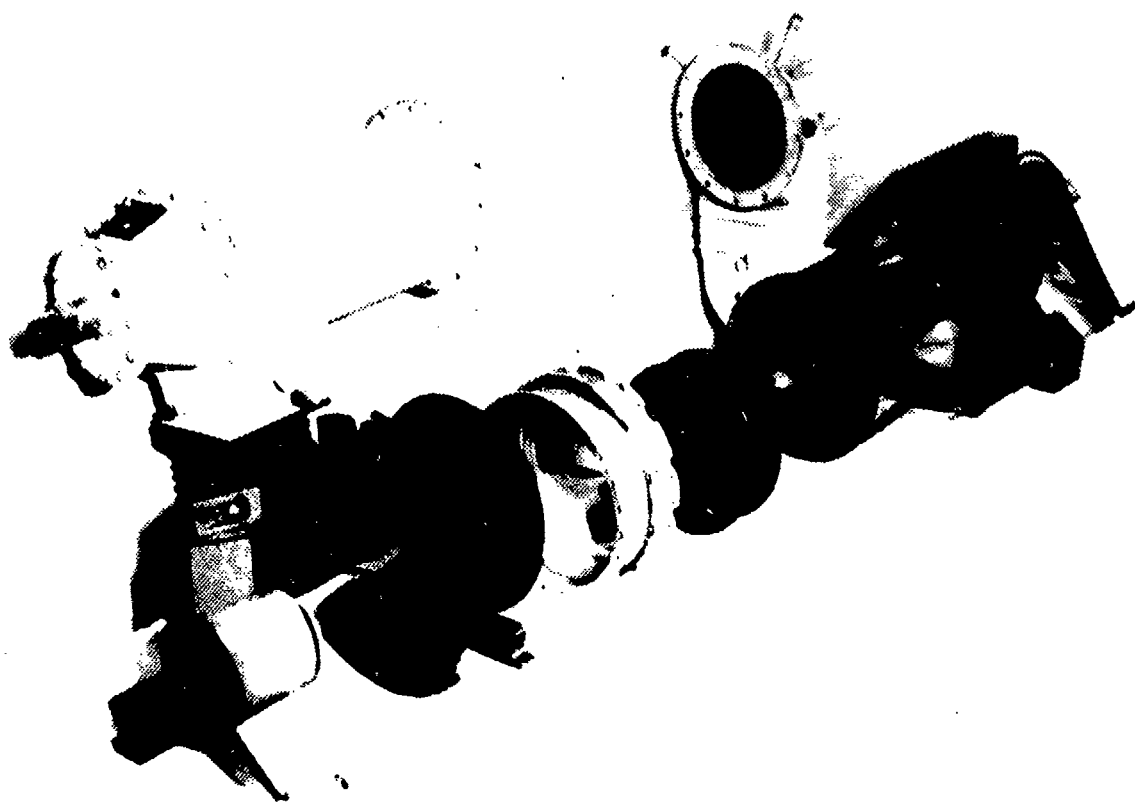


PLATE 1 EXPLODED VIEW OF THE MACHINE, 1/2 INCH SIZE MACHINE.

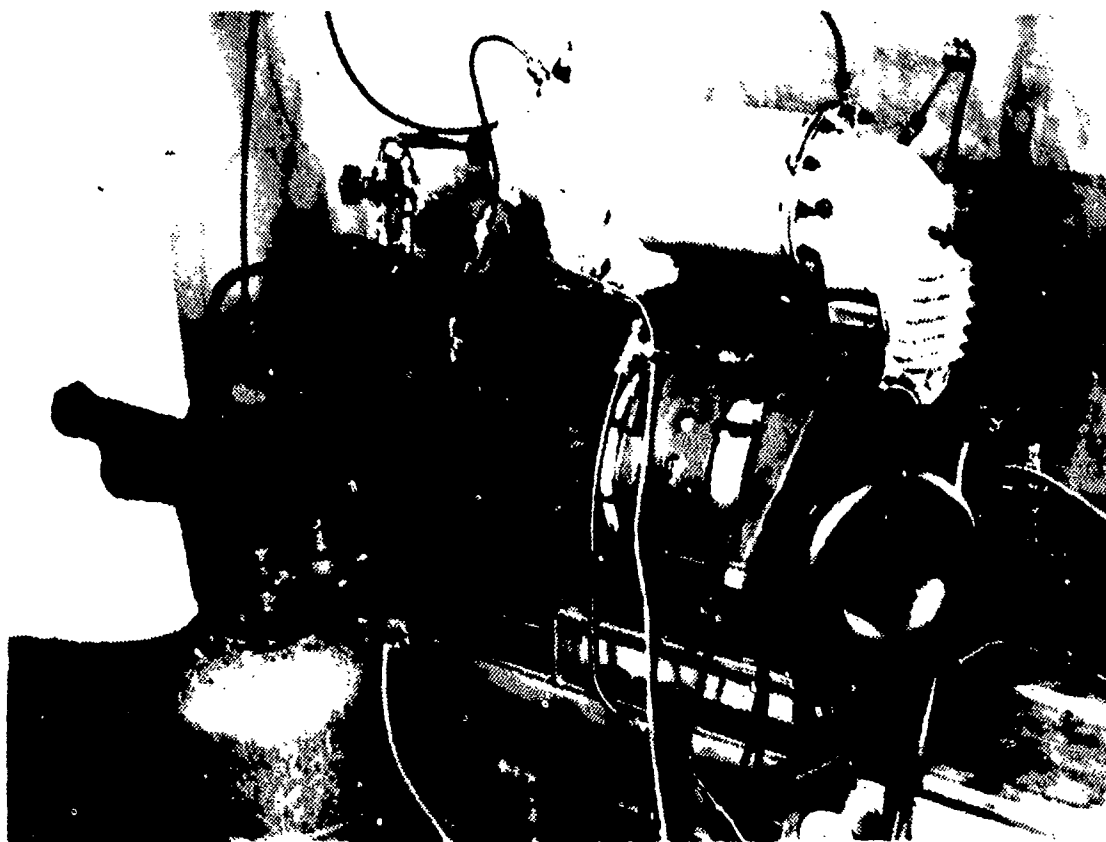


PLATE 4 ASSEMBLED VIEW OF FACTORY BUILT PRESSURE EXCHANGE ENGINE OF
9 INCH ROTOR DIAMETER.

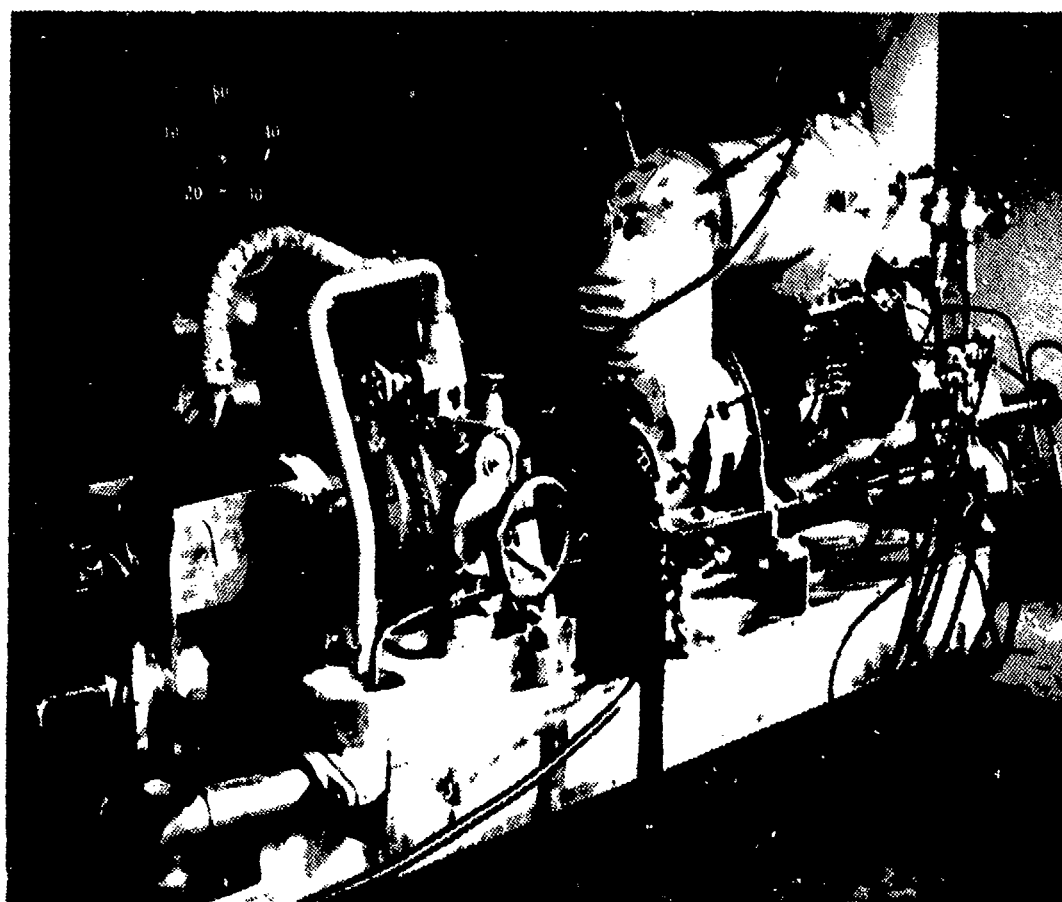


PLATE 5 THE 9 INCH PROPELLER SIZE ENGINE EQUIPPED WITH HYDRAULIC DYNAMOMETER

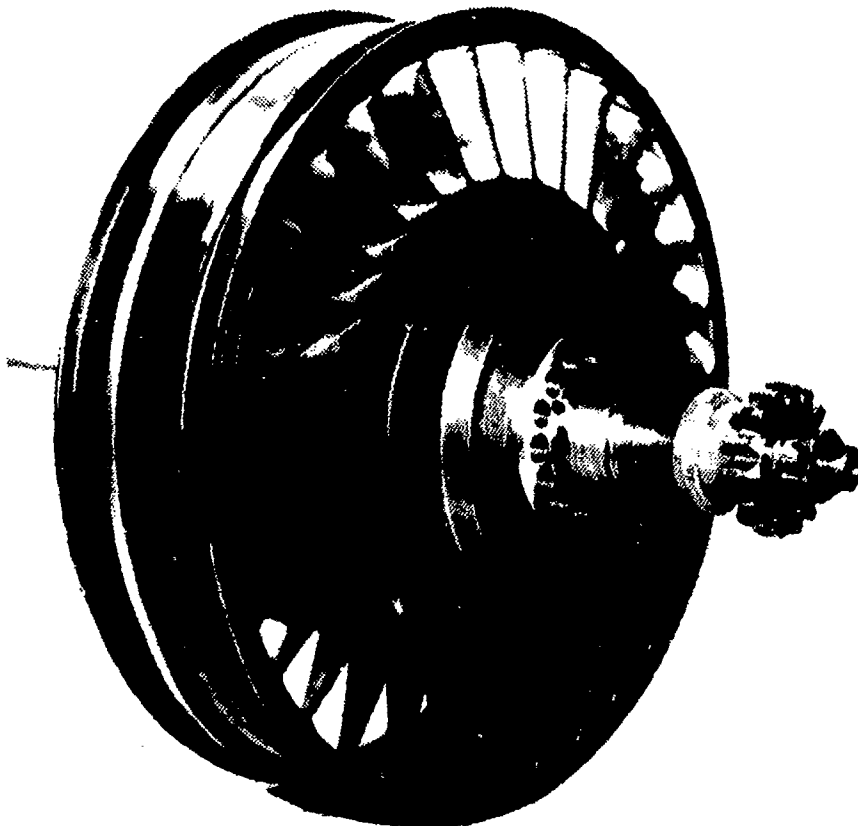


PLATE 6 9 INCH DIAMETER PRESSURE EXCHANGE ROTOR VIEWED FROM THE
INLET END AND SHOWING THE GEAR TOOTH COUPLING.

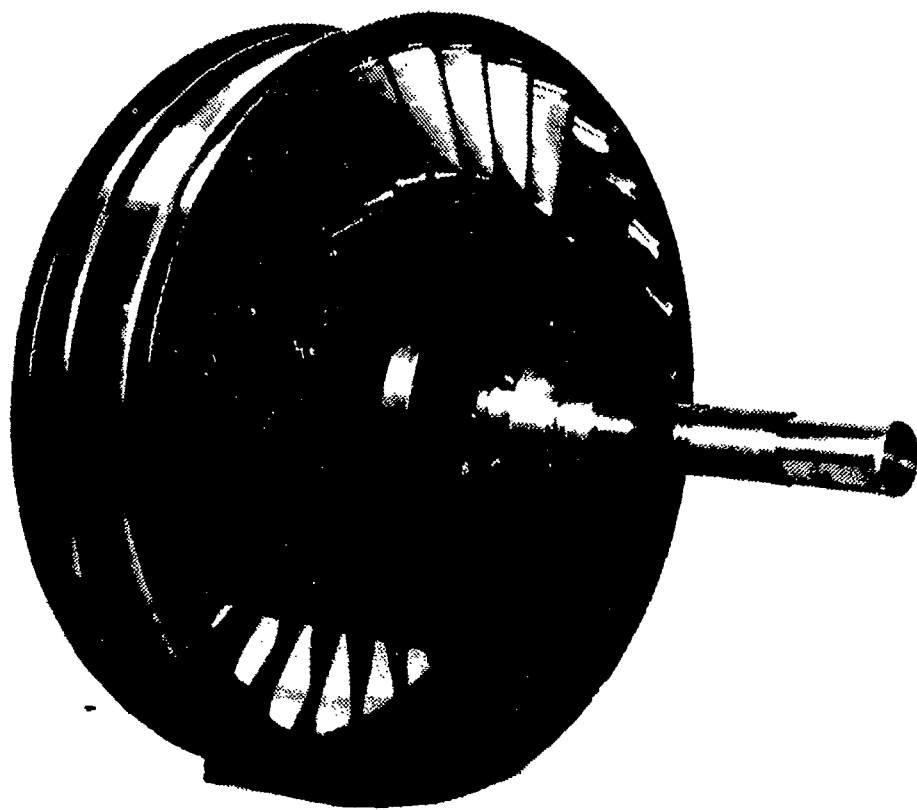


PLATE 7 9 INCH DIAMETER ROTOR VIEWED FROM THE REAR



PLATE 8 REAR VIEW OF THE 9 INCH ROTOR AFTER SUFFERING AN ACCIDENTAL
OVER SPEED AND SHOWING DAMAGE

DEFINITIONS

(1) "TURBINE"

A "Turbine" is a wheel having curved vanes at the rim as shown in FIG.1. A jet of gas, steam or liquid is directed at the vanes which deflect the fluid stream so producing a force which causes rotation. The energy of motion of the fluid (Kinetic energy) is by this means converted to another form of energy called "work" which is delivered by the rotating shaft for driving some other machine. The work per second is the "shaft power". (A windmill is a form of turbine and is now called a "windturbine".)

(2) PRESSURE-VOLUME (P-V) DIAGRAMS

So called "perfect gases" like air can be represented by the perfect gas equation:-

$$P.V = m.R.T \quad (a)$$

$$\text{so } P = m.R.T/V \quad (b)$$

Where:

P is the absolute pressure N/m (1 atm=101325 N/m)

V is volume cubic metres - m

m is mass of the gas - kg

R is the gas constant; for air R=287.1 J/kg/deg.K

T is the absolute temperature in deg. K

$$\text{i.e. } T = t \text{ deg. C} + 273.1$$

Hence, assuming for the time being that temperature remains constant, when the volume increases, the pressure falls. If a closed vessel had a moveable end, such as a piston in a cylinder, the pressure P acting on that piston of area A would produce a force F where:

$$F = P.A$$

If the piston moves a small distance, say x, then there will be an average force P acting over that distance x and mechanical work is done of amount:

$$W = P.x$$

i.e. work = force X distance moved

But this is a form of energy and is extracted from the gas which is pushing the piston, so energy is transferred from the gas so causing its temperature to fall.

But A.x is a volume increase.

So as V increases, T reduces and equation (b) shows the result of these combined effects to be an even greater fall in pressure.

If pressure is plotted against volume as in Fig.4 an expanding gas shows a falling pressure curve and since:

$$\begin{aligned} W &= P \cdot x \\ \Delta P \cdot x &= P \cdot \Delta x \\ \Delta A \cdot x &= V_2 - V_1 \quad (\text{the change in volume}) \\ \text{so } W &= P \cdot (V_2 - V_1) \end{aligned}$$

i.e. work = average pressure \times change in volume.

& this average pressure is absolute i.e. measured from vacuum state.

So the work done is equal to the area under the graph of P against V .

If in Fig.4 for the leak nozzle a piston in a cylinder converted the work starting from pressure P_2 , instead of letting the gas pass a nozzle, then first the piston will move out and have work done on it, but after the pressure has fallen to the atmospheric value P_1 it will have to return to its starting point before another "working cycle" can be executed. An exhaust valve will have to be arranged to open so that exhaust gas can be pushed out against the pressure of the atmosphere, so doing work on it. The net work gained from such a cycle is therefore the cross hatched nearly triangular area W_{p2} .

A turbine driven by the leak as the explosion cell pressure falls to atmospheric will theoretically provide the same amount of work as would the piston in cylinder but uses a different mechanism. First the available energy is converted to the kinetic form as a high speed jet in passing through the leak nozzle, then the turbine blading converts this to shaft work.

Much more work is developed from a given mass of gas discharged from the receiver, as also shown in FIG.4, by the increased area under the P - V diagram shown shaded. This is because of the extra rectangles. At pressure P_2 a volume V_2 is discharged from the receiver, doing work $P_2 \cdot V_2$ but extra work $P_1 \cdot V_2$ is done against the atmosphere so that the net extra work available is $(P_2 - P_1) \cdot V_2$.

Hence when a turbine is used to convert the work available from the expansion of a gas, the jet velocity would be much higher for discharge from the receiver, as compared with the average velocity of discharge for the leak jet. The jet from the receiver would also be steady, whilst that from the leak jet would start from the same speed and then fall steadily, finally to zero speed at the point where the pressure fell to that of the atmosphere. (Ignoring gas inertia). Gas friction heats the gas as well as heat transfer and so areas under the P - V diagram are modified. Output work now becomes this modified area multiplied by a "polytropic efficiency."

WAVE ROTOR RESEARCH & TECHNOLOGY WORKSHOP

NAVAL POSTGRADUATE SCHOOL

MONTEREY, CALIFORNIA

MARCH 26-27, 1985

A BRIEF REVIEW OF THE
G.E. WAVE ENGINE PROGRAM
(1958-1963)

ATUL MATHUR
EXOTECH INC., CAMPBELL, CALIF.

G.E. WAVE ROTOR RESEARCH PROGRAM

KEY PERSONNEL*

J.F. KLAPPROTH

A. PERUGI

J.S. GRUSZCZYNSKI

L.J. STOFFER

C.C. ALSWORTH

* omissions in the list above are unintentional

RELEVANT DATES

- 1954-1956 : EARLY WORK ON PRESSURE RISE COMBUSTORS AT NACA
SIMPLIFIED ANALYSIS OF WAVE ROTOR OPERATION
(IN VARIOUS ARRANGEMENTS). .
- 1956-1959 : ANALYSIS METHOD IMPROVED AND APPLIED AT G.E.
CYCLE STUDIES INITIATED
FABRICATION OF WAVE ENGINE RESEARCH VEHICLE
FIRST TESTING IN LATE 1959
- 1960-1961 : EXTENSIVE TESTING OF WAVE ROTOR WITH AXIAL
PASSAGES (PRESSURE EXCHANGER)
APPLICATION STUDIES
- 1961-1963 : FABRICATION AND TESTING OF WAVE ROTOR WITH
SKEWED PASSAGES
APPLICATION STUDIES, REPORTS, RECOMMENDATIONS

A BRIEF REVIEW OF THE G.E. WAVE ENGINE PROGRAM (1958-1963)

Early work done at NACA on pressure rise combustors provided part of the motivation that led to the General Electric Wave Engine program. The wave engine concept per se was initially proposed as a means of approaching constant volume combustion in a component that could be used with turbomachinery. The specific design requirements were to have controlled inflow and outflow processes, which were essentially time-steady in nature and circumferentially uniform. The combination of a wave rotor and a combustor then constituted a combustor across which, instead of a pressure loss, a net gain in pressure was effected.

During the period 1956-1959, the simplified analysis methods used at NACA were improved upon and applied at General Electric. The field method of calculating and plotting characteristics was adopted and a number of viable wave diagrams constructed. During the same time period, fabrication and installation of the test rig was carried out. Rotors with axial passages and different solidities were built and first tests were initiated in late 1959.

From 1959 to 1961, over a period of about one and a half years, extensive testing of the research vehicle was carried out and documented, along with application studies and analysis of results in an effort to improve the performance.

Initial testing and analysis had indicated that rubbing type seals were not suitable for this application and that air-gap seals were more practical. Since air-gap seals were required, it was felt that speeds approaching those of turbomachines could and should be utilized for further useful output. This led to the analysis and testing of a rotor with skewed or staggered passages along with more application studies of units with wave rotors capable of producing shaft power.

Fig.1 shows equivalent constant volume and constant pressure combustion processes on a temperature-entropy (T-S) diagram. Point 2 on this figure is the flow at inlet to the rotor, and the time unsteady induction and subsequent stagnation of the flow raises its pressure to point 3. On mixing with residual gases in the rotor at point 4, state 5 is attained and internal combustion raises the temperature and pressure level to state 6. The exhaust process leads to the gases expanding out to a final stagnation condition at point 7. Closure of the exhaust port brings the pressure of the residual gases back to point 4 and the cycle is repeated. Since the charging process is independent of the actual heat addition process, the same thing can be accomplished by means of external combustion also as shown by the process 2-3-8-9-7.

Figures 2 and 3 show the internal and external combustion processes pictorially. Note that the device has only two ports in the internal combustion mode. External combustion was chosen for the test program since it eliminated problems peculiar to internal combustion, but this was done at the expense of a more complicated mechanical arrangement as well as a timing problem. It is noted however that G.E. still intended to pursue the internal combustion alternative at a later date.

Figures 4, 5, and 6 show the essential features of the experimental setup. Note in Fig.4 that provision had been made for a starting air supply, but that this was found to be unnecessary.

Fig.5 shows the brazed construction of the axial passage rotor. A dovetail construction was envisioned originally but was abandoned due to cost of machining and rotor stability concerns. The rotor was designed to operate continuously at a temperature of 1500 degrees Fahrenheit. Fig.6 shows a photograph of the test rig, and although no details can be discerned, some idea of the essential layout can be obtained.

As mentioned earlier, a number of wave diagrams were calculated, one of them configured for the so-called 'A' type valve or port plates shown in Fig.7. Almost all the testing was based for essentially the same 'family' of wave diagrams, i.e. a counter scavenging mode where the two gas streams are brought onto and taken off the rotor from the same side by means of the inlet and transfer ports, and the delivery and exhaust ports.

Figs. 8, 9, and 10 show the computed performance for the wave engine in terms of the overall temperature ratio and the overall pressure ratio across the machine. Fig.8 shows the computed ideal performance for different exhaust pressure ratios. It was established early on that the highest overall pressure gain could be achieved with a sonic discharge through the exhaust port. For unsteady flow, sonic discharge corresponds to an exhaust pressure ratio of approximately 0.3 (for a specific heat ratio of 1.3).

Taking some losses into account, a set of reduced performance curves for the wave engine was computed for four or five different valve plates (i.e. different wave diagrams); three of these performance curves are shown in Fig.9.

Some actual data points are shown in Fig.10 with the estimated performance of 'B' type valve plates superimposed. Towards the end of 1960, fairly respectable overall pressure gains or pressure ratios of 1.2 to 1.3 could be achieved consistently, and this performance was then used to carry

out application studies with the wave rotor. Figures 11 through 15 show the outcome of these studies.

Performance of shaft engines with the wave rotor incorporated into low-cost turbomachinery is compared in Fig.11 with that of a simple shaft engine cycle (i.e. one without the wave rotor component). For a given turbine inlet temperature, a marked improvement is achieved by using the combined configuration. In the case of very small shaft engines, performance is further compromised. Fig.12 shows the estimated performance for the combined unit with specific fuel consumption (sfc) ranging from 0.75 to 2.1 as opposed to the figures for the simple cycle, (see Fig.13), of 1.3 and 3.4 respectively.

A weight and cost comparison was carried out for a production T-58 GE-06 engine with and without the wave rotor incorporated into it. Table 1 gives a detailed breakdown for the estimates made in this study. The -89 was the current production engine and the -204 was a projected production engine with upgraded performance.

A summary of the key features highlighted by this application study is given in Fig.14, showing the significant simplification achieved in the hardware by incorporating the wave rotor into the T-58. Apart from the cost reduction, a significant improvement in the sfc was also realized. The mechanical design support group involved with the program drew up the conceptual layout for the T-58 engine with the wave rotor component as shown in Fig.15.

The G.E. wave engine operated in a counterflow scavenging mode, effecting a 180 degrees reversal in the flow direction for each of the two gas streams. Consequently, staggered or canted passages (i.e.those inclined at a certain angle to the axis of the rotor) showed promise in bringing about a net angular momentum change through this flow direction reversal, making shaft power extraction from the rotor possible. This concept was also tested in further work done at G.E. from 1961 to 1963. Application studies were carried out wherein such a rotor could be used to drive a supercharging compressor. A conceptual layout for such a configuration is shown in Fig.16, which shows the wave rotor coupled to a supercharging centrifugal compressor. During this time also, extensive water table tests were conducted to gain further insight into inflow and outflow losses, the effect of port and cell wall edge geometry and mixing of the two streams inside the rotor.

The wave engine program was stopped around the end of 1963 due, in part, to General Electric's commitment to pursue large engine development exclusively.

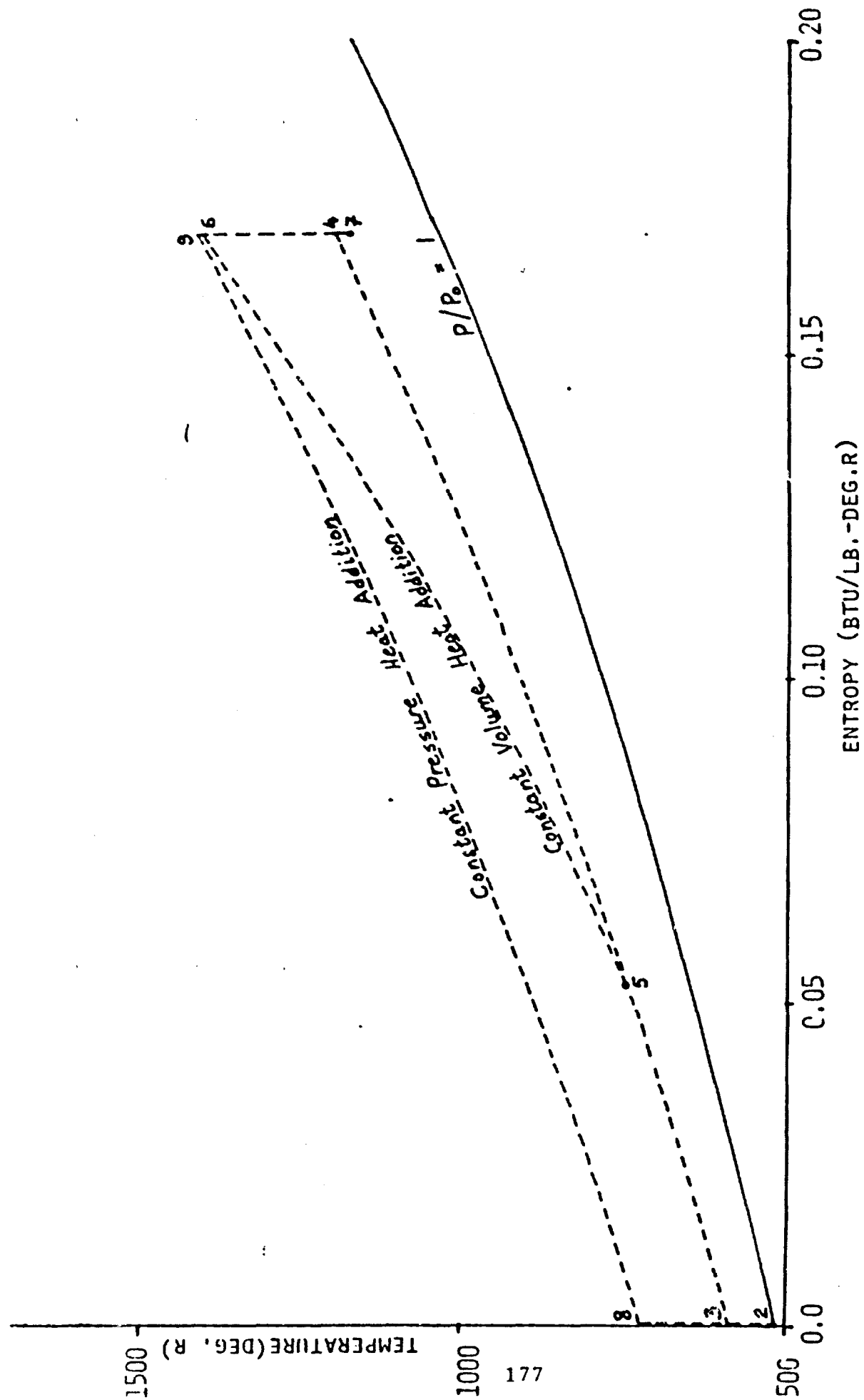


FIG. 1 IDEAL FLOW PROCESS FOR INTERNAL AND EXTERNAL COMBUSTION

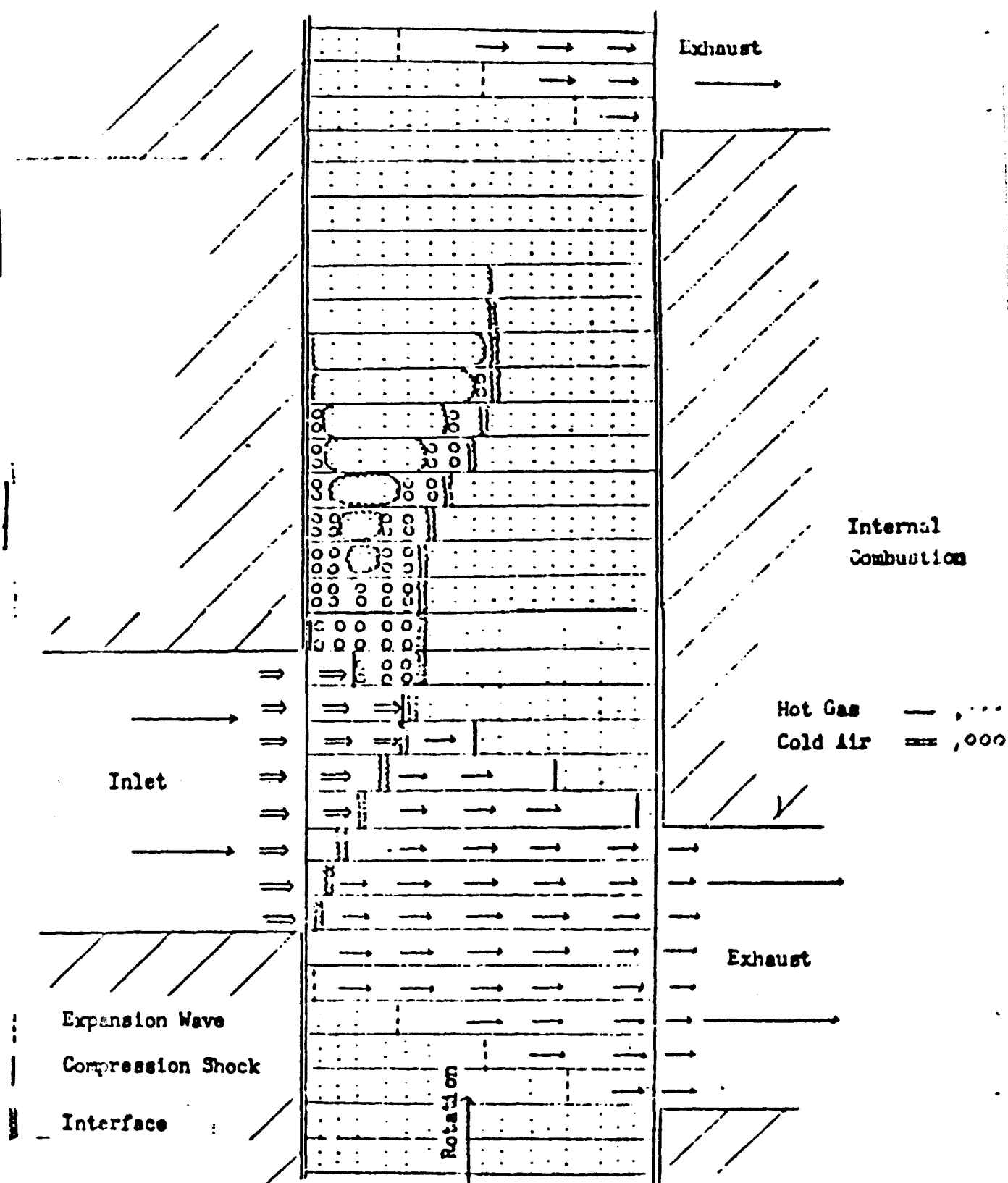


FIG. 2

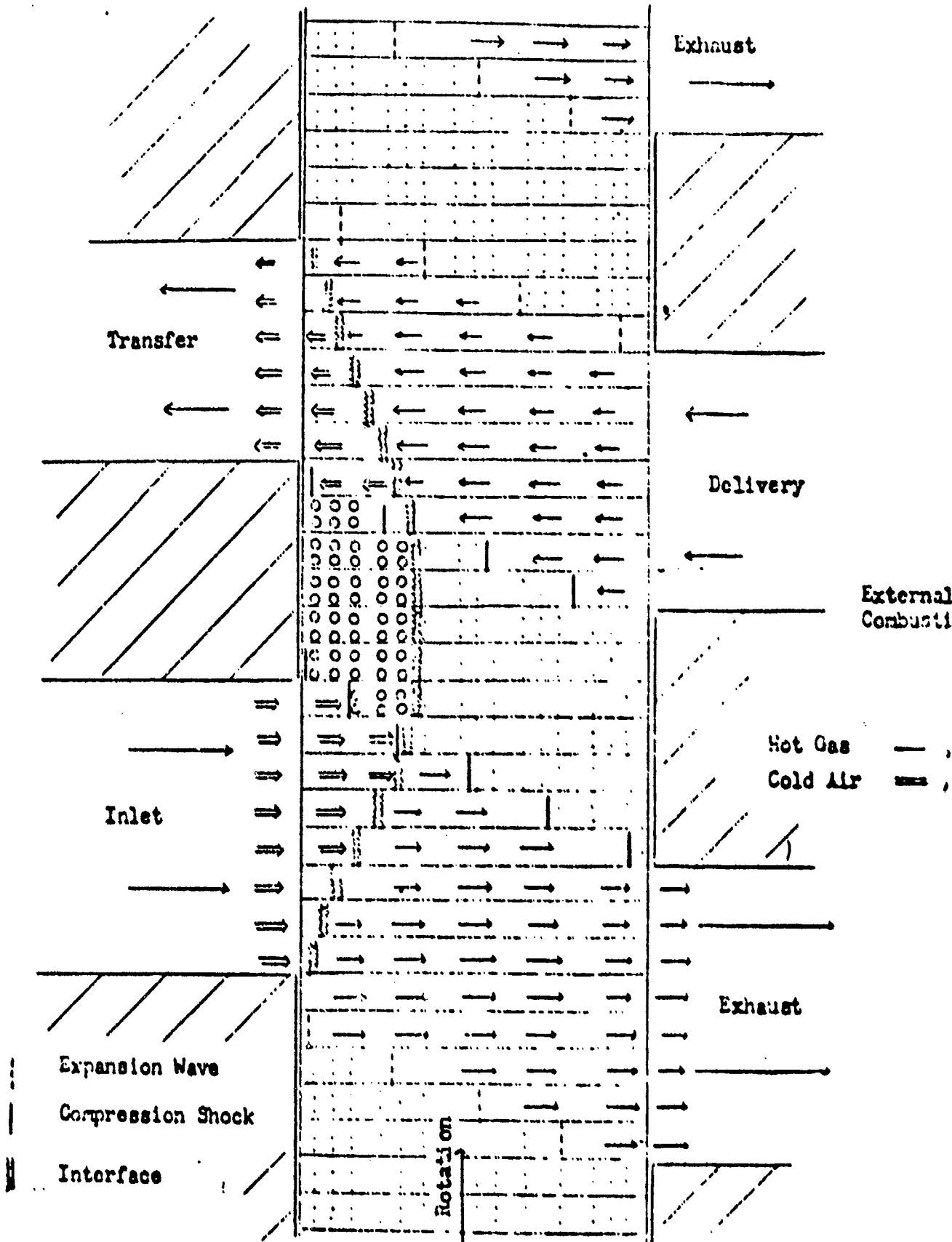


FIG. 3

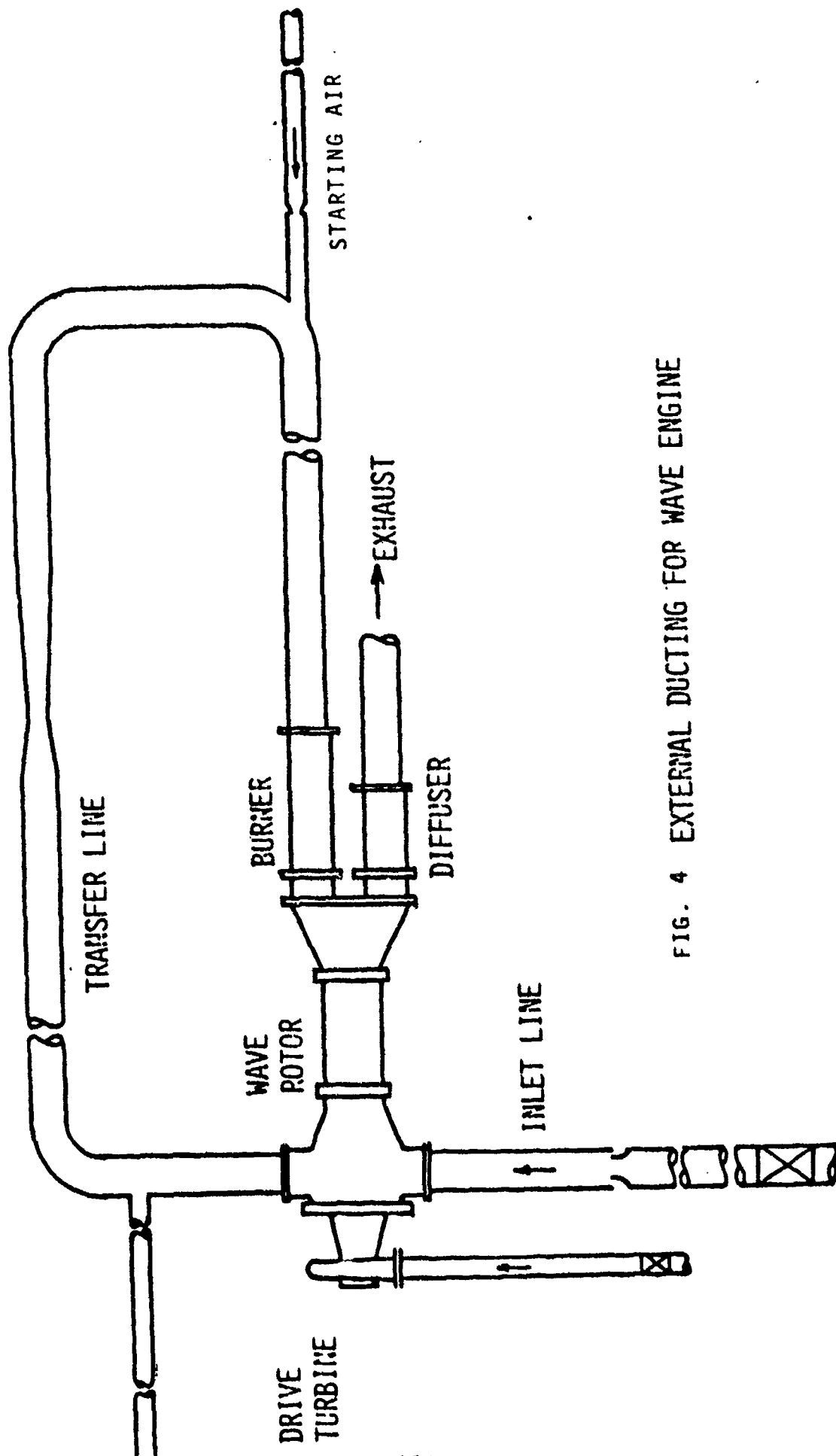


FIG. 4 EXTERNAL DUCTING FOR WAVE ENGINE

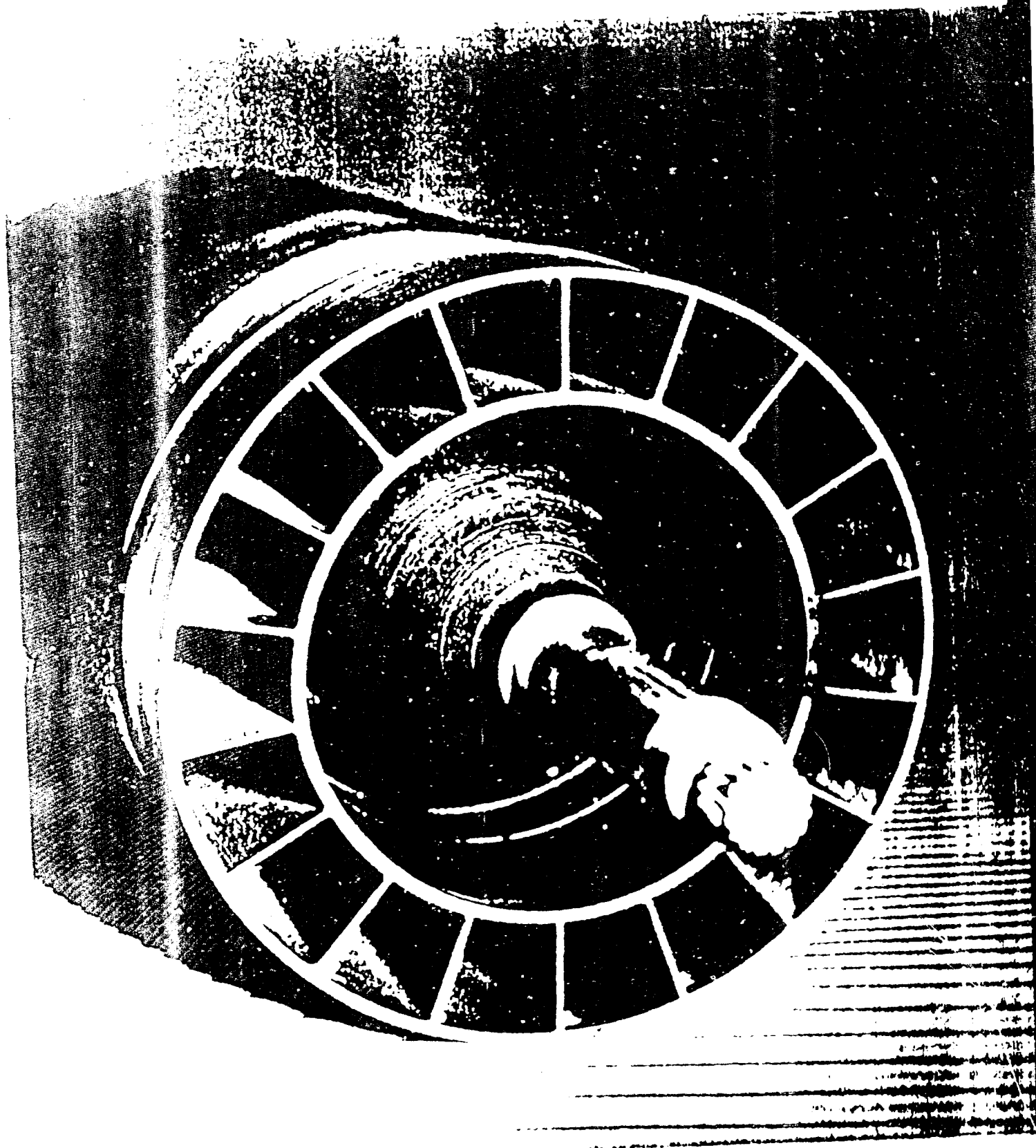
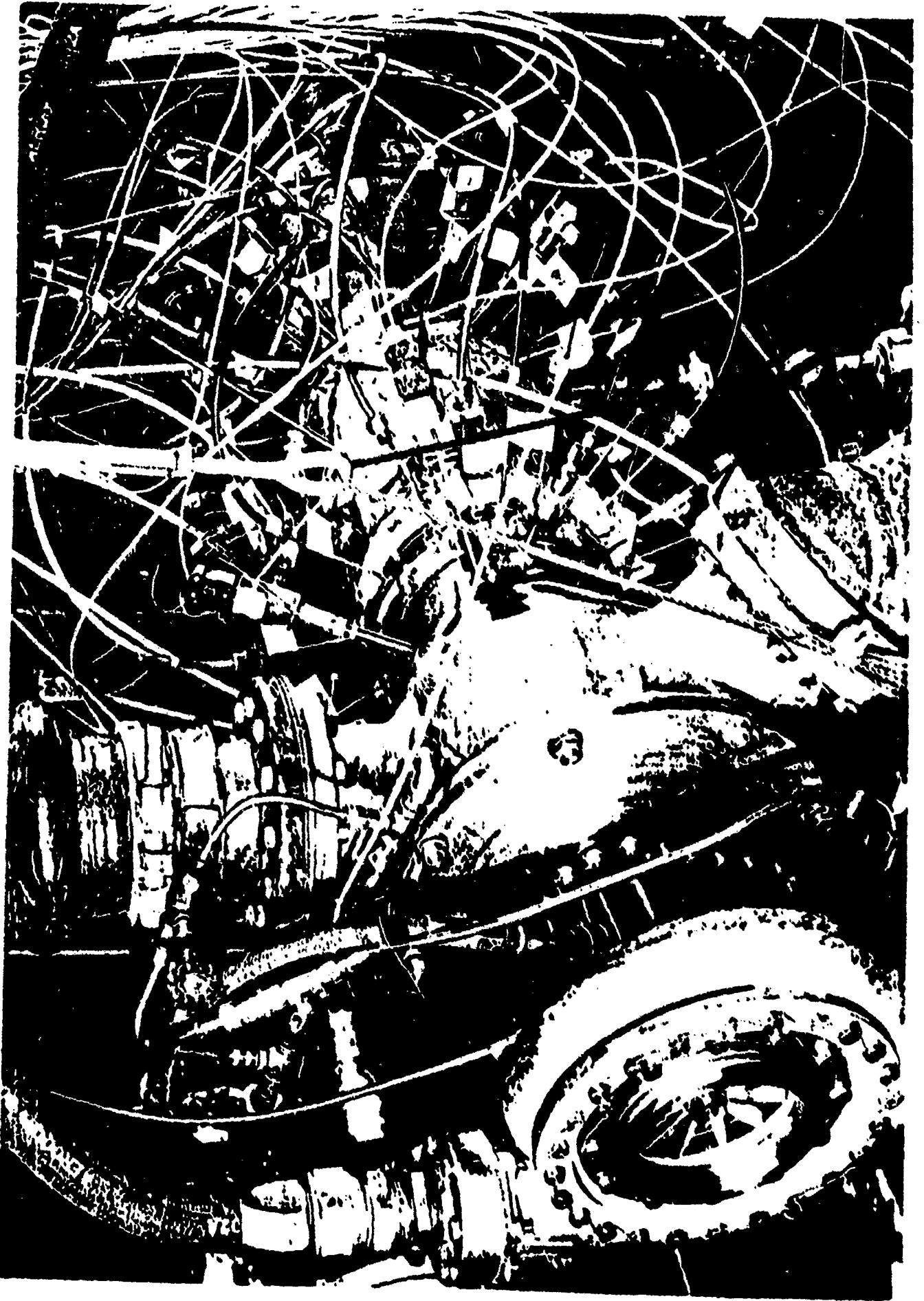


FIG. 5 C. E. ROTOR WITH AXIAL PASSAGES
(GRAZED CONSTRUCTION)

0103005



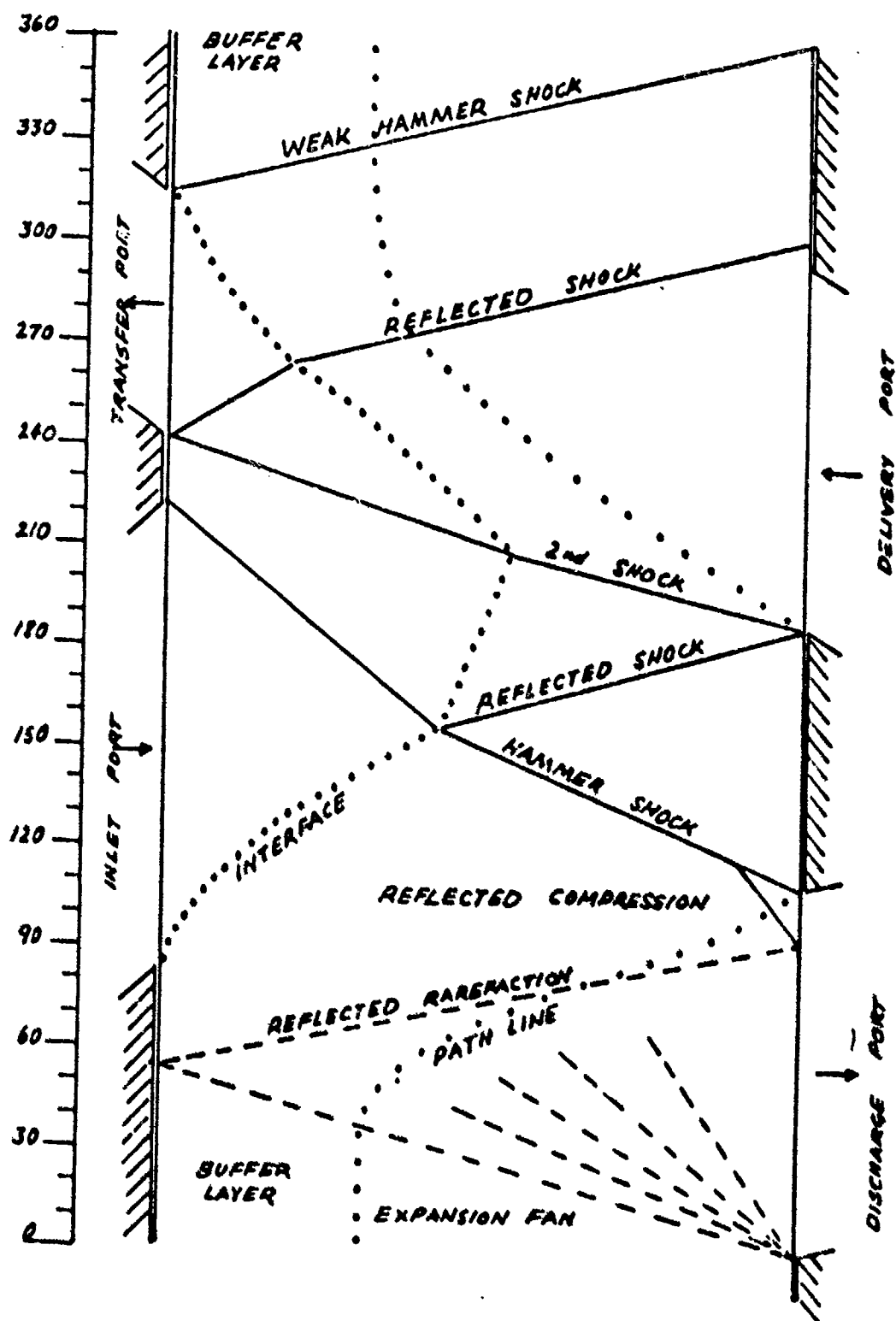
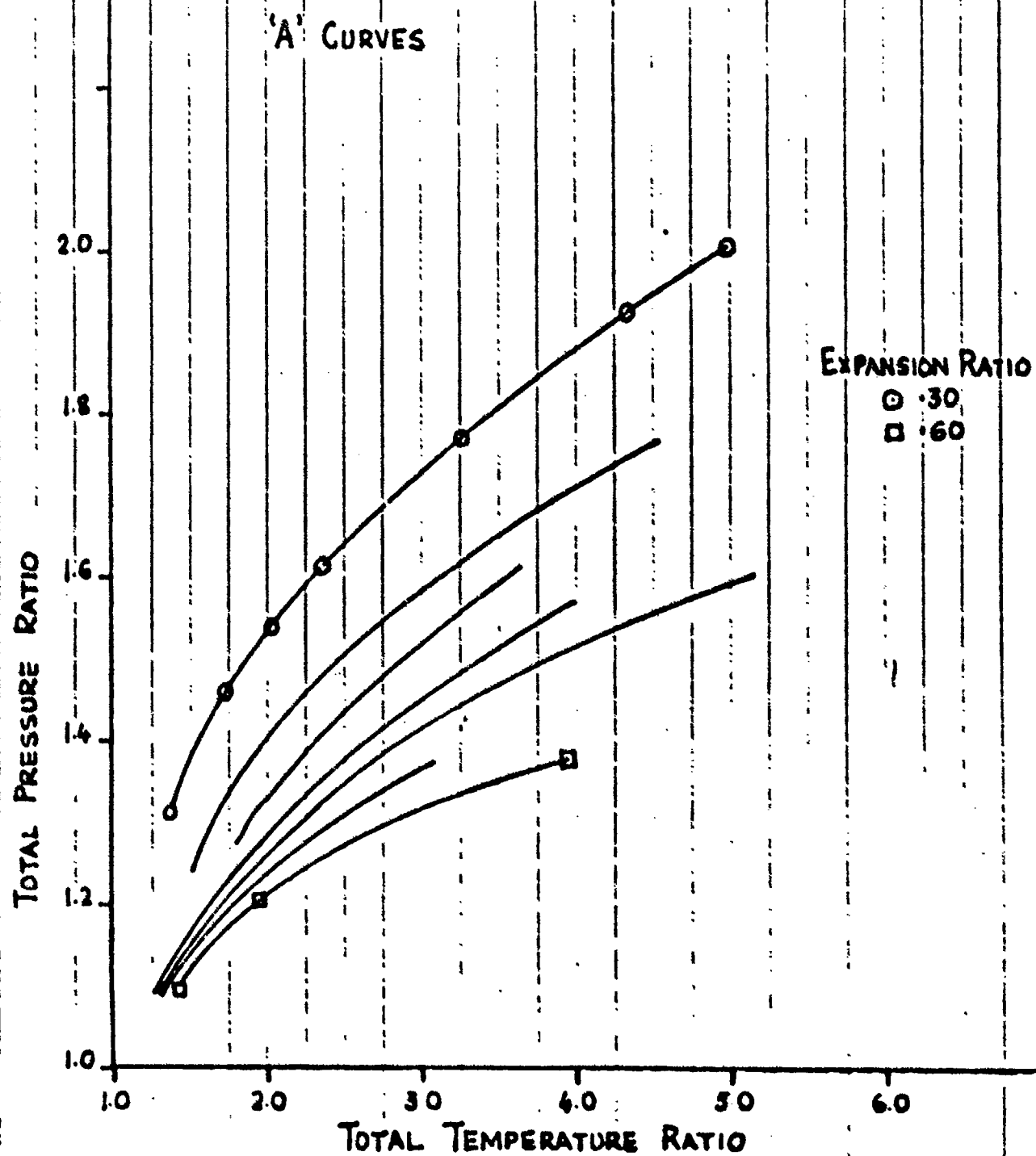


FIG. 7' WAVE DIAGRAM FOR 'A' VALVE PLATES

FIG. 8 WAVE ROTOR AS GAS GENERATOR
IDEAL PERFORMANCE CURVES



82000 40 8 10 12 14 16 18 20 22 24 26 28 30 32 34 36 38 40 42 44 46 48 50 52 54 56 58 60 62 64 66 68 70 72 74 76 78 80 82 84 86 88 90 92 94 96 98 100

FIG. 9 ESTIMATED PERFORMANCE LEVELS
FOR WAVE ROTOR

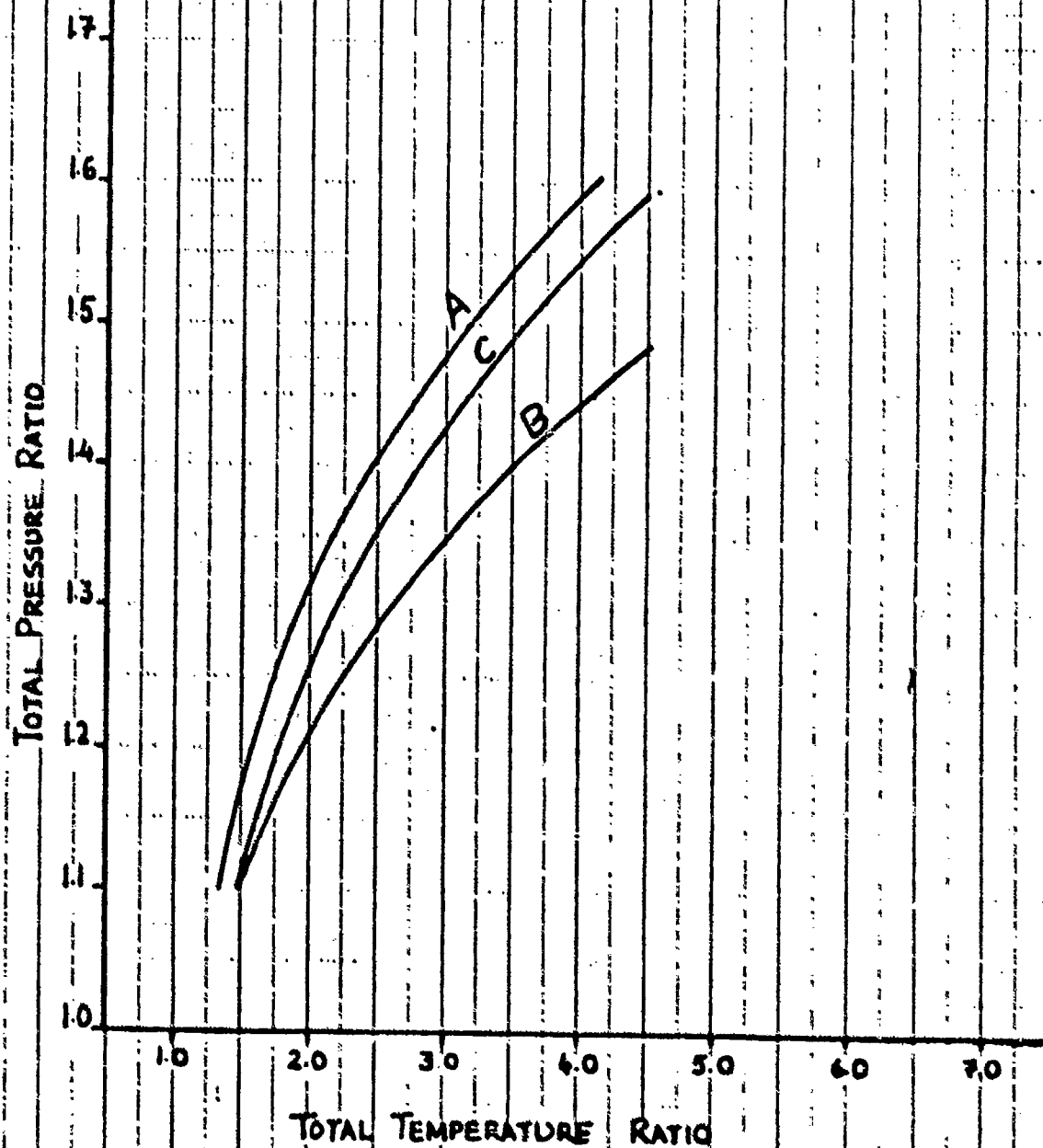
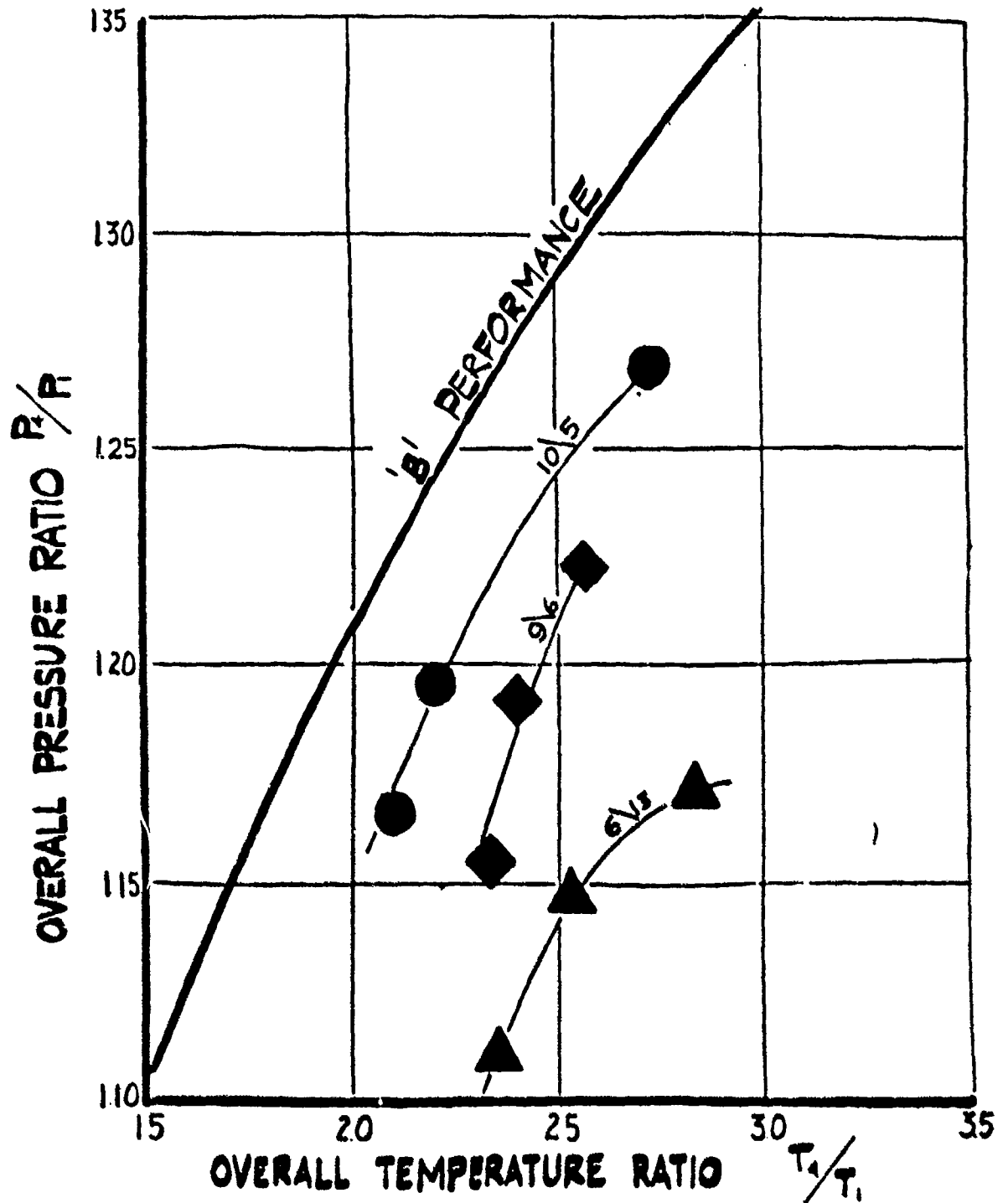


FIG. 10

WAVE ENGINE PERFORMANCE



01021031

FIG. 11

PERFORMANCE OF SHAFT ENGINES WITH WAVE ROTOR AND LOW-COST TURBOMACHINERY

'C' CURVE PERFORMANCE
ASSUMED FOR WAVE

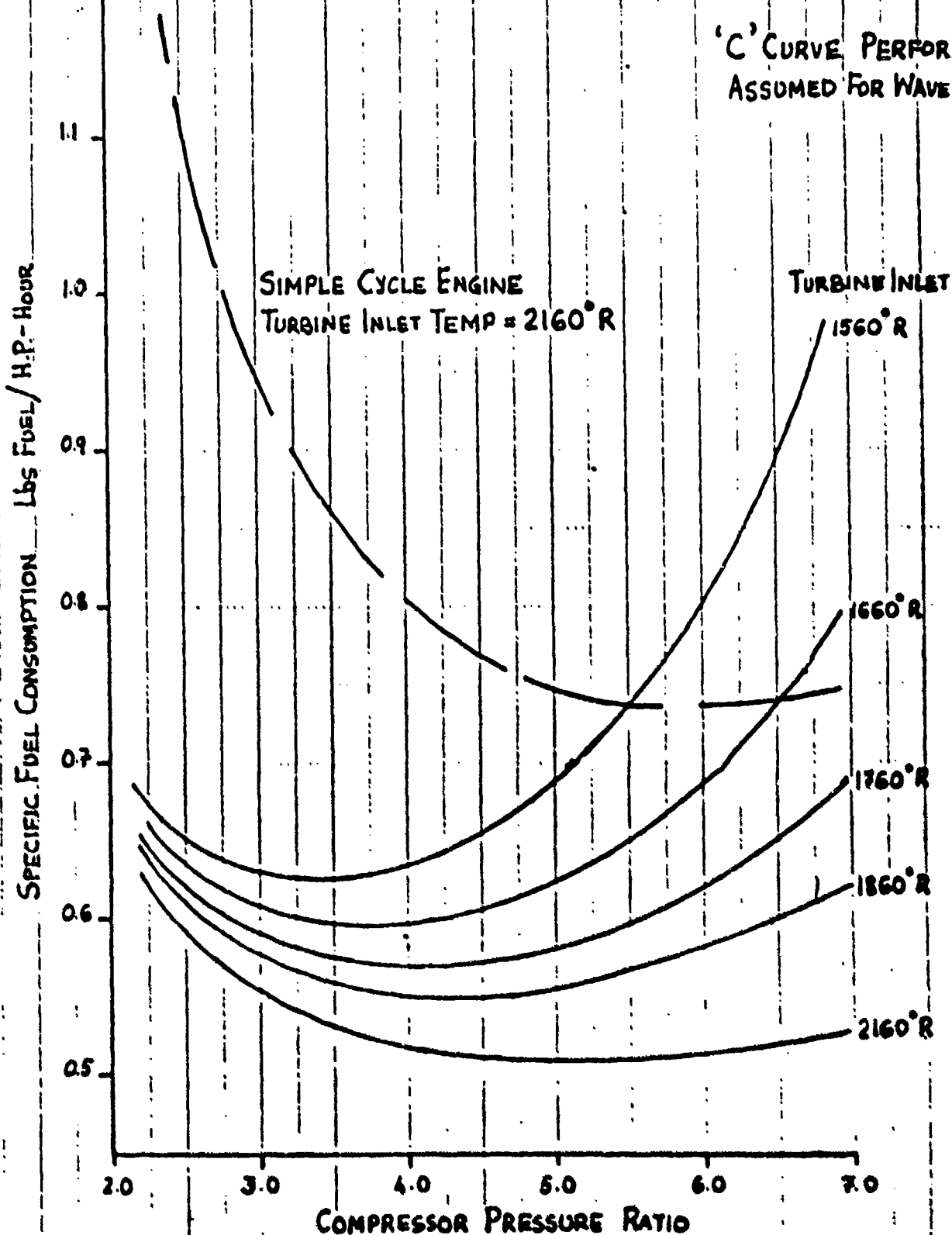


FIG. 12 PERFORMANCE OF SMALL SHAFT ENGINES
WITH WAVE ROTOR AND LOW-COST TURBOMACHINERY

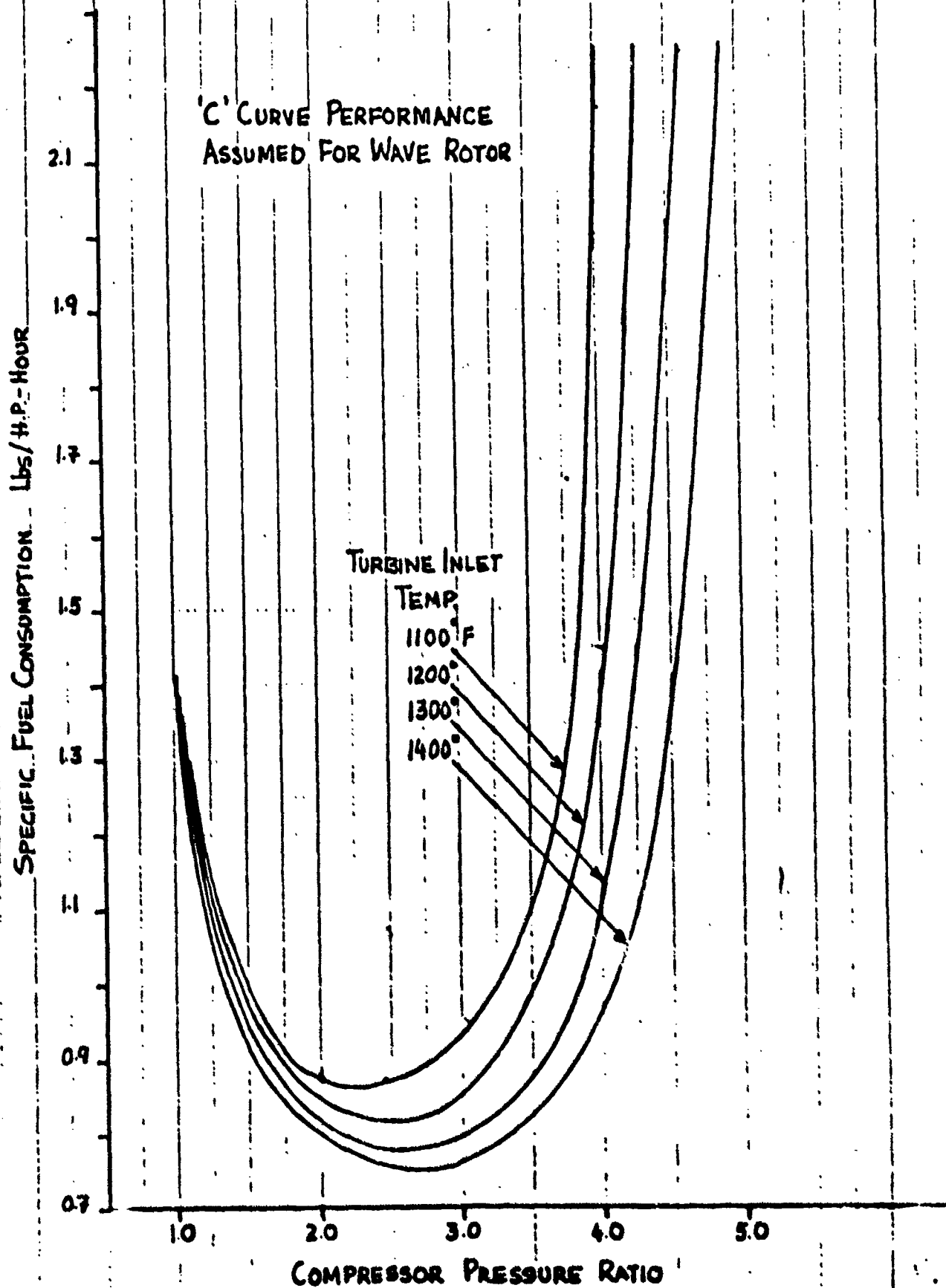
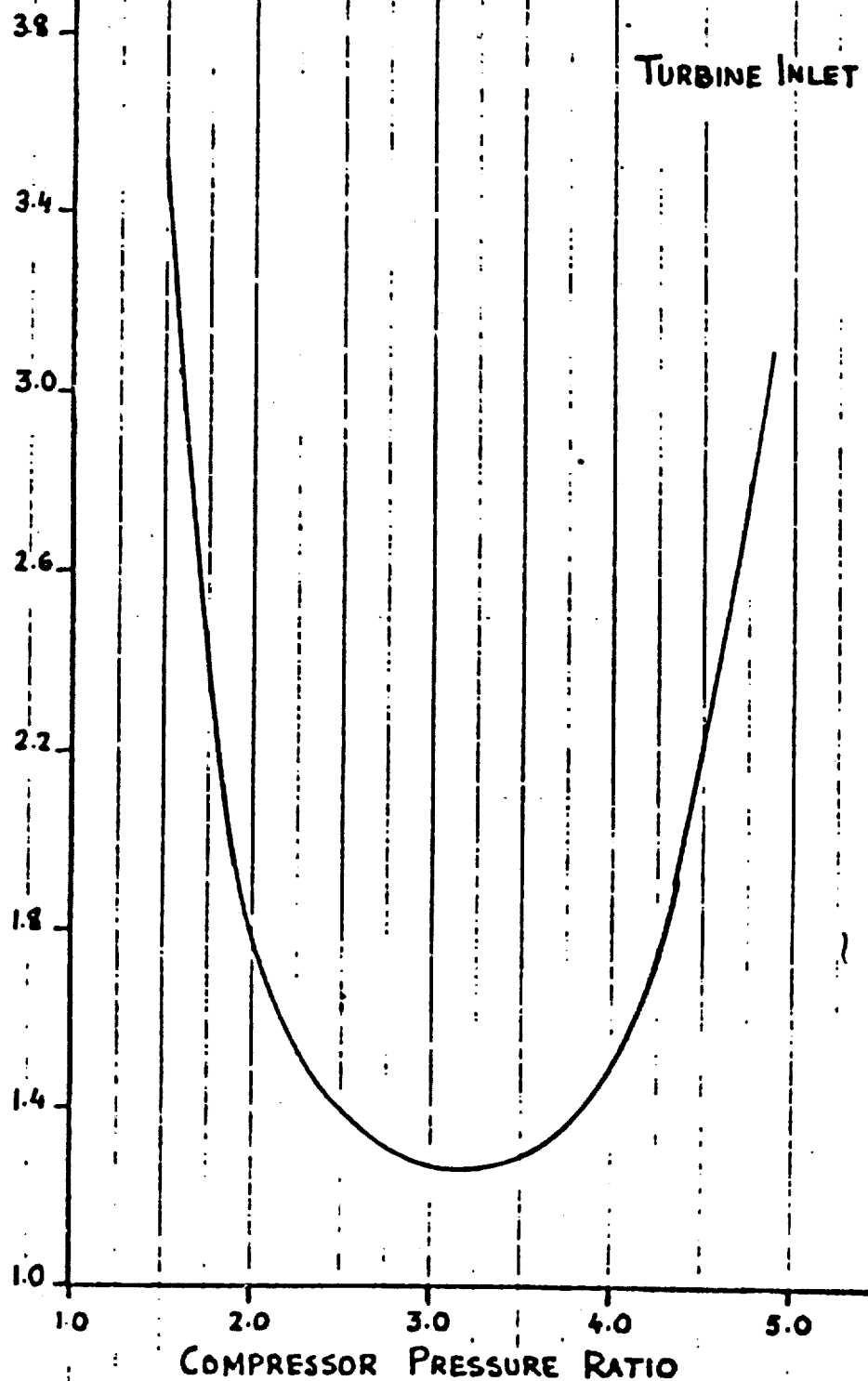


FIG. 13

PERFORMANCE OF SMALL SIMPLE CYCLE ENGINES (LOW COST TURBOMACHINERY)

SPECIFIC FUEL CONSUMPTION lbs/H.P.-Hour

TURBINE INLET TEMP = 1600°F



Description	Existing T-58 Configuration		Prototype T-58 Have Engine Configuration			
	Wgt.	Lbs.	-89 Current \$ (1)		-89 Basic \$ (2)	
			-204 Current \$		-204 Basic \$ (2)	
1. Compressor Rotor	24.5	7516	4616		15.1	
2. Compressor Stator	30.1	12114	6915		13.5	
3. Accessory Control Parts	19.1	2427	1825		17.1	
4. A/C Controls Parts (2)	23.4	9737	9044		21.4	
5. Turbine Rotor	24.0	5461	4219		18.0	
6. Turbine Stator	26.9	6539	5053		14.0	
7. Combustor Parts	11.4	1945	1129		23.0	
8. Wave Rotor	-	-	-		9.5	
9. Structures Parts	20.1	5156	3291		43.4	
10. Gear and Lube System	12.8	2483	2907		14.3	
11. Power Plant Parts	3.2	621	438		3.2	
12. Rotor Control	-	-	-		6.0	
Totals	195.5	53949	39607		193.5	
%	100	100	100		102.5	
					93.7	
					76.3	
					53.2	
					83.9	
					63.8	

1. Estimate includes only A & B parts.

2. Does not consider control simplification

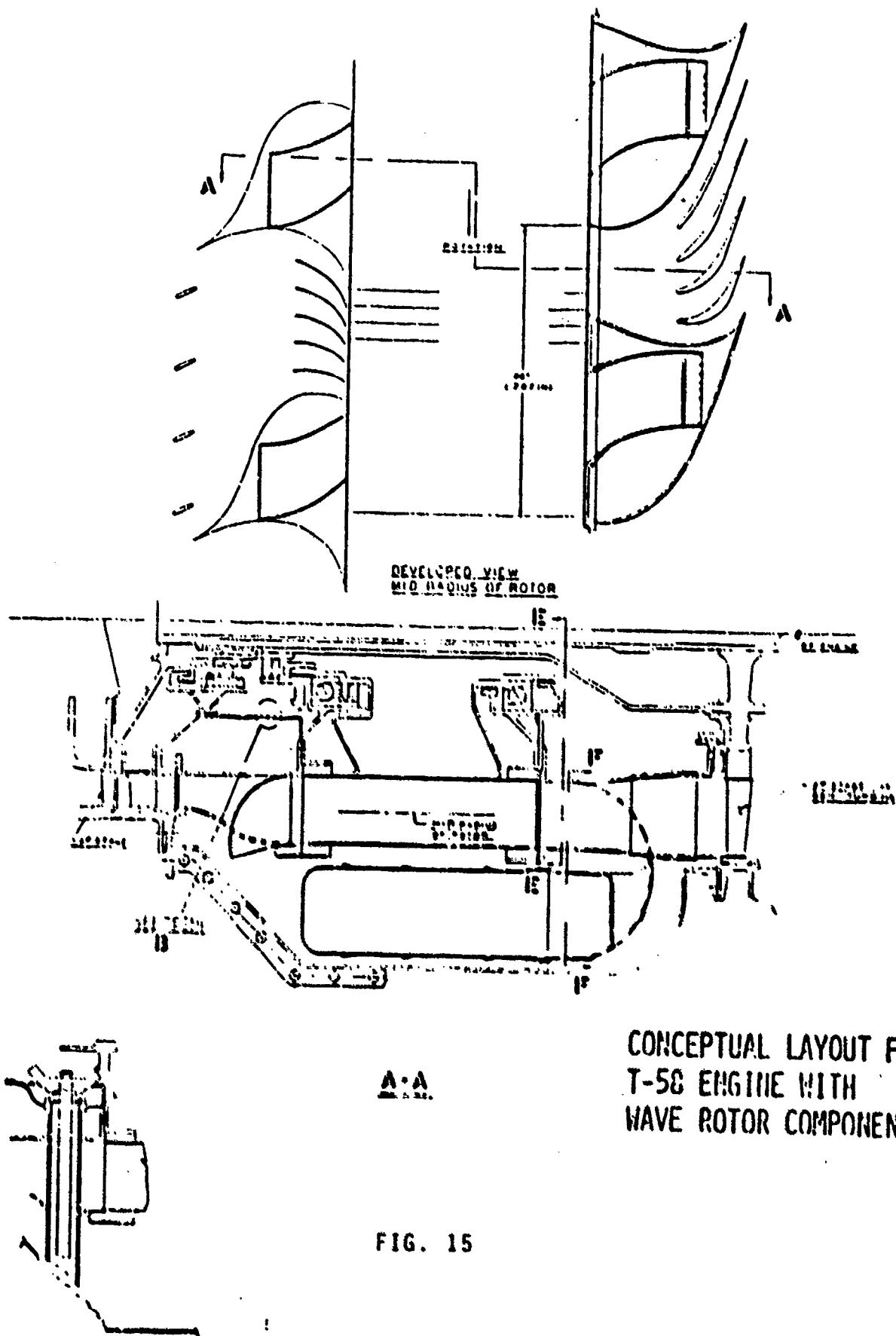
TABLE I
COST AND WEIGHT COMPARISON TABLE
-85: PRESENT PRODUCTION ENGINE (1960)
-204: PROJECTED PRODUCTION ENGINE

T-58 ENGINE APPLICATION SUMMARY

TURBOMACHINERY SIMPLIFIED THROUGH :

- APPROX. 50% REDUCTION IN COMPRESSOR STAGES
- ELIMINATION OF IGV'S AND VARIABLE GEOMETRY FOR REMAINING COMPRESSOR STAGES
- ELIMINATION OF HIGH TEMPERATURE FIRST STAGE TURBINE
- HARDWARE FIT WITHIN EXISTING ENVELOPE;
OVERALL ENGINE LENGTH REDUCED .
- 15% REDUCTION IN S.F.C. FOR SAME COMBUSTOR DISCHARGE TEMPERATURES
- SUBSTANTIAL COST REDUCTION

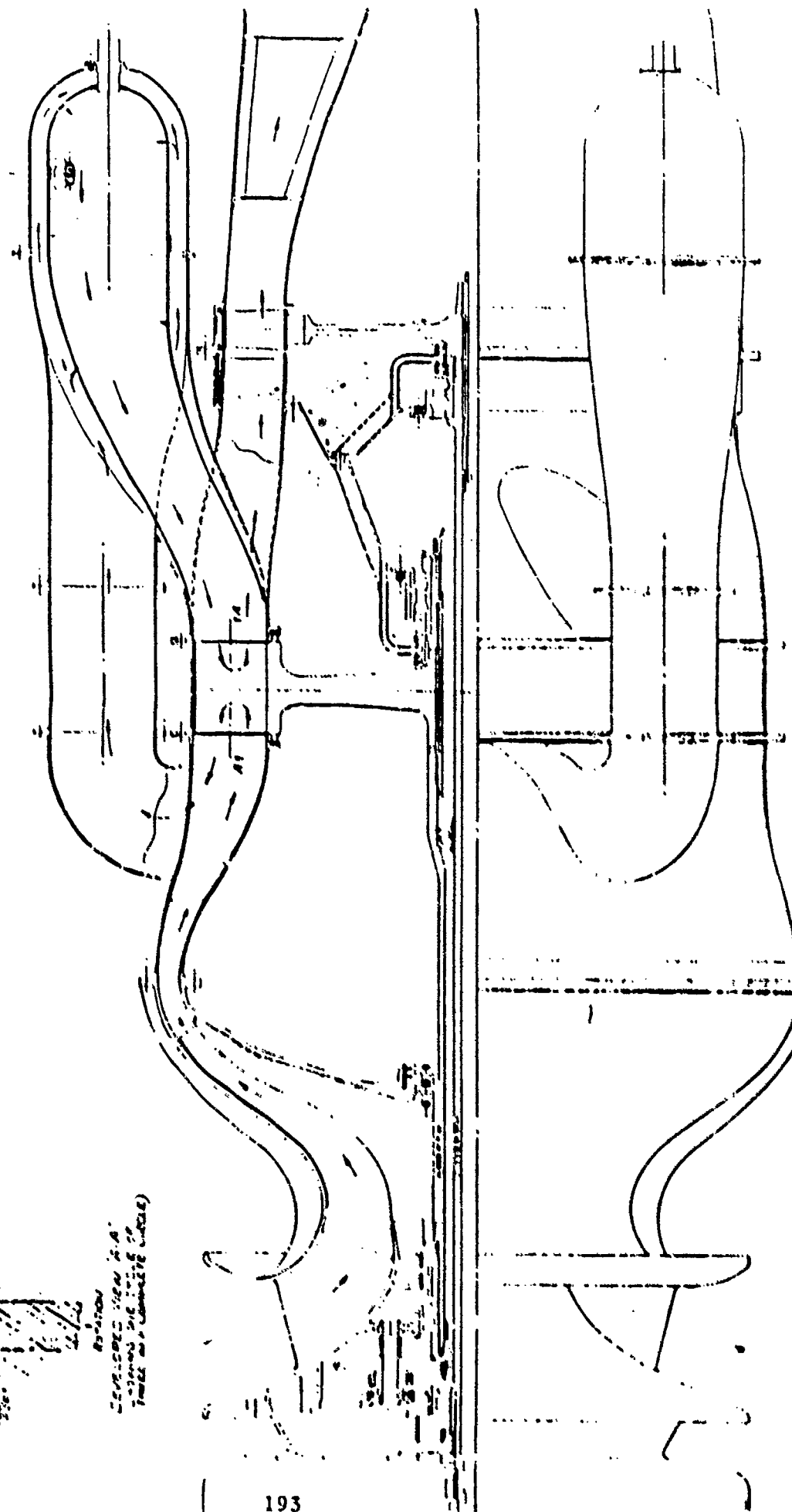
FIG. 14



CONCEPTUAL LAYOUT FOR
T-50 ENGINE WITH
WAVE ROTOR COMPONENT

FIG. 15

193



SHOCK-EXPANSION WAVE ENGINES - NEW DIRECTIONS FOR POWER PRODUCTION

BY H. E. WEBER

Professor of Mechanical Engineering, San Diego State University
and Consultant, Science Applications International Corporations

For decades prodigious amounts of money and effort have been spent on conventional turbomachinery development. Initially, improvements in performance were rapid. However, in the last two decades better performance of these machines has slowed considerably. Compressor efficiencies have been near their present limits of 88% to 92% for many years. High pressure ratios required of high performance engines are not efficiently produced in the conventional turbomachines. High cycle pressure ratios for high cycle efficiency require many stages of conventional compression. Compressors, especially in small turbomachines, decrease in efficiency as the number of stages increase due to the large amounts of surface area and relatively large leakage passages in the higher pressure stages.

The requirement for many stages of conventional compression also results in heavy machines. If high compressor pressure cannot be attained the turbine exhaust gas temperature may be considerably above the compressor discharge temperature; a regenerator or recuperator is then required for acceptable cycle efficiency. This results in considerable complication and high engine weight.

Maximum turbine inlet temperatures in conventional machines have also been near their limit for many years. High temperatures and high pressures required for light weight, high efficiency machines are inconsistent with the requirements for high strength materials. To increase permissible turbine inlet temperatures compressor discharge air has been used for blade cooling. Use of this air soon reaches its limit because the high pressure cooling air is then not available for power production. Engine power and cycle efficiency begins to decrease and a limit on turbine inlet temperature results.

Consequently, new concepts in power and thrust production are required. One class of machines which may alleviate many of the above described problems are the wave rotors or engines. These operate with time dependent flow in the moving rotor blade passages and steady flow in the stator parts. This paper deals with actual and potential performance of these types of wave machines and comparison with conventional turbomachines.

SHOCK-EXPANSION WAVE ENGINES - NEW DIRECTIONS FOR POWER PRODUCTION

by H. E. Weber

Professor of Mechanical Engineering, San Diego State University
Consultant, Science Applications International Corporation, La Jolla, CA

Abstract

For decades prodigious amounts of money and effort have been spent on conventional turbomachinery development. Initially improvements in performance were rapid. However, in the last two decades better performance of these machines has slowed considerably. Compressor efficiencies have been near their present limits of 88% to 92% for many years. High pressure ratios required of high performance engines are not efficiently produced in the conventional turbomachines. High cycle pressure ratios for high cycle efficiency require many stages of conventional compression. Compressors, especially in small turbomachines, decrease in efficiency as the number of stages increase due to the large amounts of surface area and relatively large leakage passages in the higher pressure stages.

The requirement for many stages of conventional compression also results in heavy machines. If high compressor pressure cannot be attained the turbine exhaust gas temperature may be considerably above the compressor discharge temperature; a regenerator or recuperator is then required for acceptable cycle efficiency. This results in considerable complication and high engine weight.

Maximum turbine inlet temperatures in conventional machines have also been near their limit for many years. High temperatures and high pressures required for light weight, high efficiency machines are inconsistent with the requirements for high strength materials.

To increase permissible turbine inlet temperatures compressor discharge air has been used for blade cooling. Use of this air soon reaches its limit because the high pressure cooling air is then not available for power production. Engine power and cycle efficiency begins to decrease and a limit on turbine inlet temperature results.

Reciprocating engines are cooled by both cooling jacket flow and cyclic intake of cool working air. However, these machines are heavy and suffer from friction and heat loss. They are, therefore, of limited use in high speed, light weight vehicles, or anywhere space saving and light weight are required.

Consequently, new concepts in power and thrust production are required. One class of machines which may alleviate many of the above described problems are the wave rotors or engines (1 thru 15). These operate with time dependent flow in the moving rotor blade passages and steady flow in the stator parts.

Introduction

Principles of shock compression in time dependent flow have been known for over half a century. However, in the 1940's when Brown Boveri was developing a workable pressure exchanger, the Comprex*, high strength materials for relatively high temperature applications were being developed rapidly. Because of this development, steady flow turbomachines received the attention of researchers in that field. Unsteady flow machines took a back seat even though shock compression is very efficient; e.g., single shock pressure ratios up to 2.5 are over 90% efficient compared to isentropic compression.

For the past two decades new materials development has slowed and it is time to reexamine the shock and expansion wave turbomachines. These devices are naturally cooled by the cool air ingested by the rotor; blades on the rotor pass through these regions of cool flow in each revolution resulting in moving blade temperatures about the average of the hot combustion gases and cool intake air.

Additionally these wave engines have the capability of developing pressure ratios in excess of 25. With these pressure ratios and combustion inlet temperatures of 3000°F, extremely high cycle efficiencies or low specific fuel consumption may be attained. Fig. 1 shows cycle efficiency reaching 50% and SFC less than 0.29 (for diesel fuel operation) with compression and expansion efficiencies of 0.85 and 0.9, respectively, which are attainable in wave engines. The wave engine appears like a Brayton cycle when viewed from the stator - it has adiabatic (nearly isentropic) compression; constant pressure combustion and nearly isentropic expansion.

Possibly an even greater advantage of the wave machines over steady flow turbomachinery is the considerably lighter weight of the former. This light

*Comprex is the trademark used by the Brown-Boveri company for their wave pressure exchanger, which is currently being used as a shaft driven super-charger for internal combustion engines.

weight is due to two factors:

1. Shock compression occurs in much smaller distances than does conventional steady flow compression.
2. Compression across a single shock is much greater than in a steady flow diffuser (both in stator and rotor diffusers). This much larger pressure ratio is for the same change in subsonic Mach numbers or velocities* in both shock wave and steady flow diffusion.

Still another advantage of present day wave machines over early versions is that high speed rotation results in short axial length rotors and more compact machines. These short rotors permit close control over total axial expansion and leakage between rotor and stator side walls. Also, with the small surface area, frictional effects are less important and these machines retain their high efficiency as size is reduced.

Due to all of the above factors one can expect to design wave engines or wave engine, gas generators up to ten or more horsepower per pound of engine weight. These figures are a factor of 5 to 100 better than conventional turbomachines or internal combustion engines. In general wave machines have simple blade shapes and only one or two rotors for both compression and expansion.

Seippel's original patent (1) was developed by Brown-Boveri into a successful supercharger. Its response is so rapid (12), due to shock compression, that some truck transmissions removed the lower two speeds. Mathematical Sciences Northwest (10) has done diagnostic work on the result of mixing between hot and cold gas at the interfaces by probing the flow emerging from a wave rotor. They have also measured shock patterns and shown that they compare well with calculations. Pearson (14) has done considerable research on a wave rotor designed as an engine to drive itself and produce power. In the 1950's Pearson's device produced cycle efficiencies up to 22%. Klapproth at the General Electric Co., Berchtold at ITE Circuit Breaker, Kantrowitz and co-workers at the Brooklyn Polytechnic Institute, Jenney (16) and many others have contributed to some of the earlier work in wave rotor development.

*A common misconception is that the flow on either or both sides of a shock is supersonic. This is not the case; the shock wave itself travels with supersonic speed relative to the flow into which it propagates. This flow, however, is generally subsonic.

Recently considerable progress in the development of wave machines has been made by General Power Corporation (GPC) (8,9), Mathematical Sciences Northwest (10, 11), Pearson (14) and Brown-Boveri (15).

General Power Corporation has developed and patented a very efficient wave engine which requires almost no pressure diffusion of kinetic energy outside the rotor. All pressure rise is accomplished with a three direct and reflected shock system. This is accomplished by bending the blades near the rotor exit to form nozzles as shown in Figure 4. These create a reflected shock which increases the pressure of the flow before it leaves the rotor. Thus the flow in the compressed air port stator has essentially no tangential velocity component which requires conventional diffusion to higher pressure. Thus the reflected shock which is over 95% efficient serves as a much better diffuser than a steady flow diffuser in the stator with low pressure recovery.

Wave Engines and Their Operation

The wave rotor or wave engine utilizes shock compression while both cool air and hot gas flow in the blade passages of the rotor. Thus the blades operate at relatively low temperature as they pass both hot and cold gas ports. Operation of the GPC wave rotor is described in Appendix A. Pressure ratios across a single shock are much greater than in a 100% efficient diffuser for the same change in subsonic Mach number, as shown in Figure 2. Diffuser efficiency will generally be no greater than 90%; so shock compression is even better. Additionally conventional axial flow compressors are limited approximately to the deHaller velocity ratio of 0.7 across each set of rotor or stator blades. Therefore, the number of conventional compressor stages will be very large compared to the space required on a wave rotor to achieve the same pressure ratio. Additionally shocks of pressure ratio 2.5 or less are over 90% efficient relative to an isentropic compression process as shown in Figure 3. Therefore, shock compression results in extremely light weight machinery when compared with either conventional turbomachinery or reciprocating IC engines.

High speed operation permits shortening of the rotor blade passages since flow into the rotor only occurs effectively while shocks initiated by opening or closing of a port travel down the blade passages and return. High speed

operation increases the maximum permissible port opening before the wave travels the length of the passage and returns to the upstream end. Conversely, at high speed the blade passage or rotor axial length may be shortened while the port width remains the same. Shortened blade passages result in shortened or lighter machinery as well as reduced total axial thermal expansion of the blades for temperature changes associated with varying operating conditions. This, in turn, permits reduced clearances between rotor blades and stator sidewalls, which keep leakage low.

Features of the Wave Engine with Rotor Nozzles

Researchers in unsteady wave flow have been concerned with problems of interface mixing (between hot and cold driver or driven gas), compression wave coalescence into a shock and leakage losses. Only the last is of real significance. This effect is shown qualitatively in Figure 5. As is seen the decrease in stagnation pressure in the high pressure air-combustion gas loop due to leakage is large. GPC (9) has shown that by careful control of clearances between rotor and stator side walls the predicted pressure ratio can be obtained.

The steady flow diffuser was thought to be a limitation on wave machine development for two reasons -

1. The normal diffuser is relatively inefficient for large dynamic pressure recovery and,
2. The high pressure could not be utilized in the high pressure air-combustor-hot gas loop of the wave machine.

The first concern is remedied by the reflected shock on the rotor described above. The second concern is due to a lack of understanding of the effect of boundary conditions placed on the rotor flow. If the flow from the high pressure air port is all returned through the combustor to the hot gas port, the shock system will adjust itself to produce an internally (in rotor blade passages) reflected shock or expansion wave (depending upon the nozzle to blade passage area ratio), which propagates upstream due to the back pressure imposed by the high pressure air port. This reflected shock is shown as shock "c" in Figure 4.

Maximum Cycle Efficiency

At any given rotor speed and combustion temperature there is a maximum cycle pressure as the design value of A_e/A_c varies. At the top of Fig. 8 the blade passages are straight from inlet to exit (no nozzle at exit of the blade passage, $A_e/A_c=1$). As the nozzle at the exit of the blade passages decreases in area ($A_e/A_c<1$), it becomes an increasing constriction, strengthening the reflected shock which propagates back up the blade passages. This shock slows the hot gas-cold air interface, requiring the port width at 6 to increase in order for all of the cold air to flow off the rotor into port 6. This process moves the expansion wave from closing of the hot gas port upstream nearer port 6, as shown in the second drawing from the top of Figure 8. Both shocks shown increase in strength and the stagnation pressure level in ports 5 and 6 increases (hot gas-high pressure air loop). The maximum stagnation pressure in this loop occurs when the hot gas interface and expansion wave from closing of the rotor passage by the hot gas port arrive simultaneously at the downstream edge of the high pressure air port, 6. This condition occurs at some nozzle to chamber area ratio (A_e/A_c). Decreasing A_e/A_c farther, causes decreasing air flow in the hot gas-high pressure air loop and decreasing velocity in port 5. Shock strengths begin decreasing as does the stagnation pressure in ports 5 and 6. Since this engine behaves as the Brayton Cycle when viewed from the stator, decreasing peak cycle pressure, P_{05} , decreases cycle efficiency. Thus the maximum cycle pressure ratio occurs at maximum P_{05} , as described above.

Summary Comparison of Development Opportunities in Conventional and Wave Turbo-machinery.

Conventional Turbomachinery

1. High temperature operation being limited by:
 - a. Slow progress in materials development.
 - b. Limitation on use of compressor air for turbine blade cooling.
2. Many stages of compression required because of limitations on pressure rise or on velocity ratio in each stage of diffusion. Results in heavy turbomachinery.
3. Axial flow machines are long with numerous or heavy bearings, and may pass through at least one critical speed in operating range.
4. High pressure ratio at high efficiency difficult to attain.
5. Leakage losses unimportant in large, or moderate pressure ratio machines, but serious in small high pressure ratio machines.
6. Large surface area to volume ratios result in frictional losses. Resulting low Reynolds Numbers, especially in high pressure stages of small machines, results in low compressor efficiency.

Wave Rotor Turbomachinery

1. Naturally cooled blades which pass through hot and cold gas in each revolution. Results in light weight machines. Any material advances will further benefit the wave engine.
2. Shock pressure rise very rapid and much higher than in steady flow diffusion for the same change in subsonic flow velocity for both.
3. Resulting single rotor or two separate rotor machine is stiff and requires lighter bearings. Generally no critical speeds in operating range.
4. High pressure ratios at high efficiency attainable.
5. Leakage losses must be controlled. Can be done simply with control of side and shroud clearances - especially with short axial length rotors.
6. Small surface area to volume ratios make frictional losses relatively unimportant. Scaling to small engines easily accomplished.

Conclusions

The very desirable features of a wave engine are summarized below.

1. Higher combustion temperatures; thus high specific power and light weight machines. (Rotor blades naturally cooled.)
2. Higher pressure ratios; thus high cycle efficiencies.

3. Higher pressure ratios result in expansion exhaust temperatures below compression discharge temperature; thus no regenerator or recuperator required.
4. Higher component efficiencies, especially in small engines; thus higher cycle efficiencies.
5. Smaller size due to small volume required for shock compression.
6. Stable operation, i.e., no stall as may occur in conventional turbocompressors, because shock processes are rapid, stable, and isolated from each other.

Advantages of GPC-SAIC wave rotor and engine compared to previous designs:

1. More efficient compression processes - no external (to the rotor) diffusers required.
2. Wave rotor drives entire compression process, including pre-compression.
3. Short axial length resulting in better control of side wall clearances and thus leakage. Leakage seriously affects performance.

APPENDIX A

Description of Wave Rotor Operation

One way to visualize the shock compression process occurring in the passages between blades is to imagine "sitting" on the rotor blades as they rotate past the various stator ports shown in Figure 4. Begin at the end of the hot gas expansion process. On the blade one sees new air from an external blower or compressor flowing into a blade passage pushing the spent hot exhaust gas out of the passage. When this is complete and only new air is flowing through the passage it rotates past the downstream edge of the exhaust port and the flow is shut off by the end or side wall. The sudden stopping of the flow causes a shock to propagate back upstream through the passage bringing the flow to rest relative to the blade passage. As the shock brings each portion of the flow to rest the pressure in the air increases by the pressure ratio across the shock. When the shock has reached the inlet end of the passage it rotates past the trailing edge of the inlet air port. That side wall now has trapped all of the air whose pressure has been increased on the rotor. All the blade passages go through this process and each in turn has the air in the passage compressed.

Next in the process a blade passage rotates past the leading edge of the hot gas port. A shock now is initiated which propagates down the passage bringing all the air that it passes to a still higher pressure. The hot gas moves down the passage behind the cool air forming an interface between them. The shock moves faster than the interface which moves at the subsonic gas velocity. When the shock arrives at the nozzle end of the passage it rotates past the leading edge of the high pressure air port. The nozzle behaves here as a constriction suddenly causing the flow to slow, which in turn causes a reflected shock to propagate upstream through the passage. The air that this shock passes through is further increased in pressure. This high pressure air flows through the nozzle into the high pressure air port. Each blade passage discharges its high pressure air into this port until the air-hot gas interface arrives at the nozzle end of the passage. At this point the passage rotates past the downstream edge of the high pressure air port preventing the hot gas

from entering the port. Meanwhile the reflected shock "c" has passed through the air-hot gas interface and reached the upstream or inlet end of the passage. At this time the blade passage rotates past the downstream edge of the hot gas port preventing possible back flow into the hot gas port.

The compression process is now complete. The hot gas trapped on the rotor exits through the nozzle driving the rotor and the entire compression process by its tangential momentum flow there and in a single reentry shown in Figure 4.

Summary of Special Features of GPC Wave Rotor-Gas Generator

The nozzles at the downstream end of the rotor blade passages serve two purposes:

1. At the exit to the high pressure air port the nozzles serve as a restriction to the flow causing a reflected shock to propagate upstream. This shock further increases the pressure before the flow enters the rotor nozzles and exits into the high pressure air port. Thus, at the cool high pressure air port the nozzles serve as an efficient internal (on the rotor) diffuser. Internal pressure rise due to the reflected shock is more efficient and produces a higher pressure rise than an external steady flow diffuser. See Figure 2 which illustrates the considerably larger pressure rise across a shock as compared with the steady flow diffuser, for the same change in subsonic velocities or Mach Numbers. In fact, the absolute velocity leaving the nozzles has almost no tangential component and hence no external diffusion is required.
2. At the hot gas exhaust in the flow expansion portion of the rotor the nozzles produce a reaction force to drive the rotor and entire compression process. The compressor charging air on to the rotor is also driven in this process. After leaving the rotor the hot exhaust gas is at lower pressure and temperature but available for power production in the free or separate power turbine.

Early investigations into the shock compression process occurring on a wave rotor and the associated flow did not completely understand the effect of the back pressure on the rotor at the high pressure air port. It was believed that the total pressure available at rotor exit could not be effectively utilized. Thus an efficient diffuser was not required. In fact, the early investigations concluded that the total air port flow at too high a pressure

could not be used in the return through the combustor to the hot gas inlet port. Consequently some of the flow from the combustor was diverted to a high pressure turbine. However, it has been found that if all of the flow is returned through the combustor to the wave rotor inlet that the direct and reflected shock system will adjust to produce a higher pressure in the high pressure-combustor loop increasing the cycle efficiency.

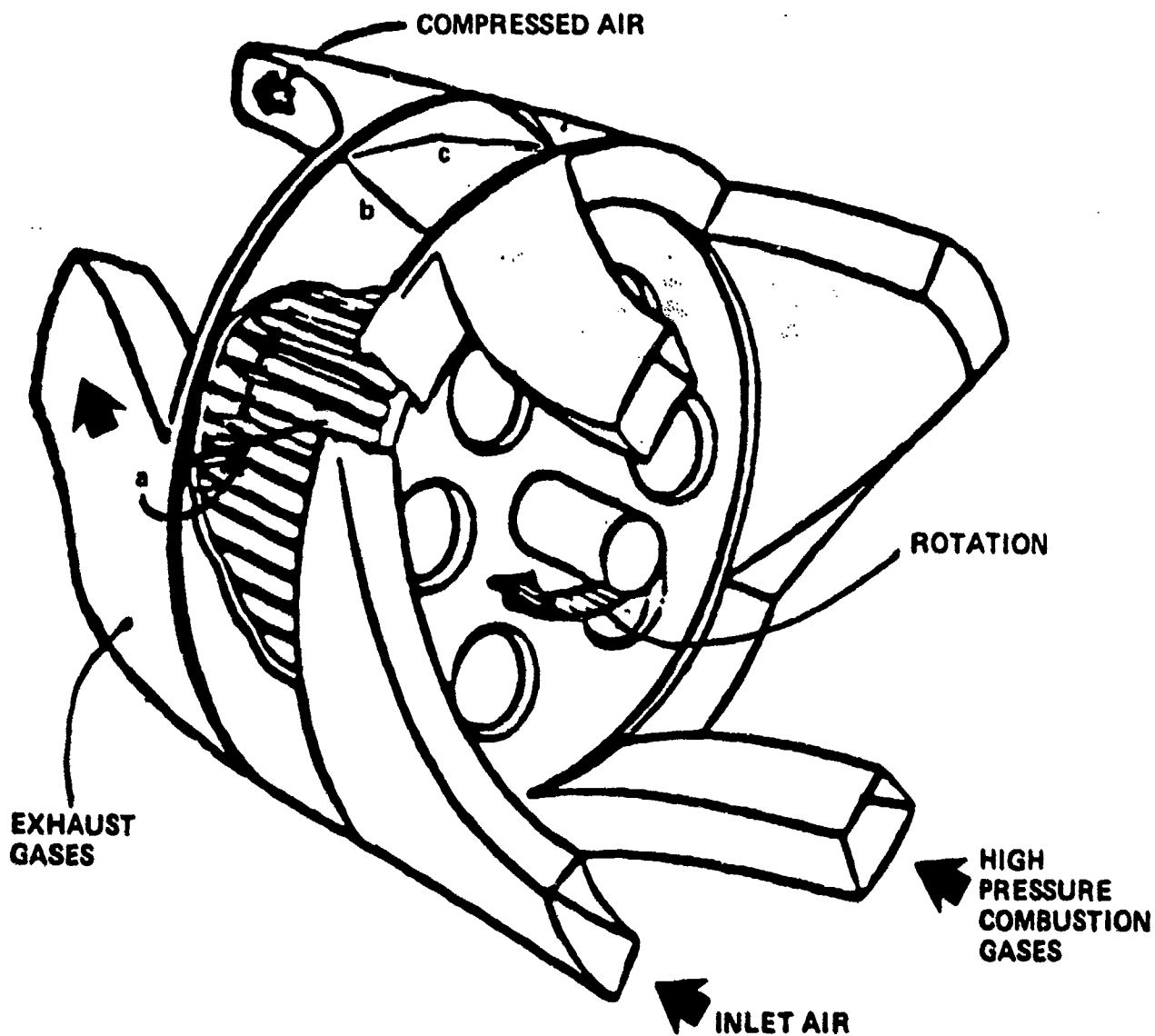


FIGURE 1 SUPERPOSITION OF WAVE FRONTS (LETTERED LINES) ON THE TUBE ROWS OF A TWO-CYCLE WAVE ROTOR (SHOCKS a, b, c AS SHOWN IN FIGURE 5).

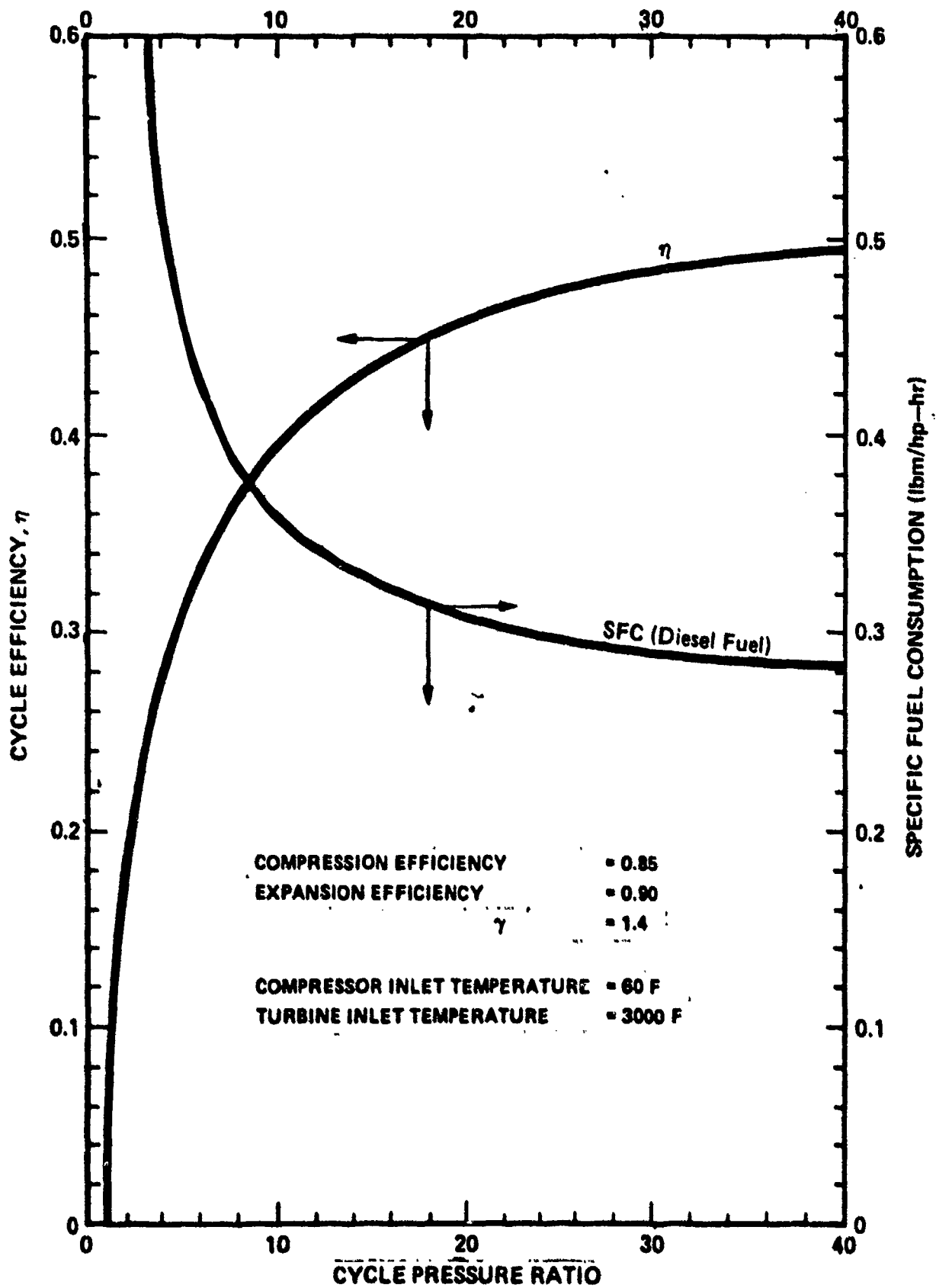


FIGURE 2 WAVE ENGINE OR BRAYTON CYCLE EFFICIENCY.

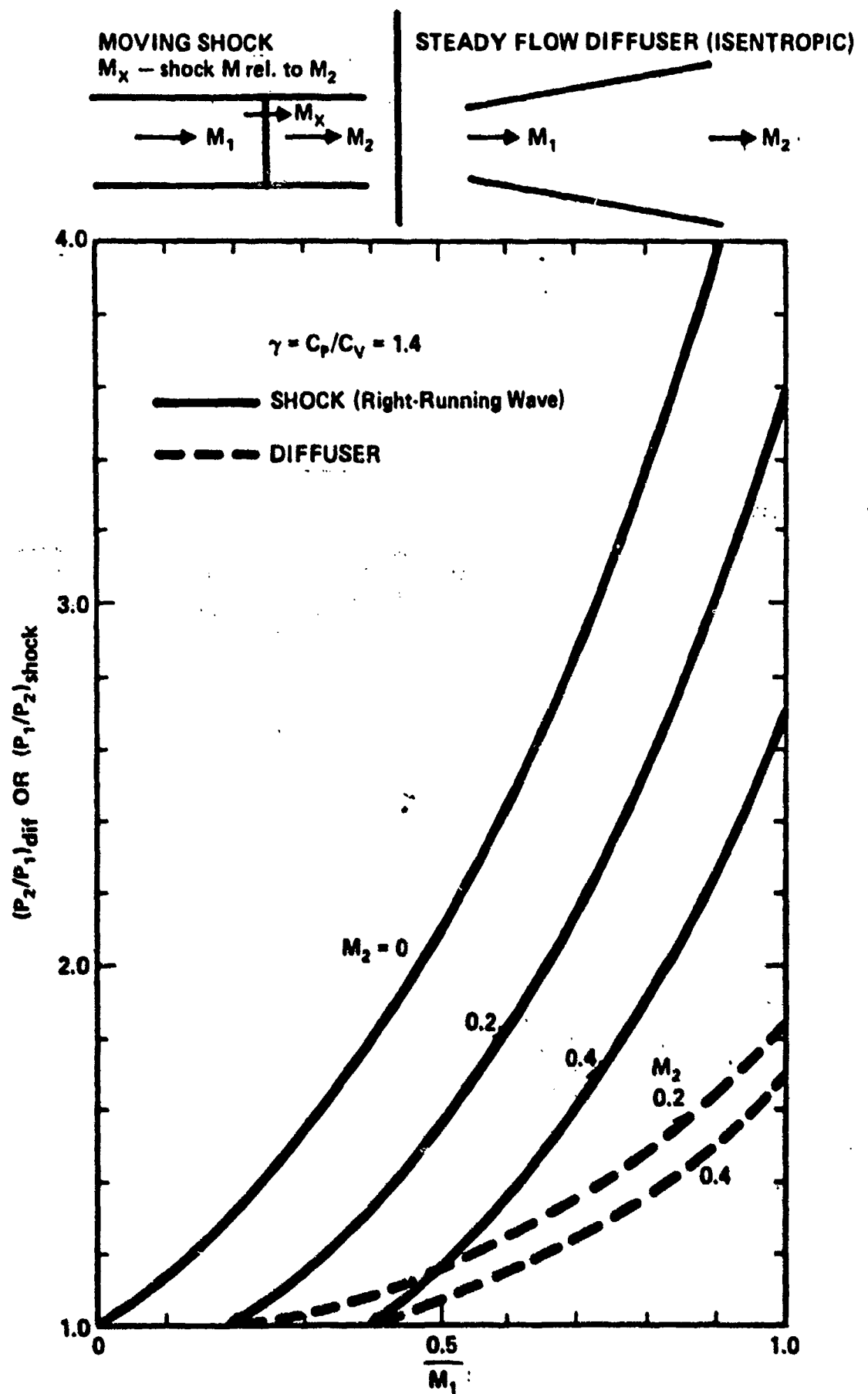


FIGURE 3 PRESSURE RATIO FOR MOVING SHOCK AND STEADY FLOW ISENTROPIC DIFFUSER.

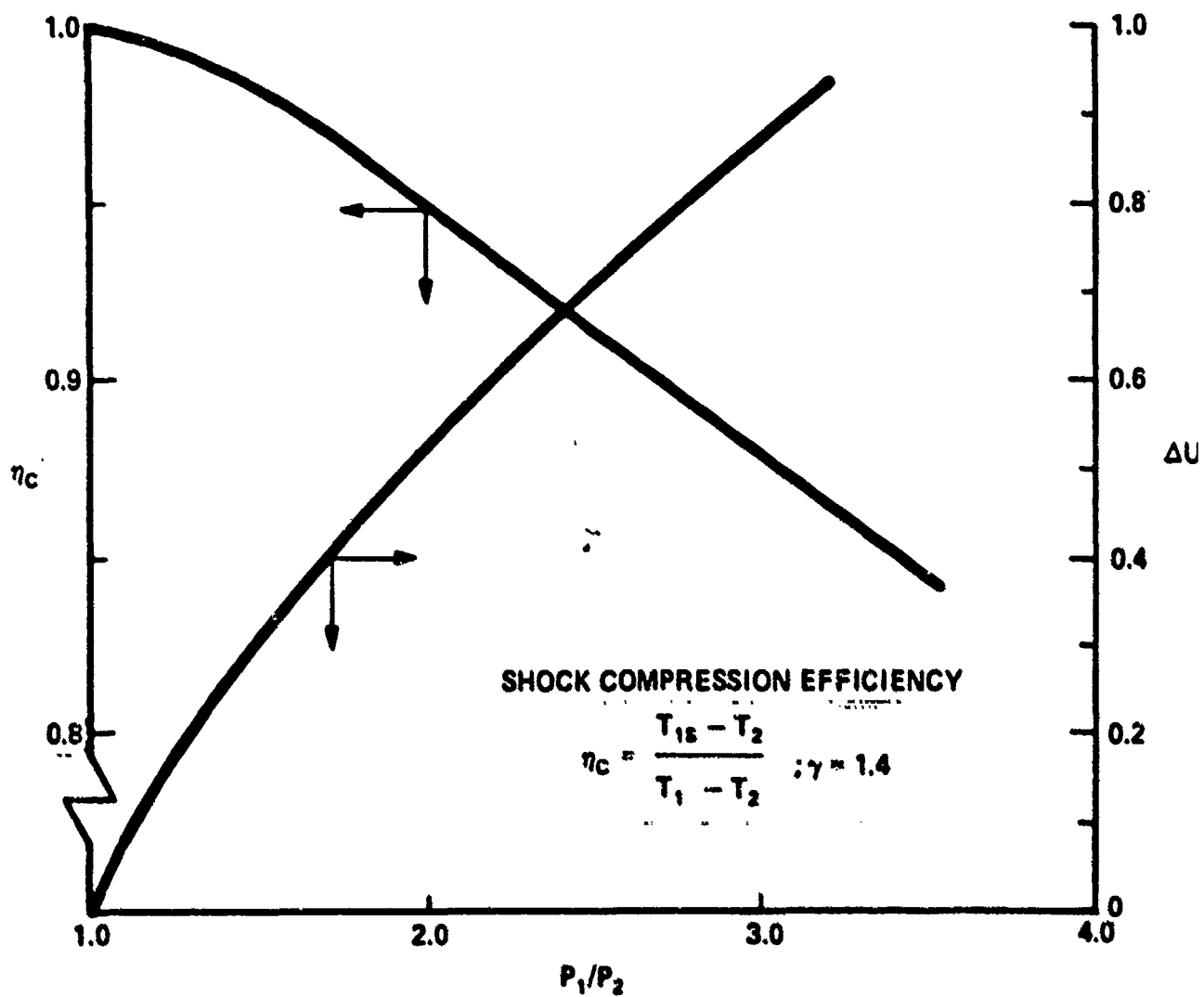


FIGURE 4 SHOCK COMPRESSION EFFICIENCY AND VELOCITY CHANGE VS. SHOCK PRESSURE RATIO.

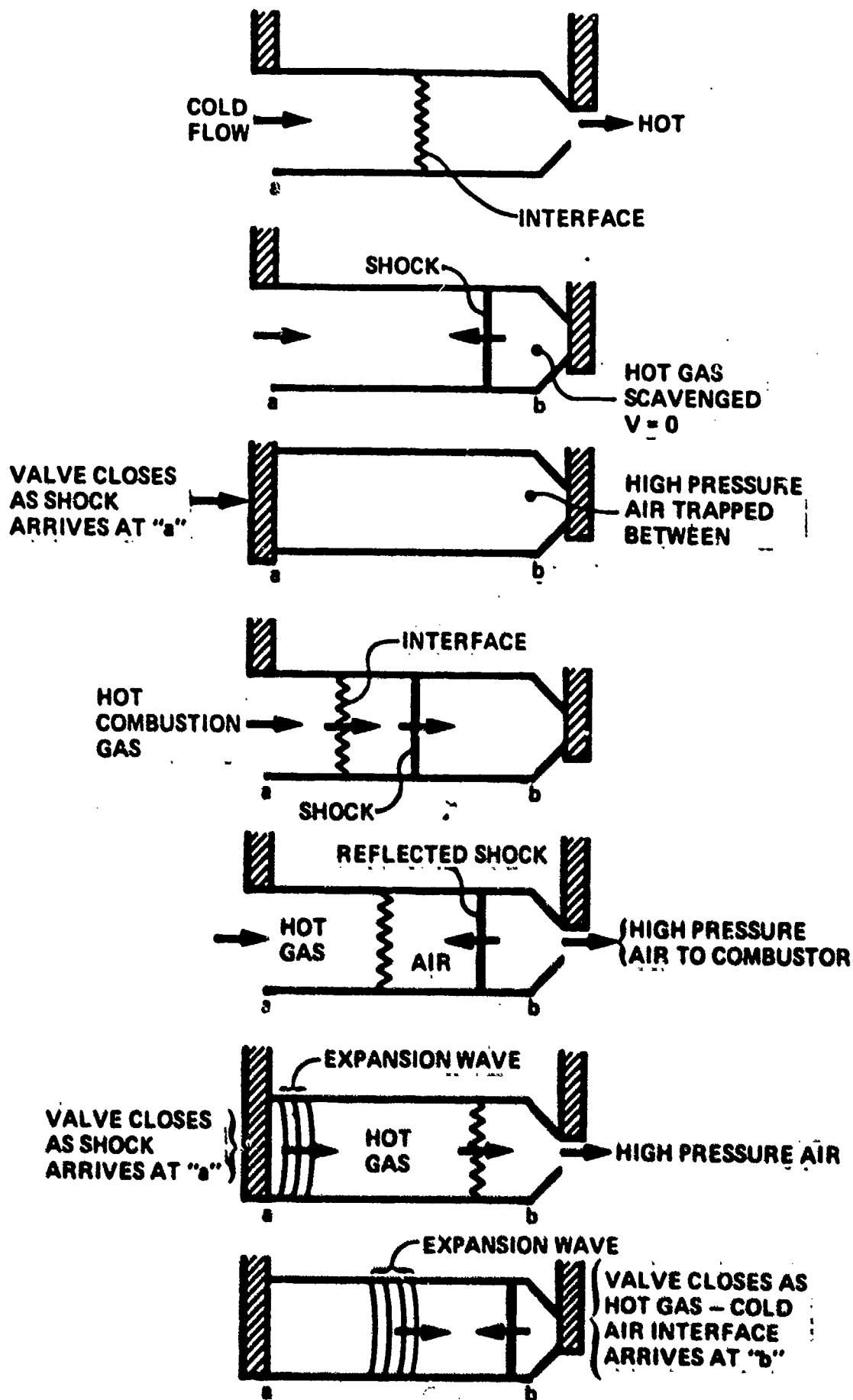
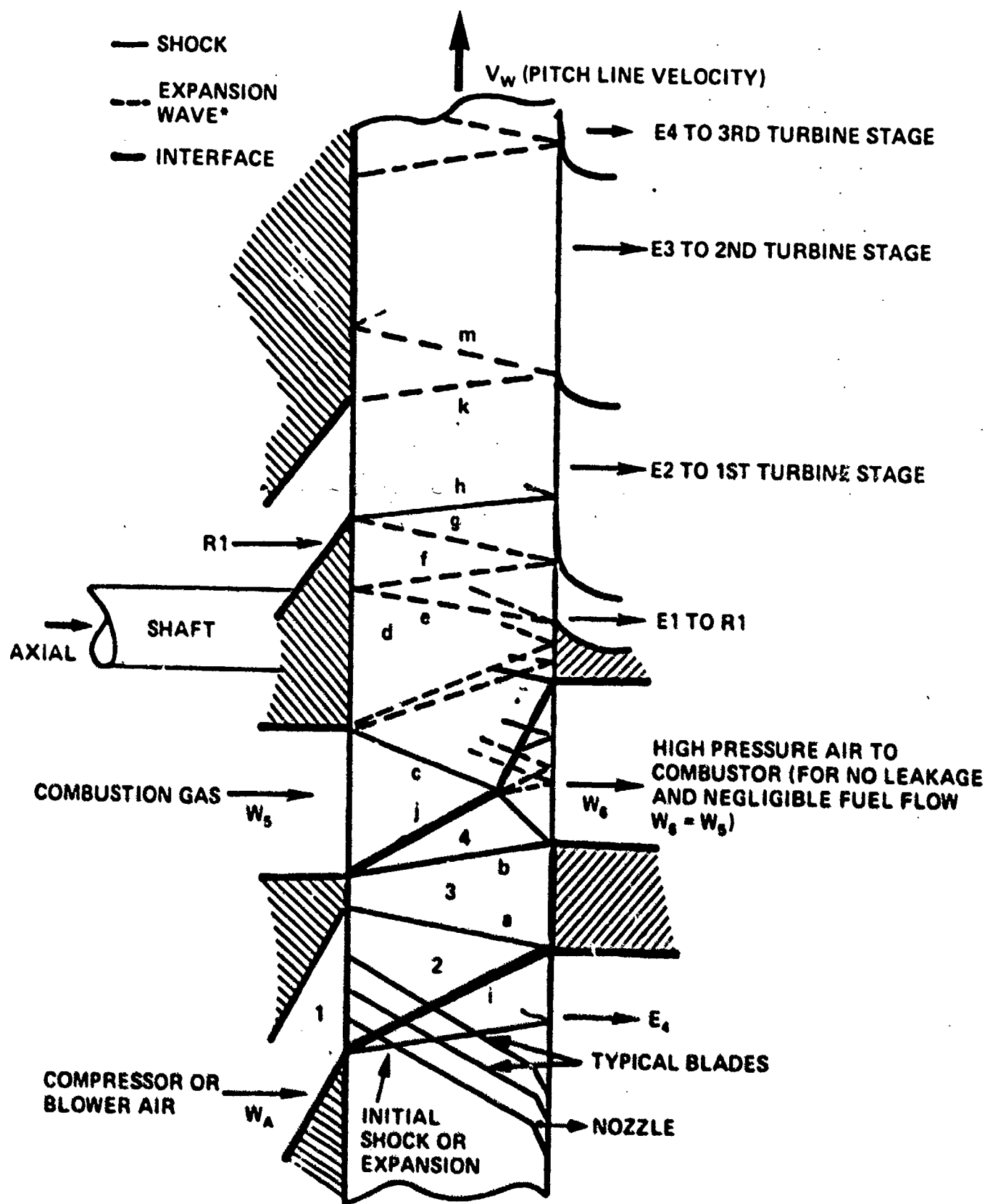


FIGURE 5 SHOCK COMPRESSION PROCESS



*Shown as single wave instead of fan for simplicity.

FIGURE 6 LOOKING DOWN ONTO PERIPHERY OF WAVE ROTOR.

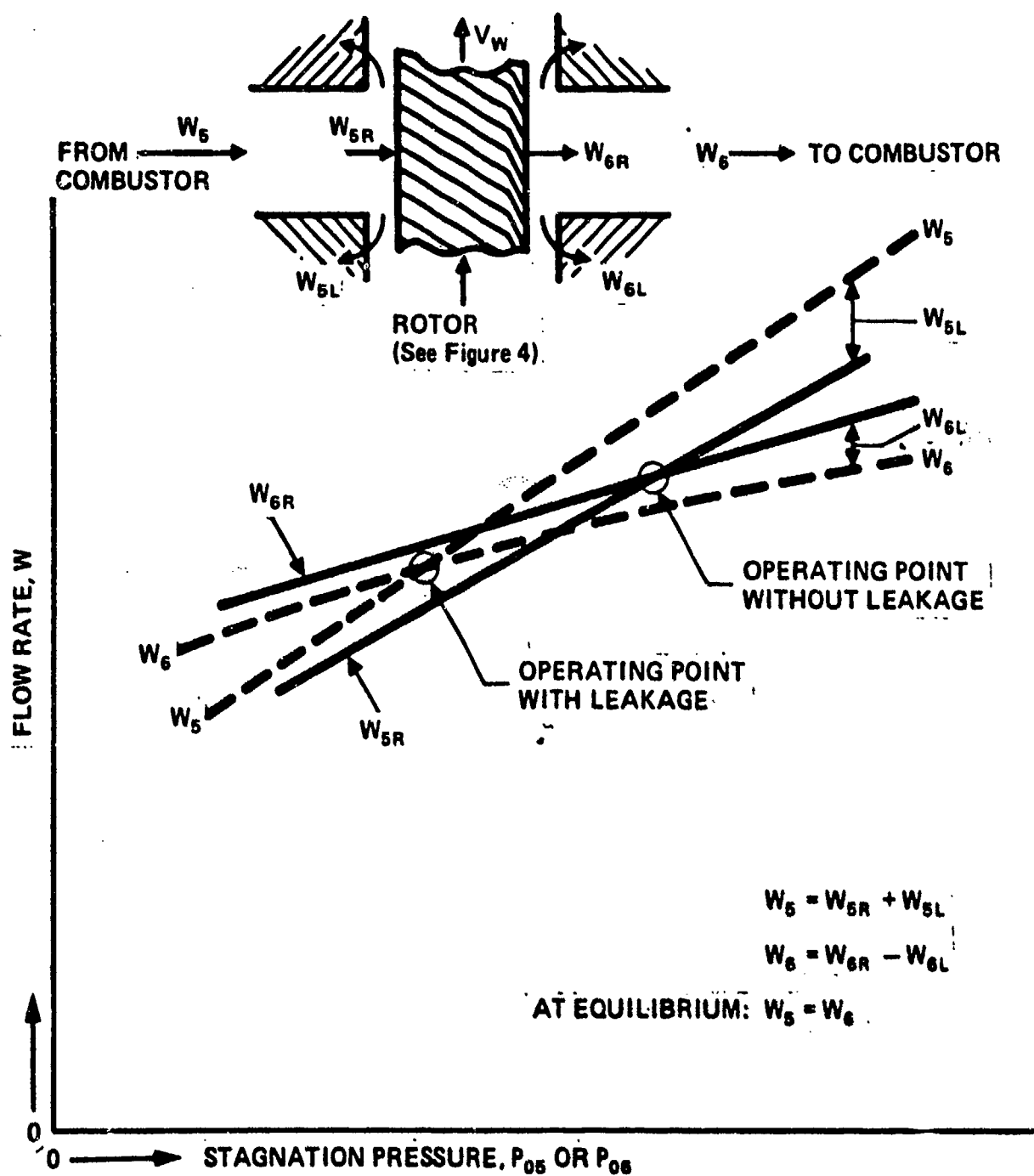


FIGURE 7 EFFECT OF LEAKAGE ON OPERATING POINT OF HOT GAS, W_5 , - HIGH PRESSURE AIR, W_6 , LOOP.

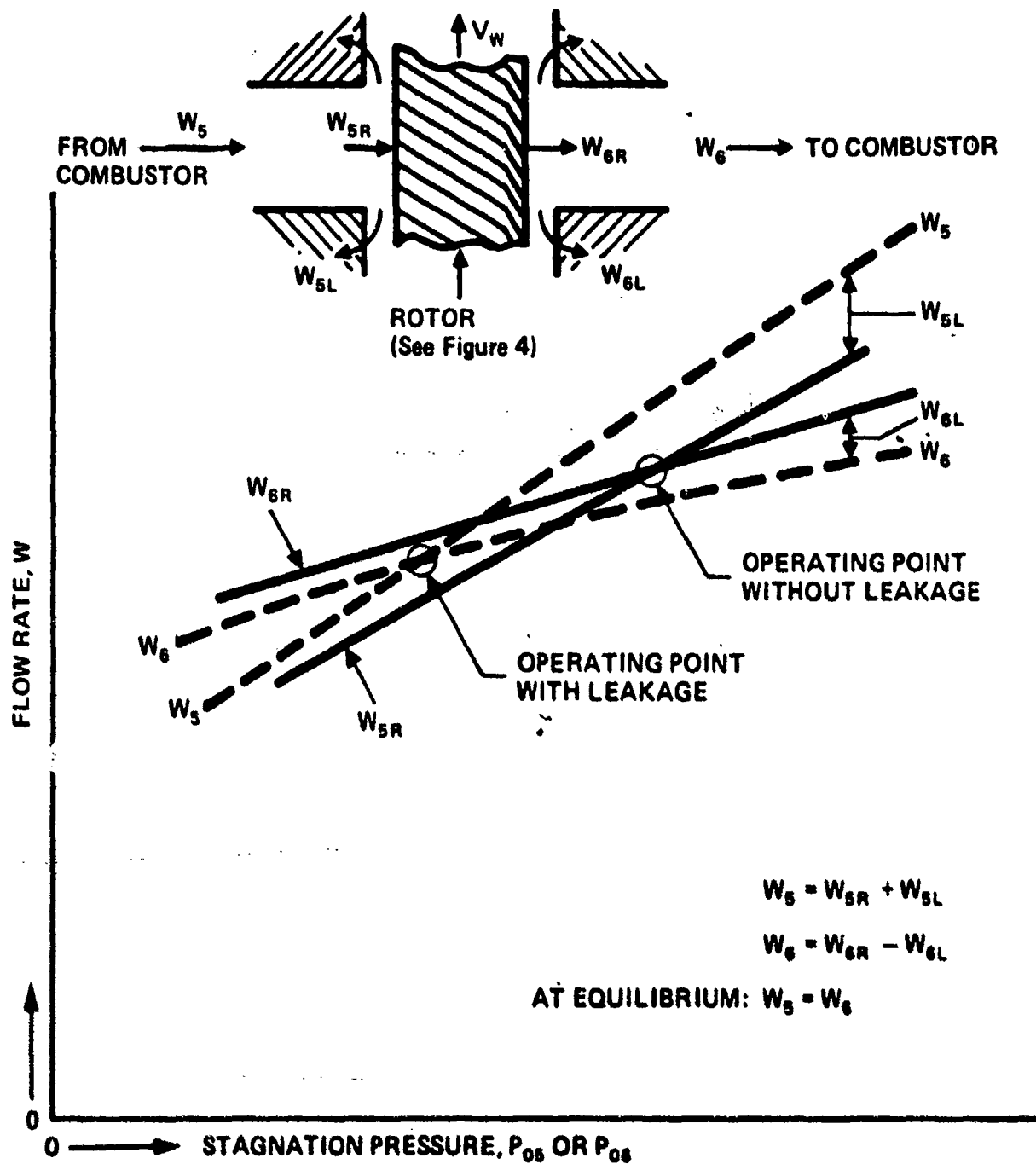


FIGURE 7 EFFECT OF LEAKAGE ON OPERATING POINT OF HOT GAS, W_5 , - HIGH PRESSURE AIR, W_6 , LOOP.

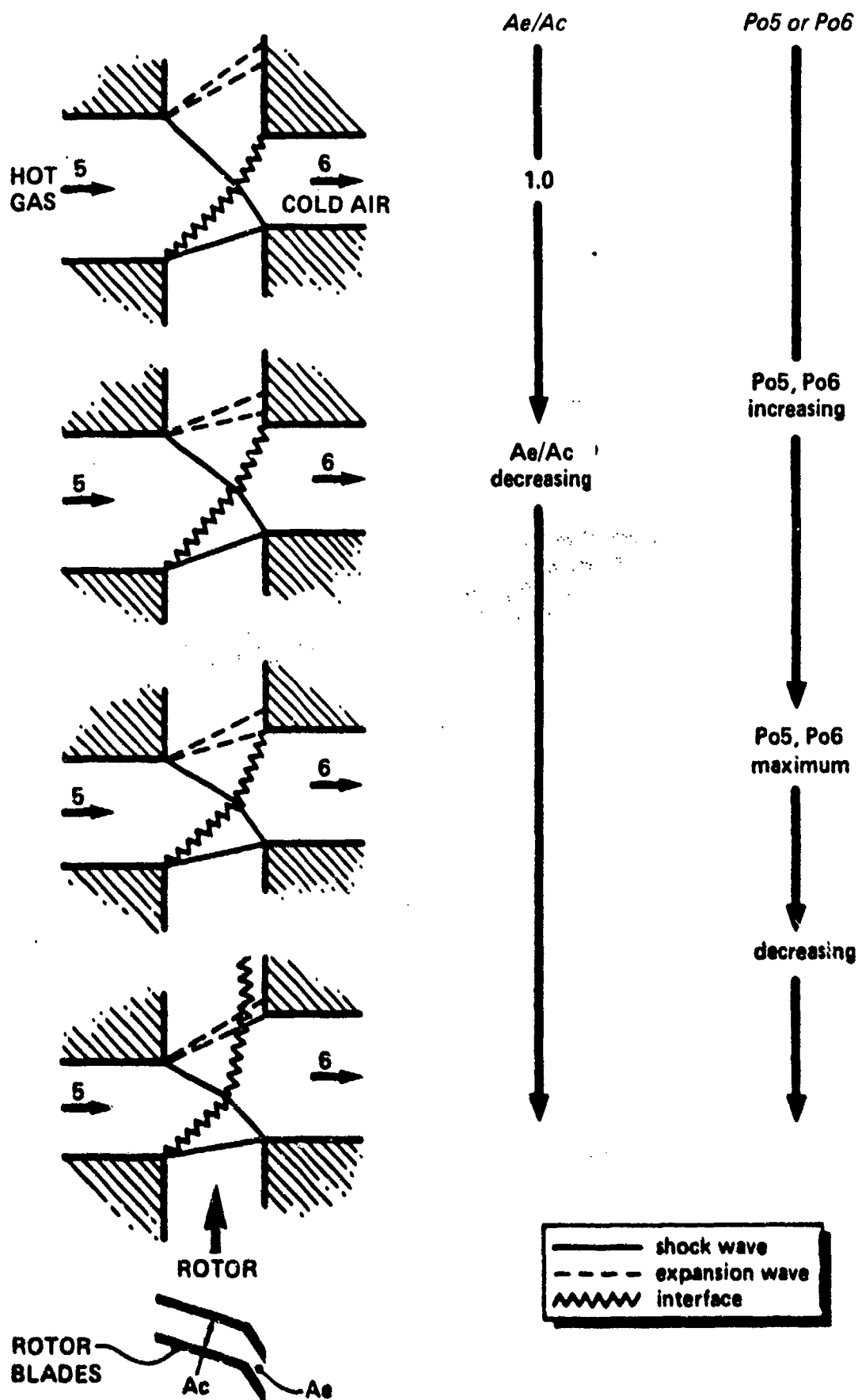


FIGURE 8 EFFECT OF A_e/A_c ON COMBUSTION LOOP STAGNATION PRESSURE

WAVE ROTOR RESEARCH & TECHNOLOGY WORKSHOP

NAVAL POSTGRADUATE SCHOOL

MONTEREY, CALIFORNIA

MARCH 26-27, 1985

DESIGN AND EXPERIMENTAL VERIFICATION

OF

WAVE ROTOR CYCLES

ATUL MATHUR

EXOTECH INC., CAMPBELL, CALIF.

DESIGN AND EXPERIMENTAL VERIFICATION OF WAVE ROTOR CYCLES

A show of renewed interest in wave devices prompted the initiation of a research effort at the Turbopropulsion laboratory of the Naval Postgraduate School, with the objective of developing an understanding of the basic flow processes and potential applications of pressure exchangers/wave engines, primarily in propulsion systems.

The effort was directed towards i) numerical studies and an unsteady flow code development, ii) basic research level (laboratory scale) experimental work, and iii) study of past and on-going efforts in this field of technology.

In the area of computational analysis, an unsteady flow code is being developed which should serve as a preliminary design tool. The code can handle the unique features that characterize typical internal processes in wave rotors, viz. multiple discontinuities and wave interactions in the flow. A further step would then be to incorporate this code into an engine performance code (both shaft and thrust power producing), to assess the potential payoffs of the combined mode operation.

The choice of the numerical technique is based on the following criteria, which need to be met as far as possible:

1. Higher order discontinuities such as shock fronts should be computed stably, i.e. without oscillations and with the proper entropy jumps.
2. The next lower order of discontinuities such as contact surfaces and gradient discontinuities should also be modelled without smearing and should be transported at the correct speeds.
3. the smooth and uniform regions of the flow should be modelled consistently.

It is often mentioned in the literature that gradient discontinuities (expansion fans, compression waves), being the lowest in the 'discontinuity heirarchy', are usually unworthy of special treatment. However, the importance of these waves in wave devices cannot be emphasized enough and any numerical code for such a flow should treat them accordingly.

Over and above the desire that these criteria be met, it was felt that for the code to be generally applicable and user-friendly, it should not require an inordinate amount of computer time, nor should it require implementation of numerical 'tricks' which render many codes quite useless except in the hands of those who developed them.

A one-dimensional method which best seems to meet the above criteria is the Random Choice Method, based on an existence proof given by Glimm (Ref.1), and developed into a numerical form by Chorin (Ref.2). The code is based on the solution of local Riemann problems. Fig.1 shows a schematic of the Riemann problem for the special case of shock-tube flow. The problem consists of the prescription of two states of a gas which are separated by a diaphragm at time $t=0$; the solution consists of charting the flow field at $t=0+$, i.e. after the diaphragm is ruptured. Each solution is an exact analytical solution obtained through shock and/or expansion transition functions (Ref.3). The method thus solves the governing Euler equations in one-dimension by solving a sequence of adjacent Riemann problems, specified as the initial conditions for each succeeding time step. The solution to each Riemann problem is then discretely represented by sampling it in a quasi-random fashion. This sampling procedure is due to Van der Corput (Ref.4), which generates equidistributed sequences of numbers belonging to a $(0,1)$ interval.

Fig.2 shows the results for a test-case for this method (due to Sod, Ref.5). Four parameters are plotted in the figure, the pressure, density, velocity and entropy. The squares on the density plot represent the magnitude and the physical location of the head wave, the tail wave, the contact surface and the shock wave (from left to right) generated by an exact solution for the test case. Note the 'infinite' resolution of the strong discontinuities as well the perfect realization of the constant states. The rarefaction wave propagating to the left is modelled well too.

The program is run in an interactive mode, and for any particular wave diagram that is being studied, all four parameters are plotted simultaneously along with an $x-t$ plot (representing the wave diagram), the latter generated by means of a suitable tracking scheme (Ref.6).

Using the Random Choice Method, a simple wave diagram was computed for the proposed wave turbine experiment at TPL. All the discontinuities are generated and tracked very well as shown in Fig.3. The propagation of the shock front in time is shown in Fig.4. Although this is an ideal representation of the waves, it still helps in visualizing the basic internal flow structure and in providing base numbers for a preliminary design. Except for the implementation of proper boundary conditions, the code requires no other input or 'tweaking', a feature that is characteristic of the Riemann problem solver type numerical codes. Even in a non-optimized form and with interactive graphics, the example shown above required about 1 minute on an IBM 370-3033AP.

A more complex diagram, which describes the low pressure side induction process of a counterflow scavenge cycle is shown in Fig.5. This is the case for a gas generator application of the wave rotor, the usefulness of the configuration being measured by the net pressure gain across the machine. This particular case can be solved in approximately 2.5 minutes of CPU time. To keep the picture in perspective, what is being solved for in this case is equivalent to the exhaust and induction processes of the internal combustion case described in Ref.7, presented elsewhere in these proceedings. The performance curves thus obtained are shown in Fig.6, which can be used in the engine performance code to get preliminary estimates of the performance of the combined unit.

Before describing the experimental effort, I would like to make note of the fact that it was encouraging to hear some of the papers presented earlier during this workshop, especially those of Dr. Kentfield and Dr. Matthews. The former British company, Power Jets Ltd., and Brown Boveri Corporation of Switzerland both recognized the need for simple tests to better understand the fundamental processes in wave rotors, something that the experiment currently being run at TPL is trying to model.

The wave turbine mode operation is essentially the cell filling and cell emptying unit processes described by Dr. Kentfield, and some of the objectives of this program are shown in Fig.7. The experiments will basically serve to validate the accuracy of the computations carried out and indicate the areas of significant deviations. A schematic of the rotor with the inflow and outflow ports is shown in Fig.8, along with a simplified representation of the corresponding wave structure. The rotor has passages which are canted at 60 degrees to the axis, and is comprised of six wafers bolted together, a feature which enables the rotor passage length to be changed should the need arise. The installation setup is shown in Fig.9.

Preliminary tests have recently been initiated and the current status of the experimentation is shown in Fig.10. Consistent self-acceleration of the rotor is achieved at approximately 5000 to 6000 RPM, indicative of shaft power production. The next step in the process is to attach an air-dynamometer to absorb the load generated and to make careful torque-horsepower-rpm measurements.

List of References

1. Glimm, J., "Solutions in the Large for Nonlinear, Hyperbolic Systems of Equations," Communications in Pure and Applied Mathematics, No.18, pp.697-715, 1965.
2. Chorin, A. J., "Random Choice Solution of Hyperbolic Systems," Journal of Computational Physics, No.22, pp.517-533, 1976.
3. Courant, R. and Friedrichs, K. O., Supersonic Flow and Shock Waves, Interscience Publishers Inc., New York, 1948.
4. Hammersley, J. M. and Handscomb, D. C., Monte Carlo Methods, John Wiley and Sons, Inc., New York, pp.31-36, 1975.
5. Sod, G. A., "A survey of Several Finite Difference Methods for Systems of Nonlinear Hyperbolic Conservation Laws," Journal of Computational Physics, No.27, pp.1-31, 1978.
6. Moretti, G., "An Improved Lambda Scheme," NASA Contractor Report CR-xxxxx, 1981.
7. Mathur, A., "A Brief Review of the G.E. Wave Engine Program," Presented at the Wave Rotor Research and Technology Workshop, Monterey, California, March 1985.

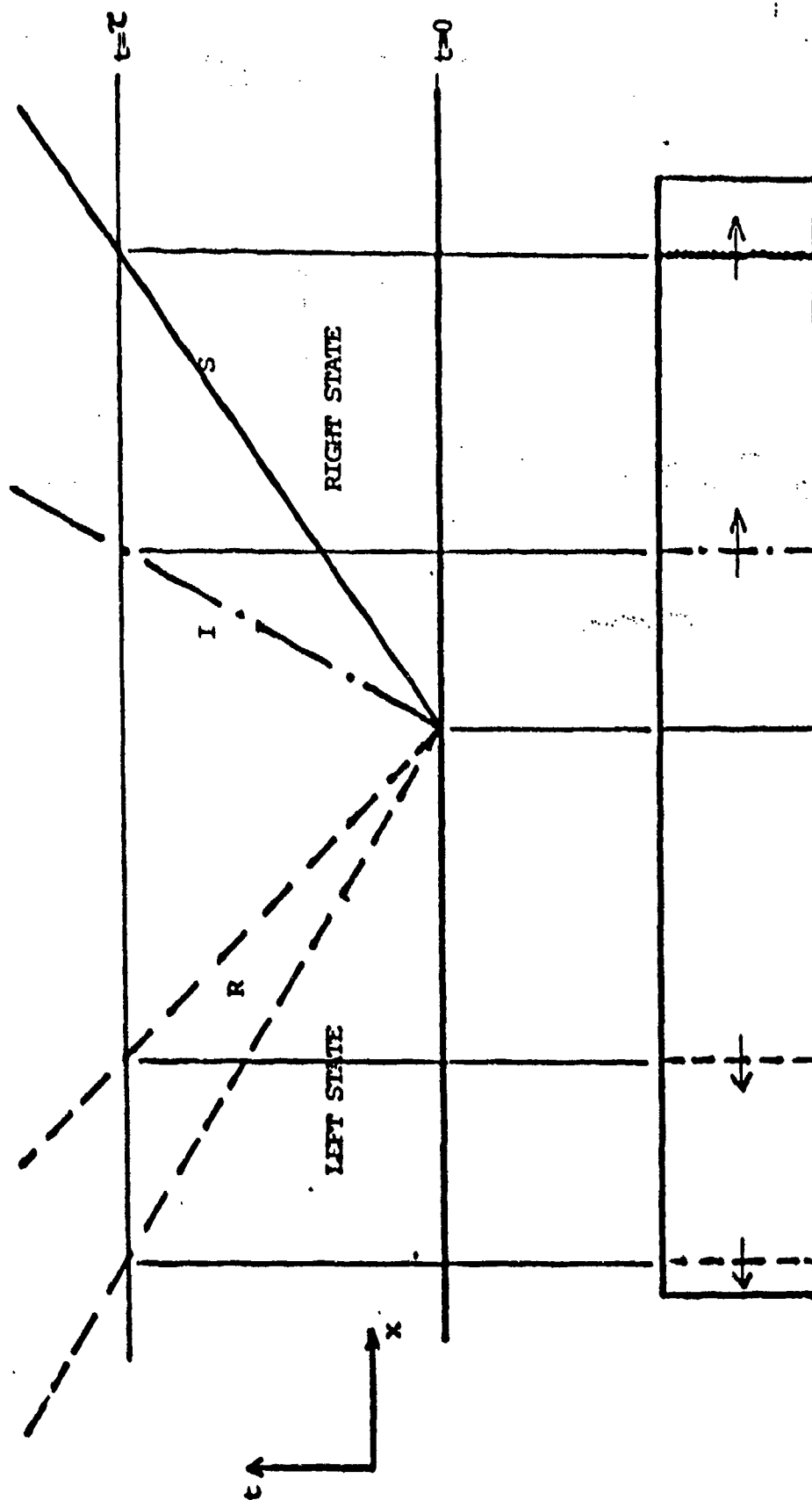


FIG. 1 THE RIEMANN PROBLEM IN GAS DYNAMICS
SPECIAL CASE OF SHOCK-TUBE FLOW

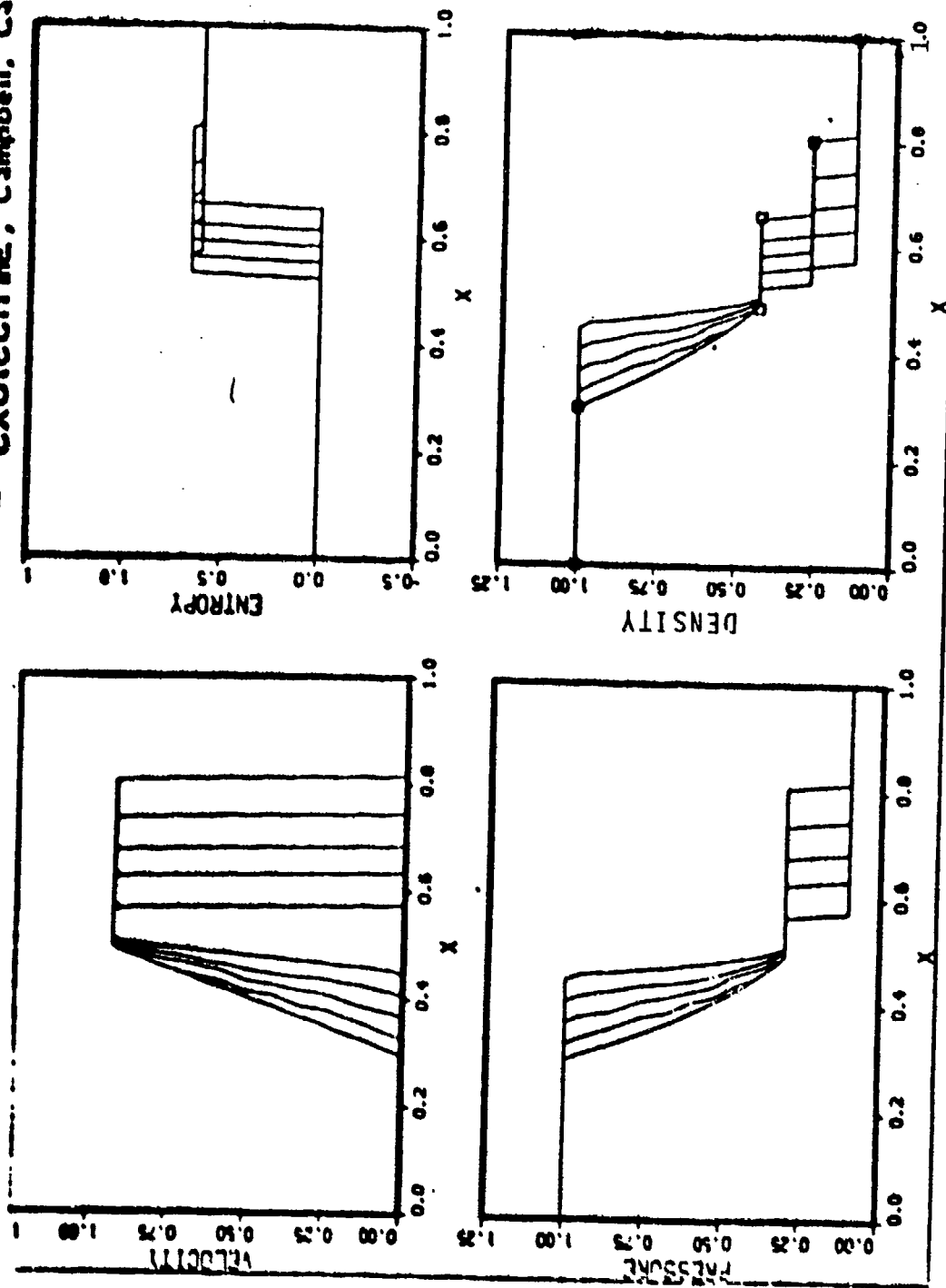
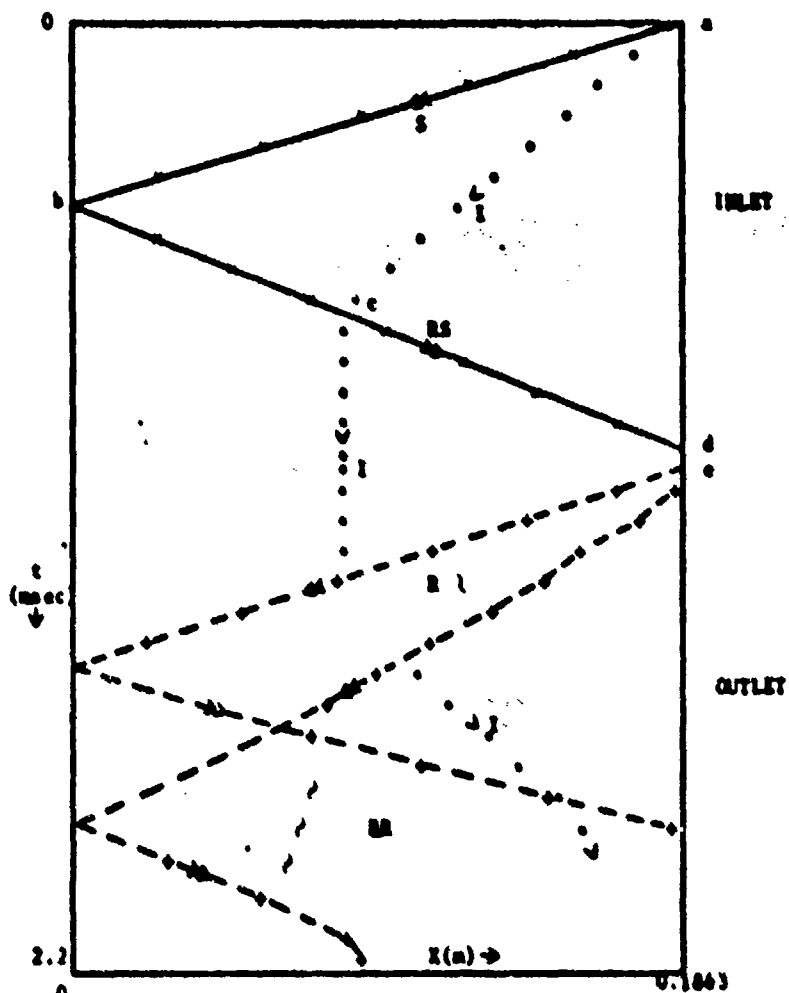
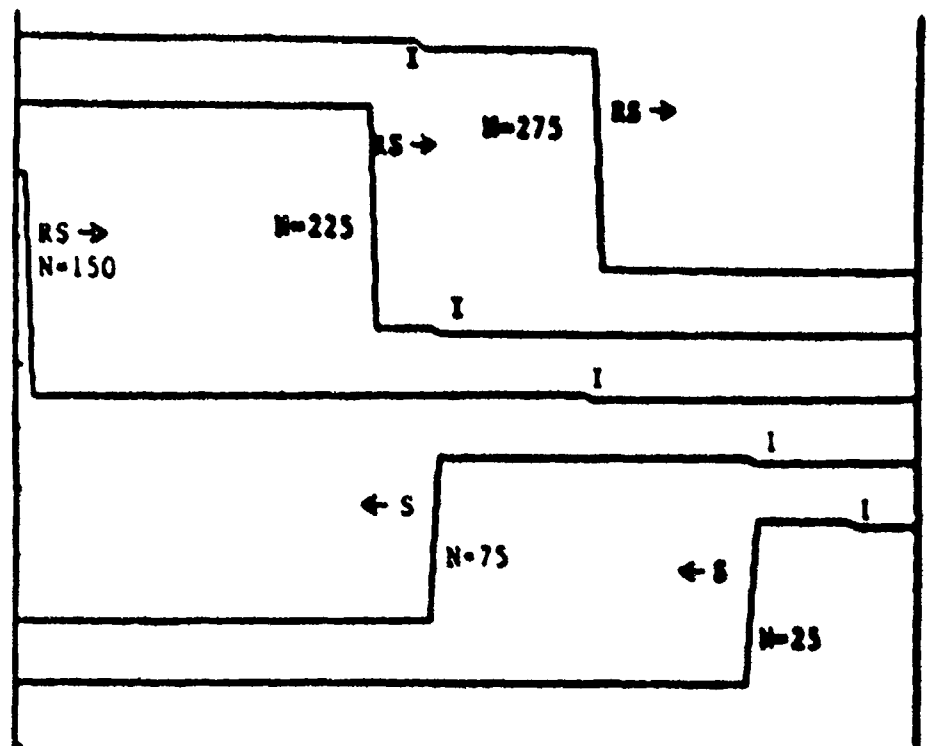


FIG. 2 TEST CASE FOR PIECEWISE SAMPLING METHOD



Wave diagram computed by 1-d Random Choice method. S-shock; RS-reflected shock; R-rarefaction fan; RR-reflected rarefaction; I-interface;

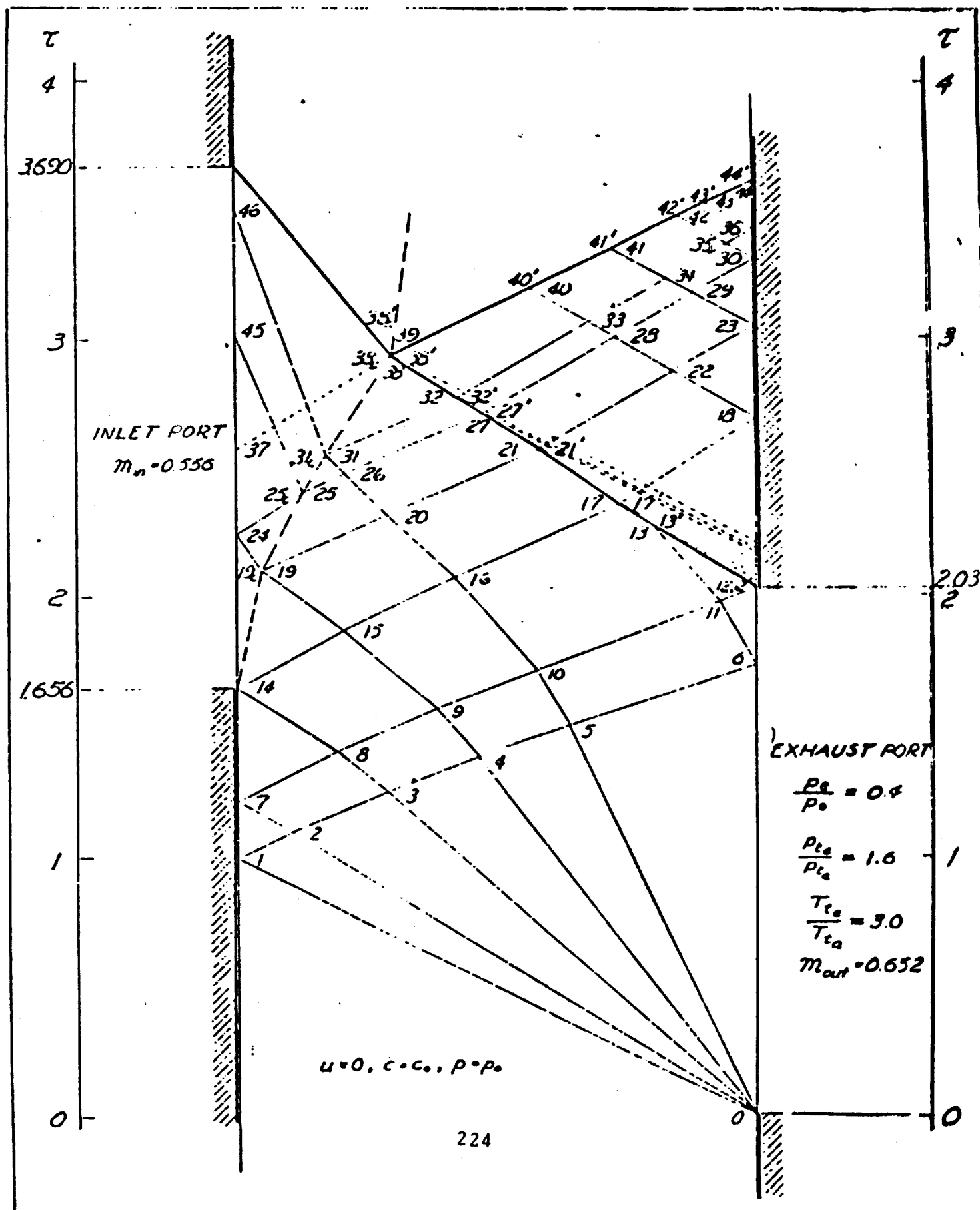
FIG. 3



Sequence showing shock and interface movement.
S-shock; I-interface; RS-reflected shock; N-timestep

FIG. 4

FIG. 5 LOW PRESSURE INDUCTION PROCESS



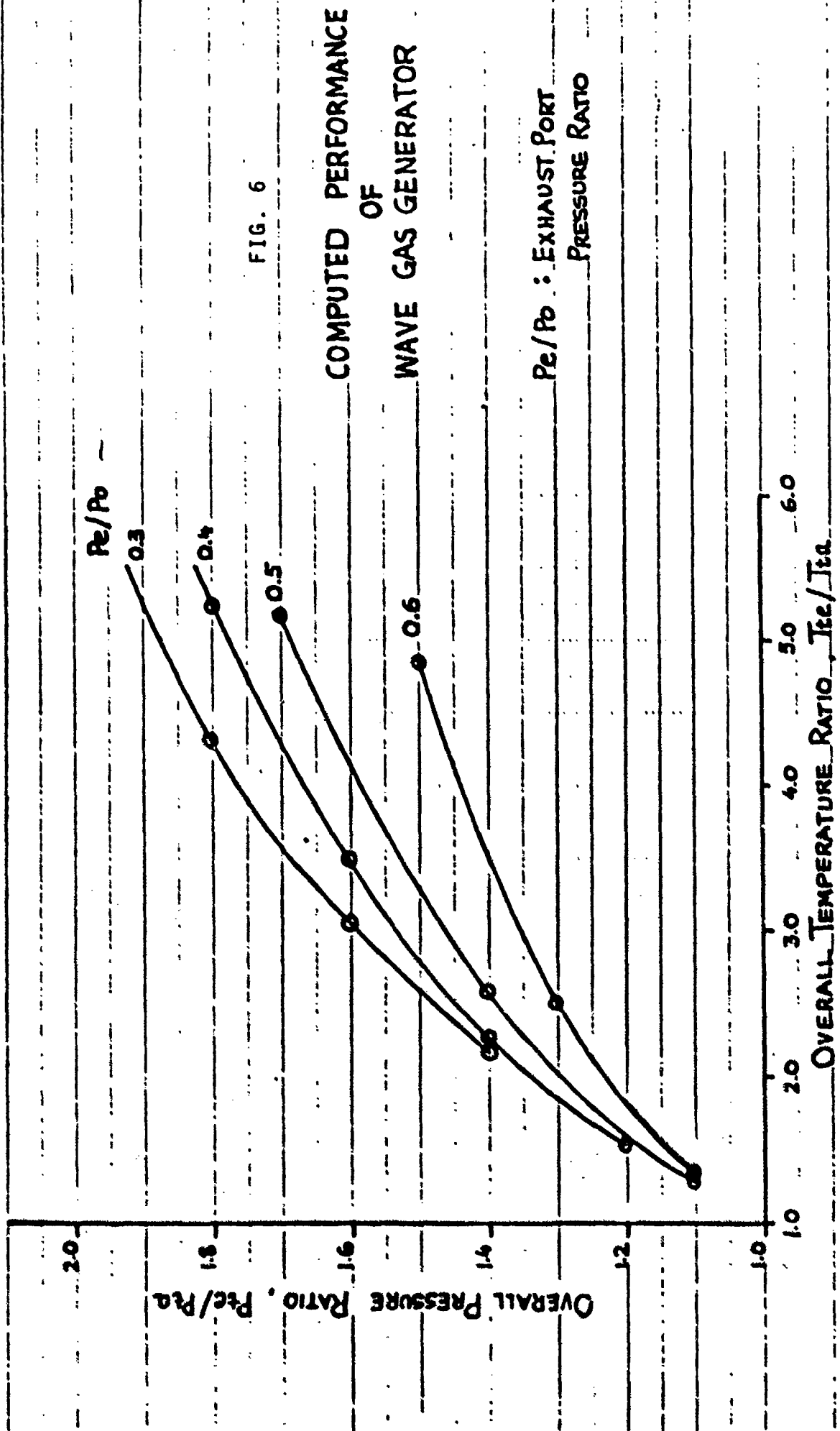


FIG. 6

EXPERIMENTAL EFFORT

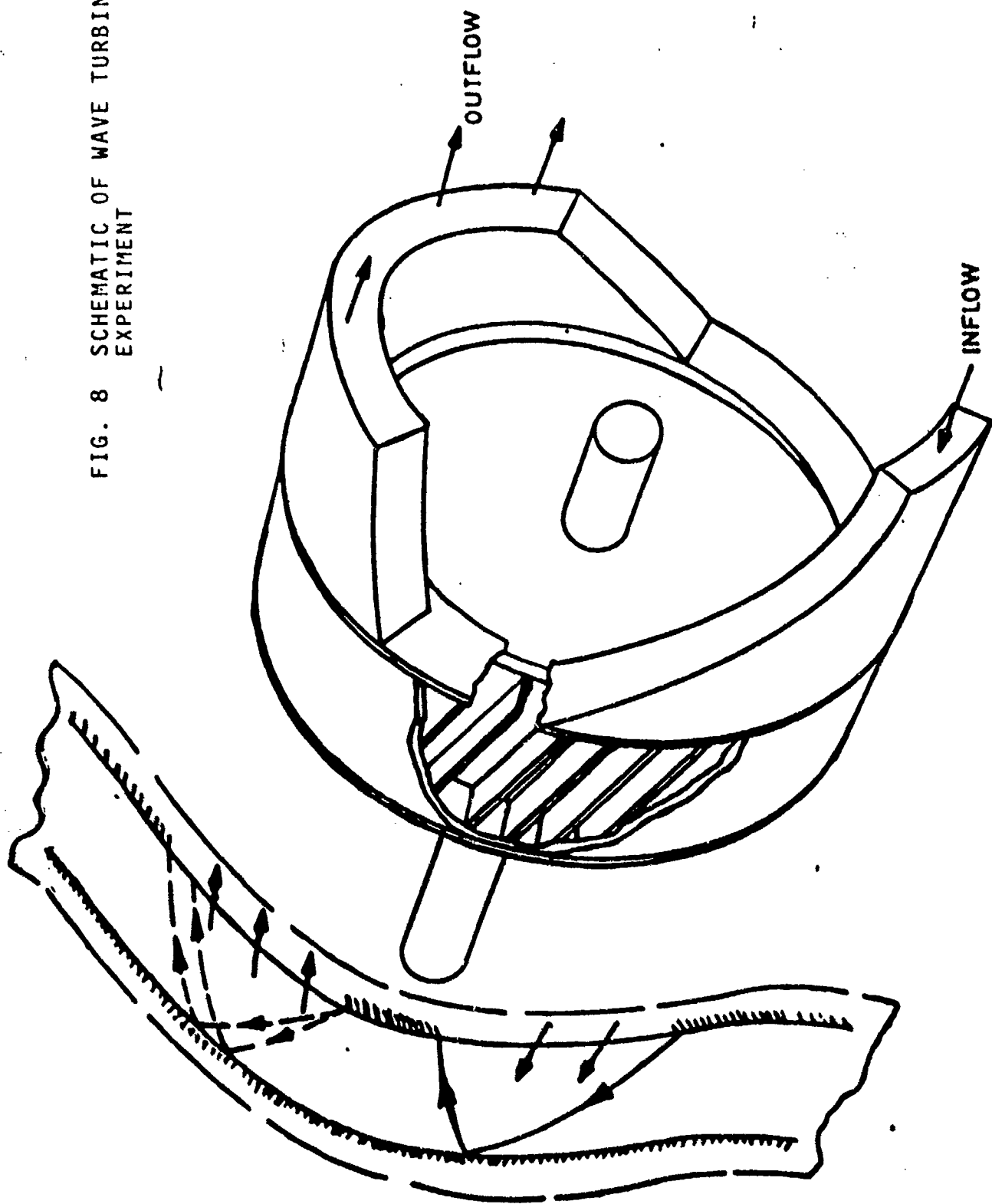
LOW-COST PRELIMINARY RESEARCH TEST RIG TO PROVIDE THE UNDERSTANDING NECESSARY TO PROPOSE A PRACTICAL ENGINE. 'WAVE TURBINE' MODE OPERATION SELECTED.

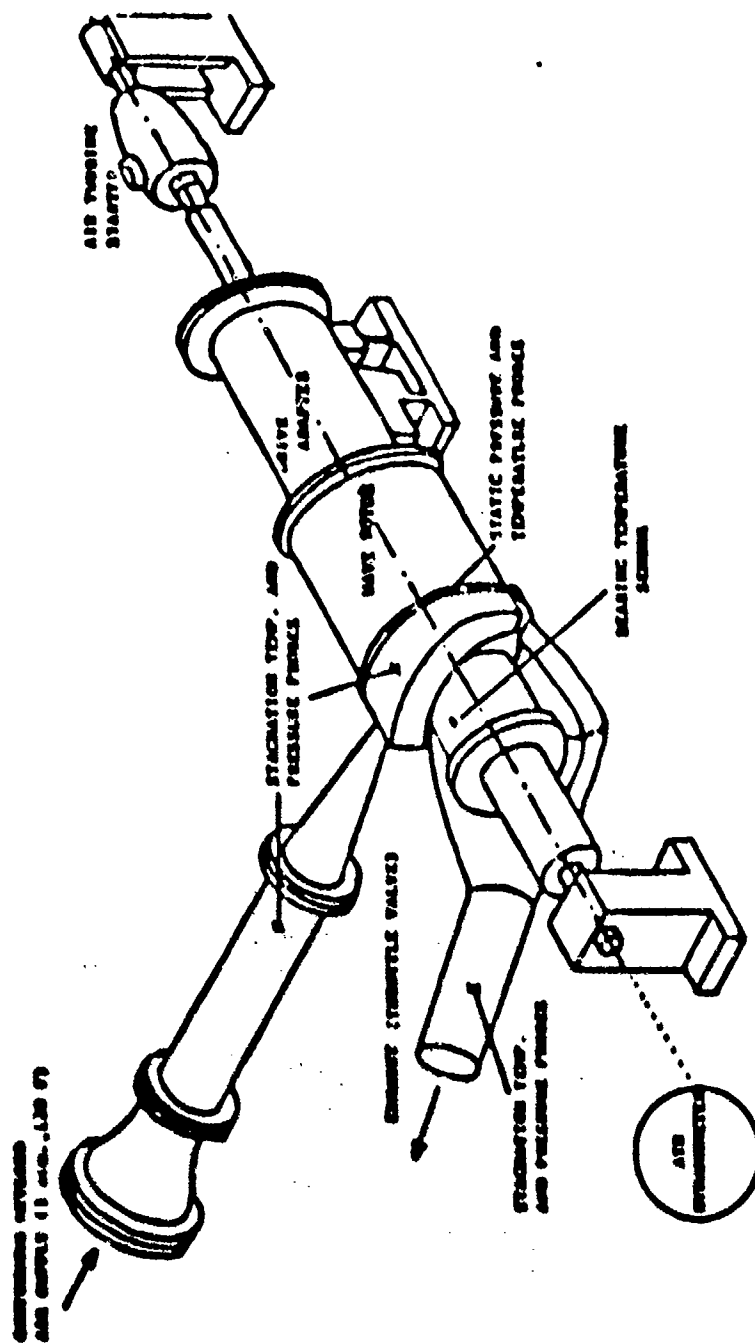
OBJECTIVES:

- DEMONSTRATE MECHANICAL RELIABILITY OF TEST VEHICLE
- COMPARE OBSERVED WEIGHT FLOW TO COMPUTED VALUE TO GAUGE INFLOW LOSSES
- COMPARE EXHAUST PROCESS WITH THE IDEAL 1-DIMENSIONAL TRANSIENT FLOW SOLUTION OBTAINED NUMERICALLY
- INTRODUCE FINITE TIME EFFECTS INTO COMPUTATION AND EVALUATE SIGNIFICANCE FOR EXHAUST PROCESSES
- (POSSIBLY) TEST EFFECT OF EDGE GEOMETRY ON INFLOW AND OUTFLOW PROCESSES

FIG. 7

FIG. 8 SCHEMATIC OF WAVE TURBINE
EXPERIMENT





ROCKET ENGINE EXPERIMENTAL TEST CELL
FIG. 9

Gradual Opening of Rectangular Axial and Skewed Wave Rotor Passages

by S. Eidelman

Science Applications International, McLean Virginia

ABSTRACT

It was shown in the present study, on the basis of numerical modeling, that the dynamics of the passage opening significantly effects the flow pattern in the passages of wave rotor devices. For rectangular axial passages, even when the velocity of the passage opening is 500 M/sec, a one dimensional flow pattern forms only in passages with length to width ratio larger than 3. In the region preceding the formation of the one dimensional flow pattern, the flow is rotational and in some instances contains shock and pressure waves which repetitively reflect from the upper and lower walls of the passage. In practice this would lead to significant mixing between the driver gas (e.g., exhaust gas) and the driven gas (e.g. fresh air) and reduce the efficiency of the engine cycle. With a reduction in the velocity of the passage opening, the volume of the mixing region increases as a result of the rotational flow which develops from the slow opening of the passage. With an increase in shock wave strength, the volume of the mixing region increases as a result of the rotational flow which develops from multiple reflections of the shock and pressure waves from the passage walls.

At the same time our modeling of the gradual opening of the skewed passage shows the way to minimize mixing losses at the inlet. Opening the skewed passages with the optimal velocity reported in this study will allow to reduce the losses and design the wave rotors with shorter passages. Our simulation shows that even if the conditions for the optimal opening are not satisfied exactly, reduction of the rotational mixing could be significant if the opening velocity is $\pm 15\%$ of the optimal value.

Numerical modeling of the process of gradual passage opening at the inlet port of the driven gas revealed that the interface between the gases will move all the way through the passage with a frozen pattern of distortion or obliqueness to the passage walls. The interface obliqueness increases when the velocity of the passage opening decreases.

In all, it can be concluded that taking into account the gradual passage opening is essential for the wave machine design, not only for proper timing and wave arrangement but also because of the losses which will occur due to mixing and wave reflections. The gap between projected and achieved efficiencies of wave machines, could be partially due to neglect of the effects of the gradual passage opening which are studied in this paper.

The Problem of Gradual Opening in Wave Rotor Passages

by S. Eidelman

Introduction

Wave rotors are devices which use wave propagation through the fluid in a rotor passage to transfer energy from one fluid to another (Ref 1) or to transfer energy from one fluid to rotor shaft and another fluid (Ref 2). "Wave rotors", "wave engines," "wave pressure exchangers," "wave equalizers," "Comprex" - are all based on the same idea of energy exchange in the unsteady waves, and the topic of the present study would be relevant to all these devices.

The principles of operation of wave rotor devices and their commercial applications can be found in References 1, 2, and 3. For completeness, the general scheme of a wave pressure exchanger will be described. Such a device is illustrated in Figure 1. One gas (driver) at high pressure is used to compress a second gas (driven). The process is arranged to occur in tube-like passages with trapezoidal cross-section located on the periphery of a rotating drum or rotor. The compression is achieved successively in each rotor passage by means of compression waves or shock waves generated by the entering driver gas. The compressed driven gas is drawn off from the end of the passage when it aligns with an outlet port. The driver gas then undergoes a series of expansions to a lower pressure and is scavenged out by freshly inducted driven gas at approximately the same pressure level. This fresh 'charge' is then compressed by the high pressure driver gas and the cycle repeats itself. Steady rotation of the drum sequences the ends of the passages past stationary inlet ports, outlet ports and endwalls. This establishes unsteady but periodic flow processes within the rotating passages and essentially steady flow in the inlet and outlet ports. The passages may be oriented axially as in Figure 1 or

at a 'stagger' angle. In general, wave machines used as pure pressure exchange (e.g., the "Comprex" Ref 1) have axially oriented passages, while-those with staggered passages may drive a shaft, since shaft work extraction is possible with this latter configuration.

It is very desirable, in the design of the wave rotor, to determine the optimal ratio between the width and length of the single passage of the rotor. Usually only two parameters are evaluated to determine this ratio: skin friction losses and by-pass losses. The number of passages on the rotor should be minimal in order to minimize skin friction losses. On the other hand the passage should be narrow compared to the port widths in order to reduce flow by-pass between inlet or outlet ports. The transient process of the passage opening or closing (as the passage end moves across a port or moves from a port to be closed by the endwall respectively) usually is not considered in the design. It is generally assumed that the passage opening or closure occurs instantaneously.

Pearson [2] tried to take into account the gradual opening of the passage assuming that the air in the passage is compressed in a series (usually three) of discrete compression waves which converged and ultimately merged to form a shock wave. This allowed him to design a complicated wave machine cycle for a rotor using relatively short passages. However, since the technique, was one dimensional it could not reveal the peculiarities of this essentially two dimensional flow and would be valid only for very weak waves.

In the present study, by means of numerical modeling, we will examine in real-time how the gradual opening influences the wave formation in the wave rotor passages and how that should affect the rotor design.

Model

Here the assumptions involved in the numerical simulations are described.

The flow in each passage of the wave rotor is unsteady and periodic. At the same time, the flow through the ports is (ideally) steady [Ref 1 & 2]. The peripheral width of the port is usually equal to several widths of a single passage, and in this study it is assumed that the flow in the inlet or outlet port remains stationary when the passage-end encounters the port. For this reason the region of the port is not included in the computational domain shown in Figure 2.

The time dependent process of the passage-end translating across the region of the inlet or outlet port will be referred as the gradual opening of the passage. The passage opening process will be referred as instantaneous, when the assumption is made that the passage instantaneously opens to the port area and is subjected immediately to the steady flow conditions at the port.

It is assumed that the flow is inviscid, and can be modeled by the Euler equations.

The unsteady two-dimensional Euler equations can be written in conservation law form as:

$$\frac{\partial U}{\partial t} + \frac{\partial F}{\partial X} + \frac{\partial G}{\partial Y} = 0$$

where

$$U = \begin{pmatrix} \rho \\ \rho u \\ \rho v \\ e \end{pmatrix}, \quad F = \begin{pmatrix} \rho u \\ p + \rho u^2 \\ \rho uv \\ (e + p)u \end{pmatrix}, \quad G = \begin{pmatrix} \rho v \\ \rho uv \\ p + \rho v^2 \\ (e + p)v \end{pmatrix} \quad (1)$$

Here, ρ is the density, u and v are the velocity components in the X and Y coordinate directions, p is the pressure and γ is the ratio of specific heats. The energy per unit of volume, e , is defined by:

$$e = \rho \left(\epsilon + \frac{u^2 + v^2}{2} \right)$$

where $\epsilon = \frac{p}{(\gamma-1)\rho}$ is the internal energy. We look for the solution of the

system of equations represented by Equation (1) in the computational domain shown in Figure 2 in time t , with the following conditions at the domain boundaries:

- a) Solid wall along segments 1-3 and 2-4
- b) Outflow along segment 3-4
- c) Inlet along segment 1-2

It is assumed that initially at time $t = 0$, the passage of the wave rotor is filled with stationary gas at ambient conditions. When instantaneous opening of the wave rotor passage was simulated, it was assumed that at time $t = 0$, the flow at the inlet 1-2 was equal to the steady flow in the port. When gradual opening of the passage was simulated, at time $t = 0$, the inlet was closed and solid wall boundary conditions were imposed at the inlet 1-2. Then, this boundary condition was gradually replaced by the flow condition at the inlet port. The length uncovered to the inlet port region, where the solid wall boundary conditions were replaced by the inlet port conditions, was determined using the elapsed time and the velocity of the passage relative to the inlet port.

The Godunov method was used to obtain a numerical solution of Equation (1) with the described boundary and initial conditions. Details of the implementation of the method and boundary conditions are given in Reference 4.

The flow field was modeled for the rectangular passage with 0.02m-width and 0.12m-length. The grid covering the computational domain of the passage is shown in Figure 2.

Results and Discussion

The following initial conditions were assumed for the air initially in the passage:

$$P_o = 1 \text{ atm} ; \rho_o = 1.2 \text{ kg/M}^3 ; U_o = 0 ; V_o = 0 ;$$

The driver gas entering through the port at the left hand end was assumed to have the following properties:

$$P_d = 1.8 \text{ atm} ; \rho_d = 1.81 \text{ kg/M}^3 ; U_d = 150 \text{ M/sec} ; V_d = 0 ;$$

These conditions correspond to a practical situation in a wave rotor when, a passage filled with a quiescent fresh charge of air at ambient conditions encounters an inlet port supplying hot, high pressure driver gas.

If the assumption is made that the passage instantaneously opens and is subjected to the conditions of the inlet flow at the left boundary 1-2 (see Fig. 2), then a perfectly one dimensional flow pattern should develop in the passage. The result of the modeling of these conditions are presented in the form of pressure contours at progressively larger time steps in Figure 3. Time $t = 0$, corresponds to the moment when the passage opens. Instantaneous opening of the passage is seen in Figure 3 to lead to an immediate formation of a shock wave and subsequent propagation in the passage from the left to the right. The flow conditions at the inlet port are matched to the parameters of the rarefaction wave which presumably would move towards the left end of the passage. For this reason the flow in the passage has no additional discontinuity. This situation is typical for a wave rotor, where flow conditions at the ports are chosen in such a way that waves do not propagate from the passages into inlet or outlet ports. The flow in the ports will therefore remain steady. In the case shown in Figure 3, the shock wave was found to propagate with a velocity, $V_{sh} = 446 \text{ M/sec}$, the interface with a

velocity $V_{in} = 150$ M/sec and all the parameters examined were confirmed accurately using one dimensional gas dynamics relationships.

Most of the approaches used in wave rotor design are based on the assumption that the waves are one dimensional in nature. When the gas is compressed by a weak shock wave for instance, assumptions are made that: the process is isentropic; the hot and cold gases are strictly separated by a planar interface; and, the flow is everywhere irrotational. This leads to the very high efficiencies projected for the compression. If the passage is wide enough, so that viscous effects can be neglected, this model of the compression in the wave rotor passage is realistic, but only for instantaneous passage opening or for a very long passage. Results presented below illustrate how the gradual passage opening effects the compression process.

In Figure 4, the pressure and Mach number contours in the passage are shown at a sequence of times for the case of a gradual opening to the inlet port with the velocity of 100 M/sec. Parameters for the gas in the passage, before opening begins, and in the inlet port are the same as for the case of instantaneous opening. The dynamics of the flow development seen in Figure 4a is very different from that shown in Figure 3. First, curved pressure waves radiate from the initial small opening appearing at the lower corner of the inlet on the left side of the passage ($t = 0.044$ Msec in Fig. 4). Subsequently, these waves reflect from the upper wall of the passage and at the time $t = 0.125$ Msec, have formed a row of compression waves which have approximately straight fronts normal to the wall of the passage. Initially, compression waves of this kind occupy a small part of the region with disturbed gas. In the region well behind the front of this quasi one dimensional propagation, compression waves are curved and are the result of the interaction between the waves reflecting back and forth between lower and upper walls of the passage and the new waves created by the progressive opening of the port to the passage.

As it is possible to see in Figures 4a and 4b for the times $t = 0.084$ Msec and $t = 0.166$ Msec respectively, the flow behind the quasi one dimensional region is highly rotational and is relatively constant pressure in the "X" direction. The passage became fully opened only at $t = 0.2$ Msec. At this time compression waves are propagating along the length of the passage and the pressure rises gradually from 1 atm at the right end to 1.8 atm at the left end. The front of converging compression waves will eventually become a shock wave, but this will occur at some later time and outside the computational domain.

It was concluded from the case presented in Figures 4a and 4b, that a length to width ratio of the passage of 6 will lead to very high mixing losses, non-uniform and inefficient compression.

In Figures 5a and 5b, pressure and velocity contours are shown for the case of gradual opening of the passage with velocity 200 M/sec. Full opening of the passage in this case occurred at $t = 0.1$ msec. A curved shock wave is formed at $t = 0.044$ msec. This shock wave (see Fig. 5a) partially reflects from the upper wall of the passage and then, gradually converging with its main front, forms an almost planar shock front at the time $t = 0.252$ msec. However, even then the flow is highly rotational behind the shock front, and the region of rotational flow occupies one third of the passage volume. In this region the gas velocity increases from $M = 0.3$ at the upper wall to $M = 0.52$ at the lower wall.

When the velocity of the passage opening is increased to 500 M/sec (see Figs. 6a and 6b) the passage becomes fully open at $T = 0.04$ Msec. Because of the fast opening of the passage the shock wave at the time $T = 0.044$ Msec. is less curved and only a small fraction of the shock front reflects from the upper wall. This reflected part of the shock front converges with the main front at $t = 0.172$ msec. From that time on, the flow pattern in the passage

is mostly one dimensional with a small and weakening region of rotational flow behind the main front. Nevertheless, even for this case, with passage length/passage width = 3, there will be very high mixing losses, with a large part of the passage volume subjected to rotational flow.

In order to study how the strength of the shock wave influences the flow pattern developing in the passage, an additional case was simulated where the parameters of the driver gas at the inlet port area were increased; namely, to

$$P_d = 2.85 \text{ atm} ; U_d = 283 \text{ M/sec} ; \rho_d = 4 \text{ kg/M}^3$$

As in the previous case the parameters of the driver gas were chosen in such a way that waves do not propagate back into the port when the passage opens. Results of this simulation, are shown in Figure 7a and 7b. The velocity of the passage opening was $V = 250 \text{ M/sec}$. It was concluded from the results presented in Figure 7a and 7b that an increase in the initial shock strength leads to stronger reflections and to substantial increases in the flow rotation. This in turn will lead to increased losses because of mixing of the driver and driven gases. The pattern of multiple reflections of the shock wave from the upper and lower walls of the passage can be seen in Figure 7a. At time $T = 0.073 \text{ Msec}$ the shock wave reflected from the upper wall is propagating towards the lower wall. Part of the reflected shock-wave front converges with the main shock wave, and part begins to reflect from the lower wall. (time 0.109 Msec) The multiple reflection weakens the reflected shock, but the reflection between the walls of the passage continues and can be followed for $t = 0.211 \text{ Msec}$ and $= 0.245 \text{ Msec}$. It is clear that for these conditions even passages with length to width ratio of 6 will have very substantial mixing losses because of the rotational flow.

A different situation is found for the passage opening to the inlet port of the driven gas. At this port, the pressure and velocity of the (driver)

gas in the passage should be matched with the pressure and velocity of the (driven) gas at the inlet. If the passage opens instantaneously, the flow field in the passage will have only one discontinuity - the interface between the fresh air and exhaust gas entering and leaving the passage respectively.

To model this condition for the gradual passage opening, it was assumed that

in the passage, $P_o = 1 \text{ atm}$, $\rho_o = 0.5 \text{ kg/m}^3$, $U_d = 150 \text{ M/sec}$ and $V_o = 0$;

in the port, $P_d = 1 \text{ atm}$, $\rho_d = 1.4 \text{ kg/M}^3$, $U_d = 150 \text{ M/sec}$ and $V_d = 0$.

The velocity of the passage opening was $V = 200 \text{ M/sec}$.

Results for this simulation are presented in Figures 8a and 8b. It can be seen that, since at the first moment most of the inlet cross-section is blocked by the wall, a rarefaction wave reflects from the inlet wall. The passage full opening occurs at $t = 0.1 \text{ Msec}$. From this time on the pressure deviation in the flow field weakens and at $t = 0.22 \text{ Msec}$ the pressure is almost completely uniform and equal to the static pressure in both the undisturbed driven air and in the exhaust gas. Figure 8b shows that the interface will carry the imprint of the gradual passage opening a long time after the passage becomes fully open. There is no dissipative mechanism included in the mathematical model used in this study to force the interface to become normal to the passage walls. Therefore the interface will "remember" the dynamics of the gradual passage opening even in passages with large length to width ratio.

Conclusions

It was shown in the present study, on the basis of numerical modeling, that the dynamics of the passage opening significantly effects the flow pattern in the passages of wave rotor devices. For rectangular axial passages, even when the velocity of the passage opening is 500 M/sec, a one dimensional flow pattern forms only in passages with length to width ratio larger than 3. In the region preceding the formation of the one dimensional flow pattern, the flow is rotational and in some instances contains shock and pressure waves which repetitively reflect from the upper and lower walls of the passage. In practice this would lead to significant mixing between the driver gas (e.g., exhaust gas) and the driven gas (e.g., fresh air) and reduce the efficiency of the engine cycle. With a reduction in the velocity of the passage opening, the volume of the mixing region increases as a result of the rotational flow which develops from the slow opening of the passage. With an increase in shock wave strength, the volume of the mixing region increases as a result of the rotational flow which develops from multiple reflections of the shock and pressure waves from the passage walls.

Numerical modeling of the process of gradual passage opening at the inlet port of the driven gas revealed that the interface between the gases will move all the way through the passage with a frozen pattern of distortion or obliquity to the passage walls. The interface obliquity increases when the velocity of the passage opening decreases.

In all, it can be concluded that taking into account the gradual passage opening is essential for the wave machine design, not only for proper timing and wave arrangement but also because of the losses which will occur due to mixing and wave reflections. The gap between projected and achieved efficiencies of wave machines (2, 6, 7), could be partially due to neglect of the effects of the gradual passage opening which are studied in this paper.

References

1. Croes, Nic, "The Principle of the Pressure - Wave Machine as Used for Charging Diesel Engines," Dept. Compres Research, A. G. Brown Boveri and Cie, Baden, Switzerland.
2. Pearson, R. D., "Pressure Exchangers and Pressure Exchange Engines," Ch. 16, Thermodynamics and Gas Dynamics of I. C. Engines, compiled by D. E. Winterbone and S. C. Low, forthcoming publication.
3. Thayer III, W. J., Taussing, R. T., Zumdieck, J. F., Vaidyanathan, T. S., and Christiansen, W. H., "Energy Exchanger Performance and Power Cycle Evaluation-Experiment and Analysis," DOE AC06-78ER01084, April 1981.
4. Eidelman, S., Colella, P. and Shreeve, R. P., "Application of the Godunov Method and Higher Order Extension of the Godunov Method to Cascade Flow Modeling," AIAA-83-1941-CP, AIAA 6th Computational Fluid Dynamics Conference, July 13-15, Danvers, Massachusetts, 1983.
5. Shreeve, R. P., Mathur, A., Eidelman, S. and Erwin, J., "Wave Rotor Technology Status and Research Progress Report," NPS67-82-014PR, Naval Postgraduate School, November 1982.
6. Coleman, R. C. and Weber, H. E., "Integral Turbo-Compressor Wave Engine," U.S. Patent No. 3,811,796, 1976.
7. "Exploratory and Advanced Development Programs," Technical Progress Report, Naval Air Propulsion Center, NADC-1-83, April 1983, Trenton.

FIGURES

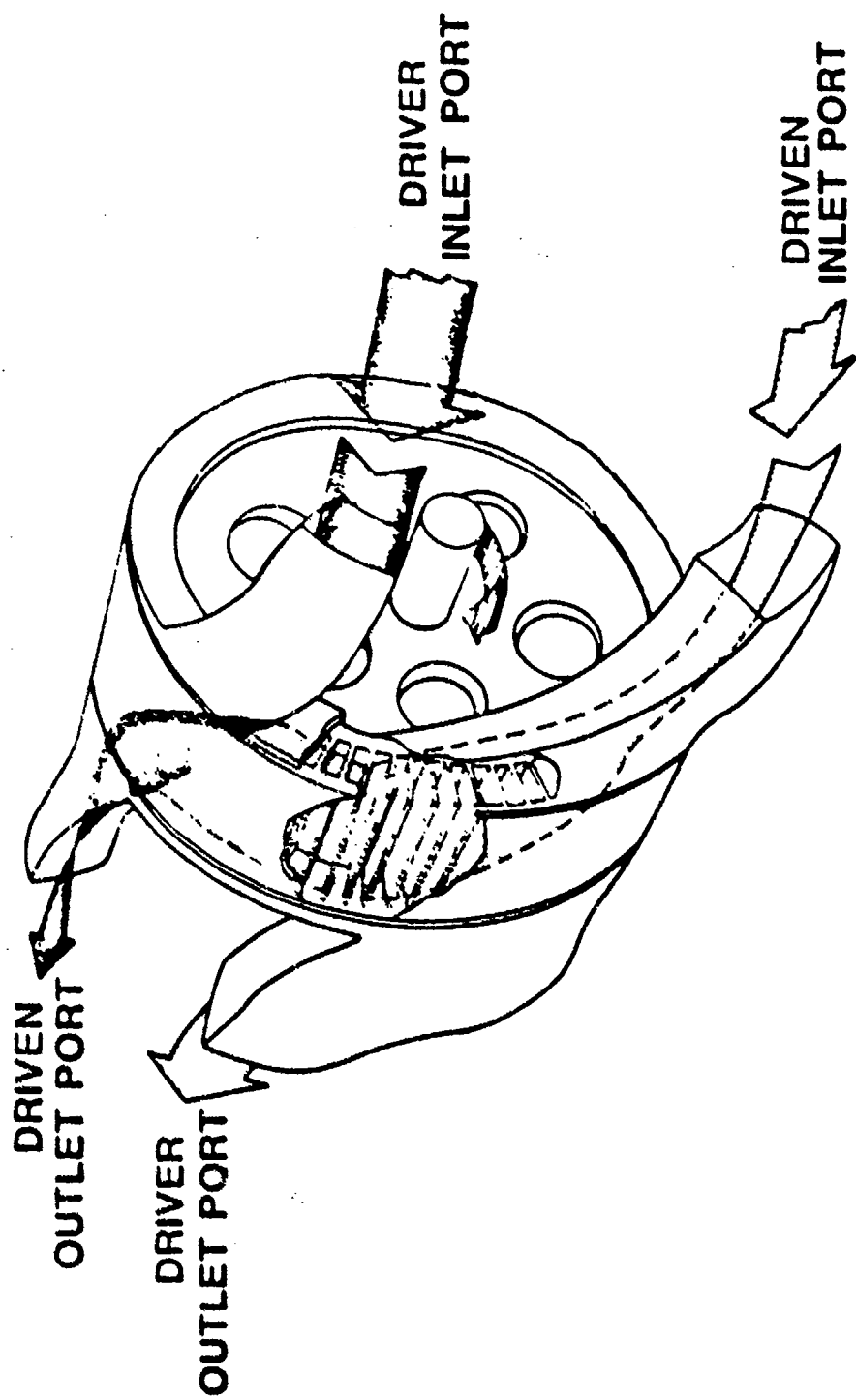


Figure 1. Wave rotor operation scheme.

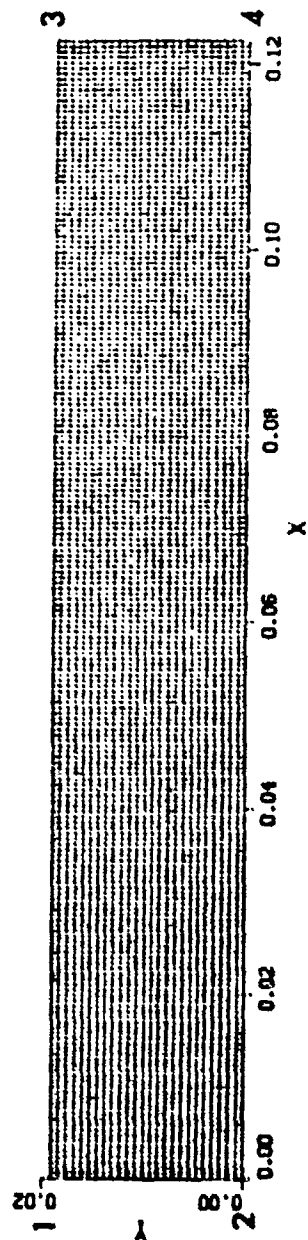


Figure 2. The computational domain.

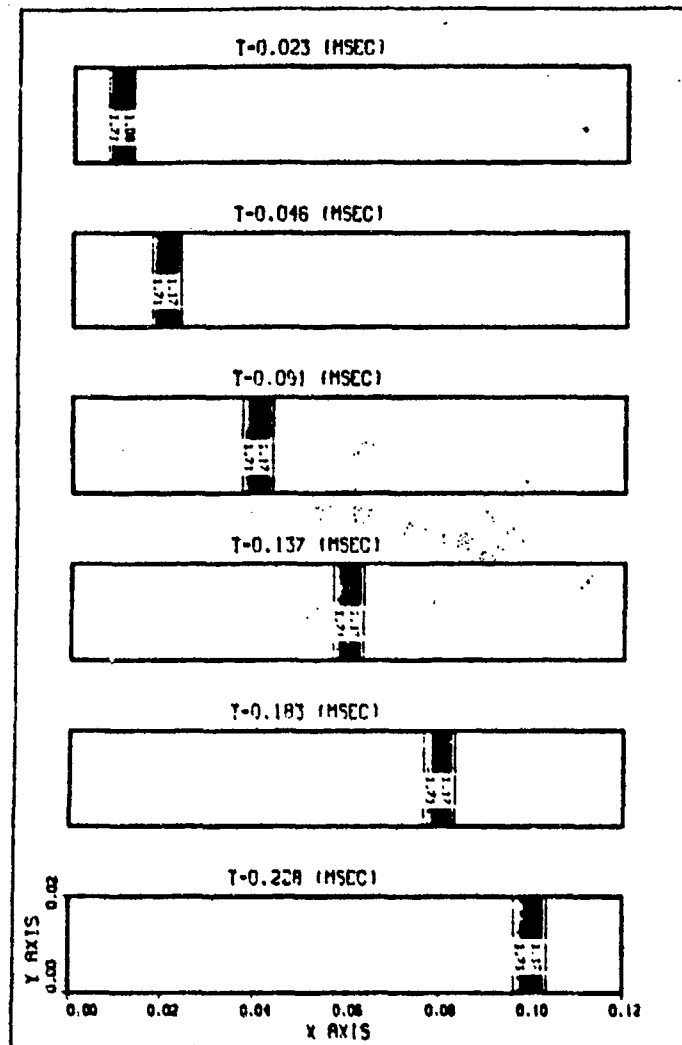


Figure 3. The evolution in time of the shock wave formed after instantaneous passage opening.

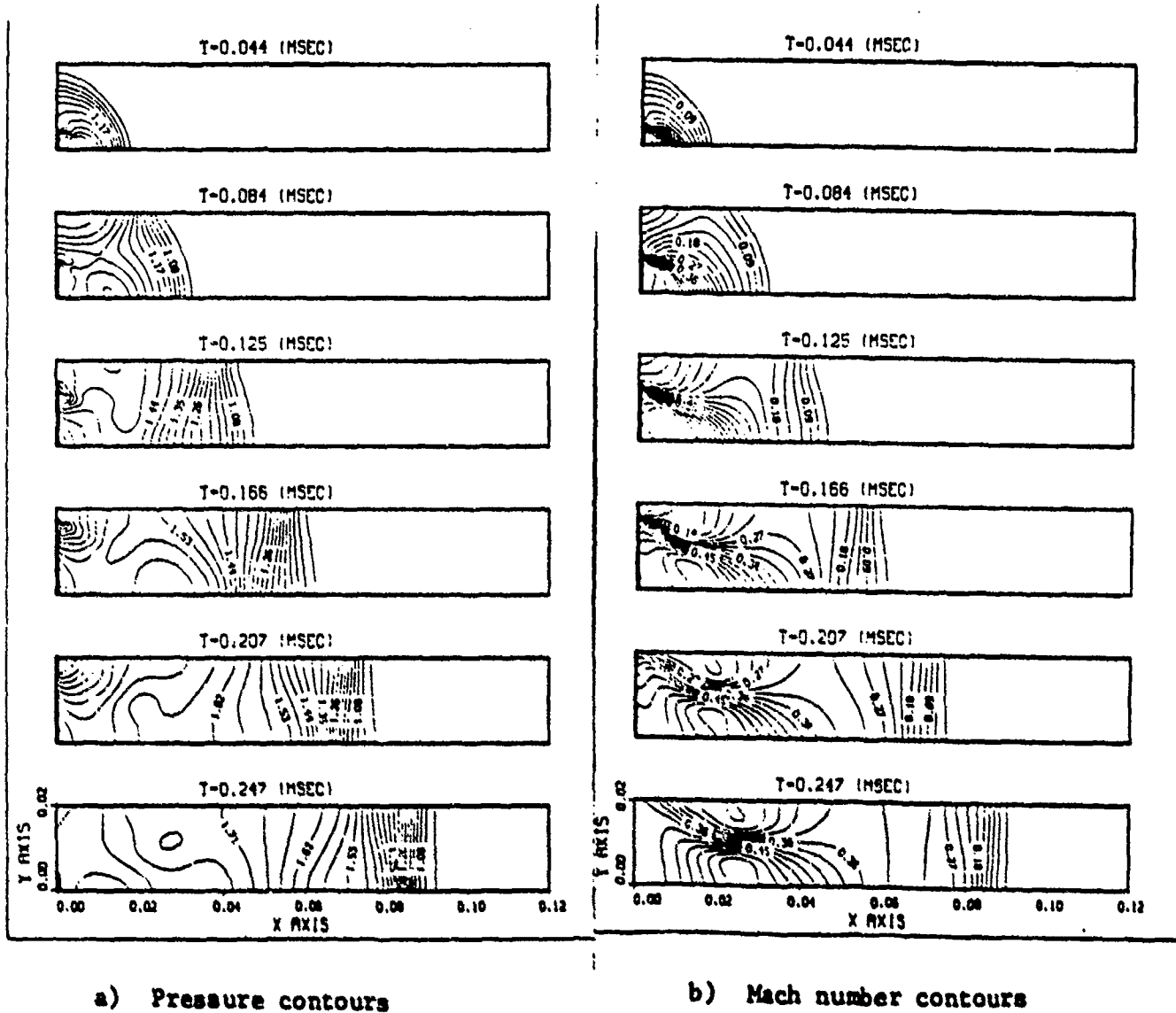
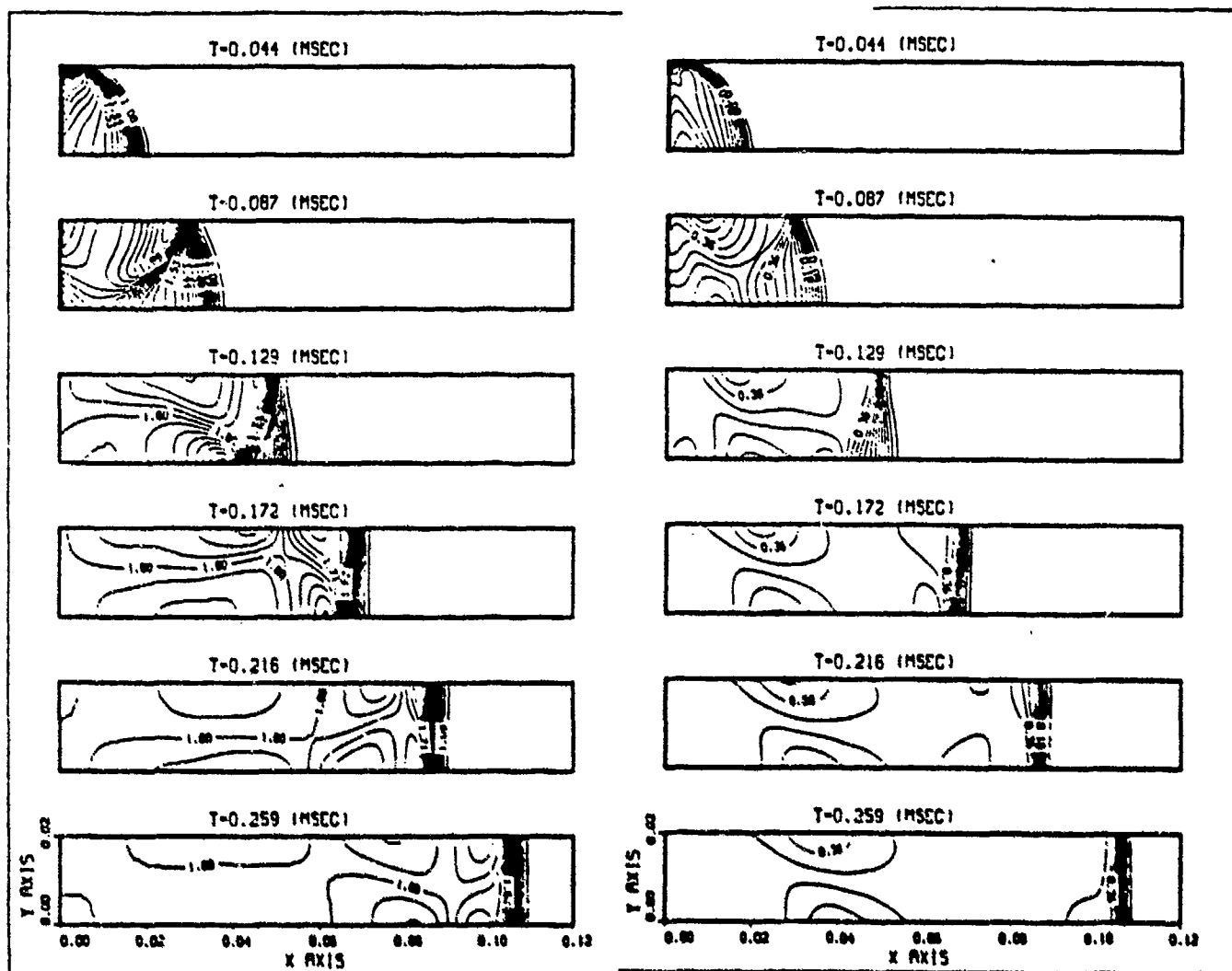


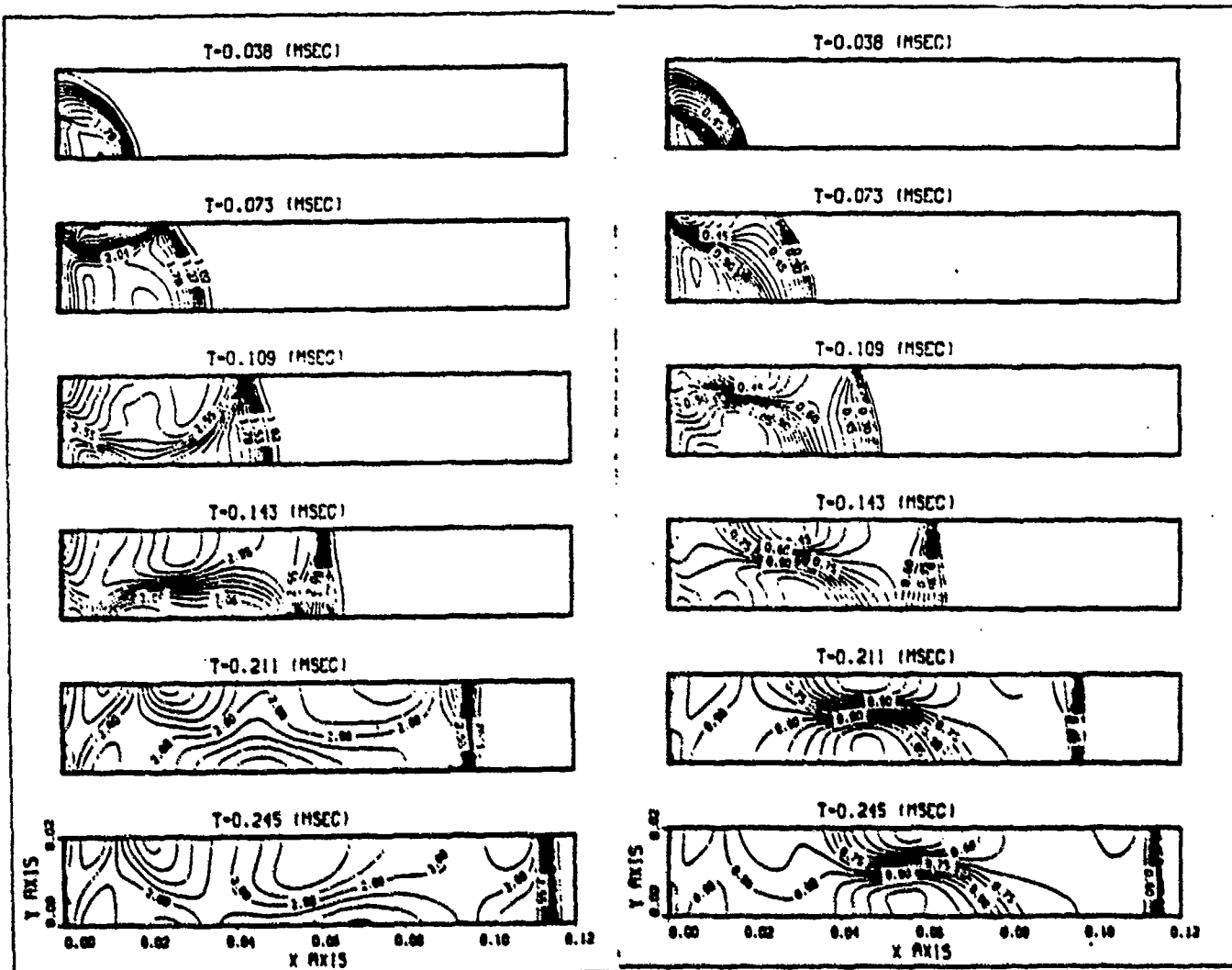
Figure 4. The flow pattern evolution for the passage gradual opening with velocity 100 m/sec.



a) Pressure contours

b) Mach number contours

Figure 6. The flow pattern evolution for the passage gradual opening with velocity 500 m/sec.



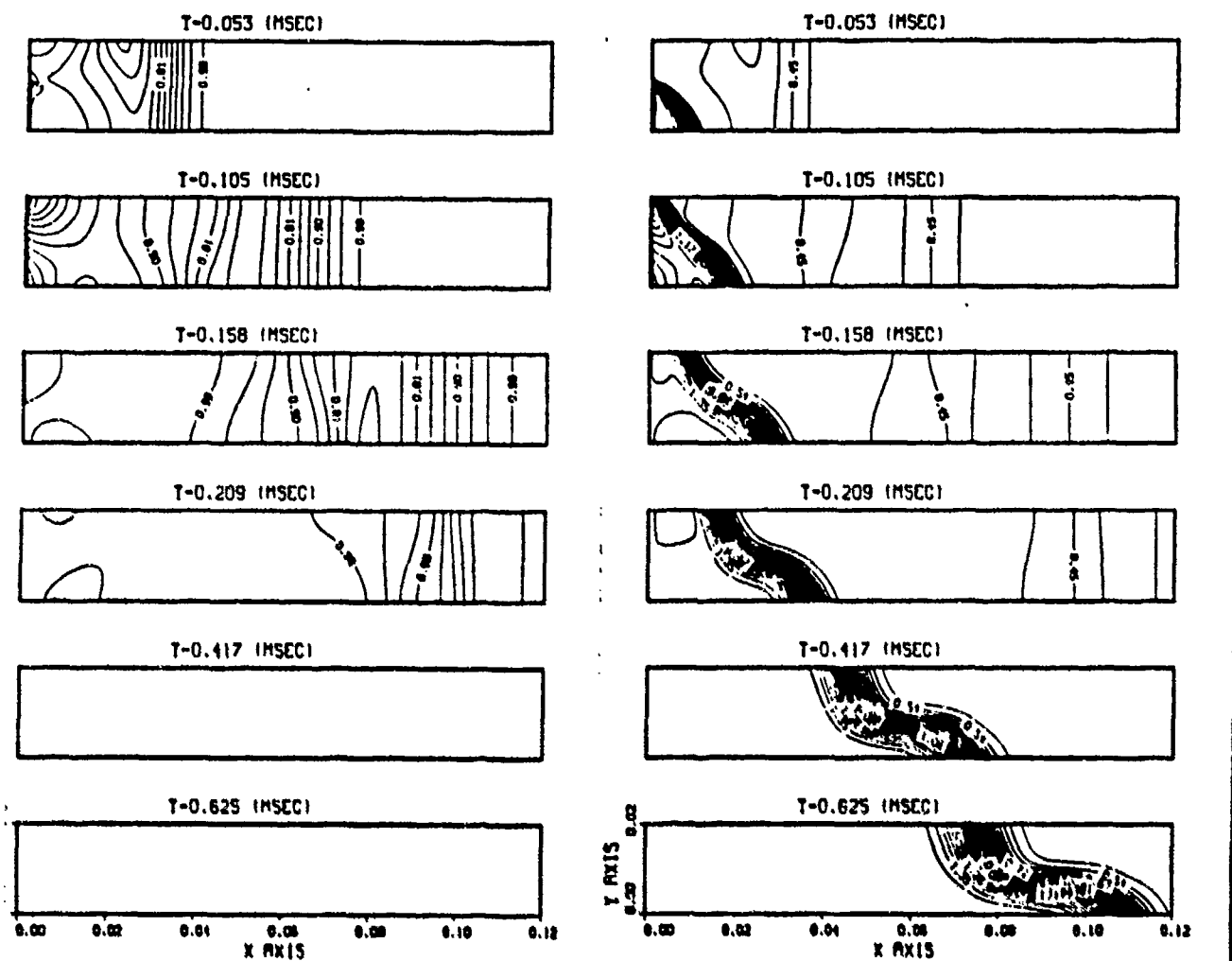
a) Pressure contours

b) Mach number contours

Figure 7. The flow pattern evolution for the gas with higher total enthalpy at the inlet port.

P200

K200



a) Pressure contours

b) Density contours

Figure 8. The evolution of the interface.

WAVE ROTORS AS SUBSTITUTES FOR GAS-TURBINE
DIFFUSER-COMBUSTOR SYSTEMS

David Gordon Wilson
Massachusetts Institute of Technology, 3-455
Cambridge, MA 02139
phone 617 253 5121

SUMMARY

Wave-rotor devices have been proposed several times in the past as the high-pressure "spools" of gas-turbine engines. A variation of these proposals is brought forward for consideration here.

The potential gains in engine performance of reducing diffuser and combustor total-pressure losses and of possibly achieving a gain in total pressure during combustion are described. Past proposals are reviewed. The potential for future development in some limited areas is discussed.

INTRODUCTION

The application of wave-rotor technology to be considered here is strictly limited. Whereas most proposals have concerned the harnessing of pressure waves in compressible fluids to transfer, as reversibly as possible, pressure energy between different streams of fluids, here we examine the interaction between a single stream of fluid and a rotor.

We have two purposes. One is to accomplish a greater degree of diffusion than is possible with conventional subsonic diffusers. The second is to approach constant-volume combustion for gas-turbine engines.

The performance of conventional diffusers

The principal performance measure of diffusers is the pressure-rise coefficient C_p , defined as the rise in static pressure as a proportion of the mean inlet dynamic pressure. A typical value of C_p for a "good" diffuser is 0.7. The maximum value of C_p is limited by several factors. The first is area ratio: if a sufficient area ratio is not provided, there is no possibility of the flow being slowed to the degree necessary to allow conversion of a high proportion of the dynamic pressure to static pressure. However, a large area ratio is no guarantee of efficient pressure recovery. Any factor that could precipitate stalling of the boundary layers along the diffuser walls, such as wall roughness, thick and sluggish inlet boundary layers, high wall curvature, flow incidence or swirling at inlet, secondary flow, or secondary vorticity, may reduce pressure recovery to a low value.

In a gas-turbine engine, the diffuser having the most impact on cycle performance is that at compressor exit. Typically the velocity at the exit of an axial compressor is 200 m/s; downstream of the radial diffuser of a centrifugal compressor the velocity is usually somewhat higher. In the axial-compressor case, a short diffuser having a velocity ratio of about 2:1 can be fitted; little additional diffusion can be incorporated downstream of a radial diffuser.

Therefore there is a considerable loss of total pressure in the form of dynamic pressure, and a smaller pressure loss due to wall friction, in the compressor-outlet diffuser in a gas-turbine engine. This loss may constitute one-third or more of the total losses in compression - eg five points in fifteen in a compressor of 85-percent efficiency.

The performance of conventional combustion systems

If combustion could be stabilized in an air stream moving at 200 m/s there would be no need for a diffuser after the compressor. However, the maximum speed of turbulent flames is less than 15 m/s. This maximum occurs at close to the stoichiometric mixture. In a standard form of combustion chamber, therefore, a "primary zone" is designed to produce near-stoichiometric mixtures at all operating conditions. The very-high-temperature gases from the primary zone must then be diluted with "secondary" air from the compressor delivery in such a way that a reasonably uniform-temperature stream is delivered to the turbine. To achieve such a flow, the diluent cooling air must be injected into the hot stream so that full penetration of the stream is achieved.

The dynamic pressure required for these dilution jets is produced from the just-slowed compressor-delivery air. The overall combustor pressure drop in gas-turbine engines that is required is generally in the range of 3-6 percent of the compressor-delivery pressure. This brings about a fall of similar percentage in the cycle thermal efficiency.

If in a typical gas-turbine engine we could eliminate diffuser losses, so bringing about a three-percent gain in compressor efficiency, and if we could eliminate a four-percent combustor total-pressure loss, we would increase the specific power output and the thermal efficiency by around five percent. This is a very considerable gain, given the large sums spent in design and development to achieve fractions of a percent improvement. If it were possible to produce an actual pressure rise in combustion, as is theoretically possible for constant-volume heat addition, the gains would be even greater.

BRIEF HISTORICAL REVIEW

The constant-volume-combustion cycle was developed actively by Holzwarth, working partly with the Brown Boveri Company, for over thirty years from 1906. It was, in fact, one of the first gas turbines to achieve successful independent operation, giving about 150 kW in 1910 (Ostarhild, 1933), but doing so at a low efficiency. A good account of the development and difficulties during the whole period, culminating in the almost-accidental switch to the development of the first fully successful industrial constant-pressure gas-turbine engine, is given by Seippel, 1980.

The Holzwarth cycle is shown in figure 1. The compressor discharges to an air receiver, acting as a capacitor. The several combustors are valved, with a rather low-frequency filling and firing cycle, and they discharge to a second capacitor, an exhaust-gas receiver. The purpose of the capacitors was to produce near-steady flow in the compressor and turbine. Although quite remarkable engineering advances were achieved during the history of the Holzwarth explosion gas turbine, it was doomed by the large throttling losses in the valves and ducting, and by the heat-transfer losses in the ducting and exhaust-gas receiver between the combustion system and the turbine, coupled with losses associated with the need for scavenging in the combustion system to bring in the new charge.

Vandermeulen, 1982, reviewed the Holzwarth cycle and what would seem to be an improvement of it due to Karavodine in which the exhaust valves and exhaust-gas receiver are eliminated, figure 2. Combustion is therefore not strictly constant volume, and the turbine handles unsteady flow. He also examined a rather strange combination of the Holzwarth and Karavodine cycles in which the turbine exhausts to a receiver which in turn exhausts through a throttle. He tested the Karavodine cycle against the constant-pressure Brayton cycle in a test rig and concluded that the losses in throttling, "dead space", and slow and incomplete combustion made the Karavodine and the Holzwarth cycles unattractive in practice.

Reynst (1955) attempted to achieve some of the theoretical benefits of constant-volume combustion without the complications and losses that accompany valves and receivers by adding fuel periodically to a toroidal vortex oscillating at a natural frequency in an appropriately shaped combustion chamber. Stability, range of operation and high heat-transfer rates to the walls were severe problems; I do not know what was the ultimate reason for the abandonment of this program.

DIFFUSION AND COMBUSTION IN PORT-ROTOR SYSTEMS

Diffusion is defined as the conversion of dynamic pressure to static pressure. In subsonic flow it is normally considered to occur in a passage of increasing cross-sectional area. Momentary diffusion also occurs when a stagnation tube is inserted into a flowing stream. The flow is brought to rest almost isentropically within the tube if the downstream end is closed. If such a tube were capped and removed from the flow it would contain fluid at the stagnation pressure. A rotor containing many such stagnation tubes that can be exposed to the flow through ports can form a type of diffuser. If the higher-pressure fluid does not escape through leakage, the tubes could be opened through another port to a higher-pressure region, and at least some of the trapped flow could be delivered.

The inertia and compressibility of the fluid forms a distributed spring-mass system, and the wave action can produce a greater degree of both filling and emptying than would be calculated from a quasi-steady model.

Because the fluid is momentarily trapped in a capped tube it offers the theoretical possibility of permitting constant-volume heat addition.

This type of diffuser-combustor combination was proposed by Gustav Eichelberg and presented by Max Berchtold of the EIH in 1949 (figure 3). In his proposed arrangement, there is a stationary annulus of diffusion-combustion tubes which are opened to compressor delivery and to the turbine nozzles at appropriate times by connected rotating disks acting as ports. The wave diagram is shown in figure 4.

A simple modification of this proposal is shown in figure 5. In this arrangement the diffusion-combustion channels rotate, and the compressor-delivery flow is therefore steady in space and reasonably steady in time. Fuel injection is from the upstream end, and would be aimed at producing a near-stoichiometric mixture at the upstream end of the channel. Ignition would be initiated either through a spark or by a crossover channel communicating with the combustion zone of the preceding channel. The combustion pressure rise would blow flame through such a channel into the fuel-air mixture of the approaching channel. After ignition, a combustion pressure wave would travel down the channel

through the compressed air, arriving at the downstream end as the port opens, reflecting a rarefaction wave that would arrive back at the inlet end of the channel as the inlet port opened.

DISCUSSION

The rotor under discussion is neither a pressure exchanger nor an engine, because the processes involve just one stream of fluid, and there is no work exchange between the fluid and the rotor. The more usual proposals, such as that by Seippel (1946, 1949), figure 6, with which the proposals of Taussig, 1984, are related, employ a dynamic pressure exchanger partly as a means of carrying out combustion at a considerably higher pressure than that of compressor delivery. The combustion chamber can therefore be much smaller, and may possibly have a smaller pressure drop.

So far as is known, no hardware for either type of gas-turbine-engine combustion system has been made and tested. Combustion within the rotor would obviously be difficult. The apparent gains are, however, large. Perhaps a test following the example of Von Ohain would be desirable. He won Heinkel's approval for the development of his first jet engine by demonstrating a crude gas-generator fueled by hydrogen. He was then able to solve the difficult problems of liquid-fuel combustion in relatively easier conditions.

Pressure leakage is a major problem in all wave-rotor systems. The two-port single-fluid systems have the possibility of using closed-ended tubes, so that fluid is brought isentropically to rest, heated and compressed by combustion, and then ported out of the upstream end. Some trapped gas would presumably remain, acting merely as a spring. Leakage would be halved, and the mechanical design of the rotor bearing system might be simplified. The turbine ducting would, however, be more complex.

In either arrangement the turbine flow would emerge striated in a hot-cold sequence. If such a pattern persisted through the turbine the blading would experience the mean temperature because neither the nozzle nor the rotor blades could respond to the high-frequency changes imposed.

REFERENCES

- Ostarhild, Karl G. (1983), letter about Hans Holzwarth sent for publication to MECHANICAL ENGINEERING, January 10, 1983.
- Reynst, F. H. (1955). PULSATING, PRESSURE-GENERATING COMBUSTION SYSTEMS OF GAS TURBINES. ASME paper 55-A-55, NY, NY.
- Seippel, C. (1949). GAS-TURBINE INSTALLATION. US Patent 2,451,186 (filed 1943).

Seippel, C. (1983). CONSTANT-VOLUME VERSUS CONSTANT-PRESSURE COMBUSTION (one chapter in the history of the gas turbine). Private communication of a translation of an earlier (1980) article in German. Baden, Switzerland.

Taussig, Robert T. (1984). WAVE-ROTOR TURBOFAN ENGINES FOR AIRCRAFT. MECHANICAL ENGINEERING, ASME, NY, NY, Nov. 1984.

Vandermeulen, H. (1982). THE CONSTANT-VOLUME GAS-TURBINE CYCLE ACCORDING TO KARAVODINE. ASME paper 82-GT-243, NY, NY.

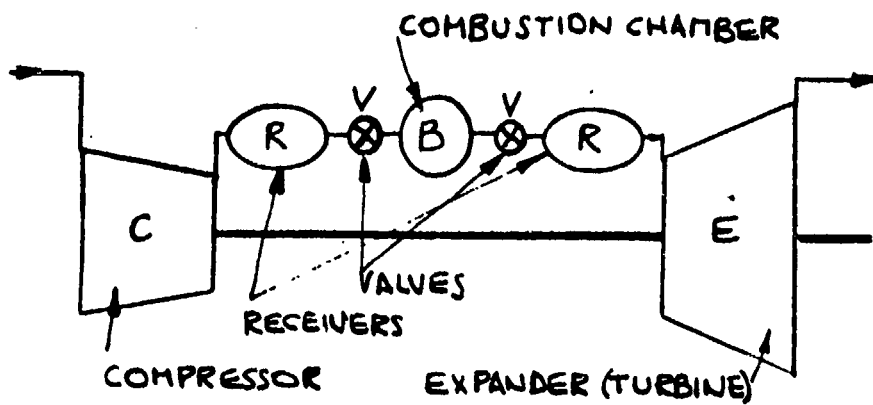


FIGURE 1 HOLZWARTH CYCLE

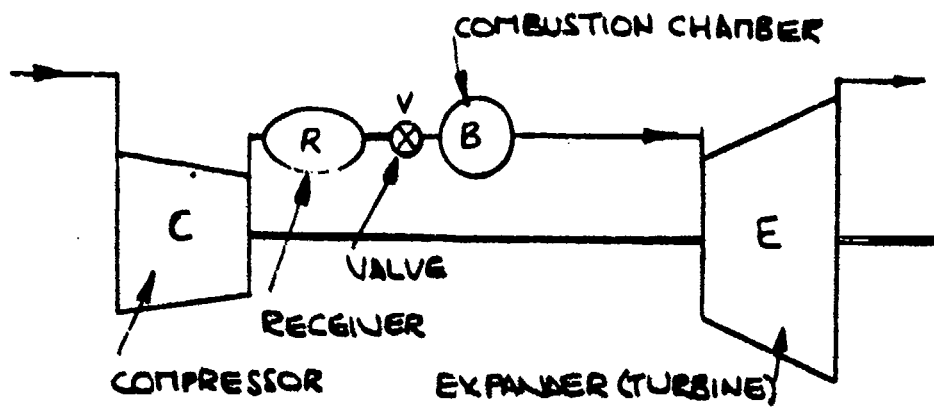
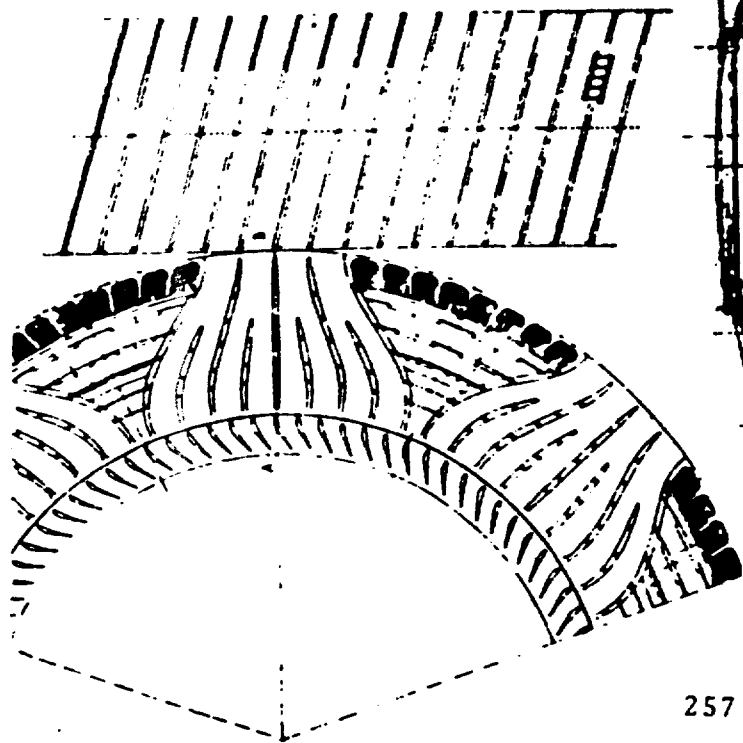


FIGURE 2 KARAVODINE CYCLE



AIRCRAFT JET ENGINE
based
ACOUSTIC COMPRESSION
Layout by Werner Howald
Maximum Thrust at sea-level
T = 20,000 lbs.
Maximum diameter = 50"

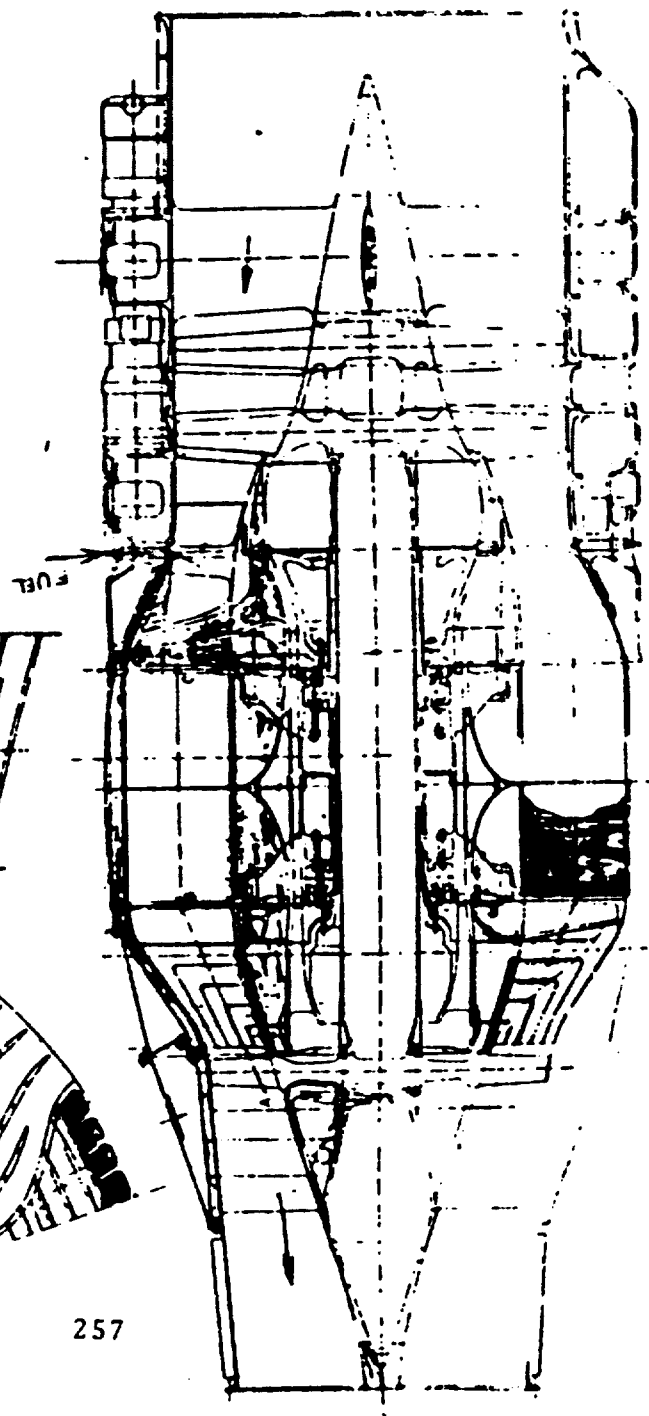
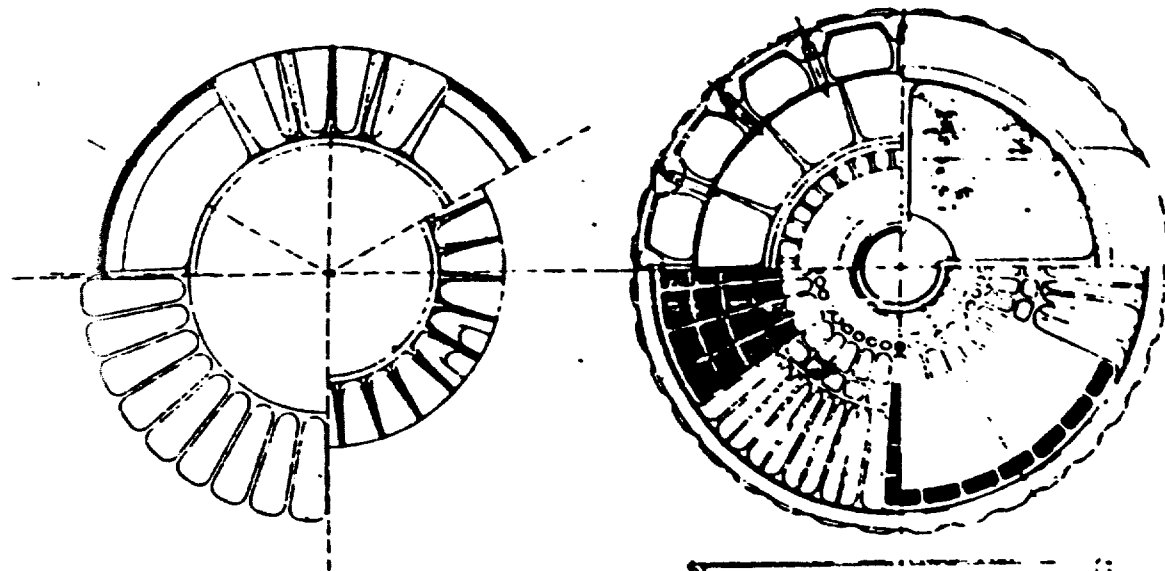


FIGURE 3 CROSS-SECTION OF THE EICHELBERG ENGINE

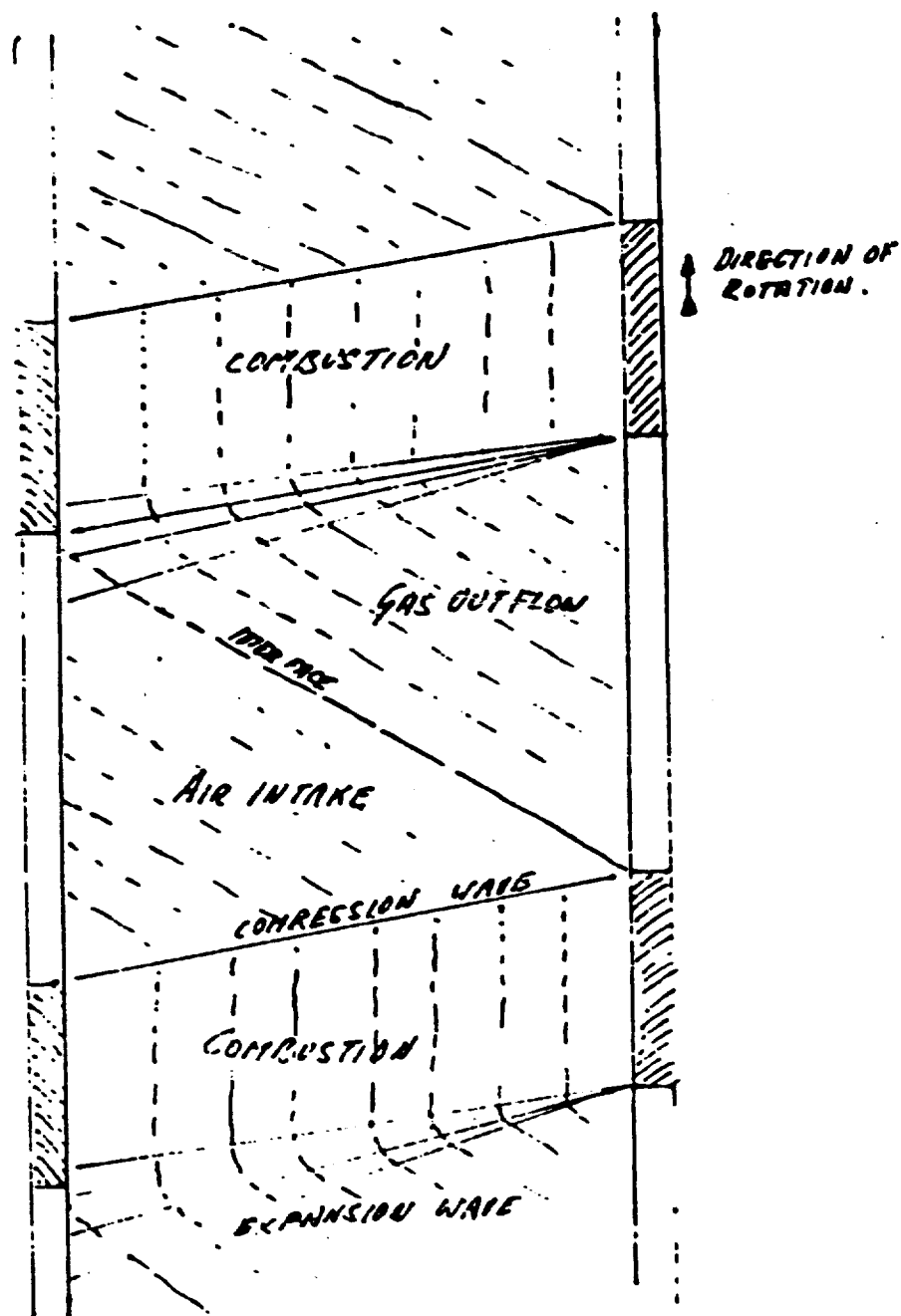
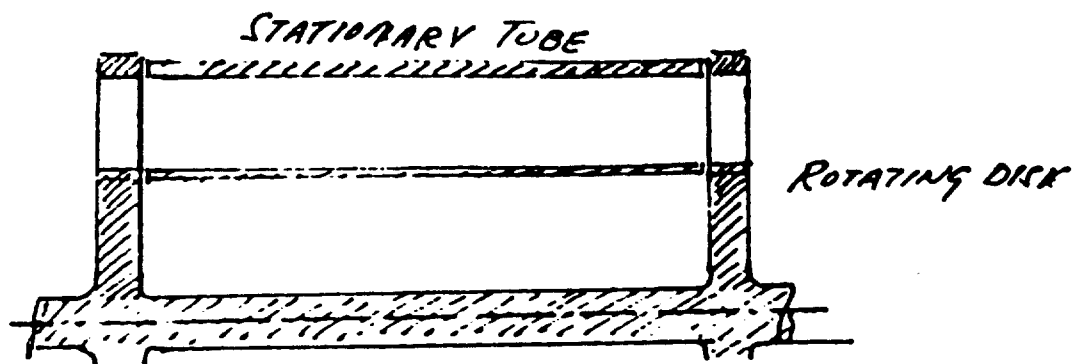


FIGURE 4 WAVE DIAGRAM OF THE EICHELBERG ENGINE

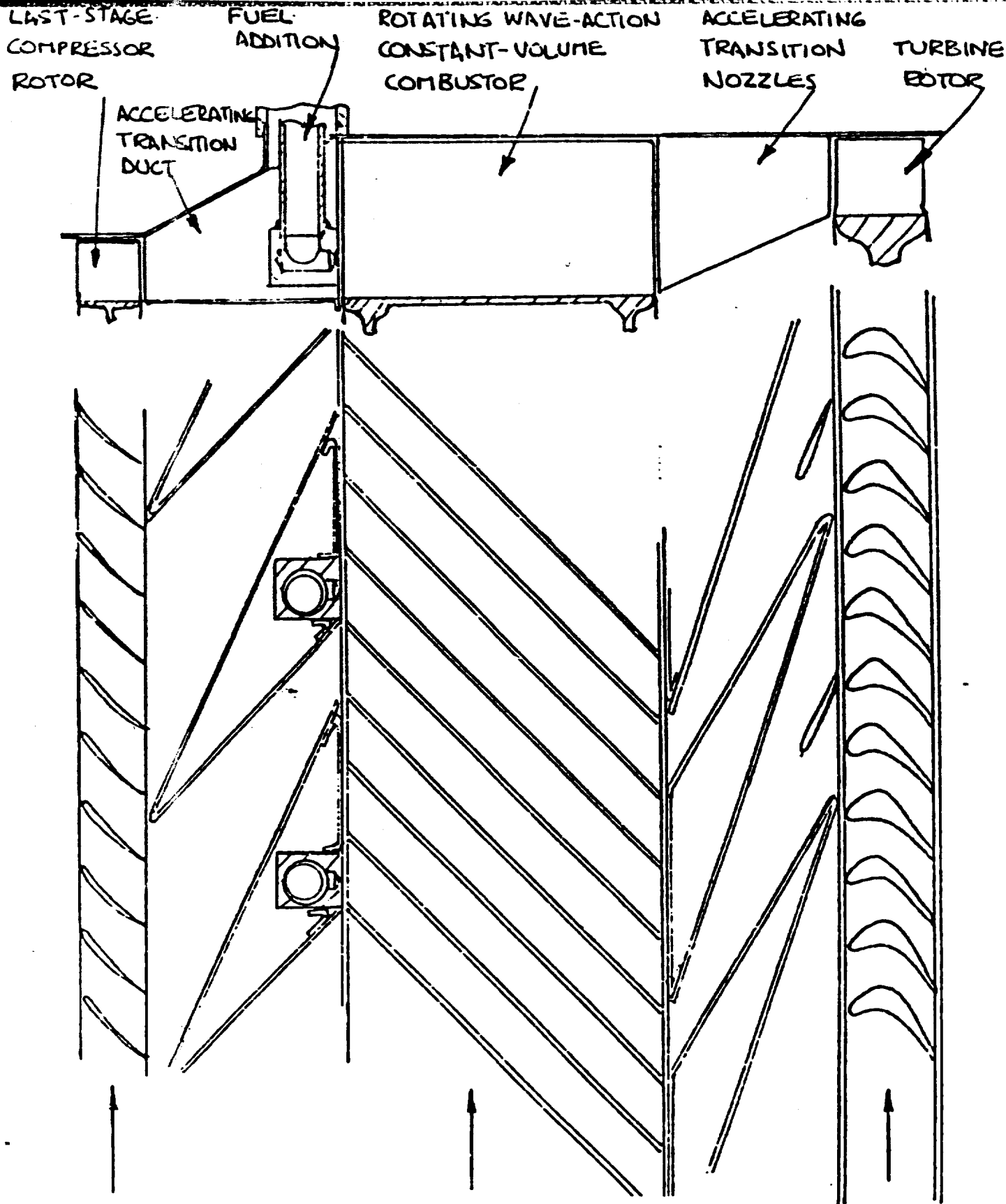


FIGURE 5 PROPOSED VARIATION OF THE EICHELBERG SYSTEM

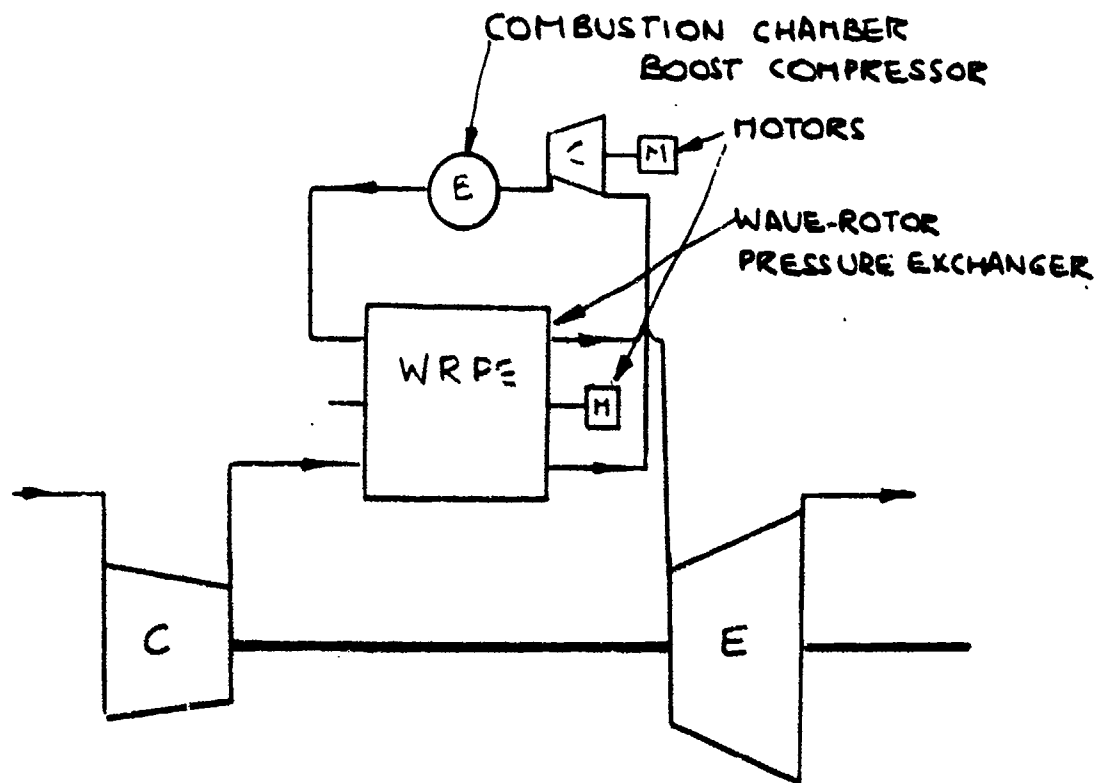


FIGURE 6 SEIPPEL SYSTEM

ABSTRACT

APPLICATION OF WAVE ENERGY EXCHANGER TO INDUSTRIAL AND ENERGY SYSTEMS

Nikolay G. Zubatov
Professor
Department of Engineering
Purdue University Calumet
Hammond, IN 46323
(219) 844-0520 Ext. 472
Home: (312) 635-8667

This presentation is based on some ideas and results developed by the author in 1968-1975 during his work in the USSR.

The development of heaters capable of preheating the oxidizer to temperatures of 2000K or higher is being vigorously pursued. This presentation reflects the study of direct energy exchange between working fluids to achieve high temperatures with existing heater materials.

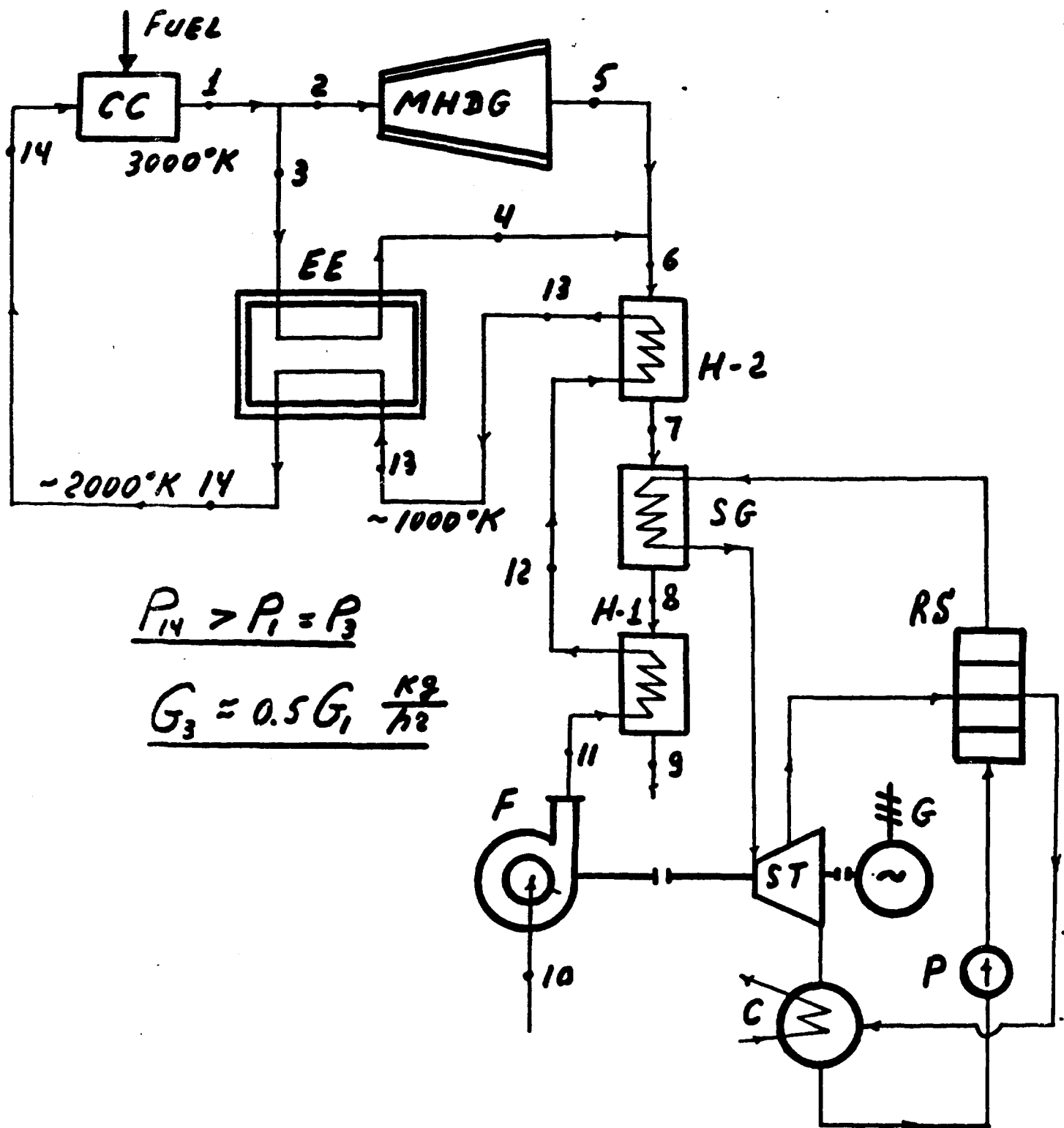
An analytical and experimental (single tube) investigation of wave energy exchanger has been performed to determine gas-dynamics characteristics of this device and to optimize the internal efficiency of direct energy transformation for high-temperature air preheating/compression in power generation (MHD-cycle) and steel production industries.

The flow within the tubes of the energy exchanger was modeled using the one-dimensional unsteady flow equations which were solved numerically. The internal efficiency of the device and the outlet temperature of the preheated air were calculated for a wide range of boundary conditions and compared with experimental results.

The new power cycles of MHD-power plants have been developed utilizing "gas-air" and "air-air" wave energy exchangers for high-temperature air preheating. Predicted thermal efficiency of these cycles approaches 52-53 percent. It has been established that the energy exchanger could operate with an energy transfer efficiency of 80-85 percent and outlet temperatures over 2000°K.

New arrangements of energy exchanger application have been also developed and analyzed economically for industrial energy systems such as steel production plants. The results will be presented at the meeting.

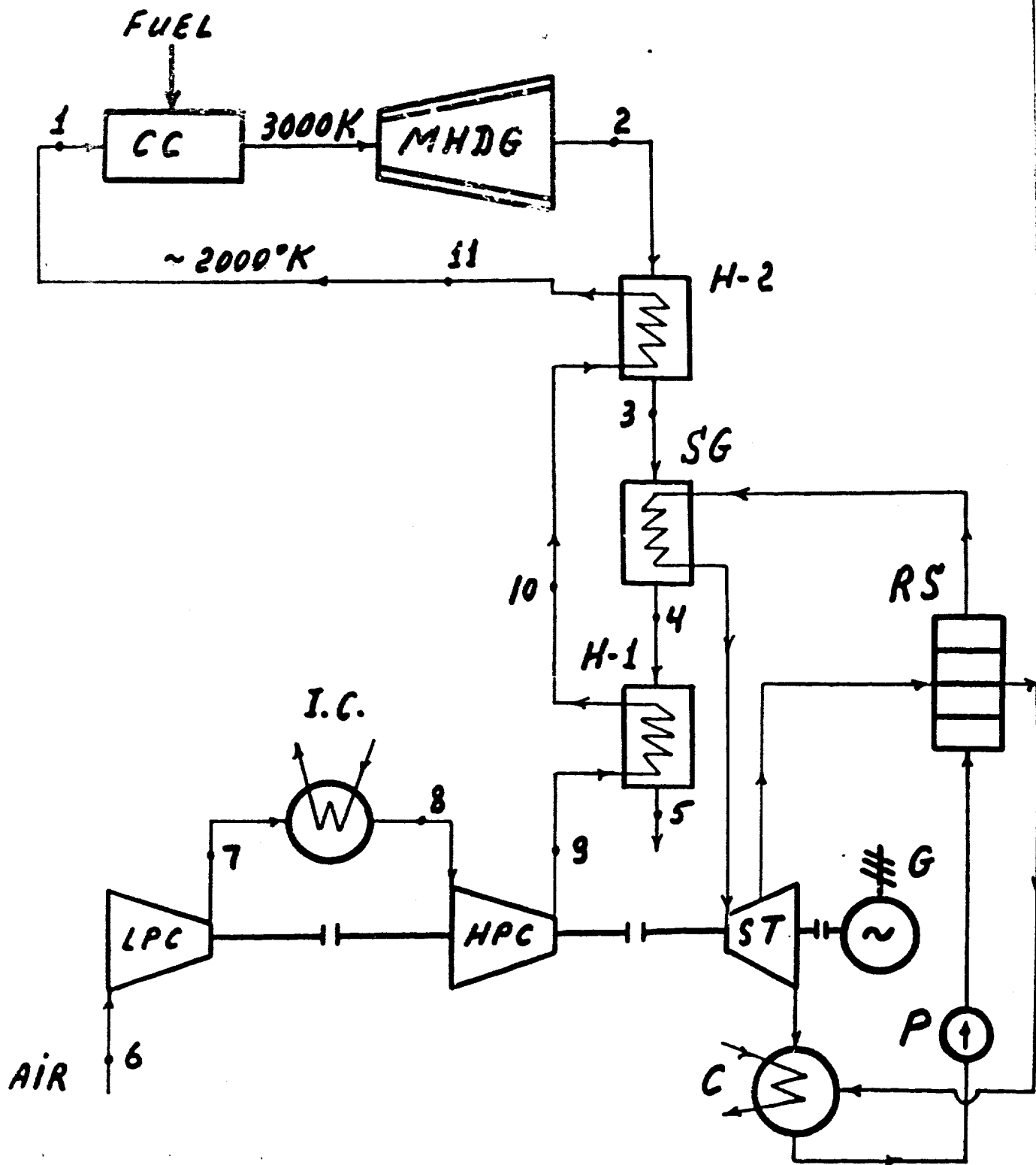
GAS-AIR CYCLE



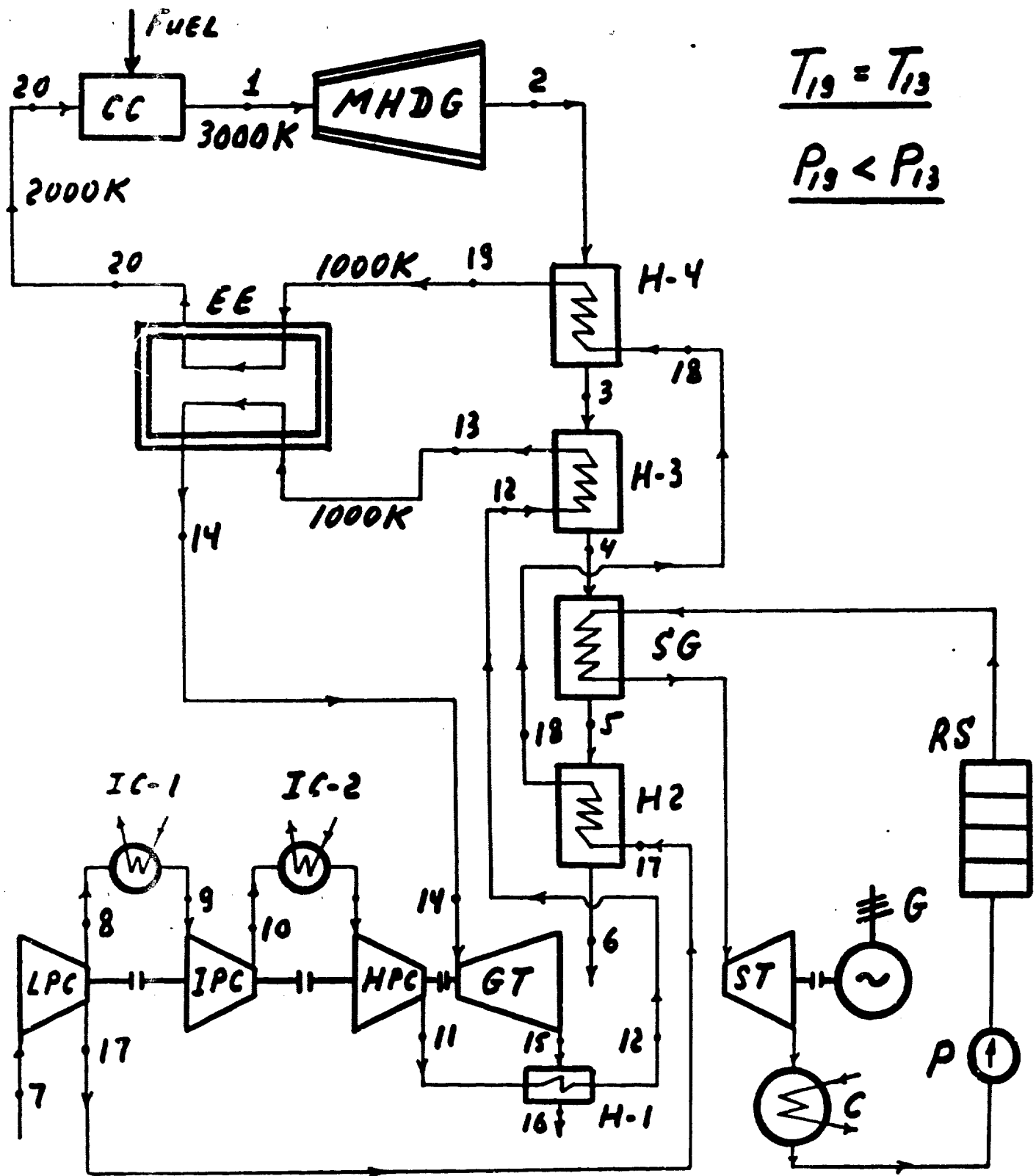
$$\underline{P_{14} > P_1 = P_3}$$

$$\underline{G_3 = 0.5 G_1 \frac{K^2}{h^2}}$$

BASIC MHD-POWER CYCLE



AIR-AIR CYCLE



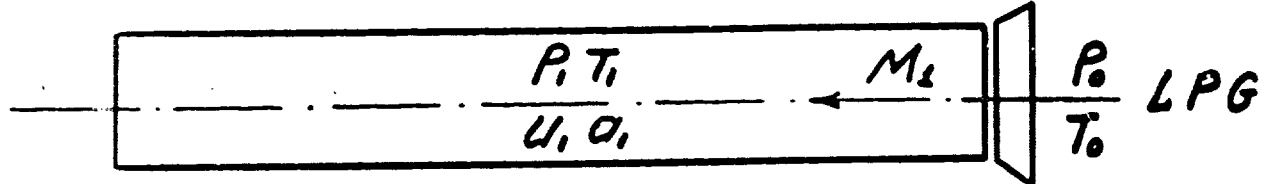
$$\underline{T_{19} = T_{13}}$$

$$\underline{P_{1,9} < P_{1,3}}$$

ENERGY-EXCHANGER BASIC PROCESSES

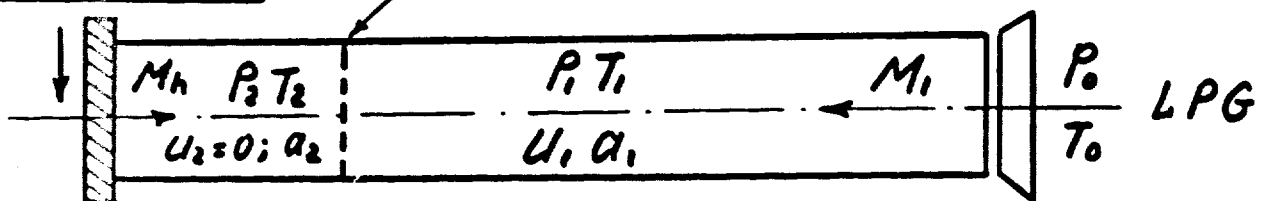
LEFT END

RIGHT END



CUT-OFF PLATE

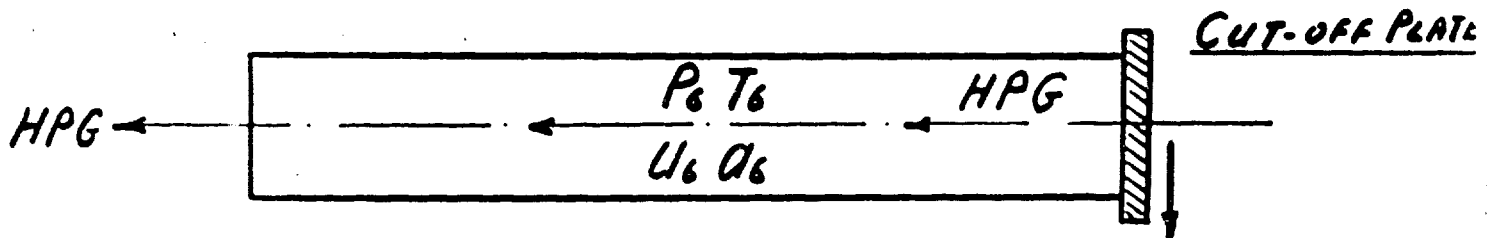
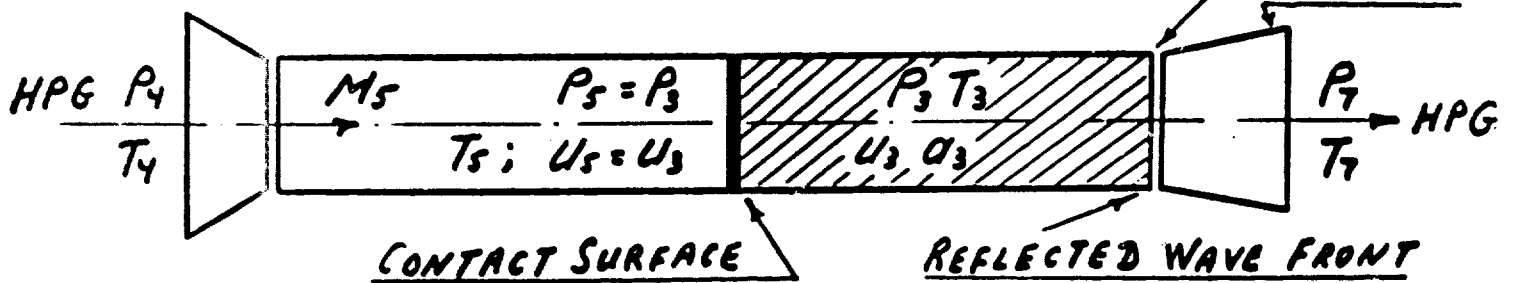
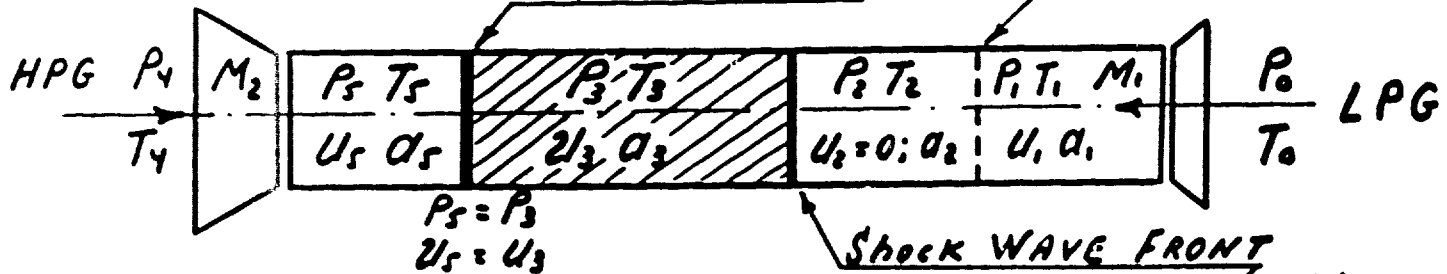
REFLECTED WAVE FRONT



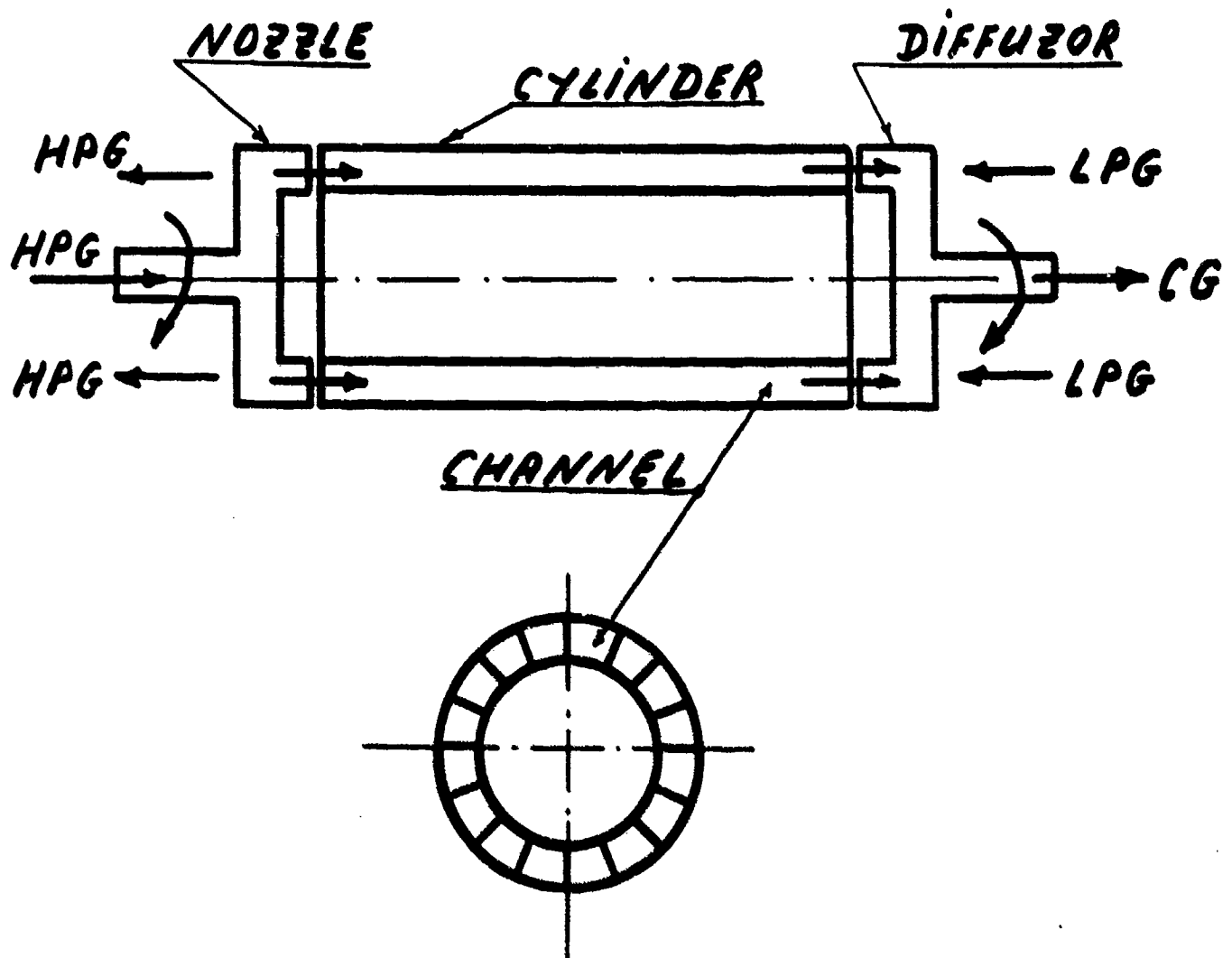
NOZZLE

CONTACT SURFACE

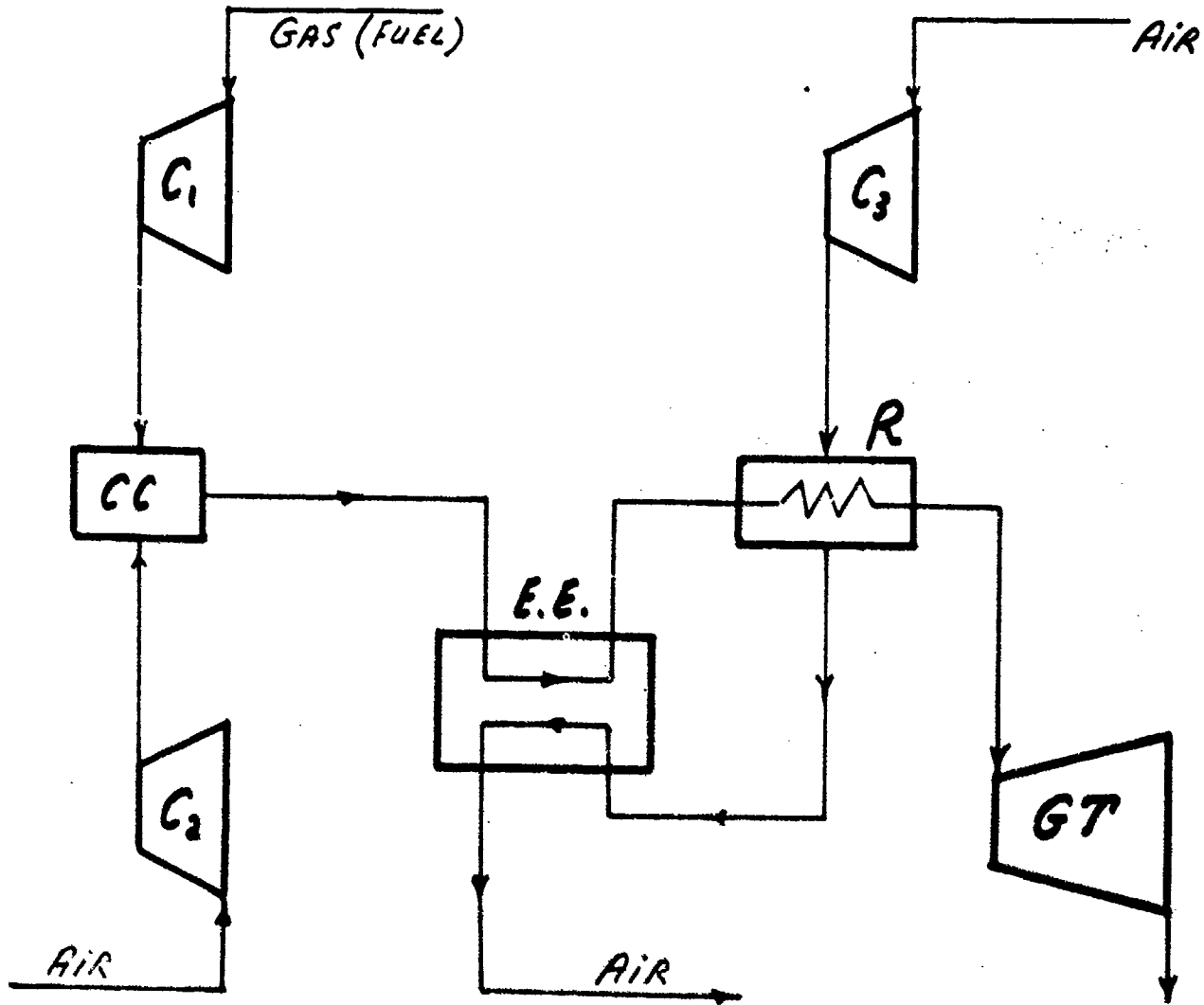
REFLECTED WAVE FRONT



ENERGY EXCHANGER ARRANGEMENT



BLAST FURNACE CYCLE (GAS - AIR)



C_1, C_2, C_3 - COMPRESSORS

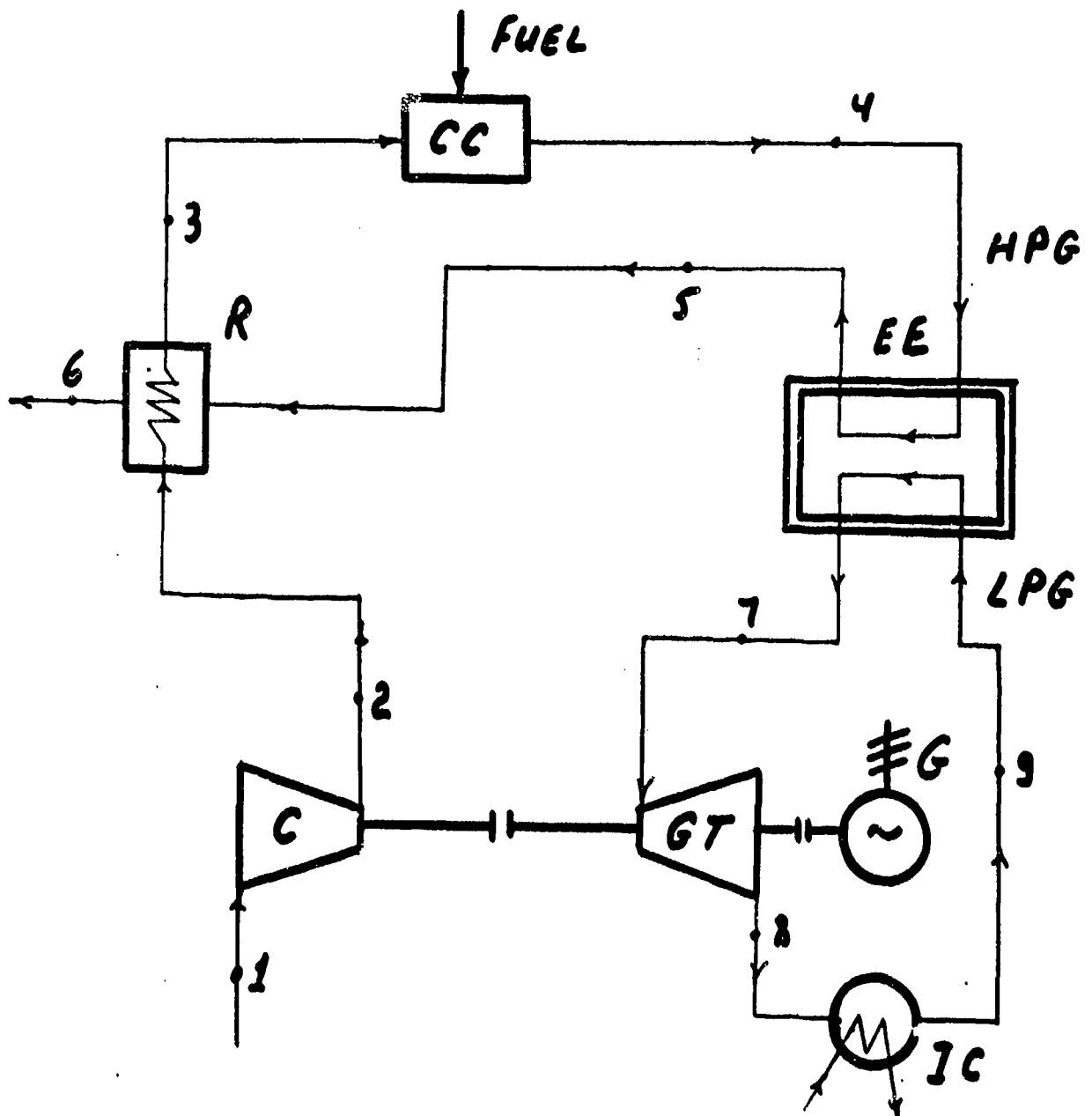
CC - COMBUSTION CHAMBER

E.E. - ENERGY EXCHANGER

R - RECUPERATOR

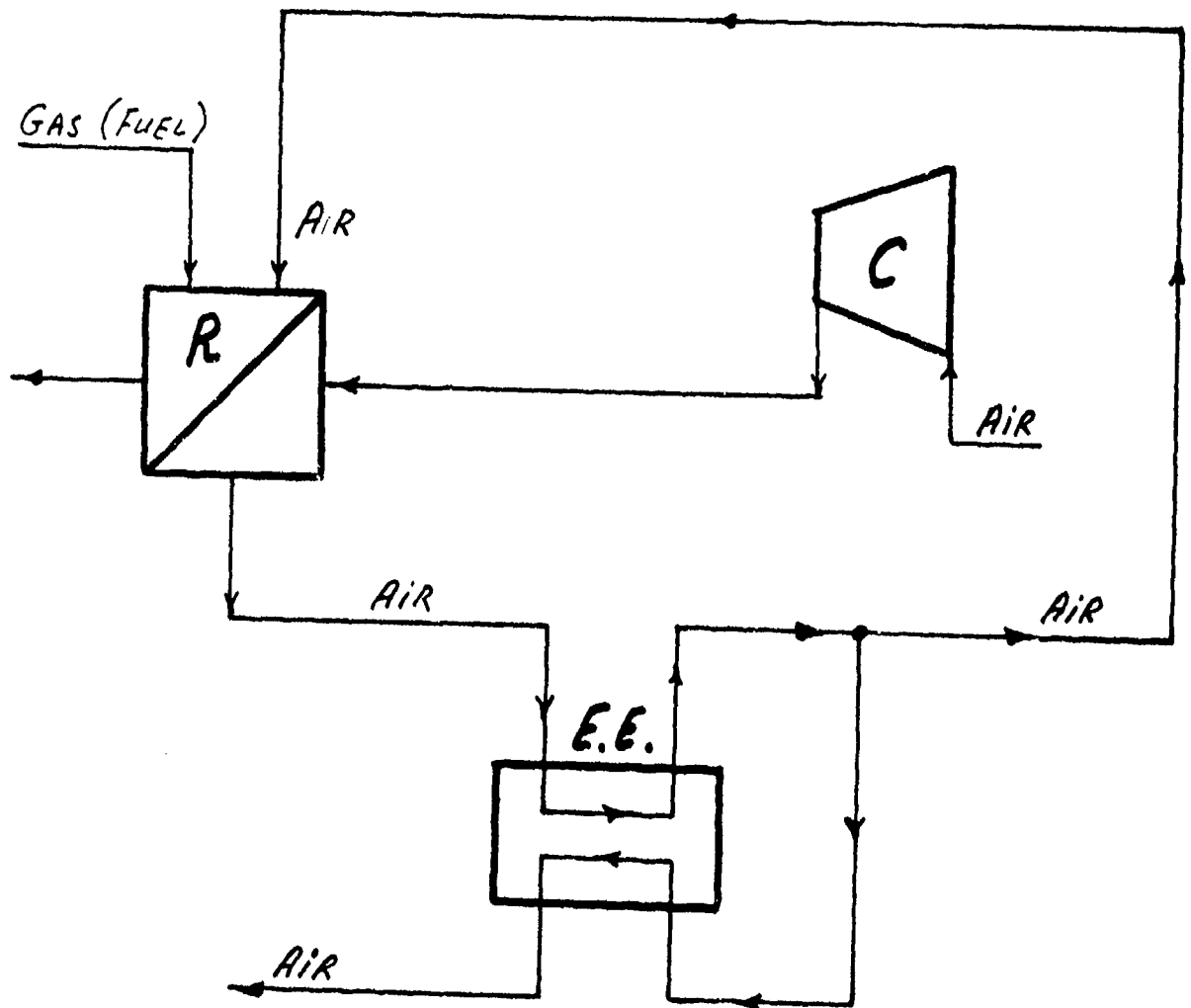
GT - GAS TURBINE

GAS TURBINE CYCLE



BLAST FURNACE CYCLE

(AIR - AIR)



C - COMPRESSOR

R - RECUPERATOR

E.E. - ENERGY EXCHANGER

LIST OF PUBLICATIONS (incomplete)

1. "Thermodynamic Analysis of Transport MHD-installation cycles with fuel combustion at constant volume."
Thermotechnical Problems of Direct Energy Conversion. Kiev, USSR, Scientific Thought Press, 1969. Issue 1., pp. 3-15.
2. "Analysis of MHD-installation cycles with low-temperature oxidizer preheating."
Third Thermodynamics Scientific Conference of the USSR. Leningrad, USSR, 1969. pp. 154-157.
3. "Perspective Efficiency of Energetic installations." Ibid., pp. 84-89.
4. "Direct Energy Exchange and its application to MHD-installations."
Thermotechnical Problems of Direct Energy Conversion. Kiev, USSR, Scientific Thought Press, 1971. Issue 2., pp. 37-44.
5. "Thermodynamic analysis of some MHD-installation cycles with Energy Exchanger."
Ibid., pp. 44-51.
6. "Energy Exchanger equilibrium wall temperature at MHD-installation cycles."
Thermotechnical Problems of Direct Energy Conversion. Kiev, USSR, Scientific Thought Press, 1972. Issue 3., pp. 56-64.
7. "Energy Exchanger's frame and efficiency as function of MHD-installation power output."
Ibid., pp. 64-71.
8. "Energy Exchanger's static characteristics at open-cycle of MHD-installations."
Thermotechnical Problems of Direct Energy Conversion. Kiev, USSR, Scientific Thought Press, 1973. Issue 4., pp. 56-60.
9. "Some characteristics of liquid-metal piston MHD-generators."
Ibid., pp. 97-104.
10. "Thermodynamic analysis of MHD-installation schemes with fuel combustion at constant volume."
New Schemes and Cycles in Thermal Energetics. Sverdlovsk, USSR, Academy of Sciences of the USSR, 1971, pp. 121-129.
11. "Application of MHD-generator in the high-temperature top cycle of the energetic installations." Ibid., pp. 146-151.
12. "Thermal schemes of Blast-furnace high temperature air heating."
Secondary energy sources use and aggregate cooling in metallurgy. Moscow, USSR, Metallurgy Press, 1972. Issue 1., pp. 74-76.
13. "The Energy Exchanger's static characteristics on scheme of Distillation installations."
The Problems of Salt Water Distillation and Waste Water Cleaning. Odessa, USSR, 1973, pp. 3-6.

PATENT CERTIFICATES:

14. "Magneto-Hydrodynamic installation."
Patent N: 160551, December 11, 1963
15. "Methods of High Temperature Air Heating and Compression for Blast-furnaces."
Patent N: 390147, April 20, 1973.
16. "Device of High Temperature Air Heating and Compression for Blast-furnaces."
Patent N: 402548, July 23, 1973.

WAVE ROTOR RESEARCH AND TECHNOLOGY WORKSHOP - MARCH 26-27, 1985

NAVAL POSTGRADUATE SCHOOL - MONTEREY, CALIFORNIA

COMPARISON OF THE WAVE-ROTOR-AUGMENTED TO THE

DETONATION-WAVE-AUGMENTED GAS TURBINE

W. ROSTAFINSKI, NASA LEWIS RESEARCH CENTER

COMPARISON OF THE WAVE-ROTOR-AUGMENTED TO THE
DETONATION-WAVE-AUGMENTED GAS TURBINE

BY W. ROSTAFINSKI

NASA LEWIS RESEARCH CENTER, CLEVELAND, OHIO

Among the numerous methods proposed to improve the SFC of small gas turbine engines, the use of burner-by-passing topping stages compares very favorably with the use of regenerators and ceramic components.

Actually one could think about these methods supplementing each other to compound the benefits. To compound the difficulty as well-unfortunately.

Two augmented gas turbine cycles are compared and discussed in this paper. One uses a wave rotor, the other a detonation wave tube. Both allow use of much higher cycle temperatures than otherwise possible, which improves efficiency. Also, both reduce compressor work, further enhancing fuel economy.

The two cycles also share uncertainties connected with hardware development. In both cases the analytical models are well understood and in the case of the wave rotor, a working prototype is available. However, in both cases, the feasibility and performance of the proposed hardware must be demonstrated by high-pressure, high-temperature, long-duration tests.

COMPARISON OF THE WAVE-ROTOR-AUGMENTED TO THE
DETONATION-WAVE-AUGMENTED GAS TURBINE

W. ROSTAFINSKI, NASA LEWIS RESEARCH CENTER

Considerable effort, both analytical and in hardware development, is devoted to improving gas turbine cycle performance and small gas turbine engines in particular. To decrease engine SFC several approaches have been proposed. The majority of them rely on increased cycle maximum temperature; others depend on better utilization of burned gas enthalpy, and finally, some other solutions use power boosting devices and thrust augmentation.

These various methods can be applied one by one or combined to compound the benefits. Unfortunately, practically all of these methods are still in the R&D stage; combining them may lead to undesirable situations: during tests poor performance of one of the new methods may also ruin predicted improvement by the other element; consequently, little would be learned from it all. A step by step approach would be more useful.

In most of the cases considered, the improvement is obtained using methods which, by the Carnot principle, must increase thermal efficiency of a cycle: that is, using higher maximum cycle temperatures or lowering the exit temperatures. On the other hand, in Brayton cycles, efficiency increases with increasing pressure ratios but small blades impose limits to PR.

To thermal cycle improvements belong: the proposed use of ceramic turbine blades, ceramic engine components (uncooled or cooled), use of a heat exchanger, and cycle modifications in which a part-flow topping stage is used. As mentioned before, use of each of these methods theoretically leads to the decrease of SFC; but in practice it all depends on efficiencies of the various components and their mass and size. Any of these may have a counter-productive effect.

The use of ceramic high temperature resisting materials in gas turbines is still in its infancy. Currently tests are limited to automotive gas turbine applications only. The metallurgical and ceramic industries, together with cooled blade designers, have a tough job on their hands. Progress in those areas is rather slow.

Because of sizeable difficulties in application of exotic materials, an easier solution seems to be to improve the gas turbine cycles using heat exchangers--to adopt cycles with regenerators. Gas turbines so equipped exist now in automotive applications. In aircraft engine application they might penalize aircraft performance by their prohibitive size and weight.

Now, novel and promising ways to reduce SFC consist in the use of direct energy transfer between burned gas and combustion air. This is obtained using intermittent operation devices. They allow:

- an increased maximum cycle temperature without the need to probe into the difficult field of ceramic materials.
- reduce the need for compressor work which is particularly important in the case of small gas turbines. High compressor pressure ratios are out of the question in such applications because of rapidly decreasing blade height with increasing pressure.

Two intermittent-operation part-flow topping cycles will be compared hereafter for their merits. Calculations have been done on two such cycles (highly idealized for ease of calculation), and in the process several general assumptions have been adopted in both cases.

The adopted conditions are: a 1000 lb. thrust, engine operating at $M = 0.75$, and an ambient pressure of 3.5 psia.

Besides this, the inlet diffusers and exit nozzles have no losses; the gas temperature at HP turbine inlet is 2500°R ; the turbine efficiencies are 0.85; and compressor efficiencies are 0.8.

Given these conditions calculations proceed along standard thermodynamic lines. The first cycle, thus, evaluated involves a wave rotor pressure exchanger. This cycle is well-known. Other papers gave its thorough description. The analysis is based on data and calculations given in an MSNW (Mathematical Sciences Northwest, Inc.) report entitled "Investigation of Wave Rotor Turbofans for Cruise Missile Engines," prepared in 1983 for DARPA (R. Taussig, principal investigator).

The second cycle relies on:

- intermittent detonations to obtain very high gas temperatures and pressures of part of flow deviated from the combustor
- an expansion chamber to reduce pressure to levels of the combustor flow
- a mixing chamber in which very high velocity flow from the detonation tube must be mixed with the combustor flow.

A wave rotor pressure exchanger prototype exists (a low pressure, low temperature model), and in the past such a rotor has been built and was successfully tested in England. In the case of a detonation augmented cycle, no detonation device nor mixing stage have been ever built. The detonation wave augmented gas turbine requires some description. This will be based on a paper entitled "Detonation Wave Augmentation of Gas Turbines" by A. Wortman, technical director of ISTAR, Inc. of Santa Monica, California presented at the Twentieth Joint Propulsion Conference in June 1984 in Cincinnati, Ohio.

In the system using a detonation wave device, the flow from the compressor is split with a part of it going through a combustor as in conventional gas turbines while the other part goes through an array of detonation ducts where it is processed by transverse detonation waves. The two flows are mixed, passed through a turbine and expanded through a nozzle. In terms of the basic mode of operation the system acts as a pure turbojet, but extensions to turbofans of arbitrary bypass ratios are obvious. Applications of the proposed system are seen primarily in the field of relatively inexpensive small gas turbines using simple centrifugal compressors. The high thrust coefficients exhibited in the model performance studies suggest applications to relatively small unmanned vehicles.

A detonation wave represents an essentially constant volume heat release and has been considered as a possible means of compression and heat release in gas turbines.

The model for the system considered here is the air standard Humphrey cycle. The significance of the benefits associated with the use of constant volume heat addition may be gauged by observing that for a pressure ratio of 4 and $\gamma = 1.4$ the efficiency of the Brayton cycle is 0.327 while that of the Humphrey cycle with $T_3/T_2 = 2$ is 0.544. An alternative way of viewing the two cycles is to note that for $T_3/T_2 = 2$ and $\gamma = 1.4$ the Brayton cycle requires four times the compression ratio of the Humphrey cycle to match its efficiency.

Comparison of the two cycles based on the adopted conditions yields the following approximate results:

Wave rotor augmented cycle

Bypass ratio	3.9	4.8	5.9
SFC	0.63	0.64	0.66

Detonation augmented cycle

Combustor flow fraction	0.2	0.3	0.4
SFC	0.61	0.65	0.76

These data differ from values given in the above mentioned reports because there was no optimization and because overly optimistic efficiencies were adopted. They are generally lower than would be estimated by more precise analysis.

This being said, it should suffice to notice that differences in SFC between the two cycles are small and that even an approximate evaluation yields very comparable results. We may, therefore, conclude that both gas turbine augmentation systems promise significant improvements. At the same time both systems need the following serious hardware R&D:

- a wave rotor able to stand very high temperature and pressures, oscillating, periodical loads; above all, it must not admit serious leakage along the periphery of the rotating tubes and at inlet parts.

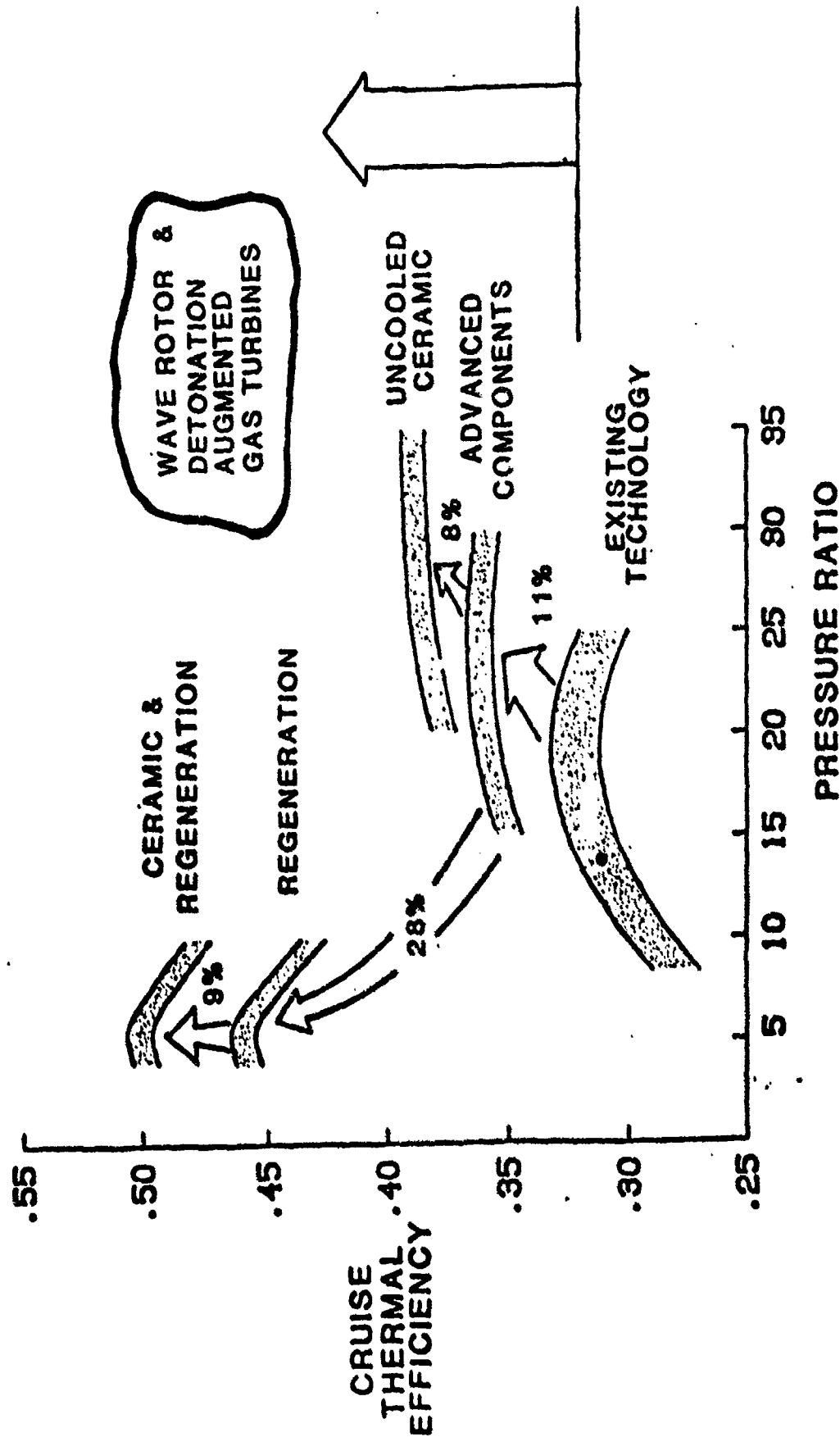
- a detonation chamber to be developed and proof obtained that sequenced detonation is feasible. Also an efficient mixing chamber must be designed.

As far as aerospace applications are concerned, the two systems are high risk, high reward initiatives.

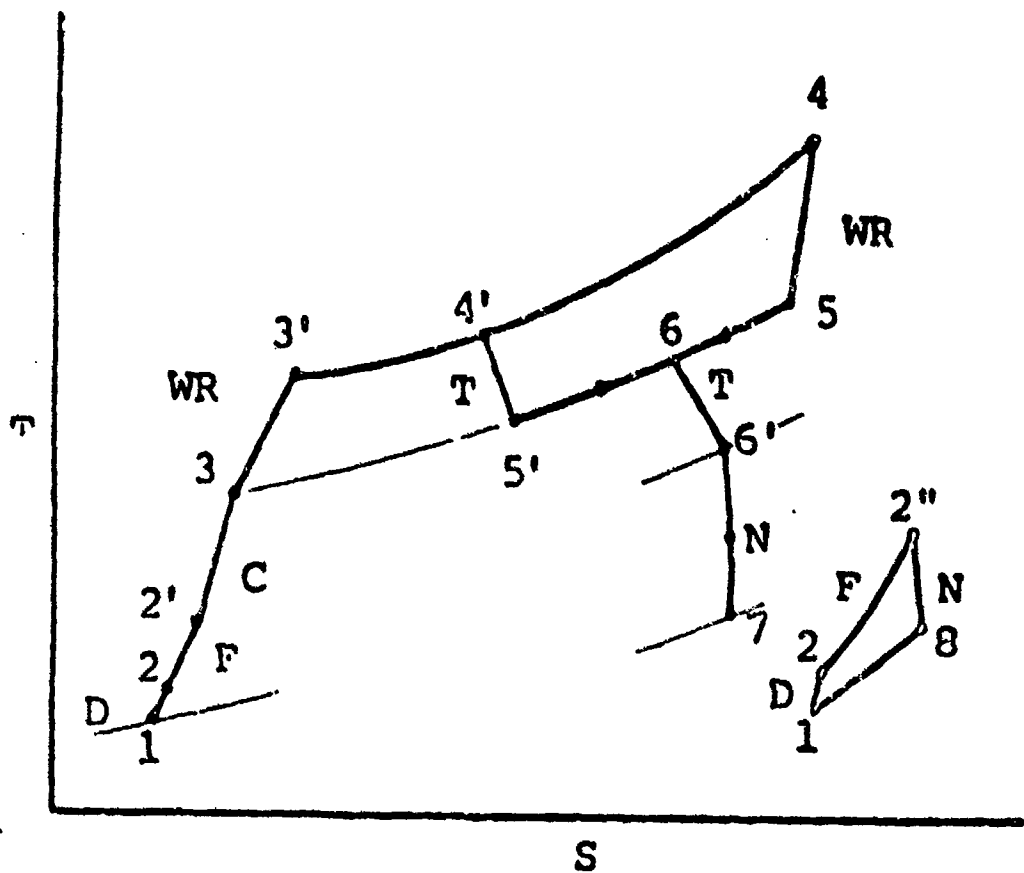
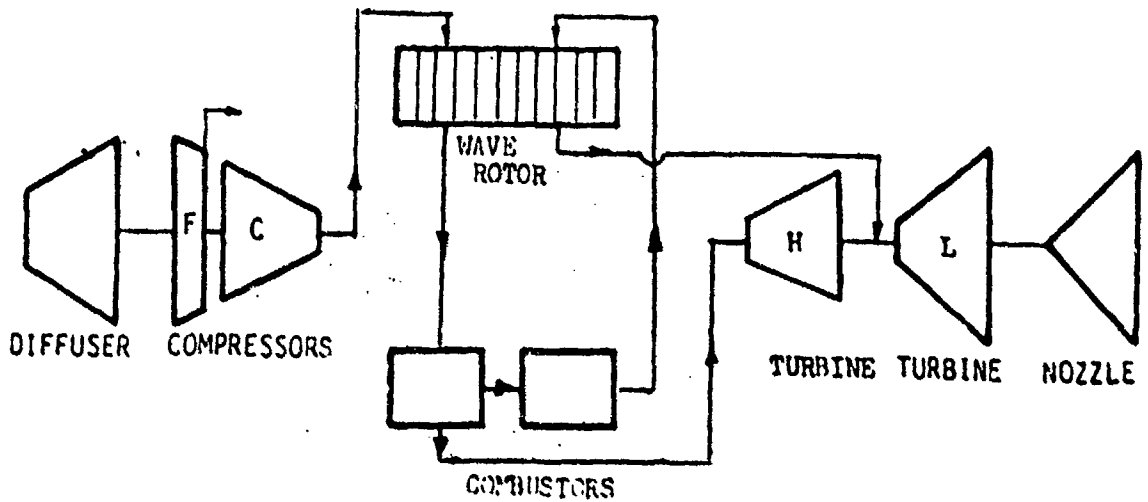
★

SMALL ENGINE TECHNOLOGY BENEFITS

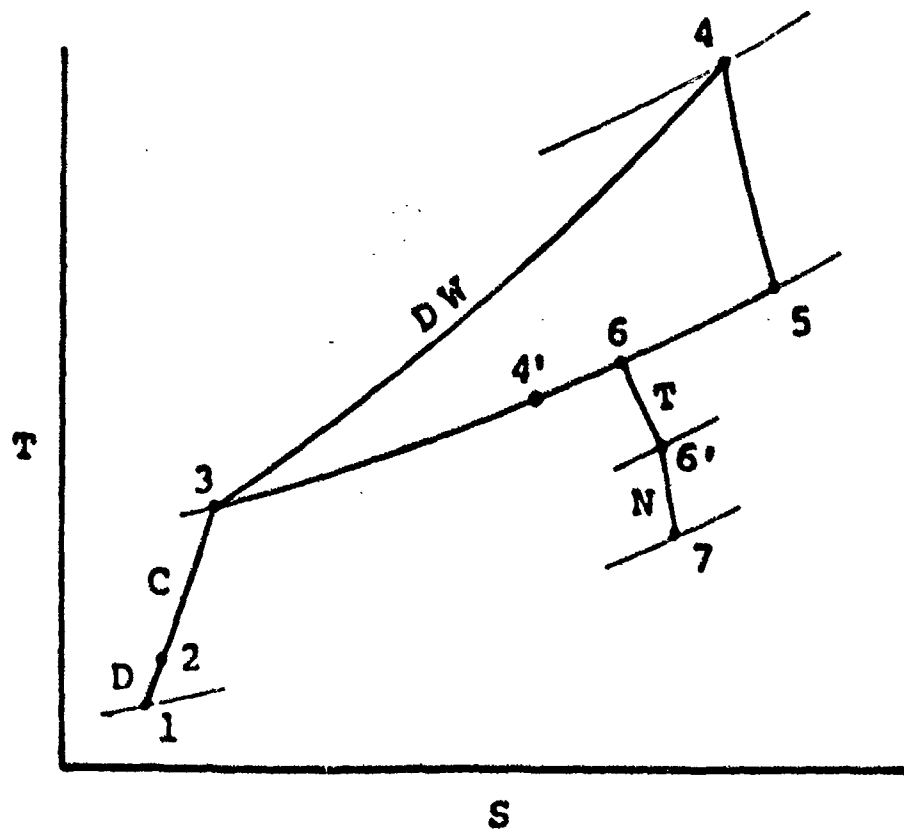
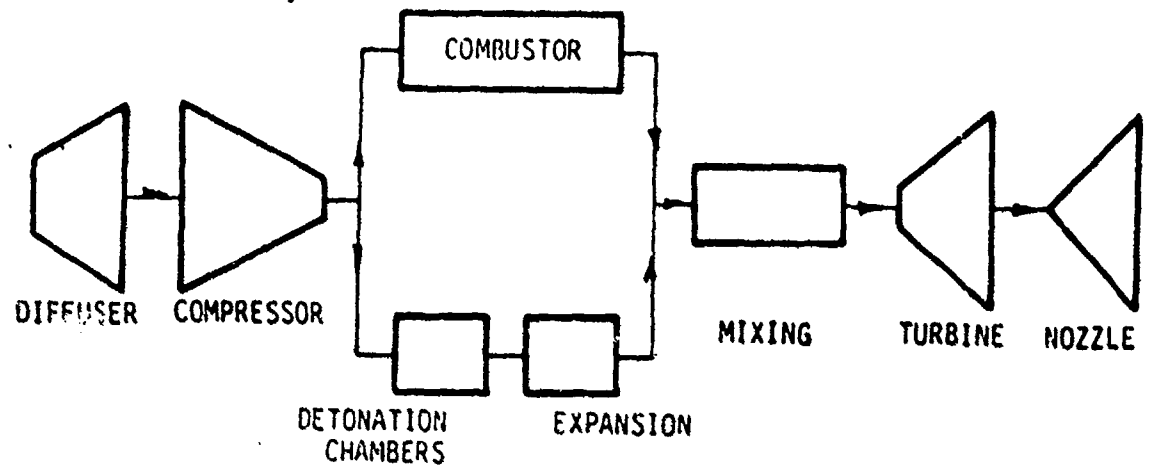
800 HP SLS
MACH 0.45/15000 FT CRUISE



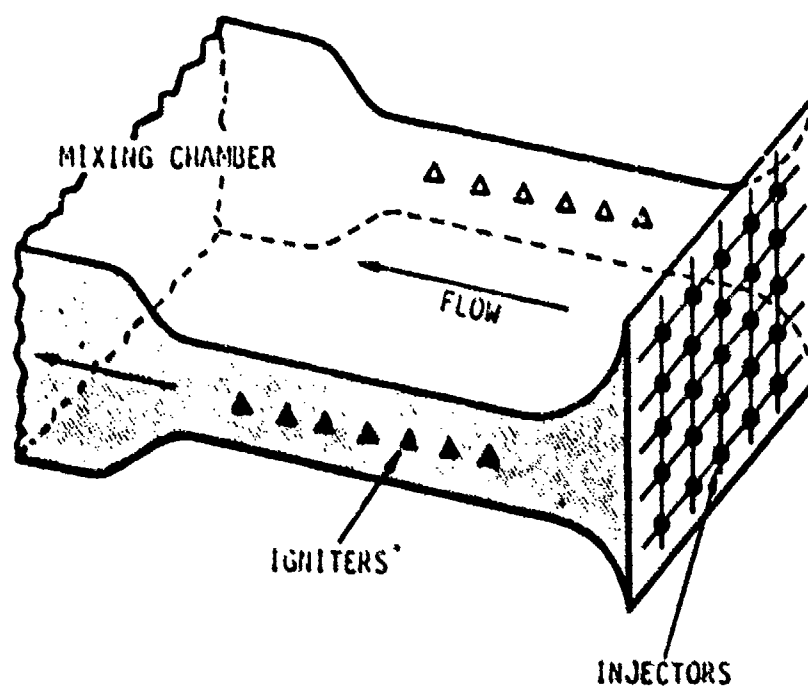
SCHEMATIC REPRESENTATION OF THE WAVE ROTOR AUGMENTED TURBOFAN ENGINE



SCHEMATIC REPRESENTATION OF THE DETONATION WAVE AUGMENTED TURBOJET ENGINE



SCHEMATIC REPRESENTATION OF THE DETONATION DUCT



DETONATION CHARACTERISTICS

- SUPERSONIC WAVE SUPPORTED BY ENERGY RELEASE. DEPENDING ON FUEL AND MIXTURE COMPOSITION DETONATION VELOCITY RANGES 1400-3500 M/SEC.
- BURNED GAS FLOWS TOWARD THE UNBURNED GAS.
- DETONATION REQUIRES A FINITE LENGTH OF PIPE TO HAPPEN.
- NO DATA ARE PRESENTLY AVAILABLE ON DETONATION CHARACTERISTICS ON JP FUELS.

PRELIMINARY COMPARISON OF WAVE ROTOR AND
 DETONATION WAVE AUGMENTATED ENGINES

WAVE ROTOR AUGMENTED TURBOFAN

BYPASS RATIO	3.9	4.8	5.9
SFC	.63	.64	.65

DETONATIONS AUGMENTED TURBOJET

COMBUSTOR FLOW FRACTION	.2	.3	.4
SFC	.61	.65	.76

CONCLUDING REMARKS

- THE TWO AUGMENTATION CONCEPTS PRODUCE SIMILAR LEVELS OF SFC
- BOTH CONCEPTS MAY BE ATTRACTIVE OPTIONS FOR FUTURE AEROSPACE APPLICATIONS
 - WAVE ROTOR GROUND TECHNOLOGY MUST BE EXTENDED TO FLIGHT.
 - DETONATION WAVE HIGHER RISK CONCEPT WHERE FEASIBILITY NEEDS DEMONSTRATION.
- FUTURE DETONATION WAVE TECHNOLOGY REQUIREMENTS
 - STUDY TO FURTHER EVALUATE APPLICATIONS AND BENEFITS
 - DETONATION CHAMBER FEASIBILITY TEST WITH JP FUELS

Prof. Max Berchtold
Swiss Federal Institute
of Technology
Zurich, Switzerland

THE COMPREX AS A TOPPING SPOOL
IN A GAS TURBINE ENGINE
FOR CRUISE MISSILE PROPULSION

Summary

In the original concept Brown Boveri Company (BBC) built and tested the Comprex wave rotor principle as a gasturbine topping cycle 45 years ago. The power-output of the wave rotor with helical blades was a surplus of compressed heated gas, which expanded in a separate turbine to the pressure level of the Comprex exhaust. The high compression- and expansion efficiencies obtained almost instantly, encouraged BBC to design and construct a complete gasturbine engine with the Comprex topping cycle. While the expected performance could be demonstrated, innumerable problems arose both in the gasturbine, as well as in the Comprex. BBC decided to concentrate their effort first to the gasturbine. Improvements in component efficiencies and the availability of metals with better high-temperature strength diminished the effort to the development of the Comprex. Only later, when work at the ITE Company in Philadelphia demonstrated the feasibility of the Comprex as a Diesel engine supercharger, BBC as a manufacturer of superchargers continued the ITE project. The advantages of the high torque in the full engine operating speed-range together with the instant response capability made the Comprex the ideal vehicular Diesel engine supercharger. This justified the effort BBC has put into this development.

In the mid sixties BBC was approached by Rolls-Royce for cooperation in the development of a topping wave rotor for a helicopter gasturbine engine. BBC delegated their cooperation in this joint effort to my laboratory. We proposed to RR a different cycle than BBC used in their GT topping cycle. We believed a cycle derived from the supercharger would allow a more practical arrangement and would bring almost the same performance gain. It was decided that RR would build a fully instrumented testrig to verify our performance prediction, which had been based on previous calibration tests. We supplied RR with an existing rotor and gave them the porting geometry for our cycle. The RR tests met our prediction quite closely. The design department in the meantime came up with a proposal for the practical realization. The project then was terminated as RR got into financial difficulties with the large jet engine program.

The potential of this engine has been looked again at the initiative of DARPA a few years ago, when the various engine concepts for more efficient cruise missile propulsion was evaluated. The results of the BBC-RR project have been reassessed in the light of the specific requirements. A preliminary study showed the potential to have some promise.

The cycle will briefly be explained and expected performance of a proposed engine arrangement will be discussed at the workshop.

The detailed cycle evaluation of the BBC-RR cycle performed by the method of characteristics is shown on Fig. 1. The analysis contains the effects of heat transfer, partial opening as well as leakage. The design parameters are

pressure ratio (comparison discharge to intake)	2.6
temperature ratio (combustion discharge to intake)	2.8
isentropic compression efficiency	0.78
isentropic expansion efficiency	0.78
pressure ratio of combustion throttling	0.92
pressure ratio (exhaust static to intake total)	1.10
pressure ratio (exhaust total to intake total)	1.18

These performance figures have been met by the Rolls Royce test. The velocity profile at the exhaust-gas exhaust port is assumed to be evened out to an average velocity based on conservation of momentum. This assumption leads to the total pressure ratio of 1.18.

Assuming the Rolls Royce Cycle as the topping cycle of the Allison Model 250 Series II gas turbine engine the thermal efficiency improves from 21% (sfc. 65 lb/H.P.hr) to 26% (sfc .525) the power output goes up from 420 HP to 550HP. The reversed flow turbine arrangement of the Allison engine lends itself favorably to the Comprex wave rotor topping cycle. On a cruise missile engine a propeller would be used.

Studies have been made to use the RR wave rotor topping cycle in conjunction with a less sophisticated gas turbine engine. A ducted fan engine using a 4:1 pressure ratio radial flow compressor at a cruise Mach number of 0.7 with a bypass ratio of 5:1 will give an sfc of .95 lb/lb hr at a thrust of 300lb (a thrust figure specified by DARPA). This sfc is not too far off to the sfc of the P & W JT 8D-17 of .87 lb/lb hr, which is a more complicated design. the thermal overall thrust power efficiency would be 19%.

Thermodynamic cycle discussion:

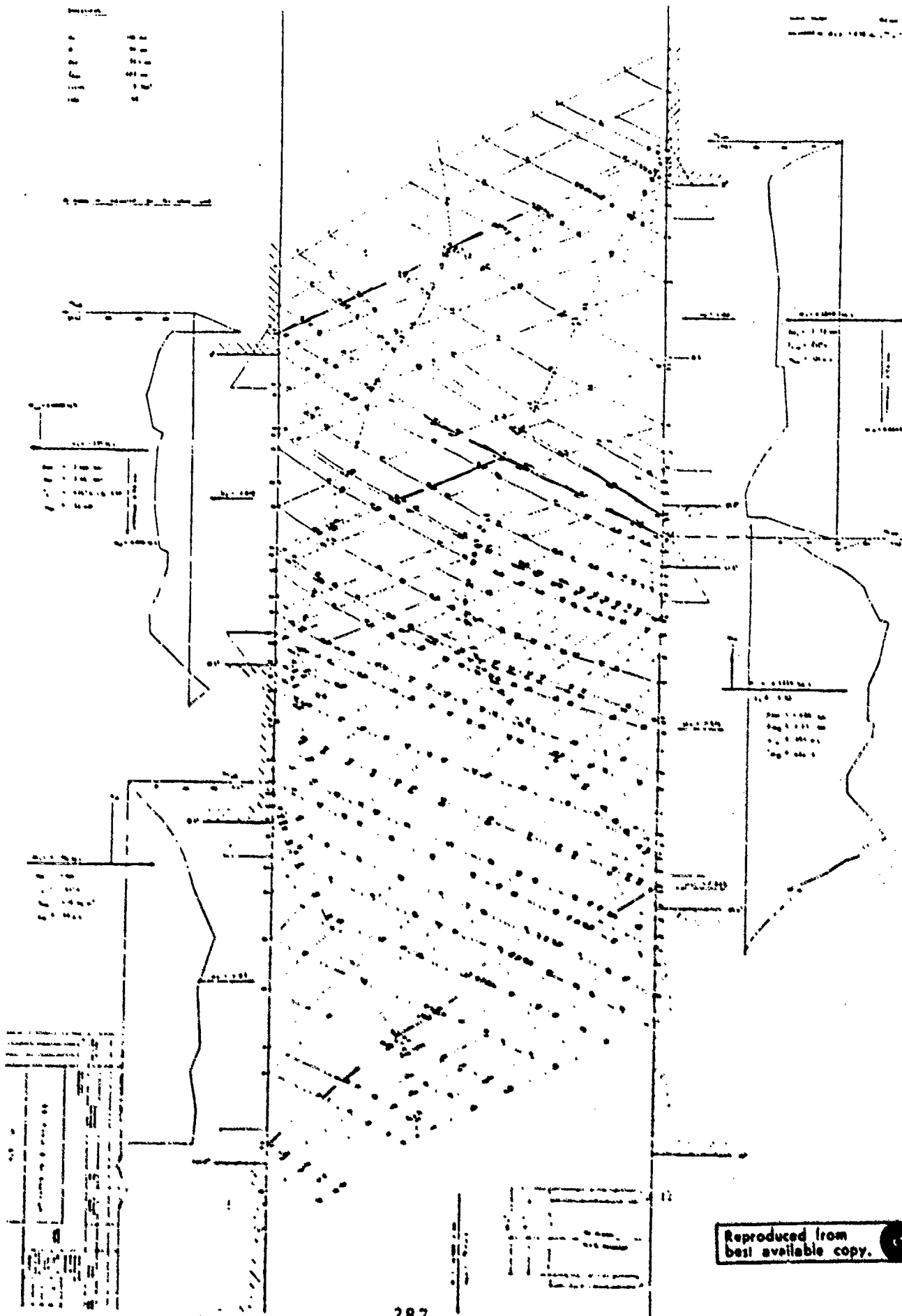
The original BBC wave rotor topping cycle is presented in Fig. 2 is the schematic component hookup, whereas Fig. 2b is the temperature entropy plot. The power output of the topping cycle is produced by the high pressure turbine B in Fig. 2a. This power is used to drive the turbocompressor A. The total flow then expands in the power turbine E. This power represents the shaft power available to drive the propeller or the fan respectively. The disadvantage of this cycle is the relatively small volume flow, which does not allow a high turbine efficiency. Furthermore it is not possible to use the full temperature potential. The turbine inlet temperature has been assumed 1000K versus 1700K at the Comprex inlet. A proposed engine arrangement of the components is shown in Fig. 3. As the wave rotor is of the through flow arrangement, it can be operated at higher gas inlet temperatures as the passages are exposed at both ends at equal time intervals to hot and cold gases.

The BBC-RR wave rotor topping cycle in contradistinction has no high pressure flow bypass. The power output is represented by a higher Comprex exhaust pressure over the Comprex intake air pressure. To the base gas turbine cycle

cycle this appears as a combustor with a pressure increase. Even though the pressure ratio gain in intake-exhaust pressure is only 1.18 versus the pressure ratio loss of .05 in a normal combustor the power output increases substantially. Fig. 4 shows the BBC-RR cycle, where Fig 4a is the schematic component hook up and Fig. 4b is the temperature entropy plot. The proposed component arrangement in the high bypass ducted fan engine is shown in Fig. 5. As it becomes necessary to reduce the gasturbine shaft r.p.m. to the propeller r.p.m. a friction planetary roller system is being applied. Preliminary tests with such systems are encouraging. A speed reducer for a small output gas turbine engine would be inexpensive and highly reliable. A similar drive is visualized to control the speed of the wave rotor. As the BBC-RR cycle is the reversed flow type, the gas intake side of the rotor will assume a higher temperature than the gas exhaust side.. As the rotor stress level is relatively low BBC has had encouraging results with ceramic rotors. They will allow the assumed wave rotor inlet temperatures of 1600R. The low coefficient of thermal expansion will permit operation at low rotor-stator clearances.

It should be kept in mind that the results presented are in many ways very preliminary. Cycle optimization with todays use of computerized wave rotor cycle analysis has not been introduced so far. Reliable calibration of test results and cycles analyzed by the characteristics method indicate a realistic the potential of the BBC-RR wave rotore topping principle.

I hope this presentation has generated the interest to further pressure a development effort in this direction.



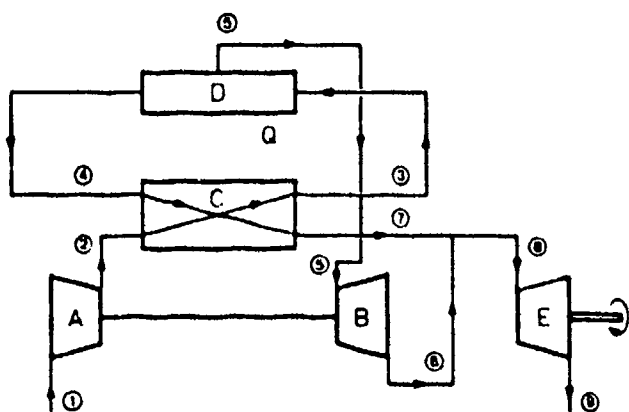


Fig. 2a Arrangement of components

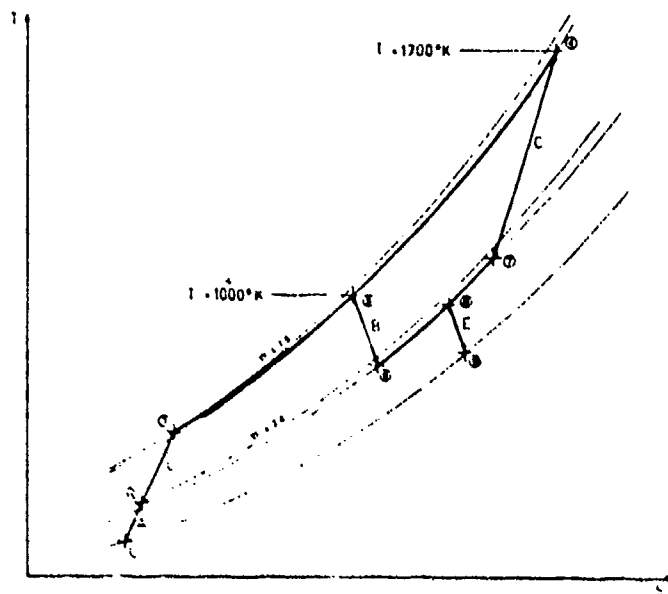


Fig. 2b Proposed H₂-O₂ cycle indicating thermodynamic state.)

Components:

- A — one-stage radial flow compressor
- B — one-stage radial flow turbine
- C — through-flow pressure exchanger
- D — condensation chamber
- E — one-stage radial flow turbine

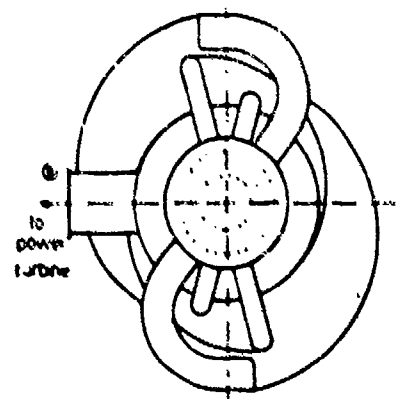
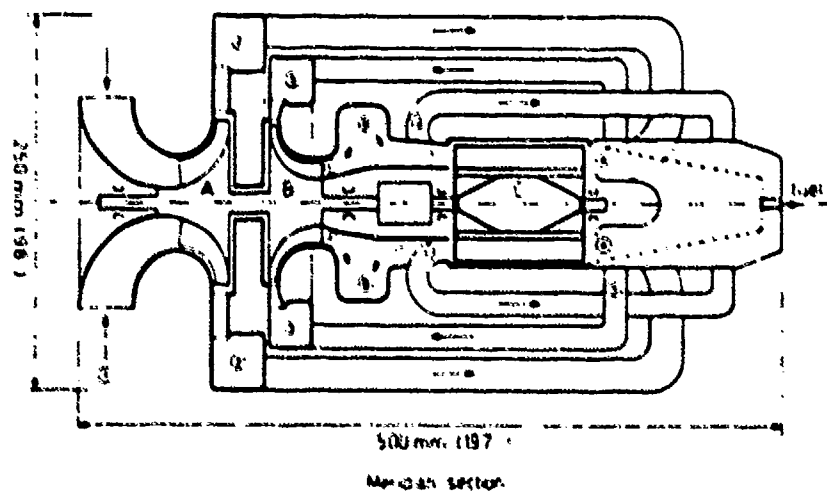


Fig. 3 H₂-O₂ gas turbine for the proposed cycle

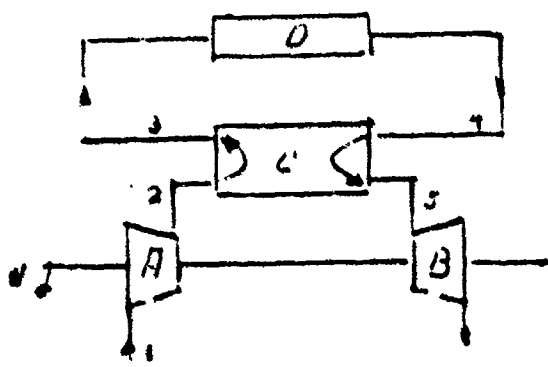


Fig. 4 a Arrangement of components

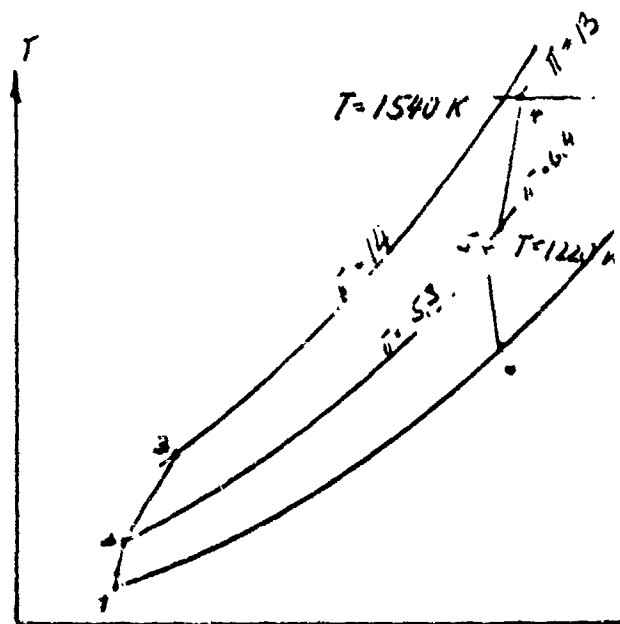


Fig. 4 b Temperature-Entropy

Components:

- A - one stage radial flow compressor
- B - two stage axial flow turbine
- C - reversed flow pressure exchanger
- D - combustion chamber

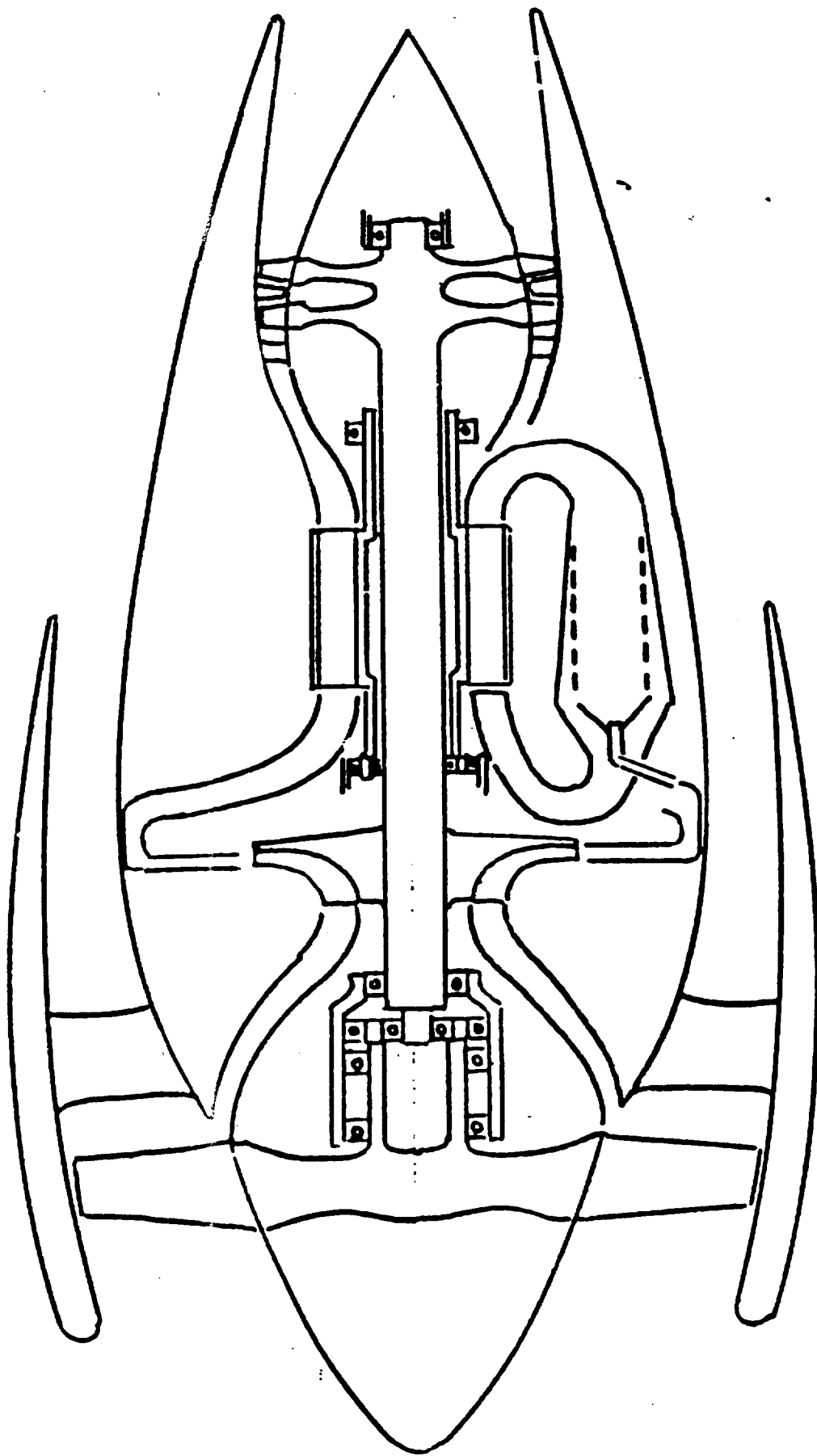


FIG. 5 CRUISE MISSILE ENGINE
Thrust 300 lbs at Mach .7 sea level, sfc .95 lbs/lb thrust.hr
Diameter 20", Length 40"

WAVE ROTOR TURBOFAN ENGINES FOR AIRCRAFT

Robert T. Taussig
Mathematical Sciences Northwest, Inc.
2755 Northup Way
Bellevue, Washington 98004

ABSTRACT

This paper describes the results of an investigation of an advanced, small turbine engine concept which uses a pressure exchanger wave rotor as the high pressure, high temperature compressor and expander stages. This work shows that thrust-specific fuel consumption in the range of 0.68 to 0.75 can be expected from engines in the 600 to 1000 lb thrust category. The low operating temperatures associated with the use of this technology will obviate the need for high temperature materials development. Concepts for integrating the wave rotor into a small gas turbine engine, computer studies of wave rotor configuration and performance optimization, and overall engine performance studies and projections are described.

WAVE ROTOR TURBOFAN ENGINES FOR AIRCRAFT

Robert T. Taussig
Mathematical Sciences Northwest, Inc.
2755 Northup Way
Bellevue, Washington 98004

Section 1 INTRODUCTION

1.1 SMALL AIRCRAFT ENGINES

A growing market for business jets, helicopters, and various types of drones has stimulated a strong interest in small turbofan engines. Competition is driving this market toward higher performance engines. Mullen and Othling⁽¹⁾ recently reviewed the status of small aircraft engines. Figure 1-1, taken from their article, compares the performance for existing small turbofans to the performance anticipated from three separate modes of engine improvement. These include improvements of existing engines, the development of new engines, and revolutionary engine concepts that require more research and development. Improvements of existing engines focus on higher temperature operation at higher engine rpm; this is the least costly and also the most limited path for increasing engine efficiency. New engines might involve the use of new, state-of-the-art materials, such as ceramics and carbon-composites, plus techniques for engine cooling better suited to small engine sizes. Figure 1-1 shows that the potential for improvement via this path is approximately a 15 to 20% decrease in thrust-specific fuel consumption (TSFC).

The revolutionary class of engines, as shown in Figure 1-1, may achieve as much as a 35% decrease in TSFC. Four advanced cycles have been considered in this context: the compound cycle turbofan, the eccentric turbofan, the recuperative turbofan, and the wave rotor turbofan, shown schematically in Figure 1-2. While each of these engines is based on the turbofan concept, the core engines are quite different. The overall performance will benefit, primarily through core engine improvements.

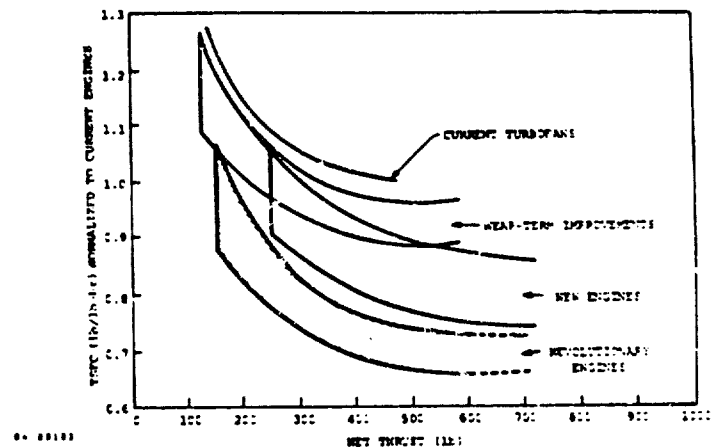


Figure 1-1 Thrust-Specific Fuel Consumption (TSFC) Improvements Available Through New and Advanced Engine Development. (Reference 1)

1.2 ADVANCED ENGINE CYCLES

The compound cycle turbofan uses a Diesel engine to generate gas and to drive an upstream compressor which supercharges the intake air.⁽²⁾ The core Diesel engine operates at high pressures and is very compact. The walls of the pistons are cooled by the intake air and by a cooling jacket. Exhaust gases expand through a power turbine that drives the fan, giving it the outward appearance of a conventional turbofan engine. The cycle efficiency of the Diesel engine core is quite high so that the overall engine efficiency is improved. To achieve the best efficiencies from this approach, the Diesel cycle peak temperatures and pressures must be very high, requiring advanced materials.

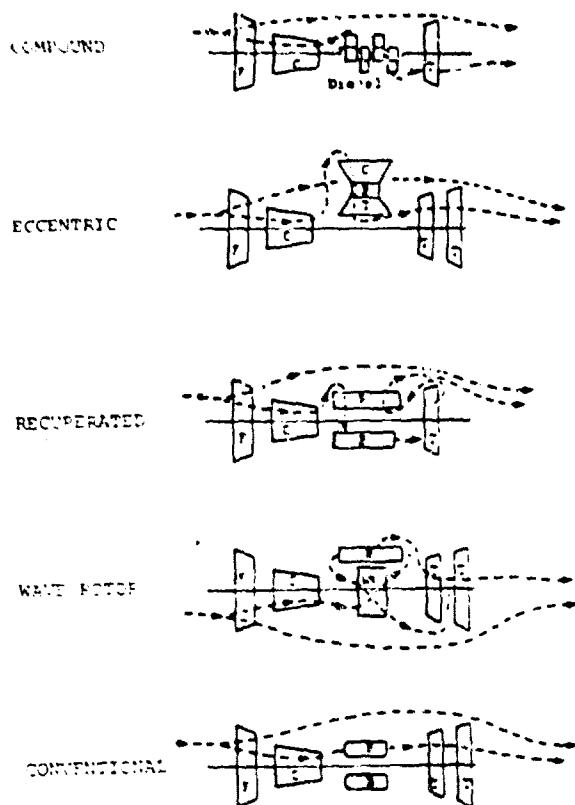


Figure 1-2 Advanced Turbofan Concepts Compared to a Conventional Turbofan. (bottom figure).

The eccentric turbofan utilizes a third high pressure spool oriented at right angles to the engine axis.⁽³⁾ Normally, as the cycle pressure ratio increases for a given mass flow, the spool diameter is reduced. By mounting this spool independently, its shaft is not constrained to be above a certain diameter as it would be for an in-line coaxial shaft configuration. Consequently, this approach achieves a high component efficiency by keeping a reasonably long blade length despite its high pressure operating regime. The high pressure spool still operates at elevated temperatures so that this approach will require materials development.

The recuperated turbofan is more efficient than an unrecuperated cycle operating at the same peak temperature.⁽⁴⁾ The recuperated cycle achieves this increase in performance at a lower pressure ratio, implying that the blade heights of the highest pressure stages will be longer and, therefore, have a higher component efficiency. A tradeoff clearly exists between added surface area for heat transfer effectiveness and the accompanying pressure drop and increased engine weight associated with the added area. This technique still requires a high temperature turbine stage and some materials development in this area but clearly not as much as is required for the eccentric turbine.

1.3 THE WAVE ROTOR TURBOFAN CONCEPT

Figure 1-3 portrays a conceptual design of a wave rotor turbofan with the high pressure wave rotor stage located co-axially with the other rotating components. The wave rotor consists of many compression tubes surrounding the periphery of a rotating drum. Each of these tubes is periodically filled with gas, which is compressed by unsteady waves over part of the rotor cycle and then released at higher pressure to drive a high pressure turbine and to supply combustion air. Figure 1-4 is a close-up view of the wave rotor component with the positions of the compression and expansion waves in each tube shown by the dark diagonal lines imposed on the tube rows. These waves propagate from one end of the tube to the other as the tube is rotated through one complete cycle. Viewed in the laboratory frame, these waves appear as stationary, standing waves through which the gas flows as it is compressed or expanded. In this cycle, air from the compressor enters the wave rotor where it rises to the peak cycle pressure. Part of this resulting high pressure air stream is heated to the peak cycle temperature in the combustor and re-enters the wave rotor to carry out the work of compressing the inlet air. The remainder of the high pressure air stream is heated to a lower temperature (1800-2000°F) where it enters the power take-off turbine.

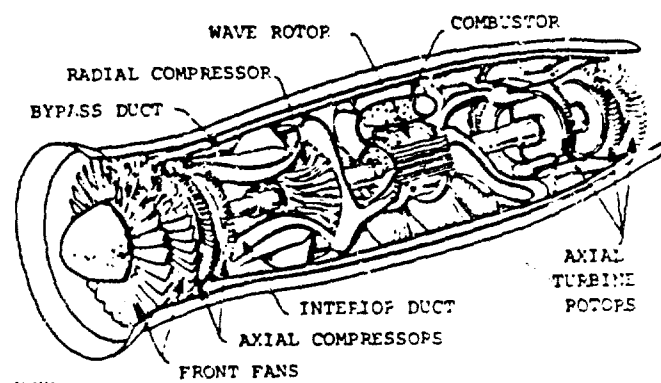


Figure 1-3 Artist's Conception of a Wave Rotor Turbofan Engine

With many tubes opening at each instant onto a given manifold, the batch processes occurring in individual tubes are converted into continuous flows within the manifold. The principal constraint for steady average flow in the stationary manifolds is wave system periodicity; that is, the wave processes must repeat themselves after some integral fraction of a revolution. Wave rotors with steady external flow can be mated with conventional steady flow machinery and are relatively easy to analyze in the fixed frame of the manifold coordinates. Some consideration has been given to matching aperiodic wave rotor flow systems to unsteady external flow systems which are tuned to an optimal operating condition, but no practical application has yet resulted for such combinations.

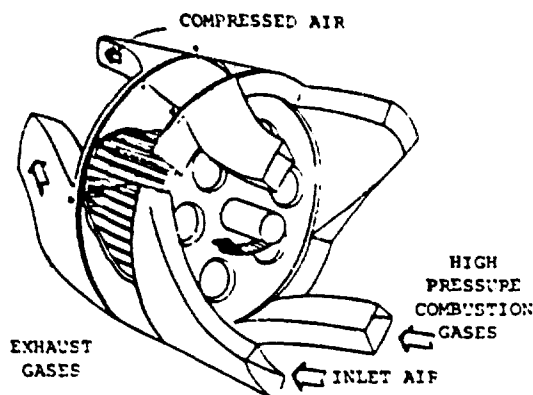


Figure 1-4 Superposition of Wave Fronts (lettered lines) on the Tube Rows of a Two-Cycle Wave Rotor.

The two main classes of wave rotors are:

1. Pressure Exchangers, which transfer work from one gas stream to another via unsteady waves, and
2. Wave Rotor/Turbines, which extract shaft power from the expanding gas stream.

Each of these is illustrated schematically in Figure 1-5. Pressure exchangers have undergone the greatest development and were amongst the earliest concepts patented. By using unsteady waves to transfer work, the compression or expansion processes are accomplished at the speed of sound or slightly faster, even though the mechanical parts of the device are moving much slower than the sound speed. No change in solid body inertia is required for it to respond quickly to load changes. Also, since the gases are being cycled in and out each tube during each wave cycle, cold inlet gases as well as hot combustion gases contact the tube walls, maintaining them at an intermediate temperature. Consequently, the rotor temperature will be substantially less than the peak temperature of any combustion gases used to drive the rotor. This feature distinguishes the pressure exchanger in a very useful way from turbines, which are limited to lower peak cycle temperatures because the turbine walls are continuously exposed to the combustion inlet temperatures.

Since there is no analog to turbine blade tip leakage in the pressure exchanger, the component efficiency of this device is comparatively high for small engines. For the same reason, the wave rotor need not have a small shaft diameter. Therefore, it can be mounted either coaxially with the lower pressure spools, or in an eccentric configuration (see Figure 1-2b).

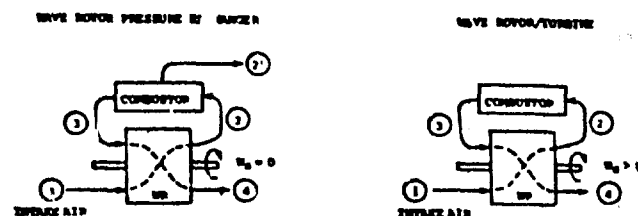


Figure 1-5 Two Main Classes of Wave Rotors

The pressure exchanger compression and expansion processes do not depend on the aerodynamic turning of flow found in turbines and compressors. Therefore, the wave rotor rotational speed does not have to match the gas velocity as it leaves the rotor, in contrast to a turbine. Since the gas exit velocity depends on its temperature, the rotor speed can be uncoupled from the peak temperature of the cycle and can be relatively slow. This fact plus cooler wall temperatures relieves the need for materials development to achieve a higher cycle efficiency.

Wave rotor/turbines extract shaft power from gases expanding from the rotor in addition to performing the supercharging function of the pressure exchanger. Shaft power is obtained by changing the direction of the flow in the same way that a turbine does. That is, the wave rotor/turbine flow tubes are bent or helical so that the direction of the exiting flow is different than the entering flow. Because a turbine must spin at a speed commensurate with the velocity of the flow leaving the turbine in order to attain a good expansion efficiency, as the gas temperature of the expanding flow increases, the flow velocity increases and so does the turbine speed. This same requirement applies to the wave rotor/turbine. Hence, some of the high temperature advantages associated with the pressure exchanger do not apply to this type of wave rotor. That is, in order for this device to operate efficiently, it also must operate at high tip speeds, in contrast to the pressure exchanger where all of the work transfer is accomplished internally at the local gas sound speed. This would imply that the wave rotor/turbine is restricted to lower peak cycle temperatures than the pressure exchanger, but possibly still higher than conventional turbines. The wave rotor/turbine does have the distinction of producing shaft power, whereas the pressure exchanger must rely on an additional turbine component to extract shaft power. A more complete description of engines based on these two concepts is presented in Sections 5 and 7.

Lastly, because the rotor wall temperature in each case lies somewhere near the mean of the combustion gas temperature and the cooler intake air temperature, the wall will transfer heat from the hotter expanding gases to the cooler compressing gases. In this mode, it automatically operates like a recuperator. If recuperation occurs too early in the compression process, it will result in an extra amount of work required to compress the gas. However, with some relatively simple additions to the flow configuration, it can be made to operate nearly as a simple recuperator, giving it some of the advantages of the recuperated turbfan engine.

1.4 WAVE ROTOR DEVELOPMENT

A variety of wave rotor devices have been developed, such as the Comprex,⁽⁵⁾ which is a commercially available supercharger for Diesel engines, and research rotors, such as the energy exchanger⁽⁶⁾ and the wave/turbine engine.⁽⁷⁾ For⁽⁸⁾ has reviewed several of the earliest propulsion applications, starting in the 1940s, which were associated with the use of the Comprex and other wave rotor concepts. Initially, the fluid dynamics of the Comprex was not well understood and it was relatively inefficient. Since that time, this concept has been developed a great deal by the Brown-Boveri Company for application in the present Diesel engine market.⁽⁹⁾

Wave rotors also were designed to supercharge aircraft engines in order to allow them to fly at higher altitudes. The wave rotor technology competed head-on in the 1950s with turbocompressor technology. Jendrassik developed one of the first concepts for wave rotor application to aircraft engines.⁽¹⁰⁾ His work was followed by several attempts to marry the pressure exchanger technology with gas turbines.^(11,12) These concepts utilized the wave rotor as a high pressure topping stage in the early turbine shaft power devices.

A completely different approach was taken by Ronald Pearson, who developed one of the first versions of the wave rotor/turbine, a device which formed a complete engine by itself to produce shaft power.⁽⁷⁾ General Electric, the ITE Circuit Breaker Company,⁽¹³⁾ and the General Power Corporation⁽¹⁴⁾ also tried to develop related technologies. Pearson's was the most successful of these efforts since he achieved overall thermal cycle efficiencies of 16% to 22% for his engine in the mid-1950s. This device produced up to 35 horsepower and ran over a wide range of operating conditions.

As a result of these efforts and because of recent research carried out under the auspices of the U.S. Department of Energy⁽¹⁵⁾ and DARPA,⁽¹⁶⁾ the wave rotor concept has advanced to the point where it can improve the thrust-specific fuel consumption (TSFC) of small aircraft engines and make them more responsive to the throttle.

1.5 OUTSTANDING TECHNOLOGY ISSUES

In the past, several obstacles have impeded the progress of wave rotor technology. These obstacles included the problem of computing unsteady flow phenomena in the wave rotor, the impact of unsteady flow effects on the efficiency of the device, and the uncertainties surrounding the selection of the best wave rotor device configuration for a particular application. The advent of modern computational capabilities in unsteady fluid dynamics, including fast computers and accurate test data on the flow behavior of the wave rotor, have made it possible to understand such phenomena and to determine the best device for specific applications.

The key issues today focus more on the engineering aspects of wave rotor technology and include problem areas such as the most effective way to seal the wave rotor against excessive leakage; the best support mechanisms for the rotor bearings and manifolds under conditions of high heat transfer; the impact of tube design on cyclic fatigue limits; and the reduction of aerodynamic losses.

Much clearer design choices are available now for each particular wave rotor application. Test data still are required for small, high efficiency wave rotors operating at high temperature and pressures before a full-fledged engine development can be undertaken. However, the basic seals and engine design problems appear to be within the limits of the state of the art. There are no evident obstacles that would prevent this engine from achieving its lightweight, high efficiency goals.

Section 2

WAVE ROTORS FOR AIRCRAFT ENGINES

2.1 PURPOSE

The preceding section introduced the concept of a wave rotor turbfan. Now the viability of this concept must be established as an attractive way to improve aircraft engine performance. Such motivation provides a strong incentive for an engine development program which, by its very nature, could be an expensive undertaking unless the intermediate steps to a near-term, working engine are recognized at the outset.

The following paragraphs address the basic reasons why a wave rotor turbfan can improve the efficiency and range of small aircraft operation and can provide an increase in their maneuverability. These arguments are quite general, relying on fundamental features of the thermodynamic cycles commonly used by turbine engines. These same arguments lead logically to scaling relations that show what

advantages this approach might have for larger aircraft engines. A straightforward estimate is made of the percentage increase in engine mass which would accompany the increase in efficiency and performance achieved with the wave rotor approach. The results show that the gain in range under normal flying conditions is much greater than the negative impact of the added weight of such an engine. That is, the decrease in fuel mass for a given range is much larger than the increase in engine mass, for all but the very shortest excursions.

The greatest uncertainties lie in the lifetime and reliability of the wave rotor component. Surer knowledge of these characteristics must come from actual engine test data, emphasizing the need for early experimental evaluations of this device from that standpoint. Wave rotor technology is poised for application in this area. It needs only to have the decision of an engine manufacturer to gather the critical, available technology together and start the process of component and engine design and evaluation.

2.2 EFFICIENCY IMPROVEMENTS

The basic advantages of the wave rotor approach are to increase the efficiency of the turbofan engine by allowing it to operate at higher peak temperatures and pressures. Higher pressures necessarily imply higher temperatures, since the gas must be heated by combustion after being compressed and the act of compressing the gas already raises its temperature. The ideal efficiency of the Brayton cycle, which is the basic thermodynamic engine cycle of the turbofan, depends only on the ratio of peak-to-inlet pressures. When real components are introduced into this calculation, their mechanical efficiencies affect the overall cycle efficiency; the addition of each new component successively detracts from the ideal efficiency. Therefore, the addition of the wave rotor component must supply enough of an increase in the ideal efficiency of this cycle to overcome the impacts of its finite component efficiency. The effect of the wave rotor efficiency is not simply a multiplicative factors times the cycle efficiency, because the cycle can still make use of the work available in the exhaust stream from the wave rotor. In this sense, the wave rotor component enjoys the privileged position of a topping cycle and can be somewhat less efficient than the lower pressure components while still augmenting the overall cycle efficiency. These arguments are quantified in Section 7.3 where we see that the wave rotor efficiency must be above ~60% for it to contribute strongly to the overall cycle efficiency.

2.3 CRUISING RANGE

The range equation for aircraft can be stated (17)

$$R = \frac{u}{\text{TSFC}} \left[\frac{L}{D} \right] \ln \left[1 + \frac{M_i}{M_f} \right] \quad (2-1)$$

where R is the distance traveled (constant flight velocity u is assumed), the initial mass of the aircraft is M_i , and the final mass is M_f after the fuel has been expended. The thrust specific fuel consumption (TSFC) must be small in order for the range to be large; similarly, the initial-to-final mass ratio must be large for long-range flight. Together, these two requirements argue for high energy fuel per pound, high efficiency engines (low TSFC), and lightweight engines.

The engine mass contributes approximately 30% of the residual mass represented by M_f . By taking the logarithmic derivative of R , we can express the impact of relative changes in both TSFC and engine mass, assuming all other variables are fixed. The resulting equation is

$$\frac{\Delta R}{R} = - \frac{\Delta \text{TSFC}}{\text{TSFC}} - \left[\left[\frac{M_i}{M_f} \right] \ln \left[1 + \frac{M_i}{M_f} \right] \right]^{-1} \frac{\Delta M_{\text{eng}}}{M_f} \quad (2-2)$$

This equation can be evaluated for small aircraft by substituting typical values for the mass ratio and the TSFC.⁽¹⁸⁾ For example, consider $M_i/M_f = 1.45$. Then the relative effect of an increase in engine mass of 27% is to decrease the range by 4% and the relative effect of a decrease in TSFC of 30% is to increase the range by 30%. The relative values chosen for these TSFC changes correspond to calculations in Section 7 for small wave rotor turbofan engines in the 600 to 1000 lb. thrust class.

An approximate value for the increase in engine mass can be obtained by assuming that the peak cycle pressure is on the order of 50 atmospheres. This pressure must be contained within two concentric shells. The outermost shell stands off a pressure difference of 25-1 = 24 atmospheres and the inner one a difference of 35-25 = 10 atmospheres. Both shells together cover 6 inches of active rotor length, yielding an active mass of 10 lbs. This value must be multiplied by a factor of 2 to 3 to cover the bearings, manifolds, and high pressure combustor shell required for this cycle, giving a combined increase in engine mass of 30 lbs. Assuming an initial total engine mass of approximately 130 lbs., the relative increase will be 30/130 = 23%. Using this result in equation shows that the percentage decrease in the range will be roughly 27%.

Even if the engine mass increase estimate is low by a factor of 2, the implications of this result are still positive. Of course, a more precise calculation needs to be carried out once a careful wave rotor turbofan engine design has been developed. Nevertheless, we can proceed with confidence that the engine mass increase will be quite manageable for the small engine applications.

2.4 MANEUVERABILITY

The principal advantage of the wave rotor for transient engine operation is to increase the speed of stable response to changes in the engine flow conditions. Normally, when an aircraft accelerates too quickly, the compressor operating points move toward and across the surge line, creating compressor stall. This phenomenon is well known and ultimately limits the performance of the aircraft. Compressor stall is due primarily to the fact that the combustor response time to the throttle is short compared to the spin-up response time of the compressor. The combustor pressure rises abruptly under such circumstances, while the compressor continues to supply air at a lower pressure. A pressure wave propagates from the combustor into the compressor, stopping the flow of air to the combustor and disrupting normal operation of the engine. When this process proceeds on a slower time scale, the compressor rotational inertia can be overcome so that its speed can increase enough to supply air at a pressure matching the combustor inlet conditions.

The wave rotor response is mediated entirely by pressure waves. Hence, its response time can be much faster than that of a conventional compressor. When the combustor pressure increase is registered at the exit of the wave rotor, it is simultaneously providing higher pressure combustion gas at the wave rotor inlet. Consequently, the re-entrant duct characteristic of the combustor automatically provides the higher pressure needed to compress the intake air up to the proper pressure level. Response times are just the rotor tube length divided by the acoustic speed of the gas. For the small engines to be considered here, these times are typically on the order of a millisecond or less, compared to several seconds or more for a compressor.

As a consequence of this advantage, a wave rotor turbofan engine can operate much closer to the compressor stall line because the wave rotor reacts quickly and buffers the upstream compressor from the combustor. This means that high performance engines can be upgraded for better cruise conditions and greater engine reliability against sudden throttle changes to give increased maneuverability.

2.5 SCALING

Due to the relative maturity of wave rotor technology in relatively small sizes (e.g., the Compress and other pressure exchangers), the most obvious near-term application should be to small engines. As we have discussed, wave rotor efficiency scales well to small sizes where more conventional turbine-compressor performance begins to deteriorate. With increased performance as a market driver for small turbofans, the existing wave rotor technology could be applied directly to existing turbofans to achieve good

reductions in TSFC without a large increase in engine mass. The result, for a variety of aircraft engines, is an increase in range, maneuverability, and reliability.

As engine size increases, the immediate advantages of the wave rotor are not so dramatic. Conventional turbine and compressor efficiencies are quite good and turbine cooling is already a highly developed art in the larger engines. The response time advantage of the wave rotor still remains, and its component efficiency also increases with size. It is true that the wave rotor will always be able to operate at higher peak cycle temperatures than the turbine, but this advantage reaches a point of diminishing returns and is ultimately limited by fuel chemistry (i.e., the flame temperature). A much more careful evaluation of wave rotor application to large turbofan engines needs to be carried out. As the earlier wave rotor applications to smaller engines develop, a sharper identification of possible large engine designs and performance will emerge. It will be possible in this development sequence to focus on intermediate improvements of wave rotors that will make the large engine applications both more specific and more attractive.

Section 3 WAVE ROTOR ANALYSIS

3.1 INTRODUCTION

In this section, the component efficiencies of several wave rotor designs are evaluated for on-design and off-design operation. The designs include pressure exchanger wave rotors and wave rotor/turbines. Gas stream properties are computed for each of the inlet and outlet ports; details of the unsteady on-rotor flows are used to illustrate the underlying phenomena which produce the port flows. A range of key design variables has been used to determine the sensitivity of wave rotor performance to these variables.

Work transfer efficiencies in the range of 70 to 75 percent appear feasible for small wave rotors designed for the 600 lb_f to 1000 lb_f thrust engine class. Off-design performance for single variable design parameter variations is very dependent on the particular parameter being varied. However, off-design performance, in which several parameters vary according to actual off-design engine operation, appears to be very good. For example, in-flight control can be exerted over rotor tip speed to accommodate the wave rotor performance to the off-design changes occurring in engine-supplied flow parameters (e.g., mass flow, pressure, and temperature). Wave rotor wall temperatures also appear to be quite acceptable (i.e., in the range of 1700 to 1950°F) for combustion temperatures in the range of 2500 to 3500°F.

The chief tool for analyzing the wave rotor component is a one-dimensional, unsteady gasdynamic computer code, called the FLOW code, which was developed specifically for wave rotor analysis.⁽¹⁵⁾ FLOW code calculations are presented in this section for wave rotors which are pure pressure exchange wave rotors. Analytic estimates are provided for wave rotor/turbines which produce shaft power. The requirements for steady inlet and outlet flows are formulated and used to define realistic classes of wave rotor designs. Specific examples are chosen for evaluation, including wave rotor/turbines such as the Pearson rotor and the GPC wave rotor, pressure exchange wave rotors such as the Rolls-Royce wave rotor, and a modern pressure exchange wave rotor designed by MSNW for high component efficiency.

The examples chosen for analysis illustrate why some of the earlier efforts were unsuccessful (and still have problems) in obtaining good performance and why other designs were more successful. The modern pressure exchange wave rotor example is explored in depth to determine the sensitivity of a high efficiency design to variations in design and operating parameters. These variations correspond to either design or operating tolerances and to off-design engine operation.

The flow code used for these calculations has been validated by detailed experimental data from MSNW's wave rotor experiments.⁽¹⁹⁾ The code is described in more detail below, but it should be pointed out here that the extension of this code to higher temperature and higher pressure conditions still requires additional validation by a hot wave rotor test in order to certify its predictive capabilities for the cases examined in this report.

Results from the code calculations include gas flow conditions for all of the inlet and outlet ports on the rotor, a discussion of the main wave phenomena responsible for these flows, the wave rotor work transfer and shaft work efficiencies, depending on the type of rotor, and presentation of preliminary sizing and operating data for rotors. The sensitivity of wave rotor performance to tip speed, port placement, and size, gas inlet and outlet conditions, tube size, number of tubes, leakage, and heat transfer has been analyzed for on-design conditions. Wave rotor response to off-design engine conditions for lower and higher flight speeds also has been investigated. The effects of heat transfer, viscosity, impedance mismatching, and gas leakage are included in all of the computations. These results also are corroborated with analytic estimates to provide a more intuitive interpretation of the results.

3.2 THE FLOW CODE

The FLOW code uses the flux-corrected transport algorithm developed by Boris and Book⁽²⁰⁾ to integrate the following one-dimensional Euler equations of unsteady, compressible gas flow:

$$\frac{\partial p}{\partial t} = - \frac{\partial}{\partial x} (pu) \quad (3-1)$$

$$\frac{\partial pu}{\partial t} = - \frac{\partial}{\partial x} (pu^2) + \frac{\partial p}{\partial x} - 0.5 \pi C_D \text{sgn}(u) pu^2 \quad (3-2)$$

$$\frac{\partial E}{\partial t} = - \frac{\partial}{\partial x} (uE) - \frac{\partial}{\partial x} (uP) + \pi C_H \left[\frac{\gamma R}{\gamma - 1} \right] p |u| (T_w - T) \quad (3-3)$$

$$\text{where } E = \frac{p}{\gamma - 1} + \frac{1}{2} pu^2$$

As Equations [3-2] and [3-3] show, the heat transfer and viscous drag terms are based on a developed pipe flow analysis where a friction factor f of approximately 2×10^{-5} has been used. These calculated unsteady tube flows are driven by the flow conditions prescribed at the inlet and outlet manifolds. These port conditions are supplied as boundary values to the FLOW code for each successive time step. The flow pattern in a single tube is computed as a function of time for several successive complete revolutions of the rotor until the solution repeats each previous cycle to within a desired level of accuracy. This periodic flow constraint is typically achieved within three complete cycles at which point the flow conditions in each manifold are accumulated to give the total mass and enthalpy flows for each manifold and to determine averaged flow properties such as the pressure, temperature, density, and velocity. In cases where shaft power is being produced, the rotor tube angles, flow velocity direction, and manifold flow angles are used to compute the tangential momentum of the gas flowing onto and off of the rotor in each port: the sum of these terms multiplied by the rotor tip speed gives the net shaft work output from the rotor. The work transfer efficiency, which measures the efficiency of pressure exchange operation, is also computed from the ratio of manifold flow conditions. These efficiencies are defined in Section 3.4.

Figure 3-1 compares the output of the FLOW code to the trace of a pressure transducer mounted near the end of one of the tubes on the MSNW wave rotor. The correspondence between the code and the experimental data is remarkably good for a wide variety of experimental conditions (see Reference 19). The code also predicts the measured work transfer efficiency reasonably well, as shown in Figure 3-2. Subsequently, the code was used for a preliminary optimization of the MSNW rotor design according to the variation in port width shown in Figure 3-3. As a result of these code calculations, some single port width modifications were made in the test rotor which led to an improvement very

close to that predicted by the codes. That is, the peak of 74 percent achieved by the experiment shown in Figure 3-4 was a direct result of the code prediction of 75 percent shown at $A_{d2}/A_{d1} = 1.05$ in Figure 3-3. The ease and speed of predicting design modifications of this sort with the FLOW code has established it as a superior tool for wave rotor analysis and design.

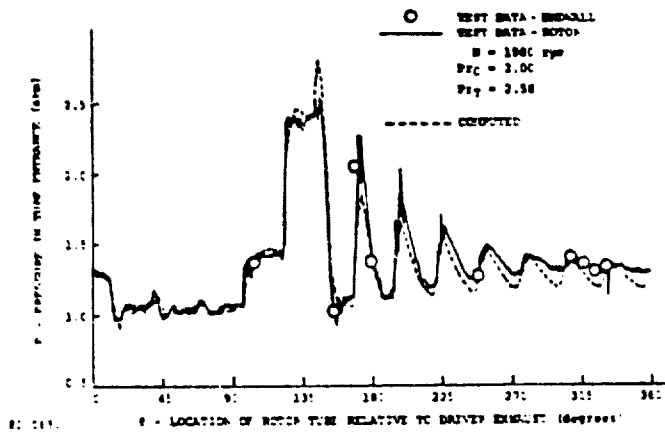


Figure 3-1. Measured and Computed Pressure History for One Wave Rotor Cycle with Wave Management for $\phi > 145^\circ$ [Ref. 19]

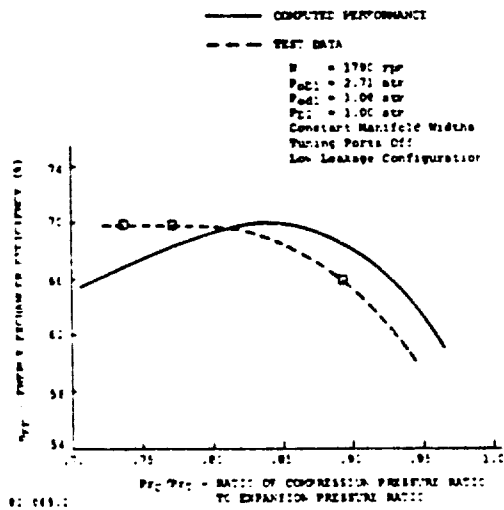


Figure 3-2. Computed and Measured Wave Rotor Efficiency [Ref. 19]

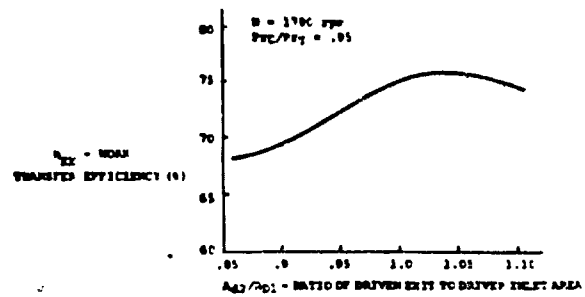


Figure 3-3. FLOW Code Optimization of Work Transfer Efficiency as a Function of Port Widths [Ref. 19]

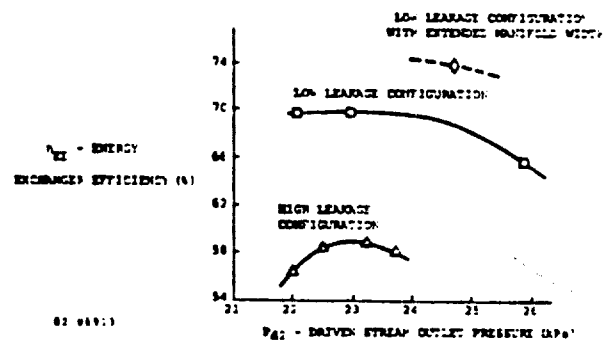


Figure 3-4. Experimental Data for Work Transfer Efficiency Variation with Outlet Port Pressure. Dashed line indicates experimental verification of FLOW code optimization [Ref. 19]

The FLOW code also treats the finite tube width opening and closing transients which create their own class of wave disturbances in the wave rotor. These transients may involve sonic flow conditions when the end of the tube is partially open. The losses associated with partially open tubes are also incorporated as pressure recovery losses in order to prescribe the tube boundary conditions properly. We follow an earlier treatment by Spaulding⁽²¹⁾ for these losses. The finite wall thickness of each tube also contributes to an area change in the stream tube dimension; we assume that the area change is gradual enough due to streamlining the ends of each tube wall so that the flow transition is isentropic. It does result in flow acceleration (deceleration) at the tube ends for inflow (outflow) and a corresponding change in the pressure boundary values computed in the flow code. Incorporation of these changes is estimated to contribute to as much as a 14% change in the computed work transfer efficiency, depending on the solidity of the wave rotor.

The FLOW code also incorporates a finite stagger angle for the tubes which allows it to represent helical wave rotor tube arrays. An additional modification permits the user to assign two stagger angles for each tube - one on the left and one on the right - with a sharp turn in the tube angle located near the right hand end of the tube. This option was developed specifically to allow reaction forces to be modeled for wave rotor/turbines (e.g., the GPC and Pearson rotors). Manifold flow angles are included so that impulsive loading of the rotor can also be calculated; that is, the flow angle of gas incident on the rotor may result in tangential gas velocities which are different than the rotor tip speed resulting in work transfer to or from the rotor. The combination of impulsive and reactive (i.e., mismatched tangential inflow and outflow) effects gives a complete characterization of the shaft power being produced by such a rotor.

Cases with and without heat transfer can be computed in order to determine the magnitude of that effect. Similarly, the tube wall temperature can be prescribed so that the amount of heat transferred to the rotor from the hot gases can be compared to the amount transferred from the rotor to the cold gases; equilibrium wall temperatures require these two quantities to be equal, which suggests a quick trial and error technique for arriving at the equilibrium wall temperature. Clearances and shroud pressures are also prescribed in order to control the amount of leakage associated with a given calculation. Tip speed, number and cross-sectional area of tubes, and angular tube width determine the basic rotor dimensions. The angular rotor speed then embodies the rotor radius once the tip speed is given. The stagger angle(s) of the tubes are set equal to zero for the pure pressure exchange applications.

3.3 BOUNDARY CONDITIONS

Flow properties at each of the wave rotor ports are supplied to the FLOW code as boundary conditions to the unsteady tube flow. These boundary conditions represent compressor outlet, combustor inlet, combustor outlet, and turbine inlet conditions for the engine cycle. Port locations and widths are derived from an initial analytic calculation involving the ideal wave pattern corresponding to the external flow conditions. Generally, the stagnation pressure and temperature are prescribed at each inlet port and the static pressure is given at the outlet ports. At each step in the calculation, the code determines whether the anticipated value of the pressure at the end of the tube is greater or less than the static pressure in the manifold. This comparison determines whether the flow must go in or out of the tube. Conditions at the tube mesh points corresponding to the ends of the tubes are calculated iteratively by using the projection of the forward or backward facing characteristic originating on the previous time step from the tube mesh points

located one spatial point in from the ends. An iterative process is then required to solve for the boundary mesh point conditions using a technique described by Spaulding for wave rotor calculations.⁽²¹⁾

This technique can be applied to partially open tubes as well as fully open tubes and to tubes with finite tube wall thickness. Flow in or out of partially open tubes can reach sonic conditions when the opening is very small. In those cases where the sonic condition is detected, the sonic flow equations replace the subsonic equations in the calculations. Finite tube wall widths are treated as isentropic converging or diverging area changes in a quasi-steady flow approximation which leads to slight increases or decreases in the flow velocities, and related flow variables also change.

As an example, consider the flow equations for fully open outflow. Figure 3-5 shows a rotor tube on the left, with wall thickness δ and interior width d . Three flow stations are distinguished: the position w inside the tube, the position th in the throat (i.e., at the very end of the tube), and the position e corresponding to the external manifold flow. As the figure shows, the flow area changes from A_w in the tube to A_e , the equivalent cross-sectional area of the stream tube in the manifold; the ratio of these two quantities, Φ , is

$$\Phi = \frac{A_e}{A_w} = \frac{(d + \delta) \cos \theta}{d \cos \beta}$$

The equations governing the flow from the tube to the manifold are

CONTINUITY

$$\rho_w A_w u_w = \rho_e A_e u_e \quad [3-4]$$

IDEAL GAS LAW

$$P_w = \frac{\rho_w A_w^2}{\gamma}, \quad P_e = \frac{\rho_e A_e^2}{\gamma} \quad [3-5]$$

ENERGY CONSERVATION

$$\frac{\gamma-1}{2} u_w^2 + a_w^2 = \frac{\gamma-1}{2} u_e^2 + a_e^2 \quad [3-6]$$

RIEMANN INVARIANT

$$QQ = u_w + \frac{2}{\gamma-1} a_w \quad [3-7]$$

ISENTROPIC CONDITIONS

$$a_w = aP_w^{\frac{\gamma-1}{2\gamma}}, \quad a_e = aP_e^{\frac{\gamma-1}{2\gamma}} \quad [3-8]$$

where Q_0 , the invariant, is known from the previous time step. The unknowns are u_w , u_o , a_w , a_o , p_w , p_o , and p_e . These seven equations may be reduced to the single equation for the variable p_w ,

$$p_w = p_o \left[\Phi^2 \left(1 + \frac{2s^2 \left[\frac{\gamma-1}{p_w^\gamma} - \frac{\gamma-1}{p_o^\gamma} \right]}{(\gamma-1) \left[Q_0 - \frac{2}{\gamma-1} s p_w^\gamma \right]} \right) \right]^{\frac{\gamma}{2}} \quad (3-9)$$

This equation can be solved iteratively in the form given with the initial guess of $p_w = p_o$. Implicit in this formulation is the assumption that the transformation of coordinates from the rotor frame to the laboratory frame does not affect the static pressure p_o , which has been assigned as the external boundary condition.

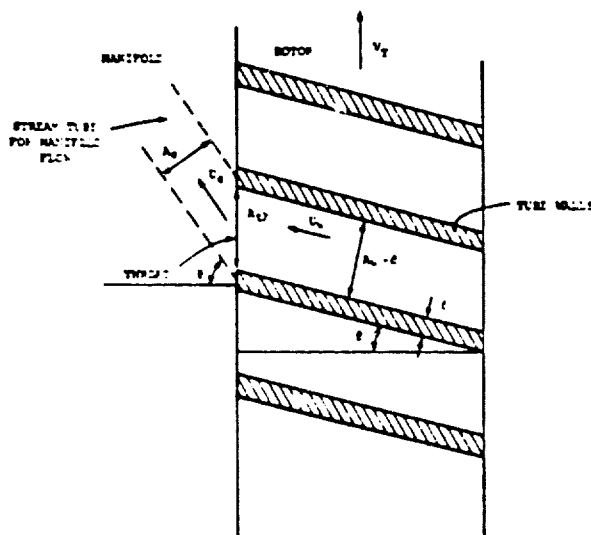


Figure 3-5. Fully Open Outflow Condition Showing Rotor Tube Geometry and Stream Tube for Flow in the Exhaust Manifold

3.4 THERMODYNAMICS AND EFFICIENCIES

Two efficiencies are used to describe the performance of a wave rotor. These are the work transfer efficiency η_w , and the shaft power output efficiency or shaft work efficiency, η_s . These are defined as

$$\eta_w = \frac{W_{d(out)} - W_{d(in)}}{W_{D(in)}} \quad (3-10)$$

$$\eta_s = \frac{W_s}{W_{D(in)}} \quad (3-11)$$

where

$$W_{Din} = mc_p T_{Din} \left[1 - \left(\frac{p_{ref}}{p_{Din}} \right)^\alpha \right],$$

$$W_{Dout} = mc_p T_{Dout} \left[1 - \left(\frac{p_{ref}}{p_{Dout}} \right)^\alpha \right],$$

$$W_{din} = mc_p T_{din} \left[1 - \left(\frac{p_{ref}}{p_{din}} \right)^\alpha \right]$$

represent the available work in the inlet driver gas, the outlet driven gas, and the inlet driven gas, respectively, and W_s is the shaft power output of the wave rotor; $\alpha = (\gamma-1)/\gamma$. The available work terms are given in terms of a reference state pressure; that is, these terms represent the work that could be obtained by an isentropic expansion to that pressure. The work transfer efficiency represents the change in the driven gas available work compared to the available work in the driver inlet stream. The shaft work efficiency represents the shaft work derived from the rotor compared to the same driver gas available work. Therefore, each of these efficiencies is a component efficiency which equals one in an ideal system but which is modified in a real system by loss terms which irreversibly use up the available energy in the driver gas inlet stream.

Losses which reduce the work transfer include entropy production in shock waves, friction losses and heat transfer at the walls of the tubes, and pressure recovery losses. Pressure recovery losses occur for partially open tube inflow where an abrupt area change exists between the external manifold stream tube dimensions and the interior tube dimensions. It also occurs, although to a lesser extent, for the reverse situation of a partially open tube with an abrupt area change and outflow conditions. The greatest losses are assumed to occur in all of the outflow manifolds where zero pressure recovery is assumed. This assumption is very conservative since it should be possible to design the manifolds with finite subsonic diffusers and finite, but not perfect, pressure recovery. Thus, the FLOW calculations presented in this document are strictly conservative in this respect.

The work transfer efficiency is related to the more conventional expansion (turbine) and compression (compressor) adiabatic efficiencies used by engine designers. Figure 3-6 shows a diagram of a wave rotor and a turbine inside a dashed box. The enthalpy-entropy states corresponding to the inlet and outlet flows of the wave rotor and the turbine accompany this diagram. The net work output from the dashed box divided by the available work of expansion of the inlet gas stream to this box is equal to the work transfer efficiency of the wave rotor when the turbine inside the box has an efficiency equal to 1. Following Thayer's derivation,⁽¹⁵⁾ the general expression for the box efficiency is given by

$$\eta_{\text{box}} = \frac{W_T}{\dot{m}_1(h_1 - h_{2s})} \quad (3-12)$$

In terms of the thermodynamic states shown in Figure 3-6, this expression can be rewritten as

$$\eta_{\text{box}} = \frac{\dot{m}_4(h_4 - h_5)}{\dot{m}_1(h_1 - h_{2s})} = \frac{\dot{m}_4(h_4 - h_{5s})}{\dot{m}_1(h_1 - h_{2s})} \eta_T \quad (3-13)$$

Using the standard definitions for adiabatic expansion and compression efficiencies

$$\eta_{TE} = \frac{h_1 - h_2}{h_1 - h_{2s}} \quad (3-14)$$

$$\eta_{CE} = \frac{h_4 - h_3}{h_4 - h_{3s}} \quad (3-15)$$

and the condition that the rotor is adiabatic

$$\dot{m}_1(h_1 - h_2) = \dot{m}_3(h_4 - h_3) \quad (3-16)$$

we can write the combination of these equations as

$$\eta_{\text{box}} = \frac{\dot{m}_4}{\dot{m}_3} \eta_{CE} \eta_{TE} \eta_T \frac{h_4 - h_{5s}}{h_4 - h_3} \quad (3-17)$$

If there is no leakage (i.e., $\dot{m}_3 = \dot{m}_4$), the pressure ratios $P_5/P_4 = P_3/P_4$, and the gases are perfect with constant specific heat (i.e., $h = c_p T$), then

$$\eta_{\text{box}} = \eta_{CE} \eta_{TE} \frac{T_4}{T_{4s}} \eta_T \quad (3-18)$$

which tends to

$$\eta_W = \eta_{CE} \eta_{TE} \frac{T_4}{T_{4s}} \quad (3-19)$$

for the case of a perfect turbine; that is, η_W represents the component efficiency of the wave rotor alone.

The shaft work efficiency η_s also can be written in terms of more conventional component efficiencies by recognizing that the work extracted from the shaft is supplied by turning the gas on the rotor in the same way that a turbine does. Detailed calculations of the change in momentum of the gas as it enters and leaves the rotor requires all of the rotor manifold flow conditions (i.e., speed, direction, and amount of mass flow) to be known. The thermodynamic expression of this work is similar to Equation (3-16) with a shaft work term added:

$$\dot{m}_1(h_1 - h_2) = W_s + \dot{m}_3(h_4 - h_3) \quad (3-20)$$

In this case, internal work is also being transferred to compress the incoming air. Unfortunately, it is not possible to give a completely independent measure of

the partition of work between shaft power and internal work transfer without specifying the ratio T_4/T_1 . That is, the fraction of the work available in the driver gas which is needed to compress the driven gas is proportional to T_4/T_1 ; a portion of the rest of the driver gas available work produces shaft work output.

Using the definition of an equivalent adiabatic turbine efficiency, we can write

$$\eta_s = \frac{W_s}{\dot{m}_1(h_1 - h_{2s})} = \frac{\dot{m}_1(h_1 - h_2) - \dot{m}_3(h_4 - h_3)}{\dot{m}_1(h_1 - h_{2s})} \quad (3-21)$$

$$= \frac{\eta_{TE}(h_1 - h_{2s}) - \frac{1}{\eta_{CE}}(h_4 - h_3)}{(h_1 - h_{2s})}$$

$$\eta_s = \eta_{TE} - \left[\frac{T_{4s}}{T_4} \frac{1}{\eta_{CE}} \right] \frac{T_4}{T_1} \quad (3-22)$$

If we consider $\eta_w = \eta_{CE} \eta_{TE} T_4/T_{4s}$ to be an equivalent work transfer efficiency under these conditions, then η_s and η_w are related by

$$\eta_s = \eta_{TE} \left[1 - \frac{1}{\eta_w} \frac{T_4}{T_1} \right] \quad (3-23)$$

For very high driver gas temperatures (i.e., $T_1 \gg T_4$), η_s tends to η_{TE} , as one would expect.

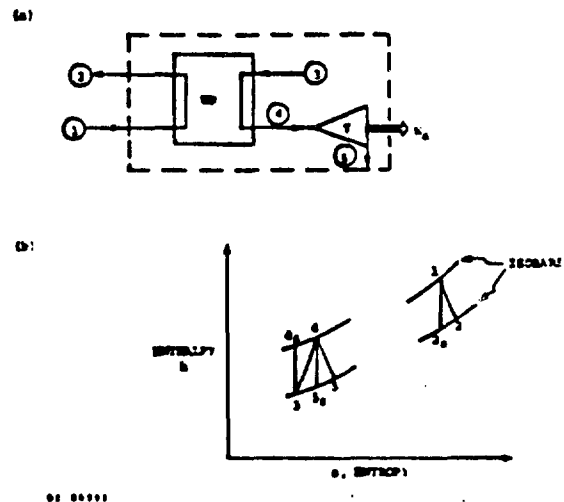


Figure 3-6. (a) Wave Rotor and Turbine Combination

(b) Equivalent Thermodynamic States. Subscript s denotes isentropic compression or expansion.

Section 4
PRESSURE EXCHANGER PERFORMANCE

4.1 SCOPE

Several wave rotor configurations for a pressure exchanger are possible including the traditional four port machines tried in the mid-fifties by Klapproth, Brown-Boveri, and others as well as the nine port machine concept developed more recently at MSNW. The earlier versions of the pressure exchanger suffered from poor scavenge and very nonuniform flows in the manifolds. The nine port design specifically resolves the problems of nonuniform port flows and poor scavenging by requiring that there be no waves incident on any port other than the relatively small tuning ports which are used to suppress wave reflections in the tubes. Both four and nine port machines are examined here in order to illustrate their differences and to quantify the advantages embodied in the design of the nine port machine. A nine port reference case is used to evaluate the sensitivity of the pressure exchanger performance to variations in its design and operating parameters.

4.2 NINE PORT ROTORS

The reference case nine port pressure exchanger design corresponds to the component which will serve as the topping stage in a 600 lb_f thrust turbofan engine flying at Mach 0.65 at sea level. With a bypass ratio of 5.0, the total mass flow of air through the engine

is 30 lb_f/sec, with 6 lb_f/sec of this flow through the core engine. The wave rotor provides the final factor of 2.5 in pressure rise from 15 atm at the compressor outlet to its peak value of 37.5 atm entering the combustor. Seventy-five percent of the air flow through the wave rotor must be heated and reinjected onto the rotor in order to provide the factor of 2.5 compression; the rest of the compressed air can be heated up to a reasonable turbine inlet temperature (e.g., by recuperating heat from the outside of the combustor can) and used in the high pressure turbine to extract shaft work. After expansion through the turbine, this flow is then recombined with the combustion exhaust gases from the wave rotor at the input to the low pressure turbine (refer to Figure 1-2d for an illustration of this cycle). The nine port wave pattern is shown in Figure 4-1 using pressure contour lines. The rotor tip speed is 15,240 cm/s (500 ft/s), the rotor diameter is 14.8 cm, and its length is 14.3 cm. The reference case design and operating values are summarized in Table 4-1. Figure 4-1 illustrates the relative port locations and size, contact surfaces, and flow code contour plots for pressure. Closely spaced parallel lines in Figure 4-1 correspond to the path taken by a compression wave. Expansion waves are represented by a fan of pressure contours radiating from the upper ports in Figure 4-1. A more detailed discussion of wave diagrams is presented in Section 6.2.

The reference case work transfer efficiency is 70 percent. A variety of related designs (i.e., port widths, port positions, rotor diameter, rotor speed) and operating conditions (i.e., driver and driven gas flow velocities, pressures, etc.) have been considered

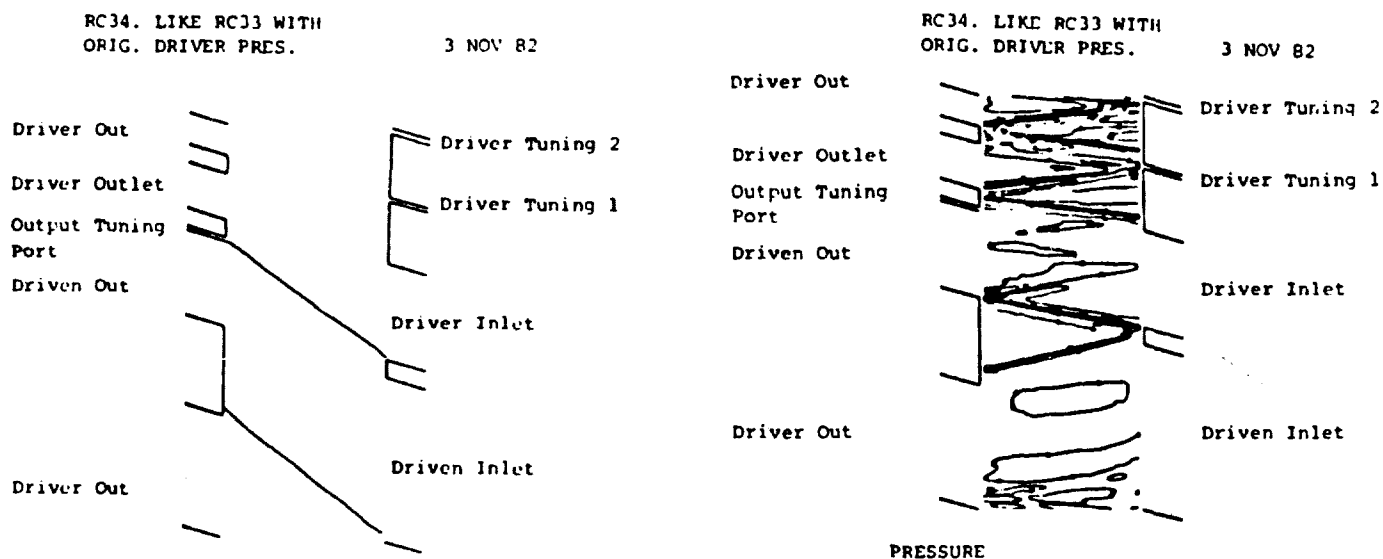


Figure 4-1. FLOW Code Results for Nine Port Pressure Exchanger Wave Rotor: Reference Case showing contact surfaces (left), port locations and relative sizes, and pressure contours (right).

in order to find ways of improving the operation of this case. These alternative designs would require a more detailed evaluation in order to assess all of their merits, but they do serve to point the way to better designs. Improvements of 3 efficiency points to 73% appear easily obtainable through minor modifications of the reference conditions and additional optimization should be possible through further design changes. Such changes should be distinguished from the more arbitrary design and operating variations discussed below, which are used to quantify the sensitivity of the reference case performance to its constituent parameters.

Table 4-1

Design and Operating Parameters for
Reference Nine Port Pressure Exchanger Wave Rotor

ROTOR DESIGN	FLOW RESULTS	
Diameter (cm)	14.8	
Length (cm)	14.3	
Tube Width (cm)	1.7	
Tube Wall Thickness (mm)	0.7	
Tube Height (cm)	1.1	
Tube Hydraulic Diameter (cm)	1.4	
Number of Tubes	24	
Number of Cycles/Revolutions	1	
Tip Speed (cm/sec)	15,240	
RPM	19,589	
Clearance (mm)	0.13	
OPERATING CONDITIONS		
Peak Temperature [$T_{D1,0}$ °K]	2240	
Peak Pressure [$P_{D1,0}$ MPa]	3.57	
Pressure Ratio	2.3	
Air Inlet Mass Flow (g/s[lb/s])	2400 (5.3)	
Combustor Mass Flow (g/s[lb/s])	1800 (4.0)	
Driven Gas Exhaust Temperature [T_{D1} °K]	1077	
Driver Gas Exhaust Temperature [T_{D1} °K]	1666	
Driven Gas Inlet Temperature [T_{D1} °K]	728	
Driver Gas Inlet Temperature [T_{D1} °K]	2209	
Wall Temperature [T_w °K]	1240	
Work Transfer Efficiency (%)	70	

4.3 PERFORMANCE SENSITIVITY

The driver gas pressure, heat transfer coefficient, and clearance were varied in order to determine the wave rotor performance sensitivity to these parameters in its operation and design. These variables are related to external duct pressure variations, to heat transfer losses, and to leakage. Each of these effects has been judged to be critical by earlier researchers as well as in our own preliminary estimates of wave rotor performance. The results of these FLOW code calculations are shown in Figure 4-2, where the vertical axis measures the percentage change in work transfer efficiency and the horizontal axis indicates the fractional variation below or above the reference value for each of these three variables.

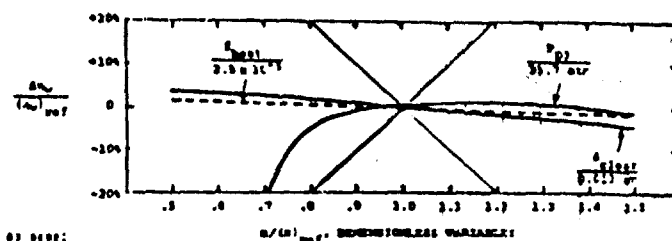


Figure 4-2. Sensitivity of Wave Rotor Work Transfer Efficiency η_w to:

Driver Gas Inlet Pressure, P_{D1}

Heat Transfer Coefficient, f_{heat}

Leakage (Clearance), δ_{clear}

Shaded regions indicate unacceptably high sensitivity. (Reference case from Table 4-2)

The strongest effects occur when the pressure at the inlet port for the combustion gas is artificially depressed below the design value. Under these conditions, the driven gas is not removed completely from the rotor by the time a tube passes by the exit port for this gas. Because of this poor scavenging, the driver gas cannot expand fully in the time allotted for it on the rotor, and less work is transferred to the driven gas than is desired. At the other extreme when the inlet driver gas pressure is higher than design, overscavenging occurs, which results in excess driver gas escaping from the driven gas exit port. This has the immediate effect of raising the work transfer efficiency somewhat at the expense of also raising the temperature of the gas mixture now exiting from the driven gas port. The temperature of the gas leaving the driver gas ports is necessarily lower. Generally speaking, the most uniform performance of the wave rotor is achieved at the reference manifold pressure or slightly higher (i.e., overscavenged conditions), a design strategy that is relatively easy to follow.

In actual engine operation, independent driver gas pressure variations would not occur because the driver gas inlet flow is linked through the combustor to the driven gas outlet port pressure and flow conditions. Therefore, actual off-design engine operation will impose a mixture of off-design wave rotor parameter values that vary in a very structured way compared to the single parameter design sensitivities being discussed here. In fact, off-design engine conditions result in off-design wave rotor performance which is much closer to its on-design performance, as will be shown in Section 4.5.

Variations in the work transfer efficiency also occur when the heat transfer coefficient and the seal clearance controlling gas leakage are changed.

Figure 4-2 shows a mild effect due to enhanced heat transfer. The reference value used for the heat transfer coefficient corresponds to the Reynolds number for the mean flow velocities in the tube. Clearly, for slower velocities the Reynolds number will also be smaller, implying a larger friction factor; however, the total heat transfer term also depends on the velocity to the first power, so that the variations in friction factor are countered by this velocity factor. Perhaps the most plausible way that the heat transfer might be much larger than in the reference case would be if a residual turbulence exists in the tube during parts of the cycle where the mean flow velocity is zero. At heat transfer levels smaller than the reference value, the heat transfer losses are negligible compared to other losses related to leakage, pressure recovery, etc.

Leakage, long recognized as a key problem for efficient wave rotor operation, has a slightly nonlinear effect on the work transfer efficiency in the vicinity of the reference case. At the lowest leakage levels shown in Figure 4-2, the work transfer efficiency increases by 4% and, at the highest leakage levels shown, the efficiency declines approximately 7%. Clearly, the leakage must be controlled, and the next series of rotor designs and tests must address this problem directly with a constructive solution.

4.4 OPTIMIZATION TECHNIQUES

Particular variations in the wave rotor design parameters can improve the reference case performance. For example, mismatches between wave and contact surface arrival times and port locations in the reference case can be used to suggest the direction of design adjustments. The wave arrival times can be adjusted to some degree by varying the rotor tip speed, since the wave speeds and rotor speeds depend on each other once the length of the rotor has been chosen.

This approach affects all of the waves in the same way and is a useful solution if the entire wave system is not yet periodic.

Another way of adjusting the design is to move one port relative to the others to better intercept the flow of a particular gas stream. Such adjustments also affect all of the other waves in the system, but not in the same way; hence, the results of such changes are much more difficult to predict without first analyzing the results of a few such changes. Port widths can be changed for similar effects. It is possible to adjust the air inlet and driver gas outlet pressures (without necessarily interfering with engine applications) to help speed or retard certain waves and thereby redirect the flows throughout the rotor cycle. These techniques represent gross adjustments.

A finer scale of modifications relate to the behavior of the tuning ports; the tube height, width, length, and number of tubes; and rotor radius. Tuning ports play an important role in cancelling unwanted waves and in allowing a broad performance range; in this sense, they are important for maintaining performance during off-design engine operation, which is discussed in more detail below. The number of tubes and tube size can be adjusted to control the amount of heat transfer by changing the wall surface area exposed to a given mass flow. The heat transfer also affects the wave pattern and efficiency of the device, as treated in Section 3. Lastly, the angular speed can be varied for a given tip speed by changing the rotor radius; for a given number of tubes, this also varies the tube wall area exposed for heat transfer as well as the hydraulic diameter of the tubes.

Without making an exhaustive appraisal of these design modifications, a few cases are illustrated in Figures 4-3 through 4-6 to show some of the possible

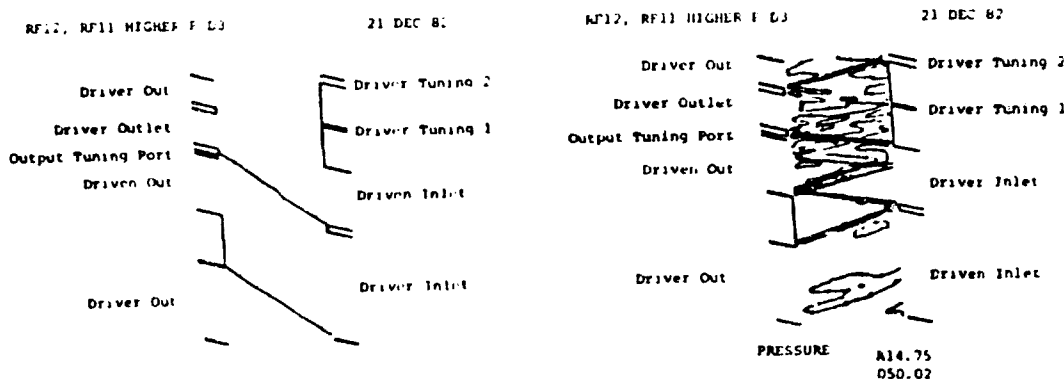


Figure 4-3. Nine Port Pressure Exchanger Wave Rotor with Overscavenged Driven Gas Flow: Contact surfaces (left) and pressure contours (right).

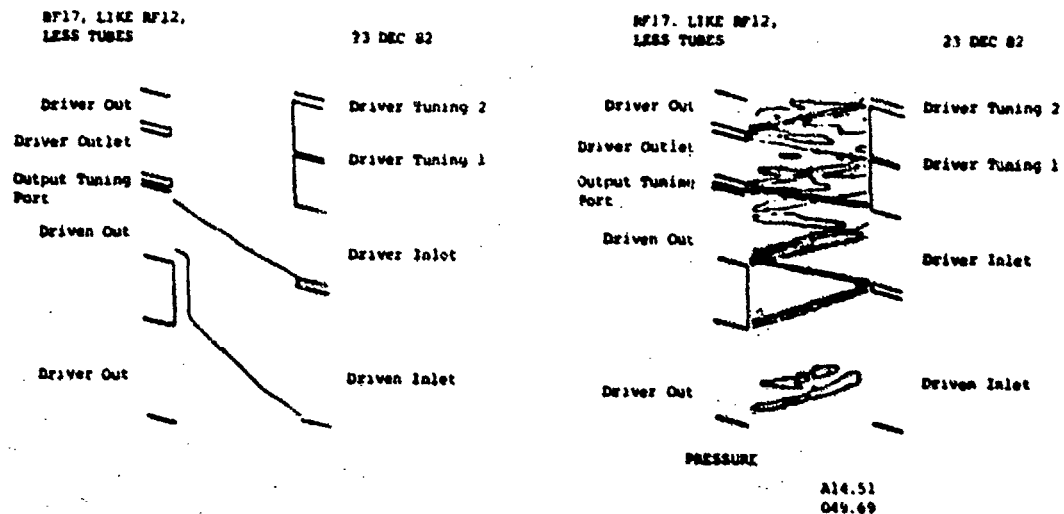


Figure 4-4. Nine Port Pressure Exchanger Wave Rotor with Decreased Number of Tubes: Contact Surfaces (left) and pressure contours (right).

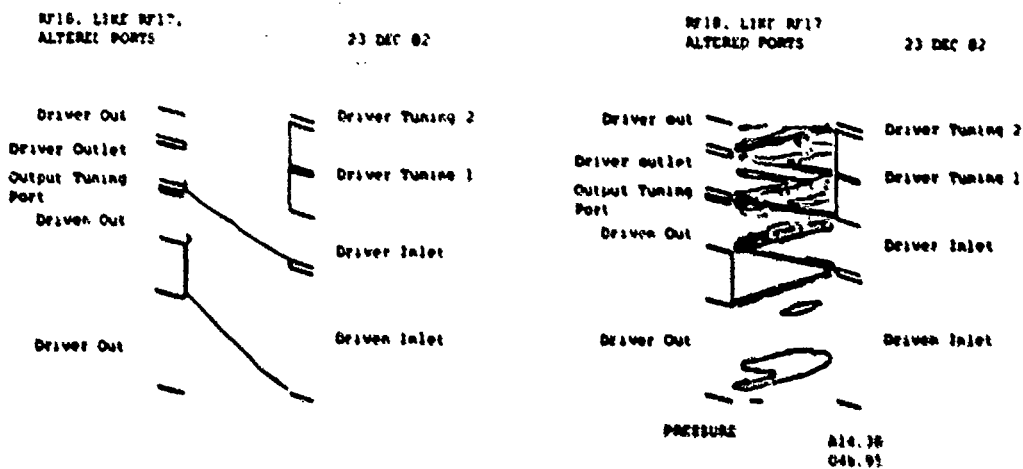


Figure 4-5. Nine Port Pressure Exchanger Wave Rotor with Altered Ports: Contact Surfaces (left) and pressure contours (right).

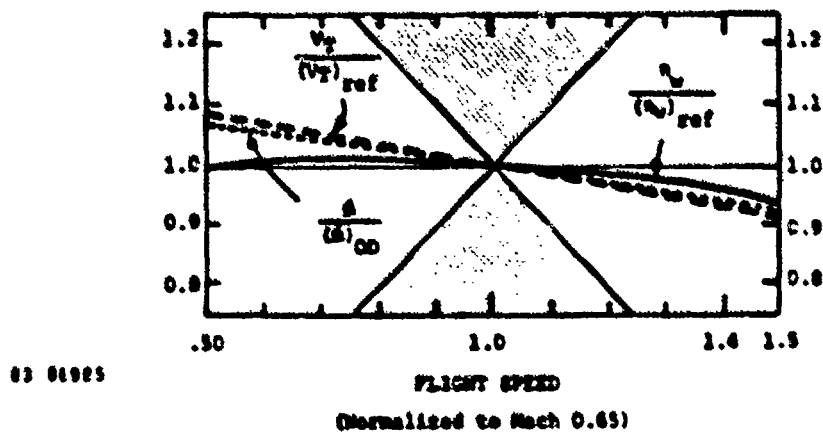


Figure 4-6. Off-Design Performance η of a wave rotor corresponding to off-design wave rotor turbofan engine operation at various flight speeds. The wave rotor tip speed V_t is varied as shown, relative to the reference value, to compensate for higher or lower mass flows. The actual wave rotor mass flow compared to the mass flow required by the off-design engine operation is indicated by $A/(A)_{OD}$.

benefits of these techniques. In some cases, such as Figure 4-3, the effect of the change is to increase the amount of overcavange relative to the reference case and in that way improve its work transfer efficiency. In Figure 4-4, the effect of decreasing the number of tubes and decreasing the heat transfer area is countered by a decrease in the collection efficiency, so that the net effect is only a small increment in performance as measured by the work transfer efficiency.

The conclusion of this set of FLOW calculations is that some very direct techniques for rotor design optimization are available via the FLOW code. These can be systematized in order to obtain the greatest design payoffs first followed by the second order improvements, once the first echelon have been put into effect. Also, because several different approaches can have similar effects benefiting the rotor performance, there is considerable choice as to how this is done. Therefore, other more pressing design considerations can be factored into the optimization to give some priority to the design modifications.

4.5 OFF-DESIGN PERFORMANCE

Off-design rotor performance has been computed from the FLOW code by assuming that the flight Mach number has been changed by changing the fuel flow conditions to the engine in such a way as to keep the combustant temperature constant. Changes in flight speed are interpreted as percentages above or below the reference case Mach II. These changes are accompanied by increases or decreases in the wave rotor port mass flows, pressures, and temperatures with resulting modifications in fuel consumption and output thrust of the engine. We have considered off-design performance ranging from 50 to 150 percent of the reference flight Mach number. The flow conditions required of the rotor and the combustor have been derived from the cycle code calculations discussed in Section 2. The rotor flow conditions have been recalculated with the FLOW code using the off-design port temperatures and pressures required by the cycle code. The off-design FLOW calculations were made first with the same design as the reference wave rotor (i.e., same port locations and sizes) and same tip speed. The resulting mass flows were close to the off-design requirements but, with a linear change in rotor tip speed proportional to the flight Mach number, a much better match was obtained as illustrated by the example shown in Figure 4-6. The results show high performance maintained (i.e., $\eta/(\eta_{ref}) = 1$) for the wave rotor over quite a wide range of flight conditions and never varying by more than 6% from the reference case.

Changes in rotor tip speed and fraction of compressed air routed through the combustor are up to the designer's discretion and, therefore, comprise the chief avenues for maintaining high performance at off-design conditions. One might also consider

variable port sizes by having movable port closure devices or by altering the flow through tuning ports at the leading and trailing edges of the main ports. The former technique has numerous sealing and mechanical problems associated with it, but the latter approach seems more practical for the lower temperature flows where simple valves are manageable. For this discussion, we have restricted the rotor adjustments to just the first method (rotor tip speed).

Similar off-design calculations were made in which the combustor temperature is varied and the Mach number is held constant. As the combustion temperature is decreased from design conditions, the acoustic speed and, hence, the typical wave speeds on the rotor are also reduced after the inlet compression wave has traversed the tube. Thus, the rotor tip speed should be reduced accordingly to allow for the longer wave transit time in the tube. However, the driver gas pressure has also been reduced at the same time, so that less gas actually passes through the driver gas port and less work of expansion is available in this gas for compressing the inlet air. This decrease in available work must match the corresponding change in inlet air flow and decreased pressure rise requirements of that flow. As a result of these coupled effects, the change in rotor tip speed is not completely effective in matching the resulting wave pattern to the manifold configuration for the on-design rotor; the amount of inlet air mass on through the combustor is varied in order to help compensate for these effects and to increase the rotor performance. Again, the performance of the wave rotor remains high over a 150% variation in combustor temperature when the simple wave rotor control strategy just described is applied.

The off-design FLOW code results illustrate an important feature of wave rotors; namely, that they can be operated off-design with good performance and that this can be achieved via an active control system which is programmable in advance via a mechanical or electronic system which senses flight speed and combustor temperature and adjusts the rotor accordingly.

Alternative passive control approaches also exist which include the plateau nozzle approach used by Pearson in his rotor,⁽⁷⁾ the end-wall "pockets" utilized by Brown-Boveri in their Compress,⁽²³⁾ and, as mentioned above, variable tuning port flows. Each of these approaches merits a more careful evaluation before deciding on the best design approach. The purpose of the particular calculations which have been discussed above was to establish that at least one attractive approach exists for operating the rotor off-design and that its performance is calculable over the whole range of desirable operating conditions.

4.6 FOUR PORT ROTORS

A moment of consideration shows that a four port pressure exchanger, with no "pockets" or other wave cancelling devices, automatically involves nonuniform inlet and outlet flows with mixing (i.e., pressure recovery) losses in the manifolds; that is, waves traverse the tubes and reach the ends of the tubes while the tube is still in the middle of a port. The main reason for this is that the gas flows in a four-port design cannot be matched with simple wave regions to make the cycle periodic. The existence of non-simple wave regions in the flow guarantees that waves will impinge on the port openings.

The consequence of nonuniform manifold flows is a mixing loss in the kinetic energy available at the outlet ports and, hence, a loss of stagnation pressure. This is manifested as a drop in the work transfer efficiency of this class of rotors relative to the efficiency of the nine port devices. A sample wave pattern taken from a FLOW code calculation for a configuration similar to those tested by Rolls-Royce is shown in Figure 4-7. A sketch of the rotor plus

manifolds is shown in Figure 4-8. In this case, three cycles of waves were designed for one revolution of the rotor and, hence, the wave system is triply periodic; each part of this triplet is identical for the subgroup of four ports shown. This particular set of flow conditions resulted in a rather strongly under-scavenged situation, as shown by the location of the contact surfaces in Figure 4-7, and a work transfer efficiency of approximately 40 percent, representing one of the lower values of efficiency for this particular design. Other FLOW calculations corresponding to very small changes in outlet driver gas pressure resulted in large motions of the contact surface, changing the scavenging but not improving the wave rotor efficiency very much (only a few percent). Experimental data for this case is rather scant, but it appears that a related version of this rotor achieved a measured product of compression and expansion efficiencies of 61 percent for the flow temperatures and velocities used in Figure 4-7.

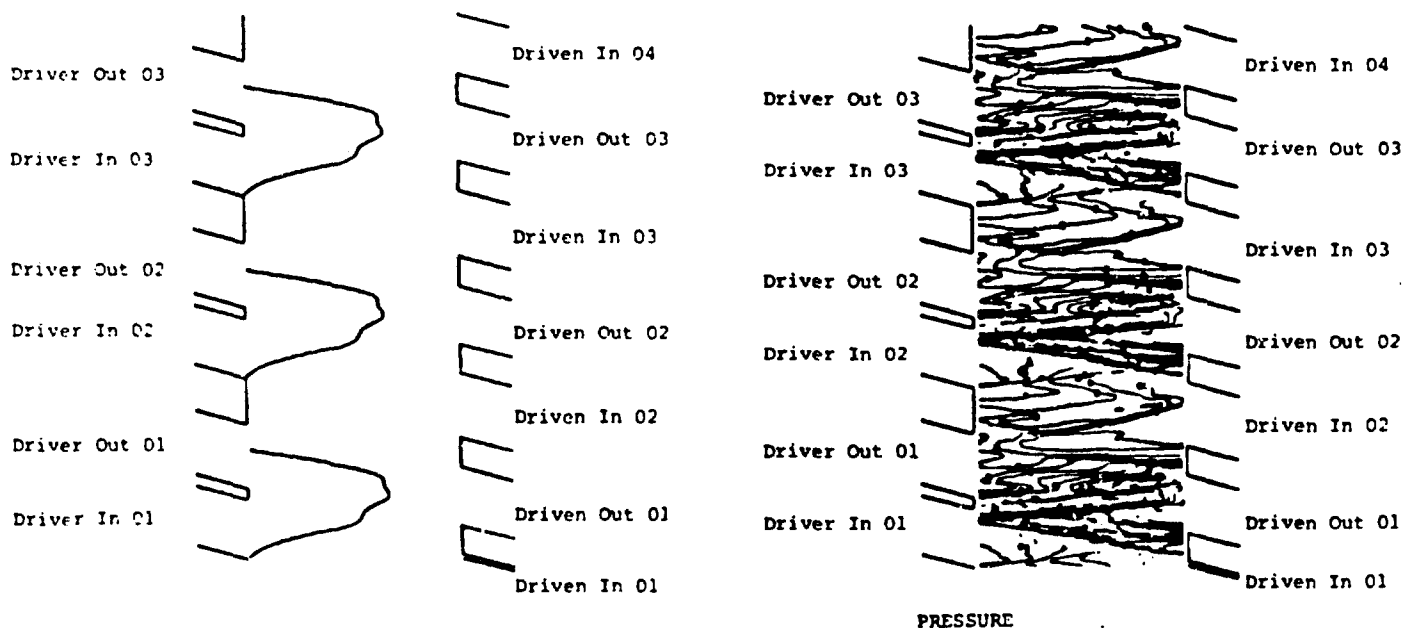


Figure 4-7. FLOW Code Contact Surfaces (left), Ports, and Pressure Contours for a Three Cycle, Four Port/Cycle Pressure Exchanger Wave Rotor.

In the simple configuration for the four port cycle shown in Figure 4-8, it would appear that the off-design performance would not be very good since the predicted on-design efficiency is so low. The use of the remedies discussed for the off-design performance of the nine port machine could also be applied here. No detailed calculations have been made to confirm their effectiveness for this wave rotor configuration, and one would need to do that before drawing more definite conclusions for this case. The four port cycles discussed here would not be appropriate for use as a topping cycle for the peak temperatures and pressure ratios (i.e., 2.5) being considered in this study since the backwork ratio approaches 1 for a wave rotor component efficiency on the order of 60% or lower. These initial code predictions are sufficiently low that other wave rotor configurations offer a better long-term potential than the four port machine.

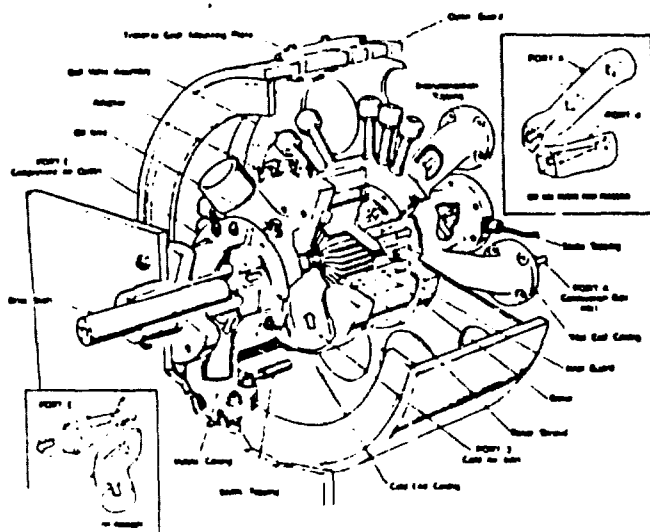


Figure 4-8. Sketch of a Three Cycle, Four Port/Cycle Pressure Exchanger Wave Rotor.

Section 5 WAVE ROTOR/TURBINE PERFORMANCE

5.1 SCOPE

Wave rotor/turbines (those wave rotors which are intended to produce shaft work in addition to pressure exchange) have been investigated previously by such companies as General Electric, Ruston-Bornaby, and the General Power Corporation.^(7,14) This type of wave rotor is generally characterized by helical tubes and may derive shaft work from both reactive and impulsive loading of the rotor tube walls, in very much the same way as an ordinary turbine blade. Most of these devices have produced a disappointingly small amount of

power output, with the notable exception of the Pearson rotor built and tested for many hundreds of hours by the Ruston-Bornaby Turbine Company.⁽⁷⁾ Both the Pearson rotor and the GPC rotor are examined here in order to contrast the two approaches to wave rotor/turbines and to extract those design elements which contribute to the success of the Pearson rotor.

5.2 PRINCIPLES OF OPERATION

The wave rotor/turbine acts as a combined compressor and turbine which produces net shaft power output. Compression is accomplished by wave action as the high temperature, high pressure combustion gases expand down to the lowest pressure on the device. The combustion gases also supply the energy to produce shaft work. In some designs, the shaft work is produced by reactive forces as the combustion gases leave the rotor. In other cases, the compressed air leaving the rotor may provide a similar reactive force or the combustion gases may be vectored impulsively back onto the rotor. In more complex systems, some of the gases exit and are re-injected back onto the rotor at a different place in the cycle without any external reprocessing; the angle of injection provides impulsive thrust to the rotor.

Shaft work extraction from a wave rotor/turbine is most effective if it is taken from low pressure scavenge gas streams or high pressure gases flowing to or from the combustor. Since the low pressure scavenge is being driven by the compressor, it makes little sense to extract shaft power from the gas taken off of the rotor during this transition; that would only increase the work which must be provided to the compressor. As we discussed above, work cannot realistically be extracted from that fraction of the compressed air leaving the rotor on the way to the combustor or from the combustion gases as they enter the rotor; the former stream needs all of the pressure it can retain to flow through the combustor, and the latter stream must retain its available work to compress the inlet air. Therefore, the most effective way to produce shaft work relies on the fact that more compressed air is produced than is actually needed as combustion gases to drive the compression processes. The extra compressed air can be re-injected onto the rotor to produce impulsive forces if the point of re-injection occurs at a part of the wave cycle where the tube pressures are lower than the compressed air pressure. This third process involves a re-entrant flow and is one of the principal reasons for the success of the Pearson wave rotor/turbine design.

It also is clear that wave rotors with substantial changes in the tube stagger angle from one side of the rotor to the other will produce large reactive forces. This implies that all of the exhaust flows from such a rotor suffer substantial stagnation pressure losses just as that fraction of shaft work is being extracted from the flow. From the foregoing discussion, this approach appears to be doomed to

failure since it causes an increase in the compressor work required to complete the low pressure scavenge and depletes the stagnation pressure rise needed to force the compressed air through the combustor and back onto the rotor. Therefore, the most efficient production of shaft work on wave rotor/turbines appears to be from impulsive loading, as described above.

5.3 THE PEARSON ROTOR

Several features of the Pearson wave rotor/turbine are unique to the process of shaft work production. Additional techniques also have been developed to make this rotor perform well over a broad range of operating conditions. When gas is exhausted from a cambered tube and reactive shaft work is produced, the gas cannot be re-introduced onto the rotor until the gas remaining in the tube has undergone sufficient additional expansion to reduce the tube pressure to the pressure in the re-entrant loop. Thus, an extra exhaust expansion is needed; that is, the exhaust port is divided in two with the higher pressure portion re-injected after the lower pressure exhaust has brought the tube pressure down to the appropriate level. This explains the presence of ports P_{L0} and L_{01} on the right side of Figure 5-1, where the flow from P_{L0} re-enters the rotor through port P_{L1} .

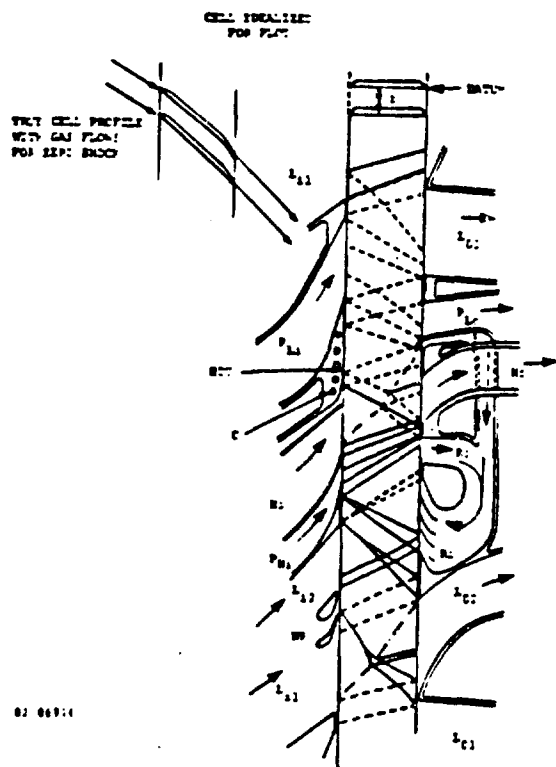


Figure 5-1. Ideal Wave Diagram for a Wave Rotor/Turbine Constructed from State, Pole, and Position Diagrams (Ref. 7).

Features which improve the rotor's off-design performance include the use of tuning ports much like those used in the pressure exchanger (e.g., P_{H1} in Figure 5-1), which are placed at the leading edge of an inlet port to help suppress the production of tube opening losses which occur from tube exposure to a sudden increase of pressure. Pearson also has introduced injection nozzles across the opening of entrance manifolds (e.g., NR in Figure 5-1) in order to exactly cancel the compression wave which reflects back through the tube to the entrance manifold. Normally this wave can be designed to reach the end of the tube just as the tube reaches the trailing edge of the manifold and is closed off. But, during off-design operation, the reflected wave may reach the manifold before this time and cause a serious disruption of the incoming flow. This nozzle design employs a "half-wave" plateau technique of pressurization where the tube pressure is raised in two equal segments as a result of the flow acceleration through the nozzles. The final pressure rise just equals the stagnation pressure in the nozzle flow so that no wave is reflected at the tube-manifold interface.

Pockets along the end wall of the rotor also help to suppress wave reflection for a variety of operating conditions for a single rotor design. The gas leaving the end of a tube as it moves into confluence with one of these pockets is accelerated by the shape of the pocket and re-enters the tube at a higher velocity and at a different angle as the tube reaches the trailing edge of the pocket. If a rarefaction wave also is incident on the same end of the tube as it moves from the beginning to the end of the pocket, this wave will not be reflected with full strength because of the re-entering flow from the pocket. Thus, the pockets can manage waves over the full range of operating conditions for which the wave is incident on the pocket.

5.4 THE GPC ROTOR

The General Power Corporation (GPC) wave rotor turbine differs in several significant respects from the Pearson rotor.⁽¹⁴⁾ The GPC rotor employs a sharp bend in the tube which constricts the flow area considerably and acts like a nozzle to accelerate the flow at a sharp angle as it leaves the rotor. In their approach, all of the shaft power appears to be extracted from reaction forces. In contrast, the Pearson rotor uses only a mild bend in the tubes to extract a small amount of reactive power; most of the shaft power is extracted through impulsive loading of the rotor blades. Also, the GPC rotor does not appear to use any technique to cancel or control reflected waves required to make the wave system periodic in one revolution of the rotor. As such, it also has no controls to maintain performance for off-design operating conditions.

The wave diagram shown in Figure 5-2 incorporates the main wave phenomena found on the GPC rotor. The rotor tubes have a stagger angle of approximately 45° relative to the rotor axis. The sharp bend in the rotor angle occurs on the right hand side in Figure 5-2; the bent portion of the tube is so short that it is not shown in this figure. Instead, the bend manifests itself in the wave diagram by reflecting incident waves and by altering the angle and velocity of gas leaving the rotor on the right. Waves separating regions 1, 2, 3, 4, 5, and 6 and denoted by double lines are compression waves. These waves compress the incoming air and prepare it for entering the combustion chamber at station 4. The combustion gas entering at 5 completes the compression but only releases part of the available work in the high pressure gas; the remainder is extracted, in theory, from the series of expansions occurring from state 7 through state 15. The GPC rotor re-injects flow leaving from regions 8 and 10 onto the rotor at station 11 to complete the expansion process.

In trying to reconstruct a plausible wave diagram for the GPC machine, several problems were encountered. Gas leaving the rotor at stations B and D to drive the re-entrant duct flow exits the rotor at two different gas pressures. In the actual GPC device, these flows are not separated so that considerable mixing losses are expected to occur as their pressures equilibrate. Reaction work also is extracted so that further pressure drop occurs, making it difficult to re-inject this flow unless the secondary expansion from 8 to 10 on the rotor is rather large. The combination of these processes is inefficient. A second problem area concerns the presence of reflected waves in the cycle which may prevent it from being truly periodic. The magnitude of the influence of the internally reflected waves needs to be determined numerically, with the FLOW code for example. The absence of wave control mechanisms in the GPC design also may contribute to poor off-design behavior for this particular rotor.

5.5 PERFORMANCE

Analytical estimates as well as actual experimental data on wave rotor/turbine performance are available. The analytic estimates can be carried out on the basis of Pearson's or GPC's wave diagrams, and the empirical data comes from the tests carried out by Ruston-Bornaby on the Pearson rotor in the 1950s.

It is possible to consider the shaft work efficiency of the wave rotor/turbine as if it were a conventional turbine and a conventional compressor working in tandem. Thus, we may substitute adiabatic turbine and compressor efficiencies for the values of η_{TE} and η_{CE} in the expression for η_s taken from Equation [3-22]. That is,

$$\eta_s = .892 - \frac{T_{4.5}}{T_4} \cdot \frac{1}{.85} \left[\frac{T_4}{T_1} \right] = .892 - 1.06 \left[\frac{T_4}{T_1} \right]$$

where the ratio T_4/T_1 is a variable parameter and the pressure ratio is 3.0. Thus, for values of $T_1 = 3000^\circ\text{F}$ (1922 K) and air inlet temperatures $T_4 = 1100^\circ\text{F}$ (870 K), the shaft work efficiency may be as high as $\eta_s = 41\%$. The virtue of using data calculated from the wave diagram is that better estimates of η_{TE} and η_{CE} are obtained. For values corresponding to Pearson's experiments, an overall cycle pressure ratio of 12.2 is appropriate to the peak temperature case of 1250 K and the value projected for η_s is 63%.

The thermal cycle efficiency of Pearson's rotor is given in Figure 5-3 as a function of shaft horsepower output. Using the conventional definition of Brayton thermal cycle efficiency with the usual adiabatic definition of turbine efficiency η_T , we can write

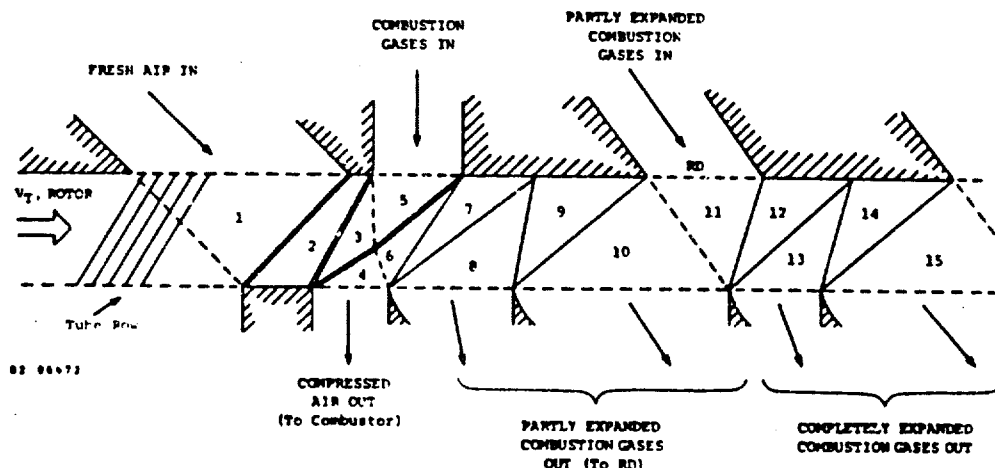


Figure 5-2. Wave Diagram for a Wave Rotor/Turbine Resembling the GPC Machine (RD = Re-entry Duct).

$$\eta_{TH} = \eta_T \left[1 - \frac{1}{p_r^\alpha} \right]$$

$$\text{where } p_r^\alpha = \sqrt{\frac{T_3}{T_1}}$$

for a maximum work cycle and where the compression work is accomplished by internal work transfer. Substituting the temperature ratio $1250 \text{ K}/300 \text{ K} = 4.167$ for the ratio T_3/T_1 in the above expression for the points corresponding to 35 shp and noting that the thermal cycle efficiency was 9.4% for that case, we can solve for $\eta_T = 19\%$. Carrying out the same steps at the peak temperature of 1070 K and 33 shp where the thermal cycle efficiency is 9.0% gives a second solution for $\eta_T = 19\%$.

From this comparison, we can see that the empirical value for η_T is substantially less than the theoretically predicted value of 63%. Pearson has discussed several sources of loss in the Ruston-Hornsby experiments, which suggest that leakage and heat transfer are two of the main contributors to this poor component efficiency.

The data in Figure 5-3 also illustrates that the wave rotor/turbine operates successfully for conditions which are considerably off-design, considering that the span of shaft horsepower was from 3 to 35 and the rotor speed varied from 9,000 to 18,000 rpm over this range. This represents a surprising capability when one understands that the wave rotor depends on the relative timing of waves relative to port opening and closing events. Further, the data supports the contention that the shaft work efficiency of the device is maintained to a large degree over this range so that the component performance is not seriously degraded. That leads to the conclusion that the rotor performance is not particularly sensitive to operating conditions once the proper design has been arrived at.

Relatively little is known at this point as to the sensitivity of the wave rotor/turbine performance to design features. However, from historical evidence it appears that it is very easy to design a poorly performing wave rotor turbine since the majority of them have not produced net shaft power output. Once the proper design principles are recognized as, for example, in the Pearson rotor, then it is no longer a hit-or-miss process to design a good wave rotor/turbine.

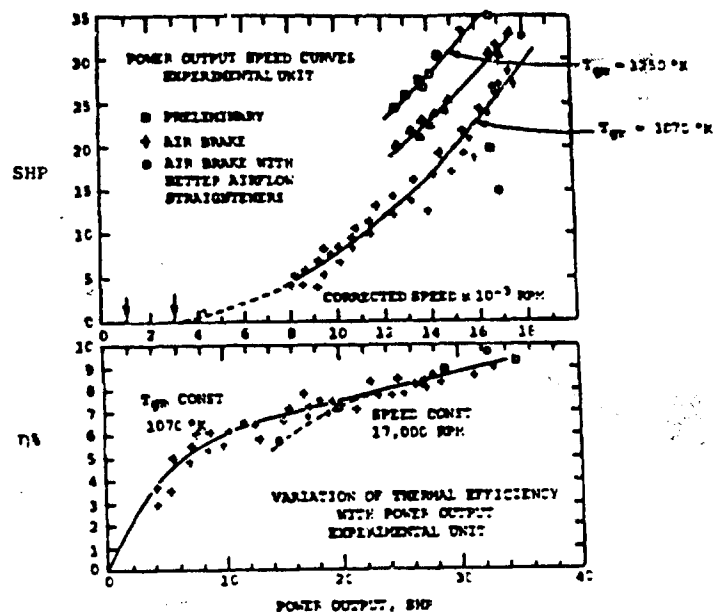


Figure 5-3. Experimental Data from the Ruston-Hornsby Tests on the Pearson Wave Rotor/Turbine. (SHP = shaft horse power, η = thermal cycle efficiency) [Ref. 7].

Section 6 WAVE ROTOR DESIGN

6.1. INTRODUCTION

Existing wave flow patterns have been used to establish preliminary wave rotor designs appropriate to a small turbofan engine. A conceptual design has been developed for a wave rotor corresponding to a turbofan engine providing 600 lb(f) thrust at Mach 0.65 and sea level flight conditions. This conceptual design emphasizes basic dimensions of the rotor (radius and length), number and shape of compression tubes, rotor tip speed, injection nozzle and exhaust manifold port placement, and flow angles relative to the rotor face. Such information is sufficient for carrying out FLOW code calculations of wave rotor performance, but a more detailed design evaluation would be required before any device of this sort is tested.

Analysis of the wave rotor design shows that the wave rotor component is small (on the order of 3 to 6 inches in diameter and length) and lightweight. Compared to the high pressure stages of conventional axial flow compressors, the size of the wave rotor tubes is relatively large. The losses in the wave rotor compression process are related to unsteady gasdynamic wave processes and nonuniform flow in the manifolds, as compared to axial flow compressor losses which are primarily aerodynamic (i.e., related to boundary layer separation and leakage at the blade tips). Specifically, the losses for wave rotors do not increase as rapidly as the losses for more conventional turbo-compressor systems as the rotor size decreases.

Unlike a turbine or compressor where tip speed must be matched aerodynamically to the gas flow in order to achieve good efficiencies, the wave rotor efficiency depends instead on the relation between the rotor period of revolution and an acoustic wave transit time within the rotor. The transit time depends on the length of the rotor. The longer the rotor, the lower the tip speed can be. Thus, the tip speed for a wave rotor can be relatively slow and still achieve good efficiency. The consequence of this feature is that the usual creep strength limits which apply to high temperature turbines are much less severe for wave rotors, allowing them to operate at higher metal temperatures. A more important concern for wave rotors is thermal cycling fatigue due to the heating and cooling of the tube walls with each cycle.

Specific effects, such as heat transfer and leakage, are design dependent and will help to determine such things as the number of tubes and tube size and shape for a given set of flow conditions. These effects are modeled analytically in this section to provide a way of estimating the amount of leakage and the equilibrium wall temperature of the rotor. Much of the design optimization can be carried out with these analytic models before invoking the FLOW code for more detailed results.

Re-entrant ducts are also discussed from a design point of view as a means for establishing the appropriate boundary conditions for the FLOW code.

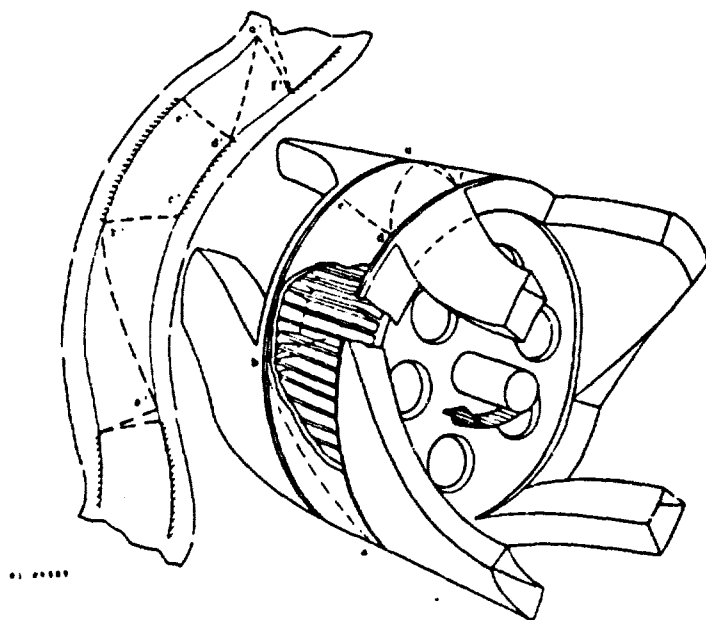


Figure 6-1. Superposition of Wave Diagram on Two Cycle Pressure Exchanger Wave Rotor Configuration.

6.2 WAVE DIAGRAMS

The fundamental flow pattern established within the wave rotor is called a wave diagram because the essential compression, expansion, and scavenging processes are caused by the propagation of unsteady gasdynamic waves along the length of each tube as the rotor spins past each of the inlet and exit ports of the device. The construction of an idealized wave diagram is the first step in the design of a wave rotor since the strength of each of the waves is related directly to the strength of the compression or expansion desired of the device and because the speed of these waves helps to determine the location and azimuthal extent of each of the ports supplying the gas to the rotor. Figure 6-1 shows a wave rotor with two complete compression and expansion cycles per revolution. It is possible to represent the wave processes occurring in the device, as shown schematically at the left in this figure. The dashed lines represent the location of wave fronts and the interface between the combustion gases and the intake air.

A basic precept for wave diagrams is the concept of periodic flow. After one revolution, the flow in a given tube must return to its original state at each point in the tube. This does not mean that the flow in the tube is uniform at this point, but it does imply that the flow is steady as observed from the stationary frame of the outside observer; in particular, the manifold or port flows are steady for a periodic wave system. A steady port flow device allows it to be mated to other steady flow devices, such as axial flow turbines or compressors, as an integrated component of an engine.

Complete periodicity is difficult to guarantee for wave diagrams in general since there may be a large number of internal reflected waves which are difficult to account for with an analytic scheme. The FLOW code does this automatically. Thus, an analytic approximation may be used to start the FLOW code calculation, and the code itself will compute a revised wave pattern with all of the wave reflections included.

There are certain classes of wave diagrams that guarantee periodic behavior within the context of the analytic approximations to be discussed shortly. These wave diagrams make use of completely uniform manifold flows, no strong waves crossing any of the contact surfaces as they traverse the tubes, and wave management ports to cancel wave reflections at the ends of the tubes. Tube opening and closing at the edges of each manifold also produce weak waves which can be partially controlled by tuning ports.

It is useful to examine one of these manifestly periodic wave diagrams as an example because it represents probably one of the most efficient forms of

the wave rotor pressure exchanger, and it allows us to give a particularly simple description of the work transfer efficiency of such a device. Figure 6-2 shows this type of wave diagram for a pressure ratio 2.5 pressure exchanger wave rotor. Note that the driven gas (air) is compressed by two shock waves of equal strength and then exits from port D3 on the left. The hot high pressure driver gas (e.g., from the combustor) enters at port D3 on the right, compressing the driven gas already in the tube by sending the second shock wave across the tube. The gas interface or contact surface between these two gases is immediately overtaken by the compression wave and travels at a slower speed across the tube. A wave management port is located at the trailing edge of the driven gas exit port D3 in order to slow the exiting gases to a zero velocity and to cancel the rarefaction wave (i.e., zero reflection) which accounts for this deceleration. The driver gas is subsequently scavenged from the tube in two separate ports, D5 and D1. A careful consideration of the Riemann invariants shows that two ports are necessary if the final gas velocity in port D1 and pressure there are to match the incoming driver gas conditions at port D1.

There are four wave management ports for this particular wave diagram. Each of these involves non-uniform flows, but generally the mass flow through these ports is so small that the port losses do not significantly affect the wave rotor efficiency. Their impact on suppression of reflected waves is considerable and represents their main contribution to device efficiency. The main inlet and outlet manifold flows are uniform since no waves from inside the device are incident on these ports. These equations do allow the two gases represented here to have different specific heats and molecular weights. A modification of these equations also allows an analytic estimate of the heat transfer (see Section 6.4). The solution procedure to the wave diagram equations is straightforward algebraic substitution; no iteration or convergence is required. Thus, the results are exact in this approximation.

A related but more complicated procedure has been used in the past for constructing wave diagrams in which internal wave reflections occur. This is an iterative technique in which one cycle is completed and then the initial parameters are adjusted to approximate the end of the first cycle; the next cycle is similarly constructed, and so on until the beginning and end of successive cycles agree well enough. This technique approximates the process followed with the FLOW code except that the FLOW code is capable of following all of the waves whereas the analytic procedures simplify the process by following only a finite number of waves which represent the main gasdynamic process in progress. The most useful format for this technique has been described by Pearson.⁽⁷⁾ He uses three Riemann invariants which relate the physical states of the gases on either side of a wave to the wave's position in the tube and to the characteristic velocities of the flow and small disturbances in the flow: the so-called

state, position, and pole diagrams. The calculation includes the same Riemann invariants used in the pressure exchange calculation for the wave diagram shown in Figure 6-2. However, the technique can be refined considerably to include finite opening and closing of each tube, losses associated with angle of attack of flow entering the tubes, and the details of wave-wave and wave-contact surface interaction within the tubes as well as wave reflection at the tube ends. Figure 5-1 shows an example of a complex wave diagram constructed by Pearson using this technique for a wave rotor/turbine which produces shaft power output. In this example the manifold flows are not uniform. However, the wave diagram is periodic, and the gases are completely scavenged in one cycle.

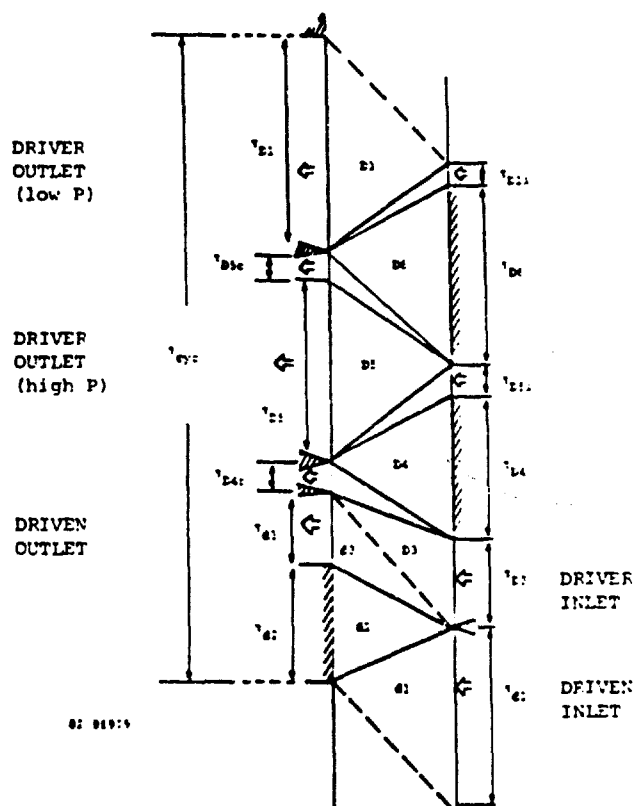


Figure 6-2. Ideal Wave Diagram for a Nine Port Pressure Exchanger Wave Rotor portraying the cycle time t_{cyt} , identification of uniform flow regions, port and endwall times.

In the four-port devices discussed in Section 4.6, incomplete scavenging occurs in one cycle so that gas entrained on the rotor undergoes a considerable amount of compression and expansion from one cycle to the next. This led to an inefficient use of the wave rotor with an equivalent high back work ratio since the entrained gases were not available at the end of each cycle to perform external work.

Further, the losses associated with these entrained gases must be kept to an absolute minimum in order to extract any useful work from the system.

6.3 DESIGN RELATIONS

The design process for a pressure exchange wave rotor begins with an assumption of the kind of wave processes which will be used to expand or compress the working gases. For example, Figure 6-2 illustrates the wave processes chosen for a pressure exchange wave rotor having the maximum work transfer efficiency. The total cycle time τ_c can be obtained from this diagram once the peak sound speed a_{D3} (i.e., combustion inlet gas temperature) and rotor length have been prescribed. That is, each of the dimensionless times shown in Figure 6-2 will be scaled to dimensional values by the acoustic transit time L/a_{D3} . The rotor tip speed v_T is thus related to the rotor radius by

$$2\pi r = v_T \tau_c (L/a_{D3}) \quad (6-1)$$

The next step is to choose the effective collection efficiency of one of the primary manifolds; for example, the driven gas outlet manifold. The collection efficiency η_{col} is a measure of how close the flow into a given manifold is to being continuous; an infinite number N of tubes opening onto a finite manifold results in a perfect collection efficiency. The actual relation is $\eta_{col} = (N-1)/N$. Thus, a prescription of the collection efficiency gives the number of tubes in the driven gas outlet manifold N_{D3} . From this quantity, the width of individual tubes may be computed:

$$d = \frac{\tau_{D3}}{\tau_c} \left[\frac{2\pi r}{N_{D3}} \right] \quad (6-2)$$

Using the mass flow into the driver gas port \dot{m}_{D3} and the accompanying flow velocity and density of that gas, one can solve the relation

$$\dot{m}_{D3} = \rho_{D3} u_{D3} h d N_{D3}, \text{ where } N_{D3} = \frac{\tau_{D3}}{\tau_c} N_{D3} \quad (6-3)$$

for the height h of each tube. Each of the other port mass flows can be derived from \dot{m}_{D3} since the flow velocities and densities and manifold sizes (e.g., in terms of the τ_i) are known from the wave diagram and are related to each other by

$$\dot{m}_i = \rho_i u_i h d \left[\frac{\tau_i}{\tau_{D3}} \right] N_{D3} \quad (6-4)$$

The flow angles of each port can be obtained by matching the tangential velocity of the rotor with the tangential flow speed in the manifold coordinate system, assuming the rotor tubes are parallel to the axis of the rotor. Thus, if u is the flow speed in the manifold coordinates and θ is the angle of the manifold flow relative to a vector normal to the rotor face, then $u \sin \theta = v_T$; therefore, the flow angle is

$$\theta = \sin^{-1} \left[\frac{v_T}{u} \right] \quad (6-5)$$

where the manifold flow speed is known from the wave diagram.

In summary, the unknowns are τ_i , r , N_{D3} , d , N , η , h , and \dot{m}_i , and the basic equations are:

$$\tau_c = \sum [\tau_i(\text{ports}) + \tau_i(\text{end walls})] \quad (6-6)$$

$$r = \frac{v_T \tau_c L}{2\pi a_{D3}} \quad (6-7)$$

$$N_{D3} = \frac{1}{1 - \eta_{col}} \quad (6-8)$$

$$d = \frac{2\pi r \tau_{D3}}{\tau_c N_{D3}} \quad (6-9)$$

$$\eta = \frac{2\pi r}{d} \quad (6-10)$$

$$\eta = \frac{v_T}{2\pi r} \quad (6-11)$$

$$h = \frac{\dot{m}_{D3}}{N_{D3} u_{D3} \rho_{D3} d} \left[\frac{\tau_{D3}}{\tau_{D3}} \right] \quad (6-12)$$

$$\dot{m}_i = \rho_i u_i h d \left[\tau_i / \tau_{D3} \right] N_{D3} \quad (6-13)$$

$$\theta_i = \sin^{-1} \left[\frac{v_T}{u_i} \right] \quad (6-14)$$

where L , ρ_i , u_i , τ_i , v_T , η_{col} , and \dot{m}_{D3} are prescribed. For purposes of FLOW code calculations where a particular tube size (i.e., h and d) is desired, several different values of L will normally be investigated. Larger values of L produce larger radii r for a given tip speed and, hence, larger values of d and smaller values of h ; the product of $h d$ depends only on the mass flow \dot{m}_{D3} , the wave diagram, and the collection efficiency. Similar variations can be obtained by varying v_T instead of L .

6.4 HEAT TRANSFER

The magnitude of heat transfer in the wave rotor has been estimated approximately using a perturbation technique to determine its effect on the rotor efficiency and design. These estimates are corroborated by the fully nonlinear FLOW code results that compare wave rotor cases with and without heat transfer.

The analysis proceeds by assuming that heat transfer in each tube follows the behavior for fully developed pipe flow with an entrance flow correction appropriate for large Reynolds numbers. No heat transfer is assumed to occur where the average flow velocity is nominally zero. Thus, the heat transfer equation is

$$\frac{dT}{dx} = \frac{0.16}{d_h^4 Re} \left[1 + \left(\frac{d_h}{L} \right)^{2/3} \right] (T_w - T) \quad (6-15)$$

where

$$d_h = \frac{2hd}{h+d}$$

is the hydraulic diameter of the tube, $Re = \rho u d_h / \mu$ is the Reynolds number, and T_w is the tube wall temperature. The solution to this equation is

$$\frac{T_w - T}{T_w - T_1} = e^{-\frac{0.16}{d_h^4 Re^{1/4}} \left[1 + \left(\frac{d_h}{L} \right)^{2/3} \right] x} \quad (6-16)$$

where T_1 is the inlet flow temperature and $T = T(x)$ is the flow temperature a distance x from the tube entrance.

Several changes occur across a wave system which requires a change in the value of T_1 . Across a shock wave, for example, the temperature ratio of the gas will be greater than 1 and will depend on the shock strength (i.e., its pressure ratio). Using Figure 6-2 as an example, we can write the heat transfer solutions for the driven gas in regions d1 and d3 as follows:

$$\left(\frac{T_w - T}{T_w - T_1} \right)_{d1} = e^{-\frac{\beta x}{d_h}} \quad (6-17)$$

$$\text{or } T(x) = T_w - (T_w - T_{1a}) e^{-\frac{\beta x}{d_h}}$$

for $0 < x < x_0$ and

$$\left(\frac{T_w - T}{T_w - T_1} \right)_{d3} = e^{-\frac{\beta y}{d_h}} \quad (6-18)$$

$$\text{or } T(y) = T_w - (T_w - T_{1b}) e^{-\frac{\beta y}{d_h}}$$

for $0 < y < y_0$ where $y_0 = L - x_0$. Using T_{d3}/T_{d1} as the ideal temperature ratio across both shock waves, we can define the entrance temperature T_{1b} for any slug of driven gas reaching the first shock wave at position x_0 in the tube as

$$T_{1b} = \left(T_{d3}/T_{d1} \right) T(x) \big|_{x=x_0} \quad (6-19)$$

$$= \frac{T_{d3}}{T_{d1}} \left[T_w - (T_w - T_{1a}) e^{-\frac{\beta x_0}{d_h}} \right]$$

Thus, the temperature of this gas slug at the driven gas exit manifold is

$$T_o(x_0) = T(y) \big|_{y=y_0} \quad (6-20)$$

$$T_w - \left[T_w - \frac{T_{d3}}{T_{d1}} \left[T_w - (T_w - T_{1a}) e^{-\frac{\beta x_0}{d_h}} \right] \right] e^{-\frac{\beta y_0}{d_h}}$$

The average value of the exit driven gas temperature is therefore

$$\langle T \rangle_{d3} = \frac{\int_0^L T_o(x_0) dx_0}{L} \quad (6-21)$$

$$T_w - \left(\frac{T_{d3}}{T_{d1}} \right) (T_w - T_{1a}) e^{-\frac{\beta L}{d_h}} + T_w \left[1 - \left(\frac{T_{d3}}{T_{d1}} \right) \right] \frac{\left[1 - e^{-\frac{\beta L}{d_h}} \right]}{\left(\frac{\beta L}{d_h} \right)}$$

A similar expression exists for the driver gas except that expansion waves are present instead of shocks. These are also modeled as discrete waves for purposes of analyzing the heat transfer. Again, the ideal temperature ratio across the wave is used to relate the exit temperature of a gas slug approaching the wave to the "entrance" temperature of the same slug of gas leaving the wave. The averaging process can again be carried out, noting that the entering driver gas at D3 actually leaves at two main exit ports, D5 and D1 (ignoring the tuning ports in this approximation), which makes the integrals somewhat more complex but still tractable.

At this point, the averaged exit port temperature with heat transfer can be compared to the wave diagram temperature computed without heat transfer to estimate the magnitude of the effect. By also calculating the amount of heat transferred to each stream, one may also determine whether or not the chosen wall temperature T_w also corresponds to an equilibrium wall temperature for that particular set of flow conditions; that is, at equilibrium, the heat transferred to the rotor from the hot gas must equal the heat transferred from the rotor to the cold gas.

While the heat transfer path is generally not known in detail, for the linearized (small perturbation) approximation used here, we can assume that the heat addition or extraction line in the T-s space is straight between the initial and final states, as shown in Figure 6-3. Thus, for example, the heat transferred out of the driver gas after a given expansion, say from state D3 to state D5, is given by

$$\begin{aligned} \delta Q_{35} &= [S_{5s} - S_5] \left[T_5 + \frac{1}{2}(T_3 - T_5) \right] \quad [6-22] \\ &= [S_{5s} - S_5] \left[\frac{T_3 + T_5}{2} \right] \end{aligned}$$

or

$$\delta Q_{35} = m_{D5} C_p \left[\ln \left(\frac{T_{5s}}{T_5} \right) \right] \left[\frac{T_3 + T_5}{2} \right]$$

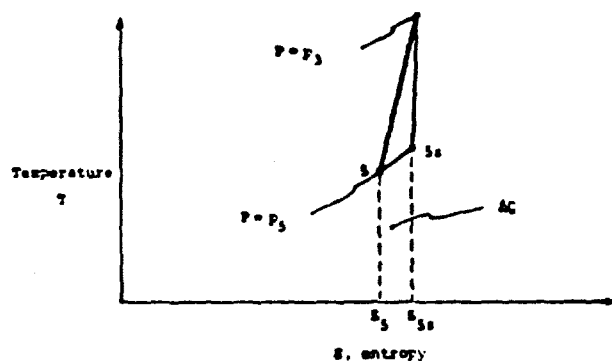


Figure 6-3. Heat Transfer from an Expanding Gas to the Wave Rotor Walls.

These estimates have been made for a variety of rotor configurations and flow conditions. An interesting effect emerges from the results which have been tabulated in Table 6-1. Comparing cases 2, 3, and 4, we see that the relative size of a tube (i.e., d, h, and L) has no noticeable effect on the equilibrium wall temperature of the wave rotor, even though the quantities of heat transferred may vary a lot with tube size. Also, it is clear that the equilibrium wall temperature in several interesting cases (e.g., 1 through 6), which correspond to combustion temperatures of 3500°F, is rather high for the basic wave diagram shown in Figure 6-2. The rotor wall temperature ranges from 1970°F to 2060°F for these cases.

It is possible to run the fully compressed air stream through the wave rotor again for extra cooling of the rotor before passing that gas on to the combustor. Some pressure losses inevitably occur with an extra scavenge of this sort, but the rotor will act as a recuperator, reducing the amount of fuel needed to reach the peak combustion temperature and thereby enhancing the efficiency of the device. A somewhat larger rotor diameter will be needed to encompass the extra cooling part of the cycle but, if it is still within the engine envelope, then this approach has a large payoff in terms of reducing the metal temperatures still further.

The work transfer efficiency is affected by heat transfer, in this approximation, by increasing the available work in the driven exit gas stream. If no other effects were present, this would represent a net increase in the work transfer efficiency. However, in actuality and in the FLOW code results, the ability of the hot gas to do work on the cold gas is reduced by heat transfer, and the work required to compress the cold gas as it heats up is also increased. As long as the overall pressure ratio of this process is fixed, the difference between these competing effects will be accommodated by changes in the mass flows of the driver and driven gases. That is, a smaller flow of driven gas per unit flow of driver gas can be compressed when heat transfer via the rotor wall occurs. This is a greater effect than the increase in the available work of the driven gas, so that the net effect is to decrease the work transfer efficiency.

6.5 LEAKAGE

Several different types of leakage can occur in a wave rotor, with differing effects on its performance. There are inner and outer radial gaps at each face of the rotor, between the rotor and the manifolds, where most of the leakage may occur. If the manifold is connected to a shroud enclosing the rotor, then the radial leakage can be reduced by pressurizing the shroud to some intermediate level which is less than the peak manifold pressure but greater than the minimum manifold pressure. An equilibrium, intermediate level of pressure may be attained quite naturally, which depends on the balance of leakage from the high pressure manifolds to the plenum and from the plenum to the lower pressure manifolds; or it can be sustained at a nonequilibrium pressure from an outside source, such as bleed air from a compressor. Other sources of leakage include azimuthal flows from high pressure manifolds to adjacent low pressure manifolds.

Leakage has been identified as a problem area affecting performance in several key experiments in the past and has been measured indirectly in several cases. Using the MSNW energy exchanger data for leakage and work transfer efficiency (see Figure 3-4), one can derive an approximate equation relating these two variables:

Table 6-1

EQUILIBRIUM WALL TEMPERATURES
AS A FUNCTION OF ROTOR DESIGN VARIABLES

Case	(T_w) _{equilib}	d (cm)	h (cm)	L (cm)	r (cm)	V_r (cm/s)	\dot{m}_{12} , driven (arg/sec)
1	1400°K	.92	1.11	9.6	3.8	15,240	6.0x10 ¹¹
2	1350°K	.41	1.24	9.6	3.8	15,240	6.0x10 ¹¹
3	1350°K	.66	.77	9.6	7.6	12,192	6.6x10 ¹¹
4	1350°K	.92	.85	12.	7.6	12,192	6.6x10 ¹¹
5	1400°K	.92	1.11	8.0	3.8	18,288	3.9x10 ¹¹
6	1350°K	.71	.87	7.6	3.0	15,240	2x10 ¹¹
7	1250°K	.90	2.63	18.0	7.5	15,240	3x10 ¹²
8	1100°K	.92	1.11	9.6	6.0	15,240	2x10 ¹¹
9	1400°K	.39	.81	9.6	3.7	15,240	6.3x10 ¹¹
10	1350°K	.53	1.19	9.6	4.2	15,240	5.3x10 ¹¹
11	1375°K	.34	1.30	9.6	3.6	15,240	7.1x10 ¹¹

NOTES

Each of these cases is for a 100 lb_f thrust engine flying at M=0.65, sea level conditions with a pressure ratio of 2.54, a peak pressure of 30.5 atm, an inlet air temperature of 757°K, and, with one exception (Case 6 @ 1 lb/sec), the inlet air flow is 2.5 lb/sec. CASE 1 is used as a guide, with 24 tubes, 1 wave cycle per revolution, and a combustion gas inlet temperature of 2200°K (3500°F). CASE 2 has 47 tubes. CASE 3 has 47 tubes and a lower tip speed. CASE 4 has 47 tubes, 2 wave cycles per revolution, and lower tip speed. CASE 5 has higher tip speed. CASE 6 has lower mass flow (1 lb/sec). CASE 7 has a lower combustion gas inlet temperature of 1922°K (3000°F), 46 tubes, and 14 lb/sec. CASE 8 has a lower combustion gas inlet temperature of 1644°K (2500°F). CASE 9 has higher peak pressure (51 atm), air inlet temperature (811°K). CASE 10 has lower pressure ratio (2.24), $P_{max}=26.8$ atm, inlet air flow = 2.4 lb/sec. CASE 11 has higher pressure ratio (2.82), $P_{max}=33.8$ atm, inlet air flow = 2.6 lb/sec.

$$\eta = \eta_o - C_1 \left[\frac{\dot{m}_{leak}}{\dot{m}_{total}} \right] = 0.835 - 1.375 \left[\frac{\dot{m}_L}{\dot{m}_T} \right] \quad [6-24]$$

where we have assumed that the loss in efficiency depends linearly on leakage. An additional adjustment has to be made to incorporate the fact that the MSNW experiment utilized only 40 percent of the periphery of the wave rotor; the remaining 60 percent was inactive but still contributed to the leakage. The corrected equation can be written as

$$\eta = \eta_o - 0.40 C_1 \left[\frac{\dot{m}_{leak}}{\dot{m}_T} \right] = 0.835 - 0.55 \left[\frac{\dot{m}_L}{\dot{m}_T} \right] \quad [6-25]$$

In order to apply this equation to situations where air is the working fluid and where the peak pressures and temperatures are different, the loss term dependence on these parameters must be modeled. To this end we assume that the radial leakage flow is choked since the gap height-to-length ratio in the clearance is very small and the gap length exceeds the critical value

$$L_{crit} = \frac{D_h}{f} \left[\frac{1-M_g^2}{\gamma M_g^2} + \frac{\gamma+1}{2\gamma} \ln \left[\frac{(\gamma+1)M_g^2}{2+(\gamma-1)M_g^2} \right] \right] \quad [6-26]$$

M_g is obtained from the relation

$$\frac{P_o}{P_o^*} = \frac{1}{M_g} \left[\frac{2+(\gamma-1)M_g^2}{\gamma+1} \right]^{1/2}$$

where P_o/P_o^* is the pressure ratio across the gap. Under these circumstances, the leakage flow rate depends directly on the acoustic speed $(\gamma RT)^{1/2}$. Thus, the change in gas species and temperature are contained in the values of γ , R , and T .

For example, consider the peak temperature to be 3000°F (1922 K) and the gas is air. Using the same gap as in the MSNW experiment for the low clearance case (i.e., 5 mils = 0.013 cm) and a rotor diameter of 15 cm, we can expect the leakage to be five times that experienced on the MSNW device or 20 percent of the inlet air flow to the rotor, yielding a work transfer efficiency of

$$\eta = 0.835 - 0.55(.20) = 0.725 \quad [6-27]$$

according to Equation [6-25].

Detailed FLOW code calculations were presented in Section 3 to support these initial estimates. The use of higher shroud pressures can be used to reduce the leakage considerably. Experiments at these elevated temperatures and pressures are clearly required to verify both these estimates as well as the more complete performance projections made with the FLOW code.

6.6 RE-ENTRANT DUCTS

Wave rotors may use outflow from one port as the inflow to another port. Every case of interest in this study involves a re-entrant duct corresponding to the combustor. In addition, wave rotors producing shaft work output may also require a second set of re-entrant ducts to complete the gas expansion and derive the final amounts of shaft work from the device.

Duct pressure losses are associated with wall friction and bends in the duct which can cause areas of flow separation. Similarly, abrupt changes in the duct cross section as well as bifurcation of the flow and rejoining the flow may lead to pressure-recovery losses. The combustor also adds heat to the flow, and other parts of the duct may extract heat from the flow because of lower wall temperatures. We shall assume a fixed relative pressure loss of 6 percent for the combustor re-entrant duct case based on accepted values in the literature (see Reference 24).

To promote flow through the combustor, at least some level of pressure recovery in the compressed air exit manifold of the wave rotor is required. The static pressure of the combustion gas entering the wave rotor is equal to the static pressure of the exiting compressed air by virtue of their intimate contact within the wave rotor. Without pressure recovery, the compressed air stagnation pressure would equal its static pressure and would therefore be less than the stagnation pressure of the combustion gases; no flow through the combustor would result. The stagnation pressure of the compressed air exiting the wave rotor can ideally be larger than the combustor exit gas stagnation pressure according to the relation

$$\frac{P_{ao}}{P_{co}} = \left[\frac{2 + (\gamma-1)M_a^2}{2 + (\gamma-1)M_c^2} \right]^{\frac{\gamma}{\gamma-1}} > 1 \quad (6-28)$$

where the important effect is due to the difference in temperatures of the two gases, each having the same velocity on the rotor (i.e., $M_{\text{combustor}} < M_{\text{air}}$). For conditions of interest, the ratio of stagnation pressures may be as large as 1.17. With a 75 percent recovery of the dynamic head in the exit flow manifold, this would yield a stagnation pressure ratio of 1.11. If the combustor pressure losses are limited to less than 6 percent (i.e., a stagnation pressure ratio of 94% in the combustor or better), then net flow through the combustor will occur.

An imbalance between the tangential flow speeds for gases entering the wave rotor and the tip speed of the rotor may also occur, which can lead to either higher or lower stagnation pressures of the compressed air exiting the rotor. These may be used intentionally to increase the compressed air flow stagnation pressure to an acceptable level. The work for raising the stagnation pressure of that stream can be taken from combustion gas flow leaving the rotor by vectoring that flow to give some reactive force to the rotor or by supplying a small amount of shaft power input to the rotor (e.g., from an external drive motor).

From this discussion one can see that pressure recovery is critical to proper operation of the combustor re-entrant loop. Detailed measurements are strongly needed in order to confirm flow loop operation for a given level of combustor pressure loss.

The FLOW code calculations proceed on the basis that a particular wave pattern results in flow speed for the compressed air outlet which can be converted at 75 percent to stagnation pressure. That stagnation pressure is then reduced by the combustor losses to give the boundary condition for the combustor inlet gas pressure to the wave rotor. A surplus of flow generally exists at the compressed air outlet so that there is no difficulty in balancing the mass in and out of the rotor at each end of this duct.

The conditions applying to the second class of re-entrant ducts, namely those providing the second stage of expansion to a wave rotor/turbine, are not so simple to satisfy since there is no excess of mass flow and substantial stagnation pressure losses may occur when the rotor develops shaft work from the flow exiting the rotor and entering the duct. In fact, an additional expansion is generally required on the rotor so that the gas fill pressure in the rotor tubes is sufficiently below the gas pressure of the re-entrant duct flow. Then it will be possible for the duct flow to scavenge the fill gas before performing work on the rotor. The treatment of this case by the FLOW code also proceeds in a similar manner to the preceding case. The initial wave diagram is designed with certain external duct losses in mind so that the fill gas is at a lower pressure than the duct flow entering the rotor after accounting for these losses.

6.7 REFERENCE DESIGN

As an example, consider the case of a 1000 lb_f thrust, 12 inch intake diameter, bypass ratio of 2.2 flying at sea level at Mach 0.65. Total intake air will be 32 lbs/sec, and the core engine will ingest 14 lb/sec air. For the wave diagram shown in Figure 6-2 and for a wave rotor compression ratio of 2.5, following a compressor pressure ratio of 11 and a diffuser compression of 1.33, the peak pressure in the engine is 37 atm. If we consider a peak (combustor) temperature of 3000°P (1922 K), then the sound speed of a_{p3} will be 2870 ft/sec (87580 cm/sec). Assigning the

values of $L = 9.6$ cm, $V_T = 500$ ft/sec (15,240 cm/sec), $\eta_{col} = 0.80$, and M_{D1} , the wave diagram yields the port flow values of u_1 , ρ_1 , T_1 , etc. summarized in Table 6-2. The rotor design values for this case are

$L = 18$ cm $V_T = 15,240$ cm/sec
 $r = 7.5$ cm $\Omega = 19,538$ rpm
 $h = 2.5$ cm $N = 46$ tubes
 $d = .90$ cm

A 600 lb_f thrust engine with the same engine inlet diameter (e.g., 12 inches) will have a similar wave diagram. The main design differences will be a smaller core engine mass throughput (e.g., 5.8 lb/sec) and, therefore, a smaller wave rotor or at least smaller tubes. The port locations and intrinsic gas flow properties will be the same as in Table 6-2; absolute mass flows for each port will be reduced in the same proportion as the core engine mass flow. In this case, the only wave rotor parameter which needs to change is the tube height (e.g., from 2.6 to 1.1 cm).

6.3 DESIGN SENSITIVITY

Several wave rotor preliminary designs related to the reference case described above have been developed to illustrate possible changes in the basic design parameters which cover the range of parameters considered in the FLOW code analysis of wave rotor performance. Table 6-1 includes the other illustrative design examples developed using the design equations presented in Section 6.2 above, such as cases 1 through 6, which correspond to higher combustion temperatures

(i.e., $T(\text{peak}) = 3500$ F); lower combustion temperatures (case 8); higher peak pressures (i.e., case 9 at $P(\text{peak}) = 50$ atm); larger number of tubes (i.e., cases 2-4 at $N=47$ tubes); higher tip speed (i.e., case 3 at $V_T=22,860$ cm/s); lower and higher wave rotor pressure ratios (2.2 and 2.8, respectively, for cases 10 and 11); and shorter rotor lengths. These cases are simply points in a continuum of design possibilities. The most impressive feature is their overall similarity. There are very slight dimensional changes amongst these cases. The greatest differences are in the equilibrium wall temperatures amongst those cases (e.g., cases 1-6 and 8) where the inlet combustion temperatures are different compared to the reference case 7.

In summary, the designer can change the tip speed, rotor length and radius, and tube height and width to accommodate a variety of flow and combustion conditions. The rotor wall temperature is within present day materials capabilities, except possibly at the highest combustor temperatures considered (i.e., $T_{comb} = 3500^\circ\text{F}$). At the upper limit of T_{comb} , an extra cooling flow of the compressed air can be used to keep the rotor wall temperature within bounds. The cooling flow also allows the rotor to act as a recuperator to help increase the cycle efficiency.

Table 6-2

EXAMPLE OF IDEAL WAVE DIAGRAM FLOW PARAMETERS
 FOR PRESSURE EXCHANGER WAVE ROTOR
 (See Figure 3-1 for Nomenclature)

Port Description	Velocity, U_1 (cm/sec)	T^* (°K)	P^* (atm)	Port Locations (°)	Density, ρ_1 (gm/cm ³)	Port Size ^a γ_1 (insec)	Mass Flow \dot{m}_1 (g/sec)	Port Flow Angles, θ_1 (°)
Driven Gas Inlet, d1	18,489	757	1.51	0 to 157	7.07	1.34	6755	80
Driver Gas Inlet, D1	19,875	1922	3.77	147 to 244	6.80	0.78	1590	76
Driven Tuning Inlet, D51	3,973	1728	2.57	295 to 298	5.14	0.03	31	76
Driver Tuning Inlet, D11	9,295	747	1.81	250 to 340	5.90	0.08	118	59
Driven Gas Outlet, d3	19,875	960	3.77	187 to 244	17.6	0.64	6755	38
Driver Tuning Outlet, D46	9,917	1841	3.76	244 to 249	6.09	0.05	97	57
Driver Gas Outlet, D5	7,946	1696	2.40	249 to 321	4.40	0.44	619	63
Driven Tuning Outlet, D56	3,973	1665	2.24	321 to 321	4.67	0.02	15	76
Driver Gas Outlet, D1	18,504	1494	1.51	321 to 314	3.51	1.24	2987	80

^a Static Values

^b Total Cycle Time = 1.07 msec

MB: These values correspond to Case 87 in Table 3-1.

Section 7
WAVE ROTOR TURBOFAN PERFORMANCE

7.1 TECHNICAL BACKGROUND

Two basic wave rotor engine cycles have been considered: those which utilize the wave rotor to produce shaft work (wave rotor/turbines) and those which use the wave rotor to produce a high pressure hot gas (pressure exchange wave rotors). Both on- and off-design thermal cycle analyses have been carried out to determine the peak engine performance capabilities in terms of thrust-specific fuel consumption and the sensitivity of that performance to design and operating parameters, particularly to those parameters associated with the wave rotor component. This evaluation has focused on the performance of engines in the 600 to 1000 lb_f class for a range of pressure ratios from 20 to 50 and peak temperatures from 2500°F to 3500°F. More specific constraints on engine core size and bypass ratio are cited below. Typically, the engine inlets are 12 to 18 inches in diameter with a core engine inlet diameter of 5 to 7 inches.

A relatively simple thermal cycle code has been used for this evaluation in order to keep the dependence of the results on wave rotor parameters as direct as possible. The cycle code calculates gas stream properties at each station in the engine, including pressure, temperature, and mass flow. Real gas effects include variations of the specific heat ratio γ with temperature and pressure and molecular weight at each flow station. A fuel having the heating value (i.e., 18,400 BTU/lb_m) and C/H mole fractions of JP4 are used throughout unless otherwise noted.

The cycle calculations suggest that a reference design wave rotor turbofan using a pressure exchange wave rotor may operate with a thrust-specific fuel consumption (TSFC) in the range of 0.65 to 0.75 for reasonable bypass ratios (i.e., 5 to 8) and peak combustor (wave rotor inlet) temperatures of 2500 to 3500°F. The wave rotor efficiency, discussed in more detail in Section 4, has been varied from 0.60 to 0.80 to bracket the values obtained by detailed FLOW code calculations. Over this range of component efficiencies, the engine TSFC varies by 5 percent (e.g., from 0.75 to 0.79 lb_m/lb_f hr for 2500°F peak temperatures).

The chief advantages of using a wave rotor are the increased cycle efficiency afforded by the automatic cooling of the wave rotor, and its high component efficiency in a small diameter, high pressure application. In particular, rotor wall temperatures do not exceed 1800°F for combustion temperatures reaching 3000°F. Additional cooling may be employed in a hybrid wave rotor/recuperator version of this engine, which will drop the rotor temperature to 1600°F or less. The exhaust from the rotor is also constrained to low

temperatures so that the turbine inlet temperatures can be kept below 1800°F for an interesting class of wave rotor turbofan engines.

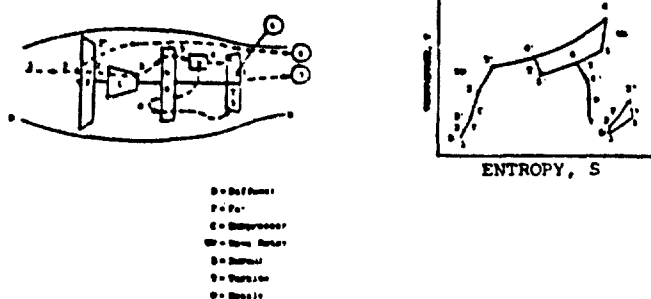
7.2 ENGINE CYCLES

The two primary engine configurations are shown in Figures 7-1 and 7-2, which illustrate the location of the wave rotor component relative to the rest of the engine, display the thermal cycle, and show engineering sketches of the engines. The pressure exchange wave rotor engine version illustrates the main flow paths for this type of engine. Partially compressed air enters the wave rotor at Station 3 from the compressor where it is compressed a factor of 2 to 3 more. The compressed air leaves the wave rotor at Station 3' and enters the combustor. Since only part of the fully heated air flow is needed to carry out compression work on the wave rotor, the rest of the air flow can be diverted at 4' to a turbine for work extraction. The diverted air flow should only be heated to the maximum feasible turbine inlet temperature; the peak cycle temperature can be much higher than turbine inlet temperature because the wave rotor is more robust than the turbine and is an actively cooled component. The flow stream at peak cycle temperature re-enters the wave rotor at 4 where it compresses the incoming cold air by expanding against it before exhausting at 5 to the lower pressure turbine. The diverted flowstream passes through the high pressure turbine and expands to a pressure at 5' equal to the combustion gas pressure (at 5) where they are recombined (Station 6) before entering the low pressure turbine at a reasonable turbine inlet temperature. Some mixing losses occur at this stage in which the higher temperature gases lose some of their available work.

In the pressure exchange wave rotor engines, the wave rotor shaft is driven independently from the other components so that the shaft can be co-axial and in line with the other rotating components or it can be mounted transverse (i.e., at right angles to the turbine). The precise orientation does not influence the cycle calculations for the model used here. In an actual engine, the rotor placement will influence the duct lengths and the amount of duct turning and will have an effect on the cycle performance, which must be included in a more detailed evaluation.

The second primary engine configuration, shown in Figure 7-2, incorporates a wave rotor/turbine. The wave rotor/turbine engine differs in several important respects from the pressure exchange wave rotor engine. First, shaft work is extracted so that the wave rotor is integrally connected to the compressor. Therefore, the wave rotor tip speed must be chosen to match the compressor speed. Also, the exhaust gases from the combustor may be expanded through the wave rotor in several passes, requiring ducts to re-route partially expanded gases back onto the rotor for further expansion. The cycle calculation also differs since the principal output from the wave rotor is shaft work instead of available work of gas expansion.

6) Thermal Cycle



(c) Engineering Sketch.

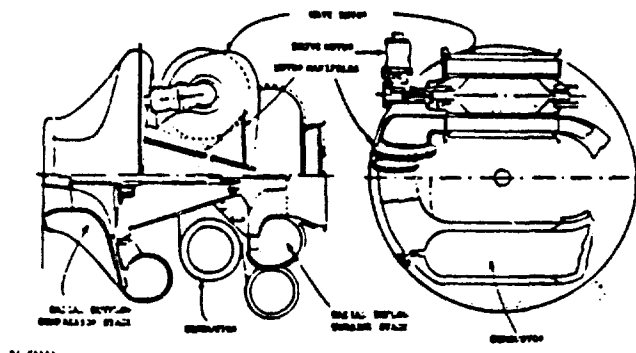
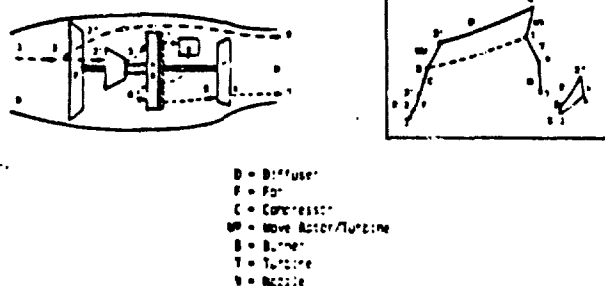


Figure 7-1. Pressure Exchanger Wave Rotor Turbofan.

(a) Flow Schematic

(b) Thermal Cycle



(c) Engineering Sketch

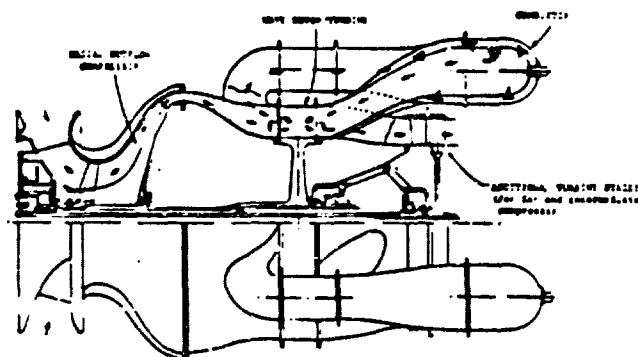


Figure 7-2. Wave Rotor/Turbine Turbofan

$$m_3[h_{(3,1)} - h_{(3,2)}] = m_4[h_{(4,1)} - h_{(4,2)}] \quad (7-1)$$

where $h = C_p T$, $m_4 = m_4 - m_3 + m_f$ and $m_4 = m_4 + m_3$, and m_f is the fuel flow. A detailed consideration shows that the wave rotor work transfer efficiency $\eta_w = \eta_{TC} \eta_{CE} T_3/T_1$ (e.g., see Section 3.4).

Calculations proceed as follows. Inputs include the flight Mach number and altitude, peak combustion temperature, and maximum inlet temperature to the high pressure turbine. Polytropic efficiencies are selected for the compressor, fan, and turbine components. A burner efficiency is also selected, and the values of η_{TC} and η_{CT} are chosen to be in the range of values computed from the flow code (as discussed in Section 4). A total engine thrust (e.g., 600 lb_f) and engine diameter (e.g., 12 inches) are selected in order to compute the required engine-specific thrust (i.e., ST in [lb_f/lbm·hr] of air). These values are then used to compute the optimum bypass ratio and fan pressure ratio that give the minimum TSFC. Alternatively, these parameters may be specified and the calculations provide the corresponding TSFC. The remainder of the cycle calculations provide the temperatures, pressures, and flow rates at each station.

7.3 ON-DESIGN PERFORMANCE

Results of on-design cycle calculations are shown in Figures 7-3 to 7-5. Figure 7-3 illustrates TSPC for several combustion temperatures as a function of the overall pressure ratio. The optimum bypass ratio and the inlet temperature to the low pressure turbine are shown as pairs of numbers at points along each curve. The low pressure turbine inlet temperature may be higher than high pressure turbine inlet temperature; realistic solutions would normally be constrained to the same temperature or lower. Figure 7-4 shows the sensitivity of the TSPC to wave rotor efficiency η_w for the engine pressure ratio 37.5 and peak temperature of 2500°R. The TSPC varies approximately 5 percent over the range of η_w values considered. The lack of TSPC sensitivity to η_w suggests that the wave rotor is a relatively low-risk approach to advanced turbofan engine development since its component efficiency is not very critical to the overall engine performance in this configuration.

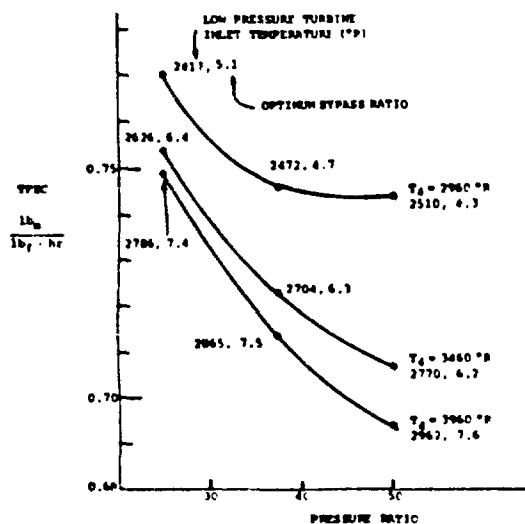
Finally, we present in Figure 7-5 a combination of fan variables (bypass ratio and pressure ratio) which indicate the minimum locus of TSFC as a function of specific thrust. The specific thrust is identified for several different engine diameters at 600 lb, and

1000 lb_f thrust. A substantial gain in TSFC is available if the engine diameter D_{eng} can increase from 12" to 14"; further improvement is possible if the engine is 16" in diameter, but at this size the bypass ratio is quite large. One would have to consider a geared fan or a derated fan efficiency if an engine of this size and bypass ratio is contemplated for 600 lb_f thrust. Figure 7-5 also may be used for any engine diameter or thrust by scaling the horizontal coordinates from

$$D = D_{eng} \left[\frac{1}{1 + 0.0089 \text{ BPR}} \right]^{1/2} \quad (7-2)$$

$$\text{Specific Thrust} = \frac{4.73 \times \text{Thrust (lb}_f\text{)}}{[D_{eng}(\text{in})]^2} \quad (7-3)$$

where D is the core engine inlet diameter assuming a 1:3 hub-to-tip ratio and M₀ = 0.65 at sea level. The minimum TSFC indicated by the dashed line in Figure 7-5 is achieved for essentially constant (e.g., 5" diameter for 600 lb_f thrust) core engine size at D_{eng} = 12", 14", and 16". That is, the bypass ratio corresponding to minimum TSFC increases just enough with engine size to eliminate any changes in the core engine diameter.



83 06987

VARIAION OF TSFC WITH OVERALL PRESSURE RATIO

M₀ = 0.65 at Sea Level

High P. Turbine Inlet Temperature = 3460 °R

No Nozzle, Diffuser Losses

Fan P.E. = 1.9

BPR = 20.6 lb_f/lb_{sec} (12" dia engine @ 600 lb thrust)

Energy Exchanger P_r = 3.5

POLYTROPIC

- Compressor Efficiency, 89%
- High P Turbine Efficiency, 87.7%
- Final Turbine Efficiency, 85.5%
- Energy Exchanger Efficiency, 89.5% Comp., 67.0% Exp.

Figure 7-3. Variation of Thrust Specific Fuel Consumption (TSFC) with Pressure Ratio for Several Peak Cycle Temperatures T₄.

M = 0.65 at sea level
High P Turbine Inlet 3460 °R
Final Turbine Inlet 3470 °R
Peak Temperature 2960 °R
Fan P_r 1.9
BPR 20.6 lb_f sec/lbm
(12" dia inlet, 600 lb_f)

Compressor P_r = 15
Energy Exchanger P_r = 3.5
POLYTROPIC EFFICIENCIES:
Compressor 0.89C
High P Turbine 0.877
Final Turbine 0.855
Bypass Ratio 4.7
No Nozzle or Diffuser Losses

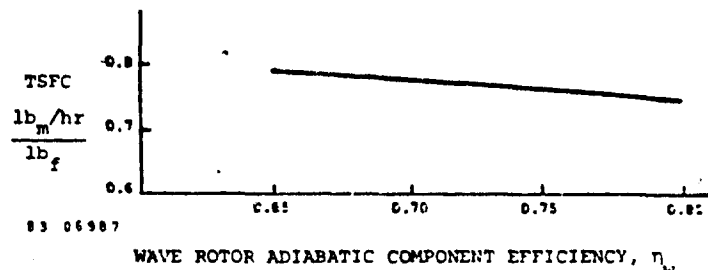
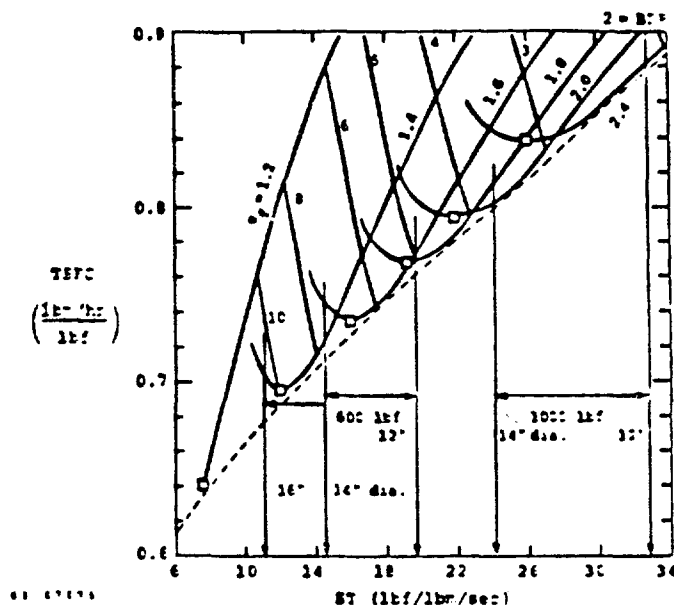


Figure 7-4. Effect of Wave Rotor Efficiency η_w on Thrust Specific Fuel Consumption (TSFC) at a particular peak pressure and temperature.



83 06987

T₄ = 2960 °R, peak cycle temperature
T₄ = 3460 °R, turbine inlet temperature
P_r = 15, compressor pressure ratio
P_r = 3.5, wave rotor pressure ratio
τ_f = 0.70, work transfer efficiency
M₀ = 0.65 at sea level
P_r = 49.8, total cycle pressure ratio

Figure 7-5. Minimum Thrust Specific Fuel Consumption (TSFC) vs. Specific Thrust (ST) for various bypass ratios (BPR) and fan pressure ratios (τ_f) for small wave rotor turbofan engines.

Similar min(TSFC) envelopes are plotted in Figure 7-6 for two values of the wave rotor work transfer efficiency. The dashed line in Figure 7-6 indicates the potential advantages of also using the rotor as a recuperator. More detailed calculations for the recuperated case need to be carried out to evaluate the effects of pressure loss during the second pass of compressed air through the rotor. The estimates shown in this figure are positive enough to warrant further study of this approach.

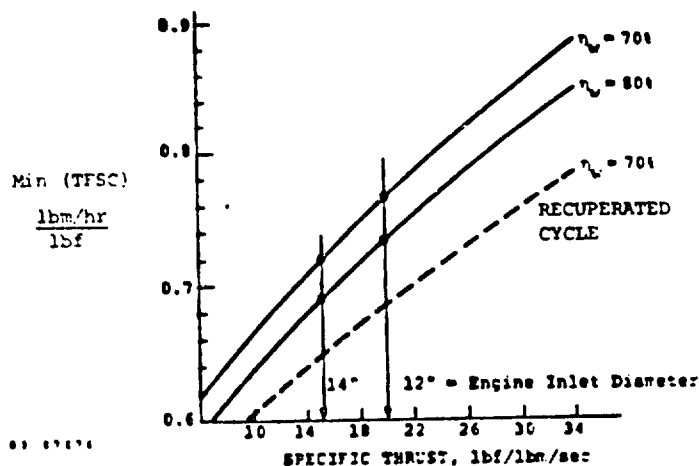


Figure 7-6. Impact of Wave Rotor Component Efficiency and Recuperation on the envelope of minimum TSFC values for the wave rotor turbofan conditions shown in Figure 7-5.

Rather little information is available on the component efficiencies of 5" diameter compressors and turbines using air and combustion gas. The most relevant recent literature comes from the development of the automotive gas turbine.⁽²⁵⁾ Earlier data also exists for small rotating turbogenerator units developed for space.⁽²⁶⁾ Each of these sources supports adiabatic turbine efficiencies on the order of 0.89 and adiabatic compressor efficiencies of 0.85. The fan efficiencies must be intuited by scaling down data from large engines. We have estimated η_{fan} as 0.885. A nominal combustion efficiency of 0.97 is assumed. Diffuser and nozzle efficiencies are taken equal to unity in order to give the uninstalled thrust-specific fuel consumption on a basis comparable to other engine studies.

Typical values for the work transfer efficiency of the wave rotor range from 65-75% for small (i.e., 5 lbm/sec) wave rotors up to 85% for large wave rotors (100-500 lbm/sec). The impact of finite wave rotor efficiencies can be computed by evaluating the ratio of the change in air stream enthalpy to the combustion gas enthalpy as the two streams traverse the rotor.

$$\frac{\text{Net } W_{out}}{W_{in}} = \frac{(T_4 - T_5) - (T_3 - T_2)}{T_4 - T_5}$$

$$= 1 - \frac{\alpha \beta}{\gamma} \left[1 - \beta + \left\{ (1 - \beta)^2 + 4\eta_w \beta \right\}^{1/2} \right]^{-2}$$

where $\gamma = T_4/T_3$, $\beta = (P_4/P_3)^\alpha$ and $\alpha = (\gamma - 1)/\gamma$. Thus, the effect of finite component efficiencies is to limit the amount of useful work that can be extracted from the topping stage gas streams. Figure 7-7 graphs the net work available from the outlet gas streams divided by the work available in the inlet combustion gases as a function of various work transfer efficiencies and the pressure ratio. As an example, for $\gamma = 2.84$ and $\eta_w = 0.65$ (e.g., for a small wave rotor engine), the wave rotor pressure ratio, P_4/P_3 , must be 2.5 or less in order for the topping stage to have a strong positive effect (e.g., $\text{Net } W_{out} > .25 W_{in}$) in the overall engine cycle. This relationship defines the minimum acceptable work transfer efficiency for any given engine cycle and sets the stage for establishing wave rotor test requirements.

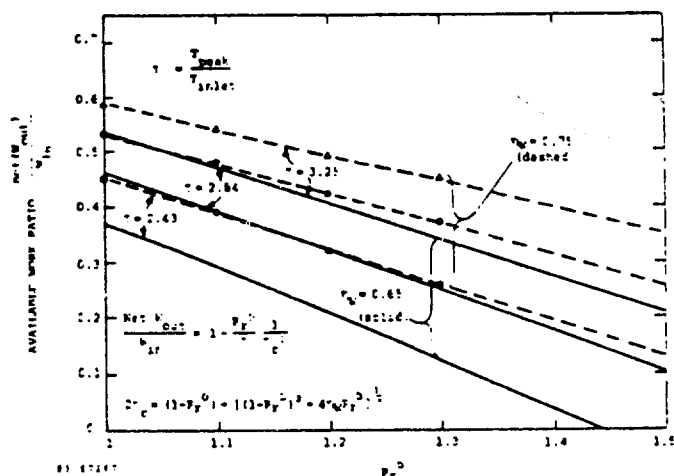


Figure 7-7. Net Output Work Available from Pressure Exchanger Wave Rotor for several component efficiencies (η_w) and peak-to-rotor inlet temperature ratios (γ) vs. wave rotor pressure ratio, P_r (P_4/P_3).

7.4 OFF-DESIGN PERFORMANCE

An analysis of off-design engine performance was conducted to determine the inlet and outlet flow requirements for the wave rotor components. These requirements are used as input parameters for the off-design wave rotor flow code calculations in order to confirm the wave rotor component efficiencies used in the cycle calculations. The chief value of these results is to determine the sensitivity of part-load engine performance to the wave rotor component.

An example of the results of off-design engine calculations are shown in Figure 7-8. These calculations allow one to examine off-design operation when the flight speed and altitude are varied. The off-design model relates the manner in which parameters such as the mass flow through the engine, shaft rpm, and internal pressures and temperatures will change in concert with each other to maintain a self-consistent set of values representing actual engine operation at part load. The model predicts the changes in engine thrust level, fuel consumption rate, and flow properties at each station for the desired off-design conditions.

We have examined off-design operation with flight Mach numbers ranging from 50% to 140% of the reference value of 0.65 in order to include dash capability during a portion of the mission.

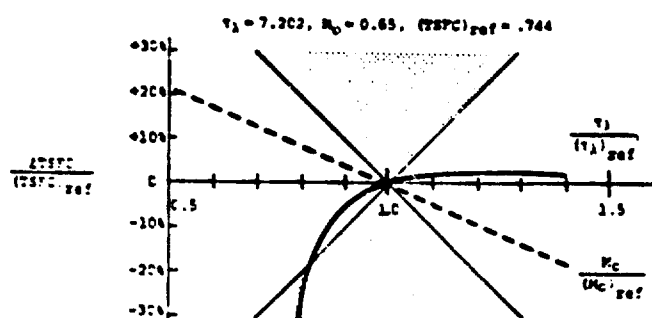


Figure 7-8. Off-Design Cycle Calculations for a Wave Rotor Turbofan Engine showing percentage changes in TSFC for variations in combustor temperature T_1 , variations in flight speed M_0 . Shaded regions indicate high sensitivity of TSFC to cycle or flight parameters.

The horizontal axis of Figure 7-8 shows the fraction greater or less than the reference value (1.0) taken by the peak cycle temperature T_1 and flight speed M_0 . The vertical axis measures the fractional change in thrust-specific fuel consumption (TSFC) compared to $(TSFC)_{ref}$; positive values of this variable imply values of TSFC lower than the reference values.

For small variations ($\pm 10\%$) about the reference flight speed and peak cycle temperatures, the fractional change in TSFC is less than $\pm 5\%$, implying local insensitivity to off-design performance.

For T_1 much less than $(T_1)_{ref}$ TSFC deteriorates rapidly. However, very reasonable off-design performance persists for T_1 higher than $(T_1)_{ref}$ suggesting that the wave rotor turbofan engine might be very well suited for missions involving a high speed segment.

The fractional change in TSFC with flight speed is essentially linear, improving at slower speeds and deteriorating at higher speeds. In every case, the percent change in TSFC is less than the corresponding percent change in flight speed, implying that off-design performance is relatively insensitive to flight speed. A more complete analysis of airframe and mission conditions is required to carry out off-design engine calculations where flight speed and peak temperature vary together. We may conclude that the wave rotor component preserves its advantages for good overall engine performance in both on- and off-design operation.

7.5 REFERENCE DESIGN PERFORMANCE

On the basis of the results presented above, it is possible to select reference design conditions for a 600 lb_f thrust wave rotor turbofan engine. This design is preliminary and involves just the first estimates of flow conditions, diameters, and performances calculated from the cycle codes. Additional analysis and design would be needed to arrive at optimized performance.

The 600 lb_f thrust engine has a TSFC = 0.776 for a 12" diameter engine; a 1000 lb_f thrust engine exhibits a TSFC of 0.89 for the same engine diameter. The design values for a 600 lb_f thrust engine are summarized in Table 7-1. Clearly, we can expect substantial improvement by moving to larger engine diameters (and correspondingly larger bypass ratios) as indicated in Figure 7-6. Further optimization would, therefore, also require a sharper definition of particular mission requirements in order to delineate such things as the maximum allowed engine diameter, bypass ratio, etc.

It is worthwhile noting from the reference design that the combustor temperature (i.e., peak cycle temperature) is 2500°F (1647 K at station 4), but the turbine inlet temperatures are maintained at 2000°F. The wave rotor wall temperatures are also below 1500°F, so that no new materials development is required for this engine.

As new high temperature materials do become available, the wave rotor will always be able to maintain a higher inlet temperature than turbines made of the same materials. Thus, the wave rotor will boost cycle performance for a given turbine materials technology and protect the turbines from excessive temperatures.

Figure 7-9 illustrates the stresses required to produce 1% creep in 10,000 hours for a variety of candidate rotor materials. The tip speeds producing these stresses are indicated on the right side of the figure. Wave rotors generally involve much lower tip speeds (e.g., 250 to 500 ft/sec) compared to gas turbines, so the material stress limits are not reached until the rotor temperature rises to considerably

Table 7-1

Preliminary Reference Design Values
for 600 lb_f Thrust Wave Rotor Turbofan Engines

Flow Stations ^a	T °K (°R)	P MPa (atm)	m kg/sec (lb/sec)
FAIN			
1	288 (519)	0.10 (1)	10.4 (22.9)
2	313 (563)	0.13 (1.326)	10.4 (22.9)
3	384 (692)	0.26 (2.62)	10.4 (22.9)
4	384 (692)	0.10 (1)	10.4 (22.9)
CORE ENGINE			
2'	384 (692)	0.26 (2.62)	2.8 (6.2)
3	744 (1340)	2.02 (20.0)	2.8 (6.2)
3'	1017 (1831)	5.04 (50.7)	2.8 (6.2)
4	1047 (1865)	4.76 (46.8)	2.8 (6.2)
4'	1365 (2457)	4.88 (48.2)	0.4 (1.0)
5	1395 (2511)	1.89 (18.7)	2.4 (5.2)
5'	1129 (2032)	1.96 (19.3)	0.4 (1.0)
6	1364 (2455)	1.90 (18.8)	2.8 (6.2)
6'	799 (1439)	0.14 (1.40)	2.8 (6.2)
7	799 (1439)	0.10 (1.0)	2.8 (6.2)

^a See Figure 2-1(b)

Thrust = 600 lb_f
Specific Thrust = 20.57
Engine Diameter = 11.75 inches
TSFC = 0.776 lb_f/lb_f/hr
Bypass Ratio = 4.68
Mach 0.65 at sea level

POLYTROPIC COMPONENT EFFICIENCIES

$$\epsilon_{\text{nozzle}} = \epsilon_{\text{diffuser}} = 1$$

$$\epsilon_c = 0.892, \epsilon_{\text{HPT}} = 0.877, \epsilon_{\text{LPT}} = 0.855$$

$$\epsilon_{\text{C}} = 0.838, \epsilon_{\text{T}} = 0.800$$

higher levels than a gas turbine can sustain. Typical values of the rotor wall temperatures computed were on the order of 1800 F or less. For the recuperated versions of the wave rotor, the wall temperature was closer to 1700 F. Figure 7-9 shows that existing nickel alloys can be used for these rotor conditions (shaded rectangle).

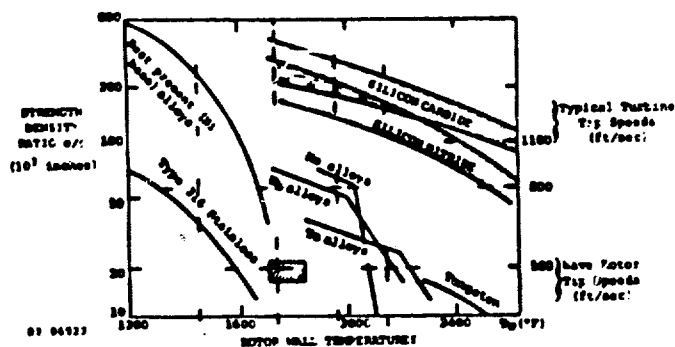


Figure 7-9. Stress to Produce 1% Creep in 10,000 Hours vs. Rotor Wall Temperatures (shaded rectangle shows wave rotor operating regime).

Another important aspect of thermal design involves the effects of thermal-mechanical fatigue. As the rotor goes through one complete cycle, both hot and cold gases are exposed to the rotor tube walls, and the tube walls also have been subjected to cyclic pressure imbalances due to the fact that the waves in adjoining tubes are located in slightly different axial positions at any given time. Initial calculations indicate that the nickel alloy cyclic fatigue limits were not exceeded for several hours of operation. However, these constraints need to be re-examined carefully for extended operation under different flow conditions.

7.6 CONCLUSIONS

Performance calculations for the wave rotor turbofan based on a pressure exchange wave rotor indicate low (0.68 to 0.75) thrust-specific fuel consumption from on-design (e.g., full load TSFC = 0.776) conditions to off-design (50% flight speed TSFC = 0.621) conditions. These results are not very sensitive to the wave rotor component efficiency for the range of values of η_w predicted by more detailed flow code calculations. The corresponding engine designs suggest that this performance may be achieved for engines in the 600 lb to 1000 lb thrust categories (at 0.65 Mach number, sea level conditions) having entrance diameters of 12 inches to 14 inches, and bypass ratios of 4 up to 8; the core engine diameter (i.e., compressor inlet diameter) for these cases was nearly constant at 5 inches (e.g., for the 600 lb_f engine) assuming a 3:1 tip-to-hub ratio for the compressor.

Wave rotor wall temperatures and turbine gas inlet temperatures are maintained at or below 1950°F so that no new materials development would be required for such engines. A preliminary reference design at 600 lbs. thrust provides the basis for a more detailed evaluation in which specific design questions involving the integration of a wave rotor with the rest of the engine may be addressed.

ACKNOWLEDGMENTS

The author acknowledges with pleasure the many important contributions to this report by W.J. Thayer III, P.E. Cassady, J.P. Zumdick, E.L. Klosterman, R. Milroy, and R. Klug at MSNW, and by Professors W. Christiansen and G. Oates of the University of Washington in Seattle. This work was supported in part by US Navy Contract No. N00140-82-C-9729 under DARPA Order No. 4361 and by US DOE Contract No. AC04-78ER01064.

REFERENCES

1. J.P. Mullen and W.P. Othling, Jr., "The Cruise Missile Technical Challenge," *Astronautics & Aeronautics*, January 1982, pp. 24-30, 53.
2. J.G. Castor, "Compound Cycle Turbofan Engine," Paper No. AIAA-83-1338, 19th Joint Propulsion Conference, Seattle, Washington, 27-29 June 1983.
3. E.J. Coleman, "Subsonic Cruise Missile Engine Needed," *Aviation Week & Space Technology*, Vol. 116, No. 26, pp. 201-203 (28 June 1982).
4. P.T. Kerwin, "Analysis of a 35 to 150 kW(e) Brayton Power Conversion Module for Use With an Advanced Nuclear Reactor," NASA Technical Note TND-6525, September 1971.
5. E. Jenny and T. Buloty, "Die Druckwellen-Maschine Complex als oberstufe einer Gasturbine," in *MTZ Motortechnische Zeitschrift* **34**, 810: 329-335 (1973) and Part 2 in **34**, 812: 421-425 (1973).
6. P.H. Rose, "Potential Applications of Wave Machinery to Energy and Chemical Processes," pp. 3-30 in *Proceedings of the 12th International Symposium on Shock Tubes and Waves*, Jerusalem, 16-19 July 1979 (The Magnes Press, Hebrew University, 1980).
7. R. Pearson, "Pressure Exchangers and Pressure Exchange Engines," Chapter 16 in *Thermodynamics and Gas Dynamics of I.C. Engines*, by D.E. Winterbone and S.C. Low (to be published).
8. J.V. Foa, *Elements of Flight Propulsion*, (John Wiley & Sons, Inc., New York, 1960).
9. P.K. Doerfler, "Comprex Supercharging of Vehicle Diesel Engines," SAE Paper No. 750335, Automotive Engineering Congress and Exposition, Detroit, Michigan, 24-28 February 1975.
10. G. Jendrassik, "Jet Reaction Propulsion Units Utilizing a Pressure Exchanger," U.S. Patent No. 2,757,509 (1956).
11. M. Berchtold and T.W. Lutz, "A New Small Power Output Gas Turbine Concept," ASME Paper No. 79-GT-111 (1974).
12. C. Seippel, "Gas Turbine Installation," U.S. Patent No. 2,461,186 (1949, filed in 1943).
13. M. Berchtold, "Aerodynamic Wave Machine Functioning as a Compressor and Turbine," U.S. Patent No. 2,867,981 (1959) assigned to ITE Circuit Breaker Company.
14. R.R. Coleman, "Wave Engine Technology Development," Final Report prepared by General Power Corporation for AFMAL (Contract No. AFMAL-TR-83-2095), January 1984.
15. W.J. Thayer et al., "Energy Exchanger Performance and Power Cycle Evaluation: Experiments and Analysis," Final Report submitted by MSNW to DOE (Contract No. AC06-78ER01084), April 1981.
16. R. Taussig et al., "Investigation of Wave Rotor Turbofans for Cruise Missile Engines," Final Report submitted by MSNW to DARPA (Contract No. N00140-82-C-9729), April 1983.
17. P.G. Hill and C.R. Peterson, *Mechanics and Thermodynamics of Propulsion*, (Addison-Wesley Publishing Co., Reading, Massachusetts, 1965) p. 145.
18. K. Teipis, "Cruise Missiles," *Scientific American*, Vol. 236, No. 2, February 1977, pp. 20-29.
19. W.J. Thayer and J.F. Zumdick, "A Comparison of Measured and Computed Energy Exchanger Performance," 13th International Symposium on Shock Tubes and Waves, Buffalo, New York, 6-9 July 1981.
20. J.P. Boris and D.L. Book, "Flux-Corrected Transport I: SHASTA, A Fluid Transport Algorithm That Works," *J. Computational Physics* **11**: 38 (1973); also J.P. Boris and D.L. Book, "Solution of Continuity Equations by the Method of Flux-Corrected Transport," pp. 85-129 in Vol. 16, *Methods in Computational Physics*, edited by B. Alder, S. Fernbach, and M. Rotenberg (Academic Press, New York, 1976).
21. D.B. Spaulding, "A Procedure for Calculating the Unsteady, One-Dimensional Flow of a Compressible Fluid, With Allowance for the Effects of Heat Transfer and Friction," Unpublished Report HTS/69/24, Imperial College of Science and Technology, November 1969.
22. J.F. Zumdick et al., "The Fluid Dynamic Aspects of an Efficient Point Design Energy Exchanger," 12th International Symposium on Shock Tubes and Waves, Jerusalem, Israel, 16-19 July 1979.
23. N. Croes, "The Principle of the Pressure-Wave Machine As Used for Charging Diesel Engines," pp. 36-55 in 11th International Symposium on Shock Tubes and Waves, Seattle, Washington, 11-14 July 1977.
24. A.E. Lefebvre, *Gas Turbine Combustion*, (McGraw Hill Book Co., New York 1983) Chapter 5, pp. 157-178.

25. R.A. Harmon, "Gas Turbines: Automotive Applications - A Look Behind the Wheel," Mechanical Engineering, April 1962, pp. 26-45.
26. "Mini-SNU/SIPS 1300 W(e) Dynamic Power Conversion System Development," Garrett AiResearch Co., NASA Report No. CR-159440 (October 1978); and J.L. Klann and W.T. Wintucky, "Status of the 2 to 15 kW(e) Brayton Power System and Potential Gains from Component Improvements," NASA Technical Memorandum TM-X-67835, August 1971.

ABSTRACT

PERFORMANCE PREDICTIONS FOR GAS WAVE TURBINES INCLUDING PRACTICAL CYCLES WITH WIDE SPEED RANGE

R.D. Pearson

A design procedure is first described which starts with "quasi-static" thermodynamic analysis based on special pressure volume diagrams. This permits overall conditions to be assessed such as total gas transfer quantities, pressures and the combustion gas inlet temperatures required. Losses are evaluated by specifying polytropic efficiencies for each stage of the cycle. Leakage and heat transfer effects are also allowed.

Design point wave diagrams follow using the data input from quasi static analysis and this introduces the author's "half wave plateau" means for permitting a speed range to be accommodated. It also minimises call opening loss and this critical area is discussed in some detail. The wave diagram starts in rudimentary form to assess overall conditions for cycle closure, then detailed maps can be finalised. These in turn allow heat transfer, leakage and friction effects to be assessed as well as integrating flows and net torque.

This calibrates the quasi-static model so permitting it to be used for performance estimation over a wide range of conditions without need to draw more wave maps. These are used as toppers for gas turbine cycles since this is their real niche. Naturally aspirated GWT's are shown to be unattractive as they would be bulky and heavy without being very energy economic. These disadvantages are shown to vanish with combined GWT-GT systems. Applications are shown to bypass jet engines for missiles and aircraft and to industrial power generation.

A very important new field is analysed for improving the utilisation of coal. The raw pulverised coal is first volatilized at high pressures of some 60 ATM using a GWT-GT combination to supply air at this pressure for providing the required heat. Oxygen is usually employed but is a much more expensive method. About 25% of the coal's energy content will be extracted as gas together with some 5% as tar. The latter is for hydrogenation to liquid fuels.

Residual char with ash is discharged for atmospheric gasification because for this stage residence times of up to 20 minutes can be required as compared with only 2 seconds for the highly reactive first stage and so pressure vessels would be very large and expensive. The gas is cooled extracting 28% of initial char energy for steam superheating. Then it is cleaned of SO_2 and ash before recompressing for use in a combined steam GWT cycle.

Here the GWT is shown to score heavily over a pure GT steam combined cycle because of its capacity to provide very high exhaust temperatures of up to 900°C . This enables the GWT-steam energy paths to be placed in series so providing true topper economy.

Plain gas turbines have to be used largely in parallel with steam sets and so do not really operate as toppers offering little energy economy, i.e. a raising of thermal efficiency from 38% to 41% is claimed but the GWT could increase this to 55%.

List of Contents

- 1.0 Introduction
- 1.1 Heat Transfer and Mixing
- 1.2 Thermodynamic Analysis based on Pressure Volume Diagrams
- 1.3 Wide speed range

- 2.0 Gas Wave Turbine Analysis (Mathematical Section)
- 2.1 Quasi Static Thermodynamic Analysis based on the P-V
Diagram (gas transfer, pressure equalisation work, leakage
and energy input by fuel)
- 2.2 Allowance for Variable Specific Heat

- 3.0 Leakage Evaluation
Table 3.I Effect of Clearance on output and
Thermal Efficiency by Thermodynamic Analysis

- 4.0 Heat Transfer and Friction

- 5.0 Port Opening and Closing Losses

- 6.0 The New Concept - Wide Speed Range
- 6.1 Illustration of the "Half Wave Plateau" Design Feature
- 6.2 Description of Fig. 10 Explaining features which confer
Wide Speed Range Capability

- 7.0 Design Wave Plotting
- 7.1 Effect of Design Mean Blade Speed on Cell Length

- 8.0 Choice of Topping Stages
Pure Pressure Exchange versus the GWT

- 9.0 The GWT as a Topper for Gas Turbine Performance Predictions
- 9.1 Early Predictions (1958)
TABLE 9.II Assumptions GWT
TABLE 9.III Assumptions Gas Turbines
- 9.2 Performance Curves (1958)

9.3 New Advanced Cycle with Boost from Transfer Gas Exchange.
Updated Predictions 1985.

TABLE 9.III Assumptions for Thermodynamic Analysis of
Advanced GWT

TABLE 9.IV Case of Zero Supercharge-Computed Characteristic

9.4 Compound Plant GWT-GT

10.0 Application to Bypass Jet Engine

11.0 Application to Coal Gasification

12.0 Application to Combined Cycles

13.0 Conclusion

14.0 List of References

15.0 Nomenclature

Appendix I Wave Cycle Closure

Appendix II Heat Transfer Equations

Appendix III Leakage Equations

List of Figures

- Fig. 1 Pressure Volume (PV) Reference Diagram for GWT analysis
- Fig. 2 Cell outlet deflections at part openings determined from water channel tests
- Fig. 3 Charts for estimating the degree of cell opening needed to generate specified rarefaction waves.
- Fig. 4 Chart for estimating the degree of cell outlet closure needed to generate specified compression waves.
- Fig. 5 Simple wave cycle.
- Fig. 6 Half wave plateau
- Fig. 7 Simple design high pressure scavenge working at 65% of design speed.
- Fig. 8 Design with half wave plateau high pressure scavenge working at 65% of design speed.
- Fig. 9 Scavenge effectiveness.
- Fig. 10 Position Diagram for pressure exchange engine (GWT already demonstrated).
- Fig. 11 Preliminary wave design (PH/PR=4.0 GWT)
- Fig. 12 Early predictions for compound cycles, temperatures and pressures.
- Fig. 13 Early predictions - Design point performance
- Fig. 14 GWT - GT Compound plant at $R_G = 5.5$
- Fig. 15 GWT - GT Compound plant at $R_G = 2.7$
- Fig. 16 GWT - GT types
- Fig. 17 Temperatures supercharged GWT (1985)
- Fig. 18 100mm Dia supercharged GWT power, airflow and fuel.
- Fig. 19 600 lb. Thrust bypass jet engine with GWT.
- Fig. 20 GWT - GT for high pressure gasifier heat supply.
- Fig. 21 GWT - GT Volatiles gasifier energy balance.
- Fig. 22 Combined cycle - Turbocharged GWT + steam.

1.0 Introduction

Gas wave turbines (GWTs) are machines which use pressure waves for compression and expansion of gases within cell rotors in the known manner of pressure exchange but also provide shaft power from the change in whirl momentum as gases enter and leave the cells. Cycles involve a low pressure scavenging stage in which cells are filled with cool air and at maximum cycle pressure a high pressure scavenging stage extracts this air and refills cells with hot combustion gas. Between these are compression and gas expansion stages where the strongest pressure wave effects are utilised. An experimental engine of 9 inch rotor size has already demonstrated feasibility (Pearson (1) & (2)). At the time this was called a "Pressure Exchange Engine", a name still retained in a new I.C. Engine publication (6) but a change to GWT seems necessary since the old name causes confusion with diesel engine superchargers. (It was classified so at the 1983 CIMAC Conference in Paris (1)).

Such engines have little to offer in naturally aspirated form except in certain small portable military electric generators and some heat and power co-generation schemes needing low maintenance and long life. However, as topping stages for gas turbines and in combined cycle applications performance calculations show that much better fuel economy and specific power should be achievable than when gas turbines are used alone. Also recuperators or regenerators are rendered unnecessary.

The GWT has an inlet port extending over only about $\frac{1}{3}$ of the rotor blade annulus and so is unable to swallow an airflow comparable with that of an axial compressor. When supercharged this becomes an advantage, however, since the high pressure blading of axial compressors become inconveniently short. But the main advantage accrues from the very high permissible gas inlet temperature made possible by the cooling effect of fresh charge alternating with admission of hot combustion gas. As a rough working rule optimum conditions are realised when the fully mixed exhaust temperature from the GWT topping stage is equal to the maximum permissible temperature of the turbine used for providing boost and this will approximate the leading edge temperature of the cell rotor - normally the hottest part.

A simple introduction giving the basic principles of pressure exchange

and describing some working cycles is given in an accompanying paper "A Gas Wave Turbine which developed 35 Horse Power and performed over a 6:1 speed range" (2). It will be assumed that the reader is familiar with these principles and basic geometry. A start will now be made by first discussing methods of performance analysis and this will be followed by detailed mathematical evaluation.

1.1 Heat Transfer and Mixing

Heat transfer calculations clearly form an important part of any analysis involving GWTs. Heating of fresh charge and cooling of hot gas reduce the effective cycle temperature ratio on which the GWT depends and so have adverse thermodynamic effects which are taken into account in the following analysis. Also the balancing of total heating and cooling effects determine the rotor temperature. During gas admission turbulent forced heat transfer is the dominant mode but there are substantial phases within the cycle when rotor blades have no forced component but natural convection in the very high acceleration produced by rotation is significant and needs inclusion. Also radiation to the cooler stators needs taking into account. Friction heating during low pressure scavenge also raises the effective minimum temperature and has a significant adverse effect apart from the friction loss itself.

To minimise the effects of heat transfer and friction the cell pitch/chord ratio should not be too small. Unfortunately losses caused by opening and closure to stator ports increase in proportion to pitch/chord ratio. So there is an optimum value which can only be determined by rigorous and detailed calculation. Greatest "port edge" losses arise as the cell outlet ends open to ducts at lower pressure since initial velocities are high and the port edge causes deflection in an adverse direction. Fig. 2 illustrates this deflection using results from water channel tests. However, a number of expedients can be used to minimise this effect and although such means are not described in the text it is assumed one has been adopted.

Another problem arises from exhaust gas left in the cell ends after low pressure scavenge. Mixing effects between air and exhaust gas were found to be much greater than anticipated in the tests so that the average effective temperature at the start of compression was excessive.

This was a primary cause of excessive gas inlet temperature and failure to achieve target performance.

Seippel (3) described how mixing could be minimised by using helical cells so that contact surfaces could move through the rotor in an axial absolute direction so avoiding centripetal acceleration which is the primary mixing agent. It is however impractical to use cells of such high stagger and so mixing will always be a problem. It can be minimised in various ways but about a 20% overscavenge seems to be needed in order to sweep out most of the mixing zone. The disadvantages are extra scavenge losses and particularly the dilution of exhaust temperature, a main advantage of the GWT being its ability to provide a hot exhaust. Cycles can be designed which minimise the net overscavenge and yet avoid trapping excessive exhaust gas.

1.2 Thermodynamic Analysis based on Pressure Volume Diagrams.

There is no substitute for wave plotting either graphically or by computer for first designing GWTs and estimating performance. These methods require considerable time and effort and for more rapid evaluation over a wide range of conditions a thermodynamic method can be used. This regards all processes as quasi static and ignores wave effects directly, but losses associated with them and other flow losses including nozzle and cell opening losses are taken into account by a polytropic flow efficiency. The latter uses one or more wave plots for its calibration and in general a value of about 60% is found to be reasonable. Reference to the "pressure volume" diagram is more meaningful than the temperature entropy state diagrams in general use for turbomachines.

Many investigators, having a background in conventional gas turbomachinery, prefer to represent pressure exchange or GWT processes on a temperature-entropy diagram and ignore pressure-volume (i.e. P-V) analysis. Whilst this is perfectly admissible for specifying end to end gas states, the approach fails to allow of sufficient detail and sometimes leads to misunderstanding and incorrect interpretation. For example, most authors refer to "compression efficiency" for these machines and apply the same criteria as for axial or centrifugal compressors. But the latter are adiabatic machines and it is admissible in such cases to calculate efficiency from measured pressures

and temperatures. Pressure exchange is essentially non-adiabatic and indeed heat transfer effects produce temperature increases some five times those attributable to friction without representing losses in compression efficiency. There is therefore no direct relation between compression efficiency and measured temperatures and pressures. Indeed it is virtually impossible to assign any meaning to the term "compression efficiency" for pressure exchange.

One instance of complete misinterpretation became evident when one researcher in the field recently stated that in the high pressure scavenging stage the contact surface must not be allowed to pass through the cells as this would cause hot gas to be discharged with the compressed air, so increasing the mean temperature and therefore reducing compression efficiency. P-V analysis immediately shows this conclusion totally invalid. Over-scavenge in the high pressure stage has no effect on losses except for the small extra friction involved in the increased mass transfer and so has virtually no effect on net power output. On the other hand air left in the cell ends is unavailable for combustion and so leads to a higher than theoretical maximum combustion temperature as the fuel flow is fixed for a given pressure ratio. To allow for mixing and stratification a degree of high pressure over-scavenge is in fact highly desirable. This shows how careful one needs to be in the understanding of pressure exchange fundamentals.

P-V analysis starts from an initial trapped charge temperature and pressure, evaluated from heat transfer and friction analysis, plus allowance for some residuals. The required hot gas inlet temperature is then evaluated by thermodynamic analysis. Indeed wave plotting cannot start until this has been fixed so is complementary to P-V based thermodynamic analysis.

Leakage effects also need taking into account. The author is of the opinion that unshrouded rotors will not be feasible for supercharged GWTs owing to the severity of fatigue stresses induced by alternating static pressures on cell walls as they pass through cycles of pressurisation and decompression. Also tip leakage is likely to be excessive owing to the large radial clearances required. Hence leakage losses fall into two categories, those associated with direct loss

through shroud and drum at each end and including any whirl momentum imparted and the intercell losses arising by leakage over blade leading and trailing edges. All these can be accommodated by thermodynamic analysis.

It is a very simple matter to include the conventional turbomachinery used for boosting the GWT and so obtain a complete cycle analysis for the plant. Analysis of the GWT itself is, as must be evident, an unusually complex matter.

TABLE 3.I - EFFECT OF CLEARANCE ON OUTPUT AND THERMAL EFFICIENCY -
By Thermodynamic Analysis.

Data: (Based on Wave diagram of Fig. 11)

T_{max}	1964°K
for rotor at	1173°K
Scavenge ratio to give 900°C (1173°K) exhaust =	1.443
T inlet to prewhirler	505.4°K
P_H/P_R (GWT pressure ratio)	4.0
Prewhirler pressure ratio	1.466
Trapping mass ratio ρ_{WT}/ρ_R	= 1.2148

The net work loss from the scavenging blower is taken as equal to the difference between blower compression work and isentropic expansion to original pressure since the energy is recovered as work by the coil rotor.

Net scavenging blower work = -1.9 KJ/Kg total air

The following table shows how the performance of the GWT will be affected by clearance variation :

<u>$\frac{g_L}{L_r}$</u>						
RELATIVE CLEARANCE	L_r	.002	.003	.004	.006	.008
Factor of Mechanical						
excellence	g_L/x	.1377	.2066	.2755	.4132	.551
Fuel/air $w_p/w_{LPS} = F'$.034	.0326	.0313	.0296	.0259
rotor output W KJ/Kg. w_{LPS}		309.6	281.0	252.1	193.2	132.8
W_o -output with shroud						
drag KJ/Kg w_{LPS}		297.6	269.1	240.1	181.2	120.8
GWT Thermal Efficiency %		19.71	18.86	17.28	14.27	10.5

The fan engine analysis to be described assumed $g_L/L_r = .003$ and means that combined clearances need to be maintained at only 20% of rotor axial expansion for single land sealing.

4.0 Heat Transfer and Friction

The reference temperature T_R based at cell rotor total exhaust Pressure P_R is the average at the end of low pressure scavenge including all heat inputs by heat transfer, friction and the trapping of residual exhaust gas.

4.1 Heat Transfer

In Appendix II forced convective cooling is considered with cell wall heat transfer assumed equal to that of impulse turbine blades. An evaluation based on the preliminary wave design of Fig. 11 and assuming an air entry temperature T_A of 386°K and a rotor temperature of 1173°K (900°C)

$$\text{gave } \Delta T_q = 47.2^\circ\text{C}$$

i.e. 6% of $T_{\text{ROTOR}} - T_A$ the mean differential

4.2 Friction

Air enters from the inlet guide vanes at absolute speed v_1 and the wave design of Fig. 11 is arranged to give zero incidence on the rotor. The relative cell gas speed w causes friction but on average finally trapped air only travels half the cell length. If friction factor f is used as in pipe flow (but increased three times for safety) it is then readily shown that :-

$$\frac{\Delta T_f}{T_A} = \frac{(K-1)}{2} \left\{ \bar{f}_{LS} \left(\frac{v}{a_A} \right)^2 + \frac{2fL}{d_h} \cdot \left(\frac{w}{a_A} \right)^2 \right\} \quad (36)$$

where ΔT_f is the temperature rise caused by friction

\bar{f}_{LS} is the stator friction loss coefficient = 0.08

also d_h is hydraulic mean dia. where H = blade height :

$$d_h = 4 \cdot H \cdot C_g / (2 \cdot H + 2 \cdot C_g) \quad (37)$$

L/C_g is the cell length/flow width ratio given by

$$\frac{L}{C_g} = \frac{L_r}{\cos \xi \cdot \delta \cdot F_B \cdot \cos \xi} \quad \text{or} \quad \frac{L_r}{F_B \cdot \delta \cdot \cos^2 \xi} \quad (38)$$

where FB = factor allowing for blade blockage of the annulus

and L_r = rotor axial length

ξ = cell stagger

For this design $L/C_g = 6$

giving $L/d_h = 3.5$

Then using the values of v_1 and w read for states (2) and (8) of Fig.11
i.e.

State	v_1/a_g	w/a_g
2	.62	.7
8	.58	.38

for $Re = 1 \times 10^5$, $f = .0046$ (pipes) and $f = 3 \times .0046$ is assumed.

The average value of $\Delta T_g/T_A$ becomes .0119 yielding

$$\Delta T_g = 4.6^\circ\text{C for } T_A = 386^\circ\text{K}$$

$$\text{But } \Delta T_q = 47.3^\circ\text{C}$$

$$\text{Total } \Delta T = 51.8^\circ\text{C}$$

If a further 9° is allowed for trapping of residuals when the cell is
overscavenged (a scavenge ratio λ of 1.2 or over) then:

$$\Delta T = 60^\circ\text{C}$$

$$T_b \text{ becomes } 446^\circ\text{K}$$

But a further 20°C needs adding to allow for heat transfer during
compression so that wave plotting can then assume isentropic processes
without excessive error. Friction heating can only account for about
10% of the total unwanted temperature gain according to this evaluation.

5.0 Port Opening and Closing Losses

Port closure losses can generally be made small during the expansion
phase but opening losses are very significant due to high initial speed
and the unfavourable deflection caused by the port edge.

In Fig. 2 deflections for two cases are given obtained from water
channel tests and these results are used in a complete analysis to

determine overall polytropic expansion efficiencies.

The results also enable rarefaction waves projected at different cell openings to be calculated and a convenient chart is given in Fig. 3. The full wave amplitude $\pi_H - \pi_P$ will be known for full opening, occurring when the datum cell wall is a distance $y = 5-t_e$ past the edge where t_e is the trailing edge thickness. It is convenient to divide this amplitude into $1/2$, $1/4$ and $1/8$ values for plotting and then the relative openings $y/5$ can be read off from Fig. 3 to specify the start of each of these fractional wave elements.

A chart giving outlet port closure progressions for similar wave fractions is given in Fig. 4. Clearly deflections will be very small and in any case will be favourable and so are ignored. Since gas speeds are also generally low, outlet port closure losses will usually be insignificant.

5.1 Cell inlet opening losses

These are most significant at start of high pressure prescavenge when pressure differentials are large leading to high stator nozzle exit speeds particularly at partial opening. Also there is an unfavourable deflection and this can again be estimated using the $\alpha = 70^\circ$ case in the experimental results shown in Fig. 2. No chart corresponding with Figs. 3 and 4 is included but the cell progressions y needed to yield specified fractional wave generation can be calculated by balancing the flow from the nozzle to the flow developing behind the compression wave front generated. If the cell is assumed to contain stagnant gas at pressure parameter π_P corresponding with the wave foot then at cell pressure π the cell gas velocity using a well known wave equation (Bannister 5) will become :-

$$W = C_R \cdot S_A \cdot \frac{2}{k-1} \cdot (\pi - \pi_P) \quad (39)$$

Whilst the absolute nozzle exit velocity v_1 will be

$$\frac{v_1}{C_R} = \sqrt{\frac{2}{(k-1)} \gamma_1 \cdot (\pi_1^2 - \pi^2) S_1^2 - \frac{2 f L}{d} \left(\frac{W}{C_R}\right)^2} \quad (40)$$

This apportions half the friction loss of the cells to each cell end boundary but incidence at cell inlet is ignored. η_1 is nozzle efficiency

$$\eta_1 = 1/(1 - \xi_{LS}) \quad (41)$$

Then equating flow from part open nozzle to gas speed in cell we have :-

$$C_d \cdot y \cdot \cos \beta \cdot V_1 = \delta \cdot F_B \cdot \cos \zeta \cdot u \quad (42)$$

where C_d is a coefficient of discharge = .9 caused by jet contraction as it leaves converging walls.

If the nozzle angle α is specified this will apply at full opening and by equating it can be shown that for the wave head amplitude π_H

$$\pi_H = \frac{\pi_F}{(1+A)} \left\{ 1 \pm \sqrt{(1 - (1+A) \cdot (1 - A(\frac{\pi_F}{\pi_F})^2))} \right\} \quad (43)$$

where:

$$A = \left\{ \frac{\cos \alpha}{F_B \cdot \cos \xi} \cdot \frac{S_i}{S_A} \right\}^2 \cdot \frac{(K-1)}{2} \cdot \frac{2}{\left\{ 1 + \frac{2fL}{d} \cdot \frac{\cos \alpha}{F_B \cos \xi} \right\}} \quad (44)$$

Note S_A - entropy function cell contents (it is assumed that $S_A = 1$)

S_1 - " " entry gas.

$$S = (T/T_R)^{1/2} / (P/P_R)^{1/\gamma}$$

Then for part openings the wave fraction ev needs to be specified, i.e.:

$$ev = (\pi - \pi_F) / (\pi_H - \pi_F) \quad (45)$$

If now variable Z is defined as :-

$$Z = (\pi - \pi_F)^2 / (\pi_1^2 - \pi_F^2) \quad (46)$$

and is calculated then from Z the value of parameter

$$C_d \cdot \frac{y}{\delta} \cdot \cos \beta \quad (47)$$

can be obtained from :

$$C_d \cdot \frac{y}{\delta} \cdot \cos \beta = F_B \cdot \cos \gamma \cdot \frac{S_a}{S_i} \sqrt{Z \cdot \frac{2}{(K-1)} \cdot \frac{1}{2} \left\{ 1 + \frac{2fL}{d_h} \left(C_d \cdot \frac{y}{\delta} \cdot \frac{\cos \beta}{F_B \cdot \cos \gamma} \right)^2 \right\}} \quad (48)$$

since C_d and $\cos \beta$ are both functions of α and y/δ the required value of y/δ can be determined.

The above expressions were derived ignoring entropy and pressure gain effects from sudden enlargement of jets entering cells partially open.

7.0 Design Wave Plotting

In Fig. 10 only the wave position diagram for an engine very similar to the one tested is given. A total of four diagrams are needed to synthesise a complete design. A wave plot such as shown in Fig. 11 is produced by the simultaneous generation of a state diagram (top left) in which pressure parameter π is plotted to a base of non dimensional relative cell velocity w/a_r , and position diagram (right) in which velocities of gases and wave propagation are plotted to an absolute frame of reference. The latter also represents one cycle of operation of each cell as it passes the fixed stator ports which are also shown. To transfer gas particle and wave propagation speeds from the state to the position diagram a pole diagram (centre) is needed. This is shown as for cells with axially oriented walls. It has the same w/a_r as the state diagram but the ordinate is non dimensional mean blade speed corrected for cell stagger angle ξ , i.e.

$$\text{pole diagram ordinate } Y_R = \frac{U}{a_r} / \cos \xi \quad (49)$$

A more complete description is given in Ref. 6.

Waves travelling along cells with reference speed a_r will displace vertically a distance Y_R as they move from an inlet to outlet or from cell outlet to inlet. Movement at other speeds C/a_r or w/a_r give vertical displacements on the position diagram in inverse proportion. Such vertical displacement will subsequently be called "progression" and is

given in cell pitches, i.e. $Y/8$. In the actual engine the stators require an angular offset with respect to each other to compensate for cell stagger.

In later designs it was found better to set up the pole diagram with cell walls at the true stagger angle in order to avoid this angular correction and give a more accurate wave interpretation. It should also be noted that π is regarded as "pressure" not speed of sound. Some authors use a vertical scale for the state diagram as a/a_R which is a big mistake because unless the ordinate is visualised as "pressure" it will not be possible to create an appropriate mental image of the flow processes taking place.

A fourth diagram (bottom left) is also shown. This is a vector diagram for cell inlet and outlet used for measuring the stator inlet angles needed to give zero incidence on the rotor or, alternatively, for giving the incidence when stator angles have been fixed. Also the outlet stator duct inclinations for zero incidence are generated.

7.1 Effect of Design Mean Blade Speed on Cell Length

From the foregoing it can be deduced that a wave at reference speed a_R travelling from cell inlet to outlet and reflecting back again to form a wave-pair will require a period in which cells progress a distance Y in time t at mean blade u given by:-

$$Y = u \cdot t = u \cdot 2 \cdot L_r / (a_R \cos \frac{\gamma}{2}) \quad (50)$$

$$\text{or } \frac{Y}{8} = \frac{u}{a_R} \cdot 2 \cdot \frac{L_r}{8} / \cos \frac{\gamma}{2} \quad (51)$$

Now regardless of mean blade speed a complete design point cycle must occur in a given number of reference wave-pairs n_T so except for adjustment of port edge angles and some consequent alteration of cell end boundary state conditions, a plot such as Fig. 11 can be used for approximate analysis with other design blade speeds and in this case $n_T = 5.18$.

If Y_T is the total cell progression for one cycle ($Y_T/8 = 18.4$ in Fig. 11) then :-

$$\frac{Y_T}{\delta} = n_R \cdot \frac{U}{a_R} \cdot 2 \cdot \frac{L_r}{\delta} / \cos \psi \quad (52)$$

But the value of Y_T/δ remains constant regardless of u for the wave plot to remain unchanged and give the same proportion of cell opening periods.

Hence rearranging :-

$$\frac{L_r}{\delta} = \frac{Y_T}{\delta} \cdot \frac{\cos \psi}{2 \cdot n_R} / \left(\frac{U}{a_R} \right) \quad (53)$$

and the cell length/width ratio L/C_g by substituting from equation (38) becomes :-

$$\frac{L}{C_g} = \frac{Y_T}{\delta} \cdot \frac{1}{2 \cdot n_R \cdot F_2 \cdot \cos(\psi) \left(\frac{U}{a_R} \right)} \quad (54)$$

Note $L/d_h = 1.8L/C_g$ from equation (37). Clearly as mean blade speed increases the cell length/width ratio and consequently L/d_h reduces and since friction and heat transfer during scavenging increase with L/d_h , it is advantageous to run at the highest possible mean blade speed in order to minimise both these effects.

It needs to be stressed that the above argument refers to design conditions only so that cell length is a variable. The ability of a given design to operate over a speed range is a totally different matter.

8.0 Choice of Topping Stages

Pure Pressure Exchange Versus the GWT.

Pure pressure exchangers provide no shaft power but give output as either a hot gas bleed from the combustor or as an elevated exhaust pressure. In either case shaft power is ultimately obtained by the use of conventional turbines operating from the availability generated. In the special case of application to diesel engine supercharging no output is obtained and it is unlikely that the GWT could be substituted to advantage. However, for gas turbine topping application for improvement of fuel consumption and specific power without need for heat exchange or regeneration, a choice needs to be made between the two. In the following a complex of factors

is discussed for rationalising this choice.

Firstly, pure pressure gain across a low pressure scavenging stage is difficult to achieve and cannot therefore be very large because of the adverse density balance of exhaust gas with respect to incoming air. Gas bleed from the combustor or from an expansion stage between HP and LP scavenging stages seem more promising alternatives but generally need either partial admission or side channel turbomachinery whose efficiency is depressed from the value of about 87% for full admission to about 65%.

This is about the same as can be achieved by the use of a GWT rotor as a turbine and so dividing the functions of pressure exchange and output turbines into separate specialised components is unlikely to achieve more than marginal advantage. Also as explained in Section 2.0 such low turbinning efficiencies are acceptable in the GWT.

Secondly existing pressure exchangers run at low mean blade speed and so a large L/dh is involved as explained in Section 7.1 yielding equation (54). This means that cell friction and heat transfer effects must be several times larger making the use of uniflow scavenging impractical. Uniflow scavenging means the same direction of flow in both high and low pressure stages and gives the most uniform rotor temperature. Contraflow scavenging on the other hand keeps the cool air inlet and outlet at one end with hot gas confined to the other. There will be a hot and cool end to the rotor and the hot end will show little advantage of natural cooling over an uncooled gas turbine.

If high mean blade speed is adopted to eliminate these disadvantages then it makes sense to abstract power from the rotor shaft by change of whirl from inlet to outlet and then the pressure exchanger will have been converted to a GWT. It will have a lower efficiency of turbine action than a dedicated turbine but the cell friction losses causing this have to be accepted in any case since scavenging is fundamental and also this friction will have been reduced by change to high speed.

Stator pockets can be employed to widen the operating speed range of pressure exchangers and involve a release of kinetic energy. This can

only be efficiently converted to shaft power by the use of high speed rotors.

The excessive mixing or stratification effects caused in high centripetal fields at contact surfaces between gases of very different density can be adequately minimised by the use of cell wall stagger $\frac{1}{2}$ of about 37 degrees. This can only be used with uniflow scavenging of course.

Pure pressure exchange involves an extra shaft which runs at relatively low speed and so increases mechanical complexity of the complete engine. The GWT on the other hand can reduce mechanical complexity. An advanced GWT could have a pressure ratio as high as 12:1 but at 8:1 would provide just the right power to drive a supercharging compressor of 4:1 pressure ratio. The overall 4 x 8 or 32:1 pressure ratio of the complete engine ought to give the fuel economy of a diesel and analysis shows very good part load economy even as low as 4% of full load. This is achieved with a very simple geometry of the kind illustrated in Fig. 16, Type B. The output is all taken from a conventional turbine operating over a 4:1 pressure ratio - equal to the compressor. If this has a separate shaft then the desirable falling torque characteristic needed for traction applications or for helicopters is readily provided.

This argument does not mean that auxiliary partial admission or side channel turbines should never be used in conjunction with GWT's. In some designs in order to maximise swallowing capacity the optimum arrangement involves such auxiliaries.

Pure pressure exchange does have several advantages however. The rotors are long and prismatic. They are simple to make and could even be extruded whilst GWT rotors have twisted complex blade shapes. Low centrifugal stresses mean thin shroud and drum which have uniform thermal response and make the use of ceramics more practical. This could partly offset the advantage of the cool rotor of the GWT which needs to be made in metal. For example, a ceramic limited to 1200°C might permit a gas inlet temperature of 1350°C for a contraflow pressure exchanger. Later it will be shown that an advanced cycle GWT with a rotor limited to 800°C would permit a gas inlet temperature of 1650°C to be used. So a 300°C advantage

still seems available to the GWT.

However, thermal and mechanical stresses are low for pressure exchangers whilst the interaction of thermal and centrifugal stresses pose a difficult problem for the GWT. For the engine tested a complete SP452 steel brazed fortiweld rotor proved reliable in withstanding numerous hot starts and stops during about 300 hours of endurance running. This involved speeds of 18,000 RPM on a rotor of 9 inch blade tip diameter (inside shroud with combustion gas temperatures of 1000°C). However, maximum rotor temperatures were only 450°C and with more exotic materials at say 800°C it may be necessary to change to a segmented running shroud and yet no extra measurable leakage can be accepted.

8.1 The GWT and the Gas Turbine

Finally when considering the GWT in relation to a conventional gas turbine working over the same pressure ratio it must be remembered that compression is achieved without need of shaft power for the former only. Since about 2/3 of the turbine output needs transfer to the compressor for the latter case it follows that the total whirl change required across the GWT for the same blade speed will be only about 1/3 of that needed for a gas turbine.

9.0 THE GWT AS A TOPPER FOR GAS TURBINES

Performance Predictions.

9.1 Early Predictions 1938

These are presented first since the assumptions still appear reasonable although the maximum metal temperatures of 670°C (1237°F) are very low by present day standards. They were never published owing to rejection by assessors on grounds of inadequate experimental data.

TABLE 9.II

The assumptions for thermodynamic analysis of
the GWT are listed as under:-

Scavenge ratio $M_{LPS}/M_{TRAPPED}$	= 1.1
Temperature rise by friction + heat transfer in LP scavenge	= 14°C
Combustor pressure loss ΔP_{CC}	= 2%
Leakage shroud and drum from P_H to P_R based on a clearance each end of	= 9% 0.022 inches
Rotor diameter (tip inside shroud)	12 inches
Rotor blade root diameter	= 8 "
Polytropic efficiency η_p for W_{p1} including transfer gas	= 65%
Polytropic efficiency η_p for W_{p2}	= 50%
(This low value was used because in the experimental engine LP prescavenge caused excessive incidence and there were other losses. These effects could now be avoided by a new design cycle)	
Mechanical and shroud drag efficiency	= 95%
Duct loss to output turbine	= 2%
Rotor Cooling total loss (drum and shaft 5% of delivery air cooled 300°C)	

TABLE 9.III

Assumptions for Gas Turbine Components

Turbine inlet temperature	= 1050°K (1430°P)
Polytropic efficiency	= 87%
Exhaust pressure loss	= 1.4%
Combustor pressure loss or duct from GWT	= 2.0%
Compressor inlet pressure loss (silencer and filter)	= 1.0%
Compressor inlet temperature	= 300°K (80°F)
Polytropic efficiency	= 88%
Input power increase factor for cooling air bleed flow and bearing losses/auxiliaries	= 1.035
Net plant output factor for bearing and gear losses	= .95

9.2 Performance Curves

In Fig. 12 the manner in which temperatures and pressures are affected by the boosting compressor pressure ratio R_C are shown.

Curve 1 shows T_0 the GWT inlet temperature rising with R_C and so reducing the cooling differential $(943 - T_0)$ so that the maximum inlet temperature T_{gm} to the GWT curve (4) needs to be progressively reduced. Both effects combine to reduce the GWT temperature ratio T_{gm}/T_0 so that the permissible pressure ratio P_H/P_0 reduces. (7) Here $P_0 = P_R$ the GWT inlet and datum exhaust pressure being equal. P_n curve (8) is 2% lower due to combustor loss and release pressure P_D/P_0 is shown by curve (9). All these progressively reduce. However the GWT power rises from 200 shp for zero boost to a maximum of 550 shp at a boost ratio of 7 ATM and the GWT pressure ratio is then only 2.8. A 12" tip diameter is assumed. (curve 12)

For high values of P_D/P_0 in excess of 2.5 an expansion stage is needed but at less than about 2.2 can be dispensed with reducing the cycle total progression Y_T/δ and so increasing rotor length and swallowing capacity. Hence at high boost, curve 13 represents GWT power.

Maximum pressure P_H rises up to $R_C = 11.5$ curve (10) and the differential between P_H and delivery pressure P_0 (curve (11)) is applied across the GWT. This differential is mostly about 8 to 11 atmospheres.

In Fig. 13 design point performance predictions are shown on the same base of boost pressure ratio. Specific output is given in terms of horse power per pound of air per second (right hand scale for dashed curves). Thermal efficiency and corresponding specific fuel consumption are shown on the left and apply to solid curves. The SFC has been converted to modern units of Kg/KWh for kerosene fuel.

The simple gas turbine, of open cycle type with no heat exchange, is shown by curves (14) and (15). Peak efficiency is 24% at $R_C = 10$ but maximum output occurs at $R_C = 6$. To give improved economy a recuperator can be fitted and if a thermal ratio of 0.8 for a penalty of 6% pressure drop is allowed curves (16) and (17) give the new efficiency and power output.

Peak efficiency is increased to 28% at $R_C = 5$ and checks well with published data for the gas turbine driven oil tanker John Sergeant shown as point J.S.

Curves (18) and (19) apply to the GWT alone but in the pressure boosted state showing a maximum thermal efficiency of only 17% at zero boost and falling off rapidly with increased boost. When added to the gas turbine section and without any recuperator the overall efficiency and specific output are shown by curves (20) and (21).

Fuel consumption is better than the recuperative set and the specific output (21) is much improved. The optimum R_C seems to be about 5.5 giving an efficiency of 30.2% and a specific output of 123hp/lb/sec as compared with 70 representing an improvement of 76% and of course absence of the large heat exchanger together with the implied reduction of airflow would make the GWT-GT set extremely light and compact in comparison.

In addition the exhaust temperature of 450°C (778°F) is higher than the 300°C (509°F) of the recuperative set making possible improved further utilisation of exhaust energy.

A layout to scale based on using the Ruston TA industrial turbine is shown in Fig. 14 arranged to operate at this optimum condition. The GWT can only drive a second stage compressor, a first stage of 3.2 pressure ratio needing to be driven by a turbine. A rather clumsy plant is the result.

A simpler and neater solution can be found by matching compressor requirements to the GWT alone. Curve (25) shows the compressor demand and (19) the GWT output. They cross at $R_C = 2.9$ but the penalty is a thermal efficiency reduced to 27% though the GWT pressure ratio is 4.1, within existing experience and equal to the design value for which the plot of Fig. 11 was drawn.

The main components of an engine of this type are drawn to scale in Fig. 15 showing a neat and compact layout. A separate power turbine would provide the falling torque characteristic demanded for traction purposes. Part load calculations showed the GWT to operate with almost unchanged pressure

ratio as the compressor boost ratio changed from 2.7 to 1.4 so thermal efficiency only fell to 17% at 1/10 of full load.

However, fuel economy would need to be improved over the whole range to meet present day competition and the more advanced design to be considered later is therefore required.

But there is further potential for improvement even with the low metal temperatures assumed. Heat exchangers either of regenerative or recuperative type cannot usefully be integrated with GWT plant but intercooled compressors can be used.

Intercooling will allow higher boost pressures without increasing air or combustor inlet temperatures so that rotor temperatures are not increased. The greater turbine expansion ratio produced will however lower the final exhaust temperature and so give improved output.

Curves (22) and (23) refer to such an intercooled plant. Optimum boost ratio is now about 8.5 with the GWT operating at $P_H/P_0 = 3.57$ so that the overall pressure $P_H/P_A = 30.3$ and yields a predicted thermal efficiency of 34.5%. This is not far short of diesel economy and specific output has been raised to 152 HP/lb/sec which is 2.17 times that of the original recuperative gas turbine.

9.3 Summary

In Fig. 16 four diagrams compare the various progressive developments which were envisaged in 1958 starting with the naturally aspirated Type A of 17% thermal efficiency for cogeneration application to Type B of 27% for traction purposes with 2.7:1 boost, then to more complex Type C of 3.5 boost ratio giving 30% and finally the 8.5 boost ratio intercooled set aimed at 34.5% thermal efficiency. All these it should be noted assume the rather high ambient of 27°C (80°F) and low rotor temperature of 943K (1237°F) with other conservative assumptions.

9.4 New Advanced Cycle with Boost from Transfer Gas Exchange

Updated Predictions 1985

The early engine had a number of features preventing high polytropic

turbining efficiencies from being realized among which were very high incidences of up to 90 degrees due to excessive prescavenging inlet velocities. A new advanced cycle has been devised which eliminates this problem and also minimises cell opening losses. It has other important advantages also.

The basic change depends on replacing the effective transfer gas turbinizing action represented by T in Fig. 1 by a GWT stage. Expansion cell pressures drop from P_{eg} to P_0 by extraction of transfer gas as before but the gas is exchanged for intermediate pressure compressed air before being returned to the main cycle to raise the pressure from P_g to P_y . The fluid labelled "Transfer gas" in Fig. 1 now becomes extra air available for combustion and so the final equalisation-compression takes place from a highly boosted state so increasing output and optimum pressure ratio. Indeed a GWT pressure ratio of 12:1 is achievable even without fan assistance in low pressure scavenge and the engine is no more complex than one in which two cycles per revolution are arranged.

There are two or more low pressure scavenging stages, at least one intermediate scavenging stage but still only one high pressure stage with single associated combustor. When carried out with a single rotor the result is a greatly reduced cell length to rotor diameter ratio so reducing rotor weight and improving acceleration.

Furthermore relative time spent at high temperature and pressure is greatly reduced and cooling effects of other stages increased, so leading to considerably reduced rotor temperature or conversely, for a given metal limit, a greatly increased permissible combustor outlet temperature. The cycle has been subjected to detailed evaluation from both the friction and heat transfer viewpoint.

TABLE 9.IV

Assumptions for Thermodynamic Analysis of Advanced GWT

Scavenge Fan pressure ratio full speed	1.4
Average L.P. scav.wave trapping P_{WT}/P_R	1.696
Clearance ratio g_1/L_T (single lands)	.003
Rotor OD (inside Shroud)	100mm
" ID	80mm
Blade Blockage Factor P_B	0.8
Blade Stagger ψ	37°
Polytropic Efficiencies (all)	75%
Number of Boost Stages	2
Main cycle Rarefaction effect P_{EH}/P_H	0.85
Boost cycle " " P_{EB}/P_B	0.8
Boost fan polytropic efficiency	80%
net loss from boost fan is allowed for in printout.	

TABLE 9.V

Case of Zero Supercharge Computed Characteristic

Results of computer printout for inlet conditions to fan
1 ATM (1.01325 BAR) 20°C (293.15°K or 68°F) Atmospheric exhaust

(1)	(2)	(3)	(4)	(5)	(6)	
P_H/P_A	P_H/P_A	$T_{max}^{\circ}K$	$T_{1cc}^{\circ}K$	$T_R^{\circ}K$	W kJ/m ³	
5	2.674	723.9	490.9	311.0	62.9	
6	2.892	819.6	521.3	312.7	122.6	
8	3.325	988.2	570.9	315.4	258.5	
10	3.746	1128.7	607.4	317.6	415.3	
12	4.182	1260	651.6	319.9	572.0	
(1)	(7)	(8)	(9)	(10)	(11)	(12)
P_H/P_A	M_{REF}	M_{LPS}	M_{TRAP}	M_{CC}	M_{KW}	SPC kg/kWh
5	12,940	0.061	0.0507	0.0226	0.635	0.738
6	18,060	0.0847	0.0704	0.0322	1.727	0.537
8	26,220	0.122	0.1014	0.0527	5.286	0.400
10	33,230	0.154	0.128	0.0725	10.764	0.344
12	39,000	0.179	0.149	0.0906	17.40	0.317

KEY

- (1) P_H - Main cycle maximum pressure
- (2) P_B - Boost cycle delivery pressure and equal to mean boost pressure of main cycle
- (3) T_{max} - Delivery temperature from combustor
- (4) T_{lcc} - Inlet temperature to combustor
- (5) T_R - reference - mean temperature after L.P.Scav.
- (6) W - work per unit cell volume
- (7) N - speed for 100 mm tip diameter
- (8)(9)(10) M - mass flows Kg/s, total, trapped and combustion inlet
- (11) W - power Kw
- (12) SFC - Specific fuel consumption

When supercharged the total flow is reduced and made 1.4 times air delivered to combustor.

9.5 COMPOUND GWT-GT

The design point parameters shown in Figures 17 and 18 all assume a GWT pressure ratio of 12, the maximum which can be handled when the main cycle expansion is limited to two outlet transfer ducts. All temperature ratios for the GWT are held constant and are equal to those with atmospheric exhaust. In this case as shown in Fig. 17 all temperatures inclusive of rotor temperature TROT increase rapidly as the boost pressure ratio R_C provided by a centrifugal compressor is increased.

The temperature at turbine inlet TGT1 is almost equal to the GWT rotor temperature and if these are limited to 800°C (1470°F) then R_C is shown to be limited to 3.6 and so overall combustor pressure will be 43 atmospheres.

Turbomachinery Assumptions

Compressor polytropic efficiency	80%
Turbine polytropic efficiency	87%
Mechanical efficiency	98%

Fig. 18 shows the calculated design point power and SPC with a corresponding scale for thermal efficiency showing that the compound plant ought to be capable of achieving a thermal efficiency of 40%. It should be noted how fast output increases with boost, the 100mm dia GWT giving 17 kW at zero boost becomes a topper for a plant giving 140 kW at $R_C = 3.6$. For most applications the compressor needs to be driven entirely by the GWT but analysis shows the GWT to be developing far too much power to give a match. Some needs therefore to be supplied as gas power from expansion stages or the GWT pressure ratio reduced.

10.0 APPLICATION TO BYPASS JET ENGINE

Calculations giving the predicted performance of two cases for bypass engines utilising GWT topping stages are summarised in Fig.19. They both satisfy a military specification for a small engine able to provide 600 pounds of thrust at sea level and a flight mach number of 0.65. The fan was specified as having a pressure ratio of 1.8.

Two cases were studied, one for the low GWT pressure ratio $P_H/P_R = 4$ and the other for the advanced cycle of $P_H/P_R = 12$ both being limited to the

same maximum rotor temperature of 900°C (1650°F).

Results show increased bypass ratio for the advanced design but the overall SFC of 0.709 lb /lb.hr is little better than the 0.731 lb /lb.hr for the lower pressure and the advantage is certainly not worth the increase in maximum pressure P_H from 21.5 ATM to 59.5 ATM which is involved. The froudjet propulsion efficiency :-

$$\eta_{jp} = 2.u/(v + u)$$

is only 63% to 64% due to the high fan pressure ratio and by dropping this the bypass ratio would increase and increase η_{jp} . This would greatly improve the SFC in each case.

13.0 CONCLUSION

A method of Design involving the interaction of pressure-volume based thermodynamic analysis and wave plotting by the Field method of Characteristics for one dimensional flow has been described. It was used for the performance prediction of gas wave turbines (GWT's). The analysis included the effects of gas friction, heat transfer and leakage. The latter included intercell leakage over blade ends as well as the total losses from circumferential clearance gaps at hub and running shroud. Data was presented for enabling wave development to be accurately plotted for finite cell width and for evaluating cell opening losses. Such one dimensional treatment can lead to workable designs as already demonstrated by the first fairly successful experimental engine but it would be valuable to give a final check using the slow but sophisticated three dimensional code developed by Professor Spalding.

Wave systems, particularly the author's "Half wave plateau" type for dealing with the triple problem of finite cell width, wave cycle closure without carry over effects and obtaining adequate speed range without adjustable ports, have been described and illustrated.

The complex of factors needing to be considered for choosing between pure pressure exchange, operating at low mean blade speed, and the high speed GWT alternative for use as topping stages was studied. The GWT was consequently chosen for further study as on balance it seemed to show the greater promise.

Application as topper for an otherwise conventional gas turbine was shown to be attractive. So far unpublished predictions for such compound plant made 22 years ago were first presented since the assumptions still appear valid though temperature limitations now seem overconservative. Even so thermal efficiencies of 30% without heat exchange or intercooling and 34% with intercooling alone and greatly improved specific power were predicted.

Then a new advanced GWT binary cycle capable of developing pressure ratios of up to 12:1 in a single rotor was introduced. It had enhanced natural cooling so permitting the use of exceptionally high combustor outlet temperatures and the cycle is capable of solving the limitations of the

earlier engine. Thermal efficiencies of 26% with atmospheric exhaust and 40% when boosted to 3.6 atmospheres using a centrifugal single stage compressor and axial turbine were predicted. A GWT of only 100 mm blade tip diameter could be the core of a compound plant developing a power output of 130 kW and the final turbine exhaust would still be quite high at 820°K (1020°F) so that further improvement by the use of an intercooler for increase of boost pressure without raising rotor temperature beyond 800°C (1470°F) is feasible.

Application to small bypass jet engines has been studied showing the advanced cycle to offer only marginal improvement in SFC as compared with a low pressure ratio GWT, the value of .709 lb fuel/hr/lb thrust at combustor pressure of 59.5 atmospheres comparing with figures of .731 at 21.5 atmospheres.

Finally application to coal gasification and to combined cycle electricity power generating schemes was described and shown to offer attractive economies in both fuel consumption and capital charges. Further effort to advance such developments is recommended.

14.0 List of References

1. Pearson, R.D.
A Pressure Exchange Engine for burning "Pyroil" as the end user
in a cheap power from Biomass System.
CIMAC Conference Papers, Paris 1983.
2. Pearson, R.D. (accompanying paper).
A Gas Wave Turbine which developed 35 HP and performed
over a 6:1 speed range.
Wave Rotor Workshop, Monterey 1985.
3. Seippel, Claude.
British Spec. No. 553,808 1941
(Pressure Exchanger for a gas turbine locomotive).
4. Pearson, R.D. and Sooton, G.E.
Improvements to Pressure Exchangers.
British Patent No. 5.
803,659 Jan 13, 1954
803,660 Oct 29, 1958
843,912 June 30, 1955
843,913 "
843,914 "
5. Bannister, P.K. (University of Nottingham)
"Pressure Waves in Gases".
Akroyd Stuart Memorial Lectures, 1958.
(Wave Plotting method with useful notation)
6. Ed. Horlock, J.H. and Winterbone, D.E.
Internal Combustion Engines, vol. 2.
Benson Memorial Volumes.
Chapter 16 - Pressure Exchangers and Pressure Exchange Engines.
Contributed by R.D. Pearson.
Oxford University Press 1985.

7. M.A.N. Turbochargers.

Single stage exhaust-gas-driven MA & MA-UP type
turbochargers with axial flow turbines.

M.A.N. - B & W Diesel Stadtbachstrasse 1
D-8900 Augsburg 1, Germany.

NOMENCLATURE

Suffices

- F - wave foot (zero wave amplitude)
- M - mid wave (amplitude)
- H - wave head (full wave amplitude)
- R - reference (state)
- i - inlet (of cells)
- o - outlet (from cells)
- r - reflected
- t - transmitted

Symbols

- a - speed of sound a_R is at reference temperature T_R measured at P_R
- b - $(k-1)/2$
- c - wave propagation speed
- i - +1 or -1 a direction marker for wave propagation
- k - ratio of specific heats
- L - cell length
- P - Pressure
- S - entropy function i.e. $S' = (T/T_R)/(P/P_R)^{\frac{k-1}{k}}$
- S' - is also the volume increase ratio produced by combustion (very nearly)
- t - time
- T - temperature absolute °K
- U - mean cell rotor blade speed
- w - gas particle speed relative to cell walls
- W = w/a_R the non dimensional gas particle speed
- x - distance along a cell
- y - rotor progression from start of L.P. scavenge measured at inlet
- Y = y/δ non dimensional progression
- Z - wave amplitude = $\pi_H - \pi_F$
- δ - cell pitch
- π - pressure parameter $\pi = (P/P_R)^{\frac{k-1}{2k}}$
- S_F - shock front (on diagrams)

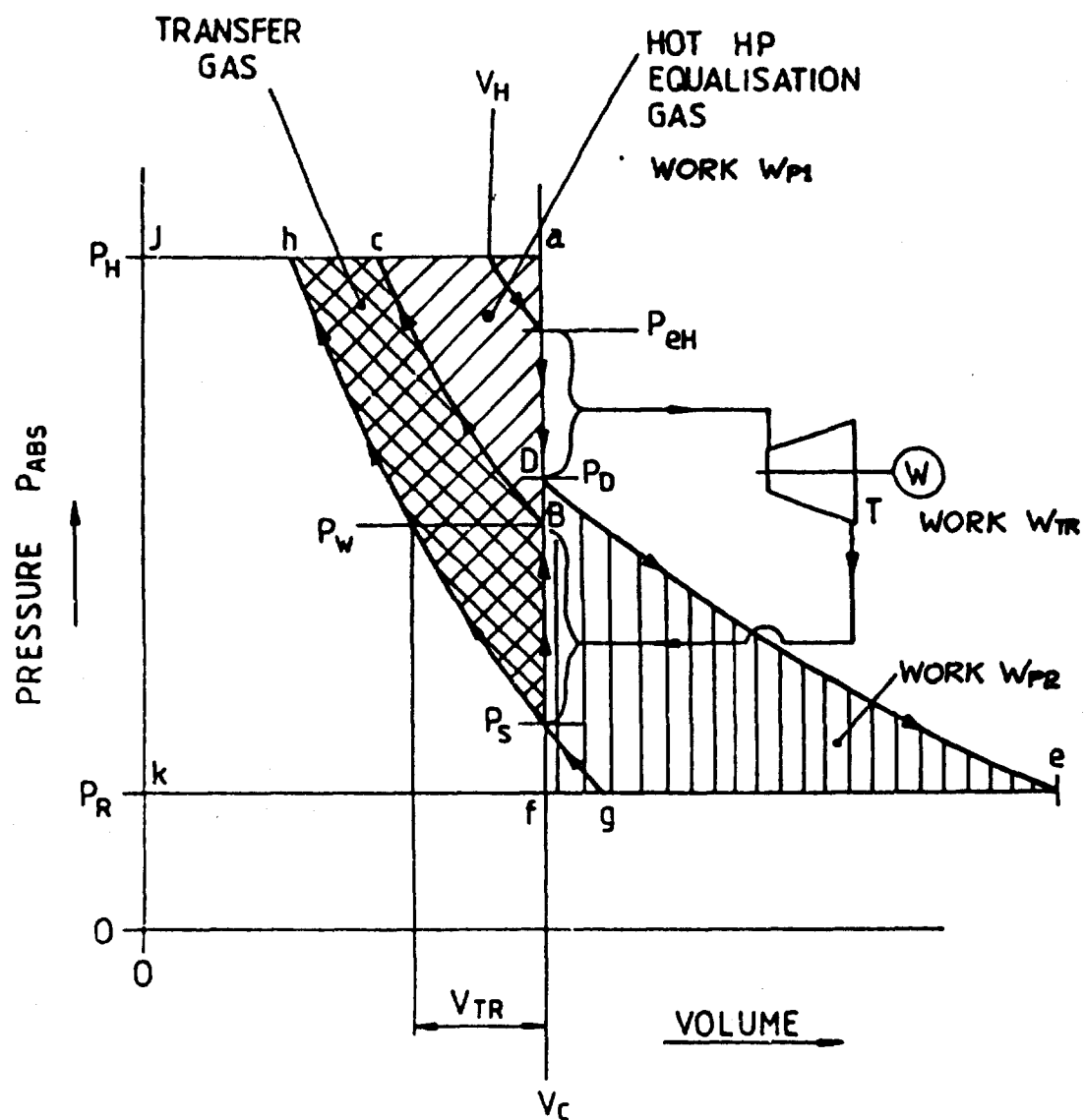
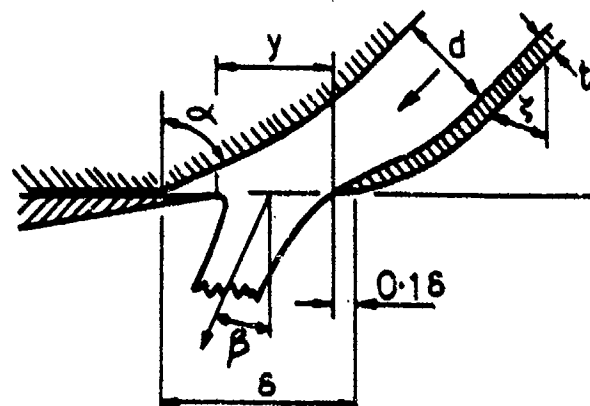
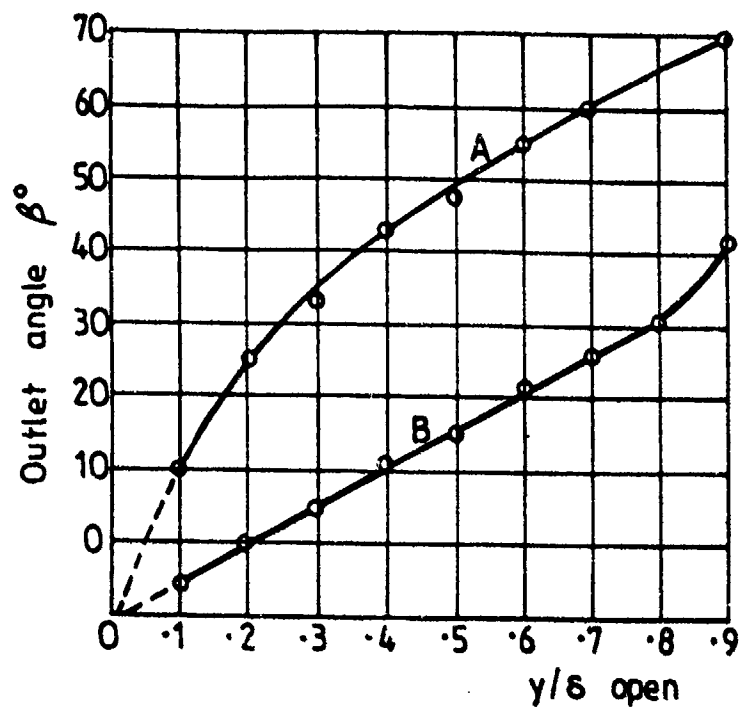


FIG.1. PRESSURE VOLUME (PV) REFERENCE
DIAGRAM FOR GWT ANALYSIS



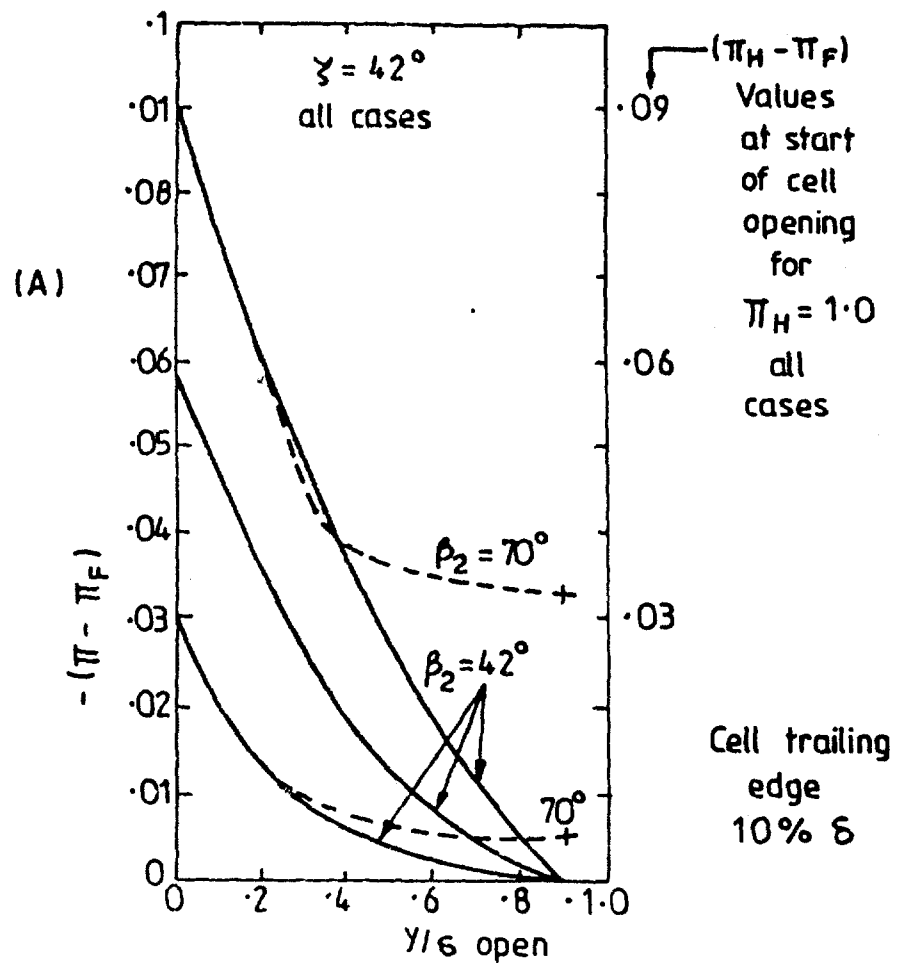
$$A - \zeta = 42^\circ \quad \alpha = 70^\circ$$

$$B - \zeta = 42^\circ \quad \alpha = 43^\circ$$

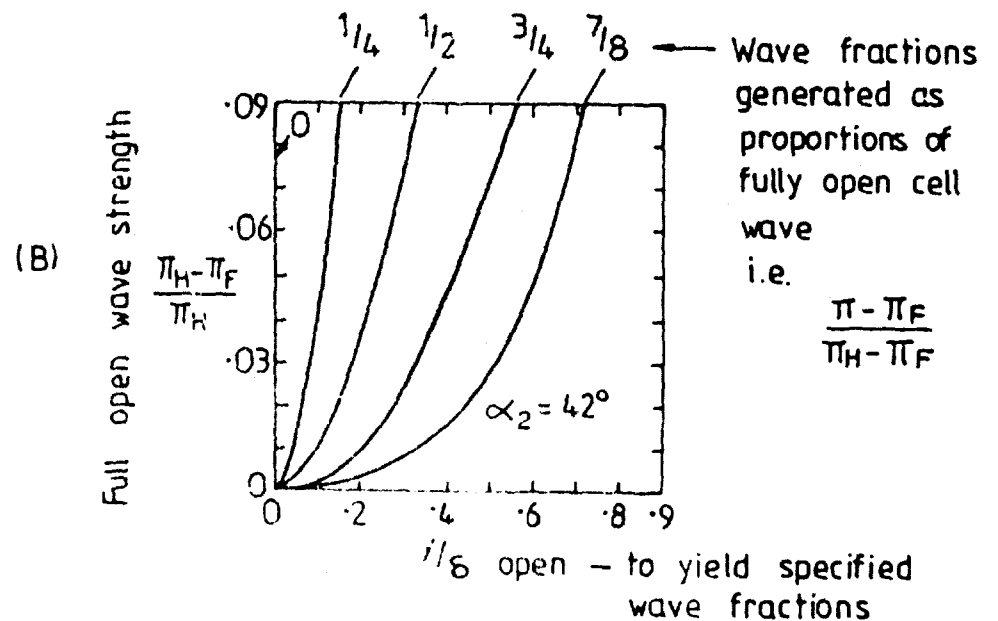
$$\frac{a}{a+t} = 0.75$$

$$\delta = 1.0", \quad H = 1.65" \text{ (Water approach depth)}$$

FIGURE 2. CELL OUTLET DEFLECTIONS AT PART OPENINGS
DETERMINED FROM WATER CHANNEL TESTS



(B) is derived from (A)



Use generalised Chart (B)

FIGURE 3 CHARTS FOR ESTIMATING THE DEGREE OF CELL OPENING NEEDED TO GENERATE SPECIFIED RAREFACTION WAVES

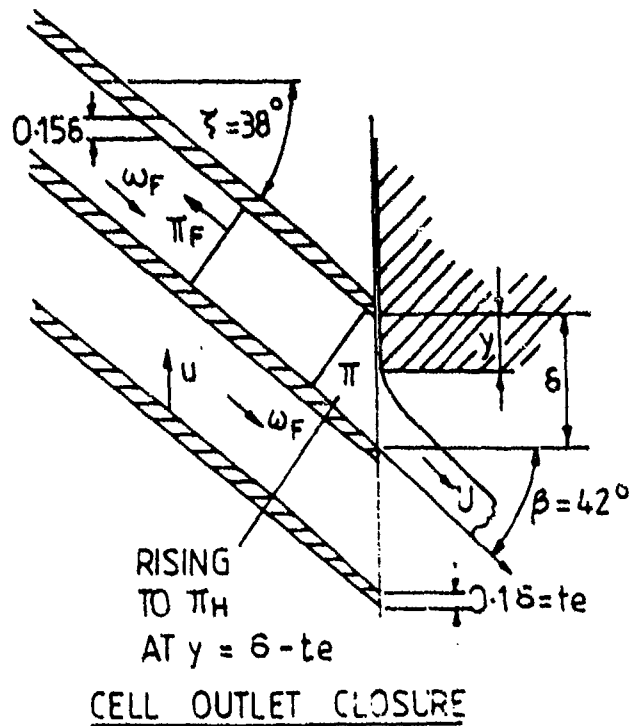
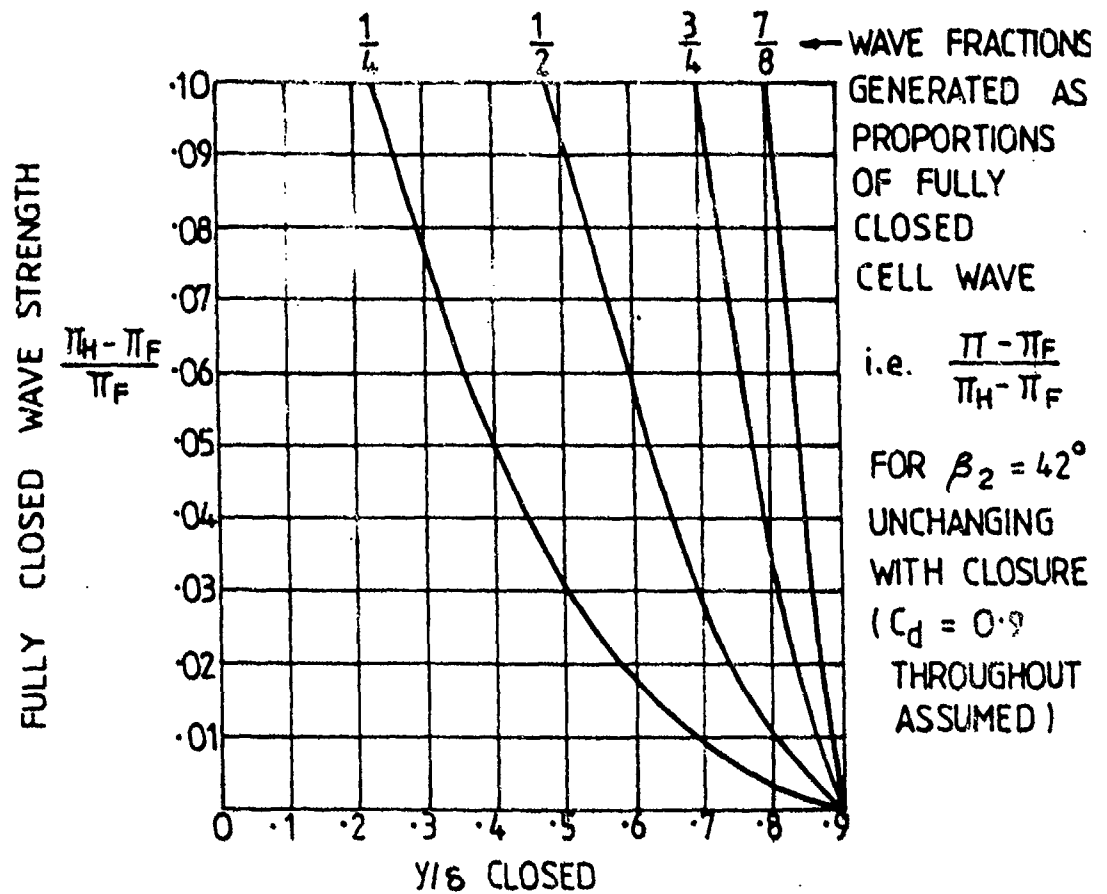


FIG. 4. CHART FOR ESTIMATING THE DEGREE OF CELL OUTLET CLOSURE NEEDED TO GENERATE SPECIFIED COMPRESSION WAVES

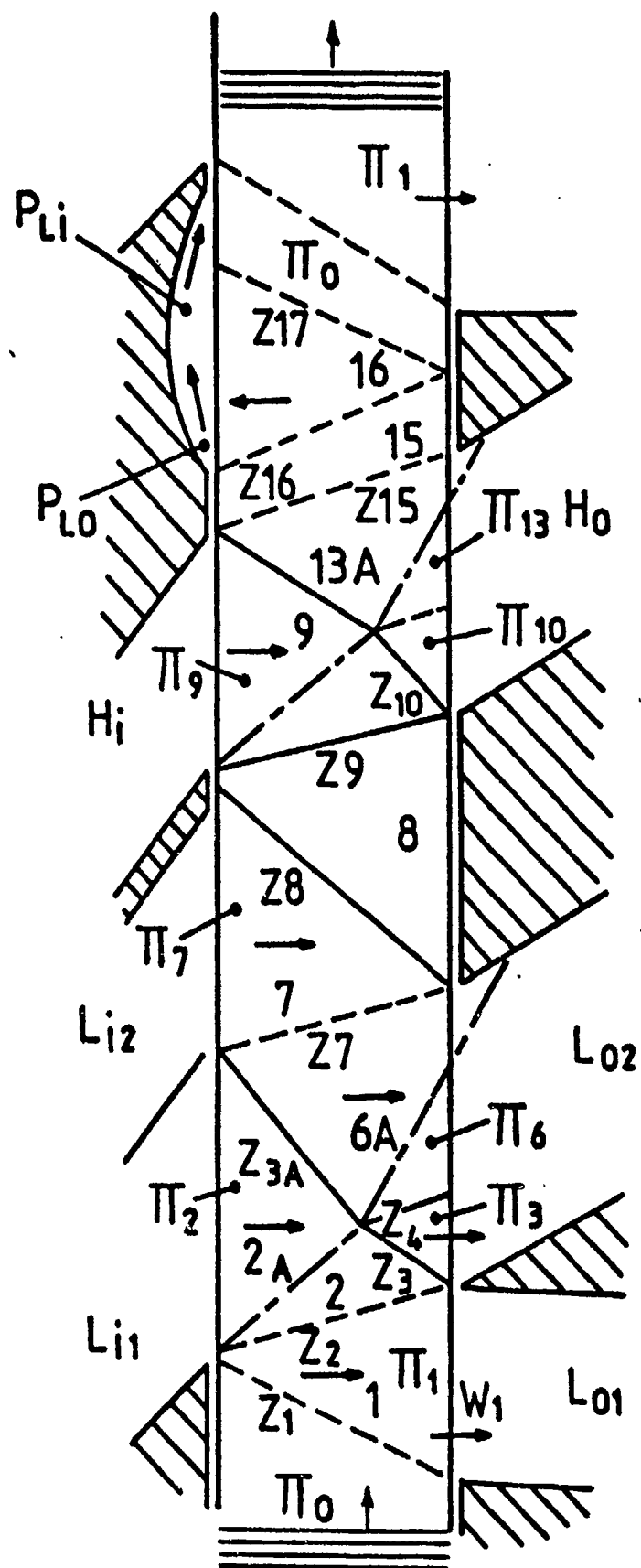


FIG. 5 SIMPLE WAVE CYCLE

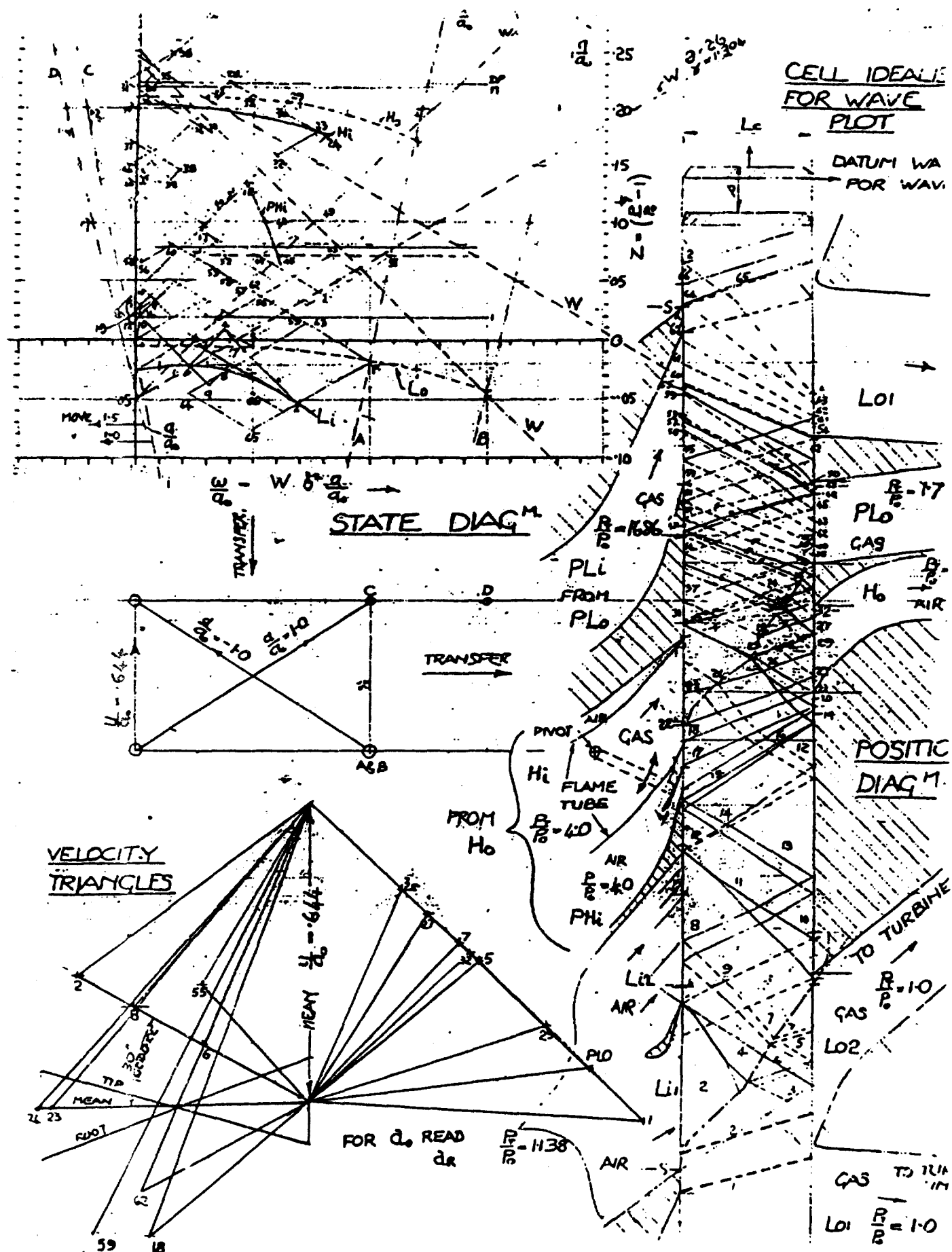


FIG.11 PRELIMINARY DESIGN (1953)

SUPERCHARGED PRESSURE EXCHANGE ENGINE FAMILY DESIGN POINTS

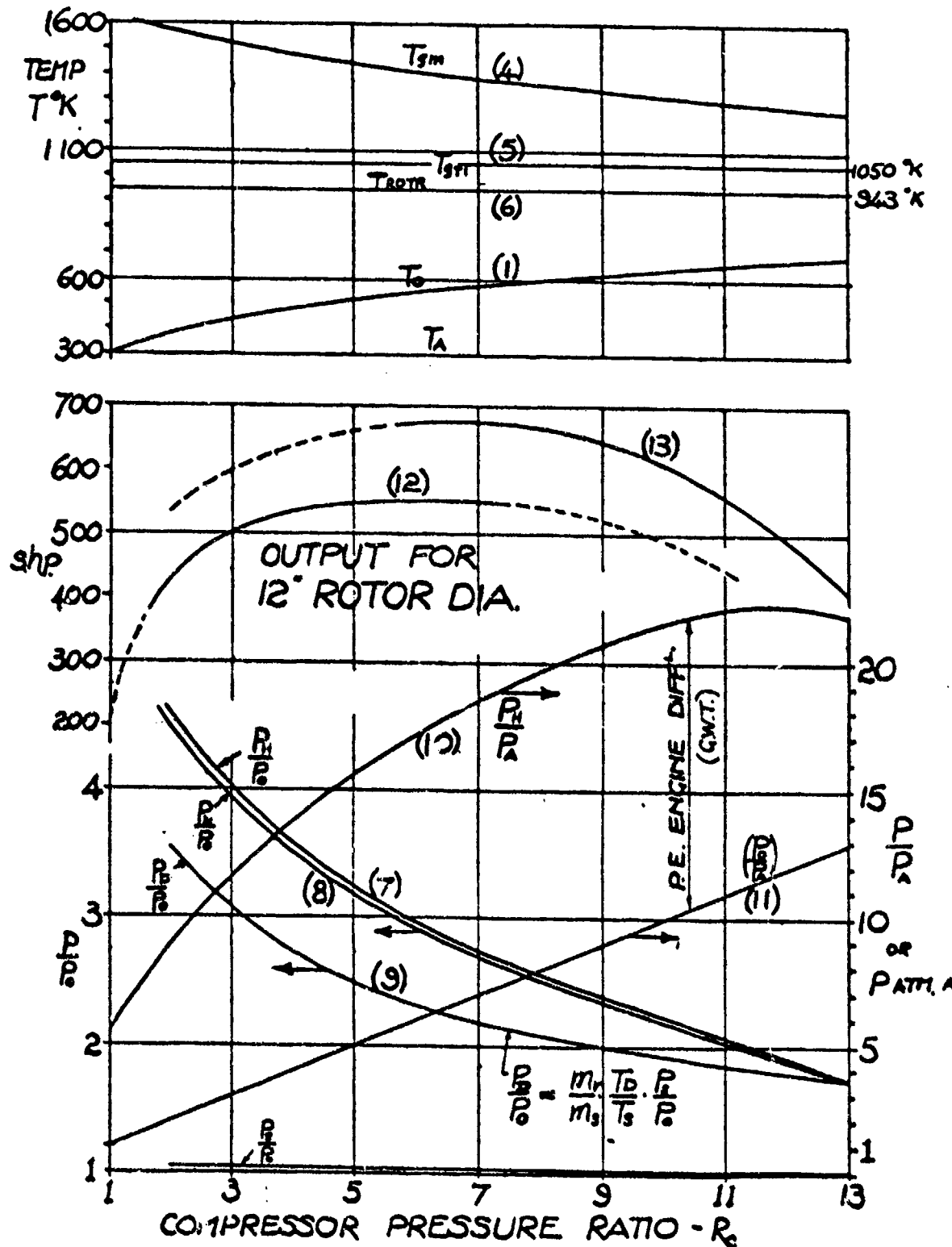


FIG. 12 EARLY PREDICTIONS FOR COMPOUND CYCLES
TEMPERATURES & PRESSURES (1958)

COMPOUND PLANT

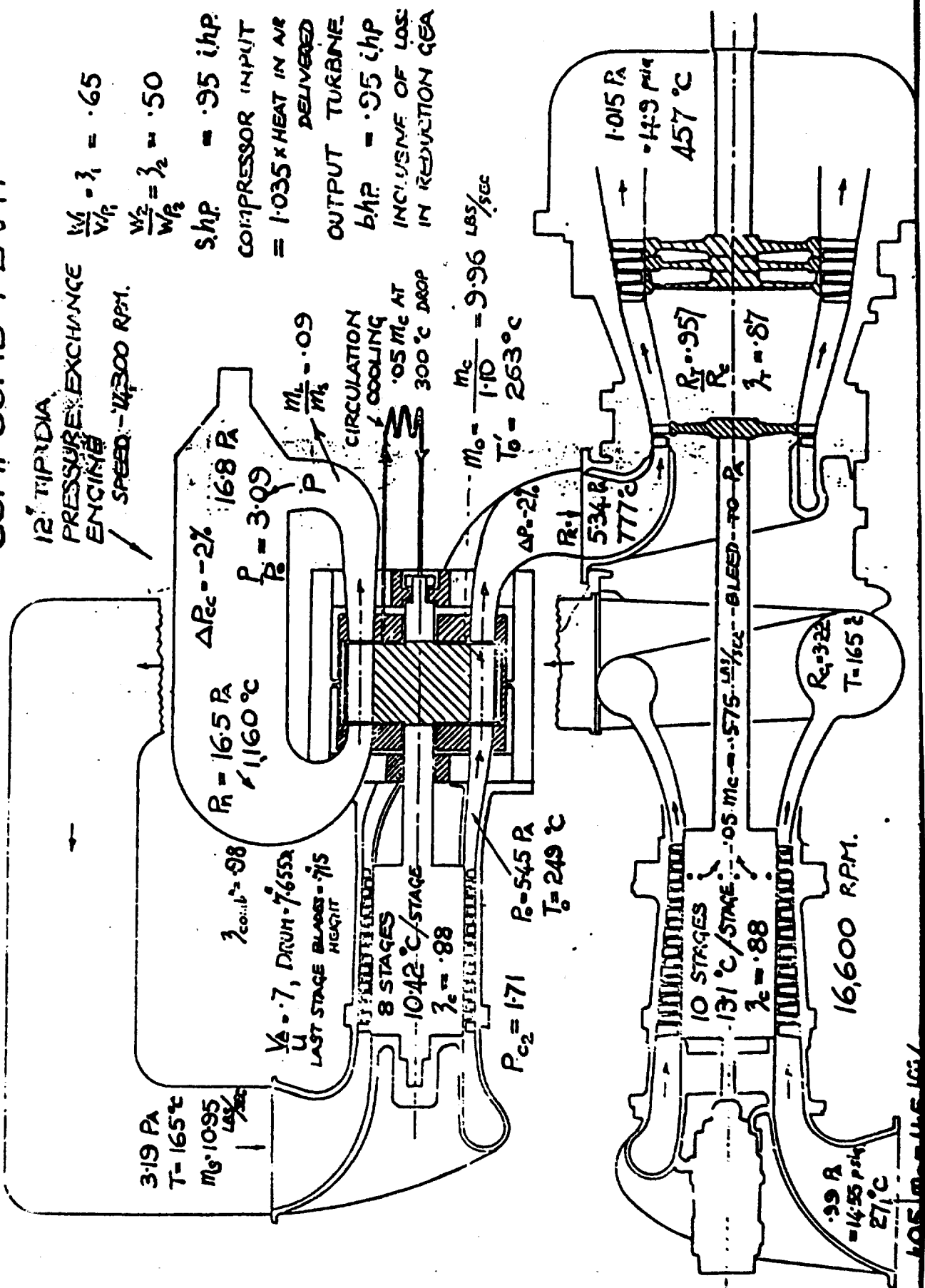
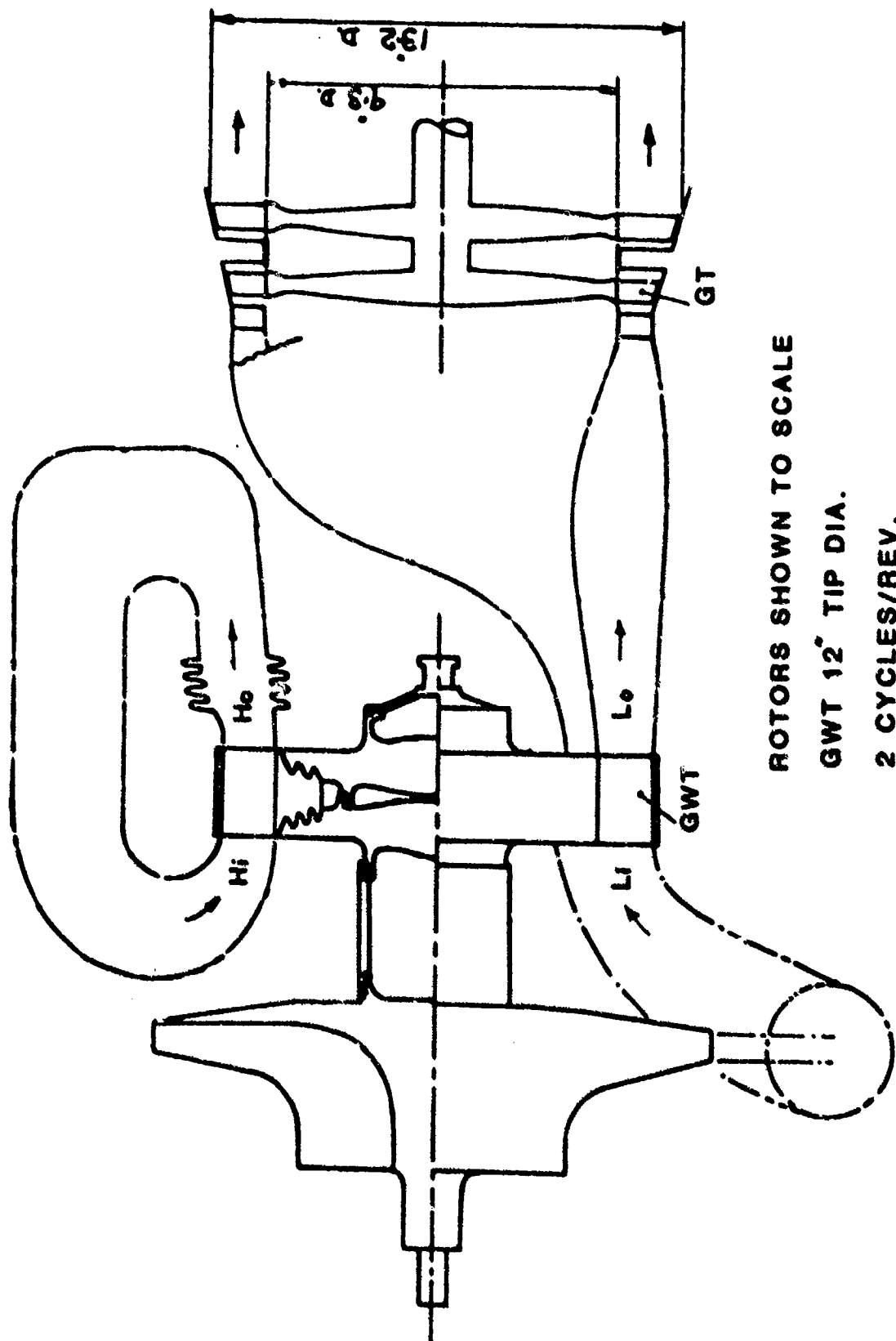


FIG.14 GWT-GT COMPOUND AT R = 5.5



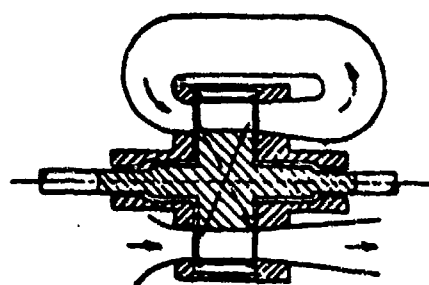
ROTORS SHOWN TO SCALE

GWT 12" TIP DIA.

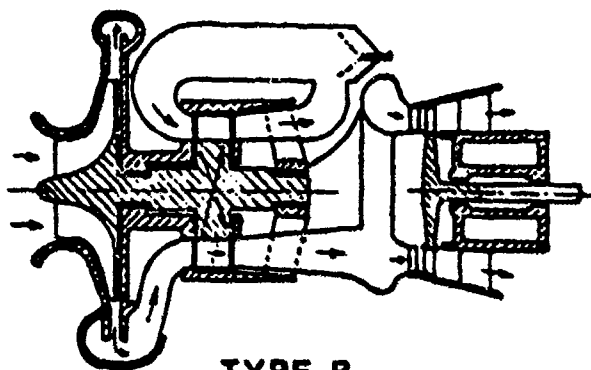
2 CYCLES/REV.

PORTING AS FIG.11

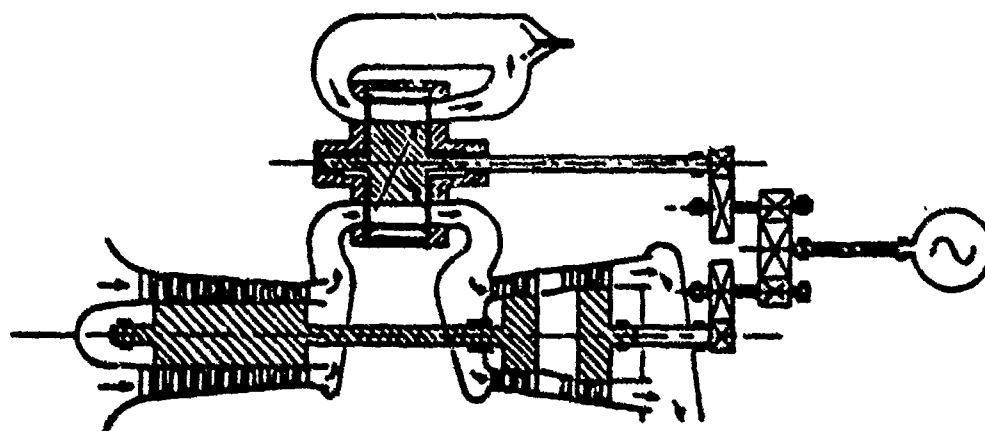
FIG.15 GWT-GT COMPOUND AT $R_e = 2.7$



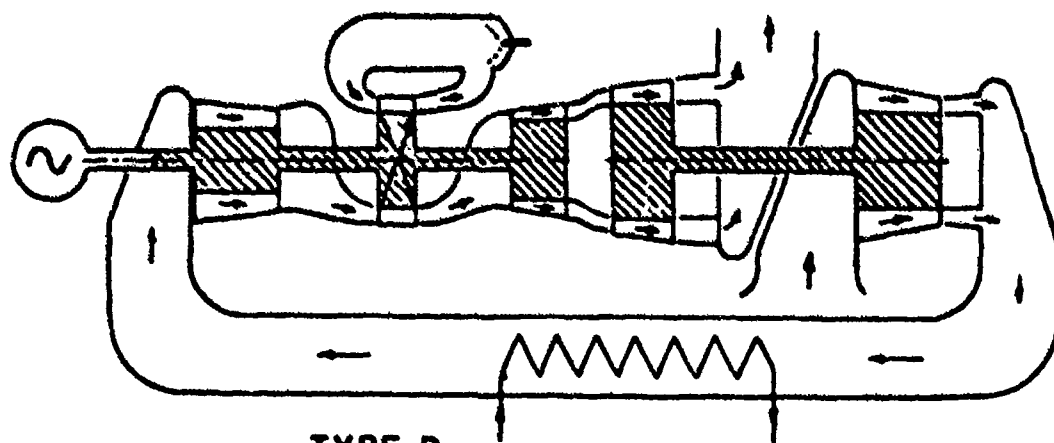
TYPE A



TYPE B



TYPE C



TYPE D

FIG.16 GWT-GT COMPOUND TYPES

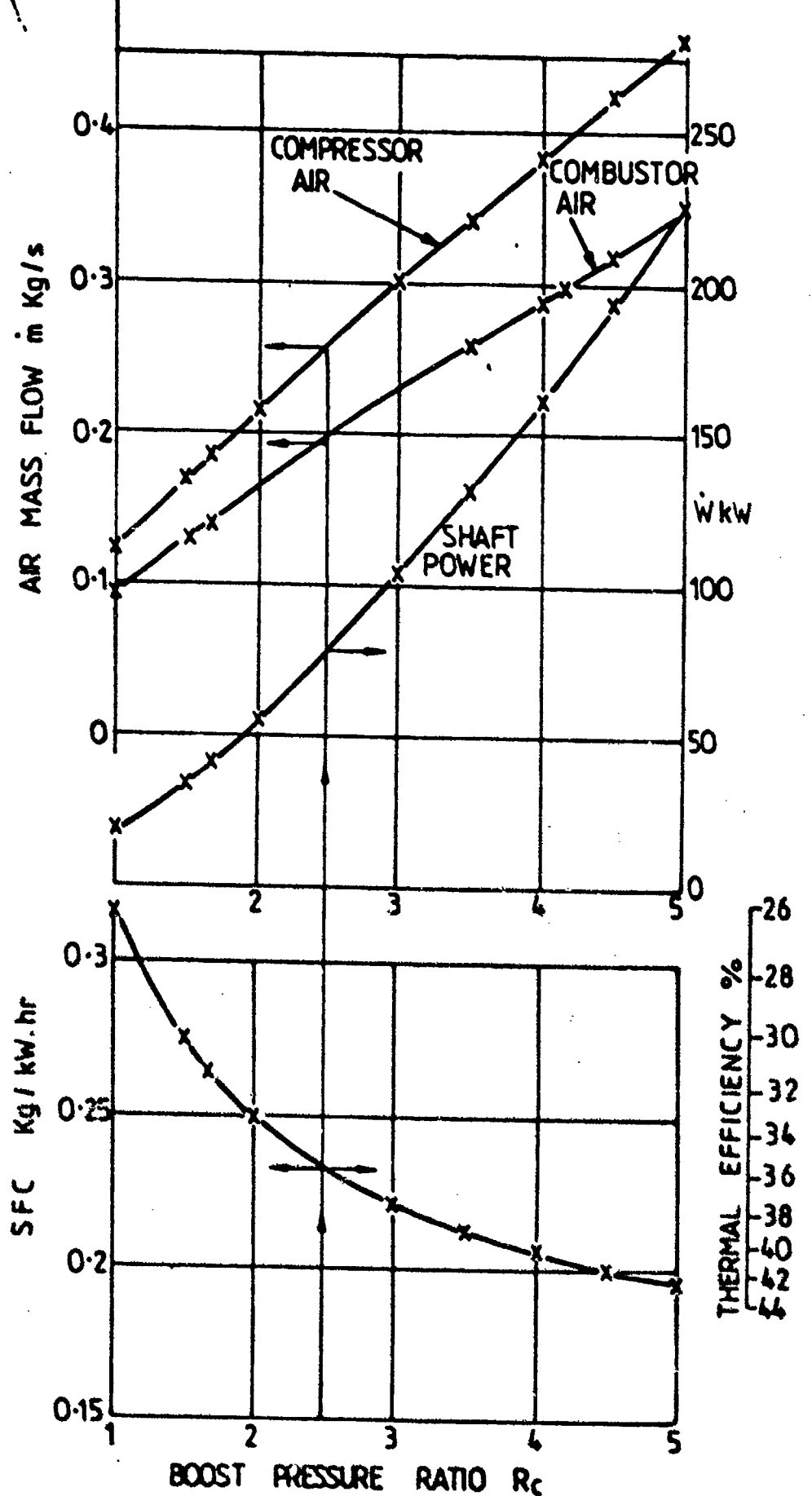
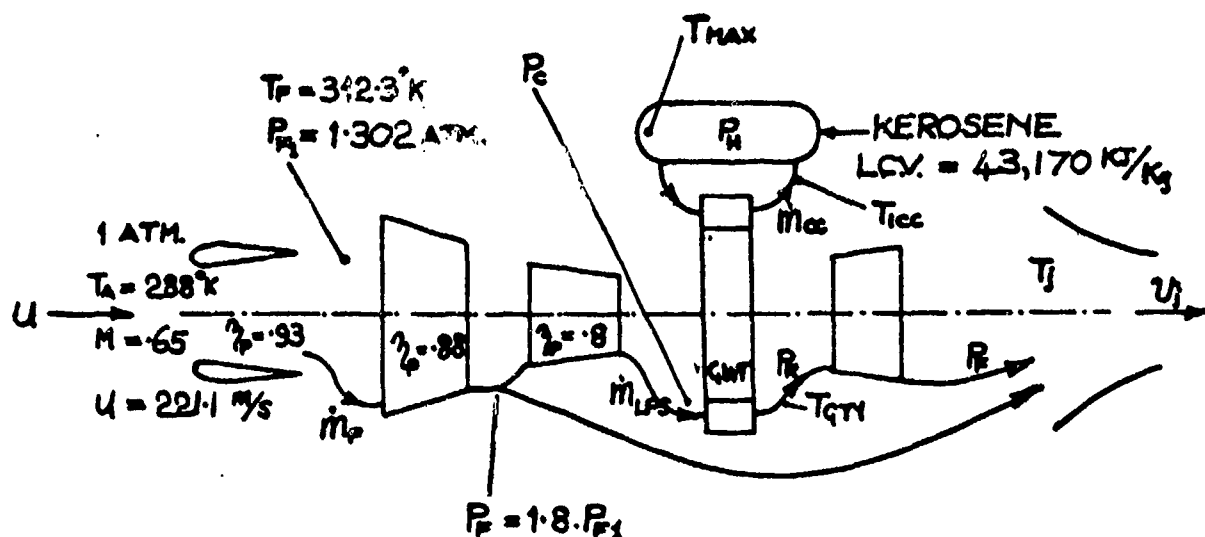


FIG.18. 100 mm DIA. SUPERCHARGED GWT (1985)
POWER , AIRFLOW AND FUEL



MECHANICAL EFFICIENCY = 0.98
CELL ROTOR AXIAL CLEARANCE $g/l/Lx$ = 0.003

PARAMETER	CASE 1	CASE 2
PR/PR	4.0	12.0
PC/PP	2.29	2.12
PH/PA	21.5	59.5
THAX	1570 C (2854 F)	1840 C (3340 F)
TROTR	900 C (1560 F)	900 C
TOTL	900 C	927 C (1700 F)
mF	10.37 kg/s (22.86 lb/s)	10.84 kg/s
mLPS	2.48 kg/s (5.47 lb/s)	2.22 kg/s
mCC	1.72 kg/s (3.79 lb/s)	1.66 kg/s
BYPASS RATIO ((mF-mLPS)/mLPS)	3.18	3.88
Tj (TOTAL JET MIXED TEMP.)	547 K	521 K
vj (jet. relative vely.) m/s	477	466
$\gamma_{jp} = 2 \cdot u / (vj + u)$ (FROUDK)	0.633	0.644
SPECIFIC FUEL CONSUMPTION		
SFC kg(FUEL)/hr/kgf(THRUST)	0.731	0.709

FIG.19 600 lb. THRUST BYPASS ENGINE WITH GWT.

IV. DISCUSSION SESSION

(i) Discussion Following Prof. Pearson's Talk.

Dr. Anthony Laganelli (Science Applications):

My first question is directed at the Rolls Royce (RR) project and perhaps even somewhat to this last figure that was put up here. On the basis of what I have heard so far in the last few days, it seems that the GPC engine could be very easily constructed into a topping engine...(garbled) I was wondering if either of you people would like to comment on that? The 2nd question is why do you always plot the dimensions; whatever happened to non-dimensional parameters?

Prof. Ronald Pearson (University of Bath):

I have always plotted non-dimensional parameters whenever relevant; all the wave parameters are non-dimensional.

Dr. Laganelli:

Yes, but when we get out the final product of thrust and specific fuel consumption I recognize they mean something, but when we are trying to compare different systems, different engines, would we be better going back to what...(garbled) taught us a long time ago? Meaning plotting dimensionless parameters, comparing different systems, why don't we do it?

Prof. Pearson:

Well, I thought we had. I mean SFC (specific fuel consumption) is non-dimensional. The thermal efficiency is, as well as the SFC because we want to look at either of them.

Dr. Laganelli:

I recognize that efficiency is non dimensional. It is conventional to give jet engine performance in specific thrust and specific fuel consumption in terms of the amount of fuel you use per hour and the amount of thrust you produce. Would you care to comment on my first question.

Prof. Pearson:

About the GPC machine?

Dr. Laganelli:

Well you suggested that the pressure ratio (could be) easily up to about 30 in the present mode just by using it as a topping cycle, as I saw that RR engine described today with the Comprex. Rather than having a Comprex you could use what you call a modified Pearson or a GPC (General Power Corp.) wave rotor on there.

Prof. Pearson:

My opinion about the GPC machine is that they haven't designed the expansion

stage properly. I don't consider the expansion stage has been properly designed.

Dr. Laganelli:

Are you talking about the simulation model or the outlet of the engine?

Prof. Pearson:

The actual machine. In my view the expansion side of the machine has not been properly designed, and until it's put right it won't run properly.

Dr. Laganelli:

Would you care to comment on that Hal (Weber)?

Dr. Hal Weber (San Diego State University and SAIC):

Well.... (garbled) it's true we haven't finished the design yet at this time. We had originally built a five re-entry device for the entire power to be taken off the one rotor. Now we plan to go to a separate power turbine. It looks just like a topping unit, it has got a compressor and a turbine and in between you put the wave rotor.

Prof. Pearson:

I think the concept is all right, the general concept is all right it's just that the detailed design of the expansion in my view has not adequately been programmed.

Dr. Laganelli:

Thank you.

Prof. John Kentfield (University of Calgary):

May I just make a comment, I noticed in your last slide you seemed to imply that you have an unsteady flow combustor in the loop as well.

Prof. Pearson:

Yes I did in fact try and do this on that particular machine. In order to put curvature on the blading and to make the efficiency of the rotor higher, but this meant the higher pressure scavenging stage was impaired. This could be put right by a pressure gain across the combustor. And I did in fact work on pulsing combustion and we finally got a pressure gain of 12% and in one particular test we got 17% which was quite enormous but that particular test was never repeated. We did get 12%, we could repeat 12% everytime. That was a valveless type pulse combustor. Running at 200HZ, the trouble was it was too big for this kind of application, far too long, and it was difficult to start. 200 cycles a second is too high to start easily.

Prof. Max Berchtold (Swiss Federal Institute of Technology):

Suppose that you were given that the efficiency was around 20%. How

confidently would you feel that you could realize this? Is this based on your analysis or do you have indications that the tests were very realistic?

Prof. Pearson:

The tests have showed a much lower polytropic efficiency of conversion along work areas than I have assumed in those calculations but that was mainly due to the fact that there was a lot of mismatching of the gases in the low pressure pre-scavenge. Just to show...(goes to overhead projector with slide and discusses it).

Prof. Berchtold:

Are you going to build one of these?

Prof. Pearson:

I am very tempted to, yes, but this isn't the right design. Yes I would like to. Starting with 8 to 1 and going to 12 later on.

Mr. X (unidentified):

At the forty percent efficiency didn't you also...(garbled) 50 to 1 compression ratio and a thousand to two thousand degrees centigrade temperatures if I am not mistaken, 50 to 1 compression ratio means that you have a combustor of 1000psi pressure. I just feel that on a small engine that certainly is an advantage in technology.

Prof. Pearson:

Not quite 2000° but not far off. There is a sort of cooling on the rotor with this new cycle but you can in fact get that and you can in fact accept that kind of temperature on the rotor.

Mr. Richard Joy (Williams International):

My name is Dick Joy, I am from Williams International and I would like to comment on the turbofan which you have chosen to focus on. As a matter of fact it has been my privilege to have laid down the preliminary design and do the performance analysis of most of the early aerodynamic design in 1964 and the engine was first drawn in 1967. This is my first introduction to wave rotors and I think I have learned two things; first thing is that they may have some application to turbines, the second thing that I have learned is that the processes that go on inside of it are so incredibly complicated as to be beyond any reasonable analysis. We people in the turbine business, what we really need is to focus less on what goes on in the turbine and more on the definition of the overall characteristics, as we would define a compressor. I have seen the pressure ratio and the temperature ratio relationships defined, but obviously in the sense of the Compress. Here we have a simple device in which are bound up relationships such as pressure ratio, temperature ratio, flow (through-flow) and corrected speed. Now we need those characteristics to put into our programs to find out defined performance, and to find out if it has any general merit. Now obviously there are some things that may come up, and if it comes to pass that we need to incorporate blow-off valves or waste

gates, what intrinsic merit there is in the wave rotor is going to be decreased, so I would like to make a plea to you people who do understand wave rotors to give us people who would like to apply the overall characteristics, the complete characteristics of pressure ratio, temperature ratio, flow and speeds. I think that can be done.

Prof. Pearson:

If we look at the arrangement I showed earlier on, which I call a simple flow where we have a cell rotor driving a centrifugal compressor, it is a 4 to 1 pressure ratio cell rotor which is within the existing experience. The net combination would give you 26% thermal efficiency only. Not a very high value, the compressor pressure ratio is only 2.4 which is not a very high overall pressure ratio. But, when the thing is turned down, the speed drops and the pressure ratio across the cell rotor remains almost constant. Only the pressure across the boost compressor tends to vary. And then this tends to keep the efficiency from falling off as fast as it would in the compressor turbine combination. When you get the engine running at full power, getting 26% efficiency, and you drop down to 10% power, the efficiency is still around 15% .

Mr. Richard Joy:

Efficiency per se is one thing, but what we really need are these defined characteristics of pressure ratio , temperature ratio, and flow so we can calculate what fuel needs to go into it. But until you give us those characteristics we can't do anything with the wave rotor in a turbine. Just simply can't do it! I mean you take the turbocharger, you put it in a car, match it up and it works beautifully at the low end but at high speed, what do you do, you waste-gate-it and throw away all the hot gas. Now if it comes to pass that the wave rotor has similar characteristics, its value is very limited.

Prof. Berchtold:

Yes.

Mr. Richard Joy:

Moreover, the old requirements that it has to accept, it has to accept flow characteristics from the compressor which has singular characteristics of flow parameters and pressure ratio:

a) to avoid surge

b) to stay in the region of maximum efficiency.

Will the wave rotor accept those characteristics?

I am from Missouri really and having done an awful lot of part-load analysis, I all too often have found that simple design point analyses lead to a great deal of trouble and very often cause you to overlook some really fundamental problems.

Prof. Pearson:

I have looked into the off-design performance and I do have some figures.

Dr. Shreeve (Director, Turbopropulsion Laboratory, Naval Postgraduate School):

If I could just put in a word here. When we first got into this, the thing that struck me immediately was there was no simplified way of doing the study of the general performance of a class of wave rotors. That is, it appeared to me we would have to construct a feasible wave diagram before we could come up with that kind of study. I would say myself that that doesn't exclude the use of the wave rotor, that just means we don't have the easy tool that we had in the past.

Mr. Y (unidentified):

I don't think we are talking the same language. All he is asking for is a compressor map.

Prof. Pearson:

Here are the test results.

Dr. Shreeve:

You only get a compressor map by modeling.

Mr. Richard Joy:

I think that you think that what you do with the computer generates test results; it generates a lot of numbers that are totally unsubstantiated. We need somehow or other these characteristics and basically we need them to be defined by tests.

Prof. Kentfield:

We've got those characteristics.

Mr. Richard Joy:

I have not seen them anywhere here. All I can say is, that is what is really needed.

Dr. William Thayer (Spectra Technology):

I think everybody here would understand that those of us that have worked in the area would say yes, great, we would really like to do it and go talk to the people who we would like to fund it. You know 3 years ago nobody in the gas turbine community was very interested in the technology at all.

Mr. Richard Joy:

Dr. Berchtold must have, he must have matched diesel engines, he must know very precisely what the pressure, mass flow and speed characteristics of these machines are. Give us something. I know you did the matching to the diesel engine and matching for a diesel is very different than matching to a turbofan which presents all sorts of new complications perhaps you haven't even thought of. And one of them I might add is the fact that the bypass

ratio and the fan pressure ratio are very intimately inter-related because of the fact that both of those two streams must co-exist at equal static pressure and that in fact defines a range of bypass ratios and makes the problem rather complicated. But we need the characteristics and maybe we can get them from BBC.

Prof. Berchtold:

...(garbled) Of course you have to have this information. But once you have settled on a cycle then we can furnish a complete map of pressures, temperatures, with everything dimensionless so you can put it into your performance.

Mr. Richard Joy:

But you showed a line of ten units there. You must have characteristics for all ten.

Prof. Berchtold:

Sure.

Mr. Richard Joy:

Maybe we can scale them up and down.

Prof. Berchtold:

Yes. You can scale them up and down.

Mr. Y:

My question is, is that data available and can we obtain those curves from you? Is that alright?

Prof. Berchtold:

Not if we don't know which engine we are talking about.

Mr. Y:

If he gives you the model number of a Comprex, will you supply him the curves for the Comprex?

Prof. Berchtold:

Yes, but then that's not the kind of Comprex he wants.

Mr. Y:

Well maybe he should decide that. He may decide that that is the kind of Comprex he wants, once he sees the curves. I don't know that it is not the one he wants.

Dr. Arun Sehra (Allison Gas Turbine Division):

My name is Arun Sehra and I am from Allison Gas Turbines. First of all I would like to say that we have exactly the same concerns that have been expressed by Dick Joy. We really want to have a map for the wave rotor otherwise we really can not make much sense of that. I also have a few questions for Professor Berchtold on the Allison 250 engine. I believe you maintain the same turbine inlet temperature while calculating the thermal efficiency?

Prof. Berchtold:

Right.

Dr. Sehra:

Okay and you have gained about 32% in shaft h.p., from 420 to 550.

Prof. Berchtold:

Yes.

Dr. Sehra:

At the same turbine inlet temperature?

Prof. Berchtold:

The same turbine inlet temperature but not the same Compress inlet temperature.

Dr. Sehra:

Okay, but you have got higher compression, and that's how you gained the thermal efficiency by going to a higher temperature.

Prof. Berchtold:

Right.

Dr. Sehra:

Are you getting some power out of the wave rotor shaft?

Prof. Berchtold:

Yes, a very small amount to just keep itself driving.

Dr. Sehra:

And at the turbine inlet you are saying that you have got the same temperature but a higher pressure as compared to the original cycle?

Prof. Berchtold:

Yes, I think that is correct.

Dr. Sehra:

Okay, and did you also look into the volume occupied by the wave rotor ? Does it fit into the silhouette of the engine itself?

Prof. Berchtold:

It fits about into the envelope of the combustion chamber . Might be a little longer in fact.

Dr. Sehra:

Thank you.

Dr. Shreeve:

Max, I am not sure whether the three people giving the performance calculations had any disagreement with each other. I tried to keep track of the numbers and tried to make comparisons of the suggested performances that these people presented . And I ask whether or not there is any obvious disagreement. John (Kentfield), did you have something.

Prof. Kentfield:

Yes but not in relation to the discussion of these three people.

(ii) General Discussion

Dr. Shreeve:

If there are no more questions on Ron Pearson's presentation, let us open it up for a more general discussion. I would like to hear comments on what people think now, having heard all of this. And we have one taker already. John Kentfield.

Prof. Kentfield:

If I may produce one viewfoil (the following is the introduction to the viewfoil). Well, I feel that we have had a very interesting couple of days, the reminiscing that was going on I think was quite useful and I would like to draw attention to the fact that there are a lot of results available on basic things done in the work of 20 years ago. The instrumentation obviously was not up to the standard of the present sophisticated instrumentation such as what Matthews was describing yesterday and BBC are currently using. But nevertheless there are a lot of cell filling, cell emptying and scavenge process data available from Power Jets, Limited. I do not have access to this but since the company doesn't exist anymore it must be possible to obtain all of these data and some of the data appear in my paper. It seems to me that there is a significant background of data available right now. It needs some coordination to bring this together. The other point I would like to make is

that with the use of these things in gas turbines several people have commented that the performance of turbine machinery is improving and that there is now perhaps no longer a need to bother with one of these machines especially since the combined efficiency is maybe slightly less than what you can get from a modern or a high pressure spool made from a turbine and a compressor with a combustion chamber in between. I tend to think of things differently, we are surely looking here at what I care to call a pressure gain combustor. That is, the Compres and its combustion chamber or possibly a pressure exchanger with combustion in its cells or if you wish to think of it this way, an I. C. engine which is highly supercharged and back pressured to a greater pressure. You can think of that as a pressure gain combustor. I think the closest approach to that was at least one version of the Napier Nomad(?) engine many years ago. But if one thinks of the need or possible need for a pressure gain combustor I think one would say that even if you make improvements in turbomachinery there is always a need to do something to improve the present combustion process. It is not the combustion efficiency which is a factor here but rather the possibility of doing something which has a greater effectiveness and one could argue this on an availability basis. This doesn't appeal to everybody, but I do so if I may for a moment; and what we have in this top picture is a TS diagram and it shows a Brayton cycle and here is a pressure loss which has been emphasized to represent a normal combustion situation and expansion through the turbine and in the next cycle shown here you see what happens if there is some sort of pressure gain in the combustion. We are going to the same T_{max} or turbine inlet temperature in both cases. One has to be careful when they say T_{max} in this sort of situation but the turbine inlet temperature is the same in both cases. There is more work available in the expansion here than there is here, (referring to the slide on the screen). You may say well, one can do this process here by effectively adding on a topping stage here to the turbo machine. Yes you can, but then it must still be possible to superimpose this type of thing on your new improved cycle. The argument based on availability says that if you want to go from point b (I can't really read my diagram here) to here, or from here to here, which is the normal combustion process, if you want to go from there to there, the availability route tells you to take the reversible...(garbled) with an expansion down to here, an isothermal process at the boundary conditions,...(garbled) If you do that and you look at the energy that is required to do this, which would be the minimum energy required, and then you compare that to the energy actually added to go from there to there, it turns out that the effectiveness of the combustion process is about 60-70%. Well now the availability argument doesn't tell you what to do about this, it just tells you there is room for improvement there. If you tried to do the same thing for the compressor or the turbine separately, there is very little difference between the isentropic efficiency and the availability effectiveness. It suggests to you that the efficiencies of those components are already quite high; there is not a big potential for improving them on the basis of a peak efficiency, maybe on worth of operating or something, yes. So what this would suggest is that the scope for improvement is in the combustion process; if you have improved turbomachinery you can take "a" in this lower diagram. Here you see, and it is probably too small for you to read, an increase in net output for the same pressure gain, meaning the same pressure gain in the combustion system or reduction of the same pressure loss. Here you see the cycle pressure ratio of the thing plotted at the bottom, and its cycle. Now what happens here, on the basis of fairly small changes like going from, say, 4% pressure loss to, say, no loss or 4% pressure loss to 3 or 4, or

5% pressure gain, that kind of small change, then what you find is that it depends where you are on this map. Now when I say that if you improve your turbomachinery you could also make it gain by still stacking on top of that some sort of pressure gain combustor, and then it seems to me that all you have to do is consult this diagram. P_i is the cycle temperature ratio, θ is the combustor temperature ratio, I can't remember which it was, so P_i is the cycle temperature ratio plotted on these dark lines and the dotted lines are the combustor temperature ratio. It depends where you move around on these. Now if you happen to be, say, down here which is about 6 to 1 pressure ratio, a cycle temperature ratio of 3, the gain is about 2% per % change in pressure loss in the combustor chamber. That is, this is the gain we get and correspondingly a reduction in the specific fuel consumption. With the same temperature ratio if you happen to have an engine out here, the gain would be 4%. So it depends where you are on that map and the gain does vary, it is true, depending on where you are on there. So if we compare, as has been spoken about, the Allison CP-50(?) machine of several years ago and then mentally redesign a model machine to get a better performance it is true you move about on here but it seems to tell you that wherever you are on here there is some potential gain from reducing the combustion pressure loss and if one cares to think about an availability argument, the availability argument conducted right through the turbine, Prof. Berchtold told me he has done this for a number of engines on an availability basis looking at all the components presumably, then what you find is that the combustor is one of the worst offenders from the point of view of indicating that there is a potential to do something about it. So it seems to me, one shouldn't think the... (garbled) has been made since the early work was done i.e. the designs started by Rolls-Royce, GE (the T-58) and so on, but now that the project has gone out the window there is no need to do anything, there is still a need to do it if you possibly can. Provided of course the penalties don't outweigh the advantages. Now one cannot say without doing more studies and obviously a lot more work, whether one could overall, on a cost-effectiveness basis or power to weight ratio basis be a winner on this. But it seems to me that one should not dismiss this thing out of hand, and I would put in a plea for any form of pressure gain combustor, speaking very generally. And as I said I would like to emphasize that I think anybody choosing to use a pressure exchanger specifically for a particular task should make sure that the thing is being used in such a way that the advantages of that particular device are maximized. In other words it's not being made to compete directly with something else that already exists now that could do the job as well or even nearly as well, because if there's only a very small benefit it's probably not worth spending money developing a new whatever it is. I think that's about all I would like to say and I'd like to give an opportunity to other speakers now. Thank you.

Dr. Shreeve:

Any comments on that?

Dr. Arthur Kantrowitz (Dartmouth College):

I would like to compliment Ray again for organizing this meeting. One of the things we ought to do is to consider how the momentum that he has created can be preserved. We have seen a history of efforts that were started, worked on with enthusiasm, stopped, (I'm guilty of both of those), and I hope that with this meeting we will start a new era, because I am persuaded, as I think most

of the people here are, that there is an enormous benefit...(garbled), in addition to the steady flow, this kind of wave equipment that will add to our potential. That transition has not been made effectively except for the marvelous advances that we heard about from BBC. I think the U.S. has some need to try and keep up with Switzerland in this respect. So I would suggest that to preserve the momentum that has been created with this meeting that we form some kind of a group which would have three functions that I can see.

- i) To encourage information exchange of the kind we've had at this meeting.
- ii) How to evaluate performance claims, which in this art, no less than in other arts, need some kind of independent evaluation.
- iii) And finally to advise the government on policy in how to utilize available funds in furthering the art. Such a group could also aid in the defense of such funding from the rigors of the budget process in this country and I think that that would be another useful outcome.

Dr. Shreeve:

Thank You. Go ahead John.

Mr. Y:

I would like to take up this opportunity to kind of continue the process the gentleman from Williams had. I once got involved in making expendable turbojets out of Garrett superchargers and found to my dismay that Garrett didn't really like to share all the characteristics of their turbo superchargers and it was a little bit frustrating to try and convert these things into turbojets. You know I respect the right of Garrett to keep that data to themselves and the right of BBC to do that also, that is in their best business interests, but on the other hand if it is possibly available it would be extremely valuable to people interested in using those machines for applications other than the ones they were intended for. In my view that is where you really ought to start. I'm really an outsider, I'm not a wave rotor builder. I think you ought to start by seeing if you can exploit the BBC off-the-shelf machines, because a guy could build his own, but it would be so valuable he couldn't afford to test it, you know, they would be really afraid to bring it up to speed for fear of losing it and then they'll be out of business. What they ought to be doing is busting a bunch of the off-the-shelf machines and if one blows up putting another one in its place to find out what its going to do. That's what you ought to do first. Next thing you ought to do is modify them, you know, e.g. if they find the rotor is too long they saw it in half, and if they don't like the pockets they fill them up with weld or something. When they've done all that then they ought to start thinking about building their own rotors, somewhere downstream, you know, maybe 10 years down the road or something like that. That's what I think.

Prof. Berchtold:

Well you see your suggestion has been followed at R.R. We gave them what equipment we had so they did not have to start from scratch. That was almost 20 years ago, when we didn't have whole room fulls of rotors and pieces available, there was a limited supply available but yet I'm sure we saved a

lot of time by giving that. Now what I said, somebody else said it very clearly also, in order to make the Comprex match the diesel engine, we had to make an awful lot of bending(?) in all directions. Having a Comprex to be used for a narrow peak of performance, we think we would do what you say, we would modify its geometry to meet the very best conditions and then we would have to measure its performance map. I think a specific performance map that's good for the diesel engine, would not be very useful for most cases that other people would be interested in. But it would be easy to make such modifications as you said and measure the more-or-less narrow speed range machine in order to get the information, and then to plug it into the application calculations. Your suggestion is very well taken.

Mr. X (Unidentified Speaker):

I would like to bring in perhaps the outsiders point of view here. We heard about several engines or gas turbines, attempts made to develop them and so forth; maybe you can correct me but I would guess a new prime mover development would cost an absolute minimum of 50 million dollars and I would give it a 15 to 20 years lead time before it even gets there. Now I have the feeling that the focus that we have seen here with this engine is very narrow; I have the feeling that this device would apply in a tremendously big variety of cycles, Brayton cycles or you name it what, steam, organic fluids, refrigeration cycles and so forth. Dr. Kentfield touched on this 15 years ago in his paper that was published a long time ago. So I have the feeling the focus is narrow, and from our point of view we are interested in industrial applications and maybe it won't be a mistake that the first commercial application is not a gas turbine or a military application but a consumer turbocharger that comes out in the market. There ought to be a message in here some place, maybe it wouldn't be a bad idea to start off with some simple devices and then go on to elaborate gas turbines.

Dr. Laganelli:

Are you going to pay for it?

Mr. X:

No, we would like to buy one of these turbochargers and bust it up in our laboratory and see what we can do with it and take it from there.

Dr. Shreeve:

It's my own opinion that you've got to be a little more exacting in designing these devices than other turbomachinery types to get to the point where they actually work. I think in turbomachinery, it takes a certain amount of knowledge to get it to function, a certain amount more to get it optimized.. I think to get a device like this to work it takes a lot more detailed calculation. I think that's what's standing in its way.

Mr. X:

Let me illuminate this from a different point of view. The suggestion was made earlier that the real answer to this problem will be to come through with a total 3-D calculation method as that is going to be the one that will give a

clear picture of what's going on. Maybe I can remind you that gas turbines are flying and have been so and there isn't really a good 3-D calculation method for gas turbines and cascades as of today.

Dr. Shreeve:

In response I would say that there are good approximate models for the behavior of the flow, and I think that's what's required here; that model has to be at least good enough to describe the processes to the point where you can get the hardware to work.

Prof. Kentfield:

I think several of us think, that some of the existing programs do this well enough, maybe not perfectly. Maybe I can speak for the people from Spectra Technology, would you agree that you think that you have the analytical capability already, which is not perfect by any means but good enough to represent something which allows you to make a workable machine. It isn't as if we need to make a huge step forward analytically to design these things. I mean the first Power Jets machine was based on...(garbled) method of characteristics and the machine worked quite well actually. As I observed yesterday, it was one of the very first gas generators, it wasn't designed for... (garbled), but the thing worked and had a peak isentropic compression efficiency of 0.8, and I can't remember after all these years, it probably is in my records, the expansion efficiency, was actually higher than that and the product of the two was around 0.68. But that was a machine that wasn't structured to cover a wide speed range, it was a very basic machine and as I showed yesterday, it had a somewhat limited speed range. I think the message is, (Prof. Berchtold touched on this), if you're going to redesign to extract the wide speed range capability of the existing Comprex, you probably will get a better result. I think one could look at Power Jets' results and say there's an implication from the experimentation that that would be the case. (And even with the analytical tools available to them in those days, hand drawn wave diagrams to calculate these machines, the thing worked quite well). And now we've got computerized methods to do this, and I don't think we need to go to those lengths to get the things working properly.

Dr. Shreeve:

Excuse me, I have to respond, I was not trying to say we do not have good enough models now. I was trying to explain we don't have the machines now, because I think the modeling tools were inadequate previously. Most of the machines have been done in a laborious way. Had we had the tools, had the previous attempts had the tools at their disposal, they would have got the machines working faster.

Prof. Kentfield:

The Prof. Spalding initiated program at Imperial College was really done after or during the death of Power Jets; that did reach the public journals and it is available now.

Dr. Shreeve:

The first thing I feel that is needed is a balanced program involving three levels of effort. But I'd like to give some other people a chance, Jerry you had something you'd like to say?

Mr. Jerry Walters (Pratt & Whitney):

Well I'd just like to make some closing remarks if I may. My name is Jerry Walters. I'm with Pratt & Whitney Aircraft. Like many of you I'm a novice to the Comprex field but very interested in it and have been since Ed Resler introduced me to it at Pratt & Whitney about five years ago. We've done some engine sizing, looking at helicopter applications where a constant speed output seemed to be the obvious choice for a first shot because we did not have to worry too much about speed cycling. That was very conceptual, and from what I've learned today, it probably would not have worked even if we had tried to make it. I think we're way too premature, with what I've heard today, in trying to approach companies like Pratt & Whitney, Williams International, G.E. and others of the industry leaders, because there's a lot of work to be done before they're going to be in a position to handle it. I think we heard a comment on that already today so I won't press it. But it seems that we all know the proper focus in this type of activity is to begin with the DARPA people and to keep the industry that you are aiming your activities at informed of what you are doing. Again, my name is Jerry Walters, and I am with Pratt & Whitney down at the Government Products Division in West Palm Beach, Florida and my phone is 305-840-2352, and any time you have something that looks like it is going to apply to my product line, I can guarantee you I will send you a ticket to come and tell me about it. I am responsible for all conceptual design activities for government products and there is no good idea that I will turn away. I will give you all the time you need to tell me about anything you have to offer. But right now I don't think I am ready to listen to anybody because there is a lot of work to be done. But that work needs to be focussed, and I think Ray, you deserve a big hand from all of us for putting this first meeting together, because it is really needed so that we understand how much activity is really going on in the world.

I did want to share a couple of things with you. I heard some technology levels that you are all working at that I think are remarkably low. I think that you would appreciate it if I gave you a little bit of insight as to what your new technology goals should be in the engines that you are working on. At P&W, we are presently running state-of-the-art turbines that run at about 2000 ft/sec. I think you ought to update all your calculations to include that kind of number. That would be with a gatorized inconel 100 material which is, its not important what the material is, the important thing is that you've got in excess of 200,000 psi strength in that type of material and you should factor that into your calculations. Clearly if you're going to have a successful flying machine you've got to have very small volume density, and by that I mean the airframe guy wants a very small nacelle, so you've got to keep your focus on very small frontal areas and to do that you've got to go to high pressures. Now, I was very fascinated that you've all zeroed in on the fact that the industry does need high pressure compressors to be supercharged by fans; you're right on track on that and I think you should pursue that. A lot of negative thinking people out there will try to convince you that with the

advent of carbon-carbons and ceramics, we can go to higher temperatures and get out of trouble. Well put on the brakes, say hold it, I've heard all that, and I don't care, because you've still got a problem with blade heights in the axial compressor and that's been expounded upon several times. I just want to tell you, you're right on board, that's exactly where the industry is. We do need the high pressure compression technique in the Comprex and as soon as you think you've got something that is really a winner, I think you should go for it. There are two applications I can think of that would be first; things that I would recommend to my company. First of all, you can circumvent the problem of speed range by going to machinery that doesn't need a big speed change; let's get the industry started with something that's rather simple. The helicopter I mentioned, that has a very small speed change requirement. I think there, when you increase the pitch on the foils, you add extra torque without any speed change and the Comprex is ideal for that from what I heard today. So that would be one area that you might want to investigate. The second one is with the President's focus now on Star Wars, we're very interested in transatmospheric vehicles and I don't know if any of you are working on that, but we certainly are starting our activities and in that arena, at Mach 5, the inlet temperatures are at about 1850°F and the industry is crying for a device, it could be a wave machine, I haven't run numbers through this so I couldn't tell you this for sure, but it sounds like a wave machine might very well be very applicable for this because of its ability to handle high temperatures. What we need out of that machine is an output of cool air to cool the components that are outboard the aircraft and in the nacelle. There are enormous thermodynamic cooling requirements onboard a machine that's going to cruise at Mach 5 or accelerate to Mach 6 or whatever, the scenario ends up being before you go into orbit. Those are going to be fairly long missions and the turbojet engine bay would have to be cooled, so there are a lot of volume flow requirements there, and you also have nozzle parts and miscellaneous accessories on the accessory boxes that have to be cooled. So there's a lot of cooling requirement, and if we insist on staying with non cryogenic materials, a thing like a Comprex machine might be the way to go. I think the Comprex has a real place in the world. My friend from Williams, (referring to Mr. Dick Joy), I'm a real admirer of his, I guess he doesn't know that, but I happened to have looked at a couple of installations on the ALCM that Boeing builds and on the Tomahawk that General Dynamics is building. To get as small a diameter as his 107 engine, you've got a job on your hands. So I would suggest that you go after maybe a third application, which would be something like what G.E., P&W. and maybe R.R., I'm sure R.R. is right in there with us, in very large bypass fans for commercial applications, there you can nest a larger Comprex machine without a big penalty in the nacelle diameter; in other words, they're not that sensitive to nacelle diameter increases, so that might be a better choice. Our mission analysis studies show that there is really no advantage in going to high pressure. Now when I say high pressure I'm talking about 40 to 60; the commercial engine people would like that and we would like it in cruise missiles, in fighter and bomber aircraft that are subsonic. But as soon as you start getting into supercruise missions and supersonic flow the high pressure ratio has no advantage. The SR-71, as you know, cruises at Mach 3 and it has a pressure ratio of 8. If we were to do that engine today it would probably be 6. So there's no big driver to have machinery which can give you large pressure ratios at high Mach number applications. So I would focus on the low Mach number machines and high bypass, especially where you can mask the probable increase in the size of the nacelle without a large penalty to the aircraft's

requirements. Lastly, I've also heard a lot of things about brazing and casting and I've got to tell you that we have something to offer you at P&W, known as Gatorizing. The Gatorizing process can give you a part, or a rotor, any one of the rotors that I've seen over the last few days, we can gatorize for you to net dimensions. In the various super alloys that I've just told you about-we can give it to you in Titanium, super nickel alloys, anything you want in that area-and they aren't terribly expensive. We have techniques now that we've developed that make the making of those parts very easy, and I think we can cooperate with you on any kind of venture like this if you want to get into this. Any questions, I'll be happy to answer any questions. We're very strong in materials technology, so any problems you have in materials, or any bonding techniques, diffusion bonding, we can do enormous things for you in that area.

Dr. Lebus Matthews (Brown-Boveri Company Ltd.):

What is Gatorizing?

Mr Jerry Walters:

O.K., P&W has developed a process called R.S.R., Rapid Solidification Rate; we take basic ingots and melt them down, drip them onto a spinning plate in an environment, and in that environment we can cool at several million degrees per second and thus rid any oxides from the material, so we end up with a pure, if you will, particulate, that we can then press into an ingot, go to a Molybdenum complex die, take the material up to its incipient melting point and press it into a net shape, any kind of a shape you can conceive of we can make. For example, let me tell you about one that is really complex that we are doing for a customer. He wanted a radial inflow turbine, and he wanted to run at high temperatures, higher than what anybody else has run in a radial inflow turbine. So we took our blade material, which we call alloy Y, it is a directionally solidified, crystal oriented material, in which we control the plane of the crystal structure. We cast that to the net shape that we wanted on the final assembly. We then took our raw powder in AF21DA (?), which happens to be a very fine grain material which you want in the bore of a disk, and we gatorized that small bore portion of the disk. Then we took a major portion of the flow path in the blades and a little bit more of the disk which you might call the rim, just where the blades attach on, and we made that out of AF21DA. We then purposely heat treated it in order to grow the crystal to get large creep strength. To the blade tip of this large crystal material, we stuck on the Alloy Y with its crystal orientation. This gives the customer a part which he can inspect with zero defect. The materials themselves have no flaws, or they are certainly undetectable flaws (with any of the techniques we have for measuring flaw sizes), that is you cannot detect the parting line between these various alloys when you do a spectrograph analysis or any other kind of analysis. Other than the visual color change of the grain boundary, you can not detect the parting line. So that's a very exciting area and that process is going into production very shortly and we have prototype parts coming out right now. So for anything where you have a complex orientation of strengths, or where you need fine grain root strengths of 220,000 psi in the core and great creep strength or stress rupture strength in the blade area, or something which doesn't have to have much strength but just survives without melting down, we'll give you something like an alloy Y tip. So there are a lot of neat things going on, I'm sure G.E. has similar types of programs. We

have them, I'm sure Williams International has them, most of the engine companies now are getting very strong in the materials area and we're very proud of the whole industry and what we're doing in the high temperature materials area. Thank you very much for your indulgence.

Mr. Clinton Ashworth (Pacific Gas & Electric):

I came here for a couple of reasons, one of which was to try and find some ideas for something to sponsor but unfortunately I feel I am going away empty handed. I represent PG&E which is the local power company here, and my name is Clinton Ashworth. We are a large company, and I was gratified to read this weeks Business Week to find that in one of the categories of the largest corporations in America, we are number 21. We're the largest single sponsor of the Electric Power Research Institute. The California utilities have considerable interest in looking at very high temperature cycles, and if we can find applications or potential applications, then putting in a little bit of seed effort into these things. I don't think I'm speaking alone on this subject, we're looking for ideas but we are very selective. We're looking for ideas that are potentially useful and we feel there is a need for the ultimate customers of whatever it is people are developing to participate in them, giving them some market oriented guidance from the onset of the works, so that we don't end up with a bunch of white elephants that someone has put a lot of money into. I got a call from Southern California Edison on Monday and the question was, (we have been thinking about MHD), what should we do next? Their apparent position has changed and we are now looking for things that are potentially useful and applicable to power generation. The hottest thing we have got going at the moment in my shop is the work we are doing on mass steam injected gas turbines (M.S.I.G.T.). The utility industry is thinking small, we're not spending a great deal of effort on the kinds of conventional things that we're noted for and accustomed to. And so I regret that I feel like I am going away without a good sponsorable idea, that is a concept with some specifics that are applicable that we can encourage the development and research on by showing a little bit of interest. We put about one million dollars last year on the M.S.I.G.T., and another \$450,000 into the so called Cheng Cycles. I think we are big on our R&D budget but small on good ideas, we are selective and we have got to have good ideas and if anyone has an idea to apply these energy exchangers to the kinds of things that the utilities would be interested in, I would be very interested in hearing about them.

Mr. George Derderian (NAVAIR):

Ray, to me this is an educational process, my knowledge of wave rotors and Complexes being meager. I am impressed by the dedication of the many people over many years in this subject area, and it appears to me, looking at what's happening here, funding has been provided on a very limited basis, on a stop/go basis. At the same time, when you look at what is available in terms of funding to cover projects of this sort, that also is very limited. Two or three things that I, from a sponsor's point of view, would like to know is could one do, in some rational and logical way, a comparative pay off of wave engines versus classical gas turbines. Because it is not apparent to me readily, although I have looked at cycles and I think I understood partially what was being said, what the potential pay-offs are, and therefore why should one fund this? The second thing is, assuming that the pay-off does exist, a

lot of work has been done in bits and pieces. I'm not sure who the key bodies are here that ought to go out and get funding, I know that I can not fund the class of project that I think this falls into. We have to find out what's been done, what's satisfactory, what's unsatisfactory, find out what state these things are in, find out what the voids are, and of the voids that exist there are only perhaps some critical items that ought to be taken care of. I spoke with Arthur (Kantrowitz) a few minutes on this subject, and I would very much encourage the kind of committee that he spoke of. You can not deal with this in bits and pieces because you will flounder for another 20 years. That's my opinion, and I say when this meeting closes there has got to be an action. You cannot just walk away. I fully agree with Dr. Kantrowitz' suggestion that action has to be taken, and I think the minutes of the meetings should reflect these actions or proposed actions.

Prof. Shreeve:

Did you have a comment, Max?

Prof. Max Platzter (Naval Postgraduate School):

I am not sure if the conclusion needs to be that there is going to be another 20 years of floundering.

Mr. Derderian:

There should not be.

Prof. Platzter:

There should not be. My impression is that the technology that is currently available be applied. I am looking at Professor Berchtold, that one can put together the partial system for the kinds of applications that have been mentioned. Examples are helicopters, high flying aircraft and so on. All we need to do at the moment seems to me is to get on with the job.

Mr. Derderian:

I see quite a bit of computational work taking place, a number of experiments over a period of time, and an industrial product that's on the market now. The tone of what's being talked about here is a device that's flightworthy. Let me give you a brief background as to my qualifications; I was the head of one of the branches which engineered and qualified engines for the Navy, helicopters and the like. Now if you were to come to me with what is available today, I would not support it. Because to put an engine up in the air, you're talking about huge resources, millions of dollars, (helicopters are five to fifteen million dollars a piece), and you are crashing substantial equipment if and when meager things fail. And if there are people in these vehicles, a crash usually means some deaths. With turbochargers the problem is not so serious, a car or a truck will just stop and pull off the road. But if we happen to have a technological failure in the case of wave rotor gas turbines we are talking of an expense running into, perhaps, a billion dollars; a technological failure for even a simple helicopter can very well run into this kind of a figure. I've undertaken some fairly sizeable projects, and I was talking to Dr. Kantrowitz about fibre optics, where we are in the

process of doing something similar. When you look at how to apply these things to aircraft controls, or aircraft engine controls, you find out that some of the control instruments and transducers etc. have not been developed. We didn't know what the voids were and where to put the dollars. I'm not saying that the work that has been done is not worthy, I'm saying that, I don't know what I should work on next if I had to fund something; what to work on next to make something happen. It appears as though there is something to this type of machinery and one must take advantage of that.

Prof. Platzer:

Do I hear that we should make specific proposals for the development plan, what should be worked on next, is this what should be done? Is this what the outcome of the meeting should be?

Dr. Shreeve:

Am I right George, that you are not yet convinced of the potential?

Mr. Derderian:

No. That is not what I said. Absolutely not.

Dr. Shreeve:

You are convinced of the potential, but you don't have a project.

Mr. Derderian:

No, that is not what I am saying. What I am saying is that the area is wide open. Bits and pieces have been done. You have a huge mosaic if you will, okay, and bits and pieces of the wall of this mosaic have been put together. Some of it is good work and some of it is, frankly, just short of disaster. I must be blunt about it, because I don't want to say everything is alright when everything is not alright. But there is substantial good work here. Now, if one were to logically fund parts of this, because there appears to be a payoff, the question is what should one fund? I don't know, and I am not sure that there is someone that can come in and say, okay, you need to do this. In this type of equipment it isn't readily apparent to me what we have to do early on to get this piece of equipment to become a successful machine.

Mr. Nick Daum (Naval Air Propulsion Center):

First of all I would like to say, Ray, that you have done a marvelous job in getting the total wave engine community together for this workshop. I have seen what I consider five different groups that have added to the total effort in this area. Mr. Pearson has piqued the curiosity of everybody in this room because he has run the thing and apparently has been successful. And yet the question burns, why can't we repeat this? And then I see Spectra (Technology) with some excellent work in the area of analysis, as I see Exotech and Science Applications Inc. Where I see Spectra coming from is that they say, well, we are either going to do more analysis to get a higher confidence level or, we are going to start cutting metal and start building something. Now I say, good luck, find somebody who will help you cut metal, and I don't know if they can

make a convincing enough proposal to do that as their next step, to get into experimenting. When I see Brown Boveri, they have apparently been successful with the Comprex. For two years we have seen the Comprex in production, but we don't see a measure of success and we are waiting for BBC to gain a greater share of the commercial market. Then we see General Power Corp. and we say they have got to run the thing in a self-sustaining mode and produce power. Only then will we start making some marks in this wave rotor community that people will take notice of.

Dr. Thayer:

I have a couple of comments. Having worked in the area, (not as many years as many people here), I heard some suggestions early on this afternoon that people take BBC's rotors and experiment with them. I think that is a very misdirected idea. I think Ray (Shreeve) probably has a little bit of appreciation for that, having taken a rotor that somebody built 20 years ago and building an experiment around it. It compromises all the objectives that you can have in doing an experiment. I think that, without mentioning specific company names, if you try to do a project that is misdirected, that deals with an idea that is possibly flawed, or tries to have too ambitious an objective without an appreciation for all the parts, (and these devices are very complex), somebody can very easily bury the whole project, the whole concept. There are several different steps that need to be taken. Some of them are analytical, I think nobody here who has talked about analysis has the wrong approach, I think there are features of everybody's work that adds to the overall understanding of this problem; however, there are a lot of mechanisms that people have really not dealt with adequately. Shmuel (Eidelman) has dealt with one problem which is an important problem. Maybe a less sophisticated way (using techniques that have been around for many years) can still contribute to the understanding of the complex unsteady fluid dynamics of what's going on. I think analysis has to be done and it has to be improved. I'm not sure that it has to be taken much further than it is now to identify the critical issues which are going to control whether a specific machine works or doesn't work. So there has to be a well founded approach in terms of analysis and experiments, and I'm not sure the analyses that are available now are not adequate to put together a machine that works reasonably well. Basic research is needed for some critical processes; maybe it will stop machines, maybe it won't. I think a multi-faceted approach to develop these machines is needed. It includes both analyses and experiments with a maximum draw on past work that's been done, which is really not available to a lot of people. I would really like to see the RR and the G.E. information exposed so that those of us that could make comparisons and analysis with past experiments have enough information to do that kind of thing. There is no way right now for us even to compare what we have done to what anyone else has done. The whole area is so fragmented, that there is no continuity of thought.

Dr. Shreeve:

The formation of the committee could help to rectify that.

Dr. Thayer:

Certainly.

Mr. Z (Unidentified Speaker):

I think that's a good point, because if your analysis is good enough, that you could for instance use it to predict the characteristics of the Comprex in terms of overall performance, then you would have some confidence in that technique. You could then apply these characteristics to other wave rotor concepts that are optimized for, let's say, turbofan engines, and give the gentleman from Williams International his map, albeit analytical, and he can do his cycle studies with it. Without that you are going to have a hard time convincing anybody that it has application capability. I think the analysts have to get together with the experimenters and verify each other's work, and be able to produce characteristics, not necessarily for the machines that have been designed and tested, but for new machines, using extrapolated analytical capability, that are designed or optimized for turbojet applications.

Dr. Matthews:

I have an assorted bag of comments. I want to say that computational and experimental efforts have to go hand-in-hand. Any advance in computation is only as good as its experimental verification. For example, the excellent predictions that Dr. Eidelman has made are only fully valuable when they can be experimentally verified; for example using the two-focus laser technique we have. Each advance in computation has to be matched with an advance in experiment and we should have an exchange of information. There could be proprietary interests which may come in the way of doing this.

Mr. Z:

But that would only be necessary to use the analytical technique to predict the overall characteristics.

Dr. Matthews:

Exactly, but when you have detailed computations showing what's happening inside a cell, then you need detailed measurements to match that. Similarly, to have global measurements and characteristics...(garbled), you need to run cycles to show whatever it maybe at whatever depth you have to match them. That's one problem. The other comment is that in this two day meeting we have had a historic review of everything that has happened in wave engines in several countries and I would like to briefly mention that recently I have been made aware of the fact that there is work going on in the People's Republic of China. They are working on the Comprex in two places, in Canton and in Peking. I don't have further details as yet, but I hope to find out some more about it. I believe that their direction is towards supercharging as well. Next, the point which you made about the lack of commercial success, there I want to say that as engineers we feel that we have made a useful machine, something that works, and we are thoroughly pleased with it. We have tested it extensively. But you have pointed out that it has not been a commercial success, and that is certainly something that bothers BBC. There I must say that a product which is being sold commercially must be perceived to be useful and not only just be useful; in fact you can sell the most useless things provided you have created the right image with the right advertising. The difficulties which we might have in making it a commercial success might not be the same that bother you in your engine program, because here in the

engine program there are engineers convincing other engineers, whereas in our situation it is a question of trying to convince the man on the street to spend one hundred dollars more on something. Just like you in America have the anti-nukes, we in Europe have the anti-motoring lobby which believes that the motor car is responsible for acid rain and that there should be much less motoring and that the speed limit should come down, and gasoline should be rationed. So there are all kinds of such social, political, and economic factors against which we have to struggle to make it a commercial success. Nevertheless we hope that this success is coming our way. Finally I want to say that this has been a fascinating educational experience for me, I'm glad to know that there is so much interest in it elsewhere in the world, I have come down from the Swiss mountains and am delighted to find that here is something which is getting a lot of attention. I want to wish my American colleagues good luck. Thank You.

Dr. Shreeve:

I would like to add one remark here. I think if there had been so much promise on paper earlier, you would probably have seen three prototype efforts going on in different companies. The days seem to have gone when it was possible to explore ideas in prototype programs, simply because of cost. I see that as the difference. I think the promise is there. Now you have to be extremely careful before you can get programs funded, and you can only do one. That puts the onus on somebody to produce. I see that as the main obstruction. It will never be possible to fund two competitive efforts in this field.

Mr. Richard Joy:

I just got an idea of how you might get some of that P.G. & E. money out of Mr. Ashworth. The Cheng Cycle is a splendid device that was patented; I thought I invented it 20 years ago. It involves putting a lot of steam into the turbine and forcing the turbine to pass maybe 20% or 30% more air than the compressor is delivering. The net result is, the turbine cannot handle that extra mass of gas, so it causes the compressor to surge. Now they would like to put in about 20% by weight more steam through the turbine than is currently going, and the only way you can do that without causing the compressor to surge is to boost the compressor ratio about 20%, i.e., we want a burner with a 20% pressure rise. Which apparently the complex will do.

Mr. Clinton Ashworth:

My only comment on that is if two Cheng Cycles are running, they don't know that they need 20% more...

Mr. Richard Joy:

You haven't fully exploited the full advantage. You haven't raised all the steam you could have in the boiler, nor put it back in, and your potential has been limited. Think about what the Complex can do for you.

Mr. Clinton Ashworth:

I think the idea of the combined topping in a Cheng cycle or a steam injected

gas turbine with an energy exchanger is something that looks good on paper, and something that we might be interested in looking into.

Dr. Shreeve:

As a result of all the remarks, I think if anything can be done, (-and I would like to thank Professor Kantrowitz for suggesting it-) it is to perhaps get together a committee as soon as possible and have them sign a letter..... summarizing the conclusions of this workshop. It might serve a useful purpose.

I appreciate all the thanks people have given to me, I would like in turn to thank Jack (King), Mike (Odell), Ray (Phillips) and Michelle (Rigterink), who have done a lot of the work, and Atul (Mathur), particularly. Atul did all the work setting this workshop up. I just started off the idea, he basically handled it. As for my own thanks I am just trying to do my job. I work for the government and it is the intent at the moment to try to look for areas in which there is a pay off. We did this initially at DARPA'S instigation and we will be meeting with the DARPA people tomorrow. I don't think the workshop was wasted in that respect, because in what happens tomorrow in talking to DARPA, they will be informed. I think the workshop has certainly done that much.

I think that some project that will work is needed. I seriously mean a project that will work. If there is going to be a project with a wave rotor in it, funded through prototype now, it has got to be successful. Otherwise, 20 more years may elapse; that's the status. The wave rotor concept has been around a long time, and I think the way it is done next time has to work. So it must not be a go-no go kind of ambitious program; it's got to be phased, planned and it has got to be supported through a logical series of steps.

I would like to thank Professor Kantrowitz for coming out and attending the meeting and giving us a very welcome address, a very good set of suggestions and interacting with everybody. And to Max Berchtold who has put in a very valuable contribution and has come a long way to do it, -thank you. Also Ron Pearson, Ron I know you are what you are, a star; thank you very much for all your input. We haven't had it all yet I know. And thank you to all the presenters. The meeting was very stimulating for me, it pulled people from all parts of the world, some of whom I knew, some I didn't and the composite was very well worth while. I thank everyone for coming to listen, both the industry and government people.

If nobody has any more remarks I declare the workshop adjourned.

Appendix A

Remarks on the Applicability of Computational Fluid Dynamics
to Wave-Rotor Technology

D. B. Spalding

WAVE-ROTOR RESEARCH AND TECHNOLOGY WORKSHOP

NAVAL POSTGRADUATE SCHOOL
MONTEREY
CALIFORNIA

26 and 27 March 1985

REMARKS ON THE APPLICABILITY OF COMPUTATIONAL FLUID DYNAMICS TO WAVE-ROTOR TECHNOLOGY

by

D Brian Spalding
Computational Fluid Dynamics Unit
Imperial College
February 1985

Despite the enthusiasm and inventiveness of a large number of talented individuals, sometimes backed by considerable industrial resources, wave-rotor devices (also known as 'pressure exchangers', and, developed by Brown Boveri, as 'complexes') have achieved remarkably little commercial success.

What is the reason for this? Are such devices basically inferior to their competitors? Or have their possibilities not yet been properly evaluated?

In the view of the present writer, there still remain good prospects for commercial success: but this will come only when as-yet-unexplored geometrical and operational possibilities are systematically investigated.

For the most part, wave-rotor research has concentrated on designs in which the cells containing the working fluid are wrapped around cylindrical surfaces, and have cross-sectional areas which are uniform along their length. The patent literature shows examples of cells on conical and other surfaces, with variations of cross-section, and with a variety of curvatures applied to the cell walls. However, there has been little systematic investigation of these possibilities by practical experiment.

Theoretical analyses of wave-rotor performance have been based, perhaps exclusively, on one-dimensional analyses, often those of the 'characteristics' type, which leave out of account the effects of heat transfer, friction, etc. Therefore, whether the changes in geometry envisaged by inventors would actually improve the

performance, and if so by how much, are not known.

The present writer was associated with the research on pressure exchangers, as they were called by the team with which he was working, in the late 1950's and early 1960's. The project in question had been initiated by Mr G Jendrassik, in associated with Power Jets Limited of London. When Mr Jendrassik died prematurely, the present author was hired by Power Jets to persist with the theoretical developments. In charge of the work on the Power Jet side was Mr J Hodge, followed by Mr J E Barnes; and experimental work was conducted at Ricardo's Limited. In those days, the experimental approach was the only practical one; and a program was set up in which some of the geometrical variables would be systematically varied, and the corresponding performance changes observed. However, although the first results were extremely promising, improving them was found to be difficult; and the project was abandoned because funds ran out. Computers, and computational procedures, were too little developed for any extensive theoretical analysis to be made, although the writer's students did, at Imperial College subsequently, continue with research of that kind.

Interpretation of the experimental results showed one thing very clearly, the flow was not one-dimensional. Departures from the behaviour postulated by the theoretical analysis were caused by several factors including:-

1. friction and heat transfer at the cell walls;
2. non-uniformities of flow across the cell cross-section while the ends of the cells were passing the entry and exit ports; and
3. the tendency of the centrifugal forces operating on the gases in the cell to cause heavy cold gas to go to the outside while hot light gas went to the inside.

In the writer's opinion, it is the latter effect which was most productive of poor performance, and it is one which has been partially remedied by the introduction of cells which have radial sub-divisions.

No investigations were made by the Power-Jets team of non-cylindrical rotors, or of blades with curvature.

Computational fluid dynamics has now advanced to the point at which it becomes practical to include in simulations of wave-rotor phenomena all those effects which were formerly omitted and which proved so troublesome. It is now a comparatively easy matter to

simulate the three-dimensional flow in a wave-rotor cell, and to take account of the body forces which promote 'stratification' of the hot and cold gases and of the turbulent-mixing effects which tend to oppose such stratification. The non-uniformities of flow resulting from the gradual opening of the ports can be accounted for; it is also possible to introduce the effects of using cells of varying cross-sectional area, and the influence of having them wrapped on an arbitrary body of revolution rather than a cylinder.

In the opinion of the present writer, therefore, it is desirable that those who remain interested in wave-rotor research should adopt the computer simulator as the main means by which they will conduct their investigations, and will resort to experimental confirmation only when the computer has indicated where performance is likely to be especially good, or where phenomena of interest are likely to be especially easily detected.

There is no need for anyone wishing to perform this work to begin constructing a computer code especially for the purpose. The PHOENICS Computer Code, with which the present writer is associated, is capable of doing the job very well; and the investigator will have only to introduce the initial and boundary conditions which concern him, and then, when he has exhausted the possibilities of the existing turbulence models, to make modifications in that particular area. Otherwise, all he needs is a computer, and the ability to operate it for long periods of time in order that performance trends, and other interesting features of the simulation, can be detected.

This program is available on a royalty- and licence-free basis to academic researchers; and the present writer would be particularly pleased if he could supply copies to those who wanted to use it for investigating the still-insufficiently explored possibilities of wave-rotor machines.

Appendix B

Wave Rotor Workshop Program

ONR/NAVAIR SPONSORED
WAVE ROTOR RESEARCH & TECHNOLOGY WORKSHOP

LOCATION: INGERSOLL HALL RM 122
NAVAL POSTGRADUATE SCHOOL
MONTEREY, CALIFORNIA

CHAIRMAN: R. P. SHREEVE
(408) 646-2593

Tuesday 26th March

0730 REGISTRATION (COFFEE & DONUTS)

INGERSOLL HALL 122

0830 WELCOME

M. F. PLATZER
NAVAL POSTGRADUATE SCHOOL

0840 OPENING ADDRESS

A. KANTROWITZ
Dartmouth College

0910-1200 SESSION 1 - PRESSURE EXCHANGERS

"The Pressure Exchanger; An
Introduction, Including a
Review of the work of Power
Jets (R&D) Ltd".

J. Kentfield
University of Calgary

The Comprex

M. BERCHTOLD
Swiss Federal Institute

The Gas Dynamics of Pressure
Wave Superchargers

L. MATTHEWS
Brown-Boveri Ltd.

The MSNW Energy Exchanger
Research Program

W. J. THAYER
Spectra Technology Inc.

1400-1700 SESSION 2 - WAVE ENGINES

A Gas Wave-Turbine Engine which
Developed 35 HP and Performed over
a 6:1 Speed Range

R. PEARSON
Univ. of Bath, U.K.

A Brief Review of the G. E.
Wave Engine Program of 1958-63

A. MATHUR
NPS/Exotech Inc.

Studies and Rig Tests of a Wave
Rotor for a Helicopter Engine.

R. K. Moritz
Rolls-Royce Ltd.

Comparison of Wave and Steady
Flow Machines

H. E. WEBER
San Diego State University

The General Power Corporation
Engine Program

M. BERCHTOLD/H. E. WEBER
Swiss Federal Institute
San Diego State University

1715-1900 SOCIAL HOUR

Del Monte Room, Herrmann Hall

Wednesday 27th March

0730 (Coffee and Donuts)

0800-1600 SESSION 3 - RESEARCH AND APPLICATIONS STUDIES

A. Mathur, Naval Postgraduate School (Exotech Inc).
Design and Experimental Verification of Wave Rotor Cycles

S. Eidelman, Naval Postgraduate School (SAI, Inc).
Gradual Opening of Axial and Skewed Passages in Wave Rotors.

D. G. Wilson, Massachusetts Institute of Technology
Potential for Use of Wave-Rotor Technology to Approach Constant-Volume Combustion for Gas-Turbine Engines.

N. Zubatov, Purdue University
Application of Wave Energy Exchanger to Industrial & Energy Systems.

W. Kostafinski, NASA Lewis Research Center
Comparison of the Wave-Rotor-Augmented to the Detonation-Wave-Augmented Gas Turbine.

1130-1315 LUNCH

M. Berchtold, Swiss Federal Institute, Zurich
The Comprex as a Topping Spool in a Gas Turbine Engine For Cruise Missile Propulsion.

R. Taussig, Spectra Technology Incorporated
Wave Rotor Turbofan Engines for Aircraft.

R. Pearson, University of Bath
Performance Predictions for Gas Turbine-Wave Engines Including Practical Cycles with Wide Speed Range.

1445-DISCUSSION SESSION

Opportunity for questions and for the expression of opinions and recommendations.

1600 (APPROX) CLOSING REMARKS & ADJOURNMENT

NOTE: A VISIT TO THE TURBOPROPULSION LABORATORY WILL BE AVAILABLE ON REQUEST FOLLOWING ADJOURNMENT.

CONFERENCE PHONE & MESSAGE CENTER (408) 646-2362
ARRANGEMENTS- ATUL MATHUR, MICHELLE RIGTERINK
POST CONFERENCE PHONE (408) 646-2165

Appendix C

List of Attendees

List of Attendees
(Alphabetical Order)

1. Clinton P. Ashworth
Supervising Mechanical Engineer
Pacific Gas & Electric Company
77 Beale St., Rm 2547
San Francisco, CA 94106
(415) 972-2910
2. Max Berchtold*
Professor
Swiss Federal Institute of Technology
Zurich, Switzerland
ETH Zentrum, CH 8092
ZURICH, Switzerland
01-256-2479
3. Oscar Biblarz
Code 67B1
Department of Aeronautics
Naval Postgraduate School
Monterey, CA 93943
(408) 646-2312
4. Tibor Bornemisza
Principal Engineer Adv. Tech.
TURBOMACH DIV. SOLAR TURBINES INC.
4400 Ruffin Rd.
San Diego, CA 92123
(619) 238-3090
5. Robert Bullock
President
Bullock and Bullock Inc.
P. O. Box 6037
Scottsdale, AZ 85261
(602) 947-9314
6. George Cheklich
Chief Engine Research Function
Army Tanks Command
Warren, Michigan 48397-5000
(313) 574-6319 autovon: 786-6319
7. Thomas T. Coakley
Research Scientist
Computational Fluid Dynamics
NASA Ames Research Center-STE Branch
Moffett Field, CA 94035
Mail Stop 229-1
(415) 694-6451
8. Nicholas Daum
Program Manager/Wave Rotor Dev. Prog.
Naval Air Propulsion Center PE34
P. O. Box 7176
Trenton, NJ 08628
(609)896-5747
9. George Derderian
Propulsion Manager
Naval Air Systems Command, Code 310E
Washington, D. C. 20360
Autovon: 222-7447
10. Shmuel Eidelman*
Research Physicist
Science Application International Co.
1710 Goodridge Dr. Mail stop G-8-1
Mc Lean, VA 22306
(202) 767-3254
11. Robert Erdmann
Senior Vice President
Science Applications Intl. Corp.
P. O. Box 2351, Mail stop 8
La Jolla, CA 92037
(619) 456-6152
12. Joseph Foa
School of Engineering and Applied Sciences
The George Washington University
Washington, D.C. 20052
(202) 676-6149
13. Steven Freedman
Executive Scientist/Technology Evaluation
Gas Research Institute
8600 West Bryn Mawr Ave.
Chicago, IL 60631
(312) 399-8390
14. John Glancy
Science Applications International Co.
P. O. Box 2351
La Jolla, CA 92037
(619) 456-6152

* Speaker

15. Darryl W. Hall
Senior Staff Scientist
Science Applications Intl. Corp.
994 Old Eagle School Rd. Suite 1018
Wayne, PA 19087
(215) 687-5080
16. James Hammer
President, HESCO
9 Sierra Vista Dr.
Monterey, CA 93940
(408) 372-5697
17. William Ingle
Manager Research
Gas Research Institute
8600 Bryn Mawr
Chicago, IL 60631
(312) 399-8337
18. Richard J. Joy
Senior Engineering Specialist
Williams International
2280 W. Maple Road
P. O. Box 200
Walled Lake, MI 48088
(313) 624-5200 Ext. 1362
19. Arthur Kantrowitz*
Dartmouth College
213 Cummings Hall
Hanover, NH 03755
(603) 646-2611
20. John Kentfield*
Professor
Dept. of Mechanical Engineering
Faculty of Engineering
University of Calgary
Calgary, Alberta, CANADA
(403) 284-5777
21. Dr. Anthony L. Laganelli
Chief Scientist
Science Applications International Corp.
994 Old Eagle School Rd.
Wayne, PA 19087
(215) 687-5080
22. Atul Mathur*
Code 67Xu
Department of Aeronautics
Naval Postgraduate School
Monterey, CA 93943
(408) 646-2888
23. Lebius Matthews*
Senior Research Engineer
BBC Brown-Boveri
Baden, Switzerland
01 056 75-2869
24. Robert Moritz*
Senior Project Engineer
Rolls Royce Inc.
1895 Phoenix Blvd., Suite 400
Atlanta, GA 30349
(404) 996-8400
25. Hal Moses
Ex-NAVAIR Professor
Department of Mechanical Engineering
Randolph Hall, VPI & SU
Blacksburg, VA 24061
(703) 961-7188
26. Ian Moyle
Exotech Inc.
1901 S. Bascom Ave.
Suite 337
Campbell, CA 95008
(408) 559-7616
27. Badri Narayanan
Code 67Ba
Department of Aeronautics
Naval Postgraduate School
Monterey, CA 93943
(408) 646-2165
28. Friedrich Neuhoff
Code 67Nf
Department of aeronautics
Naval Postgraduate School
Monterey, CA 93943
(408) 646-2880
29. Ivan Oelrich
Research Staff Member
Institute of Defense Analyses (IDA)
1801 N. Beauregard Street
Alexandria, VA 22311
(703) 845-2289

30. Ronald D. Pearson*
Lecturer
School of Engineering, University
University of Bath, Claverton Down
Bath, Avon, BA2 7AY, United Kingdom
Bath 61244 Ext. 375
31. Ray Phillips
Code 67Sf
Department of Aeronautics
Naval Postgraduate School
Monterey, CA 93943
(408) 646-2165
32. Michael J. Pierzga
Aerospace Engineer/Small Turbine Technology
NASA Lewis Research Center Mail Stop (5-9)
21000 Brookpark Road
Cleveland, OH 44212
(216) 433-4000 Ext. 5376
33. Max Platzer*
Code 67
Department of Aeronautics
Naval Postgraduate School
Monterey, CA 93943
(408) 646-2312
34. Edwin Resler Jr.
Professor
Cornell University
204 Upson Hall
Ithaca, New York 14853
(607) 256-5081
35. Wojciech Rostafinski*
Aerospace Engineer
Advanced Planning & Analysis Office
NASA Lewis Research Center
Cleveland, OH 44135
(FTS) 294-6132
36. Nicholas Rott
Stanford University
Palo Alto, CA 94305
37. Arun K. Sehra
Supervisor, Compressor Research
Allison Gas Turbine, Speed Code T14
P. O. Box 420, Indianapolis, IN 46206
(317) 242-4807
38. Raymond Shreeve (Chairman)
Code 67Sf
Department of Aeronautics
Naval Postgraduate School
Monterey, CA 93943
(408) 646-2593
39. Fred Sidransky
Principal Engineer
Sundstrand Aviation Operations
4747 Harrison Ave. P. O. Box 700
Rockford, IL 61125
(815) 226-6767
40. Edward Stawski
Research and Development
Naval Propulsion Center
P. O. Box 7176
Trenton, NJ 08628
(609) 896-5948
41. Robert Taussig*
Director, Energy Technology
Spectra Technology, Inc.
2755 Northup Way
Bellevue, WA 98004
(206) 827-0460
42. William J. Thayer*
Director of Flow Technology
Spectra Technology Inc.
2755 Northup Way
Bellevue, WA 98004
(206) 827-0460
43. John Tuzson
Manager
Gas Research Institute
8600 W. Bryn Mawr
Chicago, IL 60631
(312) 399-8234
44. Thomas Vitting
Research Scientist
Exotech Inc.
1901 S. Bascom Ave
Suite 337
Campbell, Ca 95008
(408) 559-7616

45. Jerry Walters
Government Products Division
P. O. Box 2691
Pratt & Whitney
West Palm Beach, FL 33402
(305) 840-2352
46. William F. Waterman
Sr. Supervisor, Compressor Aerodynamics
Garrett Turbine Engine Co.
111 So. 34th St. P. O. Box 5217
Phoenix, AZ 85010
(602) 231-2059
47. Helmut E. Weber*
Professor
Mechanical Engineering Dept.
San Diego State University
San Diego, CA 92182-0191
(619) 265-6067
48. Denis S. Whitehead
Whittle Laboratory, Engineering Dept.
Cambridge University
Trumpington Street
Cambridge, U. K.
Cambridge (0223) 66466
49. David Wilkinson
Aerospace Engineer
AFWAL/PORA
Wright Patterson AFB
Dayton, OH
(513) 255-5451 Autocon: 785-5451
50. David Gordon Wilson*
M. I. T. Mech. eng. room 3-455
Cambridge, MA 02139
(617) 253-5121
51. Oswald L. Zappa
Program Manager, Energy Directorate
AVCO Everett Research Laboratory, Inc.
2385 Revere Beach Parkway
Everett, MA 02148
(617) 381-4696
52. Nikolay Zubatov*
Professor
Purdue University, Calumet
Hammond, IN 46323
(219) 844-0520

Distribution List

WORKSHOP ATTENDEES (52) AND FOLLOWING ADDRESSEES
RECEIVE 1 COPY, EXCEPT WHERE INDICATED

1. Commander
Naval Air Systems Command
Washington, DC 20361

Attention: Code AIR 310
Code AIR 320D
Code AIR 530
Code AIR 536
Code AIR 7226
Code AIR 03D
2. Office of Naval Research
800 N. Quincy Street
Arlington, VA 22217
Attention: Code 200
Code 400
3. Commanding Officer
Naval Air Propulsion Center
Trenton, NJ 08628
Attention: V. Lubosky
4. Commanding Officer
Naval Air Development Center
Warminster, PA 19112
Attention: AVTD
5. Naval Postgraduate School
Monterey, California 93943

Attention: Code 1424 (4)
Code 012
Code 67Sf (10)
6. Library
Army Aviation Material Laboratories
Department of the Army
Fort Eustis, VA 23604
7. Air Force Office of Scientific Research
AFOSR/NA
Bolling Air Force Base
Washington, DC 20332
Attn: Mr. James Wilson
8. National Aeronautics & Space Administration
Lewis Research Center (Library)
21000 Brookpark Road
Cleveland, OH 44135
9. Library
General Electric Company
Aircraft Engine Technology Division
DTO Mail Drop H43
Cincinnati, OH 44135
10. Library
Pratt & Whitney Aircraft Group
Post Office Box 2691
West Palm Beach, FL 33402
11. Library
Pratt-Whitney Aircraft Group
East Hartford, CT 06108
12. Library
Curtis Wright Corporation
Woodridge, NJ 07075
13. Library
AVCO/Lycoming
550 S. Main Street
Stratford, CT 06497
14. Library
Teledyne CAE, Turbine Engines
1330 Laskey Road
Toledo, OH 43612
15. Library
Williams International
Post Office Box 200
Walled Lake, MI 48088
16. Library Detroit Diesel Allison Div.
Post Office Box 894
Indianapolis, IN 46202
17. Library
Garrett Turbine Engine Company
111 S. 34th Street
Post Office Box 5217
Phoenix, AZ 85010
18. Dr. Robert Williams
Defense Advanced Research Projects
Agency
1400 Wilson Blvd.
Arlington, VA 22209

Distribution List (Cont.)

19. Erich E. Abell
Technical Director
U.S. Air Force Dept. of Defense
Wright-Patterson AFB
Dayton, OH 45433
20. Dr. Edward T. Curran
Chief Scientist
Aero Propulsion Laboratory
Wright-Patterson AFB,
Dayton, OH 45433
21. Fredrick I. Ordway
Director Special Projects
Department of Energy
Washington, DC 20585
22. Staff Specialist, Propulsion
OSD/OU SDRE (R & AT/MST)
Room 3D1089
The Pentagon
Washington, DC 20301
23. Mr. R. A. Langworthy
Army Aviation material Laboratories
Department of the Army
Fort Eustis, VA 23604
24. Dr. Arthur J. Wennerstrom
Chief, Compressor Research
AFWAL/POTX
Wright-Patterson AFB
Dayton, OH 45433
25. Dr. Marvin E. Goldstein
Chief Scientist
NASA Lewis Research Center
21000 Brookpark Road
Cleveland, OH 44135
26. Mr. Melvin Hartman
Research & Technology Assessment MS 3-7
NASA Lewis Research Center
21000 Brookpark Road
Cleveland, OH 44135
27. Mr. Ziemianski
Chief, Propulsion Systems Projects Div.
NASA Lewis Research Center
21000 Brookpark Road
Cleveland, OH 44135
28. Director, Propulsion Laboratory
U. S. Army Research and Technology Lab.
NASA Lewis Research Center
21000 Brookpark Road
Cleveland, OH 44135
29. Mr. Larry Fishbach
NASA Lewis Research Center MS 6-12
21000 Brookpark Road
Cleveland, OH 44135
30. Calvin Ball, Small Gas Turbine Engines
NASA Lewis Research Center MS 77-6
21000 Brookpark Road
Cleveland, OH 44135
31. Mr. Bert Phillips
NASA-Lewis Research Center
21000 Brookpark Rd. MS 500-203
Cleveland, OH 44135
32. Dr. Robert E. English
Distinguished Research Associate
NASA-Lewis Research Center
21000 Brookpark Rd. MS 60-2
Cleveland, OH 44135
33. Mr. Wayne Wheelock
DRSTA - RGR
U. S. Army Tank Automotive Command
Warren, MI 48090
34. Mr. John Hansen
Defense Advanced Research
Projects Agency
1400 Wilson Blvd.
Arlington, VA 22209

Distribution List (Cont.)

- | | |
|-------------------------------------------------------------------------------------------------------------------------------------|---------------------------------------------------------------------------------------------------------------------------------------------------|
| 35. Mr. R. C. Coleman Jr.
General Power Corporation
224 Planck Avenue
Paoli, PA 19301 | 43. Mr. Frank Parry
Research and Development Assoc.
P. O. Box 9695
Marina Del Rey, CA 90291 |
| 36. Director, Research and Development
Ford Motor Company
P. O. Box 2053
Dearborn, MI 48121 | 44. Mr. Francis X. Dolan
Creare Incorporated
P. O. Box 71
Hanover, NH 03755 |
| 37. Dr. Charles E. Treanor
Calspan-UB Research Center
P. O. Box 400,
Buffalo, New York 14225 | 45. Mr. Ted Pasternac
Science Applications, Inc.
P. O. Box 2351
La Jolla, CA 92038 |
| 38. Mr. Anil K. Nijhawan
Teledyne, CAE
1330 Laskey Road
Toledo, OH 43612 | 46. Mr. Earl F. Krapp
Solar Turbines Incorporated
Subsidiary of Caterpillar
Tractor Co.
P. O. Box 85376
San Diego, CA 92138-5376 |
| 39. Mr. Peter C. Tramm
Allison Gas Turbine Division of
General Motors
P.O. Box 420,
Indianapolis, IN 46206-0420 | 47. Mr. Earl J. Slanker
General Electric Company
Gas Turbine Division
Onve River Road
Building 500, Room 210
Schenectady, NY 12345 |
| 40. Dr. Adrian Pallone
Chief Scientist
AVCO Systems Division
AVCO Corporation
201 Lowell Street
Wilmington, MA 01887 | 48. Director of Research
Sun Oil Research
Matson Ford Road
Radnor, PA 19087 |
| 41. Dr. Shuang Huo
Marine Division
Westinghouse Electric Corp.
Hendy Avenue
Sunnyvale, CA 94088 | 49. Mr. P. W. Runstadler, Jr.
Box B-1170
Veron Corporation
Hanover, NH 03755 |
| 42. Dr. Wayne G. Burell
Director of Research
U. T. R. C.
Silver Lane
East Hartford, CT 06108 | 50. Mr. Archie H. Perugi
Manager, Energy Technology
Energy Systems and Tech. Div.
General Electric Company
Schenectady, NY 12345 |

Distribution List (Cont.)

- | | |
|------------------------------------------------------------------------------------------------------------------------------------------------------------|-----------------------------------------------------------------------------------------------------------------------------------------------|
| 51. Mr. Heldeubrand
Military Propulsion & Tech.
The Garrett Turbine Eng. Co.
111 South 34th St.
P. O. Box 5217
Phoenix, AZ 85010 | 59. Dr. Hans von Ohain
Room No. 3305
National Air and Space Museum
7th Independence, S. W.
Washington, D. C. 20560 |
| 52. Dr. D. C. Prince Jr.
General Electric Company
Aircraft Engine Tech. Div.
Cincinnati, OH 45215 | 60. Mr. Arthur H. Lefebvre
Purdue University
Thermal Sciences and Propulsion
School Of Mech. Engineering
West Lafayette, IN 47907 |
| 53. Mr. L. J. Stoffer
General Electric Company
Aircraft Engine Tech. Div.
Cincinnati, OH 45215 | 61. Mr. George Serovy
Iowa State University
Turbomachinery Components
Research Laboratory
Ames, Iowa 50011 |
| 54. Mr. David H. Archer
Manager, Chemical Engineering Res.
Westinghouse Electric Corp.
1310 Beulah Road
Pittsburgh, PA 15235 | 62. Mr. Eugene Covert
M. I. T.
Gas Turbine and Plasma Lab.
Department of Aeronautics
and Astronautics
Cambridge, MA 02139 |
| 55. Mr. Richard W. Foster-Pegg
Westinghouse Electric Corp.
CTSD, MS lab 100
P. O. Box 251
Concordville, PA 19331 | 63. Prof. R. S. Hickman
Dept. of Mechanical and
Environmental Engineering
Univ. of California,
Santa Barbara CA 93106 |
| 56. Dr. Eric Thornton
Manager, International Relations
The Gas Research Institute
8600 West Bryn Mawr Ave.
Chicago, Illinois 60631 | 64. Prof. B. T. Zinn
Aerospace Engineering, North Ave.
Georgia Institute of Technology
Atlanta, GA 30332 |
| 57. Mr. Robert Wilson
The A. D. Little Co.
25 Acorn Park
Cambridge, MA 02139 | 65. Dr. George Rudinger
State University of New York
327 Engineering East
Amherst, NY 14260 |
| 58. Dr. Paul Hermann
Head, Turbomachinery Tech. Staff
Sundstrand Aviation Operations
4747 Harrison Avenue
P. O. Box 7002
Rockford, IL 61101 | 66. Professor Gordon Oates
Department of Aeronautics
and Astronautics
University of Washington, MS FS-10
Seattle, WA 98195 |

Distribution List (Cont.)

67. Professor J. Sladky
Kinetics Group Incorporated
P. O. Box 1071
Mercer Island, WA 98040
68. Professor Frank E. Marble
Jet Propulsion and Mech. Eng.
California Institute of Tech.
MS 205-45
Pasadena, CA 91125
69. Professor James P. Johnston
Mechanical Engineering
Stanford University
Stanford, CA 94305
70. Professor Mitsuru Kurosaka
University of Tennessee
Tullahoma, TN 37388
71. Dr. Thomas C. Adamson, Jr.
Professor and Chairman
Department of Aeronautics
University of Michigan
Ann Arbor, MI 48109
72. Dr. Jack L. Kerrebrock
Department Head and Professor
Department of Aeronautics
Mass. Institute of Tech.
Cambridge, MA 02139
73. Dr. Lakshminarayana
The Pennsylvania State Univ.
153 Hammond Building
University Park, PA 16802
74. Mr. Sanford Fleeter
Purdue University
Thermal Sciences and Propulsion
School of Mechanical Engineering
West Lafayette, IN 47907
75. Mr. Jean Fabri
ONERA
29 Ave de la Division Leclerc
92 Chatillon
FRANCE
76. Professor Dr.-Ing. Heinz E. Gallus
Lehrstuhl und Institute Fur
Strahlantriebe und Turboarbeitsmaschinen
Rhein.-Westf. Techn. Hochschule Aachen
Templergraben 55
5100 Aachen
West Germany
77. Professor J. P. Gostelow
School of Mechanical Engineering
The New South Wales Institute of Tech.
New South Wales
Australia
78. Dr. Geoffrey P. Howell
Rolls-Royce Ltd.
P. O. Box 31
Derby, England DE28bj
79. Dr. K. N. C. Bray
Professor of Gas Dynamics
University of Southampton
Southampton, SO95nh
ENGLAND
80. Dr. F. Breugelmans
Von Karman Institute for
Fluid Dynamics
Turbomachinery Department
72, Chaussee de Waterloo
1640 Rhode-Saint-Genese
BELGUIM
81. Dr. R. S. Fletcher
Cranfield Institute of Tech.
School of Mech. Engineering
Cranfield, Bedford MK43 0AL
ENGLAND
82. Dr. George Gyarmathy
Swiss Federal Institute of Tech.
Lab of Mechanical Engineering
Sonneggstrasse 3, 8092 Zurich
SWITZERLAND

Distribution List (Cont.)

83. Dr. E. Brocher
Institut de Mecanique des Fluides
1, Rue Honnorat
13003 Marseille
FRANCE
84. Prof. D. Brian Spalding FRS
Head of CFDU and Professor
of Heat Transfer
Room 440 M.E. Building
Imperial College of Science and Tech.
Exhibition Road
London SW7 2BX, ENGLAND
85. Dr. F. A. Hewitt
Advanced Research Lab
Rolls-Royce Ltd.
P. O. Box 31
Derby, England DE2 8BJ
86. Mr. J. A. Barnes
Dept. of Mechanical Engineering
Imperial College
South Kensington
London, ENGLAND
87. Dr. G. B. R. Feilden
Feilden Associates, Ltd.
Greys End
Henley-on-Thames
Oxfordshire RG9 4QT
ENGLAND